IAEA RADIATION TECHNOLOGY REPORTS No. 3

Development of Novel Adsorbents and Membranes by Radiation-induced Grafting for Selective Separation in Environmental and Industrial Applications

IAEA
International Atomic Energy Agency

Development of Novel Adsorbents and Membranes by Radiation-induced Grafting for Selective Separation in Environmental and Industrial Applications

The following States are Members of the International Atomic Energy Agency:

AFGHANISTAN
ALBANIA
ALGERIA
ANGOLA
ARGENTINA
ARMENIA
AUSTRALIA
AUSTRIA
AZERBAIJAN
BAHRAIN
BANGLADESH
BELARUS
BELGIUM
BELIZE
BENIN
BOLIVIA
BOSNIA AND HERZEGOVINA
BOTSWANA
BRAZIL
BULGARIA
BURKINA FASO
BURUNDI
CAMBODIA
CAMEROON
CANADA
CENTRAL AFRICAN REPUBLIC
CHAD
CHILE
CHINA
COLOMBIA
CONGO
COSTA RICA
CÔTE D’IVOIRE
CROATIA
CUBA
CYPRUS
CZECH REPUBLIC
DEMOCRATIC REPUBLIC OF THE CONGO
DENMARK
DOMINICA
DOMINICAN REPUBLIC
ECUADOR
EGYPT
EL SALVADOR
ERITREA
ESTONIA
ETHIOPIA
FINLAND
FRANCE
GABON
GEORGIA
GERMANY
GHANA
GREECE
GUATEMALA
HAITI
HOLY SEE
HONDURAS
HUNGARY
ICELAND
INDIA
INDONESIA
IRAN, ISLAMIC REPUBLIC OF
IRAQ
IRELAND
ISRAEL
ITALY
JAMAICA
JAPAN
JORDAN
KAZAKHSTAN
KENYA
KOREA, REPUBLIC OF
KUWAIT
KYRGYZSTAN
LAO PEOPLE’S DEMOCRATIC REPUBLIC
LATVIA
LEBANON
LESOTHO
LIBERIA
LIBYA
LIECHTENSTEIN
LITHUANIA
LUXEMBOURG
MADAGASCAR
MALAWI
MALAYSIA
MALI
MALTA
MARSHALL ISLANDS
MAURITANIA
MAURITIUS
MEXICO
MONACO
MONGOLIA
MONTENEGRO
MOROCCO
MOZAMBIQUE
MYANMAR
NAMIBIA
NEPAL
NETHERLANDS
NEW ZEALAND
NICARAGUA
NIGER
NIGERIA
NORWAY
OMAN
PAKISTAN
PALAU
PANAMA
PAPUA NEW GUINEA
PARAGUAY
PERU
PHILIPPINES
POLAND
PORTUGAL
QATAR
REPUBLIC OF MOLDOVA
ROMANIA
RUSSIAN FEDERATION
RWANDA
SAUDI ARABIA
SENEGAL
SERBIA
SEYCHELLES
SIERRA LEONE
SINGAPORE
SLOVAKIA
SLOVENIA
SOUTH AFRICA
SPAIN
SRI LANKA
SUDAN
SWEDEN
SWITZERLAND
SYRIAN ARAB REPUBLIC
TAJIKISTAN
THAILAND
THE FORMER YUGOSLAV REPUBLIC OF MACEDONIA
TUNISIA
TURKEY
UGANDA
UKRAINE
UNITED ARAB EMIRATES
UNITED KINGDOM OF GREAT BRITAIN AND NORTHERN IRELAND
UNITED REPUBLIC OF TANZANIA
UNITED STATES OF AMERICA
URUGUAY
UZBEKISTAN
VENEZUELA
VIETNAM
YEMEN
ZAMBIA
ZIMBABWE

The Agency’s Statute was approved on 23 October 1956 by the Conference on the Statute of the IAEA held at United Nations Headquarters, New York; it entered into force on 29 July 1957. The Headquarters of the Agency are situated in Vienna. Its principal objective is “to accelerate and enlarge the contribution of atomic energy to peace, health and prosperity throughout the world’’.

IAEA Radiation Technology Reports Series No. 3

DEVELOPMENT OF NOVEL ADSORBENTS AND MEMBRANES BY RADIATION-INDUCED GRAFTING FOR SELECTIVE SEPARATION IN ENVIRONMENTAL AND INDUSTRIAL APPLICATIONS

INTERNATIONAL ATOMIC ENERGY AGENCY
VIENNA, 2012

COPYRIGHT NOTICE

Marketing and Sales Unit, Publishing Section
International Atomic Energy Agency
Vienna International Centre
PO Box 100
1400 Vienna, Austria
fax: +43 1 2600 29302
tel.: +43 1 2600 22417
email: sales.publications@iaea.org
http://www.iaea.org/books

For further information on this publication, please contact:

Industrial Applications and Chemistry Section
International Atomic Energy Agency
Vienna International Centre
PO Box 100
1400 Vienna, Austria
email: Official.Mail@iaea.org

Printed by the IAEA in Austria
November 2012

IAEA Library Cataloguing in Publication Data

Development of novel adsorbents and membranes by
radiation-induced grafting for selective separation
in environmental and industrial applications. –
Vienna : International Atomic Energy Agency, 2012.
p. ; 30 cm. – (IAEA radiation technology reports
series, ISSN 2225-8833 ; no. 3)
STI/PUB/1572
ISBN 978-92-0-134010-8
Includes bibliographical references.

1. Radiation chemistry. 2. Membrane technology.
3. Fuels cells – Research. I. International Atomic
Energy Agency. II. Series.

IAEAL 12-00769

FOREWORD

Radiation-induced grafting is a powerful technique for the preparation of novel materials based on easily available and low cost synthetic and natural polymers. The materials to be developed by radiation-induced grafting include special adsorbents and membranes for use in environmental and industrial applications. Grafting is used in situations where the requirements for bulk properties and surface properties cannot be readily met using a single polymeric material. Radiation provides a highly advantageous means of grafting. A large concentration of free radicals is produced in the irradiated material without the use of chemical initiators, and these radicals undergo reaction with a monomer of choice to produce macromolecular chains that are covalently bound to the irradiated specimen. Different geometries, including films, powders and macroscopic objects, have had surface grafted layers attached in this way. The current trend in research and development studies shows that, at present, radiation grafting on polymers is developing in three main directions: polymeric adsorbents, polymeric membranes and track etched membranes.

The recommendation for further research and development in this field was intensively discussed at the 7th International Symposium on Ionizing Radiation and Polymers (IRaP 2006), held from 23 to 28 September 2006, in Antalya, Turkey, and by the consultants meeting on radiation-induced grafting of polymers held from 29 September to 3 October 2006 in the same venue.

The coordinated research project (CRP) on Development of Novel Adsorbents and Membranes by Radiation-induced Grafting for Selective Separation Purposes has been launched with the objective of using gamma rays, electron beams and swift heavy ions for grafting of various monomers onto natural and synthetic polymers for the development of novel adsorbents and membranes for environmental and industrial applications.

The first Research Coordination Meeting (RCM) of the CRP was held in Vienna, from 19 to 23 November 2007. The meeting summarized the current status of investigations in this field and discussed the ways to meet the CRP goals. The second RCM, held in Aargau, Switzerland, from 15 to 19 June 2009, reported on the progress achieved since the first meeting, critically evaluated the results obtained by different groups and formulated the work programme and networking activities until the end of project. The final meeting was held in Budapest, Hungary, from 6 to 10 December 2010, and summarized the project results, with conclusions and recommendations for the future.

The IAEA wishes to thank all the participants in the CRP for their valuable contributions and E. Takacs for technical editing of this publication. The IAEA officers responsible for this publication were M.H. de Oliveira Sampa and S. Sabharwal of the Division of Physical and Chemical Sciences.

EDITORIAL NOTE

The papers in these Proceedings (including the figures, tables and references) have undergone only the minimum copy editing considered necessary for the reader's assistance. The views expressed remain, however, the responsibility of the named authors or participants. In addition, the views are not necessarily those of the governments of the nominating Member States or of the nominating organizations.

Although great care has been taken to maintain the accuracy of information contained in this publication, neither the IAEA nor its Member States assume any responsibility for consequences which may arise from its use.

The use of particular designations of countries or territories does not imply any judgement by the publisher, the IAEA, as to the legal status of such countries or territories, of their authorities and institutions or of the delimitation of their boundaries.

The mention of names of specific companies or products (whether or not indicated as registered) does not imply any intention to infringe proprietary rights, nor should it be construed as an endorsement or recommendation on the part of the IAEA.

The authors are responsible for having obtained the necessary permission for the IAEA to reproduce, translate or use material from sources already protected by copyrights.

Material prepared by authors who are in contractual relation with governments is copyrighted by the IAEA, as publisher, only to the extent permitted by the appropriate national regulations.

CONTENTS

REPORTS BY PARTICIPANTS OF THE COORDINATED RESEARCH PROJECT

SUMMARY

1. INTRODUCTION

Radiation-induced grafting is a powerful technique for the preparation of novel materials based on easily available and low cost synthetic and natural polymers. The materials to be developed by radiation-induced grafting include special adsorbents and membranes for use in environmental and industrial applications.

Grafting can impart surface properties highly different for those of bulk properties and radiation provides a highly advantageous means of initiation of polymerization reaction in the process. A large concentration of free radicals are produced in the irradiated material without the use of chemical initiators and these radicals initiate the polymerization reaction with a monomer of choice to produce macromolecular chains that are covalently bound to the irradiated trunk material. Different geometries, including films, powders and fibres have had surface grafted layers attached in this way.

Research on grafted materials to meet a variety of other surface property requirements remains active. Examples in recent years include radiation grafting of styrene onto crosslinked polytetrafluoroethylene (PTFE) and subsequent sulfonation for fuel cell application, surface modification of nanoparticles for radiation curable acrylate clear coatings. Adsorbents having specific functional groups have been prepared and used for the removal of valuable metal ions from seawater and hazardous organic pollutants from wastewater.

The current trend in research and development studies show that at present radiation grafting on polymers is developing in three main directions: polymeric adsorbents, polymeric membranes, and track etched membranes:

Polymeric adsorbents

- The graft polymerization has been industrially applied especially in Japan for the production of high performance adsorbents for metal ions and undesired gases in the last 10 years despite their relatively high cost;
- In order to reduce the manufacturing cost of radiation-grafted polymeric adsorbents, more efficient grafting techniques need to be developed. The R&D works carried out in Japan Atomic Energy Agency, JAEA, have shown that with the use of emulsion systems in grafting, the irradiation doses can be highly reduced;
- The economic aspects of using radiation-grafted polymeric sorbents can be further enhanced by using high surface area and cheaper substrates such as fibres and polymers of natural origin;
- With the proper selection of ligands and controlling the functionality of grafted chains higher selectivity and more efficient adsorption properties can be imparted onto adsorbent materials;
- The availability of low-energy, low cost electron accelerators especially for surface grafting have been considered to improve the economics of the overall process of grafting.

Polymeric membranes

- The fuel cells offer advantages in terms of high power densities and water as the by-product which makes them an environmentally friendly alternative for energy production. The membranes to be used in fuel cell applications should possess high stability, durability under the extreme conditions of relatively high temperature and oxidative atmospheres. The modified fluorinated polymers meet these requirements at the expense of their high chemical inertness. The functionalization of these materials for fuel cell applications are best achieved by using radiation-induced grafting;

- Radiation-grafted membranes serve as low cost alternative to commercially available perfluorinated membranes (Nafion®, Aciplex™, Flemion®, etc.) for low temperature fuel cells to be used in stationary and mobile devices i.e. automotive industry;
- The performance in terms of current-voltage properties of fuel cells containing poly(tetrafluoroethylene-co-hexafluoropropylene) (FEP) based radiation-grafted membranes was found to be comparable to Nafion® 112, and the durability of several thousand hours has been reported which shows high promise for automotive applications.

Track etched membranes

- Swift heavy ions allow the creation of nanopore membranes and nanostructured templates for nanotechnology. Radiation-induced grafting onto such devices increases their applications for medical purposes especially in ultra and nanofiltration fields.

2. CRP OVERALL OBJECTIVE

The overall objective of this Coordinated Research Project (CRP) was to use gamma rays, electron beams and swift heavy ions for grafting of various monomers onto natural and synthetic polymers for the development of novel adsorbents and membranes for environmental and industrial applications.

2.1. Specific research objectives

- Adsorbents suitable for the collection and recovery of significant metal ions;
- Development of adsorbents for removal of undesired anions from aqueous systems;
- Development of low cost membranes with improved durability and performance characteristics for potential applications in fuel cell fabrication;
- Development of methods for the preparation of membranes with 1-50 nm pore sizes and functionalization of inner pore surfaces;
- Development of new adsorbents with enhanced heavy metal ion uptake capacities;
- New fabrication methods of radiation-grafted specialty adsorbents for environmental and industrial applications;
- Production of radiation-grafted membranes with smaller pore sizes selective for proteins, polysaccharides and metal ions.

2.2. Salient aspects of the CRP

The CRP participants used radiation processing technology for grafting of various monomers onto natural and synthetic polymers for the development of novel adsorbents and membranes for environmental and industrial applications, and the work done during this CRP was envisaged to yield the following results:

Environmental applications

- Removal of heavy metal ions and hazardous toxic ions from aqueous media, using low-cost, reusable, highly selective advanced adsorbents developed through radiation technology;
- Understanding the mechanisms of grafting processes towards the optimization of desirable properties;
- Establishing guidelines for grafting processes.

Industrial and medical applications

- Development of low cost, durable and high performance membranes for fuel cell membranes and battery separators;
- Development of separators for biopolymers and cell sheets for health care applications;

- Understanding the mechanisms of grafting processes towards the optimization of desirable properties;
- Establishment of guidelines for grafting processes.

3. ACHIEVEMENTS

3.1. Argentina

The objective was to obtain membranes using heavy ions of low and high energy with new properties that facilitate its use in diverse areas like: fuel cells, materials that respond selectively to the ambient conditions, membranes for removal of metals from wastewaters and drug entrapment in polymer matrices of biomedical interest for use in medical treatment or industrial processes. The development during this CRP involved two fields: a) Grafting on submicroscopic wall track and b) New membranes obtained by grafted implanted PVDF foils. Concerning the *grafting on submicroscopic wall track,* polymer surface modifications were obtained by the application of radiation treatments and other physico-chemical methods: swift heavy ions etching and grafting procedures. The present work is part of a systematic study that involves different polymeric substrates and monomers with the purpose to induce grafting on etched tracks. The residual active sites produced by heavy ion beams, remaining after the etching process, were used to start the grafting process. In order to produce tracks on foils of poly (vinylidene fuoride) (PVDF), samples were irradiated with ^{208}Pb of 25.62 MeV/n or with 115 MeV Cl ions. Moreover, foils of polypropylene (PP) were irradiated with ^{208}Pb of 25.62 MeV/n. Irradiated samples were etched and grafted with N-isopropylacrylamide (NIPAAm) monomers or with acrylic acid (AA) monomers, respectively. Experimental curves of grafting yield as a function of fluency and the etching time were measured. Also, the grafting yield as a function of the grafting and etching time was obtained. The replica method allowed the observation of the shape of the grafted tracks using transmission electron microscopy (TEM). In addition, NIPAAm grafted foils were analysed using Fourier transform infrared spectroscopy (FTIR). The permeation of solutions, with different pH, through PP grafted foils was measured. This opens the possibility to control the passage of medical substances through membranes. For the fuel cell experiments, samples of PVDF grafted by ion track procedure, were initially characterized by SEM and FTIR and any special morphology was observed for PVDF not treated; its surface presented smooth and its cross-section was homogeneous; styrene grafting on PVDF showed little round cavities on surface but this morphology was not observed on the bulk of material. The ATR-FTIR spectra of grafted samples showed the characteristic absorption bands for styrene in 1060 cm^{-1} and 760 cm^{-1}, and this can be attributed to successful styrene grafting procedure on PVDF. The supplied samples had different irradiation treatment in each side of films, but no difference was observed in styrene grafting in quality and quantity terms. The sulfonation procedure (methodology previously described for perfluorated polymers) was applied on grafted PVDF. The success of sulfonation was measured by mass gain after this reaction. It was observed that percent water uptake in little styrene grafting PVDF was poor compared to Nafion®, but this parameter increases at higher styrene grafting specimens. The ion exchange capacities are higher than Nafion®, in lower or higher styrene grafted samples. In the development of n*ew membranes obtained by grafted implanted PVDF foils***,** this part of the work describes a new method to produce a thin layer of polyacrylic-acid (membranes) that grows on the surface of PVDF foils implanted by an Ar beam with energies between 30–150 keV. Different combinations of monomers in water solutions were used such as: acrylic acid (AAc); acrylic acid-glycidyl methacrylate (AAC-GMA); acrylic acid − styrene (AAc-S), acrylic acid − N-isopropyl acrylamide (AAc-NIPAAm) and acrylic acid − N-isopropyl acrylamide − glycidyl methacrylate (AAc-NIPAAm-GMA). Then the grafting induced on the implanted surface of PVDF, was analysed. The experimental results show that for particular optimized values of ion fluence and energy, AAc concentration, sulfuric acid and PVDF form (alpha or beta) a large percentage of grafting was obtained. Furthermore at certain point of the grafting process the development of the PolyAAc-Xmonomer produce a detachment from the irradiated substrate and continue its grafting outside the irradiated substrate. A membrane can be produced by this method that is an increased replica of the original implanted surface. Finally, PVDF films implanted by an Ar beam with energies about 100 keV and for 10^{13} cm^{-2} of fluence were grafted using different AAc solutions for the following purpose: absorption of different ions, biocompatibility, and immobilization of compounds of biological interest such as immobilization of enzymes (urease) or hormone (insulin) and the study of their activity.

3.2. Brazil

Brazil has been working on radiation grafting for many years. On the scope of this CRP, the Brazilian project promoted the application of radiation grafting of polymers for fuel cells membranes, for medical or food polymer packaging studies and for mathematical modelling or simulation of the diffusion aspects involved on chemical species migration. The DMAEMA grafting of PVC was performed by classical gamma irradiation and an innovative process by EB. The degree of grafting was determined in both cases and these results were discussed. Migration process from these grafted PVC samples into biological simulating media, DEHP (a PVC plasticizer) was quantified by classical gas chromatography and UV spectrophotometry. It was verified that PVC plasticizer migrates at lower concentration when grafted samples are used. The numerical method to simulate diffusion process evolved is simple and fast; it can use different diffusion coefficients for each different layer of medium: polymer, solution or grafting, and it's possible to add partition coefficient between each interface of different materials. The use of this numerical method as a modified Cottrell equation solution will permit to fit the voltammetry assay results and to determine the diffusion coefficient and to model the behaviour of the grafted membrane during the ionic conduction. The diffusion numerical procedure was applied to fit the water uptake results in Fe^{+++} absorbed by PP-g GMA, in collaboration with Egypt. Details of the experimental conditions had been included on the mathematical model. The investigation of fluorinated and perfluorinated polymeric films styrene grafted by EB showed promising results when the mutual irradiation was performed under warming and vacuum conditions. In this case, PVDF films achieved about 15% of styrene grafting that allowed high percent of water uptake when this copolymer film is sulfonated. Also, the mechanical properties and IEC characteristics of these film samples were evaluated and these values were close to that presented by Nafion® films. These results indicate mutual styrene grafting performed by industrial EB accelerator can be a fast alternative to produce ionomers that can compete with commercial Nafion® films. Finally, it was fruitful the Argentina collaboration work, where their ion tracked PVDF films were sulfonated in our laboratory and we could evaluate some parameters like percent of water uptake, ion-exchange capacity (IEC) and tensile strength maximum as a mechanical property. Some sulfonated styrene grafted PVDF films showed an intense water uptake even in sulfonated films with low degrees of grafting; this advantage was achieved due to the improvement in the amount of reactive surface done by the micrometric-nanometric pores obtained by ion tracking nuclear process, and were covered by styrene and sulfonated subsequently. Some properties of these films were compared to Nafion® films and ion tracked PVDF films were observed to be a new ionomer material and it can be used in process that require a great uptake of water. The electrochemical I-V behaviour of ion tracked films was analysed by polarization curves, and charge transfer region was observed in higher potentials, close to those of Nafion®.

3.3. Egypt

The direct radiation grafting technique was used to graft glycidyl methacrylate (GMA) monomer containing epoxy ring, onto polypropylene fibres. The ring opening of the epoxy ring in GMA by different amino groups was studied to introduce various chelating agents. The characterization and some selected properties of the prepared grafted fibres were studied and accordingly the possibility of its practical use for water treatment from iron and manganese metals was investigated. On the other hand, the synthesis of highly selected polymers prepared from poly(vinyl alcohol) (PVA), 2-acrylamido-2-methyl propane sulfonic acid (AMPS) and grafted with acrylic acid (AAc) or acrylamide (AAm) monomers using gamma rays as initiator was studied. In this work, the cationic/anionic membranes were also prepared by radiation-induced grafting of styrene/methacrylic acid (Sty/MAA) binary monomers onto low density polyethylene (LDPE) films. To impart reactive cationic/anionic characters in the grafted membranes, sulfonation and alkaline treatments for styrene and carboxylic acid groups, respectively, were carried out. Characteristics and some properties of the prepared grafted polymers were investigated. Also, the possibility of their applications in the selective removal of some heavy metals was studied. The prepared grafted materials had a great ability to recover the metal ions such as: Ni^{2+}, Co^{2+}, Cu^{2+}, Cd^{2+}, Mg^{2+}, Zn^{2+}, Mn^{2+}, and Cr^{+3} from their solutions. It was found that AMPS content in the graft copolymers is the main effective parameter for the selectivity of the copolymer towards metal ions. The higher the AMPS content the higher the selectivity towards Co and Ni ions. Also, in case of LDPE-g-P(Sty/MAA), the sulfonation and alkaline treatments are the most effective parameter for metal absorption and swelling behaviour of the prepared membranes. The graft composition, irradiation dose, and pH also have a great influence on the membrane characteristics and applicability in wastewater treatments from heavy and toxic metals. Results revealed that the prepared grafted materials with different functionalized groups are promising as ion selective membranes and could be used for wastewater treatment.

3.4. France

Track etched functionalized nanoporous β-PVDF membrane electrodes, or functionalized membrane electrodes (FME), are thin-layer cells made from track etched, poly(acrylic acid) (PAA) functionalized nanoporous β-poly(vinylidene fluoride) (β-PVDF) membranes with thin Au films sputtered on each side as electrodes. The Au film is thin enough that the pores of the membranes are not completely covered. The PAA functionalization is specifically localised in the walls of the nanoporous β-PVDF membrane by radio grafting. The PAA is a cation exchange polymer that adsorbs metal ions, such as Pb^{2+}, from aqueous solutions thus concentrating the ions into the membrane. After a calibrated time the FME is transferred to an electrochemical cell for analysis. A negative potential is applied to the Au film of the FME for a set time to reduce the adsorbed ions onto the Au film working electrode. The other metalized side of the FME functions as a counter electrode. Finally, square-wave anodic stripping voltammetry (SW-ASV) is performed on the FME to determine the metal ion concentrations in the original solution based on calibration. The calibration curve of charge versus log concentration has a Temkin isotherm form. The FME membranes are 9 µm thick and have 40 nm diameter pores with a density of 10^{10} pores/cm^2. This high pore density provides a large capacity for ion adsorption. Au ingress in the pores during sputtering forms a random array of nanoelectrodes. Like surface modified electrodes for adsorptive stripping voltammetry, the pre-concentration step for the FME is performed at open circuit. The zero current intercept of the calibration for Pb^{2+} is 0.13 ppb (µg/L) and based on 3S/N from blank measurements a detection limit of 0.050 ppb is obtained. Voltammetry (CV) and chronoapmerometry (CA) were used to characterize the system.

3.5. Hungary

Based on EPR (electron paramagnetic resonance) measurements it was found that in cellulose samples radicals formed during irradiation were stable and the crystalline content did not change significantly due to grafting. Therefore, grafting is supposed to occur mainly on the surface of the crystalline region. The radiation induced degradation of cotton-cellulose starts at very low doses (5–10 kGy) resulting in a decrease in DP (degree of polymerization). However, the degradation does not result in a significant change in the mechanical properties. Optimum conditions for obtaining highest grafting yield with low degradation depend on the monomer structure both for pre-irradiation grafting and for simultaneous grafting. In the case of pre-irradiation grafting for acrylamide, acrylic acid, N,N-methylene bis-acrylamide, and hydroxypropyl methacrylate the highest grafting yield was obtained at: irradiation with 20 kGy absorbed dose, grafting in solution with 2 mol dm^{-3} monomer concentration, at 40°C, 60 minutes. For glycidyl methacrylate (GMA) the optimum conditions were: 40 kGy absorbed dose, grafting in solution with 1.5 mol dm^{-3} monomer concentration, at 50°C, 60 minutes. In the case of simultaneous grafting for acrylamide, acrylic acid, N,N-methylene bis-acrylamide, and hydroxypropyl methacrylate the highest grafting yield was obtained at: irradiation with 20 kGy absorbed dose, monomer solution with 2 mol dm^{-3} concentration, room temperature. For glycidyl methacrylate (GMA) the optimum conditions were: 5 kGy absorbed dose, monomer solution with 0.38 mol dm^{-3} concentration, room temperature. The swelling in water of cotton-cellulose can be increased by grafting with acrylamide, acrylic acid and N,N-methylene bis-acrylamide, it can be decreased by grafting with hydroxypropyl methacrylate and glycidyl methacrylate (GMA). The first three monomers can be applied for adsorption of heavy metal ions. GMA grafted cellulose functionalized with cyclodextrine can be applied for the adsorption of phenol and its derivatives. The adsorption properties tested using UV/VIS spectroscopy proved to be better for samples grafted with GMA using simultaneous grafting (SG) due to their more hydrophobic nature than the samples grafted using pre-irradiation grafting (PIG). The functionalization by cyclodextrine (CD) resulted in a further increase in adsorption capacity. Using the mutual grafting method at higher doses the samples were covered by a thick layer while in the case of the pre-irradiation method the samples disintegrated possibly due to phenomena of over-grafting. The difference in the appearance of over-grafting between mutual and pre-irradiation grafting is due to the difference in the reaction mechanism. During irradiation radicals are produced not only on the outer surface of the cellulose but also inside. In the pre-irradiation technique applied in this work peroxide groups are incorporated both inside and outside. In the heated aqueous solution where the polymerization was carried out, initiation occurs both outside and inside as the monomer could diffuse inside the fibres swollen in aqueous medium. The growing chains inside the fibres cause disintegration. In the case of mutual grafting cellulose radicals initiate the grafting. The grafting starts at surface of the cellulose fibres and the long grafted chains form a dense film on the surface of the fibres forming a barrier layer hindering the diffusion of further monomer molecules inside the fibre.

3.6. India

In the framework of the CRP radiation grafting of different monomers onto various backbone polymers, depending on their proposed applications were investigated. Grafting of acrylonitrile onto thermally bonded non-woven porous polypropylene fibre sheet using electron beam (EB) was carried out by pre-irradiation grafting technique. Grafting extent of ~125% using technical grade chemicals was achieved under optimized experimental conditions. The grafted nitrile groups were amidoximated and studied for uranium uptake from sea water and heavy metal ions such as Co^{2+}, Ni^{2+}, Mn^{2+}, and Cd^{2+} from simulated samples. Adsorption and elution of adsorbed ions in suitable eluents were studied. The grafting process was upgraded to pilot scale to obtain sheets of 1×1 m^2 for further applications of grafted sheets. Mutual radiation grafting technique was used for grafting of vinylbenzyltrimethyl ammonium chloride, [2-(methacryloyloxy)ethyl]trimethylammonium chloride, and [2-(acryloyloxyethyl)]trimethylammonium chloride on to cotton cellulose substrate. The grafted matrices showed significantly higher water uptake and retention properties. The grafted matrices were evaluated for their antibacterial properties against *Escherichia coli*, *Pseudomonas flourescens*, *Staphylococcus aureus and Bacillus cereus*. The antibacterial efficacies of the grafted products samples were found to be a function of extent of grafting and the type of bacteria tested against. PVBT-*g*-cotton was studied for its protein adsorption behaviour in continuous column process using Bovine serum albumin (BSA) as a model protein. Mutual radiation grafting technique was used to graft acrylic acid on micrometre thick micro-porous polypropylene membrane. Contact angle measurement studies of the grafted and radiation treated polypropylene showed that initial grafting as well as radiation treatment of polypropylene in aqueous medium and in presence of Mohr's salt enhances its affinity towards the grafting solution. The enhancement in the polar component of surface energy of treated polypropylene membrane is the primary cause of grafting enhancement. The membranes grafted to an extent of ~20 % were found to perform comparably with the battery separator presently being used by battery industry. Acrylic acid was covalently linked to Teflon® scrap by mutual radiation grafting technique. The grafting extent decreased with increasing dose rate and thickness of the substrate. The SEM studies indicate significant difference in bulk and interface due to change in thickness of the Teflon® backbone.

3.7. Japan

Fibrous adsorbent for removal of toxic metal ions have been synthesized by radiation-induced graft polymerization. In this study, to reduce the dose, that was an important factor to decrease the cost, it was adopted the emulsion grafting technique instead of general organic solvent system for making metal adsorbent. Especially, emulsion system which disperses monomer micelles in water with assistance of surfactant was found to accelerate the graft polymerization. In the emulsion grafting, smaller micelles could improve the grafting yield, because the smaller micelles could cover a large surface area of trunk polymer. The micelle diameter of emulsion was controlled by monomer and surfactant concentration. Glycidyl methacrylate (GMA) micelle diameter was 0.08 μm at 5% GMA with 0.5% Tween 20 (surfactant). In this emulsion condition, degree of grafting reached 100% within only one hour, when the graft polymerization was carried out at a dose of only 10 kGy and reaction temperature of 40°C. By using this emulsion system, the fibrous graft adsorbent for ultra-pure water production was commercialized. From the point of reduction of environmental burden, natural polymer-based metal adsorbents were synthesized by this system onto the nonwoven cotton fabric and the nonwoven polylactic acid (PLA) fabric as trunk polymers, and their subsequent amination. The cotton-based metal adsorbent could be degraded by microorganism in compost during 120 days. The cotton part of graft adsorbent was firstly decomposed within 30 days, and subsequently the degradation of graft chains occurred after 60 days. The PLA-based metal adsorbent, which has poor resistant to chemical compounds such as alkali, was synthesized by the control of both grafting yield and PLA hydrolysis. The order of metal ion selectivity of the PLA-based metal adsorbent with iminodiacetic acid was $Cu^{2+} > Pb^{2+} > Ni^{2+} > Zn^{2+} > Cd^{2+} > Co^{2+} > Ca^{2+} > Mg^{2+}$.

3.8. Malaysia

In the framework of the CRP concerning development of less-water dependant membranes for high temperature proton exchange membrane fuel cell, two types of proton exchange membranes for fuel cell application for operation below and above 100°C were developed using radiation induced grafting (RIG) methods. The first membrane containing sulfonic acid moiety was developed using RIG of sodium styrene sulfonate (SSS) onto electron beam (EB) irradiated poly(vinylidene fluoriede) (PVDF) films in a single-step reaction for the first time using synergetic effect of acid addition to grafting mixture under varying grafting conditions. The reaction parameters were optimized and grafting levels suitable for fuel cell application were obtained. The fuel cell related properties of the obtained membranes were evaluated and the performance was tested in situ in a single H_2/O_2 fuel cell, under dynamic conditions, and in comparison with a similar sulfonated polystyrene PVDF membrane obtained by two step conventional RIG method i.e. grafting of styrene and subsequent sulfonation. The newly obtained were found to have better (specifically less water uptake) properties than conventionally prepared grafted membranes. Moreover, the newly prepared membrane having 53% grafting percentage (G%) showed an improved fuel cell performance marked by a 30% increase in the stability compared to conventionally prepared one at the same G% at temperature of 60°C. This coupled with a cost reduction mainly as a result of elimination of sulfonation reaction. The performance of these membranes can be further improved toward high temperature operation by impregnation of inorganic filler such as zirconium phosphate or zirconium oxide. Also, crosslinking during the grafting reaction would help to improve stability. This could result in low cost membranes suitable for use in low temperature fuel cells. In the second part, acid-base composite membrane for fuel cell operating temperature above 100°C was studied. EB irradiated poly(ethylene-*co*-tetrafluoroethylene) (ETFE) films were first grafted with N-vinylpyridine (NVP). The effects of the reaction parameters such as monomer concentration, irradiation dose, reaction time, film thickness, temperature and film storage time on the degree of grafting were established to obtain grafting levels suitable for fuel cell. The membranes were subsequently doped with phosphoric acid under controlled condition with. The proton conductivity of the obtained phosphoric acid doped membranes was investigated under no free water conditions in correlation with the variation in G% and temperature (30–130°C). The thermal stability, thermal properties, and crystalline structure of the membranes were found to maintain sufficient level after grafting and acid doping. The performance of 34 and 49% grafted and doped membranes was tested in a single fuel cell at a temperature of 130°C under dynamic conditions with a respective power density of 146 and 127 mW/cm^2 obtained. The polarization and power density characteristics together with the initial stability of the membrane showed a promising electrolyte candidate for fuel cell operation above 100°C. The performance of these membrane need to be further investigated under various conditions including concentration of doping acid and temperature of doping followed by stability test, all of the which are currently undergoing.

3.9. Poland

The reported investigations carried out in the frame of this CPR were focused on the preparation of sorbents of heavy metal ions via modification of polymer surface by radiation-induced grafting of selected functional groups. The final product can be potentially exploited for the preconcentration and removal of cations including lanthanides from very dilute solutions as well as for the decontamination and treatment of radioactive wastewater. In the first stage of the studies the efforts were concentrated on the elucidation of the most important factors influencing radiation-induced grafting, particularly (i) the effect of radical population generated in polymeric matrix on degree of grafting, (ii) parameters determining grafting processes and their procedures, (iii) correlation between layer structure formed via copolymerization and content of monomers in the initial solution. Characterization of the sorbents at each step of their production was carried out using gravimetric method, EPR spectroscopy, ATR-FTIR, thermal and contact angle measurements. Sorption properties of the prepared materials were determined using constructed at the Institute of Nuclear Chemistry and Technology LG-1 gamma radiometer applied for the measurements of solutions radioactivity before and after sorption. Sorption capacity of the absorber prepared by radiation grafting was evaluated using $^{152}Eu^{3+}$ as a model marker monitoring depletion of the radioisotope from the aqueous solution. The coordination chemistry of trivalent lanthanides does not differ neither along the series nor from the actinide series, therefore, the data can be extrapolated for both groups of elements. The studies carried out by electron spin resonance spectroscopy (EPR) and gas chromatography (GC) confirmed that population of radiation-induced radicals increases in the following order polystyrene<polypropylene<polyethylene. The same relationship was found for efficiency of radiation grafting. It was concluded that under comparable conditions the content of radicals in polymeric matrices significantly determines degree of grafting. In the second stage of investigations it was found that application of the simultaneous method of grafting introduces to the grafted layers crosslinking or/and branching as well as degradation of functional groups. All these phenomena reduce access of metal ions to the studied sorbent therefore sorption capacity of the polyamide functionalized via pre-irradiation (indirect) method by acrylamide is higher than that determined for the sorbent prepared by simultaneous method of grafting. When two monomers, acrylic acid (AAc) and acryl amide (AAm), contribute in the formation of grafted layer, their input into copolymerization was not proportional to their concentrations in the feed solution. It was found that grafting of the monomers shows synergetic effect as the yield of copolymerization exceeds degree of grafting achieved for individual components. The macromolecules constructed from two types of monomers, namely AAc and AAm, affect matrix crystallinity, particularly when AAm is used. Only external layers of the grafted homopolymers (PAAc and PAAm) and copolymers (P(AAc+AAm)) contribute in sorption of radioactive europium ions. Depletion of the radionuclide is above 95% for all prepared adsorbents. Radiation-induced grafting of the selected functional groups forming complexes with chosen metal ions seems to be promising way for working out novel sorbents of potential application in separation techniques. The results might contribute in the development and implementation of radiation technologies for the production of adsorbents of metal ions, e.g. trivalent cations of lanthanides.

3.10. Republic of Korea

Micro-porous polyethylene separator was modified by radiation grafting of methyl methacrylate in order to improve its affinity with a liquid electrolyte. The degree of grafting (DOG) increased with the monomer concentration and grafting time. The morphological change of the modified separator was investigated by scanning electron microscopy. The degree of crystallinity upon grafting was reduced due to the formation of an amorphous PMMA layer. The electrolyte uptake and the ionic conductivity of the separator increased with an increase in the DOG. The ionic conductivity reached 2.0 mS/cm for the grafted polyethylene separator with 127 wt% DOG. The prepared separators were characterized by using charge/discharge cycling test, AC impedance, and thermal stability analyses. Thermal shrinkage of the PE-g-PMMA separators decreased with an increasing degree of grafting up to 70% above which it was saturated. The PE-g-PMMA separators showed better oxidation stability on the anode up to 5 V and a better cycle life performance than the original PE separator. Also, micro-porous poly(methyl methacrylate)-grafted polyethylene separators (PE-g-PMMA) were prepared by a radiation-induced graft polymerization of methyl methacrylate onto a conventional PE separator followed by a phase inversion. After the phase inversion, the micro-pores were generated in the grafted PMMA layer. The prepared micro-porous PE-g-PMMA separators showed an improved electrolyte uptake and ionic conductivity due to their improved affinity with a liquid electrolyte and the presence of pores in the grafted PMMA layer. The PE-g-PMMA separators exhibited a lower thermal shrinkage compared to the original PE separator. The PE-g-PMMA separators showed better oxidation stability up to 5.0 V when compared to the original PE separator (4.5 V). A novel polymer electrolyte membrane, poly(vinylbenzyl sulfonic acid)-grafted poly(tetrafluoroethylene-co-hexafluoropropylene) (FEP-g-PVBSA), has been successfully prepared by simultaneous irradiation grafting of vinylbenzyl chloride (VBC) monomer onto a FEP film and taking subsequent chemical modification steps to modify the benzyl chloride moiety to the benzyl sulfonic acid moiety. The chemical reactions for the sulfonation were carried out via the formation of thiouronium salt with thiourea, base-catalysed hydrolysis for the formation of thiol, and oxidation with hydrogen peroxide. Each chemical conversion process was confirmed by FTIR, elemental analysis, and SEM-EDX. A chemical stability study performed with Fenton's reagent (3% H_2O_2 solution containing 4 ppm of Fe^{2+}) at 70°C revealed that FEP-g-PVBSA has a higher chemical stability than the poly(styrene sulfonic acid)-grafted membranes (FEP-g-PSSA). An EDX analysis was also used to observe the cross-sectional distribution behaviours of the hydrophilic sulfonic acid groups and hydrophobic fluorine groups. The characteristics of an ion-exchange capacity (IEC), water and methanol uptake, methanol permeability, and proton conductivity as a function of the degree of grafting were also studied. The IECs and water uptakes of membranes with different degrees of grafting (36% to 102%) were measured to be in the range of 0.8 meq/g to 1.62 meq/g, and 10% to 30%, respectively. The proton conductivity was higher than that of a Nafion® 212 membrane (6.1E-02 S/cm), when the degree of grafting reached 60%. The methanol permeability and uptake of the FEP-g-PVBSA membrane was significantly lower than that of the Nafion® 212 membrane, and even the degree of grafting reached 102%.

3.11. Switzerland

The Electrochemistry Laboratory of Paul Scherrer Institut looks back of nearly two decades of development of solid polymer electrolytes for fuel cell applications by the radiation grafting technique. Imbedded in this major activity, the Insitut contributed over the past three years parts of this development to the IAEA-CRP, in particular the development of α-methylstyrene-methacrylonitrile (AMS/MAN) grafted membranes based on FEP- and ETFE-commodity films, exhibiting better life time stability under fuel cell operating conditions as the formerly exploited styrene grafted membranes. Fundamental investigations concerned the radiation stability of the two base polymers, FEP-and ETFE-films, typically 25 μm thick, to minimize radiation damage, in particular to the mechanical properties of the films. Further, the grafting kinetics for the two component monomer solution (AMS and MAN) was investigated and optimized with respect to some fuel cell relevant properties, e.g. specific conductivity, graft component degradation, etc. The kinetics was followed by post synthesis analysis of the grafted films by confocal Raman spectroscopy. Further, thermal characterization, e.g. DSC, TGA, and small angle neutron (SANS) and X rays (SAXS) scattering have been utilized to learn more about the morphology of pristine and grafted films, as well as the sulfonated membranes, the latter in dry and swollen state. Reconstruction of the polymer morphology in dependence of water content could be achieved by applying a core-shell model available in literature. Extensive testing of these membranes in fuel cells under conditions of relevance to mobile applications revealed that the concept of substituting the α–hydrogen atom in the styrene monomer to AMS results in the expected stability improvements. Crosslinking further adds to stability, as experienced for styrene/DVB as graft component. However, the grafting of the AMS/MAN component as well as the crosslinking of this graft component has to be further optimized. Further, outside of the contribution to CRP, ideas have been developed to scale-up the laboratory preparation of these membranes in terms of increased membrane area and number of membranes prepared in one batch.

3.12. Syrian Arab Republic

The effective treatment of heavy metals in the environment has become one of the major issues of public interest due to their toxicity. The treatment of aqueous waste, including soluble heavy metals, needs concentration of the metallic solution into small volume, followed by recovery or secure disposal. Polymer membranes (PP and PE) had been grafted with basic and acidic functional groups using gamma radiation. Two binary mixtures had been used for the grafting reactions: acrylic acid/N-vinyl pyrrolidone, and acrylic acid/N-vinyl imidazole. The influence of different reaction parameters on the grafting yield had been investigated as type of solvent and solvent composition, comonomer concentration and composition, addition of inhibitors, and the irradiation dose. Water uptake with respect to the grafting yield had also been evaluated. The ability of PP films, grafted with acrylic acid/vinyl pyrrolidone, to uptake heavy metal ions such as Hg^{2+}, Pb^{2+}, Cd^{2+}, Co^{2+}, Ni^{2+} and Cu^{2+} was elaborated. The uptake of the metal ions increases with increasing the grafting yield. Furthermore, the Pb^{2+} uptake was much higher than the uptake of the Hg^{2+} and Cd^{2+} ions that the membranes may be considered for the separation of Pb^{2+} ions from Hg^{2+} or Cd^{2+} ions. The ability of PE films, grafted with acrylic acid/N-vinyl imidazole to uptake heavy metal ions such as Pb^{2+}, Cd^{2+}, Co^{2+} and Ni^{2+} was elaborated. An increase in the uptake of the metal ions was observed as the grafting yield increases. Because of their basic/acidic character the prepared membranes may be considered for removing of the studied ions from wastewater. Further work is in progress to elaborate this use of the prepared membranes in separation processes.

3.13. Thailand

Metal adsorbent containing hydroxamic acid groups was successfully synthesized by radiation induced graft copolymerization of methyl acrylate (MA) onto two natural polymers, cassava starch and cellulose fibre. The optimum conditions for grafting were studied in terms of % grafting. Conversion of the ester groups present in grafted copolymer into hydroxamic acid was carried out by treatment with hydroxylamine (HA) in alkaline solution. The adsorbent was characterized by FTIR, TGA, and DSC. The presence of electron donating groups in adsorbent containing hydroxamic acid groups provides the ability to form polycomplexes with metal ions. The ability to adsorb various metals was investigated in order to evaluate the possibility of its use in metal adsorption. It was found that adsorbent containing hydroxamic acid groups can adsorb various metal ions. Each metal has a specific pH at which it shows maximum percentage adsorption. The adsorbent exhibited a remarkable % adsorption for Cd^{2+}, Al^{3+}, UO_2^{2+}, V^{5+} and Pb^{2+} at pH 3, 4, 5, 4, and 3, respectively. The selectivity of metal adsorbent toward the metal ions used is in the following order: $Cd^{2+} > Pb^{2+} > Al^{3+} > UO_2^{2+} > V^{5+}$.

3.14. Turkey

The research and development activities carried out under the scope of this CRP have been directed at the synthesis of specialty adsorbents for environmental applications particularly for the removal of hazardous anions and cations from aqueous systems. The target pollutants chosen were arsenate, chromate and phosphate anions. Nonwoven fabrics based on polyethylene (PE) and coated polypropylene (PP) were used for radiation grafting of glycidylmethacrylate (GMA) and dimethylaminoethyl methacrylate (DMAEMA) and 4-vinyl pyridine (4VP) via accelerated electrons. The experimental parameters such as dose rate, absorbed dose, monomer concentration and temperature, were optimized for every grafting process. The grafted polymers were characterized spectroscopically by FTIR, XPS, and by thermal analysis. The uptake of various forms of chromium as well as arsenate and phosphate ions was systematically investigated by using PE/PP nonwoven fabrics grafted with 150% of the respective polymer. Two different approaches were followed for functionalizing of grafted polymers. In the case of GMA grafts the epoxy rings were opened by attaching 1,2,4-triazol, dipyridyl amine and picolylamine groups which were later complexed with copper ions. Cu(II) ions were held very firmly by the corresponding amine groups leading to the formation of so-called polymer-ligand exchangers. The polymer ligand exchangers thus obtained were shown to be very efficient in removing various forms of hexavalent chromium anions as well as arsenate from mixtures of other anions. The removal efficiency was determined to be 108 mg chromium per gram of adsorbent which is far superior to the other adsorbents reported in the literature. DMAEMA grafted nonwoven fabrics were first quaternized by using dimethyl sulphate which was later treated with HCl to replace sulphate counter ions with chloride. The polycationic structure thus obtained was used to remove phosphate anions in the presence of other anions. The selectivity towards phosphate was found to be very good in low concentration ranges of anions. Quaternized DMAEMA grafted fabrics were also used for the removal of chromate and found to be very effective by showing an uptake capacity of 125 mg chromium per gram of adsorbent. When the uptake was measured against the amount of grafted DMAEMA only, it was observed that for every two DMAEMA group one chromate was removed. Most of the anion uptake studies were carried out in batch form while in some cases continuous adsorption was studied and breakthrough curves were constructed.

3.15. United States of America

Various irradiation techniques have been used to graft vinyl and acrylic monomers to polymer (including biopolymer) substrates by simultaneous and pre-irradiation methods. Pulse radiolysis is a method for study of the graft polymerization kinetics; electron paramagnetic resonance (EPR) spectroscopy can be used to determine the chemical structure of the radiolytically produced free radicals and their decay mechanisms. The pulse radiolysis experiments involve the application of a pulse of electrons to a sample to produce ionized species, followed by the observation of their time-resolved absorption characteristics. This type of measurement enables the determination of the rate coefficients associated with various reactions taking place, with the main focus on the role of intermediate species. The report will involve the following two ionizing radiation grafting projects: a) Advances in the electron beam grafting of isopropylacrylamide to a poly(ethylene-terephthalate) membrane for cell sheet detachment, and b) Ionizing radiation-induced grafting methods for the synthesis of polymer electrolyte membrane fuel cells.

4. CONCLUSIONS

The work done under the CRP has contributed to the following developments: preparation of radiation grafted adsorbents for environmental application, radiation grafted surfaces for biomedical applications, and radiation grafted membranes for fuel cells and battery applications.

4.1. Adsorbents

- Synthetic polymers such as PE, non-woven polypropylene (NWPP) have been grafted with a variety of monomers and applied for the removal of toxic compounds, e.g. heavy metal ions from water and wastewater (Egypt, Japan, India, Poland, and Syrian Arab Republic);
- Functionalized adsorbents containing amine and carboxylic acid groups have been developed by radiation grafting and high adsorption capacity was achieved. Some of these adsorbents could be used several times after regeneration for removal of valuable metals. Such grafted/modified materials showed a potential for the removal of lanthanides and actinides such as $^{152}Eu^{3+}$ and ^{99m}Tc, and separation of zirconium from uranium in low level nuclear waste (Egypt, Poland, and Turkey).
- Natural polymers such as cellulose, starch, polylactic acid have been grafted with various monomers for adsorption of toxic compounds from polluted waters (Egypt, Hungary, Japan, and Thailand).

4.2. Ion track membranes

- Radiation grafting on ion track membranes has been proven to be a good technique to immobilize chelating groups for detection sub-ppb level heavy metal ions in treated wastewaters. Based on this technique novel low cost sensor has been designed. The final small device is a disposable sensor, which is now in the stage of technological transfer to industry (France and Turkey).
- Grafted submicroscopic track membranes with selective permeability obtained using the residual active sites after the etching procedure can be used to control the pore as a function of pH (Argentina).

4.3. Battery separators

- Grafting of polymethylmethacrylate (PMMA) onto the PE separator has been shown to improve the separator performance of lithium battery related to thermal stability, electrolyte uptake and ionic conductivity. The process of production PP based radiation grafted battery separator is being upgraded to satisfaction of industry (India and the Republic of Korea).

4.4. Biomedical applications

- A uniform grafting of N-isopropylacrylamide onto poly(ethyleneterephthalate) membrane dishes was achieved using the pre-irradiation method and under anaerobic conditions with relatively low dose of 25 kGy. Cell sheets of 1×10^6 human prostate epithelium cells were successfully detached from these grafted membrane dishes without any damage and within very short period of time of 20 minutes at 25°C (the USA).
- Antibacterial bandages and membranes for separation of protein have been developed in laboratory scale by grafting on cellulose. 2-(acryloyloxyethyl)]trimethylammonium chloride grafted cotton (AETC-g-cotton) has shown bactericidal properties against gram positive bacteria. The MAETC grafted product was tested for skin grafting studies on rats and found to be better than steam sterilized cotton (India).
- The grafting of heparin-DMAEMA on PVC for non-thrombogenic applications has been investigated, and the migration of plasticizer di-2-ethyl hexyl phthalate (DEHP) has been evaluated experimentally. The grafted samples showed reduced migration (Brazil).
- Incorporation of specific chain transfer agents called RAFT agents brings a control over the molecular mass and distribution of grafted chains not obtained with conventional free radical grafting technique. This has been shown for controlled radiation induced grafting of styrene with molecular mass range of 2000–50 000 with a dispersity of 1.1–1.2 on both natural and synthetic polymeric substrates. The precise control of grafted chain length and narrow molecular mass distributions is very important for tissue engineering applications as well as development of sensors (Turkey).

4.5. Fuel cell applications

- Progress has been achieved with respect to fuel cell applications of radiation grafted membranes at different levels. Basic understanding of the grafting process has been improved for various combinations of base polymers and monomers also with respect to simplifying later scale-up processes. The importance of the stability of the grafted component under fuel cell conditions has been recognized and addressed. However, a full understanding is still missing. Radiation grafted membranes have the potential to substitute more expensive membrane materials as solid polymer electrolyte in future fuel cell applications. Simultaneous electron beam irradiation of FEP and styrene followed by post-irradiation heat treatment has been demonstrated to be a successful technique for production of a polymer electrolyte membrane of substrate thicknesses of 25–125 µm. Higher grafting density with oligomer sized grafts was achieved using pulsed electron irradiation with high dose per pulse and higher pulse repetition rate (Brazil, Switzerland, Republic of Korea, Malaysia, and the USA).
- Membrane with improved properties containing sulfonic acid moiety was obtained by electron beam (EB) induced grafting of sodium styrene sulfonate (SSS) onto poly(vinylidene fluoride) (PVDF) films using a shorter (single-step) method for fuel cell operation below 100 °C. Less water dependent acid-base composite membrane for fuel cell operating above 100 °C was also obtained by grafting of N-vinylpyridine onto ETFE followed by doping with phosphoric acid. The performance of the membranes needs to be further improved (Malaysia).
- VDF films with submicroscopic ion tracks were prepared, grafted, and sulfonated for fuel cells application. More assays are on-going to obtain a final product (Argentina, Brazil).

REPORTS BY PARTICIPANTS OF THE COORDINATED RESEARCH PROJECT

SURFACE MODIFICATIONS OF POLYMERS INDUCED BY HEAVY IONS GRAFTING

R.O. MAZZEI, J. LOMBARDO, D. CAMPOROTONDI, D. TADEY, G.G. BERMÚDEZ

National Atomic Energy Commission
Ezeiza Atomic Centre, Ezeiza,
ARGENTINA

Abstract

Polymer surfaces are modified by the application of swift heavy ions etching and grafting procedures. The residual active sites produced by heavy ion beams, remaining after the etching process, were used to start the grafting process. In order to produce tracks on foils of poly(vinylidene fluoride) (PVDF) they were irradiated with ^{208}Pb of 25.62 MeV/n or with 115 MeV Cl ions. Moreover, foils of polypropylene (PP) were irradiated with ^{208}Pb of 25.62 MeV/n. Then, they were etched and grafted with N-isopropylacrylamide (NIPAAm) monomers or with acrylic acid (AAc) monomers, respectively. The replica method allowed the observation of the shape of the grafted tracks using transmission electron microscopy (TEM). In addition NIPAAm grafted foils were analyzed using Fourier transform infrared spectroscopy (FTIR). The sulfonation procedure (methodology previously described for perfluorated polymers) was applied on grafted PVDF. A new method is described to produce a thin layer of poly-acrylic-acid (membranes) that grows on the surface of PVDF foils implanted by an Ar^+ beam with energies between 30–150 keV. Different combinations of monomers in water solutions were used such as: acrylic acid (AAc); acrylic acid-glycidyl methacrylate (AAc-GMA); acrylic acid-styrene (AAc-S); acrylic acid-N-isopropyl acrylamide (AAc-NIPAAm) and acrylic acid-N-isopropyl acrylamide – glycidyl methacrylate (AAc-NIPAAm-GMA). The experimental results show that for particular values of: ion fluence and energy, AAc concentration, sulphuric acid and PVDF polymorphous (alpha or beta) a huge percentage of grafting was obtained. At certain point of the grafting process the development of the PolyAAc-Xmonomer produce a detachment from the irradiated substrate and continue its grafting outside it. This method produces a membrane that is an increased replica of the original implanted surface. Finally, PVDF films implanted by an Ar^+ beam with energies about 100 keV and a fluence of 10^{13} cm^{-2} were grafted using different AAc solutions for different purposes: improvement of their biocompatibility, absorption of different ions and immobilization of compounds of biological interest (enzymes, hormones).

1. OBJECTIVE OF THE RESEARCH

The major objective of research was to obtain membranes with new properties using heavy ions of low and high energy that facilitate its use in diverse areas as: fuel cells, materials that respond selectively to the ambient conditions, membranes that facilitate the removal of metals from wastewaters and drug entrapment in polymer matrices of biomedical interest for use in medical treatment or industrial processes.

2. INTRODUCTION

2.1. Grafting on submicroscopic wall track

The radiation graft polymerization is one of the methods for obtaining the so called *intelligent materials* [1, 2]. A graft copolymer may be obtained when an active site in a polymer A, initiates the polymerization of the monomer B [3]. There are two methods to prepare graft copolymers: in the simultaneous irradiation or mutual method the active sites formed during irradiation are in contact with reactive monomer, initiating the polymerization and chains grafted to the polymer substrate. In the other method, the polymer A is at first irradiated in the presence of air which leads to formation of either hydroperoxides or diperoxides on the trunk polymer. They are stable and can be decomposed at high temperatures. In a second step, the irradiated polymer is immersed in the monomer solution to initiate the grafting reaction. When an ion with atomic number Z and energy per nucleon E/n falls on a polymer film it produces a damage zone around the incident axis. In this way, the charged particle creates a cylindrical region that is easily attacked by a suitable reagent. The etching solution creates holes along and around the particle path [4]. Solid state nuclear track detectors (SSNTD) have found widespread applications [5]. The nuclear track technology allows in wide margins the independent choice of pore diameter, shape, inclination and membrane porosity forming the nuclear track membranes (NTM). An intelligent material is a material with specific characteristics that responds to environmental conditions. NTM can be combined with a polymer that responds to environmental conditions. The active sites remaining after the etching procedure were used to graft N-isopropylacrylamide (NIPAAm) and AAc on the track without using any supplementary irradiation source such as gamma or electron beams.

2.2. New membranes obtained by grafted implanted PVDF foils

Heavy ions of low energy, which have ranges of approximately a few hundred nanometres in polymers, are able to induce changes near the surface of the material. Therefore, the process of grafting using heavy ion beams which can modify the physical and chemical properties of a surface layer and leaving the bulk properties not modified in the irradiated samples, is a method to obtain new materials. This could open the possibility to merge the chemical and physical properties of the substrate with the characteristics of the grafted monomer in order to produce new advanced materials [6]. The present study describes a new method to produce a thin layer of monomer combinations (membranes) that grow on the surface of PVDF foils implanted by an Ar^+ beam with different energies and different combinations of monomers in water solutions. A novel effect is described.

2.3. Fuel cell

For the fuel cell experiments, films irradiated with different ions from TANDAR and GANIL accelerators or a ^{252}Cf source were used. To obtain submicroscopic pores with different diameters, different etching times were used. The etching conditions were: 6N KOH + 0,1N KMnO4 at 81°C. Finally, the films were irradiated with 30 kGy of gamma rays and grafted with styrene. In all the cases the grafting time was 22 hours at 61°C using 100% styrene solution. The fuel cell experiments were carried out by Mr J. Manzoli and his group (Brazil) and they are described in this report.

3. MATERIALS AND METHODS

3.1. Membranes and films preparation

3.1.1. PVDF-NIPAAm

The irradiated materials were β and α poly(vinylidene fluoride) (PVDF) foils from Solvay (Belgium) of 9 or 25 µm thickness. The foils were extracted prior irradiation in boiling toluene for 24 h. The monomer NIPAAm (Sigma Aldrich Ltd.) was used as received for the grafting process. The experimental set-up consisted stacks of foils placed perpendicular to the ion direction. For the irradiation in vacuum, heavy ion beams of ^{35}Cl (115 MeV) provided by the Tandar accelerator (Buenos Aires, Argentina), were used. To irradiate PVDF foils of 7.4 cm^2 in air, beams of ^{208}Pb (25.62 MeV/n) provided by the GANIL laboratory (Caen, France), were used. Due to the ions high energy, the electronic stopping power could be considered as constant throughout the foil. Some of the foils were irradiated with fission fragments (PVDF-Cf foils) using a ^{252}Cf source. An important parameter in order to analyze the etching experiment is to measure the bulk velocity of the process (Vb). To this end, foils previously irradiated with fission fragments (PVDF-Cf) were immersed in each etching experiment and, after an etching time of 24 h, a bulk velocity of 3 µm/day was measured. In order to produce pores, the irradiated foils with Cl and Pb ions were chemically etched using an aqueous solution of 6N KOH + 0,1N $KMnO_4$ at 81°C during an etching time not greater than 40 min. To stop etching process, the films were quickly washed in distilled water and the remaining water at the surface was absorbed with filter paper. Then the foils were quickly immersed in the monomer solution to start the grafting process. Two grafting solutions were used: 10 wt% NIPAAm aqueous solution (solution 1) and 11 wt% NIPAAm + 20 wt% methanol + 0.1 wt% Mohr salt aqueous solution (solution 2). The grafting reaction was carried out by placing ampoules with the foils, deoxygenated previously by means of bubbling nitrogen, in a water bath at 62°C. The last step of the process which consisted in the extraction of the homopolymer was performed in the following way: grafted foils were first washed during 24h with distilled water at 62°C and then 24h with distilled water at room temperature. No extensive homopolymer formation was observed. Neither grafting nor homopolymer formation were observed in blank experiments with non-irradiated foils.

Finally, the foils were dried until they reached a constant weight at room temperature. The grafting yield is defined as Y(%) = (mf -mi)/mi. For solution 1, mi and mf are the weights of the dried samples before etching and after grafting, respectively. In previous experiments low values of the grafting yield measurements after the etching, were found. The weights after the etching and before the grafting were not measured in order to begin the grafting process as soon as possible. On the other hand, for solution 2, mi and mf are the weights of the dried samples (after etching) before and after grafting, respectively. Infrared transmission measurements were carried out at a resolution of 4 cm^{-1} using a Nicolet Impact 410 spectrometer, equipped with a DTGS detector. To analyze the shape of the nuclear tracks, transmission electron microphotographs of the PVDF pores were obtained using the two-step replica technique for non-dissolved materials [7]. A polycarbonate chloroform solution (PC) was used on the etched PVDF foils and after drying the solution, the PC replica was obtained. As a second step, the technique which performs a Pt/C (platinum/carbon) replica of the previous PC replica was applied. The Pt/C replicas were observed using a Philips 300 electron microscope.

3.1.2. PP-AAc

The material used was a biaxially oriented coextruded 20 μm PP film (RADICIFILM, S.P.A., Italy). The acrylic acid (Merck Ltd.) for the grafting process was used as received. The experimental set-up consisted of different stacks of foils of 7.4 cm^2 irradiated perpendicularly to the ion beam direction. Beams of ^{208}Pb (25.62 MeV/n) provided by the GANIL laboratory (Caen, France) were used. To produce tracks the irradiated foils were chemically etched using 8 M H_2SO_4 + $K_2Cr_2O_7$ (saturated) aqueous solution at 50°C and at different times. After this process, the foils were carefully washed in distilled water for 1 h, dried with a filter paper, and finally weighed before the grafting procedure starts. The etched foils were placed in closed tubes containing the aqueous grafting solution that consists of 79 vol% AAc, 0.4 M H_2SO_4 and 0.1 wt% Mohr salt (to prevent homo polymerization). After deoxygenating the tubes with bubbling nitrogen, they were placed in a 62°C water bath to carry out the grafting reaction. After a certain period of time and to stop the grafting process, the PP samples were taken out from the monomer solution and washed for 1 h in distilled water at 62°C and then for 3 days in distilled water at room temperature.

Finally, the samples were dried in an oven at 70°C up to a constant weight. In blank experiments with no-irradiated sheets, neither grafting nor homo polymer formation were observed. The grafting yield Y was calculated by Y (%) = 100 (wf - wi)/wi, where wi and wf are the foil weights before and after grafting, respectively. The conductivity (C) was measured using a conductometer Altronix CT-1 model (0–200 lS scale). For the calibration of the permeation measurement, a Film Millipore (NYSE: MIL, http://ir.millipore.com) with 5 μm pore diameters and a pore density of 6 x 10^5 tracks/cm^2 and 10 μm thickness was used. NaCl solutions with different values of pH were produced. The final concentration of salt was chosen to obtain approximately the same conductivity for all of them. A drop of a solution of a given pH was put onto the membrane of PP that also separated it from the compartment with pure water (downstream compartment) where the conductivity was measured. The measured conductivity (C) follows the expression $C = C_\infty(1 - e^{-t.k})$. Each determination, as a function of time, consists in measuring the ratio, $C_R = C/C_\infty$ (1) and from the fitting the value obtained was $\tau = 1/k$ (2). For each combination of membrane and solution, the experiment was repeated six times and a mean value τ was obtained. The fraction of the sample area that is covered with pores is $F\pi r^2$, where F is the ion fluence and r is the effective radius of the pore. In the following, τ is assumed inversely proportional to this fraction and then result in $\tau/\tau_0 = F_0 \pi r_o^2 / F \pi r^2$ (3). To measure τ, first it's necessary to determine the constant τ_0 and for this purpose it was used a Millipore film of 10 μm of thickness with known pore diameters of 5 μm (r_0 = 2.5 μm) and a density of $F_0 = 6 \times 10^5$ pores/cm^2. Then, τ was measured using (3) with the previous value of τ_0.

3.2. Implanted PVDF foils

Argon ion beams between 30–125 keV, provided by a VARIAN 200 kV ion implanter (Tandar Laboratory) were used to irradiate polymer films with fluencies between 0.1×10^{13} and 50×10^{13} cm^{-2}. The targets were films of β and α-PVDF with different thicknesses. Synthesis quality styrene, glycidyl methacrylate, N-isopropyl acrylamide monomers, vinyl sulfonic acid, and AAc monomer (from Merck Ltd.) were used as received. All foils were stored at –20°C temperature in air until the grafting experiment was performed. Grafting time was 3 hours in all cases. Absorption experiences were carried out using two grafting solutions: a) 79 vol.% AAc + 0.2 M H_2SO_4, + 0.1 wt% Mohr salt (solution 1); and b) 77 vol.% AAc + 0.2 M H_2SO_4 + 0.1 wt% Mohr salt + 5.4 vol.% vinyl sulphuric acid (solution 2).

For the biocompatibility experiments, films of PVDF were irradiated with Ar 50 keV with 10^{13} cm^{-2} and then introduced in a solution of AAc 79 vol.% + 0.2 M H_2SO_4 + 0.1 wt% Mohr salt [8]. Membranes were washed in distilled water for several days at room temperature and/or 62ºC. The polymer to be implanted was washed with saline solution and with antibiotics and then with MEM Eagle medium. The laboratory animals were managed according to the norms of the NIH and sacrificed 45 days post implant.

In order to determine the biocompatibility of the obtained material, intra peritoneal and subcutaneous surgical implant of poly-AAc were carried out in male mice BALB/c 8 weeks old and 25 g of weight. 0.5 mg intra muscular anesthesia was administered to the animal allowing working conditions of 20 minutes. The animals were maintained with balanced diet and water ad libitum. 200 micro grams of wet polymer was used for each implant. The clinical state of the animals was evaluated during 45 days, after which autopsy was carried out and the pathological and hystopathological study completed. In order to study the immobilization of compounds of biological interest, immobilization of enzymes (urease) or hormones (insulin) and the study of their activity, β-PVDF films were irradiated with Argon beams of 100 keV with fluencies from 5×10^{12} cm^{-2} to 1.4×10^{13} cm^{-2}. Film thickness of 4.5 or 25 µm were used. The grafting solution was acrylic acid 79 vol.%, 0.1 wt% Mohr salt, 0.2 M H_2SO_4 and 20 vol.% distillated water, bubbled 15 minutes with N_2. Urease enzyme (solution, Wiener Lab.) was incorporated into the solution during the grafting procedure, while the control films were carried out without the enzyme. The membranes with the immobilized enzyme were maintained at 2–8°C in 50 mM, pH 7.4 phosphate buffer.

3.2.1. Urease enzymatic activity determination (Method 1)

The enzymatic activity of the urease was determined after measuring the amount of remaining urea from 5 mL solution of 300 mg% of urea in phosphate buffer solution (pH 7.4, 50 mM, 0.9 wt% NaCl), after an hour of incubation of the films at 37°C. The indophenol colorimetric method was used, in which the produced ammonia reacts with phenol in alkaline media producing a colored product whose absorbance is determined at 540 nm.

The amount of remaining urea is considered as a percentage regarding a control with free enzyme, in substitution of the film with immobilized enzyme. The amount of ammonia produced is calculated proceeding to the colorimetric determination, previous incubation with urease, to estimate the production of ammonia from the remaining urea, without the contribution of the free ammonium due to membrane interference.

3.2.2. Enzymatic activity determination (Method 2)

The enzymatic activity of the urease was determined after measuring the amount of remaining urea from 5 mL a solution 320 mg% urea after a hour incubation of it films at 37°C. The method kinetic urea UV was used (Fig.1.), in which produced ammonia is incorporated to the α-ketoglutarate by action of the glutamate dehydrogenase with parallel oxidation of NADH to NAD^+:

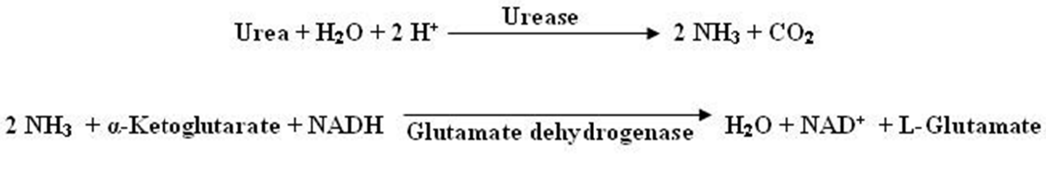

FIG. 1. Scheme of enzymatic activity of the urease.

The increase of NAD^+ concentration is proportional to urea concentration in the sample. Absorbance is determined from the NAD^+ at 340nm, at 60 seconds and 120 seconds of having begun the reaction, by way of eliminating interferences, in such way that the absorbance corresponding to the NAD^+ result from the difference between both times. The amount of remaining urea is considered as a percentage regarding the concentration of initial urea in each solution.

3.2.3. Insulin hormone activity determination

The insulin hormone activity was determined using the following procedure: insulin usage: H.M. Penfill Actrapid (Human insulin injection solution). Composition biosynthetic human insulin (DNA origin produced in Saccharomyces cerevisiae recombinanate, 1 IU corresponds to 0.035 mg). Experimental animals: Mice BALB/c male and female aged 10 weeks of average weight of 25 g. (In compliance with the national Laws Relating to the Conduct of animal experimentation). Anesthesia was carried out using intramuscular ketamine in single dose of 5 mg and in some cases double dose of 2.5 mg. To take a blood sample to assess blood glucose levels in animals implanted, mice were punctured in a vein in the back of the tail. Determination of blood glucose in mice was performed using test strips and ACCU-CHEK ACTIVE instrument. Inoculation of polymer, in the case of fractions folia (all implants were foils of 1.0 × 0.8 cm) were implanted surgically on the back animals properly anesthetized (see Fig.2.) while milled disintegrated films were made with a mechanical disintegrator using a potter. The approximate weight of dry polymer was 50 mg.

4. EXPERIMENTAL

4.1. PVDF-NIPAAm

Figure 2 shows a microphotograph of a 9 µm track length from a ^{208}Pb irradiated sample of 9 µm thickness, etched during 30 min.

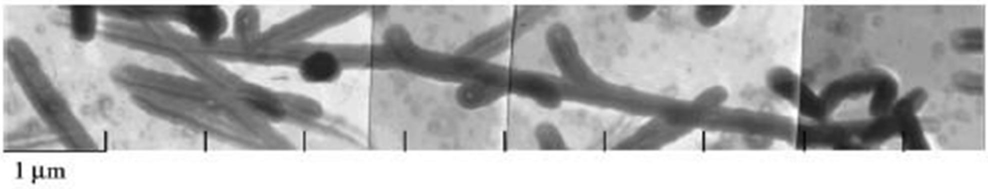

FIG. 2. Microphotograph of a sample.

Figure 3 shows several FTIR spectra measured for non etched grafted foils (labels 1–4) and for etched grafted foils (labels 5–7). The characteristic absorption bands of PNIPAAm can be identified from the sample spectra (label 1–4) such as: (i) NH amide stretching vibration at 3300 cm^{-1} (broad peak because NH are bonded), (ii) the Fermi resonance enhanced overtone of the amide II at 3078 cm^{-1}, (iii) amide I at ca. 1650 cm^{-1} and (iv) amide II at 1548 cm^{-1}. As it can be observed in Fig. 4 (label 1–4), the presence of PNIPAAm is clearly identified by the absorption bands at 1650 cm^{-1} and 1548 cm^{-1}. These spectra were taken with different ions and fluencies with the purpose of showing that their intensities are strongly correlated with the grafting yields and not with the irradiation parameters. Furthermore a decrease in their intensities is clearly observed for etched foils (labels 5–7) and the low grafting yield values were estimated by comparing labels 5−7 spectra with label 4 spectra as approximately 3%. In addition, Fig. 3 shows that this low intensities peaks, namely 1548 and 1650 cm^{-1} which are typical of PNIPAAm, are not observed for non-grafted foils. The infrared spectra obtained from irradiated foils with 10^{11} cm^{-2} Pb beam for etched and grafted foils (Fig. 2, labels 1–3) is compared to the control spectra of irradiated non etched foils (label 5) and irradiated etched foils (label 6), both without any grafting. The infrared spectra obtained using a 3 µm pore diameter PVDF foil (label 4), post irradiated with gamma rays and finally grafted with 3% aqueous solution used in a previous experiment [12], was included for comparison purposes (15% grafting yield). In this case the peaks at 1548 and 1650 cm^{-1} related with PNIPAAm are clearly observed. From the last observation we can conclude that the characteristic PNIPAAm peaks are not present in spectra of non-grafted foils.

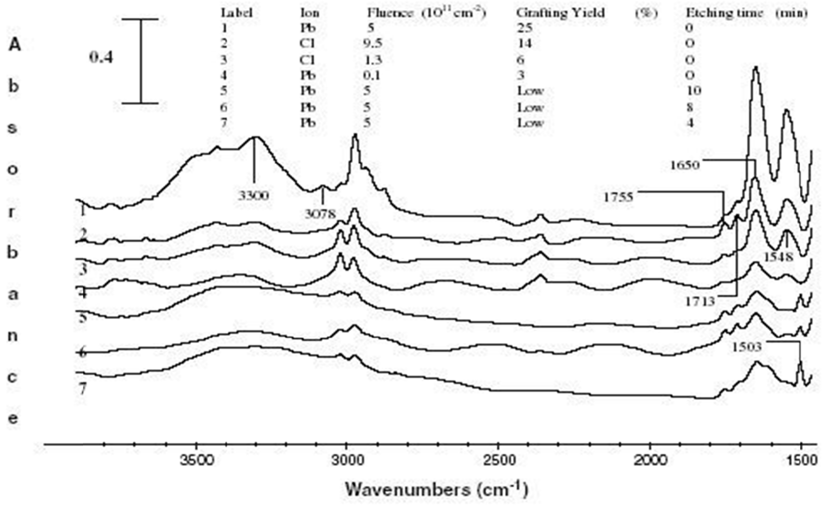

FIG. 3. Infrared spectra of PNIPAAm grafted foils of 9 μm thickness, using solution 1 for 22 h grafting time. The inset shows the etching and grafting conditions. The bar in the figure indicates the scale. 10 wt% NIPAAm aqueous solution.

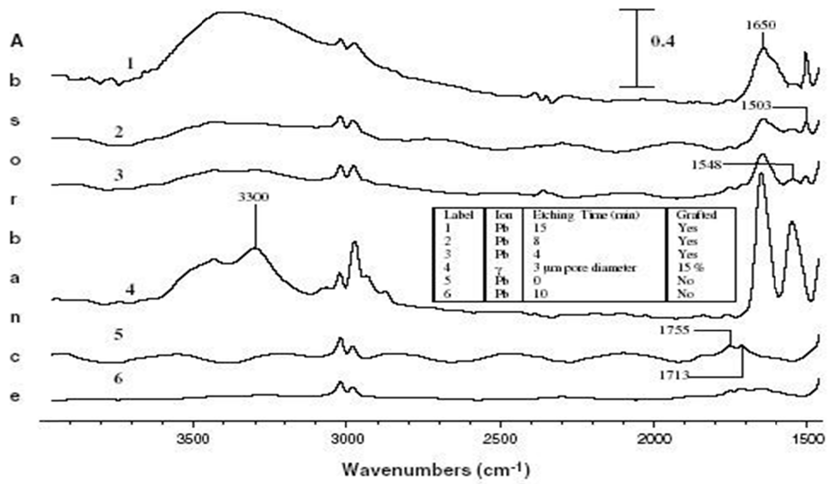

FIG. 4. Comparison of infrared spectra for 9 μm thickness foils, using solution 1 for 22 h grafting time irradiated with 10^{11} cm^{-2} ^{208}Pb ions. For irradiation, etching and grafting specifications see the inset in the figure. Bar indicates the scale. 10 wt% NIPAAm aqueous solution.

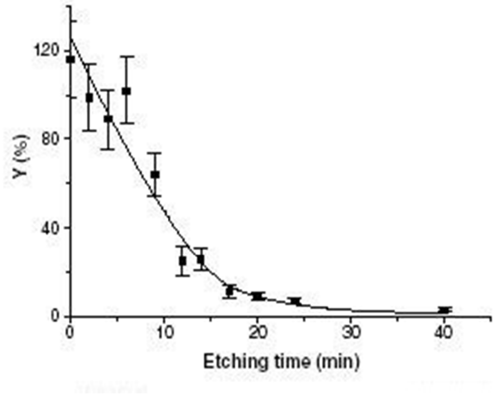

FIG. 5. Grafting yield Y as a function of the chemical etching time for ^{208}Pb ions using solution 2 and 25 μm thickness foils, for 10^{10} cm^{-2} fluence and 22 h of grafting time. 11 wt% NIPAAm + 20 wt% methanol + 0.1 wt% Mohr salt aqueous solution.

It is known that chemical etching produces pores and gradually removes the active sites resulting in a decrease of grafting yield. The diameters of theses pores increase with the etching time. The idea of an interference effect between cylindrical holes produced by the etching process explains the decrease of the grafting yields as a function of the etching time (Fig. 5). The diameter of the pore increases as a function of the etching time, reducing the active sites for grafting and the grafting yield values [9].

4.2. PP-AAc

The etching removes the active sites of the latent tracks producing pores in the films. First, pores promote the monomer diffusion inside the foils, but the etching continues and the grafting yield starts to decrease due to the active sites removal [10]. Previous experiments provided the optimum conditions such as fluence, etching and grafting time in order to obtain an adequate grafting for the permeation experiments. The adopted approach was to select the smallest possible fluence, maximum etching time and grafting times that assure a measurable grafting yield. Therefore, 1010 cm^{-2} fluence, 10 h or 12 h etching times and 3, 5 and 15 min grafting times were selected. NaCl solutions with different values of pH were produced. Final salt concentration was chosen to obtain approximately the same final conductivity for all of them.

A drop of a solution of a given pH was put onto the membrane of PP, separated from the compartment with pure water (downstream compartment), where conductivity was measured. The determination consists of measuring $C_R = C/C_\infty$ (1), using $C = C\infty(1 - e^{-t.k})$ and from experiment the value obtained was $\tau = 1/k$ (2) and $\tau/\tau_0 = F_0\ \pi\ r_o^2 /\ F\ \pi\ r^2$ (3). To measure τ, first was determined the constant τ_0 using a Millipore film of 10 µm of thickness with known pore diameters of 5 µm ($r_0 = 2.5$ µm) and a density of $F_0 = 6\ 10^5$ pores/cm^2. Then, τ was measured using (3) with the previous value of τ_0. Fig. 6 shows the evolution of the effective diameter calculated using (3) as a function of pH for different membranes. The initial pore diameter before grafting was calculated from weight loss measurements. For 10 and 12 h etching time 800 Å and 900 Å pore diameter values were obtained, respectively (50% and 63% of porosity). As can be observed (Fig. 6) for low grafting yield, the effective pores have greater diameter than high grafting yield.

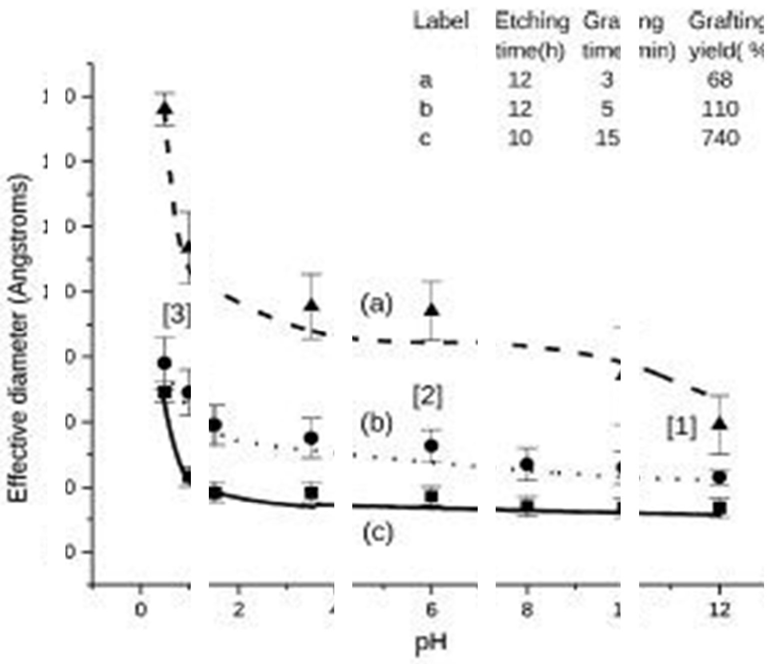

FIG. 6. Effective pore diameter obtained using relations [1–3] for 10^{10} cm^{-2} fluence. The inset shows etching and grafting conditions.

4.3. New membranes obtained by grafted PVDF and PP foils

These experiences describe a new method to produce a thin layer of poly(acrylic-acid) (membranes) that grows on the surface of PVDF films implanted by an Ar beam with energies of 100 keV and for 10^{13} cm^{-2} of fluence, PP membranes with porous post grafted with hydroxyethyl methacrylate and PVDF membranes with porous post grafted with styrene. These membranes were used to study: the absorption of different ions, their biocompatibility, immobilization of compounds of biological interest, immobilization of enzymes or hormones (insulin) and their activity, and their behaviour in a fuel cell.

Figure 7 shows the grafting yield as a function of the fluence for 79 vol% AAc + 0.2 M sulphuric acid + 0.1 wt% Mohr salt in aqueous solution and for 22 hours of grafting time. A maximum is observed for 10^{13} cm^{-2} fluence. In these conditions, and during the grafting reaction, the grafted poly acrylic acid was detached from the original substrate continuing the grafting reaction separated from it.

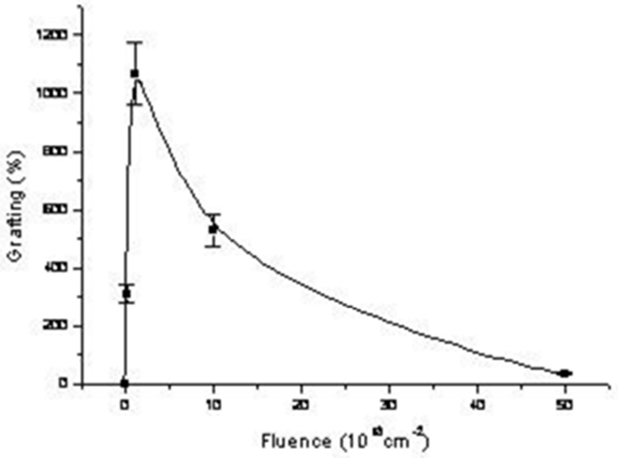

FIG. 7. Grafting yield as a function of fluence for 100 keV Ar^{+} ions and for 79 vol% AAc water solutions. The observed maximum in the grafting yield is obtained about 10^{13} cm^{-2}.

Figure 8 shows a photography from the substratum obtained for 50 keV of energy ions and for the grafting conditions used for Figure 7. To the side of poly acrylic acid film, the original substratum can be observed and the superior part of the figure shows the corresponding grafting film replica, and in the Figure 9 can be observed the different stages of the new membranes obtained with different grafting times.

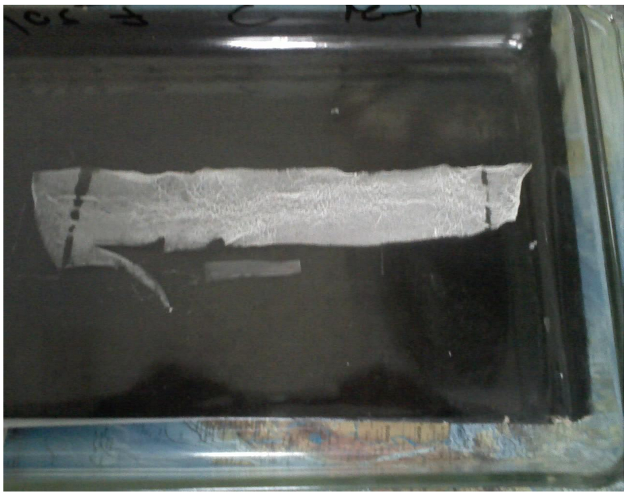

FIG. 8. Membranes of poly(acrylic-acid) that grows on the surface of PVDF films implanted by an Ar beam. In the inferior part of the figure the substratum is observed.

FIG. 9. Different stages of the new membranes obtained.

4.4. Detachment effect for monomer combination

Figure 10 shows the maximum grafting yield as a function of GMA concentration. The sum of both monomers was 78.25% in water solution. Until 2.5% GMA monomer grafted film detached from the irradiated substrate. Fig. 11 shows that grafting yield has a maximum as a function of styrene concentration and Fig. 12 shows the grafting yield as a function of the NIPAAm concentration. The total monomer concentration was 78 vol% in water solution and the grafted film detached from the irradiated substrate. Figure 13 shows the grafting yield as a function of GMA percentage. The grafting solution was 69 vol% AAc + 9.8% NIPAAm + X% GMA + 0.2 M sulphuric acid + 0.1 wt% Mohr salt in water solution. As the GMA percentage increase, the grafting yield increase and the poly (AAc-co-NIPAAM-co-GMA) film detach from the substrate.

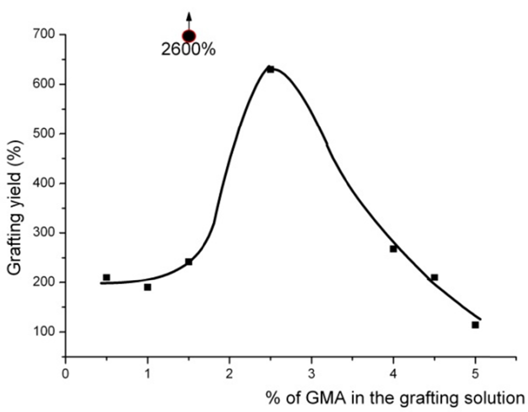

FIG. 10. Grafting yield as a function of the GMA percent.

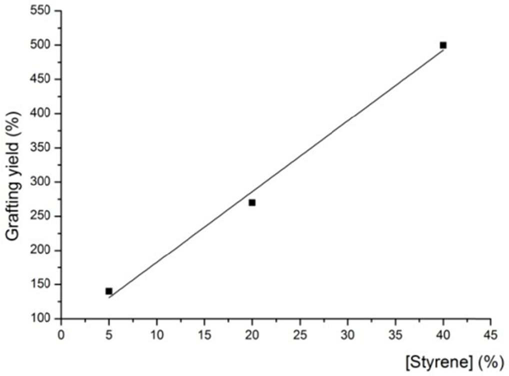

FIG. 11. Grafting yield as a function of the styrene percentage.

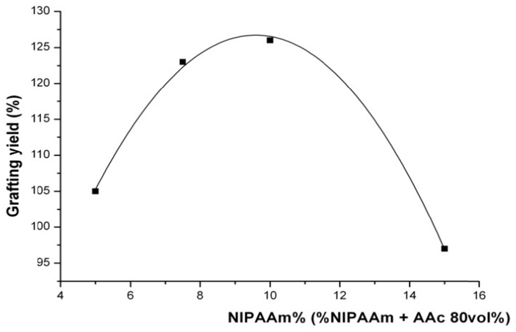

FIG. 12. Grafting yield as a function of the NIPAAm concentration.

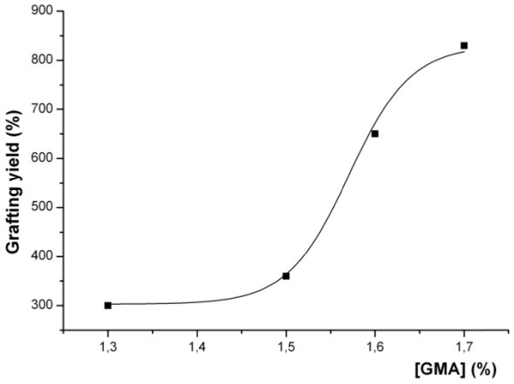

FIG. 13. Grafting yield as a function of the GMA percentage.

4.5. Applications

4.5.1. The absorption of different ions

Figures 14 to 19 show absorption percentage using solution 1 and solution 2 as a function of the Ni^{2+}, Zn^{2+}, Co^{2+}, Mn^{2+}, Cu^{2+}, and Cr^{3+} concentration. The addition of vinyl sulfonic acid to the grafting solution introduces $-SO_3$ groups in the membrane that give to the same one the capacity to exchange ions with a liquid. They were carried out assays for the cations Cu^{2+}, Cr^{3+}, Ni^{2+}, Mn^{2+}, Zn^{2+} and Co^{2+}, obtaining positive results in all cases. The differences among the capacity to adsorb ions in membranes with vinyl sulfonic acid are significant for Zn^{2+}, Co^{2+} and Cu^{2+} regarding membranes with acrylic acid.

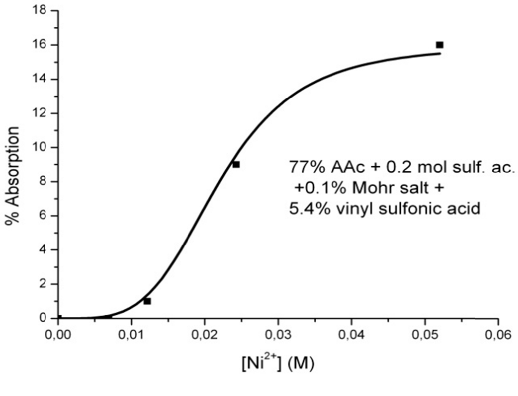

FIG. 14. Absorption percentage as a function of Ni^{2+} concentration.

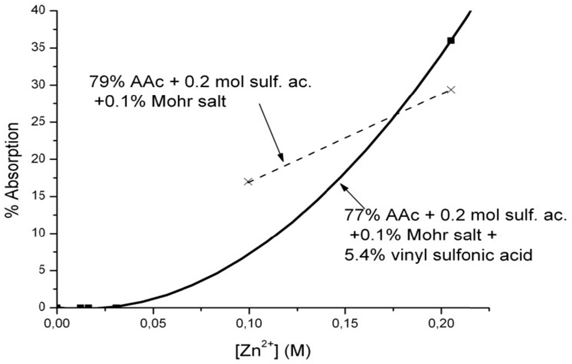

FIG. 15. Absorption percentage as a function of Zn^{2+} concentration.

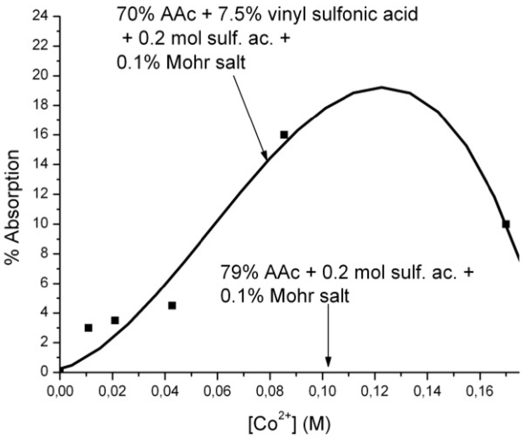

FIG. 16. Absorption percentage as a function of Co^{2+} concentration.

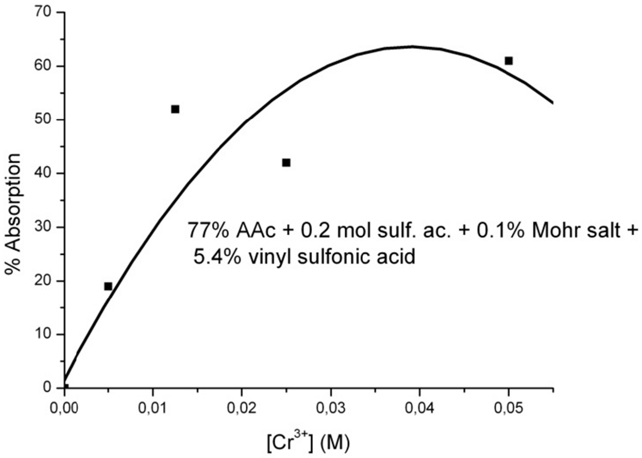

FIG. 17. Absorption percentage as a function of Cr^{3+} concentration.

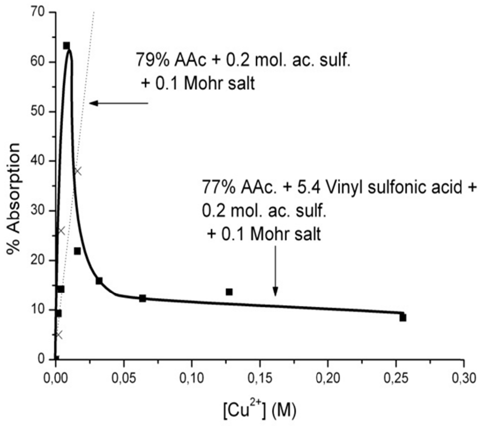

FIG. 18. Absorption percentage as a function of Cu^{2+} concentration.

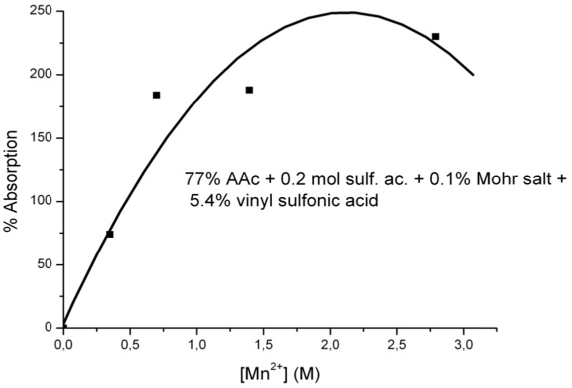

FIG. 19. Absorption percentage as a function of Mn^{2+} concentration.

4.5.2. Experiences of implants in animals

The structures of polymers, carried out with fibres of the textile industry, have been used to develop different types of animals and human cell cultures, and therefore, they have become in kind of a matrix frame for artificial organs development. These structures can be used to create artificial skin with the purpose of treating the serious burns and the ulcers taken place by the diabetes. Alive cells are grown in culture and next, sowed in the structure of the polymer. If it is applied in the patient's wound, the material protects it against mortal infections and loss of fluids liberating factors of chemical growth, signs that stimulate the normal cellular growth in the area of the wound.

It was developed a grafting technique that allows polymeric membranes of acrylic acid that are not dissolved in water to take place because in the grafting process they incorporates to the membrane part of the substrate [8]. It is sought to investigate the possibility to use this new material as cellular support in processes of tissue repair. Figure 20 shows the anaesthetized animal and subjection form foresaw to the chirurgical act. Figure 21 shows the skin separation for subcutaneous (or abdominal cavity) and the previous polymer to be subcutaneous (or abdominal) implanted. Figure 22 shows a microphotograph of the polymeric membrane (1200 X). Figure 23 corresponds to an implant in the abdominal cavity where the colored fibres are observed as consequence of having incorporated proteins of the media (album), control experiment with the original films shows that they don't incorporate colouring. Reaction of rejection is not appreciated in which case an encystment would be observed. In Figures 24 and 25 neoangiogenesis, knitted connective and colored polymer by incorporation of proteins of the media are observed. Figure 26 shows the biocompatibility of the material with the biological tissue, muscle, knitted connective is observed integrated to the material.

FIG. 20. Anaesthetized animal.

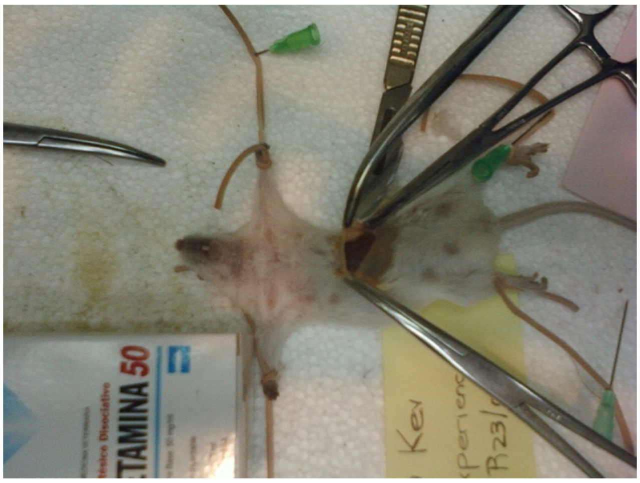

FIG. 21. Skin separation for polymer subcutaneous implantation.

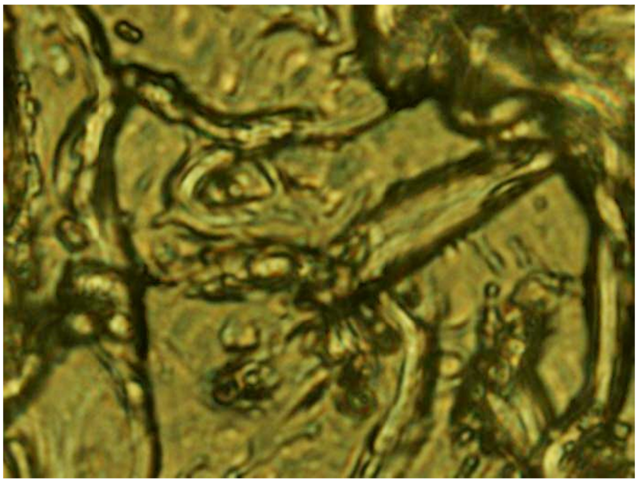

FIG. 22. Microphotograph of the polymeric membrane (1200 X).

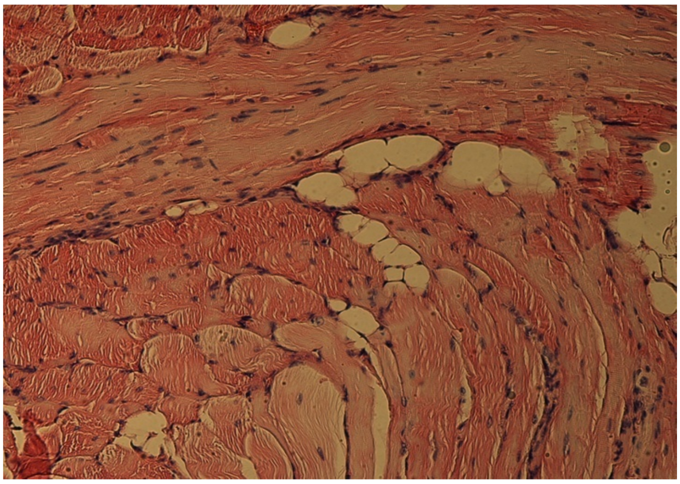

FIG. 23. Implant in the abdominal cavity.

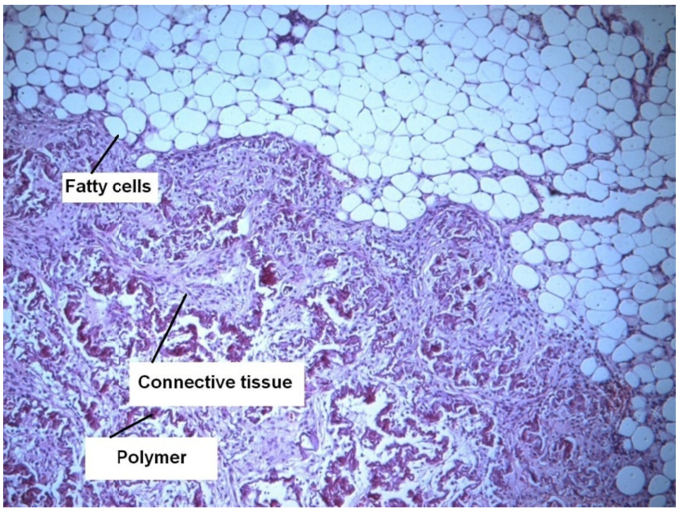

FIG. 24. Intraperitoneal implantation (45 days post-implant).

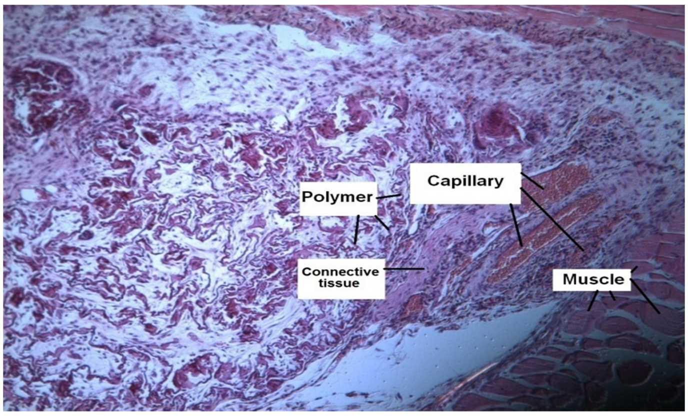

FIG. 25. Intraperitoneal implantation (45 days post-implant).

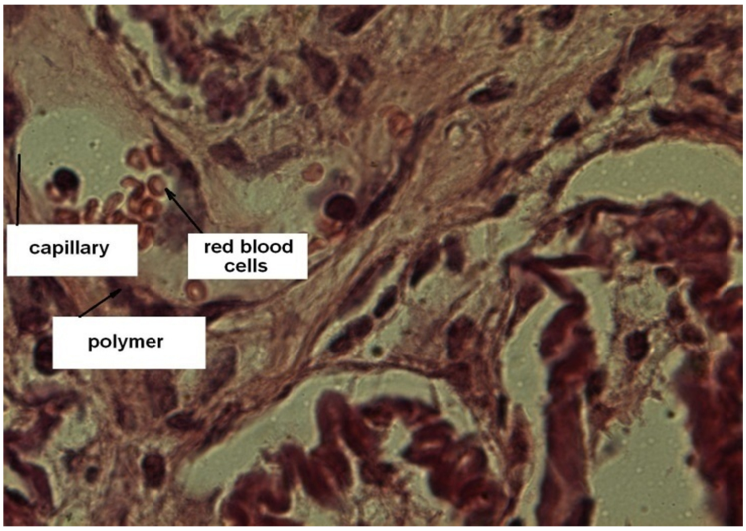

FIG. 26. Biocompatibility of membranes.

4.5.3. Immobilization of urease in membranes obtained grafting PVDF implanted with Ar$^+$ ions

To evaluate the effect of the film of poly acrylic acid (PAA) in the determination of ammonium and urea, different assays were carried out using a membrane obtained under the same methodology, without the urease incorporation. In the ammonia blank sample, the capacity of retention of the ammonium cation was determined by the film, incubating at 37°C during 10 minutes in 5 mL solution of urea in phosphate buffer solution pH 7.4 in presence of free enzyme, comparing to a control in absence of the film. Later on, ammonia remaining on the resulting solution was colorimetric determined. A percentage of free ammonia is obtained in presence of the film, regarding the control without membrane. In the urea blank sample, the capacity of retention of urea was determined by the film, incubating at 37°C during one hour in presence and absence of the film in 5 mL of urea solution in phosphate buffer solution pH 7.4. (Table 1). Later on, the remaining urea concentration was colorimetric determined. No significant decrease was observed in the solutions after incubation. (Table 2). Urease activity of 0.45 UI represents 100% relative activity.

In order to study the effect on storage stability of immobilized urease, free urease and immobilized urease were left in buffer phosphate solution pH 7.4 50 mM at 2–8°C, and activity was determined at 7, 14, 21, and 28 days.

TABLE 1. PERCENTAGE OF UREA FOR DIFFERENT MEMBRANES

Thickness (μm)	Fluence (cm^{-2})	% decrease in urea (%) Method 1/Method 2	Percentage of urease in the grafting solution (mg%)
4.5	1.4×10^{13}	14/26	2.0
4.5	1.2×10^{13}	23 /29	4.5
4.5	1.2×10^{13}	21 /9	1.1
25	5.0×10^{12}	13 /9	4.5
25	1.0×10^{13}	32 /37	2.3
25	1.0×10^{13}	47 /41	3.4

TABLE 2. UREASE CONCENTRATION IN THE GRAFTING SOLUTION FOR THICKNESS OF 25 μm AND FLUENCE 10^{13} cm^{-2}

Urease concentration (mg%)	Urea decrease (*) (mg^{-1})
2.3	1.6
1.2	1.9
0.55	1.3
0.28	1.4

(*)Calculated as: catalyzed urea hydrolysis × initial urea $concentration^{-1}$ × weight of $film^{-1}$

Figure 27 shows the percentage of activity retained during the time for free enzyme regarding immobilized enzyme in the membrane. It was observed that although the initial value is smaller, the storage stability is greater for immobilized enzyme regarding free urease. Under the same storage conditions, the activity of immobilized urease decreases slower than free enzyme.

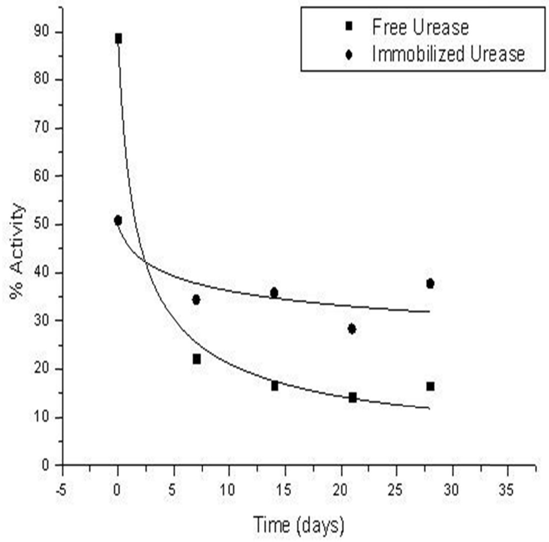

FIG. 27. Percentage of activity maintained in time for the free enzyme (in phosphate buffer solution pH 7.4, 50 mM) versus the immobilized enzyme in the foil.

In order to study the effect of pH of the medium on the activity of immobilized urease, the activity of free and immobilized enzyme was determined in different buffer solutions at values of pH 2.5–8.5. Remaining urea was measured after 1 hour incubation at 37°C on buffer solution, and was compared to a solution in which 100% urea was hydrolyzed to ammonia at pH = 7.5. Immobilized enzyme on AAc-g-PVDF membranes showed a broader range of functionality at different pH, though lower activity obtained with the optimum pH for free enzyme (Fig. 28). Optimum pH of immobilized enzyme was pH 5.0, is close to AAc pK_a and the COOH groups do not charge, minimizing electrostatic repulsion between enzyme and membrane.

In order to study the effect of incubation temperature on the activity of urease, free and immobilized urease were incubated at different temperatures for an hour, and urea concentration was determined colorimetrically. According to Fig. 29. free enzyme showed better activity percentage at all temperatures than immobilized enzyme. However, urease attached to membranes was still functional, showing less dependence on temperature.

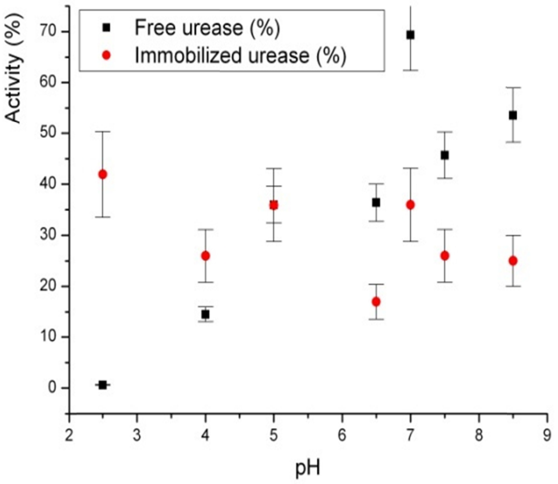

FIG. 28. The effect of pH on the activity of free urease and immobilized urease.

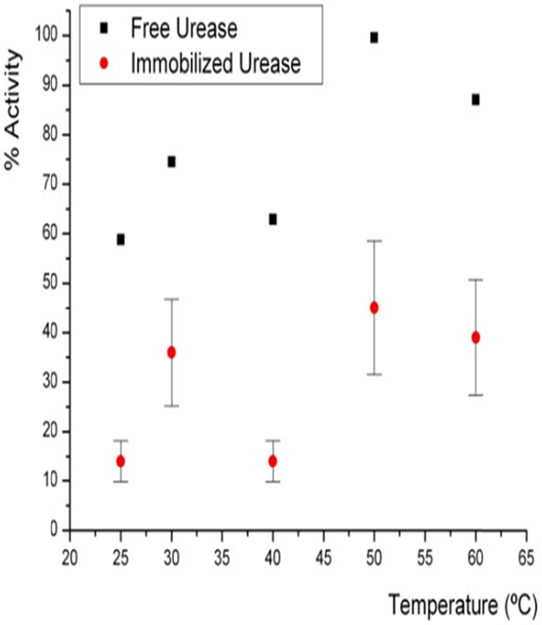

FIG. 29. The effect of incubation temperature on the activity of immobilized and free urease.

Preliminary studies on determination of blood glucose in mice implanted with polymeric membranes obtained grafting PVDF implanted with Ar^+ ions were carried out. It was studied the drug entrapment in polymer matrices of biomedical interest for use in medical treatment or industrial processes. Insulin decreases glucose blood levels because it facilitates glucose uptake after insulin binding to receptors found on cells muscle and fat and the simultaneous inhibition of glucose production from the liver.

Analysis of blood glucose at different times post-inoculation and routes of administration in films weight of 50 mg, insulin units per film: 0.375. All animals were fed regular (permanent), even prior to analysis. Results are shown in Table 3.

TABLE 3. BLOOD GLUCOSE LEVELS AT DIFFERENT TIMES FOR SUBCUTANEOUS INJECTION AND INTRAPERITONEAL INOCULATION OF COMPLETE MEMBRANE AND MILLED MEMBRANE. INITIAL VALUE WAS 140 mg% IN 6 CONTROL MICE

Time (Hours)	Post subcutaneous injection -complete membrane- (mg%)	Post intraperitoneal inoculation -milled- (mg%)	Post subcutaneous inoculation -milled- (mg%)
0	145	163	147
0.5		110	
4		91	132
24		100	97
40		99	
48	101	100	
96			127
120	117	120	128

4. CONCLUSIONS

New films of poly acrylic acids using the pre-irradiation grafting method were obtained and a new effect was observed. The best conditions for the detachment effect obtained were: 10^{13} cm^{-2} fluence, 100 keV Ar ions and 25 µm PVDF films. This effect is probably due to the stress suffered by the substratum when the grafting proceeds, causing the detachment of the grafted film taken with part of the substratum. These membranes were used for studies on absorption of different ions, the biocompatibility, and immobilization of compounds of biological interest: enzymes (urease) and the study of their activity.

Immobilized urease showed a better behaviour on pH and temperature dependence, as well as greater storage stability with less critical loss of activity in time. Although in some cases, the activity obtained was not the optimal; the advantages of immobilized enzyme outweigh this, allowing the reusing of enzyme, retention at the reaction site, and potential application in biosensors. Anatomy pathological and histological studies indicate the biocompatibility of the implanted material. During the 45 days post implant manifestations of clinical pathologies were not observed.

REFERENCES

[1] OMICHI, H., Synthesis of intelligent materials using ion beams, Nucl. Instr. Meth. Phys. Res. **105** B (1995) 302.

[2] REBER, N., OMICHI, H., SPOHR, R., TAMADA, M., WOLF, A., YOSHIDA, M., Thermal switching of grafted single ion tracks, Nucl. Instr. Meth. Phys. Res. **105** B (1995) 275.

[3] CHAPIRO, A., Radiation induced grafting, Radiat. Phys. Chem. **9** (1977) 55.

[4] MAZZEI, R., The relationship between tracks in solid state nuclear track detectors (SSNTD) and the submicroscopic kinetic theory, Radiat. Meas. **26** (1996) 577.

[5] FLEISCHER, R.L., PRICE, P.B., WALKER, R.M., Nuclear Tracks in Solids. Principles and Applications, University of California Press, Berkeley (1975).

[6] MAZZEI, R., GARCÍA BERMÚDEZ, G., MASSA, G., FILEVICH, A., Grafting of polypropylene and poly(vinylidene fluoride) films implanted with Ar^+ ions, Nucl. Instr. Meth. Phys. Res. **255** B (2007) 314.

[7] MAZZEI, R., GARCÍA BERMÚDEZ, G., BETZ, N., CABANILLAS, E., Swift heavy ion induced graft polymerization in track etched membranes' submicroscopic pores, Nucl. Instr. Meth. Phys. Res. **226** B (2004) 575.

[8] MAZZEI, R., M. DEL GROSSO, G.G., CHAPPA, V., ARBEITMAN, C., “Surface modifications of polymers induced by heavy ions grafting”, Report of the 2^{nd} RCM on Development of Novel adsorbents and Membranes by Radiation- induced Grafting for Selective Separation Purposes, IAEA (2009)19.

[9] FERNÁNDEZ, A., TORRES, A., BETZ, N., TADEY, D., Grafting of PNIPAAm on PVDF submicroscopic tracks induced by the active sites remainders of the etching process, Nucl. Instr. Meth. Phys. Res. **266** B (2008) 937.

[10] MAZZEI, R., FERNÁNDEZ, A., GARCÍA BERMÚDEZ, G., TORRES, A., GUTIERREZ, M.C., MAGNI, M., CELMA, G., TADEY, D., Grafting of acrylic acid on etched latent tracks induced by swift heavy ions on polypropylene films, Nucl. Instr. Meth. Phys. Res. **266** B (2008) 937.

DEVELOPMENT AND APPLICATION OF CHLORINATED, FLUORINATED AND TECHNOLOGICAL POLYMER FILMS MODIFIED BY GRAFTING PROCESS USING ELECTRON BEAM AND GAMMA RADIATION

J.E. MANZOLI[1,4], A.B.C. GERALDO[1], E. MOURA[1], E.S.R. SOMESARI[1],
C.G. SILVEIRA[1], H. OIKAWA[1], N.S. MOREIRA[1], C. FORBICINI[1],
E. TENÓRIO[2], C.G. AUGUSTO[3,4], L.C.G.A. PANZARINI[5]

[1]Nuclear Energy National Commission
Nuclear and Energetic Research Institute
São Paulo, BRAZIL
[2]FATEC, Tatuí, BRAZIL
[3]IFSP, São Paulo, BRAZIL
[4]Universidade São Judas Tadeu, São Paulo, BRAZIL
[5]FEI, São Bernardo do Campo, BRAZIL

Abstract

The ionizing irradiation (electron beam and gamma irradiation) induced grafting to fluorinated and chlorinated polymeric films were studied. Styrene grafting onto fluorinated and perfluorinated polymers and their ulterior sulfonation constitute a process to produce ionomers for many applications. The modification of polyvinylchloride with dimethylaminethylmethacrylate-heparin grafting attempt for the fact that grafting can be applied in packaging industry as an alternative for decreasing of plasticizer or another chemical species migration, in many cases nocivus contaminant for human health, and, in the specific study of this project, to obtain a less thrombogenic polymer surface to be used in medical applications. The results indicate mutual styrene grafting performed by industrial EB accelerator can be a fast alternative to produce ionomers that can compete in market. The numerical method to simulate diffusion process evolved is simple and fast and applied to fit experimental results.

1. OBJECTIVE OF THE RESEARCH

The objective was to utilize the radiation grafting technique to modify the chlorinated, fluorinated and technological polymer films by gamma and electron beam irradiation grafting. The focus was on developing an ion exchange membrane for fuel cell application and quantification of the influence of radiation grafting on the migration behaviour of plasticizer from packaging into material, for food or medical applications. Suitable analytical methods were developed to evaluate and achieve information about the surface, chemical and physical characteristics of these materials, and model developed to simulate the diffusion characteristics of the target materials.

2. INTRODUCTION

On the scope of this CRP, the Brazilian promote the study of application of radiation grafting of polymers for fuel cell membranes, for medical or food polymer packaging technology and for mathematical modelling or simulation of the diffusional aspects involved on chemical species migration.

Grafting is a powerful surfacing modification process to produce new polymeric materials with an intimate molecular interaction, not present in simple processes like adhesion, traditional blending and co-polymerization. Grafting process by ionizing radiation has been more attractive lately due to the fast free radicals production without chemical intermediates, as initiators. The evaluated properties are related to the application of the modified polymer materials as ion exchange membrane for fuel cells and as food/medical packaging with reduced plasticizer diffusion. A first set of materials studied were polytetrafluoroethylene (PTFE), polyvinyl difluoride (PVDF) and polypropylene (PP) films grafted by irradiation with styrene and finally sulfonated. These will be applied as a PEM (proton exchange membrane, also called polymer electrolyte membrane) into a hydrogen fuel cell.

The radiation induced grafting of polymers became important lately because it can be used to produce material that can be alternative for Nafion® substitution in PEM fuel cells. Nafion® membrane acts as an electrolyte that allows cations conduction only. Also, the low chemical reactivity and the high mechanical and thermal resistances are important attributes for its utilization as catalyst support. Disadvantages like long-time preparation, methanol permeation and high cost are limiting factors to use Nafion® membranes in fuel cells. Nafion® membrane composites obtained as of heteropolyacids [1] and acid silicon oxides [2] improved some characteristics like high water retention and high conductivity in operation temperatures up to 100 °C, but it does not solved high costs problem yet.

Fluoropolymers and polypropylene have been grafted with aromatic monomers like styrene and divinylbenzene [3, 4]. These polymer matrices have high melting temperatures that are advantage for their utilization in fuel cells. However, they have high crystallinity degrees and this characteristic is not appropriate for modification using ionizing irradiation. Many studies proposed a previous polymer crosslinking to improve irradiation and mechanical resistances [5, 6]. When styrene is the grafted monomer at high degrees of grafting the degradation causes deterioration of the mechanical properties and it can be related to the high polystyrene crystallinity [7].

In this work, fluorinated polymer and PP films were grafted with styrene monomer by electron beam and/or gamma irradiation. Simultaneous and pre-irradiation in controlled temperature and pressure were used. Other parameters like monomer, solvent, dose and dose rate were considered. The grafted polymer film was sulfonated and the cation exchange membrane obtained was characterized by gravimetry, thermal analysis, vibrational spectroscopy, microscopy and electrochemical analysis. The performance and durability of cation exchange membrane will be tested in a fuel cell prototype in the near future.

Polyvinyl chloride (PVC) flexible films were prepared, radiation grafted with dimethyl aminoethyl methacrylate (DMAEMA) monomer. This monomer traps heparin molecules in the PVC surface [8] for desired applications. This PVC-g-DMAEMA-heparin polymer presents less thrombogenic surface for medical applications in contact with blood. It would be desirable that migration or diffusion of plasticizers [9] (and other undesired substances inside flexible PVC) be reduced due to the grafting, when contact of this polymer occurs with stomach acids (by drips) or blood. This material could be applied as a new packaging material to prevent thromboembolism when packaging in blood banks. Diffusion/migration of plasticizer, like di-2-ethyl hexyl phthalate (DEHP) from PVC packaging to the food/hemoproducts, could be a source of possible chemical food or medicine contamination. It was proposed to apply a procedure and evaluate grafted film samples in order to quantify the amount of phthalate that migrates, comparing the grafted and non-grafted migrated amounts. Polymeric biomaterials with surface hemo-compatibility properties had been successfully synthesized by the grafting of hydrophilic monomers onto commercial polymeric films by the simultaneous gamma irradiation process [10]. DMAEMA is a monomer with amine and acrylate groups that are responsible by hydrophilic characteristics in grafted polymer. Heparin is a disaccharide which has the main characteristic to avoid hemorrhages, but this biomolecule does not make a covalent bond with the PVC matrix; to fix it to the polymeric substrate it is necessary to graft a specific monomer with physical and/or chemical affinities to bind heparin. Here, the DMAEMA grafting on PVC was performed by an innovative process using EB radiation. In the experimental migration process from these grafted PVC samples into biological simulant media, DEHP was quantified by classical UV spectrophotometry into the media. It was verified that PVC plasticizer migrates at lower concentration when grafted samples are used.

The numerical method to simulate diffusion process evolved is simple and fast**;** it can utilize different diffusion coefficients for each different layer of medium (polymer, solution or grafting) and partition coefficient can be added between each interface of different materials. The use of this numerical method as a modified Cottrell equation solution will permit to fit the voltammetry assay results and to determine the diffusion coefficient as well as to model the behaviour of the grafted membrane during the ionic conduction. The diffusional numerical procedure was applied to fit the water uptake results in Fe^{3+} absorbed by PP-g GMA, in collaboration with Prof. Hegazy from Egypt. Details of the experimental conditions have been included on the mathematical model.

3. MATERIALS AND METHODS

3.1. Radiation facilities

In this work, electron beam and gamma radiation were used to initiate grafting. Electron beam (EB) radiation was supplied by electron beam accelerator JOB 188 (Dynamitron®) energy 1.5 MeV, beam current 25 mA, scan 60–120 cm, and beam power 37.5 kW. Gamma radiation was carried out by a ^{60}Co Gamma cell model 220 from AECL (4 kCi).

3.1.1. Vacuum or special gases chamber

The simultaneous and pre-irradiation EB grafting methods under vacuum or inert gas conditions were achieved using the stainless steel irradiation chamber shown in Fig. 1 specially designed for this project. It is sealed through screws that pressing a metal O-ring in the top cap, which has titanium foil window. This window allows penetration of electron beam.

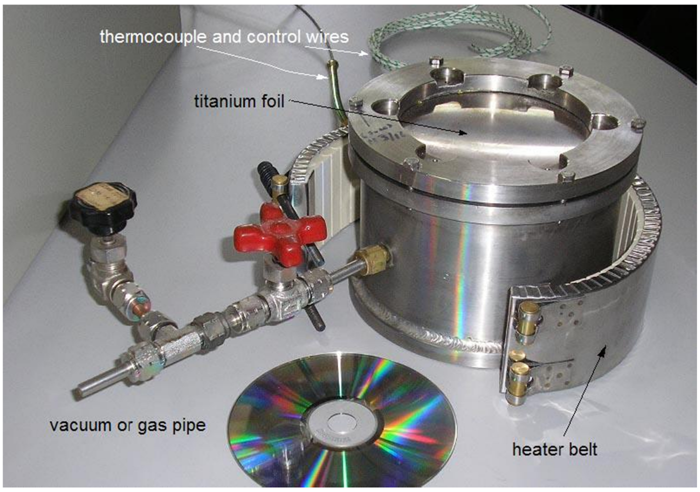

FIG. 1. Irradiation chamber with heating set.

3.2. Samples and chemicals

3.2.1. PVC radiation grafting and migration of DEHP

Commercial blood bags of flexible PVC were cut into 1 cm×1 cm pieces. These pieces were immersed in a solution of 0.25% sodic heparin/30% DMAEMA, the same medium used for grafting by gamma irradiation [8]. The solution and the polymeric substrate were irradiated at 5 and at 15 kGy EB irradiation doses, at a dose rate of 11.29 kGy/s.

The degree of grafting was determined by gravimetry and the MID-ATR-FTIR method was performed to verify DMAEMA-Heparin presence on polymeric substrate.

After grafting the samples were immersed in sodium chloride solution and with 0.5 mol dm^{-3} of glycerine (biological simulant medium). This procedure was three times repeated. The irradiated substrates were immersed in these solutions and aliquots of 2 mL were sampled after 24 hours. Each aliquot was mixed in 2 mL of hexane to extract DEHP of these polar solutions. The DEHP concentration in hexane was determined by UV-spectrometry.

3.2.2. Styrene grafting by ionizing radiation

Fluoropolymer films (Goodfellow) were grafted with styrene monomer (Acros Chemical) dispersed in toluene and/or xylene. Gamma and electron beam irradiations were applied to perform the grafting process in simultaneous and/or pre-irradiation modes. Some parameters, like dose, dose rate, temperature, vacuum and pressure of inert gas/air, were studied to optimize the grafting. Finally, the grafted polymer films were sulfonated by chlorosulfonic acid and/or sulfoacetic method.

The characterization of cation exchange membrane obtained by the above process was performed by FTIR, gravimetry (to obtain the degree of grafting), SEM and electrochemical analysis (IEC and conductivity).

The optimized samples will be tested in the fuel cell prototype (PROCEL/IPEN/CNEN-Brazil Programme) to evaluate the performance and the durability parameters.

3.3. Diffusion process - 1D numerical simulation

The diffusion simulation method is not intended to be applied in a rigorous metrological sense. It will be used as a guide to understand the mass movement through the grafted membrane. The use of this numerical method as a modified Cottrell equation solution, coupled with electromagnetic influence, will permit to fit the voltammetry assay results and to determine the diffusion coefficient and to model the behaviour of the grafted membrane during the ionic conduction. This will be the scope of a future work. In this paper is presented the main and innovative characteristics of the algorithm.

The grafting causes the creation of new and different slices or layers in the surface of the backbone polymer. This multiphase system has different diffusion coefficients for each material phase concerning the diffusion species which can vary under temperature changes. In the PEMFC, proton diffusion could not be described by a simple Cottrell's function, due to this multiphase aspect. As the thickness is much smaller than the area dimensions, diffusion can be assumed as one dimensional, at orthogonal direction. Description of the process is made by the Fick´s second law which, in one dimension:

$$\frac{\partial}{\partial t}C = \frac{\partial}{\partial x}\left(D\frac{\partial}{\partial x}C\right) \tag{1}$$

where C is the concentration of the migrant, generally in µg/mL, and is a mathematical function which depends on space and on time (x and t), or it is said $C = C(x,t)$. D is the diffusion coefficient. The parameter x is dependent for many systems and its quantity is [distance]^2/[time]. It is necessary to define the *initial condition*, which is $C_o = C(x,t=0)$, called here *initial concentration profile* (ICP) and the *contour conditions*. Starting from C_o, C evolves in time, changing its profile, or mathematical form, as function of x. The numerical solution uses a non-uniform mesh of points for the discretization of x domain. The density of points is higher close to interfaces. In order to numerically solve Fick´s equation, Eq.(1), the x domain was discretized in n points by using a three-point finite difference scheme, which generates the following form for the left side of Eq. (2):

$$\begin{aligned}
&\frac{d}{dx}D(x)\frac{d}{dx}C(x) \overset{N}{\cong} \frac{d}{dx}D(x)\left[\frac{C_{i+1/2}-C_{i-1/2}}{\Delta_i+\Delta_{i-1}}2\right] = \\
&= \left(D_{i+1/2}\frac{C_{i+1}-C_i}{\Delta_i} - D_{i-1/2}\frac{C_i-C_{i-1}}{\Delta_{i-1}}\right)\frac{2}{\Delta_i+\Delta_{i-1}} = \\
&= \left(\frac{2D_{i+1/2}}{\Delta_i(\Delta_i+\Delta_{i-1})}\right)C_{i+1} + \\
&-\left(\frac{2D_{i+1/2}}{\Delta_i(\Delta_i+\Delta_{i-1})} + \frac{2D_{i-1/2}}{\Delta_{i-1}(\Delta_i+\Delta_{i-1})}\right)C_i + \\
&+\left(\frac{2D_{i-1/2}}{\Delta_{i-1}(\Delta_i+\Delta_{i-1})}\right)C_{i-1} = OC
\end{aligned} \tag{2}$$

Δ_i (or ΔX_i) is the non-constant distance between successive points i.

D is diffusion coefficient. Operator O condenses notation.

After some algebraic manipulations of operator O, Eq.(2) becomes:

$$\left(1-\frac{O\Delta t}{2}\right)C_{t+\Delta t} = \left(1+\frac{O\Delta t}{2}\right)C_t = f_i \tag{3}$$

The f_i is a known value, easily calculated, and Δt is the time step.

Equation (3) is the time evolution of the concentration function, C. It is a tridiagonal system of n linear equations, where n is the total number of points, which is easily solved by the Thomas algorithm [11].

4. RESULTS

4.1. Radiation grafting of fluorinated and perfluorinated polymer samples

Table 1 shows the results of percent of mutual styrene grafting performed in both kinds of irradiation sources: electron beam (22.4 kGy/s of dose rate) and gamma rays (4.7 kGy/h of dose rate); the absorbed dose of 100 kGy was the same at both irradiation sources. Distinct types of polymer films were immersed in distinct grafting media: styrene and butanol-1 at concentration 1:1 (both irradiation sources) and styrene and toluene at concentration 1:1 (only gamma rays). The irradiations were performed in air, at room temperature and under pressure (both irradiation sources) and under vacuum and at 60°C (only electron beam). High degree of grafting was observed by electron beam when the monomer was dispersed in alcohol as a grafting media and vacuum and warm conditions. When gamma rays were applied high degrees of grafting was obtained when the monomer was dissolved in toluene and the irradiation was conducted in air at room temperature and pressure.

TABLE 1. PERCENT OF MUTUAL STYRENE GRAFTING IN DISTINCT TYPES OF POLYMERIC FILMS, IRRADIATION SOURCES, GRAFTING MEDIA AND PHYSICAL CHEMICAL CONDITIONS

Samples	Styrene grafting % (standard deviation)			
	Electron beam, dose:100 kGy, dose rate: 22.4 kGy/s		Gamma rays, dose: 100 kGy, dose rate: 4.7 kGy/h	
	Air, room T and P	Vacuum, 60°C	Air, room T and P	
	Styrene: butanol-1, 1:1		Styrene: butanol-1, 1:1	Styrene: toluene 1:1
PTFE	0.5 (0.1)	3.3 (0.1)	4.6 (0.1)	7.4 (0.5)
PFA	1.0 (0.0)	6.2 (1.1)	5.8 (1.3)	11.3 (2.0)
PVDF	0.9 (0.1)	15.4 (0.7)	5.1 (0.2)	14.1 (0.3)

In comparison of the grafting carried out on warm and vacuum conditions, the PTFE had a grafting yield three times greater than that for the ambient condition, although this perfluorinated polymer always had the lowest grafting yield and the PVDF had the highest grafting yield, where it was around 15 times greater than that for the liquid phase.

These behaviours can be related to the observations of Chapiro [10], where PTFE swells slightly in styrene and this monomer diffuses into the partially grafted layers; in the same way, PVDF should have a low monomer diffusion resistance at the polymer-vapour interface.

The result where PTFE films shows low degree of grafting, PFA films have values higher than PTFE and PVDF films present the highest values, also should be related to radicals formation characteristics for each film type. The reactivity of radicals formed on each polymer substrates and the G values (number of species formed or the number of chemical changes of a particular type induced on the deposition of 16 aJ (100 eV) of energy for radical formation are important factors to explain the experimental results in this work. For example, some typical G values for radical formation on gamma radiolysis under vacuum at ambient temperature are PTFE, 0.14 [12], PFA, 0.93 [13] and PVDF, 3.3 [14, 15]. By analogy, the high grafting yield onto PVDF and the observed decreasing grafting yields for PFA and PTFE respectively could be related to the number of radicals generated on these polymer matrices.

The conditions of warm and vacuum performed in this experimental system suggested grafting occurs in a specific mechanism that can be proposed as:

$$\begin{array}{lllllll}
R\text{-}OH & \rightarrow & R\text{-}O^{\bullet} & + & {}^{\bullet}H & \text{(Solvent radiolysis)} & (4) \\
M\text{-}H & \rightarrow & M^{\bullet} & + & {}^{\bullet}H & \text{(Monomer radiolysis)} & \\
R\text{-}O^{\bullet} & + & P\text{-}H & \rightarrow & R\text{-}OH + {}^{\bullet}P & & (5) \\
M^{\bullet} & + & P\text{-}H & \rightarrow & M\text{-}H + {}^{\bullet}P & & \\
H^{\bullet} & + & P\text{-}H & \rightarrow & H\text{-}H + {}^{\bullet}P & & \\
{}^{\bullet}P & + & {}^{\bullet}M & \rightarrow & P\text{-}M & & (6)
\end{array}$$

Where the first step of process (slow step), the irradiation allow the radiolysis of each component of grafting media, that results in high reactive radicals, mainly the alcoxy radical ($R\text{-}O^{\bullet}$ or specifically n-butoxy radical); in a second step, this more reactive radical scavenger a hydrogen atom of polymeric chain, even hydrogen scavenging can be achieved by other radicals originated in the first step. Finally, the polymer grafting by monomer radicals occur in the last step [15, 16].

Sulfonation is a kind of process performed to give a hydrophilic characteristic to these styrene grafted films by inclusion of sulfonic groups ($-SO_3H$) in the grafted chains. The PTFE, PFA and PVDF films grafted in the conditions of warm and vacuum under electron beam irradiation were sulfonated and this process converts these films into an ionomer. High water swelling and cation exchange are some characteristics of these films.

Figure 2 shows the increase of mass and the water uptake for each solfonated film type. A mass increase was observed after sulfonation of the grafted polymer films and these percent values are close correlation with the percent of grafting. It suggests that sulfonation process was accomplished, where one sulfonic group is bonded to one aromatic ring of styrene. The water uptake characteristic is coherent with the degrees of styrene grafting and increase of mass after sulfonation. Low degree of water uptake for PTFE films was observed that presented low degree of grafting and low gain of mass after sulfonation process. The value of percent of water uptake for PVDF film is close to that for Nafion® film and it suggest sulfonation and styrene grafting process are enough to achieve the values of this parameter for Nafion®.

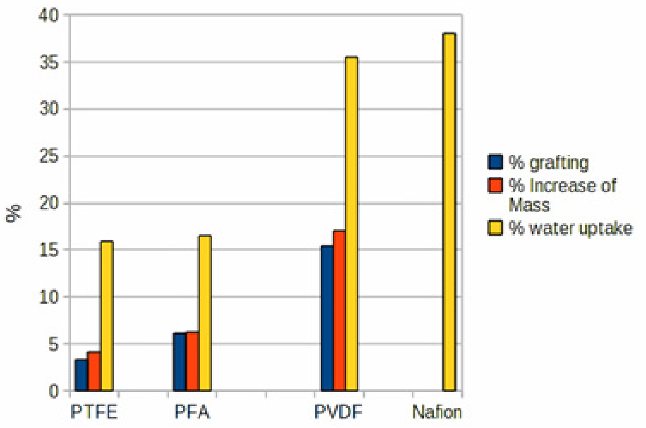

FIG. 2. Percent gain of mass of polymer films after sulfonation process and their percent of water uptake. Comparison with degree of water uptake of Nafion®.

The sulfonated films were characterized by their ion exchange capacity and the results are shown in Fig. 3. Here, the values of IEC are coherent with degrees of grafting, gain of mass after sulfonation and water uptake for each polymer film type. Again, the PVDF film presents a value of IEC close to that for Nafion® film.

The tensile strength maximum was measured to evaluate the mechanical resistance for these polymer films that suffered aggressive process like irradiation grafting followed by sulfonation (Fig. 4). It was observed that fluoropolymer films like PTFE and PFA had low value for this parameter and it should be related to high crystallinity and the agressivity of applied process (grafting and sulfonation), where it was contributed for the weakness of final product. However, PVDF film showed a value of tensile strength maximum close to this parameter for Nafion®; it suggests PVDF styrene grafted and sulfonated film can be an alternative material to be compared to Nafion® films and to be tested in fuel cells.

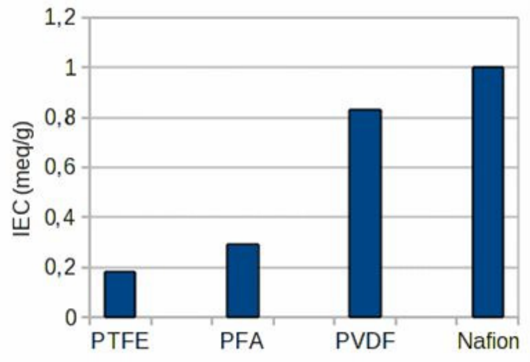

FIG. 3. The IEC values for polymer films styrene grafted by electron beam under mutual grafting mode, warm and vacuum conditions. Comparison to Nafion® film.

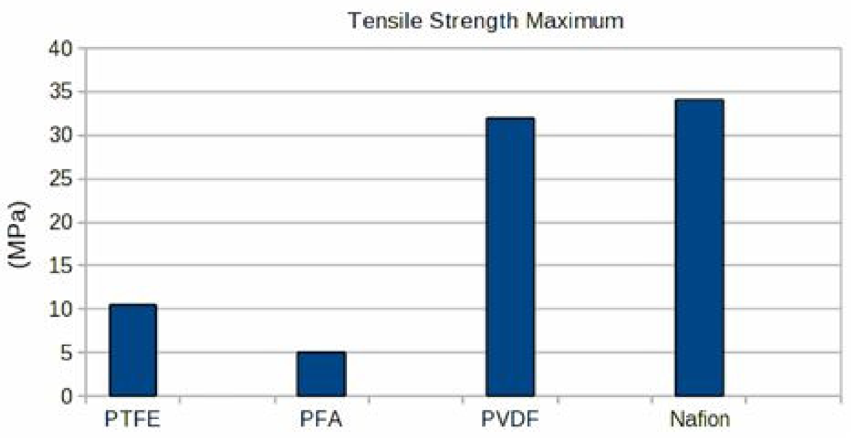

FIG. 4. The tensile strength maximum values for polymer films styrene grafted by electron beam under mutual grafting mode, warm and vacuum conditions. Comparison to Nafion® film.

In the same way, the PVDF styrene grafted film by ion tracking process received from Argentina (cooperation with Mr Rubén Mazzei, Argentina) presented gain of mass after sulfonation process as it is observed in Fig. 5. These films showed very high water uptake (minimum 50% to above 400% in mass) and it is related to the increase of surface proportioned by ion tracking process.

Table 2 shows the characteristics and parameters for ion tracking PVDF films and after sulfonation of these styrene grafted films. It seems that IEC is favourable when pore size is high, but it should be confirmed. The film with 14 µm thickness can be a good candidate to be compared to Nafion® films because of its high values of IEC and tensile strength.

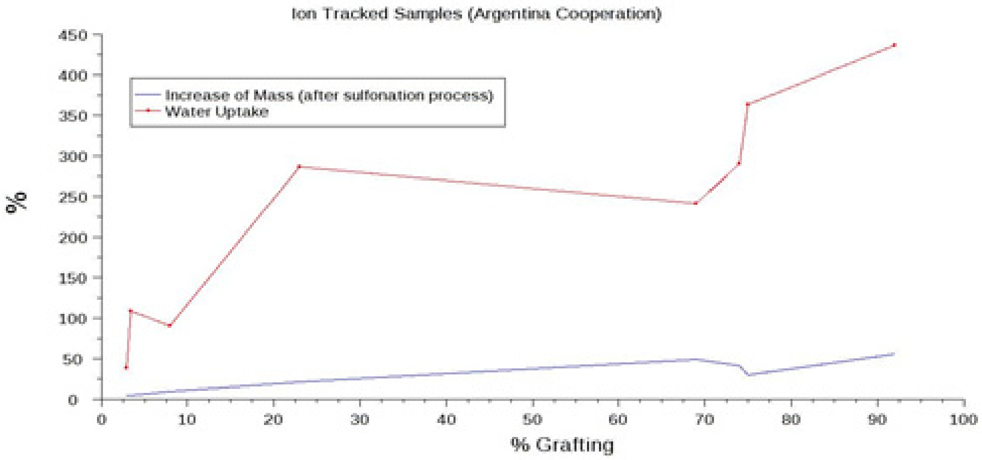

FIG. 5. Percent gain of mass of ion tracking PVDF styrene grafted films after sulfonation process and their percent of water uptake.

TABLE 2. CHARACTERISTICS AND PARAMETERS FOR OBTENTION OF ION TRACKING PVDF STYRENE GRAFTED FILMS AND AFTER THEIR SULFONATION PROCESS

Sty. graft (%)	Irradiat. type	Fluence (cm^{-2})	Etch. time (h)	Pore size (µm)	Film thickn. (µm)	Water uptake[1] (%)	IEC (meq/g)	Tensile strength (MPa)
3	Fission fragment (^{252}Cf)	10^{12}	0.75	0.25	25	38		
3.5	S 110 MeV	10^{11}	0.75	0.42	25	108	3.15	7
8	S 110 MeV	10^{11}	0.75	0.33	25	90		
23	S 110 MeV	10^{11}	0.75	0.19	14	286	1.18	11
69	S 110 MeV	10^{11}	1		25	241	3.97	
74	S 110 MeV	10^{11}	1.5		25	290	4.17	
74	S 110 MeV	10^{11}	1.5		25	290	4.17	
75	S 110 MeV	10^{11}	2		25	363		
92	S 110 MeV	10^{11}	0.5		25	436	6.3	
Nafion®					25	50*	1.0	13**

[1] From dry membrane conditioned in water at 25 °C for overnight (dry weight basis).

* From dry membrane conditioned in water at 100 °C for overnight (dry weight basis).

** From machine direction and water soaked at 23 °C (R.C. McDonald, C.K Mittelsteadt, E.L. Thompson, Fuel Cells **4** (2004) 208-213.

Figure 6 shows the polarization curves for PVDF grafted films in a Pt/membrane/Pt electrochemical system; the Nafion® curve and Pt-Pt behaviour were compared. The current-potential behaviour results show for all curves five distinct regions: hydrogen evolution region (-500 mV – 400 mV), equilibrium potential, charge transfer (-400 mV – 200 mV), mixed control region (-100 mV – 600 mV), mass transport (450 mV – 600 mV) and oxygen evolution (above 650 mV).

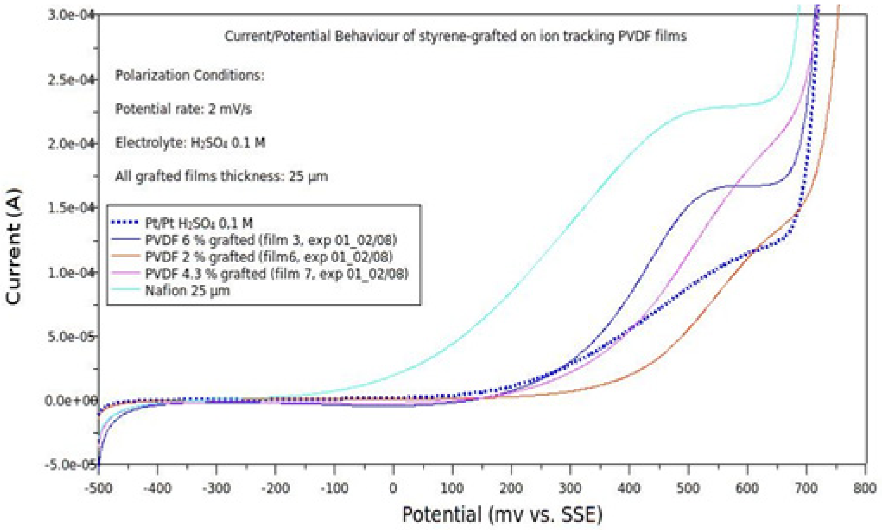

FIG. 6. Polarization curves for ion tracking PVDF styrene grafted films. Comparison with polarization of Nafion® film and Pt electrodes.

The equilibrium potential refers to Nernstian behaviour and the charge transfer is related to the Butler-Volmer equation that describes the electrochemical system kinetics and it shows the way in which current density varies with exchange current density, over potential and the transfer coefficients. The mixed region is an intermediate situation where there is a control of the current by mass and electron transfer steps and it corresponds to much of the rising part of I-E curve. The mass transport region relate the current to the chemical changes at the electrode by equation the flux of electroactive species with the flux of electrons; in this case, the electroactive species concentration on electrode surface is a function of potential but the current is not and under a maximum concentration flux, the current is limited (I_L) by electroactive species diffusion.

The principal changes are in value of potential where charge transfer start (obtained by Tafel curves) and the potential interval that mixed control occur. The Pt-Pt curve shows mixed control anodic region interval of 450 mV; in Pt/Nafion/Pt curve, this region has an interval of 650 mV. Polarization curve of Pt/PVDF film 6% grafted/Pt is observed an interval of 400 mV and the 4.3% and 2% grafted films have values of 400 mV and 300 mV, respectively. The values that define the mass region can be extracted of these curves: to Pt-Pt curve the mass region starts in 600 mV (I_L around 1.0×10^{-4} A), to Pt/ Nafion/Pt curve the mass region starts in 500 mV (I_L around 2.25×10^{-4} A) and to Pt/ PVDF film 6% grafted/Pt curve the mass region starts in 550 mV (I_L around 1.7×10^{-4} A); another PVDF grafted films did not present well defined limit current.

These results show a lower potential range in mixed control region for Pt-Pt system in H_2SO_4 0.1 mol dm^{-3} than those observed in Pt/Nafion®/Pt system and it suggests mixed control is important for Nafion® system. The high limit current value observed in mass region for Nafion® system suggests the maximum electroactive species concentration flux occur in high intensity when this membrane is used compared to Pt-Pt system (without membrane), it means that diffusional phenomena of electroactive species is favoured if Nafion® membrane is used; Nafion® potentialize the conduction nature of electrolyte. More electrochemical studies should be performed in PVDF grafted membranes to verify the behaviour between degree of grafting/sulfonic groups available and this electrochemical parameters; the Pt/PVDF film 6% grafted/Pt curve shows electrochemical potentialities if this membrane is used and it can be a good electrolyte.

4.2. Radiation grafting of PVC and migration of DEHP

In Table 3 the degree of grafting of DMAEMA into PVC for different EB irradiation doses is shown, and in Fig. 7 shows the Mid-ATR-FTIR spectra of irradiated and non-irradiated samples which have the absorption bands indicating the grafting.

TABLE 3. DEGREE OF GRAFTING OF DMAEMA-HEPARIN INTO PVC, ACCORDING TO IRRADIATION DOSE AT DOSE RATE 11.29 kGy/s

Dose	Degree of grafting (%)	Average (standard deviation)
5 kGy	5.09 4.91 4.93	4.98 (0.10)
15 kGy	8.53 7.84 8.72	8.36 (0.46)

Figure 7 shows absorption bands at 1500–1700 cm^{-1} region that is related to C-N bond vibration. These bands are present in both heparin and the DMAEMA, however, the absence of absorption band at 760 cm^{-1} characteristic of S-O vibration bond present at heparin molecule does not confirm its presence at irradiated substrate. The use of FTIR methodology for sample analysis is inadequate to verify the heparin presence because it was used in very small quantities at grafting solution (0.25% of heparin); the next step in this characterization will be another sample preparation methodology, like substrate dissolution and later film sample formation on KBr support. For gamma radiation at these doses, even at simultaneous grafting, the degradation of heparin does not happen [8]. So it was understood that this degradation was not happening in this electron beam procedure, but as the reaction mechanism is different, new characterizations should be made.

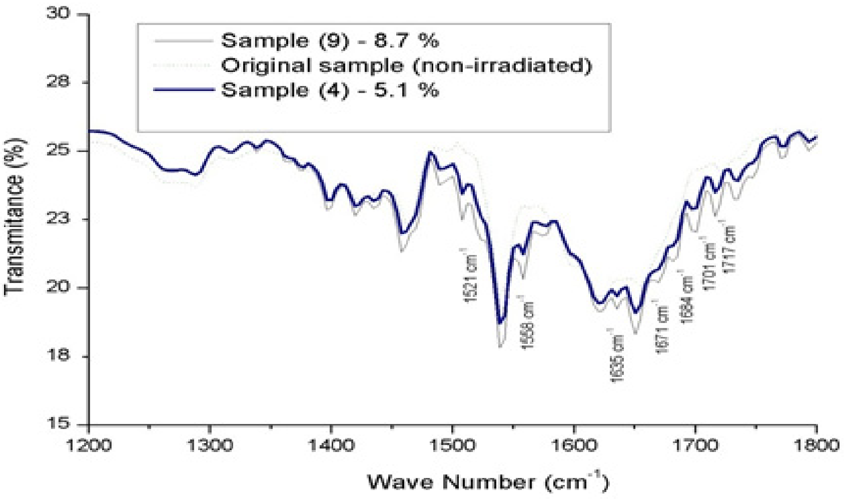

FIG. 7. Mid-ATR-FTIR spectra of irradiated and non-irradiated samples.

The developed analysis by UV spectrophotometry had a linear response and it is a simple method that was successfully used for DEHP determination. Figure 8 shows the calibration curve for DEHP quantitative analysis.

The DEHP concentration determined by UV spectrophotometry at irradiated (15 kGy dose) and non-irradiated samples after immersion essay was 1.95 ppm and 4.47 ppm, respectively. It shows that DEHP migration is lower at irradiated samples than non-irradiated samples; this irradiation methodology could be an alternative to decrease the DEHP migration effect at blood packages but more experiments in this way must be performed.

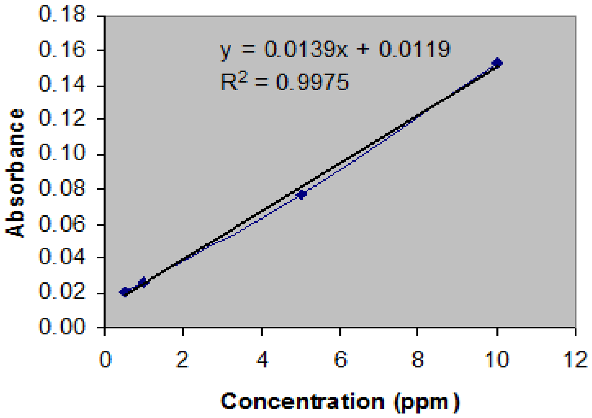

FIG. 8. Calibration curve of DEHP quantitative analysis by UV spectrophotometry.

4.3. Diffusion of Fe^{3+} absorbed into PP-g GMA

The use of the diffusion simulation was applied to the system shown in Fig. 9 on the effect of treatment time on the Fe absorbed by glycidyl methacrylate, GMA, into polyprolylene (PP) treated with ethanol 120% grafting (work in collaboration with Prof. E.A. Hegazy, from Egypt). For this case, the Fick differential equation was solved and the obtained results are shown in orange line in Fig. 10.

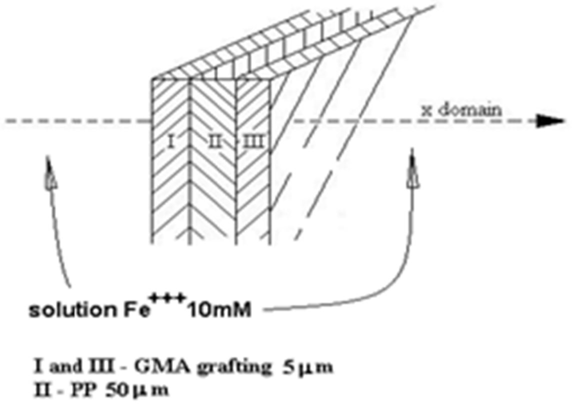

FIG. 9. Sketch of the system simulated in the diffusion of iron ions.

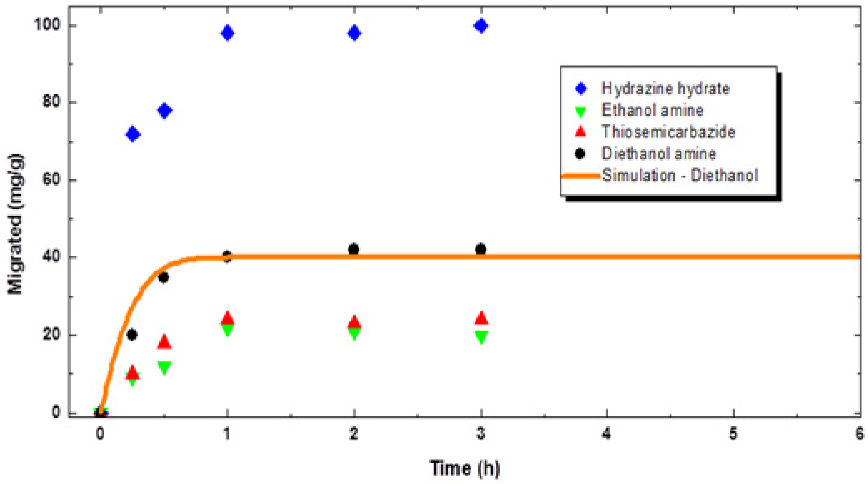

FIG. 10. Comparison of experimental results (measurement by Prof.E.A. Hegazy, Egypt) and simulation in solid orange line.

The diffusion coefficients were estimated as 8.6×10^{-14} m^2/s into the PP and 6×10^{-6} m^2/s into the grafting layer and into the iron solution.

Geometrical considerations, inclusion of experimental parameters like pH, chemical potential, concentration, porosity etc. are necessary in order to continue with this simulation study. When kinetic migration experiments were done, this simulation will be applied in order to evaluate the diffusion coefficient of DEHP in PVC.

5. CONCLUSIONS

The high dose rate present in electron beam accelerators was not a limiting factor in the grafting process. The mutual grafting is an attractive technique since it has shown good reaction yields, which depend on the parameters chosen besides the polymer/monomer system. The degree of grafting of DMAEMA into PVC films has strong dependence on dose rates and it reduces the migration of DEHP. The styrene grafting occurs always in all studied parameters. The mutual styrene grafting can be performed at industrial EB accelerators under warm and vacuum conditions to achieve better process yields.

Functionalized ion tracked PVDF have potential to be used in polymer electrolyte membrane for fuel cell (PEMFC). The water uptake is always above 50%, due the high surface area done by ion tracking, even in low percent of grafting. The excellent degree of water uptake does not compromise the mechanical properties of polymer films. Enhanced properties of grafted materials concerning better mechanical resistance and decrease of additive migration may be useful to optimize the new materials for packaging industries.

ACKNOWLEDGEMENTS

The staff of this project wishes to thanks the following researchers and technicians. Without their help these results could not be obtained: Dr. Maria Helena de O. Sampa, Carlos Silva, Dr. Celina Duarte, Dr. Magali Monteiro, M.Sc. Djalma B. Dias, Dr. Olga Z. Higa, Wanderlei Andrade and Paulo Pirolla.

REFERENCES

[1] TAZI, B., SAVADOGO, O., Effect of various heteropolyacids (HPAs) on the characteristics of Nafion® HPAS membranes and their H_2/O_2 polymer electrolyte fuel cell parameters, Journal of New Materials for Electrochemical Systems, **4** (2001) 187-196.

[2] ADJEMIAN, K.T., SRINIVASAN, S., BENZIGER, J., BOCARSLY, A.B., Investigation of PEMFC operation above 100 degrees Celsius employing perfluorosulfonic acid silicon oxide composite membranes*,* Journal of Power Sources, **109** (2002) 356-364.

[3] LI, J.Y., ICHIZURI, S., ASANO, S., et al., Preparation of ion exchange membranes by preirradiation induced grafting of styrene/divinylbenzene into crosslinked PTFE films and successive sulfonation, Journal of Applied Polymer Science E, **101** (2006) 3587-3599.

[4] BÜCHI, F.N., GUPTA, B., HAAS, O., SCHERER, G.G., Study of radiation-grafted FEP-g FEP-g-polystyrene membranes as polymer electrolytes in fuel cells, Electrochimica Acta, **40** (1995) 345-353.

[5] TABATA, Y., IKEDA, S., OSHIMA, A., Radiation-induced crosslinking and grafting of polytetrafluoroethylene, Nuclear Instruments and Methods in Physics Research B, **185** (2001) 169-174.

[6] DARGAVILLE, T.R., GEORGE, G.A., HILL, D.J.T., et al., High energy radiation grafting of fluoropolymers, Progress in Polymer Science, **28** (2003) 1355-1376.

[7] SATO, K., IKEDA, S., IIDA, M., OSHIMA, A., TABATA, Y., WASHIO, M., Study on polyelectrolyte membrane of crosslinked PTFE by radiation grafting, Nuclear Instruments and Methods in Physics Research B, **187** (2003) 424-428.

[8] CONSUELO, L.C.G.A.,"Estudo da Enxertia e Heparinização Simultâneas do Poli(Cloreto de Vinila), via Radiação Gama", Doctorate Thesis, IPEN, São Paulo, Brazil (2003).

[9] GOTARDO, M.A., MONTEIRO, M., Migration of diethylhexyl phtalate from PVC bags into intravenous cyclosporine solutions, J. Pharm. Biomed. Anal. **38** (2005) 709-713.

[10] CHAPIRO, A., 1959, Influence de la temperature sur le greffage du styrène sur des films de polytetrafluoroéthylène et de Poly(chlorure de vinyle) par la méthode radiochimique directe, J. Polym. Sci. **34** (127) 481-501.

[11] VON ROSENBERG, D.U., "Methods for the numerical solution of partial differential equations - Modern Analytic and Computational Methods" in Science and Mathematics, Elsevier (1975) New York.

[12] OSHIMA, A., SEGUCHI, T., TABATA, Y., ESR study on free radicals trapped in crosslinked polytetrafluoroethylene (PTFE), Radiat. Phys. Chem. **50** (1997) 601-606.

[13] DARGAVILLE, T.R., HILL, D.J.T., WHITTAKER, A.K., An ESR study of irradiated poly(tetrafluoroethylene-*co*-perfluoropropyl vinyl ether) (PFA), Radiat. Phys. Chem. **62** (2001) 25-31.

[14] DARGAVILLE, T.R., GEORGE, G.A., HILL, D.J.T., High energy radiation grafting of fluoropolymers, Progr. Polym. Sci. **28** (2003) 1355-1376.

[15] SEGUCHI, T., MAKUUCHI, K., SUWA, T., TAMURA, N., ABE, T., TAKEHISA, M.J., Radiation effects on poly(vinylidene fluoride). III. Electron spin ressonance study on irradiated poly(vinylidene fluoride), Chem. Soc. Jpn. Chem. Ind. Chem. **7** (1974) 1309-1315.

[16] LEHRLE, R.S. AND PATTENDEN, C.S., Gamma radiolysis of dilute polyisobutylene solutions: influence of solvent, Polym. Degrad. Stab. **63** (1999) 139-146.

[17] RÄTZSCH, M., ARNOLD, M., BORSIG, E., BUCKA, H., REICHELT, N., Radical reactions on polypropylene in the solid state, Progr. Polym. Sci. **27** (2002) 1195-1282.

DEVELOPMENT OF NOVEL ABSORBENTS AND MEMBRANES BY RADIATION-INDUCED GRAFTING FOR SELECTIVE PURPOSES

E.A. HEGAZY, H. ABDEL-REHIM, D. HEGAZY, A.A. ALI, H. KAMAL, A. SAYED

National Center for Radiation Research and Technology, Atomic Energy Egypt
P.O.Box 29, Nasr City, Cairo
EGYPT

Abstract

The direct radiation grafting technique was used to graft glycidyl methacrylate (GMA) monomer containing epoxy ring, onto polypropylene fibres. The ring opening of the epoxy ring in GMA by different amino groups was studied to introduce various chelating agents. Some properties of grafted fibres were studied and the possibility of its practical use for water treatment from iron and manganese metals was investigated. The radiation initiated grafting of acrylic acid (AAc) or acrylamide (AAm) monomers onto poly(vinyl alcohol) (PVA), a 2-acrylamide-2-methyl propane sulfonic acid (AMPS) polymer was studied. Cationic/anionic membranes were also prepared by radiation-induced grafting of styrene/methacrylic acid (Sty/MAA) binary monomers onto LDPE films. To impart reactive cationic/anionic characters in the grafted membranes, sulfonation and alkaline treatments for styrene and carboxylic acid groups, respectively, were carried out. The possibility of their applications in the selective removal of some heavy metals was studied. The prepared grafted materials had a great ability to recover the metal ions such as: Ni^{2+}, Co^{2+}, Cu^{2+}, Cd^{2+}, Mg^{2+}, Zn^{2+}, Mn^{2+} and Cr^{3+} from their solutions. It was found that AMPS content in the grafted copolymers is the main parameter for the selectivity of the copolymer towards metal ions. The higher the AMPS content the higher the selectivity towards Co and Ni ions. In case of LDPE-g-P(STY/MAA), the sulfonation and alkaline treatments are the most effective methods to influence metal absorption and swelling behaviour of the prepared membranes. Graft composition, dose and pH have also a great influence on the membrane characteristics and applicability in wastewater treatments from heavy and toxic metals. Results revealed that the prepared grafted materials with different functionalized groups are promising as ion selective membranes and could be used for wastewater treatment.

1. OBJECTIVE OF THE RESEARCH

The objective of this work is to use gamma rays and electron beam irradiation for grafting of various monomers containing reactive functional groups such as carboxylic acid, amide, nitrile, oxime groups onto different kinds of natural and synthetic polymers. New grafting techniques are used to reduce the irradiation dose and overall cost of manufacturing of adsorbents. Some additives like acids and organic salts were used to obtain high grafting chains by chemical modification to enhance the functionality of the supported materials. The new adsorbents should be showing selectivity toward different kind of heavy metal ions. Material supported-reactive agents are common to many separation technologies, such as water softening, removal of heavy metal ions from industrial waste water, recovery of precious metals, separation, selection and purification of metal elements.

2. INTRODUCTION

Material supported-reactive agents are common to many separation technologies, such as water softening, removal of heavy metal ions from industrial wastewater, recovery of precious metals, separation, and purification of metal elements. There are a number of techniques for the removal of metal ions from water but solvent extraction and ion exchange methods are the most widely used ones. Solvent extraction has the advantage of fast kinetics, high capacity and selectivity for the target metal ions [1, 2] but it is normally not considered for dilute solution of the metal ions due to the large requirement of the extractants. One of the important materials which could be used for such treatments is the functionalized polymers are capable of metal chelation and/or complexation with their reactive functional groups such as carboxylic acid, amide, nitrile, oxime groups.

Functional groups can be introduced in the polymeric materials by radiation grafting technique. Researches on fibrous reactive agents have shown many advantages over their resin counterparts. The high specific surface areas of fibrous supports improve the accessibilities of functional groups resulting in higher reaction rate than the resin type agents.

Metal chelating radiation grafting supported hydrogels as ion exchangers can be used to remove the target metal ions at lower concentrations though the kinetics are slower than that of solvent extraction.

They are synthesized either by graft polymerization of functionalized monomers or by incorporation of chelating groups into the polymer matrix by stepwise functionalization of existing polymers. Although the number of known chelating ligands is large [3-6], the donor atoms in most cases are N, O, P and S. Grafted hydrogels containing amide, amine, carboxylic acid and ammonium groups, can bind metal ions and be a good polychelatogens for water purification applications [7]. The selective removal and recovery of metal ions has a potential in vast range of applications in conservation of the environment and use of resources. In respect of this point, polymeric materials have been extensively studied and many reviews are available in the field [8, 9].

In this work, PVA containing AMPS-co-AAc of AMPS-co-AAm units were prepared using gamma irradiation. The selectivity and affinity of the prepared terpolymer towards Co, Ni, Cu and Cr from aqueous solutions were investigated. Polypropylene (PP) was used as a substrate for various reasons; it is a highly useful thermoplastic, broadly used as a molding in many extruded forms and it can be grafted with acrylate monomers. Therefore, the direct radiation grafting technique was used to graft glycidyl methacrylate (GMA) monomer containing epoxy ring, onto PP. Also, in this work, the cationic/anionic membranes were also prepared by radiation-induced grafting of Styrene/methacrylic acid (Sty/MAA) binary monomers onto LDPE films followed by sulfonation and alkaline treatments. Properties of the radiation grafted membranes were studied. The possibility of their practical applications for different separation and wastewater treatment from heavy and toxic metals were studied and evaluated.

3. MATERIALS AND METHODS

3.1. Preparation of chelating fibres

The grafted fibre PP-g-GMA containing an epoxy group, 1,4-dioxane, which acted as medium, and an amine compound such as diamino ethane, hydrazine hydrate, thiosemi carbazide, ethanol amine and ammonia were put into a 100 mL Wolff bottle equipped with an electromagnetic stirrer, a reflux condenser, and a heating bath. After the reaction, the obtained chelating fibres were washed with deionized water.

3.2. Batch procedure

The adsorption amount and distribution coefficients, K_d of metal ions between the chosen reactive polymer and dissolved metal ions were investigated out at constant temperature by a batch procedure. 500 mL solution of metal ions and known weight of the reactive polymer were stirred for 24 h. The reactive polymer was previously pre-cleaned with 2.0 M HNO_3. The concentration of ion remaining in the solution was detected by atomic absorption instruments (AAs) and confirmed by inductively coupled plasma-mass spectrometer (ICP-MS). The adsorbed metal was calculated as follows:

$$A= [V (C_1 - C_2)]/W$$

where A is adsorbed metal (mg/g), W is the weight of the chelating fibre (g), V is the volume of solution (L); and C_1 and C_2 are the concentrations of metal ions before and after adsorption, respectively (mg/L).

The distribution coefficient (K_d), can be calculated using the following equitation:

$$\frac{Kd}{K_d} = \frac{\text{wt. of metal ion on the polymer (mg)/wt. of the reactive groups (g)}}{\text{wt. of metal ion in solution (mg)/volume of solution (cm}^3\text{)}}$$

3.3. Metal determination by AAs and ICP-MS

Trace metal concentration in the remaining solution were determined according to the operating instructions of the manufacturer (Unicam model Solaar 929 atomic absorption) and (TJA solutions; plasma optical emission-mass spectrophotometer POEMS3). Synthetic metal standards having 2.0 mol dm^{-3} HNO_3 as the experimental samples were used for calibration.

3.4. Selectivity coefficient

$FeCl_3$ and $MnCl_2$ solutions (about 1 mmol dm^{-3}) are prepared in a citrate buffer (10 mmol dm^{-3}) at pH 5.6 to prevent precipitation of the hydroxides of the metal ions. A mixture of 10 mL of a Fe^{3+} solution and 10 mL of a Mn^{2+} solution was added to about 40 mg of fibre. The mixture was rotated at 25°C for 24 h. The contents of Fe^{3+} and Mn^{2+} remaining in the solution were determined by AAs. For determining the amounts of Fe^{3+} and Mn^{2+} chelated on the fibre, the fibre was washed, added to 10 mL of 1 mmol dm^{-3} HNO_3, and rotated for 24h, at 25°C to desorb the chelated metal ions. The amounts of desorbed Fe^{3+} and Mn^{2+} were measured by (AAs). The selectivity coefficients Ks, were calculated for the selective chelation reaction:

$$\text{F—Mn} + Fe^{3+} \leftrightarrow \text{F—Fe} + Mn^{2+}$$

$$Ks = ([Fe^{3+}]^2/[Mn^{2+}]^3)f \times ([Mn^{2+}]^3/[Fe^{3+}]^2)s$$

where F represents the fibre, s, the solution.

4. RESULTS AND DISCUSSION

The direct radiation grafting technique was used to graft glycidyl methacrylate (GMA) monomer containing epoxy ring, onto polypropylene (PP). The effect of preparation conditions on the grafting yield and the optimum conditions at which the grafting process proceeds homogeneously were determined.

4.1. Effect of solvent

Solvents are basically used in radiation grafting processes to enhance the degree of accessibility of monomer to grafting sites within the polymer. The influence of different kinds of solvents on the grafting yield is investigated and shown in Fig.1. It can be seen that the highest degree of grafting was obtained with 1,4-dioxane as solvent. The results could be attributed to ability of 1,4-dioxane to swell the base polymer and enhance the efficiency and uniformity of the grafting.

4.2. Reactivity of the epoxy group

The pendant epoxy group in GMA offers a facile way of introducing a wide variety of novel functionalities into preformed supports. The epoxy group is characterized by a high reactivity and ability to enter into a vast number of reactions. This reactivity is caused by the presence of the highly strained three-membered ring with deformed valency angles, and shortened bond between the carbon atoms. The epoxide reacts with nucleophiles such as different amines; hydrazine hydrate, ethanol amine, diethanol amine, thiosemi carbazide, and ammonia by a ring-opening reaction. The possible use of such prepared fibre in some practical applications such as water treatment from iron and manganese metals was investigated.

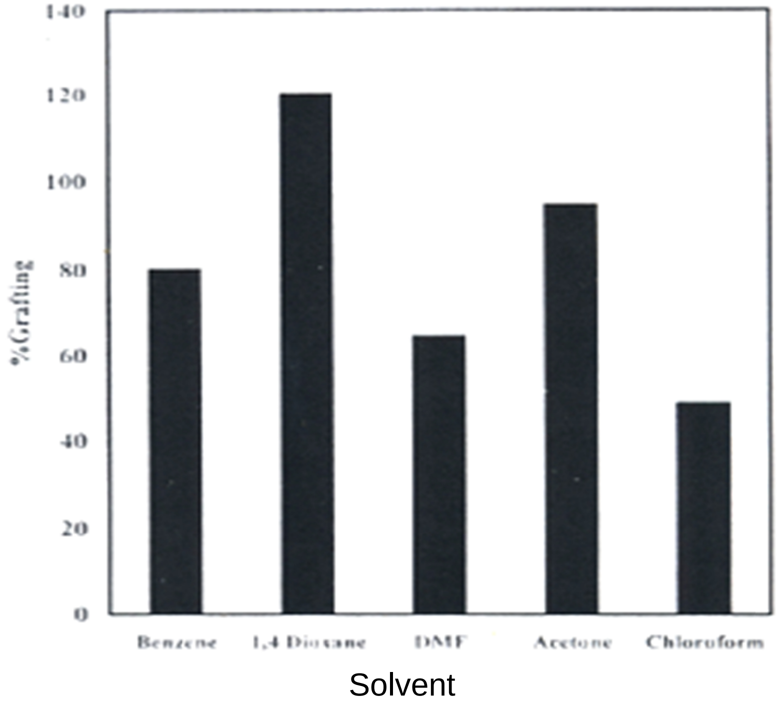

FIG. 1. Effect of different solvents on the GMA grafting yield onto PP fibres.

Table 1 shows a comparative study for the variation of iron and manganese uptake according to the type of reactive groups in the grafted polymer and distribution coefficient (K_d) for PP-g-GMA having 120% degree of grafting treated with different types of amino groups, individual concentration of metal feed solution, 500 ppm, time of treatment, 1 hour. It can be seen that the iron uptake is higher than that of manganese which follows the order of valency of the investigated metal ions.

The maximum metal uptake of the two metals by these reactive polymers is investigated; it can be seen from Table 1 that all the investigated reactive fibres have high chelation ability towards the individual metal ions existing in the feed solution.

TABLE 1. MAXIMUM METAL UPTAKE (mg/g) AND DISTRIBUTION COEFFICIENT (K_d) FOR PP-g-GMA HAVING 120% DEGREE OF GRAFTING

	Fe^{3+}		Mn^{2+}	
Amino group	Metal uptake (mg/g)	K_d	Metal uptake (mg/g)	K_d
Hydrazine hydrate	99.6	332	80	266
Ammonia	55.5	185	27.1	90
Diethanol amine	43.6	145	34.6	115
Thiosemi carbazide	26.4	88	21.8	72
Ethanol amine	24.9	82	40	133

4.3. Selectivity of the reactive polymer towards iron and manganese

The knowledge of the selectivity of different reactive polymers towards iron and manganese allows choosing the most suitable polymer for a given metal ion in order to have a high recovery of such metal. The selectivity of different reactive polymers is investigated using mixture of iron and manganese in the same feed solution. A batch system containing an equimolar feed solution from iron and manganese is prepared. The selectivity ratio uptake of PP-g-GMA grafted fibre having 120% degree of grafting, treated with different amino groups, towards iron and manganese mixture in the same feed solution, and distribution coefficients are listed in Table 2.

Since the different reactive polymers have a high affinity towards Fe^{3+} it might be possible that the polymer will show some selectivity between Fe^{3+} and Mn^{2+}. The selectivity coefficient of fibre for Fe^{3+} and Mn^{2+} metal ions was investigated and the results are given in Table 3. It can be seen that the affinity of the polymer fibre was much higher for Fe^{3+} than Mn^{2+} metal ions. The selectivity coefficient observed for Fe^{3+} was 1.3×10^2.

TABLE 2. SELECTIVITY RATIO UPTAKE AND DISTRIBUTION COEFFICIENT FOR IRON AND MANGANESE MIXTURE

	$Fe^{3+} + Mn^{2+}$				
	Metal uptake mg/g	K_d	Metal uptake mg/g	K_d	Selectivity ratio (M1/M2)
Hydrazine hydrate	74	247	35	117	2.11
Ammonia	27	90	26	87	1.03
Diethanol amine	34	113	24	80	1.4
Thiosemicarbazide	22	73	10	33	2.2
Ethanol amine	26	87	20	67	1.3

TABLE 3. SELECTIVITY COEFFICIENTS OF PP-G-GMA FIBER HAVING 120% DEGREE OF GRAFTING, TREATED WITH HYDRAZINE HYDRATE FOR Fe^{3+} TO Mn^{2+}

Fe^{3+} (mmol)		Mn^{2+} (mmol)		
On fibre	In solution	On fibre	In solution	*Ks*
0.82	0.515	0.24	1.57	1.3×10^2

From the results of individual metal uptake and also, the selectivity of two metals, it can be seen that the reactive polymer of PP-g-GMA having 120% degree of grafting and treated with hydrazine hydrate shows the maximum metal ion uptake if compared with other reactive polymers treated with other amino groups. Also, the results revealed that all the treated reactive polymers had some selectivity towards iron rather than manganese.

4.4. Efficiency of the reactive polymer

To explore the applicability of the sorbent reactive polymer, it was important to obtain knowledge on its sorption capacity towards iron and manganese ions. These are carried out by equilibrating a fixed amount of the sorbent with a series of metal ion solutions of gradually increasing concentration. A maximum amount of metal ion can be removed from the solution when the chelating sites of the sorbent are saturated.

Table 4 presents the effect of initial feed concentration of Fe^{3+} and Mn^{2+} on its uptake by PP-g-GMA having degree of grafting of 120%, treated with hydrazine hydrate. It can be seen that increasing the concentration of metal ions results in increasing the amount of iron and manganese uptake (ppm) to reach a certain limiting value. Thereafter, it levels off at higher feed concentration.

TABLE 4. EFFECT OF INITIAL CONCENTRATION OF Fe^{3+} AND Mn^{2+} ON ITS UPTAKE BY PP-g-GMA

Initial concentration (ppm)	Max.Fe^{3+} uptake (ppm)	uptake (%)	Max.Mn^{2+} uptake (ppm)	uptake (%)
25	24.43	97	23.52	94
50	48.12	96	46.65	93
100	94.84	94	92.2	92
500	296.64	60	212.47	42
1000	298.54	29	214.2	21
1500	299.4	19	215.4	14

4.5. Effect of salt anion type

The effect of salt anion type on the uptake of metals under investigation was determined. Table 5 shows the maximum uptake of iron and manganese by PP-g-GMA having 120% degree of grafting and treated with hydrazine hydrate, using different anion type of iron and manganese.

TABLE 5. EFFECT OF METAL SALT ANION TYPE ON THE UPTAKE OF THE OTHER METALS (mg/g).

	$Fe_2(SO4)_3$		$Fe(NO3)_3$		$FeCl_3$	
	Fe	Mn	Fe	Mn	Fe	Mn
$MnSO_4$	74	35	75	30	73	29
$MnCl_2$	73	33	69	36	74	30
$Mn(NO_3)_2$	69	36	67	33	66	34

From Table 5 it can be seen that the maximum uptake of iron and manganese and selectivity ratio are almost the same at different anion type. So it can be concluded that, maximum uptake and selectivity of the prepared reactive polymers is not affected by changing the salt anion.

4.6. Synthesis of metal ions selected grafted polymers from poly (vinyl alcohol), 2-acrylamido-2-methyl propane sulfonic acid and acrylic acid or acrylamide.

The graft-polymers were prepared from poly(vinyl alcohol) (PVA), 2-acrylamido-2-methyl propane sulfonic acid (AMPS), acrylic acid (AAc) or acrylamide (AAm) monomers irradiated using gamma rays as initiator. Characteristics and some properties of the prepared grafted polymers were investigated. Also, the possibility of their applications in the selective removal of some heavy metals was studied. The prepared grafted polymer had a great ability to recover the metal ions such as: Ni^{+2}, Co^{+2}, Cu^{+2} and Cr^{+3} from their solutions.

4.7. Effect of AAc and AAm terpolymer content on the swelling % in water

The effect of feed solution composition i.e. AAc and AAm copolymer content on the swelling of the prepared grafted PVA/AMPS-AAc or PVA/AMPS-AAm terpolymer hydrogels in water was studied. An irradiation dose of 20 kGy was applied and water as used a diluent, monomer/copolymer concentration was 20% and the results are presented in Fig. 2. It can be seen that the swelling behaviour of the copolymer is greatly influenced by grafted polymer composition and the type of crosslinked polymer used for the polymer formation (AAc or AAm). For PVA/AMPS-AAc system, the swelling degree decreases as the AAc content in the graft-polymer increases. Whereas, for PVA/AMPS-AAm system, the swelling degree increases as the AAm content in the graft polymer hydrogel increases to reach a maximum at grafted-polymer containing 80% AAm. Thereafter, the increase in AAm content leads to decrease in grafted-polymer water absorbency. From Figure 2, it can be observed also that the swelling of PVA/AMPS-AAm is much higher than that for PVA/AMPS-AAc. These results may be due to the association of the carboxylic groups and the intermolecular hydrogen bonding between the COOH and OH of AAc and PVA. As the AAc content increases, the number of the associated groups increases and consequently, the intermolecular hydrogen bonding also increases

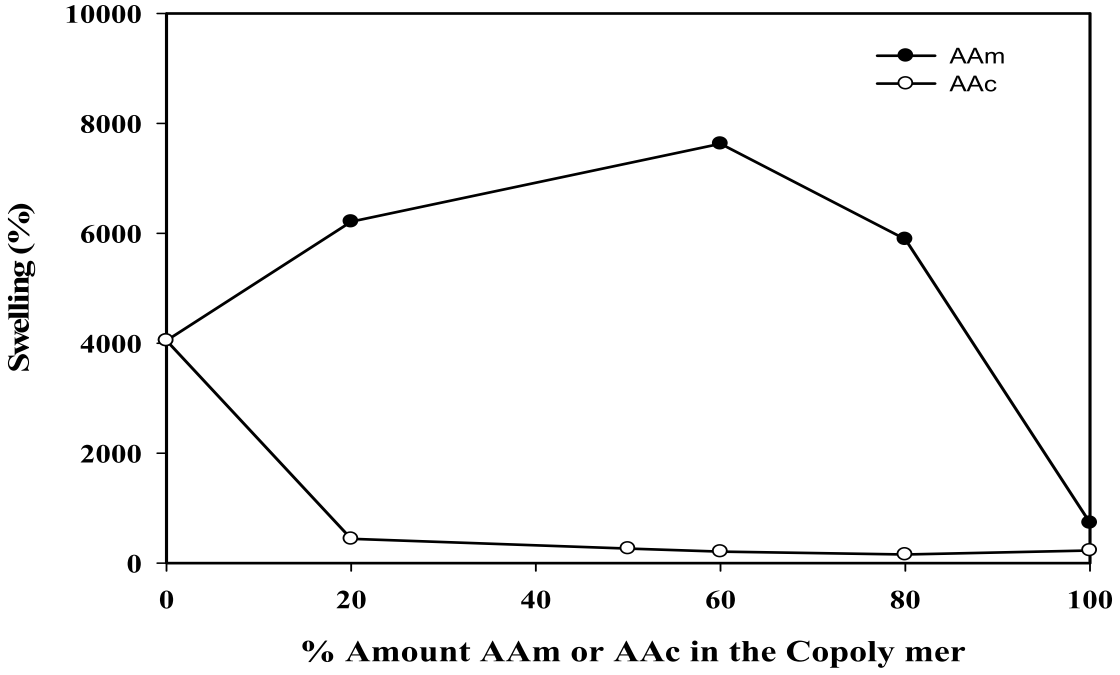

FIG. 2. Effect of AMPS/AAm or AMPS/AAc composition in the swelling behaviour of PVA-AMPS/AAm graft copolymer.

4.8. Possible applications of the prepared graft copolymer

Studies have been made to investigate the ability of the prepared grafted materials in the removal of some toxic metals from their wastes such as Co, Ni, Cu and Cr ions. PVA/AMPS-AAc or PVA/AMPS-AAm ter-polymers of different compositions were prepared and the affinity of such terpolymers towards Co, and Cu individually was investigated and shown in Fig 3 and Fig. 4. In general, it is clear that, the affinity of PVA/AMPS-AAc or PVA/AMPS-AAm grafted polymers of different compositions towards the metals under investigation decreases with increasing the AAm or AAc acid content in the prepared grafted terpolymers. The affinity decreases due to the increase in crosslinking density as a result of increase in AAc or AAm content in the grafted polymers. Such increase in crosslinking density restricts the diffusion of metal ions into the bulk of copolymer.

It is clear that, for Co removal by PVA/AMPS-AAc graft copolymer, the uptake is higher than that of PVA/AMPS-AAm grafted polymer at a given composition. However, the affinity of PVA/AMPS-AAm grafted polymer towards Cu ions is higher than that of AAc grafted polymer. This opposite behaviour may be due to functional groups affinity towards metal; AAc has higher affinity towards Co and form strong complex with them.

The metal uptake by PVA-AMPS/AAc or PVA-AMPS/AAm from two different metal ions was investigated by different graft copolymer hydrogels having various compositions. The selectivity is determined for each copolymer and metal ions.

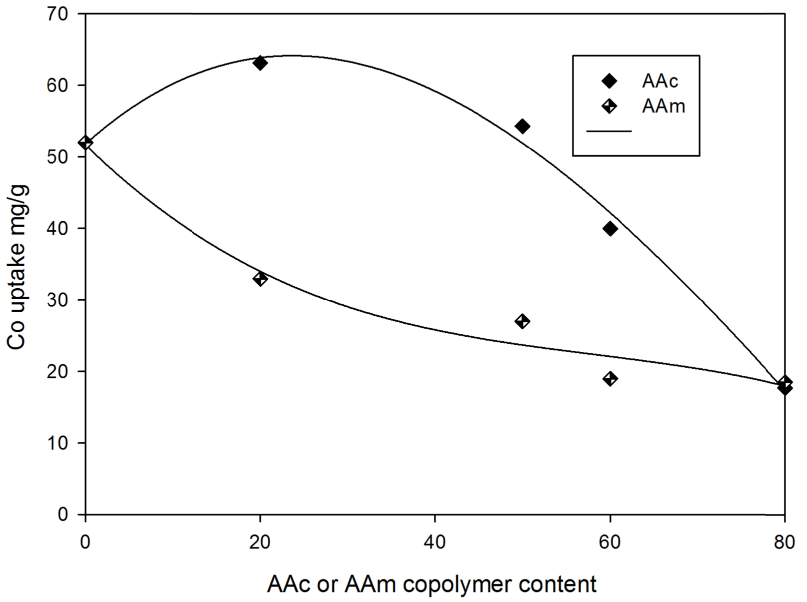

FIG. 3. The affinity of PVA/AMPS-AAc or PVA/AMPS-AAm grafted polymers (30 kGy) of different compositions towards Co.

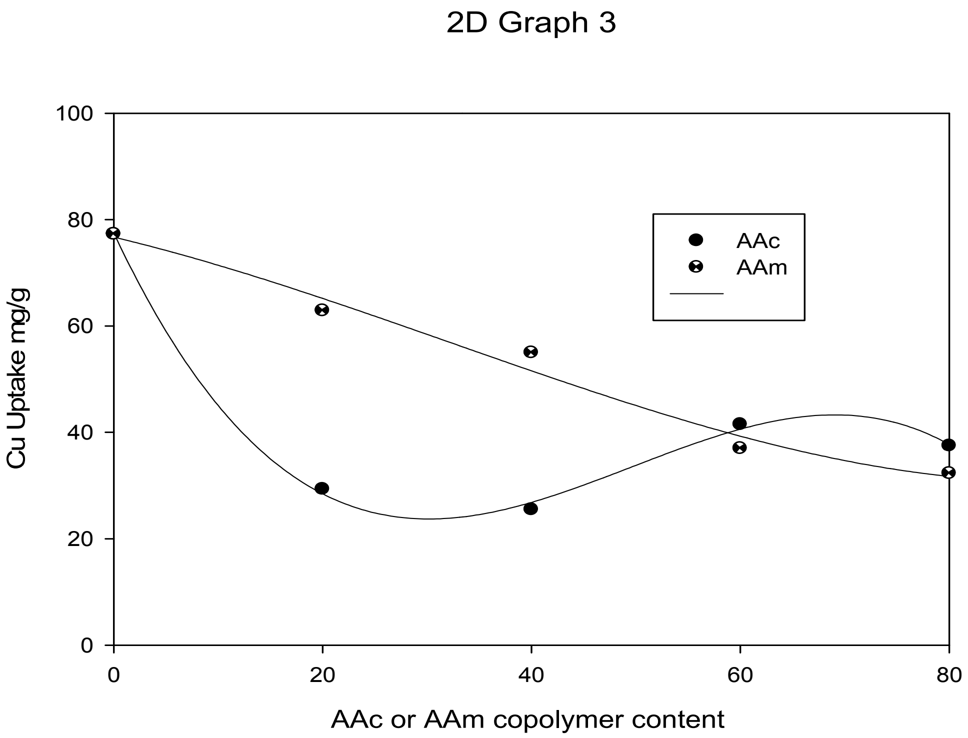

FIG 4. The affinity of PVA/AMPS-AAc or PVA/AMPS-AAm grafted polymers (30 kGy) of different compositions towards Cu.

4.9. Selectivity of the copolymers towards different metal ions

4.9.1. Selectivity of PVA-AMPS/AAc of different AMPS contents towards different metals in binary system

Metal uptake by PVA-AMPS/AAc of composition (10:8:2) is shown in Fig. 5. The selectivity of the copolymer towards Co is higher than that of other metals such as Cr, Ni, and Cu. The results show that AMPS has a great ability to adsorb Co rather than other metals under investigation. The selectivity of PVA-AMPS/AAc of composition (10:8:2) towards Co, Cu, and Cr in binary system was investigated and shown in Fig. 5. The selectivity of the copolymer towards Ni is higher than other metals such as Cu, and Cr. The results show that the AMPS have a great ability to adsorb Ni rather than other two metals Cr, or Cu.

The selectivity of PVA-AMPS/AAc of composition (10:8:2) towards Cu, and Cr in binary system is also investigated and shown in Fig. 5. The figure shows that the selectivity of the copolymer towards Cu is higher than Cr.

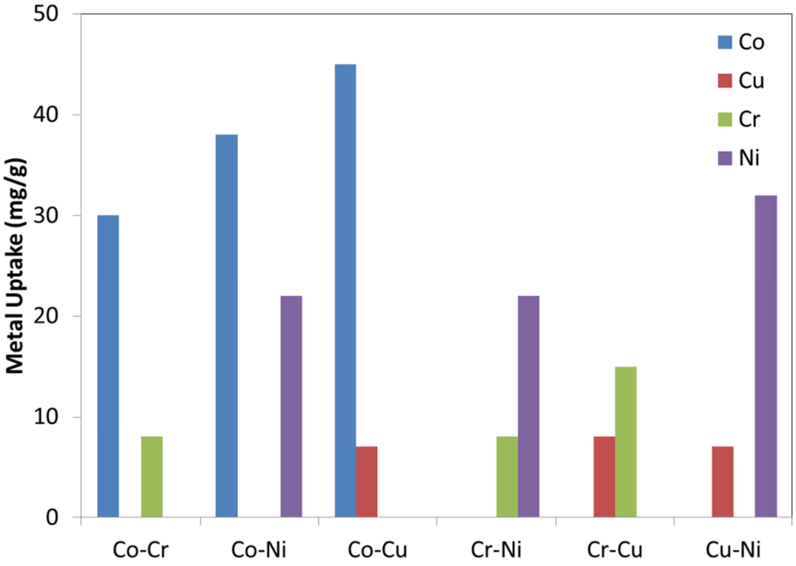

FIG. 5. Selectivity of PVA-AMPS/AAc of (10:2:8) composition towards Co in the presence of Ni, Cu, and Cr in binary system.

4.9.2. Radiation-induced molecular imprinted graft polymers based PVA for metal recognition and selective separation

The synthesis of highly specific molecular imprinted polymers (MIPS) has been the goal of many research groups in the past decade. Molecular imprinting is becoming recognized as a technique for ready preparation of polymeric materials containing recognition sites of predetermined specificity.

Metal ion-imprinted PVA were prepared by ^{60}Co gamma rays technique. Improvement of the selectivity and the affinity of PVA polymer towards some heavy metal ions such as Co and Ni were investigated. For preparing imprinted polymers PVA, and its binary system with AAc, AAm or AMPS, were used as a matrix in presence of metal ions and N,N'-methylene bisacrylamide crosslinker. Preparation conditions of metal ion-imprinted polymers including the nature of the polymer or monomer, metal ion concentration, polymer-monomer composition and degree of crosslinking, which may influence their affinity and selectivity towards metal ions at different pH values, were studied. The affinity of PVA towards Co or Ni was enhanced by mixing it with AAc, AAm and AMPS. Such affinity was improved in the order PVA/AAm < PVA/AAc < PVA/AMPS. Co or Ni-imprinted

PVA/AAc has a great affinity towards Co rather than Ni, when these metal ions exist in a mixture. However, Co or Ni-imprinted PVA/AAm and Co or Ni-imprinted PVA/AMPS have almost the same affinity towards Co or Ni. Effect of different PVA/AAc compositions on the selectivity of a mixture of Co and Ni was investigated. It was found that as AAc content increases the selectivity towards Co, however, the selectivity towards Ni decreases by increasing AAc content.

Figure 6 shows that the affinity of Co-imprinted PVA/AAc towards Co is higher than that of Ni, meanwhile, Ni-imprinted polymer shows high affinity towards both Co and Ni. This is probably due to the strong ionic interaction between PVA and AAc which may increases the stability of the complex formed between the copolymer and imprint molecule.

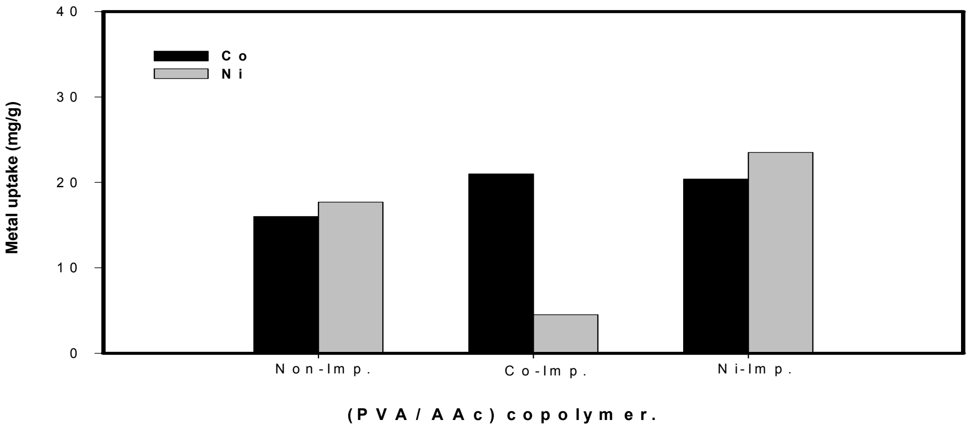

FIG. 6. Metal uptake using metal-imprinted and non-imprinted PVA/AAc of composition 1:1 wt%.

In general, it can be concluded that, the imprinted polymers prepared by radiation grafting in order to compete with heavy metals and extract them from wastewater, especially, that prepared from (PVA/AAc) copolymer and PAMPS, gave higher selectivity towards heavy metal ions such as Co and Ni.

4.9.3. Effect of different PVA/PAAc compositions on the selectivity towards Co and Ni in a mixture

The effect of different compositions of non-imprinted and imprinted polymers on the affinity and selectivity towards Co and Ni was studied and shown in Figures 7–9. It was found that, as the AAc content increases in the copolymer, the selectivity towards Co increases, meanwhile, the selectivity towards Ni decreases. The data shows also that imprinting the polymer with Co or Ni metals or by increasing the AAc content in the copolymer decreases the affinity of polymer towards Ni. The affinity as well as the selectivity of Co-imprinted polymer increase with increasing poly(AAc) content in the copolymer compared with that obtained for non-imprinted or Ni-imprinted polymer. However, the selectivity and affinity for Co and Ni-imprinted polymer towards Co is higher than that for non-imprinted ones. The affinity of Ni towards Ni-imprinted polymers is higher than that of Co-imprinted.

4.10. Separation of Cu^{2+} from solution containing Fe^{3+}

Poly(vinyl alcohol) membrane (PVA) was modified by radiation graft copolymerization of acrylic acid/styrene (AAc/Sty) comonomers and the Cu and Fe ions-transport properties of these membranes were investigated using a diaphragm dialysis cell. In the feed solution containing $CuCl_2$ or a mixture of $CuCl_2$ and $FeCl_3$, the PVA-g-P(AAc/Sty) membranes showed high degrees of perm-selectivity towards Cu^{2+} rather than toward Fe^{3+}. The permeation of Cu^{2+} ions through the membranes was found to increase with the decrease in the grafting yield. The role of carboxylic acid and the hydroxyl groups of the grafted membranes in the transportation process of ions is discussed.

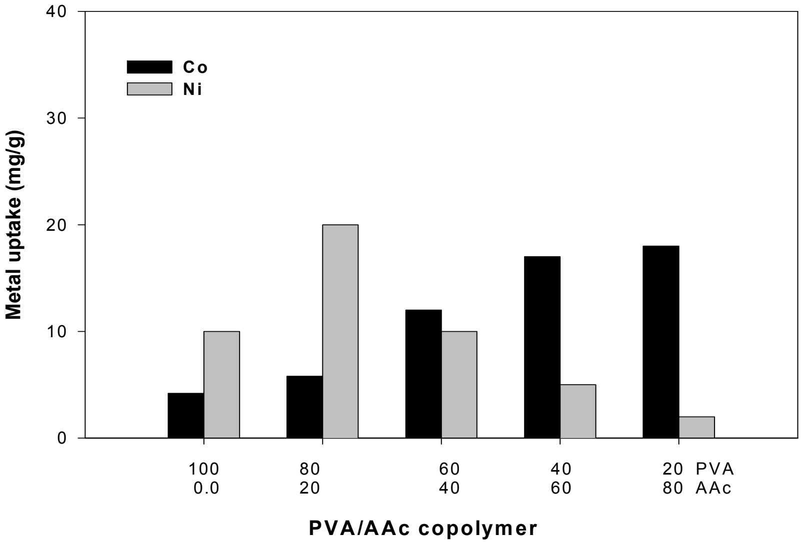

FIG. 7. Metal uptake from their mixture solutions, using non-imprinted PVA/AAc of different compositions.

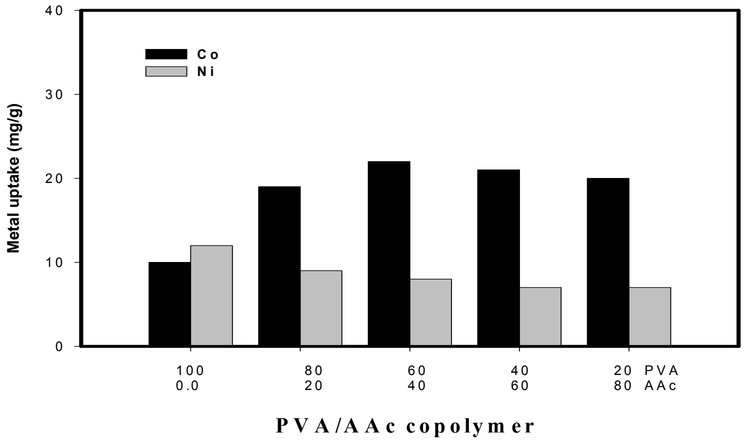

FIG. 8. Metal uptake from their mixture solutions, using Ni- imprinted PVA/AAc of different compositions.

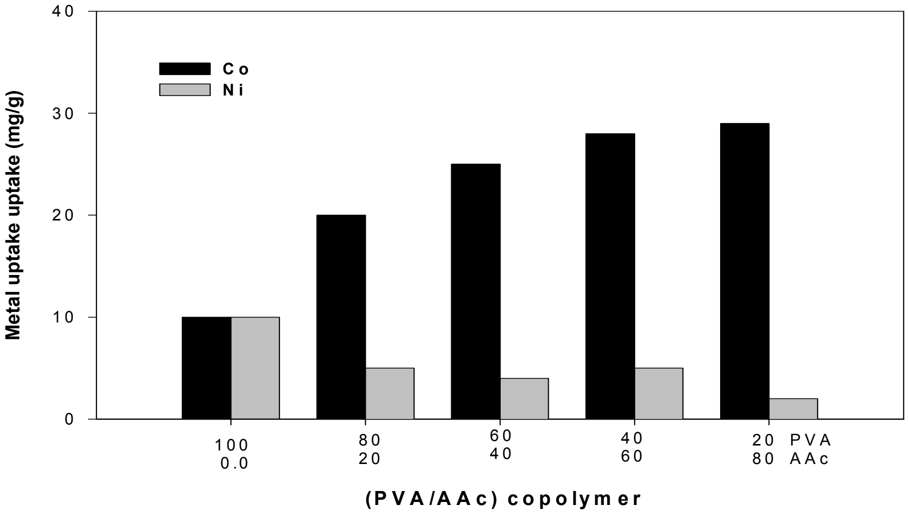

FIG. 9. Metal uptake from their mixture solutions, using Co- imprinted PVA/AAc of different compositions.

To determine the selective transport of Cu and Fe through the grafted membranes of PVA-g-P(AAc/Sty) membranes, the transport properties of PVA-g-P(AAc/Sty) membranes toward Cu, Fe, and a mixture of Cu and Fe ions were studied and the results are shown in Figures 10 and 11. It is obvious that, in the feed solution containing $FeCl_3$ or a mixture of $CuCl_2$ and $FeCl_3$, the PVA-g-P(AAc/Sty) membrane does not allow Fe^{3+} to transport through the received solution. However, Cu^{2+} ions can penetrate through the membrane either if the ions exist alone in the feed solution or in presence of Fe^{3+} ions. Also, it was observed that the presence of Fe^{3+} ions in the feed solution enhances the rate and the amount of Cu^{2+} ions transported through the membranes.

This result can be explained by taking into account that Fe^{3+} is chelated with reactive functional groups of the membrane to form a stable complex. This is may be due to the trivalent property of Fe. As a result, the hydrogen bonding of the carboxylic acid and hydroxyl functional groups broke down and the penetration rate of Cu from the feed solution to the receiver solution increased.

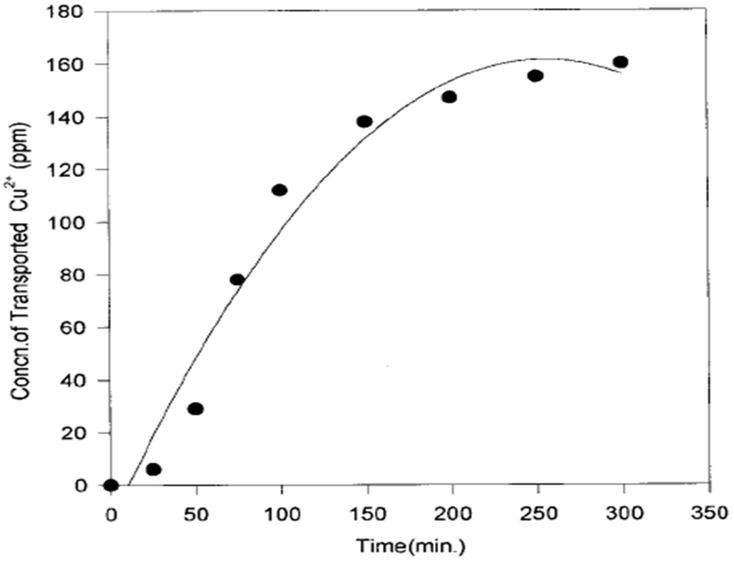

FIG. 10. Transport of Cu^{2+} through PVA-g-P (AAc/Sty) membrane having degree of grafting of 55%; pH of feed solution/received solution, 4.7/6.7.

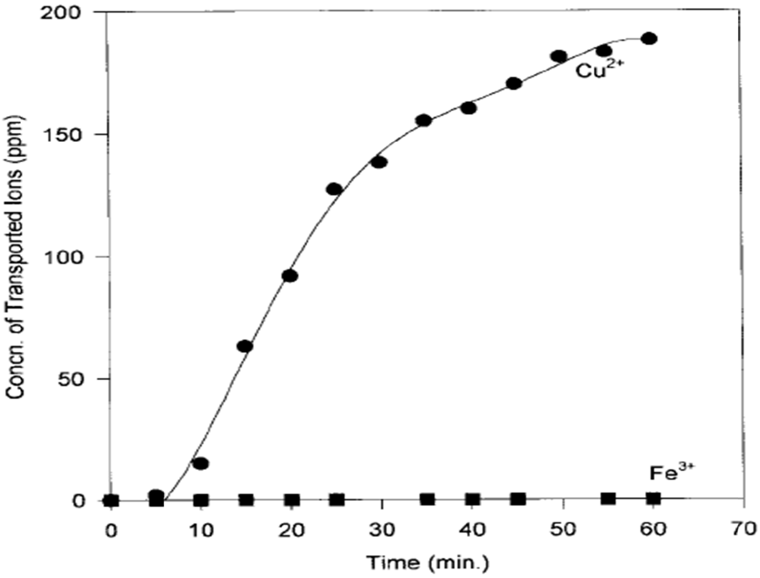

FIG. 11. Transport of Cu^{2+} from solution containing Fe^{3+} through PVA-g-P(AAc/Sty) membrane having a degree of grafting of 52%; pH of the feed solution/ received solution, 4.03/6.7; and Cu/Fe composition, 1/1 (ppm/ppm).

4.11. Radiation induced graft copolymerization of binary monomers (MAA/Sty)

Preparation of graft copolymers by radiation induced graft copolymerization of methacrylic acid (MAA) and styrene (Sty) in a binary monomers mixture onto low density polyethylene films was studied. The graft copolymerization was carried out using the direct method in which the polymer substrate, monomers and solvent were subjected to ^{60}Co gamma rays. The effect of grafting conditions, such as solvent monomer concentration and composition and dose on the grafting process was determined.

4.11.1. Effect of solvent on the grafting of MAA/Sty binary monomers onto LDPE

From Table 6 shows the effect of the mixture MeOH/H2O composition on the degree of grafting of MAA/Sty binary monomers of composition 50:50 (wt%), comonomer concentration 20 (wt%), film thickness 40mm, and irradiation dose 20 kGy. It can be seen that the degree of grafting increases as the water content in the reaction mixture increases. The presence of water resulted in an enhancement of the grafting yield as compared to that obtained when MeOH was used alone.

TABLE 6. EFFECT OF MeOH/H_2O COMPOSITION ON THE DEGREE OF GRAFTING OF MAA/Sty BINARY MONOMERS

MeOH/H_2O Composition (wt %)	Degree of grafting (%)
100:0	170.0
90:10	250.4
80:20	300.3
70:30	351.3

4.11.2. Effect of irradiation time and dose on the grafting of MAA, MAA/Sty onto LDPE

Figure 12 shows that the grafting rate increases with irradiation time up to 8 h, and then slows down at longer times. From Figure 13 it can be seen that the degree of grafting increases with dose to reach the maximum, 80 and 211 wt% graft yield at 15 kGy, respectively, and then decreases as the dose increases. These results indicate that, there is a critical dose at which maximum radical yield occurs leading to an increase in percentage of grafting. The decrease in percentage of grafting beyond optimum dose may be attributed to the fact that at higher doses, chain degradation of poly(methacrylic acid) may occur [10].

4.12. Effect of comonomers composition

Figure 14 shows the effect of comonomers composition on the grafting yield of MAA/Sty onto LDPE. Increasing the Sty content in the binary mixture resulted in increasing the degree of grafting. This is due to the inhibition and protection effects of styrene on the degradability of PMAA graft chains. Also the presence of Sty may inhibit the homopolymerization of MAA by resonance stabilization of its benzene rings.

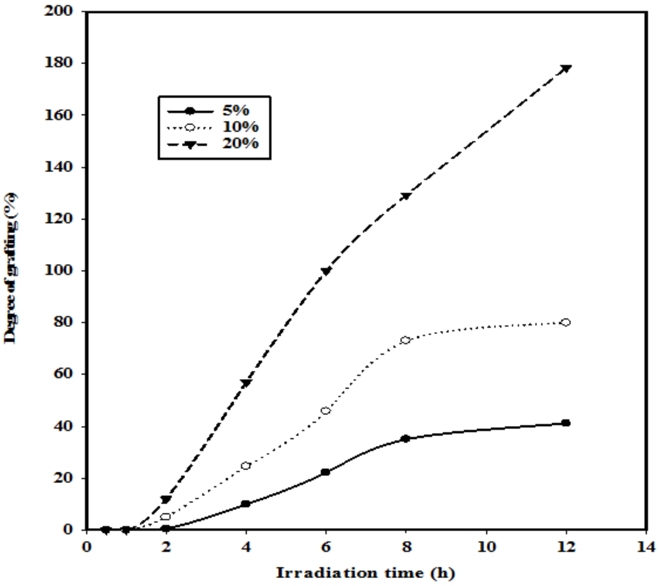

FIG. 12. Degree of grafting vs. irradiation time for various MAA concentrations (wt%).

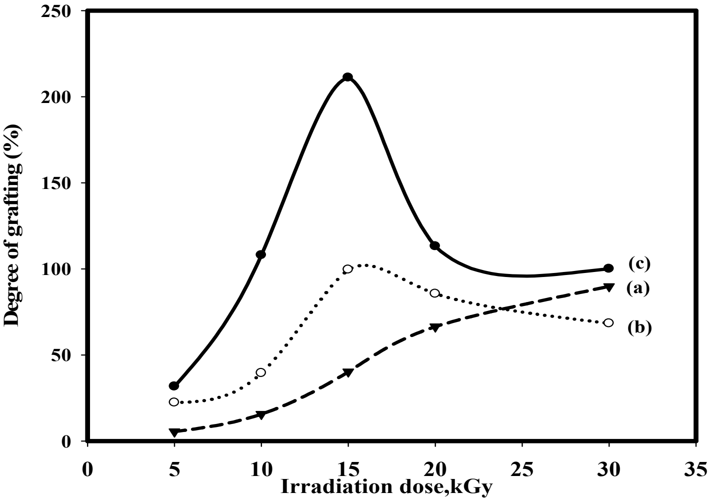

FIG. 13. Effect of dose on the grafting of MAA and Sty onto LDPE films of thickness 40 µm, in MeOH as a diluent. Comonomer concentration 20 wt%, (a) LDPE-g-Sty (b) LDPE-g-MAA and (c) LDPE-g-MAA/Sty (50/50 wt%).

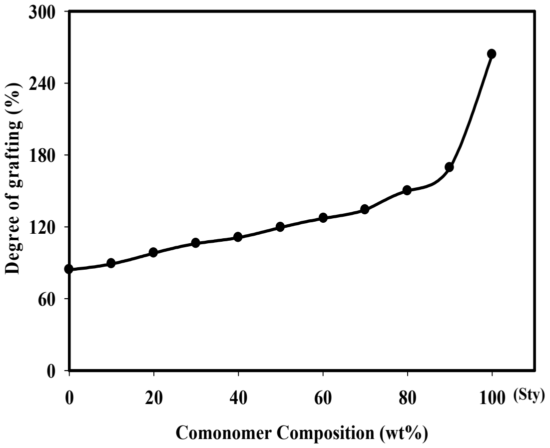

FIG. 14. Effect of Sty/MAA composition on the degree of grafting in presence of methanol as a diluent. LDPE film thickness 70 µm; comonomer concentration 20 (wt%); dose 15 kGy.

4.12.1. Sulfonation and alkaline treatment of the grafted copolymers

Further chemical treatments have been carried out to impart excellent properties for use in the field of ion-exchange membranes in wastewater treatments and separation processes. The physical and chemical properties of the grafted membranes and their applications as ion exchangers were studied. The hydrophilic properties of the chemically treated grafted copolymers significantly increase by sulfonation and alkaline treatments (Figures 15–16). The swelling increases continuously as the degree of grafting increases. Such behaviour may be expected from the increase in the ionic content of the membrane as the graft content increases.

The perm-selectivity of this graft copolymer may be high towards different metal ions. This can be achieved by introducing such easily ionizable groups (anion and cation) by sulfonation and/or alkaline treatment. Introducing of these electrolytic groups into the grafted chains improve the hydrophilic properties.

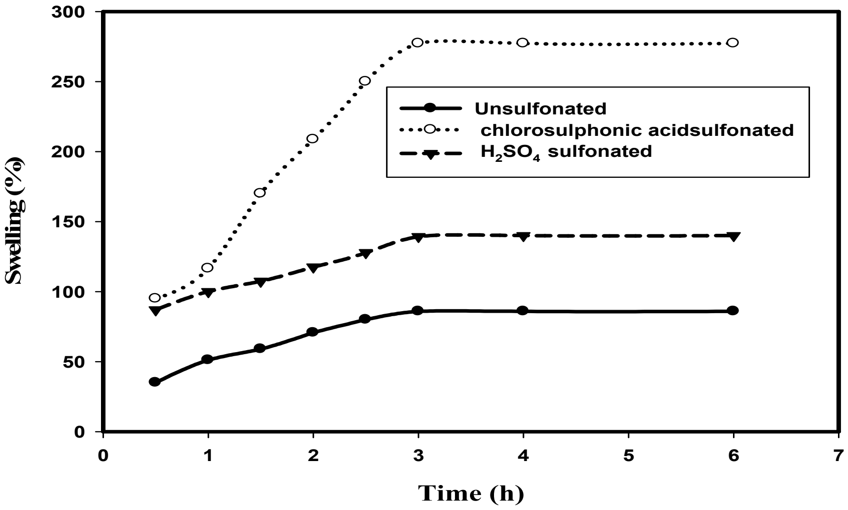

FIG. 15. The equilibrium swelling of non sulfonated and sulfonated LDPE-g-(MAA/Sty) 50/50 wt%, graft percentage 100%.

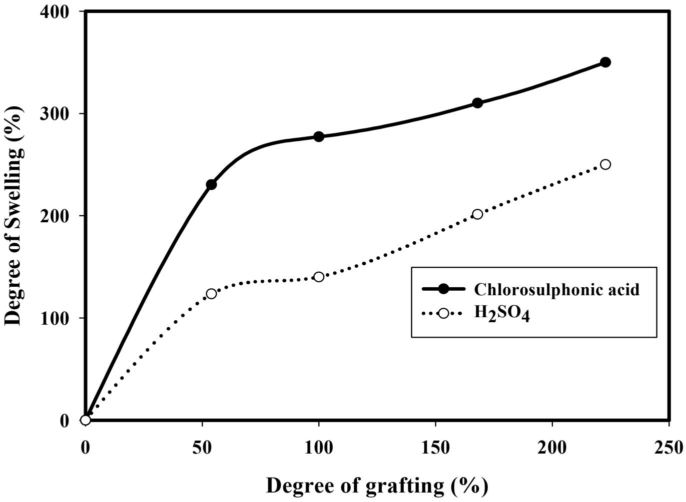

FIG. 16. Effect of degree of grafting on degree of swelling of sulfonated LDPE-g- (MAA/Sty)(50/50), 3h.

4.12.2. Effect of grafting yield on the ion exchange capacity of the grafted membranes

The IEC of membranes of comonomer composition (90/10) MAA/Sty and the results are shown in Fig. 17. It can be seen that, the higher degree of grafting the higher IEC of the membrane which reflect the increase in carboxylic acid groups content with grafting. However, the increase in IEC is not pronounced. The effect of grafting percentage and sulfonation reagent (concentrated sulphuric or chlorosulfonic acid) on the ion exchange capacity was investigated and the results are shown in Fig. 18. It is observed that, the higher the degree of grafting, the higher is the ion exchange capacity of a membrane for both membranes that sulfonated with chlorosulfonic or sulphuric acid. As the degree of grafting increases, the number of ionic sites in a membrane also increases. The IEC is increased significantly by sulfonation and alkaline treatments of the functional groups in the graft copolymer.

It can be seen from Fig. 18 that the sulphuric acid treated membranes have little exchange capacity with K^+ ions than that chlorosulfonic acid sulfonated membranes (the sulfonation time for both H_2SO_4 and chlorosulfonic acid was the same, 1.5 h). The grafting of poly (MAA/Sty) into LDPE films and subsequent sulfonation with H_2SO_4 for 1.5 h results in ion exchange capacities in the range of 1.9–3.4 meq/g of the dry polymer depending on the degree of grafting in the range of 60–220%. However, when the sulfonation was carried out with chlorosulfonic acid, the ion exchange capacity of 4.2 meq/g was achieved; this value is acceptable with respect to common ion exchangers (Amberlite IR 3–5 meq/g).

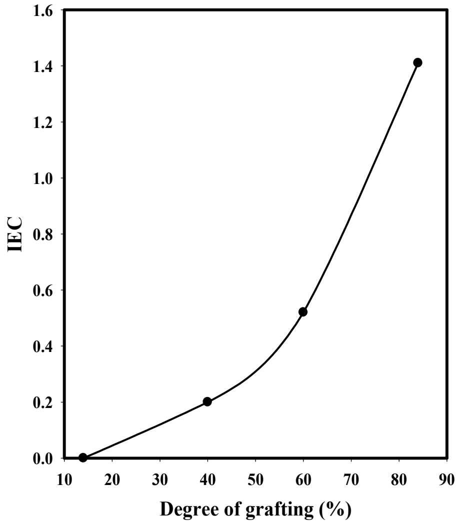

FIG. 17. Effect of degree of grafting of LDPE-g-(MAA/Sty) (90/10wt%) on ion exchange capacity (IEC).

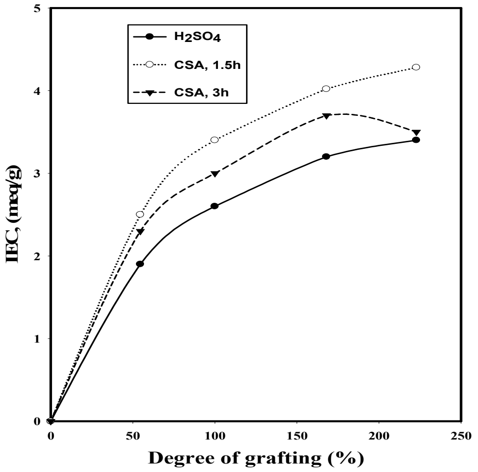

FIG. 18.IEC vs. degree of grafting of sulfonated LDPE-g-MAA/Sty (50/50 wt%).

4.12.3. Competitive adsorption of metal ions

The applicability of the prepared membranes in heavy metal separation was also investigated (Figs 19–21). The adsorptive properties and/or exchange between the ionic membrane and metals in the feed solution seems to be changed by introducing two ionic groups COOH, SO_3H in the grafted membrane.

Adsorption percent of the carboxyl/sulfonic acid grafted membranes for different metal ions under competitive conditions (adsorption from solutions containing mixture of two metal ions) for Ni/Cd, Ni/Mg, Ni/Co, Ni/Zn, Hg/Cu and Zn/Mn was investigated and the data are shown in Fig. 19–21. As can be seen from the figures, the adsorption capacity of metal ions in a single solution is higher than that of the metal ions in a mixture. Thereby, for mixtures of two metal ions, it is a competition process between the different metals and functional groups. It should be noted that, the competitive adsorption percent of the membranes for all metal ions were lower than the non-competitive conditions. The presence of the other metal ions decreases the adsorption capacities as expected.

The non-competitive adsorption percent are 98.8 for Zn where the chelating ligand MAA/Sty (90/10 wt%) and 98.7 for Hg and Mn where the chelating ligand was MAA/Sty (50/50 wt%). The competitive adsorption percent are 82.2 for Zn in a mixture with Mn and 86 for Hg in a mixture with Cu while it reduced to 16.05 for Mn in a mixture with Zn where the chelating ligand was MAA/Sty (90/10 wt%). The results in Fig. 19 revealed that Cd^{2+} can be separated in a mixture of Ni and Cd by the use of MAA grafted membranes of K-type with high efficiency more than 86%. It is also observed that, the selectivity of such membrane towards Cd is higher than Mg when both metals in a mixture with Ni. Moreover, from Fig. 21 for mixture of Zn^{2+} and Ni^{2+}, Zn^{2+} and Mn^{2+} can be separated by sulfonated KOH treated MAA/Sty grafted membranes of composition 50/50 with adsorption efficiency of 76%. From the aforementioned data, it is obvious also that, the membranes have great affinity towards Hg when exists in a mixture with Cu. In some mixtures such as, Zn/Mn the membranes (90/10) MAA/Sty shows great affinity towards Zn and the sorption efficiency of Zn was 82% (Fig. 20). This means that, the grafted membranes is excellent exchanger for both transition and alkali metal ions.

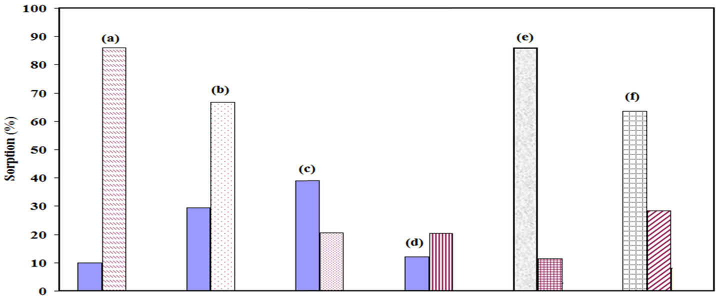

FIG. 19. Competitive adsorption of two different metal ions existing in a mixture of feed solution by LDPE-g-MAA KOH treated, degree of grafting 100% (a) (Ni/Cd), (b) (Ni/Mg), (c) (Ni/Co), (d) (Ni/Zn), (e) (Hg/Cu) & (f) (Zn/Mn).

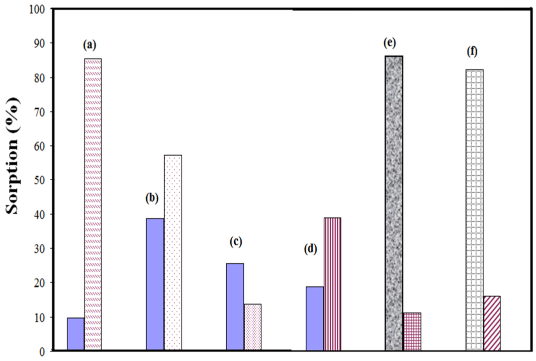

FIG. 20. Competitive adsorption of two different metal ions existing in a mixture of feed solution by LDPE-g-MAA/Sty (90/10 wt%) KOH treated, degree of grafting 100% (a) (Ni/Cd), (b) (Ni/Mg), (c) (Ni/Co), (d) (Ni/Zn), (e) (Hg/Cu) & (f) (Zn/Mn).

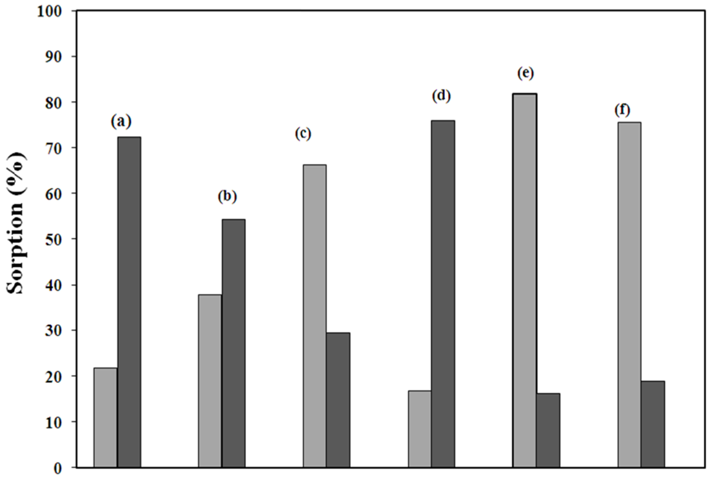

FIG. 21. Competitive adsorption of two different metal ions existing in a mixture of feed solution by sulfonated LDPE-g-MAA/Sty (50/50 wt%) KOH treated degree of grafting 100% (a) (Ni/Cd), (b) (Ni/Mg), (c) (Ni/Co), (d) (Ni/Zn), (e) (Hg/Cu) (f) (Zn/Mn).

5. CONCLUSIONS

PVA and PP fibres were modified by radiation induced graft copolymerization of different monomers and comonomers such as GMA, acrylic acid/styrene (AAc/Sty), 2-acrylamido-2-methyl propane sulfonic acid (AMPS), acrylic acid (AAc), or acrylamide (AAm) monomers. Some properties of the prepared grafted polymers were investigated. Also, the possibility of their applications in the removal of some heavy metals was studied. From the obtained results, it can be seen that the presence of functional groups in the prepared graft copolymers, improve their selectivity towards different metal ions. The affinity to metal ions depends mainly on the incorporated groups in the grafted membranes and the composition of the copolymer must control the sorption of the metal ions. The diffusion of these metals is mainly dependent on the type of metal, electronic configuration and ionic radii of these metal ions. The ion with the lowest hydrated ionic radius i.e. highest electro-positivity showed the highest metal uptake. The amount of metal ions adsorbed by such grafted membranes is influenced not only by the physical properties and molecular size of the metals investigated but also on the functional groups of the grafted side chains and their compositions.

REFERENCES

[1] MASSOUMI, A., HEDRICK, C.E., Solvent extraction of metal ions and surface-active agents from saturated sodium chloride brine, J. Chem. Eng. Data **14** (1969) 52–54.

[2] WATARAI, H., FUJIWARA, M., TSUKAHARA, S., SUZUKI, N., Construction of an internet compatible database for solvent extraction of metal ions, Solv. Extr. Res. Dev., Jpn. **7** (2000) 197-205.

[3] SENNA, M.M., SIYAM, T., MAHDY, S., Physico-chemical studies on Cu(II) complexes of acrylate chelating polymers, J. Macrom. Sci. Pure Appl. Chem. A **41** (2004) 1187-1203.

[4] LI, W., ZHAO, H., TEASDALE, R.R., JOHN, R., ZHANG, S., Synthesis and characterisation of a polyacrylamide–polyacrylic acid copolymer hydrogel for environmental analysis of Cu and Cd, React. Funct. Polym. **52** (2002) 31-41.

[5] DURMAZ, S., OKAY, O., Acrylamide/2-acrylamido-2-methylpropane sulfonic acid sodium salt-based hydrogels: synthesis and characterization, Polymer **41** (2000) 3693-3704.

[6] OKAY, O., SARIISIK, S.B., ZOR, S.D., Swelling behavior of anionic acrylamide-based hydrogels in aqueous salt solutions: Comparison of experiment with theory, J. Appl. Polym. Sci. **70** (1998) 567-575.

[7] PHILIPPOVA, O.E., RULKENS, R., KOUTUNENKO, B., ABRAMCHUK, S.S., KHOKLOVI, A.R., WEGNER, G., Polyacrylamide hydrogels with trapped polyelectrolyte rods, Macromolecules **31** (1998) 1168- 1179.

[8] KAYAMAN, N., GÜREL HAMURCU, E.E., UYANIK, N., BAYSAL, B.M., Interpenetrating hydrogel networks based on polyacrylamide and poly(itaconic acid): Synthesis and characterization, Macrom. Chem. Phys. **200** (1999) 231-238.

[9] RIVAS, B.L., POOLEY, S.A., MATURANA, H.A., VILLEGAS S., Metal ion uptake properties of acrylamide derivative resins, Macrom. Chem. Phy. **202** (2001) 443-447.

[10] HEGAZY, E.A., TAHER, N.H., KAMAL, H., Preparation and properties of cationic membranes obtained by radiation grafting of methacrylic acid onto PTFE films, J. Appl. Polym. Sci. **38** (1989) 1229-1242.

FUNCTIONALIZED NANOPOROUS TRACK ETCHED β-PVDF MEMBRANE ELECTRODES FOR LEAD (II) DETERMINATION BY SQUARE WAVE ANODIC STRIPPING VOLTAMMETRY

H. BESSBOUSSE[1], I. NADHAKUMAR[2], M. DECKER[1], M. BARSBAY[3],
M-C. CLOCHARD[1], T.L. WADE[1]

[1]Laboratoire des Solides Irradiés,
CEA-CNRS-Ecole Polytechnique,
91128 Palaiseau, FRANCE

[2]School of Chemistry
University of Southampton
University Road
Southampton S017 1BJ, UK

[3]Hacettepe University
Department of Chemistry
Polymer Chemistry Division
06800 Beytepe Ankara, TURKEY

Abstract

Track etched functionalized nanoporous β-PVDF membrane electrodes, or functionalized membrane electrodes (FME), are thin-layer cells made from poly(acrylic acid) (PAA) functionalized nanoporous β-poly(vinylidene fluoride) (β-PVDF) membranes with thin Au films sputtered on each side as electrodes. The Au film is thin enough that the pores of the membranes are not completely covered. The PAA functionalization is specifically localised in the walls of the nanoporous β-PVDF membrane by grafting. The PAA is a cation exchange polymer that adsorbs metal ions, such as Pb^{2+}, from aqueous solutions concentrating the ions into the membrane. After a time the FME is transferred to an electrochemical cell for analysis. A negative potential is applied to the Au film of the FME for a set time to reduce the adsorbed ions onto the Au film working electrode. The other metalized side of the FME functions as a counter electrode. Finally, square-wave anodic stripping voltammetry (SW-ASV) is performed on the FME to determine the metal ion concentrations in the original solution. The calibration curve of charge versus log concentration has a Temkin isotherm form. The FME membranes are 9 μm thick and have 40 nm diameter pores with a density of 10^{10} pores/cm^2. This high pore density provides a large capacity for ion adsorption. Au ingress in the pores during sputtering forms a random array of nanoelectrodes. Like surface modified electrodes for adsorptive stripping voltammetry, the pre-concentration step for the FME is performed at open circuit. The zero current intercept of the calibration for Pb^{2+} is 0.13 ppb (μg/L) and a detection limit of 0.050 ppb based on 3S/N from blank measurements. Voltammetry (CV) and chronoapmerometry (CA) were used to characterize the system. The apparent diffusion coefficient (D) for Pb^{2+} in the PAA functionalized pores was determined to be 2.44×10^{-7} cm^2/s and the partition coefficient (pK_M) was determined to be 3.08.

1. OBJECTIVE OF THE RESEARCH

Toxic metals content in water is usually on ppb (μg/L) levels. Reliable quantification of these low concentrations is difficult and the analysis equipment is not portable. The objective of the present research was to construct portable equipment with cation exchange polymer elebrode which is applicable for the analysis of aqueous solutions containing metal ions in ppb concentration.

2. INTRODUCTION

The maximum allowable levels for toxic metals in water are now set at low ppb (μg/L) levels. The maximum levels of Pb^{2+} in potable water established the European Environmental Agency (EEA) the United States Environmental Protection Agency (EPA) and recommendations from the World Health Organisation (WHO) are 7.2, 15.0, and 10.0 ppb respectively and the goal of the United States EPA is zero [1−3].

Reliable quantification of these low concentrations is difficult time consuming and expensive. Also, the analysis equipment is not portable so the samples have to be sent a centralised lab which typically involves a 24 hour turnaround time, which means that pollution events can be missed, or detected too late.

Electrochemical analysis techniques, such as anodic stripping voltammetry (ASV), are generally inexpensive, rapid and portable. The electrode of choice for measuring trace levels of toxic metal ions by ASV has been the dropping mercury electrodes (DME) [4]. DMEs and mercury film electrodes are very sensitive, due to their high capacity to preconcentrate ions for analysis by electro reduction, and DMEs can measure a large range of ions [5−7]. The problem with mercury is that it is unacceptable for environmental applications because of its toxicity. Also, DMEs are expensive and difficult to use. Currently, there is interest in finding replacement electrodes for the DME and mercury films [8].

A new industry, based on thick-film screen-printed electrodes, has evolved to exploit the growing interest in environmental sensors and to replace mercury [9−11]. Screen-printed electrodes are cheap and disposable but the quoted limits of detection (LOD) are barely able to measure the required low concentration levels [9−14]. Also, these quoted LODs for screen-printed electrodes can be misleading because they are based on 3S/N background measurements made in ideal laboratory environments.

There have been very impressive results for the detection of Ag^+ and As^{3+} by ASV using electrodes that do not contain mercury with LODs as low as 0.0005 ppb for Ag^+ and 0.005 ppb for As^{3+} [15−19]. Pb^{2+} LODs are somewhat higher on non-mercury electrodes with the lowest Pb^{2+} LOD being 0.020 ppb using in situ bismuth-films on a glassy carbon electrodes modified with calixarene [20]. Other good Pb^{2+} LODs of ~0.1 ppb have been obtained on silver rotating disks electrodes, carbon electrodes modified with poly(pyrrole-malonic acid) and in situ bismuth modified gold or carbon paste electrodes [21−23]. The quoted LODs for mercury free screen-printed electrodes for Pb^{2+}, however, are about 0.4 ppb [9−11].

A new type of thin-layer cell has been developed for use as electrochemical sensors for voltammetric analysis, Figure 1a. The new cell is based on track etched poly(acrylic acid) (PAA) functionalized nanoporous β-poly(vinylidene fluoride) (β-PVDF) membranes with porous gold electrodes on each side that function as working and counter electrodes for voltammetry, functionalized membrane electrodes (FME). The polymer film of a FME has chemically functionalized parallel nanopore channels of uniform diameter (Figure 1b). The nanopore channels are formed by heavy ion irradiation and chemical etching [24]. The heavy ion irradiation produces damage tracks in the form of radicals from broken carbon-carbon bonds. These radicals are very stable in β-PVDF due the crystallinity of the polymer [24]. The radical tracks are chemically etched to reveal nanopore channels and the channel diameters are proportional to the etching time. After the etching, however, there are still radicals within the pores.

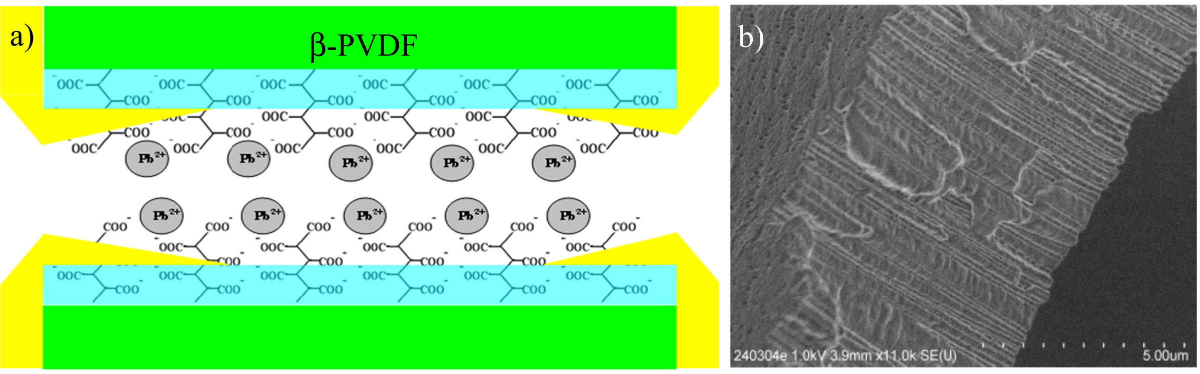

FIG. 1. a) Scheme of a nanopore from a gold coated PAA functionalized radio-track etched β-PVDF membrane (FME) after absorbing Pb^{2+} ions from polluted water. The β-PVDF membrane is shown as green and the $RCOO^-$ as blue represents the PAA gel that is radio grafted into the 40 nm diameter nanopores of the membrane. The 35 nm thick gold coating is shown as yellow. The grey balls represent the absorbed Pb^{2+}. b) FESEM image of a track etched β-PVDF membrane cross-section.

These remaining radicals can be reacted with different monomers, such as RCOOH from acrylic acid (AA) to impart chemical functionalization to the nanopore interior without blocking the pores. The functionalized nanoporous β-PVDF membranes are then transformed into electrodes by the deposition of a thin gold or conductive layer onto the membrane surfaces to make an electrically conductive thin film. The metallic layer is thin enough (35 nm) that is does not completely cover the pores. The gold partially ingresses the nanopores during the sputtering [25].

When the FMEs are immersed in a liquid sample they can selectively absorb certain ions, such as Pb^{2+}, depending on their functionalization. They can then be removed from the sample, rinsed, and placed in an electrochemical cell for ASV analysis. β-PVDF is a very durable material with chemical and mechanical properties similar to Teflon and is nontoxic.

3. MATERIALS AND METHODS

Materials: β-poly(vinylidene fluoride) (β-PVDF) films of 9 µm thickness were provided by PiezoTech SA. Toluene, potassium hydroxide, potassium permanganate, potassium disulfite, acrylic acid (AA), Mohr's salt ($(NH_4)_2Fe(SO_4)_2$ $6H_2O$), sulphuric acid, $C_8H_{17}N_3$ HCl (EDC), phosphate buffer saline (PBS), *t*-BuOH (C_4H_9OK 95%) were purchased from Sigma-Aldrich. Alexa Fluor R 488 hydrazide ($C_{21}H_{15}N_4NaO_{10}S_2$) was purchased from Invitrogen.

Irradiation: Prior to the swift heavy ion irradiation β-PVDF films are toluene-extracted for 24 h. The irradiation was performed at the GANIL irradiation centre (Caen, France). Films were irradiated with Kr ions (10.37 MeV/amu, fluence 10^7 to 10^{10} cm^{-2}) in a He atmosphere. The irradiated films were stored at -20°C in a N_2 atmosphere until chemical etching and radio grafting.

Chemical etching: β-PVDF irradiated films were chemically etched using permanganate solution (0.25 M) in a highly alkaline medium (KOH, 10 M) at 65°C for 30 min. After etching the membranes obtained were washed in potassium disulfite solution (15%) and deionized water.

Radiografting: Etched β-PVDF films were immersed at room temperature into a radio grafting solution containing AA and Mohr's salt (0.25%w/w) in a purgeable glass tube and then connected to a Schlenk line. After 15 min of N_2 bubbling at room temperature, the glass tube is sealed and put into a thermostated water bath at 60°C for 1 h. The radio grafted film is washed with water and then Sohxlet extracted in boiling water for 24 hours in order to extract free homopolymer. The membrane was dried at 50°C under vacuum overnight.

Field-emission scanning electron microscopy (FESEM): FESEM micrographs were acquired with a Hitachi S-4800 microscope.

Infra-red spectroscopy: FTIR spectra of PVDF were obtained with a Nicolet Magna-IR 750 spectrometer equipped with a DGTS detector. Spectra were recorded in attenuated total reflexion mode (ATR) using a diamond-crystal with single reflection. Spectra were collected by cumulating 32 scans at a resolution of 2 cm^{-1}.

Confocal scanning laser microscopy (CSLM): Measurements were performed with a Leica TCS-SP2 using an Ar laser (488 nm). Samples were observed in water with a 40× dry objective of numerical aperture 0.85.

Atomic force microscopy (AFM): AFM images were acquired by tapping mode in air on a Multimode AFM system equipped with a Nanoscope III controller.

Solutions: The Pb^{2+} solutions were diluted from 1.000 µg/mL AAS calibration standards (Alfa Aesar) or from $PbCO_3$ powder 99% (VWR). The electrolyte for the voltammetry measurements was 0.1 M sodium acetate (Sigma-Aldrich). 18 Mohm deionised water (Aquadem Veolia) was used. 100 mL polypropylene containers (VWR) were used for dilution and analysis to avoid loss of Pb^{2+} due to surface adsorption on glass [26].

Connections: The functionalized membrane was metalized by gold sputtering on both sides with a K550 gold sputter (EMITECH). Gold sputtering targets were purchased from NewMet (New Metals & Chemicals LTD). The metalized sides are then connected to 0.5 mm diameter stainless steel wires with silver paste (FERRO, CDS Electronique). The connections were water proofed with hot wax and fingernail polish. Kapton tape (3M) was used to cover the surface of the electrode for some experiments.

Voltammetry: The voltammetry was performed in a three-compartment electrochemical cell controlled by a PalmSens potentiostat (PalmSens) or a BiStat 3200 (Uniscan). An Ag/AgCl (3M KCl) reference electrode (METROHM) was used for all measurements.

4. RESULTS AND DISCUSSION

The synthesis of functionalized radio grafted β–PVDF membranes was developed at the Laboratoire des Solides Irradies [24, 27–32]. β–PVDF polymer films are first bombarded by swift heavy ions (Figure 2a) and the tracks formed along the ion passage are revealed under alkaline chemical treatment (Figure 2b). The obtained nanoporous polymer membranes do not need to undergo subsequent e-beam irradiation to increase radicals in the polymer bulk for submicron pore diameters. After etching times less than one hour, the radical residues within the nanopore walls were sufficient for radio grafting [24]. In the presence of vinyl monomers such as AA, a radical polymerization takes place by a radio grafting to specifically functionalize the nanopore walls with a polymer hydrogel as demonstrated from FTIR spectra (Figure 2c). The double peak for CH_2 vibrations in both films are seen at ~3000 cm^{-1} and a new peak is seen for O-C=O stretching at 1710 cm^{-1} from the grafted PAA.

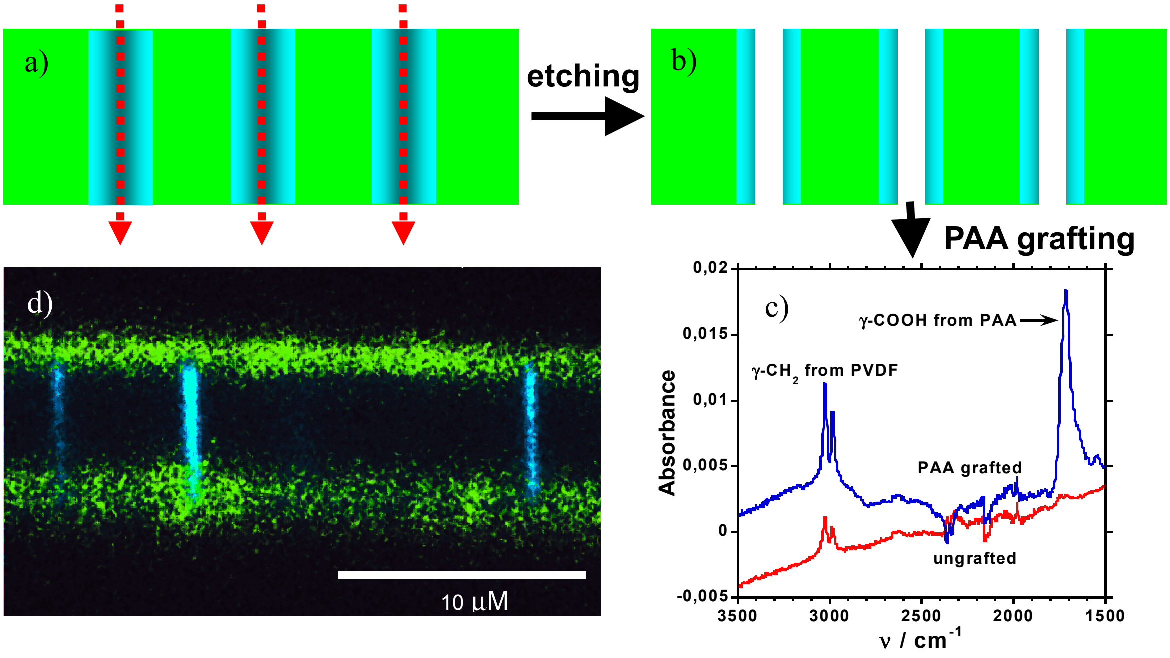

FIG. 2. a) 9 µm thick β-PVDF films were irradiated with Kr ions (10.3 MeV/amu, fluence 10^7 to 10^{10} cm^{-2}) under a He atmosphere. The dashed red arrows indicate the path of the Kr ions and the black/grey areas indicate the zone of irradiation damage in the film. b) The ion tracks were revealed under chemical etching. c) AR–FTIR spectra of etched (red) and grafted (blue) PAA β–PVDF films. d) Fluorescein isothiocyanate labelling reveals amine groups (green), i.e. surface oxidation and Alexa Fluor R hydrazide labelling reveals carboxyl group (blue), i.e. PAA.

A confocal laser imaging study clearly shows that the PAA is localized inside the pores (Figure 2d). Surface oxides on the film were modified with ethylenediamine before grafting. After grafting, the film was labelled with fluorescein isothiocyanate, specific for amine groups, and Alexa Fluor® hydrazide, specific for carboxyl groups. The green coloured fluorescence reveals surface oxidation and the blue coloured fluorescence reveals grafted PAA [24].

The PAA grafting yields used for the FMEs were usually 10 to 15%. Higher grafting yields resulted in pores that were mostly filled by PAA hydrogel so it was impossible to have open pores for ion adsorption after the gold sputtering. Lower grafting yields indicated that the grafting did not work probably due O_2 contamination from insufficient N_2 purging of the grafting tube or the grafting tube was not well sealed.

FESEM and AFM images indicate the nature of the radiografted PAA (Figure 3). For the ungrafted membrane the pore diameter is about 40 nm (Figures 3a-c) while the diameter of the PAA grafted membrane is about 30 nm (Figures 3d–f) showing that about a 5 nm of PAA is grafted onto the walls of the nanopores. This further indicates that there are radicals within the pore walls and the PAA is intercalated into the β–PVDF matrix as well as the surface of the pore walls. The lighter grey areas around the pores in the FESEM image (Figure 3d) indicate a higher density material which is the PAA intercalated into the β–PVDF.

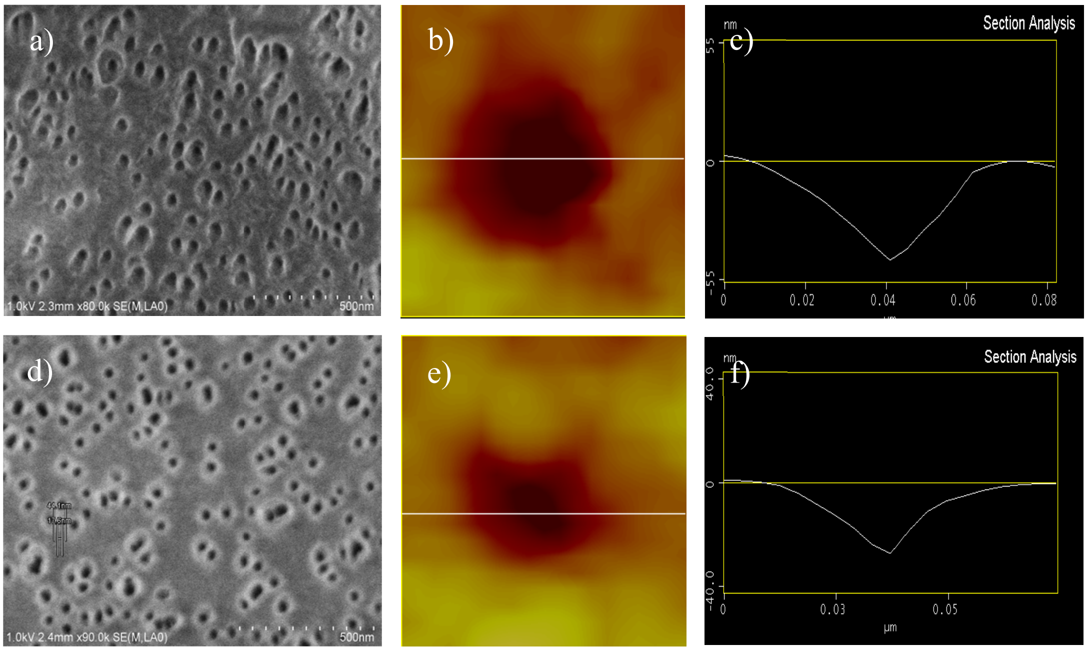

FIG. 3. a-c) FESEM photo, AFM image and AFM line profiles of an ungrafted β–PVDF membrane irradiated with a fluence of 1x10^{10} ions/cm^2 and 30 minutes of etching and d–f) the same membrane after PAA grafting.

To transform the functionalized membrane into an electrode, a thin (35 nm) Au film is sputtered through 0.4 cm diameter holes in a homemade aluminium mask onto each surface (Figures 4 and 5a). From the FESEM micrograph in Figure 4b it is clearly seen that the pores of the film remain open after sputtering, however, Au does ingress the membrane pores [25]. The Au, which protrudes into the membrane's pores, forms 30 nm diameter, 100 nm long nanoelectrodes. The result is a membrane of with random array of 10^{10} parallel nanoelectrodes/cm^2 separated from the counter electrode by 9 µm long 30 nm diameter pores. After sputtering the Au film through a mask (Figure 5a) a 1.5 x 0.6 cm square of membrane is cut out, Figures 5b and 5c, and connected to stainless steel wires with silver paste. The contacts are first protected with hot wax and then fingernail polish (Figure 5d).

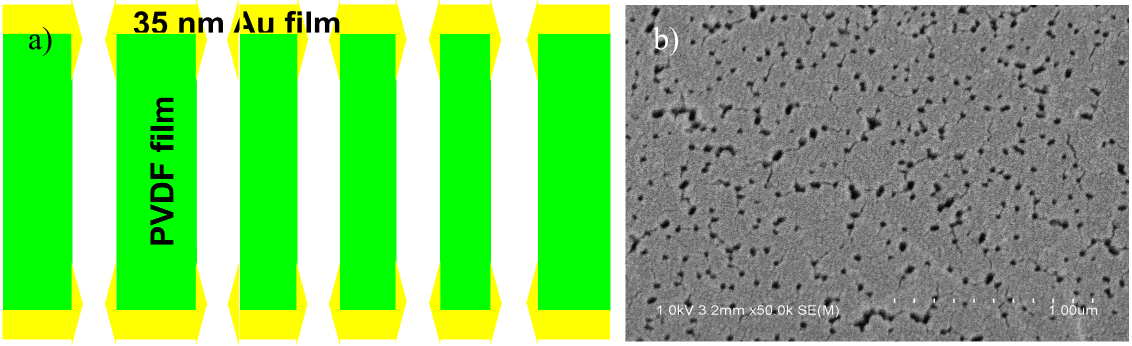

FIG. 4. a) Scheme of a 9 μm thick functionalized β-PVDF membrane (green) with a 35 nm sputtered gold film (yellow) on each side. b) FESEM photo of a 9 μm thick functionalized β–PVDF membrane with a 35 nm Au film sputtered on the surface.

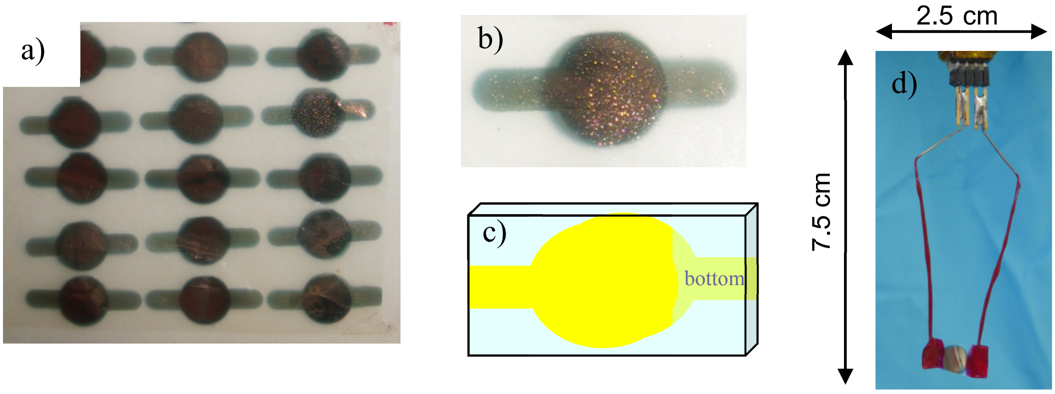

FIG. 5. a) Photo of a 35 nm thick gold layer sputtered on each side of the functionalized β–PVDF membrane through a mask. b) and c) Photo and scheme of a metalized membrane cut out from the large surface from photo a). d) Photo of a membrane attached to wire leads with silver paste and protected with wax and fingernail polish for connection to a potentiostat.

Before a FME is used, a cyclic voltammogram (CV) is performed in a blank solution (0.1 M sodium acetate pH 4.5, Figure 6a). In spite of the fact that the gold layer on the PVDF membrane is only 35 nm thick the CV shows the typical profile of a polycrystalline Au electrode [33]. The CV was performed on the membrane starting at 0.0 V and ramped at a scan rate of 20 mV/second to +1.2 V where the scan was reversed until the scan was stopped at +0.2 V. The other side of the FME was the counter electrode. This configuration of the working and the counter electrodes is essentially that of a thin-layer cell [34–36].

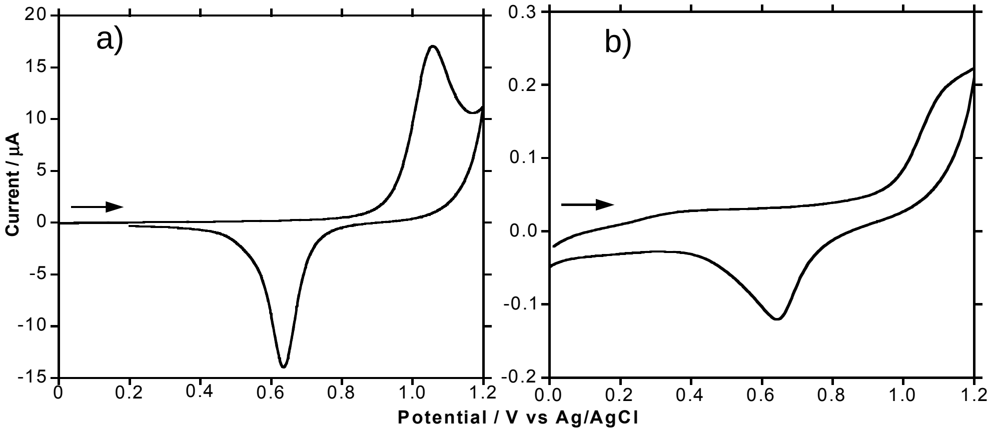

FIG. 6. a) 0.4 cm diameter Au CV in 0.1 M CH_3COONa, pH ~4.5 (scan rate = 20 mV/s), b) surface covered with Kapton tape. The arrows indicate the sense of the scan.

The reduction peak at 0.62 V in Figure 6a is the reduction of one monolayer of Au oxide formed at potentials more positive than 0.850 V during the positive scan [33]. Integration of this reduction peak between 0.400 and 0.800 V gives a charge of 75 μC. The charge for the oxidation of a monolayer of gold (111) is 482 μC/cm^2 [33]. This gives an area of 0.1556 cm^2, however, the visual area of the FME is 0.126 cm^2, 0.40 cm diameter, so the roughness factor (RF) of the electrode is 1.24. This high RF is likely due to the gold ingress in pores of the membrane during the sputtering, Figures 1a and 4a [25]. Figure 6b shows the same experiment as Figure 6a except the surface of the working was covered with Kapton tape in order to limit the measured current to the gold which ingresses in the pores of the membrane. This gives a surface area of 0.00229 cm^2, based on the same calculation as Figure 6a. If we consider that the Au inside of the pores is 30 nm diameter disks then a geometric calculation of the surface gives a surface area of 0.00879 cm^2 so what we have measured by the CV in Figure 6b is about 25% of the disk model, however, is probably in the form of Au tubes with an outside diameter of 30 nm with an unknown internal diameter and unknown length. The obvious thing to do would be to dissolve the membrane and observe the membranes side of the gold surface as was done by Vaidyanathan et al. [25] with polycarbonate membranes with 200 nm diameter pores. β–PVDF is, however, difficult to dissolve and 30 nm structures are still a bit of a challenge to characterize so this is an on-going study.

A CV of the FME in the same solution as Figure 6a with 0.025 mM Pb^{2+} added at a scan rate of 100 mV/s (curve I) shows the electrochemical behaviour for the reduction and oxidation of the Pb^{2+} (Figure 6b). The Pb^{2+} reduction current peak occurs at -0.054 V and the oxidation peak occurs at -0.033 V. The reduction peak current is ~14 μA and the oxidation peak current is ~9 μA. Even though the peak separation is only 0.021 V the difference in currents indicates the irreversibility of the Pb^{2+} on Au. This could be the result of alloy formation or oxidation of the deposited Pb by oxygen present in solution since no purging of the solution was performed. At a scan rate of 2 mV/s (curve II) the CV is sigmoid indicating that at long times the diffusion steady-state.

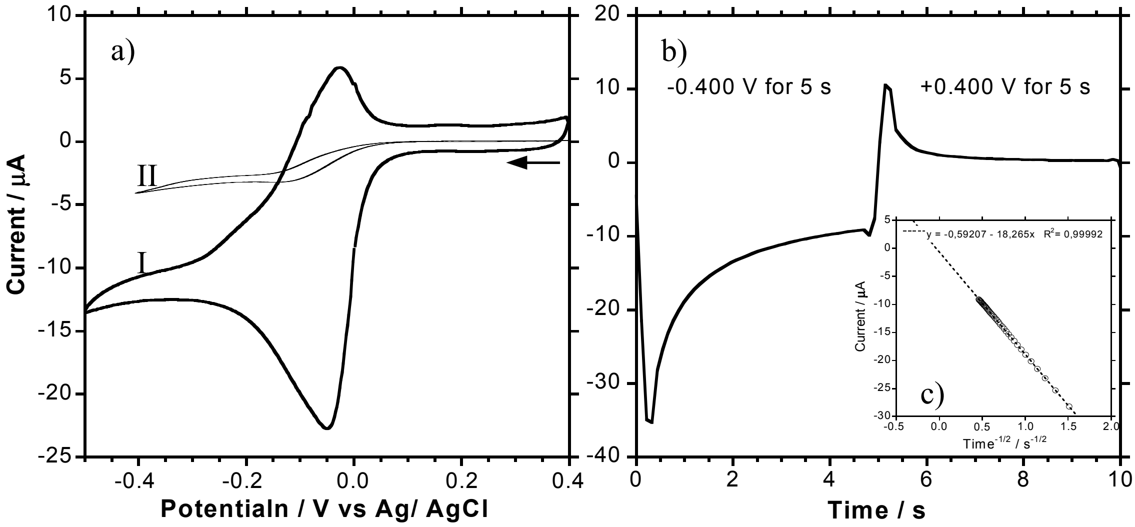

FIG. 7. a) CVs of a FME in a 0.025 mM Pb^{2+} solution with 0.1 M CH_3COONa, pH ~4.5 (curve I scan rate = 100 mV/s and for curve II scan rate = 2 mV/s). b) Chronoamperometric plot of a FME in a 0.0966 mM Pb^{2+} solution with 0.1 M CH_3COONa, pH ~4.5. c) Current versus time$^{-1/2}$ plot of the reduction part of the chronoamperometric plot.

Chronoamperometry experiments were performed based on the potential window seen for the CVs in Figure 7a and 7b. The potential was switched from +0.400 V to -0.400 V and held for 5 seconds then switched back to +0.400 V and held for 5 seconds in order to measure the diffusion limited current (I_{diff}), the solution concentration was 0.100 mM Pb^{2+}. The ratio of the oxidation current to the reduction current (i_O/i_R) at a given time after the potential step ranges from -0.124 to -0.030 which is much lower than predicted for a simple reversible reaction of -0.293 [37]. A plot of the current for the reduction step versus 1/t$^{-1/2}$ yields a straight line with a good fit for the linear regression (Figure 7c).

During the immersion of a FME in a sample containing heavy metal ions, the membrane absorbs some of the metal cations by the PAA grafted in the nanopores of the β–PVDF membrane, Equation 1. The pK_M of Pb^{2+} in bulk PAA is 4.0 at pH < 4.0, determined by potentiometric titrations and ion-selective electrodes [44].

$$M^{n+} + \text{R-COO}^- \text{ <--> } \text{R-COO}^-M^{n+} \qquad (1)$$

For the electrochemical analysis the FME is connected to a potentiostat and placed at a negative potential. The negative potential reduces the absorbed metals ions that are very close to the working electrode, from the poly (acrylic acid) in the pores to their metallic state at the Au surface, Equation 2.

$$\text{R-COO}^-M^{n+} + ne^- \text{ --> } M(Au) \qquad (2)$$

After the reduction, square wave anodic stripping voltammetry (SW-ASV) analysis is performed in order to oxidize the metal from the working electrode surface and measure the resulting current, Equation 3.

$$M(Au) \text{ --> } M^{n+} + ne^- \qquad (3)$$

The parameters for the SW-ASV analysis were a frequency of 25 Hz, step amplitude of 25 mV and a potential increment of 4 mV. The optimisation of the deposition potential, time and immersion time follows: The deposition potential was determined by immersing a FME in 50 mL of stirred 3 µg/L Pb^{2+} sample for 10 minutes followed by SW-ASV. The charge increases with decreasing deposition potential (Figure 8a). There is, however, a local minimum at – 0.9 V. This is likely due to the hydrogen gas bubbles from proton reduction at the FME that could impair Pb^{2+} deposition, Equation 4.

$$2H^+ + 2e^- \text{ --> } H_2\,(g) \qquad (4)$$

Also, for potentials more negative than -0.8 V there was a problem with the gold electrode adhesion due to the formation of hydrogen gas bubbles. Therefore, a deposition potential of -0.8 V was used for further studies. The absorption time was determined by immersing a FMS in 50 mL of a 3 µg/L Pb^{2+} sample for different times followed by deposition at – 0.8 V (Figure 8b). After 30 minutes equilibrium is established. Figure 8c shows the charge versus the deposition time. After 100 seconds a plateau is reached so a minimum deposition time of 100 seconds is used for further studies.

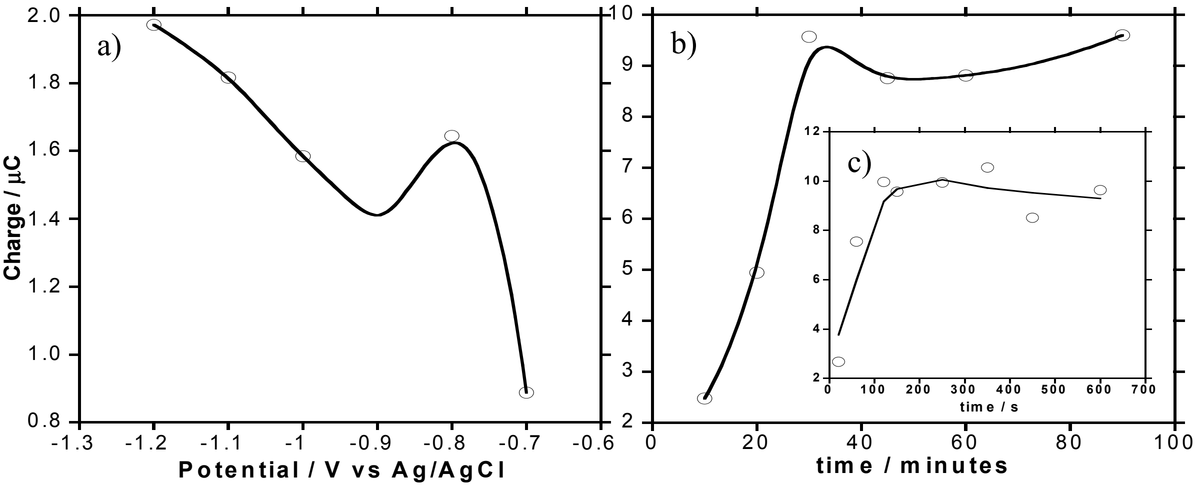

FIG. 8. a) A plot of oxidation charge from SW-ASV scans of FMEs that were immersed in 50 mL of stirred 3 µg/L Pb^{2+} samples for10 minutes with different deposition potentials. b) A plot of the charge versus immersion time in 50 mL of stirred 3 µg/L Pb^{2+} samples using a deposition potential of -0.8 V. c) A plot of deposition time versus charge for a membrane that been immersed in 50 mL of stirred 3 µg/L Pb^{2+} samples for 30 minutes with a deposition potential of -0.8 V.

Figure 9a is a plot of superimposed SW-ASV current peaks for different concentrations of Pb^{2+} along with a blank scan. Each curve was obtained using a different FME. At concentrations higher than 3 to 4 µg/L current/voltage curves do not increase much in height but become very broad. For this reason the calibration curve was plotted with the charge and not peak current.

Figure 9b is a curve of the charges found from Figure 9a versus the concentrations of the solutions measured. Different isotherms were used to fit the curve in Figure 9b and a Temkin isotherm gave the best fit with a R^2 of 0.98979. The Temkin isotherm indicates that there is a decrease in the heat of adsorptions with increasing coverage within the pores [38]. The intercept of the charge versus log $[Pb^{2+}]$ plot has a $[Pb^{2+}]$ value of 0.13 ppb. The 3S/N, standard deviation (σ), of eight blank scans was 0.05 ppb.

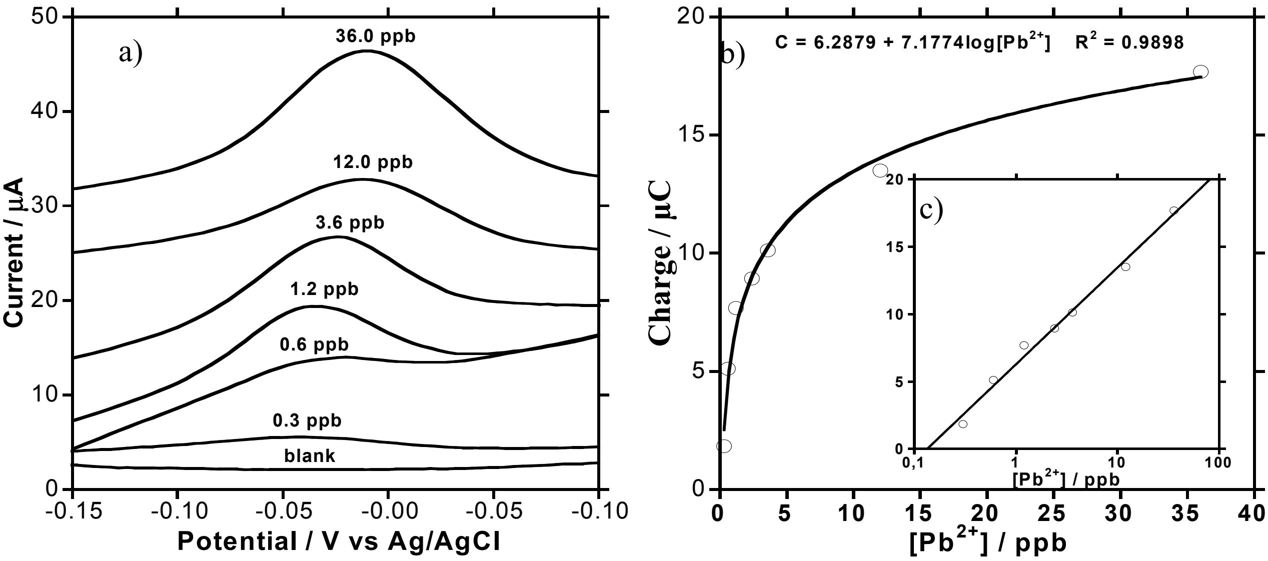

FIG. 9. a) SW-ASV analysis plots of FMEs after immersion in 50 mL of stirred Pb^{2+} ion solutions for 30 minutes using different concentrations. The curve from a blank analysis is also plotted. b) A calibration curve for Pb^{2+} ions determined from Figure 8a. c) A charge vs. log concentration curve.

A SW-ASV measurement of tap water showed no indication of Pb^{2+}. When the same tap water sample was spiked with 3 ppb of Pb^{2+} the charge recovered was 88.5% of the charge corresponding to 3 ppb from the calibration curve in Figures 8b and c, however, this charge only corresponds to a concentration of 1.2 ppb. This could be due to the logarithmic nature of the calibration curve so it is very sensitive to slight charge variations at low concentrations. Or the discrepancy could be due to a masking of Pb^{2+} by something in the tap water or perhaps complex formation by an anion such as Cl^- or F^-.

5. CONCLUSIONS

The FME is very sensitive to sub-ppb concentrations of Pb^{2+}. The membrane preparation is done in bulk and is very inexpensive in materials. The most expensive step is the gold metallisation. We are in the process of functionalizing the PVDF membranes with polymers other than PAA to evaluate different ion adsorption efficiencies and selectivities. Because of their versatility, the FME can be thought of as a template for electroactive polymers as ion sensors.

The Temkin isotherm indicates that the energy of adsorption of Pb^{2+} is inhomogeneous in the PAA functionalized membrane so there is a need to develop techniques to improve the uniformity of the PAA polymerisation. The group is currently working on improving the reproducibility of the grafting yield by studying Reverse Addition Fragmentation Transfer Polymerization inside tracks. The kinetics of the adsorption isotherm needs also to be addressed in order to understand and better optimize the adsorption.

The adsorption is done at open circuit and the SW-ASV analysis is very fast, less than 3 minutes. The ability to preconcentrate the ions at open circuit means that many samples can be collected in parallel and stored for later analysis.

REFERENCES

[1] EUROPEAN ENVIRONMENT AGENCY, Directive 2008/105/EC (2008) 10.

[2] WORLD HEALTH ORGANISATION, Guidelines for Drinking-water Quality **1**, (2008) 392.

[3] UNITED STATES ENVIRONMENTAL PROTECTION AGENCY, National Primary Drinking Water Regulations May (2009) 3.

[4] BRETT, C.M.A., BRETT, A.M.O., Electrochemistry Principles, Methods, and Applications. 1st ed. Oxford University Press, Oxford (2005).

[5] BAHRAMI, S., ABBASI, S., GHORBANI, Y.A., MIRAN-BEIGI, A.A., High sensitive determination of trace amount of cobalt by catalytic adsorptive stripping voltammetry, Russian Journal of Electrochemistry **45** (2009) 208-214.

[6] FISCHER, E., VAN DEN BERG, C.M.G., Anodic stripping voltammetry of lead and cadmium using a mercury film electrode and thiocyanate, Analytica Chimica Acta **385** (1999) 273-280.

[7] JAKUBOWSKA, M., ZEMBRZUSKI, W., LUKASZEWSKI, Z., Thallium determination at the single picomole per liter level by flow-injection differential-pulse anodic stripping voltammetry, Electroanalysis **20** (2008) 1073-1077.

[8] HUTTON, E.A., HOCEVAR, S.B., OGOREVC, M., Ex situ preparation of bismuth film microelectrode for use in electrochemical stripping microanalysis, Analytica Chimica Acta **537** (2005) 285-292.

[9] LASCHI, S., PALCHETTI, I., MASCINI, M., Gold-based screen-printed sensor for detection of trace lead, Sensors and Actuators B-Chem. **114** (2006) 460-465.

[10] RENEDO, O.D., ALONSO-LOMILLO, M.A., MARTINEZ, M.J.A., Recent developments in the field of screen-printed electrodes and their related applications, Talanta **73** (2007) 202-219.

[11] RICO, M.A.G., OLIVARES-MARIN, M., GIL, E.P., Modification of carbon screen-printed electrodes by adsorption of chemically synthesized Bi nanoparticles for the voltammetric stripping detection of Zn(II), Cd(II) and Pb(II), Talanta **80** (2009) 631-635.

[12] KHALED, E., HASSAN, H.N.A., HABIB, I.H.I., METELKA, R., Chitosan modified screen-printed carbon electrode for sensitive analysis of heavy metals, International Journal of Electrochemical Science **5** (2010) 158-167.

[13] RENEDO, O.D., MARTINEZ, M.J.A., Anodic stripping voltammetry of antimony using gold nanoparticle-modified carbon screen-printed electrodes, Analytica Chimica Acta **589** (2007) 255-260.

[14] YANTASEE, W., DEIBLER, L. A., FRYXELL, G.E., TIMCHALK, C., LIN, Y.H., Screen-printed electrodes modified with functionalized mesoporous silica for voltammetric analysis of toxic metal ions, Electrochem. Commun. **7** (2005) 1170-1176.

[15] JAVANBAKHT, M., DIVSAR, F., BADIEI, A., FATOLLAHI, F., KHANIANI, Y., GANJALI, M.R., NOROUZI, P., CHALOOSI, M., ZIARANI, G.M., Determination of picomolar silver concentrations by differential pulse anodic stripping voltammetry at a carbon paste electrode modified with phenylthiourea-functionalized high ordered nanoporous silica gel, Electrochimica Acta **54** (2009) 5381-5386.

[16] FEENEY, R., KOUNAVES, S.P., On-site analysis of arsenic in groundwater using a microfabricated gold ultramicroelectrode array, Anal. Chem. **72** (2000) 2222.

[17] SONG, Y., SWAIN, G.M., Development of a method for total inorganic arsenic analysis using anodic stripping voltammetry and an Au-coated, diamond thin-film electrode, Anal. Chem. **79** (2007) 2412-2420.

[18] JENA, B.K., RAJ, C.R., Gold nanoelectrode ensembles for the simultaneous electrochemical detection of ultratrace arsenic, mercury, and copper, Anal. Chem. **80** (2008) 4836-4844.

[19] DAI, X., NEKRASSOVA, O., HYDE, M.E., COMPTON, R.G., Anodic stripping voltammetry of arsenic(III) using gold nanoparticle-modified electrodes, Anal. Chem. 76 (2004) 5924-5929.

[20] TORMA, F., GRUEN, A., BITTER, I., TOTH, K., Calixarene/Nafion-modified bismuth-film electrodes for adsorptive stripping voltammetric determination of lead, Electroanalysis **21** (2009) 1961-1969.

[21] BRAND, M., ESHKENAZI, I., KIROVAEISNER, E., The silver electrode in square-wave anodic stripping voltammetry, Determination of Pb^{2+} without removal of oxygen, Anal. Chem. **69** (1997) 4660-4664.

[22] HEITZMANN, M., BASAEZ, L., BROVELLI, F., BUCHER, C., LIMOSIN, D., PEREIRA, E., RIVAS, B. L., ROYAL, G., SAINT-AMAN, E., MOUTET, J. C., Voltammetric sensing of trace metals at a poly(pyrrole-malonic acid) film modified carbon electrode, Electroanalysis **17** (2005) 1970-1976.

[23] BALDRIANOVA, L., SVANCARA, I., VLCEK, M., ECONOMOU, A., SOTIROPOULOS, S., Effect of Bi(III) concentration on the stripping voltammetric response of in situ bismuth-coated carbon paste and gold electrodes, Electrochimica Acta 52 (2006) 481-490.

[24] CUSCITO, O., CLOCHARD, M.C., ESNOUF, S., BETZ, N., LAIREZ, D., Nanoporous beta–PVDF membranes with selectively functionalized pores, Nucl. Instr. Meth. Phys. Res. B **265** (2007) 309-313.

[25] VAIDYANATHAN, R., STICKNEY, J.L., COX, S.M., COMPTON, S.P., HAPPEK, U., Formation of In2Se3 thin films and nanostructures using electrochemical atomic layer epitaxy, J. Electroanal. Chem. **559** (2003) 55-61.

[26] PINHEIRO, J.P., BOSKER, W., Polystyrene film-coated glassware: a new means of reducing metal losses in trace metal speciation, Analytical and Bioanalytical Chemistry **380** (2004) 964-968.

[27] BETZ, N., MOEL, A.L., PIREAUX, J.-J., Ionizing radiation & polymers, Nucl. Inst. Meth. B **236** (2005) VII-VIII.

[28] CLOCHARD, M.C., BEGUE, J., LAFON, A., CALDEMAISON, D., BITTENCOURT, C., PIREAUX, J.J., BETZ, N., Tailoring bulk and surface grafting of poly(acrylic acid) in electron-irradiated PVDF, Polymer **45** (2004) 8683-8694.

[29] CLOCHARD, M.C., BETZ, N., GONCALVES, M., BITTENCOURT, C., PIREAUX, J.J., GIONNET, K., DELERIS, G., LE MOEL, A., Peptide immobilization onto radiation grafted PVDF-g-poly(acrylic acid) films, Nucl. Instr. Meth. Phys. Res. B **236** (2005) 208-215.

[30] CLOCHARD, M.C., WADE, T.L., WEGROWE, J.E., BALANZAT, E., Influence of asymmetric etching on ion track shapes in polycarbonate, Nucl. Instr. Meth. Phys. Res. B **265** (2007) 325-329.

[31] GRASSELLI, M., BETZ, N., Electron-beam induced RAFT-graft polymerization of poly(acrylic acid) onto PVDF, Polymer **45** (2005) 8683-8694.

[32] MAZZEI, R., BERMUDEZ, G.G., BETZ, N., CABANILLAS, E., Swift heavy ion induced graft polymerization in track etched membranes' submicroscopic pores, Nucl. Inst. Meth. B **223** (2004) 575-584.

[33] HOOGVLIET, J.C., DIJKSMA, M., KAMP, B., VAN BENNEKOM, W.P., Electrochemical pretreatment of polycrystalline gold electrodes to produce a reproducible surface roughness for self-assembly: A study in phosphate buffer pH 7.4, Anal. Chem. **72** (2000) 2016-2021.

[34] HUBBARD, A. T., ANSON, F. C., Linear potential sweep voltammetry in thin layers of solution, Anal. Chem. **38**, (1966) 58.

[35] HUBBARD, A.T., ANSON, F.C., Determination of adsorbed cobalt and iron ethylenedinitrilotetraacetate complexes on platinum electrodes by thin layer electrochemistry, Anal. Chem. **38** (1966) 160.

[36] HUBBARD, A.T., ANSON, F.C., New electrodes for chronopotentiometry in thin layers of solution, Anal. Chem. **36** (1964) 723.

[37] RIEGER, P. H., Electrochemistry. Prentice-Hall, Inc., Englewood Cliffs, NJ, (1987) pp 508.

[38] BOND, C.G., Catalysis by Metals. 1st ed., Academic Press Inc., London (1962) **1**, pp 519.

GRAFTED CELLULOSE BASED ADSORBENTS FOR SELECTIVE SEPARATION PURPOSES

E. TAKÁCS, L. WOJNÁROVITS

Institute of Isotopes
Hungarian Academy of Sciences
Budapest
HUNGARY

Abstract

The effect of high energy ionizing radiation on cotton-cellulose was studied. It was found that degradation of cellulose started at low doses, below 5 kGy, resulting in decrease in the degree of polymerization. However, the mechanical properties of cotton-cellulose samples only slightly changed with the dose up to 40 kGy. Acrylate type monomers were successfully grafted to cellulose by mutual and by pre-irradiation grafting technique. With both techniques the grafting yield increased with increasing dose and monomer concentration. In the case of pre-irradiation grafting the increase in grafting time also resulted in an increase in grafting percentage. Cotton-cellulose was functionalized using pre-irradiation grafting (PIG) and simultaneous grafting (SG) of glycidyl methacrylate (GMA). The adsorption properties of this material were further enhanced by β-cyclodextrin (CD) immobilization. This molecule is known for its unique ability to form inclusion complexes among others with aromatic compounds like phenols, pesticide, dyes, etc.

1. OBJECTIVE OF THE RESEARCH

Phenol and its derivatives are toxic causing serious health problems even at very low concentration. Therefore, it is very important to remove them from drinking water and from wastewater, as well. Among other techniques, cellulose based adsorbent produced by radiation induced grafting can be used for this purpose.
The objective of the present work focuses on the optimization of synthesis of specific adsorbents based on cellulose, and characterization of the grafted samples. The final objective is to produce cellulose samples with selective adsorption properties and optimize the conditions for adsorption.

2. INTRODUCTION

Heavy metal ions, pharmaceutical compounds, and pesticides are mostly toxic and carcinogenic even at low concentration causing ecological disequilibrium and severe public health problem [1–6]. Prolonged exposure in the aquatic environment causes adverse effects in the ecosystem. Wastewater treatment plants are ineffective in eliminating these toxic compounds, and most part of them passes through the treatment plants without any change.

Various methods, such as chemical precipitation, oxidation, reduction, coagulation, ion exchange, reverse osmosis, solvent extraction, flocculation, membrane separation, filtration, evaporation, electrolysis and adsorption have been used to remove and recover heavy metal ions from sewage and industrial effluents [2–3, 7−10]. A series of advantages and disadvantages are associated with each of these techniques. Among all the treatment processes mentioned, adsorption using the chelating properties of adsorbents is one of the most effective and economically feasible alternative methods [2, 4, 7].

Several adsorbents have been developed for removing heavy metal ions from aqueous solutions, e.g. different types of clays, activated carbon, chelating resins containing amidoxime or iminodiacetic acid groups, simple and binary metal oxides, activated sludge, bone char, canola meal, red mud and metallurgical slag [3, 11]. After investigating 200 functional groups, Tamada et al. [12] found that amidoxime shows the best chelating properties. The conventional adsorbents such as synthetic cation exchange resins are non-renewable and non-biodegradable [6]. The natural materials including cellulose, chitosan (a cellulose derivative) are renewable, biodegradable, cheap and available in large amount [9]. Natural materials can be chemically modified for enhancing metal-binding ability by addition of new functional groups [9, 13]. There is an intensive research nowadays for their application in metal ion adsorption from aqueous wastes.

Several agricultural products and by-products such as cotton, hemp, flax, rice husk, sugarcane bagasse, sawdust of wood, wheat straw, onion skins, palm kernel husk, peanut skin, pinus bark, corn cobs, cane stick, jute stem etc., have been applied as efficient adsorbents for heavy metal, especially for divalent metal cation removal [4, 6, 14, 17]. These by-products are accessible in huge amount and as shown in Table 1, they consist of cellulose, hemicellulose, lignin and some protein, lipids, wax, etc. [6].

TABLE 1. α-CELLULOSE, HEMICELLULOSE AND LIGNIN CONTENT (%) OF DIFFERENT PLANTS

Plant type	α-cellulose	Hemicellulose	Lignin	Ash	Reference
Cane stick	39.37	27.61	26.2	1.29	[14]
Corncobs	38.4	40.7	9.1	1.3	[6]
Cotton stalks	58	14.38	21.45	2.17	[15]
	48				
Jute	58-63	20-22	13-15		[16]
Jute stem	37.07	32.17	24.48	0.55	[14]
Olivepruning	35.67	25.80	19.71	1.36	[15]
Rice straw	41.20	19.50	21.90	9.20	[15]
Sorghumstalks	41.50	24.43	15.64	4.85	[15]
Sugarcane bagasse	40-50	25-30	20-25		[1]
Sugarcane bagasse	50	27	23		[5]
Sugarcane bagasse			19.80	2.1	[15]
Sunflower stalks	37.60	29.30	10.80	7.9	[15]
Vine shoots	41.14	26.00	20.27	3.49	[15]
Wheat straw	39.72	36.48	17.28	6.49	[15]

The use of ionizing radiation increases the reactivity of cellulose towards certain reagents [18]. The radiation-induced reactions in the macromolecules of the cellulose materials are known to be initiated through rapid localization of the absorbed energy within the molecules to produce very reactive intermediates, long- and short-lived free radicals, ions and excited states [19, 20]. Some of the radical species decay rather slowly: they are observable by EPR spectroscopy days after the irradiation [21]. Arthur [22, 23] published reviews on the structure of radicals produced in cellulose by a large variety of initiation. On gamma irradiation of cellulose radicals are formed with localized unpaired electrons in positions 1 and 4 of the pyranose ring, the formation of which is accompanied by rupture of the glycoside bond. Thermal transformations of these radicals cause their degradation: dehydration of the radicals with double bond in the pyranose ring forming by that allyl type radical is the most probable process (Fig. 1) [24–27].

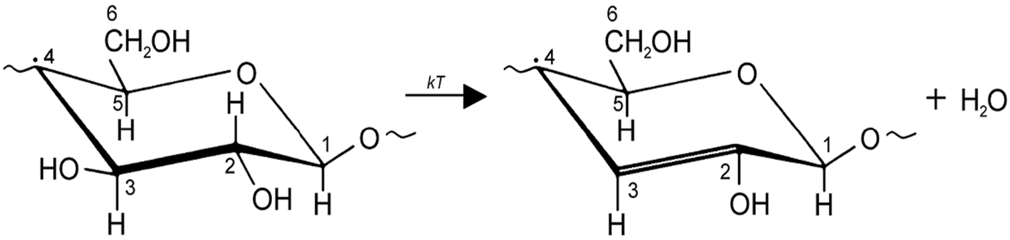

FIG. 1. Dehydration of C4 centred radical to allyl type radical.

These intermediates cause the secondary degradation of materials through chemical reactions such as chain scission (decreasing the molecular weight of polymer), cross-linking (increasing the molecular weight of polymer) [19, 33]. Cross-linking increases the tensile strength, elongation, modulus of elasticity, hardness and softening temperature. On the other hand, chain scission decreases these properties [33]. The efficiency of these two types of reactions depends on the structure of the polymer and the conditions of treatment before, during and after irradiation [19, 20]. Cellulose belongs to the class of degrading polymers.

Interactions of high-energy radiation in required conditions with polysaccharides, such as starch, cellulose, lignocellulose and pectin result in dehydrogenation, oxidative degradation by a cleavage of glycosidic bonds, and destruction of the basic monomer unit [19, 33, 34]. Irradiated either by neutrons, X rays or gamma rays the relative viscosity and the degree of polymerization (DP), number of glucose units in the polymer chain, of cellulose decreases and the concentration of carboxyl and carbonyl groups increases with increasing the absorbed dose due to the cleavage of the glycosidic bonds. However, there is only a slight modification in the mechanical properties [33, 34]. The electron beam radiation degrades the cellulose or cellulose derivatives less severely than the gamma ray radiation. At the same dose, the concentration of radicals is higher in electron beam irradiation, due to the high dose rate, and the chance of the termination reaction between two macroradicals is higher. The irradiation with high dose rate is more efficient for crosslinking reaction due to the higher average radical concentration during the irradiation treatment [33].

There is also another phenomenon, called ‘after effect’ [19]. Ionizing radiation causes microstructural changes in cellulose and improves the accessibility of the crystalline regions to reagents [35]. During the irradiation, radicals produced in amorphous regions will decay quickly, while others which are trapped in the crystalline and semi-crystalline regions of the cellulose structure can decay at a certain period and cause a further degradation of (e.g. the viscosity of cellulose decreased at even two weeks after irradiation) [19].

When cellulose is irradiated in the presence of air, the radicals on the polymer backbone react with oxygen forming peroxy radicals as it was shown by EPR measurements [36]. Radical signal is well detectable even after a month’s storage at room temperature, however, its intensity decreases and its shape also shows some changes indicating altered radical structures. The decrease of intensity is due to formation of hydroperoxides and peroxides. The reactions below show on a simplified reaction scheme:

$$\text{Cellulose} \rightsquigarrow \text{R}^{\bullet} \tag{1}$$
$$\text{R}^{\bullet} + \text{O}_2 \longrightarrow \text{ROO}^{\bullet} \tag{2}$$
$$\text{ROO}^{\bullet} + \text{Cellulose} \longrightarrow \text{ROOH} + \text{R}^{\bullet} \tag{3}$$
$$2\ \text{ROO}^{\bullet} \longrightarrow \text{ROOR} + \text{O}_2 \tag{4}$$

Radiation grafting offers some unique advantages over the conventional grafting method. Radiation grafting of cellulose has been studied to impart and improve many desired properties like flame retardancy, high absorbancy, water impermeability, abrasion resistance, anti-crease properties, rot resistance, thermo-responsive property and properties for bio-medical applications [37]. Ionizing radiation induced grafting may take place both by radical and ionic propagation mechanisms. Since ionic polymerization needs 'ultrapure' conditions, e.g. absence traces of water, which can act as chain breaker, in practice the grafting occurs with a free radical chain mechanism. In the pre-irradiation grafting (PIG) technique the polymer is irradiated in inert gas (N_2, Ar) or in vacuum, during irradiation free radicals form on the polymer backbone. The irradiation results in forming of radicals on the surface of cellulose fibbers and inside the fibrilles [38]. These radicals are surprisingly long lived, by EPR method they can be detected days after the irradiation [24, 25].

Usually the pre-irradiation is carried out in the presence of air or oxygen. Under such conditions the peroxy radicals formed on the polymer backbone transform slowly to relatively stable ROOH type hydroperoxides and ROOR type peroxides. (The method is also called peroxidation grafting method [39].) The peroxy products can be stored for long periods before performing the grafting step. During grafting the irradiated polymer is immersed in the liquid monomer or in solution of monomer and the system is heated to approximately 40–70°C. The peroxy products undergo decomposition to radicals, these radicals initiate the grafting. Since in the pre-irradiation method the monomer is not exposed to radiation the obvious advantage is that the final product is free from homopolymer. During irradiation of the base polymer some degradation takes place, which is a disadvantage.

$$\mathrm{ROOH} \longrightarrow \mathrm{RO}^{\bullet} + {}^{\bullet}\mathrm{OH} \qquad (5)$$

$$\mathrm{ROOR} \longrightarrow 2\mathrm{RO}^{\bullet} \qquad (6)$$

In the mutual or simultaneous irradiation grafting (SG) technique the monomer and the polymer are irradiated simultaneously to form free radicals for polymerization. When irradiation is carried out in solution, free radicals form in the decomposition of monomer, polymer and solvent. Generally the mass of the solvent is much higher than the masses of the monomer and polymer. As an approximation it is generally assumed that the energy of ionizing radiation is absorbed by the solvent and the free radicals formed from the solvent react both with the monomer and the polymer. In aqueous solutions the radiolysis of water supplies hydroxyl radical (radiation chemical yield, G–value = 0.27 μmol J^{-1}), hydrogen atom (0.07 μmol J^{-1}) and hydrated electron (0.27 μmol J^{-1}) reactive intermediates [40, 41]. The hydroxyl radicals and to smaller extent the hydrogen atoms are capable of removing hydrogen atoms from cellulose producing by that radicals on the polymer backbone. All the three intermediates may react with the monomer in radical addition reaction yielding radicals that can take part both in homopolymer formation and grafting.

The disadvantage of the method is the homopolymer formation in the liquid phase. Higher grafting yields are expected at higher monomer concentrations, as any instant radicals generated on the backbone are able to interact with more monomer molecules. However at high monomer concentrations, as more monomer radicals will be generated in the bulk, homo-polymerization will be equally favoured.

Homopolymer formation, and by that the loss of a considerable part of the monomer, is usually suppressed by adding inhibitors to the liquid. In most cases Mohr–salt ($Fe(NH_4)_2(SO_4)_2(6H_2O)$) and Cu^{2+} sulphate ($CuSO_4 \times 5H_2O$) are used for this purpose. The adsorption of these metal ions on the cellulose surface may inhibit also grafting. In hydrophilic backbones like cotton cellulose, dissolved oxygen can diffuse into the backbone and quench the radicals generated on the backbone; this may lead to decrease in the grafting yield. Presence of oxygen hinders the homo-polymerization and grafting reaction to the same extent.

After the grafted polymer is prepared it is washed thoroughly in water or in other solvent (e.g. methanol, water-methanol mixtures, acetone) at elevated temperature (~70°C) in order to remove the un-reacted monomer and the homopolymer. Then the graft is dried at 40–60°C in oven, in a vacuum drying system, or in desiccator. The mass of the dried sample measured before and after grafting is used to calculate the grafting yield.

The polymer that will become grafted on the cotton surface is crucial from the point of view of the end-product properties. Acrylate and methacrylate type monomers were used for the experiments.

Glycidyl methacrylate (GMA) is an interesting choice under increasing interest [42, 43], because it has the highly reactive epoxide group at one end. The grafted materials containing the epoxide groups can be used for the adsorption of water contaminants [44]. The adsorption properties of this material could be enhanced by further functionalization. The desired functionality can be introduced via chemical reaction with the epoxy group. Amino type adsorbent was synthesized for the removal of mercury ions [43] from GMA grafted nonwoven cotton fabric.

β-cyclodextrin (CD) is known for its unique ability to form inclusion complexes with aromatic (mainly phenol derivatives) compounds, metals and dyes [45, 46]. In most cases CD functional group is attached to the base material (e.g. cellulose) by chemical reaction using crosslinking or coupling agents [45–47]. The accessibility of CD may be limited in these cases due to its controlled mobility. This problem can be solved by coupling CD to the GMA grafted cotton using GMA as a spacer.

3. MATERIALS AND METHODS

3.1. Materials

Analytical grade monomers were purchased from Sigma Aldrich, CD from CycloLab and were used as received. Purified water was obtained from an ion exchanger equipment type ELGA Option 4. Bleached cotton fabric samples (110 g/m^2, Colortex Kft., Hungary) were washed first in 1% acetic acid solution at 50 °C for 5 minutes, then in deionised water and the samples were dried. Carboxymethylation using monochloroacetic acid and sodium hydroxide was carried out by the technology described previously [48]. The degree of substitution was 0.05. This slight modification resulted in high improvement of accessibility: accessible surface characterised by iodine sorption capacity (IS), [49] increased by about 200%. The IS of slightly carboxymethylated cellulose was 119 mg/g, while that of untreated one 38 mg/g.

3.2. Grafting methods

Simultaneous grafting (SG): First the monomer solution (containing Mohr salt to avoid homopolymerization) was deaerated for about 5 minutes by N_2 or Ar bubbling, then the cotton samples were immersed in the monomer solution (liquor ratio: 0.1 g sample/10 mL solution) and the bubbling was continued for a further 15 minutes. The ampoules were flame sealed in inert atmosphere and irradiated at room temperature by ^{60}Co gamma rays up to 40 kGy doses (dose rate 10 kGy/h). After irradiation the samples were washed in deionised water and the unreacted monomer was removed by extraction at 40°C with deionised water for 6 hours. The samples were dried in air until constant weight and weighted (w_g).

Pre-irradiation grafting (PIG): Cotton-cellulose fabric samples were irradiated in air, at room temperature up to 40 kGy doses (dose rate 10 kGy/h). Immediately after irradiation the samples were immersed in 1 mol dm^{-3} aqueous monomer solutions at 40°C for 1 hour (liquor ratio: 0.1 g sample/10 mL solution). N_2 bubbling was applied to deoxygenate the monomer solutions. Bubbling was started about half hour before grafting and continued during the whole grafting procedure. Grafted samples were washed and extracted as described before.

3.3. β-cyclodextrin (CD) immobilization

CD was successfully immobilized during SG. 0.017 mol dm^{-3} CD was added to the grafting solution (33% H_2O, 33% methanol, 33% dimethyl formamide, DMF). The rest of the procedure was the same as in normal SG.

3.4. Characterization of samples

The grafting yield (= 100% × $(w_g-w_0)/w_0$) was determined by weighting the dried samples before (w_0) and after (w_g) grafting. The yield was also determined by following the IR absorption using a Unicam

Mattson Research Series 1 FTIR instrument, with diffuse reflexion detection. The absorption peak at 1740 cm^{-1} assigned to the stretching vibrations of C=O group was used to characterize the grafting yield. The band at 2900 cm^{-1} assigned to the stretching vibrations of aliphatic C-H bonds served as internal standard.

The X ray diffraction (XRD) patterns were taken on textile samples of ~20 × 30 mm using a Philips instrument equipped with a Bragg-Brentano parafocusing goniometer, secondary beam graphite monochromator and proportional counter.

The advance of grafting was checked by scanning electron microscopic (*SEM) images* of cotton fabric samples covered with evaporated gold in vacuum. JEOL JSM 5600LV type instrument was used for taking images.

The determination of the degree of polymerization (DP) was based on the viscosity measurements of the sample dissolved in cupriethylenediamine (Cuen) solution [50].

The tensile strength was measured on fabric samples of 5 cm width using Instron type equipment.

The Swelling = 100 % × $(w_s-w_g)/w_g)$ was determined by weighting the wet grafted samples after blotting them with filter-paper (w_s) and after drying in air (w_g).

The UV-spectroscopy of an aqueous solution of 0.2 mmol dm^{-3} 2,4–D and phenol before and after adsorption on the grafted samples was performed with a JASCO U-550 UV/VIS spectrophotometer.

4. RESULTS AND DISCUSSION

4.1. Effect of irradiation on cotton–cellulose

The degradation of pure cotton-cellulose starts at relatively low doses. As shown in Fig. 2 the degree of polymerization (DP) was 1680 for the untreated sample and it decreased down to 400 already after 5 kGy absorbed dose. The further decrease in DP was not as fast as it was at smaller doses: the DP was 480 after 10 kGy, finally 230 after 40 kGy. The change in tensile strength with dose was not as drastic as it was with DP. Only a slight change in tensile strength was observed up to 40 kGy dose.

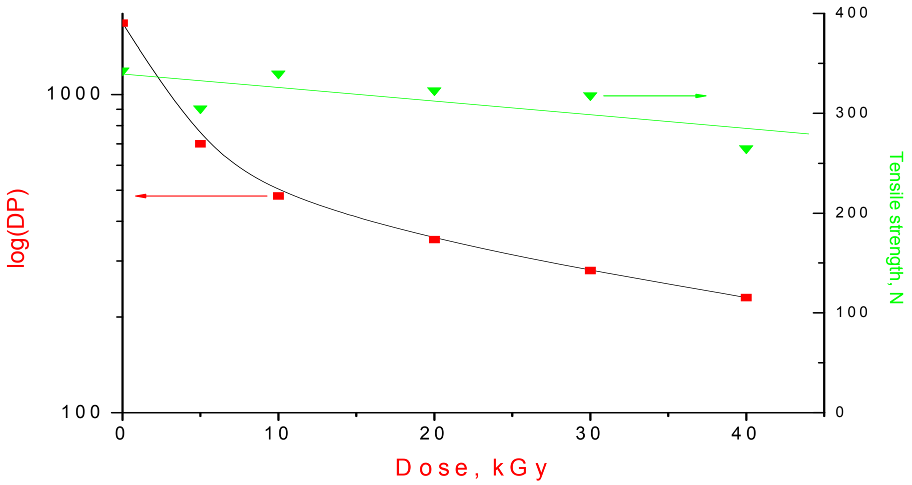

FIG. 2. Degree of polymerization on logarithmic scale (logDP) and tensile strength of cotton–cellulose as a function of dose.

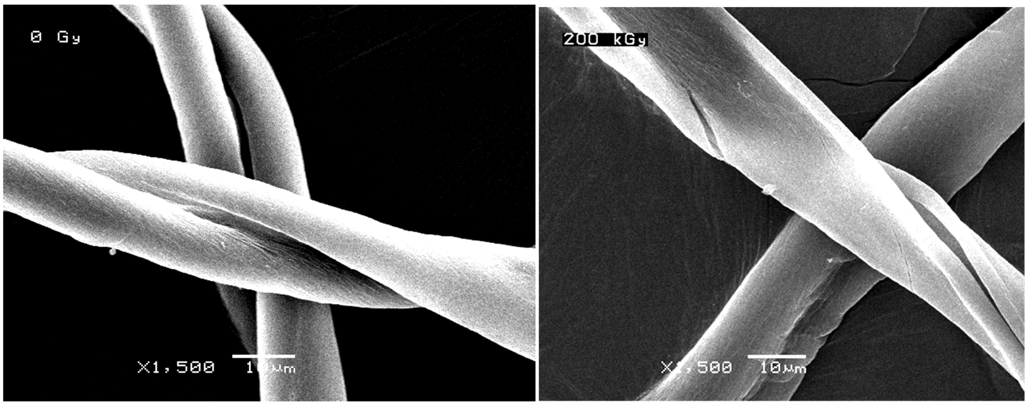

FIG. 3. SEM photos of cotton cellulose–before irradiation (left) and after 200 kGy irradiation (right).

Various methods were used to follow the high–energy radiation induced degradation of cellulose. SEM pictures in Fig. 3 show that after 200 kGy the structure of the fibres has changed and micro cracks can be observed on the surface. Radicals formed on the cellulose chains initiated chain reaction resulting in degradation. As the samples were irradiated in air carbonyl groups were formed and their concentration was followed by measuring the characteristic FTIR absorbance belonging to the carbonyl group (Fig. 4A).

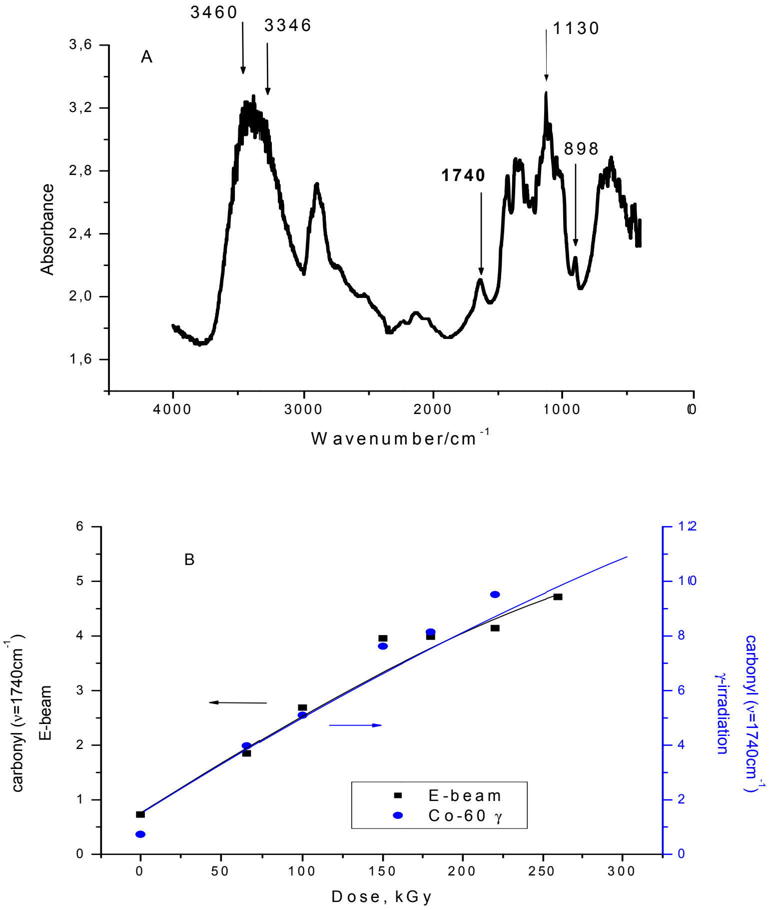

FIG.4. (A) FTIR spectrum of cotton-cellulose; (B) Absorbance of C=O groups versus absorbed dose measured by FTIR at 1740 cm^{-1}.

As Fig. 4A shows the infrared spectrum of cellulose is rather complex due to the large number of different chemical bonds, due to the interactions between the polymer chains, crystalline and amorphous regions, and the absorbed water also complicates the spectrum. The absorbance above 3000 cm^{-1} is basically connected to the OH groups and H atoms. The wide absorption band is due to a large number of overlapping absorption peaks. The well resolved peak at about 2900 cm^{-1} is assigned to the symmetrical CH_2 stretching vibration. The absorbancies in the 1500–500 cm^{-1} range are due to a large number of asymmetrical and deformation vibrations. At about 1700 cm^{-1} appears the C=O stretching vibration. In pure, un-oxidized cellulose this absorbance is weak. The absorbance increases with irradiation of the sample. This absorbance at 1740 cm^{-1} linearly increased by the dose as indicated on Fig. 4B. Due to self-termination reaction of the radicals formed on the cellulose chain the carbonyl concentration was lower with the EB irradiated samples than those with the gamma irradiated samples of about three order of magnitude lower dose rates. Based on the results obtained in radiation degradation doses above 40 kGy were never applied.

4.2. Grafting

4.2.1. Pre-irradiation grafting

The effect of dose, grafting time, temperature and monomer concentration in grafting solution was studied. The effect of monomer structure and the structure of the trunk material were also studied. As mentioned in the introduction, in the case of PIG some degradation of the trunk material starts already during irradiation. Therefore, the grafting conditions should be very carefully optimized because during grafting this degradation may continue resulting in samples of pure mechanical stability.

The grafting yield increased almost linearly with the absorbed dose in acrylic acid solution as Fig. 5 shows. However, with this monomer in 2 mol dm^{-3} concentration, the samples started to disintegrate above 20 kGy. Similar phenomena were observed when the effect of grafting time and monomer concentration was studied. Although grafting yield rapidly increased with grafting time, in 1 mol dm^{-3} AAm solution, above 60 minutes the disintegration of the samples started again (Fig. 6). Concerning the effect of monomer concentration with AAc sample irradiated with 20 kGy the disintegration of the samples started above 2 mol dm^{-3} (Fig. 7). In *PIG* the doses applied were below 30 kGy. The mechanical properties of cellulose irradiated with 30 kGy are not much different from those of the unirradiated sample. Therefore it's supposed that the interaction between the irregularities caused by the radiation in the cellulose structure and the monomer together with the swelling of the cellulose in the aqueous solution lead to destruction of the structure resulting in disintegration of the samples.

The presence of crosslinking agent N,N–methylene bis-acrylamide, (BAAm) in the AAm containing grafting solution resulted in a remarkable increase in the grafting yield (Fig. 8). In the case of simple cellulose the grafting yield with only AAm was 70%. Addition of 1% BAAm (with respect to AAm) increased the grafting yield to 155% while with 5% it was ~200%. BAAm resulted in a considerable (50%) decrease in the water uptake as compared to the sample grafted without this additive. In the case of CMC BAAm additive did not result in a considerable improvement in the grafting yield, the yield increased by about 20% (Fig. 8). Here, too, there is a decrease in the water uptake as shown on Fig. 8.

It was supposed that the increase in grafting yield observed in the presence of crosslinking additive is partly due to the homopolymer trapped into the loose crosslinked structure formed in the reaction of AAm and BAAm. This homopolymer may form interpenetrating network resulting in a dense structure. This idea is supported by the fact that the swelling of the sample decreases with increasing grafting yield in the presence of the crosslinking monomer (Fig. 8), although both AAm and BAAm are hydrogel forming monomers.

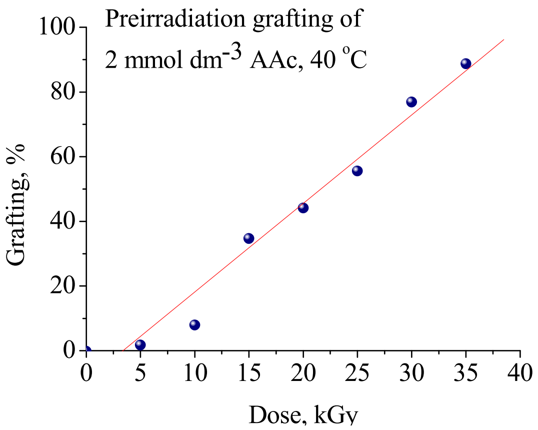

FIG. 5. Effect of absorbed dose on grafting yield in PIG.

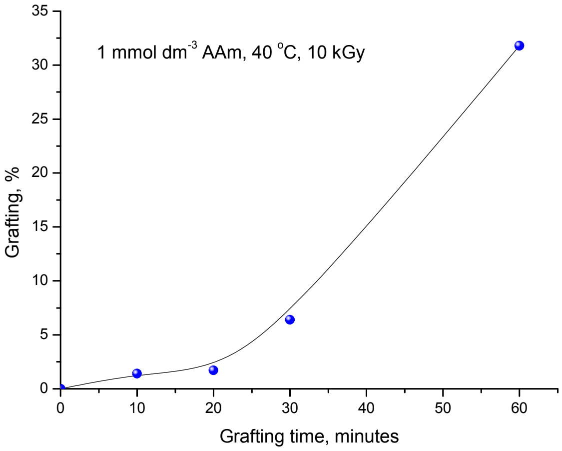

FIG. 6. Effect of grafting time on grafting yield in PIG.

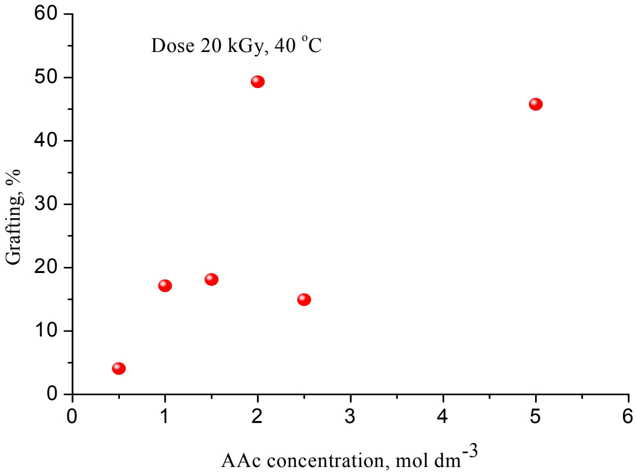

FIG. 7. Effect of monomer concentration on grafting yield in PIG.

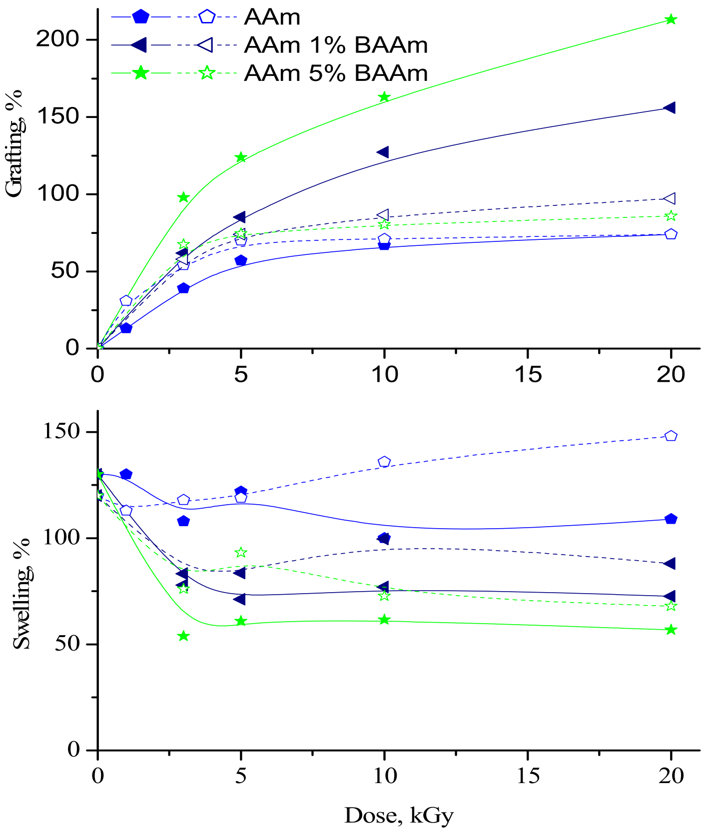

FIG. 8. Effect of bifunctional monomer and the structure of cellulose on grafting yield in PIG. Closed symbols belong to cellulose opened symbols to slightly carboxy-methylated cellulose.

4.2.2. Simultaneous grafting

The mutual grafting procedure is complicated by homopolymer formation. In this case radicals are formed not only on the cellulose but on the monomer, too. The homopolymer formation can be supressed by different additives which react with radicals in the solution: it was used Mohr salt which has a good solubility in water. When optimizing the grafting conditions with mutual grafting of acrylic acid onto cotton-cellulose it was found 0.02 mol dm^{-3} as optimum for Mohr salt concentration.

With increasing dose the grafting yield increased, however, above 25 kGy no further increase was observed (Fig. 9). At higher doses the samples were covered by a thick dense layer of grafted polymer. Polymer formation was excessive in these cases and we called this phenomenon over-grafting. The film which persisted after solvent extraction appears to be crosslinked polymer. Therefore, the values measured for these samples may not be true indication of grafting but rather a combination of grafting and interpenetrating network formation (crosslinked polymer, and trapped homopolymer in the matrix of the cellulosic substrate).

With increasing monomer concentration from 0.5–2 mol dm^{-3} the grafting yield increased (Fig. 10), but above this monomer concentration over-grafting occurred even at lower doses.

4.3. Comparison of pre-irradiation and simultaneous grafting of GMA to cellulose

Glycidyl methacrylate (GMA) grafted samples are often applied for further functionalization with CD. The effect of absorbed dose and monomer concentration were compared for PIG and SG grafted samples.

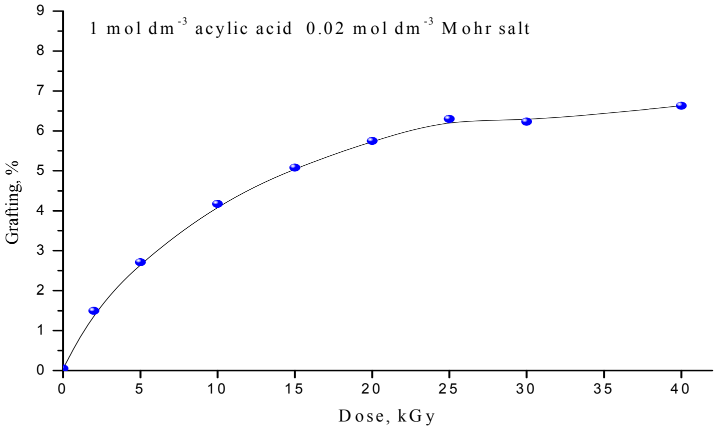

FIG. 9. Effect of dose on grafting yield in SG.

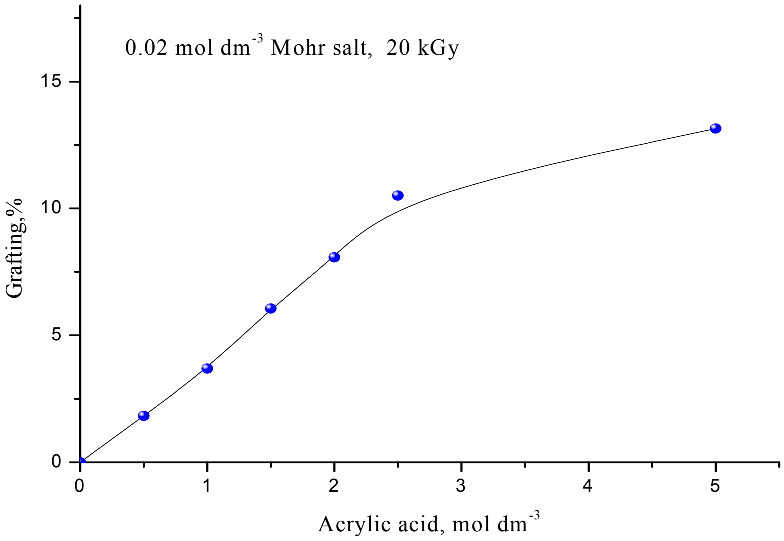

FIG. 10. Effect of monomer concentration on grafting yield in SG.

4.3.1. *Effect of the absorbed dose*

Great difference was found between the samples grafted by PIG and SG concerning the DG. While in the case of PIG grafted in 1.5 mol dm^{-3} GMA solution DG below 75% was measured, SG lead to much higher degrees of grafting, a concentration of 0.38 mol dm^{-3} GMA at doses of 20 kGy resulted in DG (wt %) of over 350% (Fig. 11).

The grafting of GMA on cotton was also clearly observed using FTIR spectroscopy. The IR spectrum of GMA shows absorption peaks at 907 cm^{-1} due to the stretching vibration of the epoxy group, at 1728 cm^{-1} due to the carbonyl group and at 1153 and 1255 cm^{-1} because of the C–O stretching of the ester group. The progress of grafting was observed by following the change in the absorbance assigned to the carbonyl group at 1728 cm^{-1} appearing in the spectrum of GMA, since there are no peaks in this region in the spectrum of cellulose.

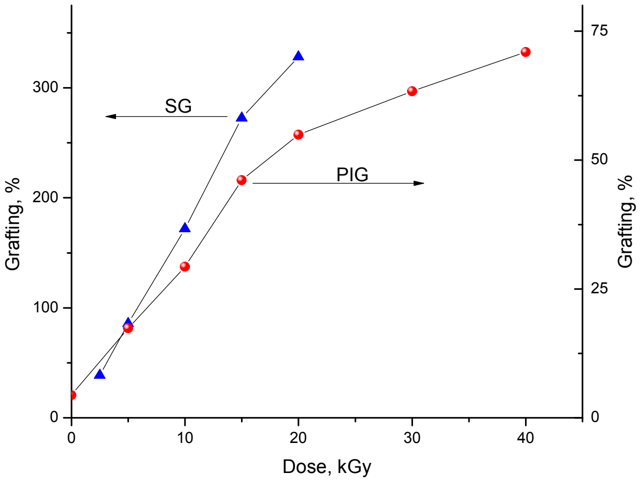

FIG. 11. Degree of grafting as a function of the absorbed dose, SG grafted in a 0.38 mol dm^{-3} GMA solution, PIG grafted at 50 °C for 1 h in 1.5 mol dm^{-3} GMA grafting solution.

Although the FTIR spectra for simultaneously grafted fibres could be expected to be the same as for the pre-irradiated grafted fibres, there is a remarkable difference (Fig. 12). The spectra of the SG samples show some extra peeks in the 2900–3000 cm^{-1} and in the 1600–1500 cm^{-1} regions. These peeks demonstrate the incorporation of *styrene homopolymer suppressor* co-grafted to the cellulose. A similar case was already reported by Badawy and co-workers [51] in the simultaneous grafting of acrylonitrile on cellulose in the presence of styrene. In their experiments small amounts of styrene were also consumed serving as a comonomer in the graft copolymerization reaction.

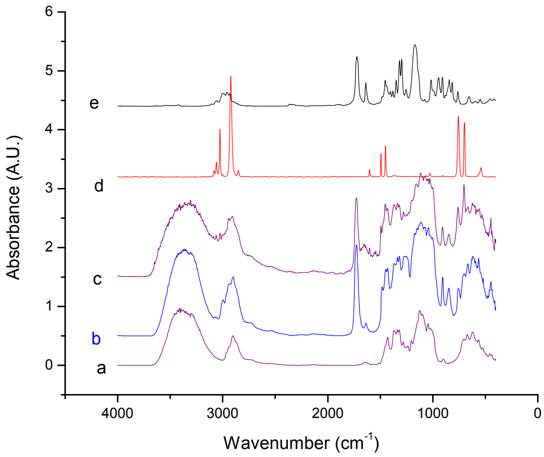

FIG. 12. FTIR spectra of a: cellulose, b: GMA-grafted cellulose using PIG, c: GMA-grafted cellulose using SG, d: styrene, e: GMA.

For both PIG and SG the degree of polymerization (DG) increases with the absorbed dose although the reaction mechanism is different. SG leads to a higher DG than PIG at the same dose.

In PIG during the pre-irradiation phase, the amount of generated radicals is expected to be linearly dependent on absorbed dose. These radicals will then react with the oxygen and form peroxy compounds. However, a part of the radicals decays in self-termination or another reaction (e.g. reacting with some impurities). Dissociation of the peroxy compounds by heating the grafting reaction mixture initiates grafting more or less the same time at all peroxy groups and chains can start growing simultaneously. An important side effect is degradation since the sample is irradiated directly, for this reason 30–40 kGy dose is a practical maximum.

Together with radical formation there is a second effect of irradiation that is the degradation of the cellulose, the extent of degradation also increasing with the dose. At an absorbed dose of 32 kGy the degree of polymerization (DP) of cellulose has already decreased by a factor 8 [25] and at 50 kGy the DP decreased to such an extent that the tensile strength of the cellulose is reported to be just half of its initial value [43]. Since such a drastic decrease in mechanical properties is not desired, 40 kGy is recommended as an absolute maximum value.

At PIG the slope of the DG versus dose curve is decreasing for higher absorbed doses, probably since higher concentrations of radicals will have an increased chance to follow other reaction routes (decay, degradation).

For SG on the other hand, radiation creates radicals both in the solvent molecules and on the cellulose sample. These solvent radicals may react with both the GMA and with the cellulose substrate. This leads to the formation of grafted PGMA chains as well as homopolymer (in spite of homopolymer suppressor added). After some time, the surface is completely covered with PGMA which blocks the further penetration of GMA inside the fibre. Most possibly, further irradiation will then mainly result in a thickening film of PGMA homopolymer. At 5 kGy dose, there is already a DG (M%) of approx. 100%, which means that for every present AGU there is a GMA molecule. The whole reaction happens in one step in a closed system and more radicals will result in a polymerization reaction.

4.3.2. Effect of monomer concentration

Increasing monomer concentration resulted in increase in DG both in PIG and in SG. Samples procured upon the same doses and monomer concentrations have much higher yield in SG as in PIG. In PIG, the highest DG, about 65%, was measured when GMA–monomer concentration was 2 mol dm^{-3} (Fig. 13), in SG more 300% DG was obtained in solution containing 1.5% monomer.

For PIG, a maximum DG is reached at a 2 mol dm^{-3} GMA concentration. Initially, as the concentration of reactant (GMA) increases, the polymerization rate increases as well, and more GMA is grafted on cellulose. At higher concentrations, viscosity effects start playing a role and also homopolymerization may occur by a radical transfer mechanism, decreasing the concentration of monomer available for the grafting reaction and slowing down the grafting.

For SG, the yields are so high: at 1 mol dm^{-3}, the apparent DG (M%) exceeds 200% (while in PIG this it is approx. 40–70%). Together with the visual assessment this leads to the belief that there is already a significant amount of homopolymer present, rendering experiments at even higher concentrations inaccurate. Concentrations higher than 0.5 mol dm^{-3} are thus not recommended.

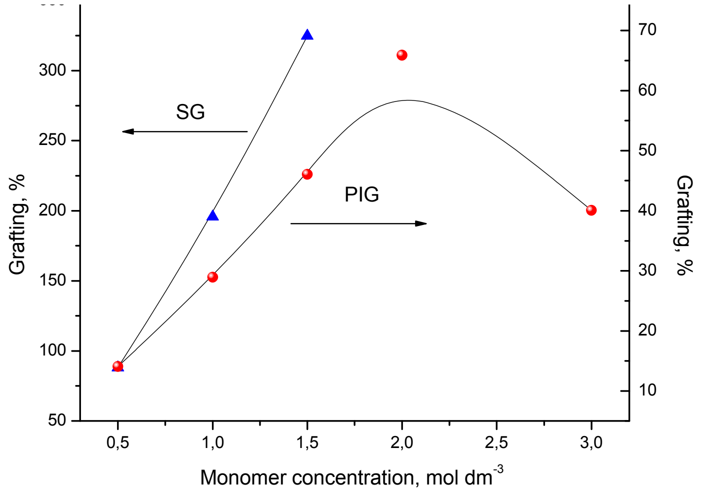

FIG. 13. Degree of grafting as a function of the GMA-monomer concentration. PIG: 20 kGy, 50 °C, 1 h, SG: 5 kGy.

4.3.3. Immobilization of β-cyclodextrin during SG and adsorption properties of the samples

Further functionalization of the GMA grafted samples by CD using chemical methods resulted in a low degree of immobilization for CD. The experiments were more successful when CD was added directly to the grafting solvent mixture in SG. The surface of the samples grafted in the presence of CD (Fig. 14) was different from those grafted without CD. The small pearls appearing on the surface of the fibres indicate the formation of CD polymer.

The degree of immobilization was followed by gravimetry; however, the change in the adsorption properties was a more direct indication of the presence of immobilized CD as indicated on Fig. 15. Grafting improved the adsorption properties of cellulose and this effect was more pronounced with samples prepared by SG than with those prepared by PIG.

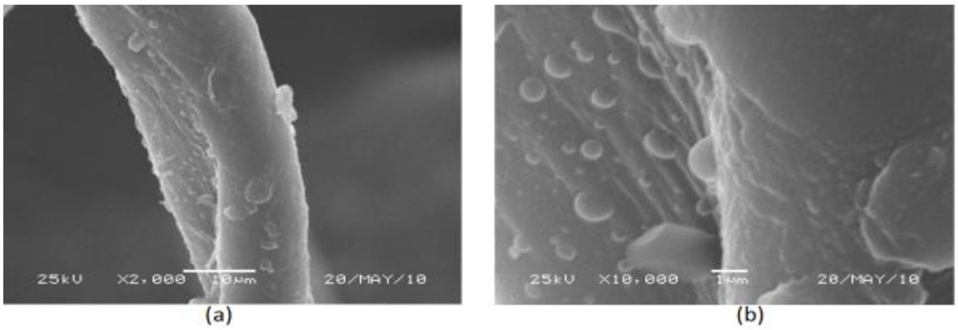

FIG. 14. Surfaces of fibres simultaneously grafted with CD. Magnifications (a) X2000 and (b): X10 000.

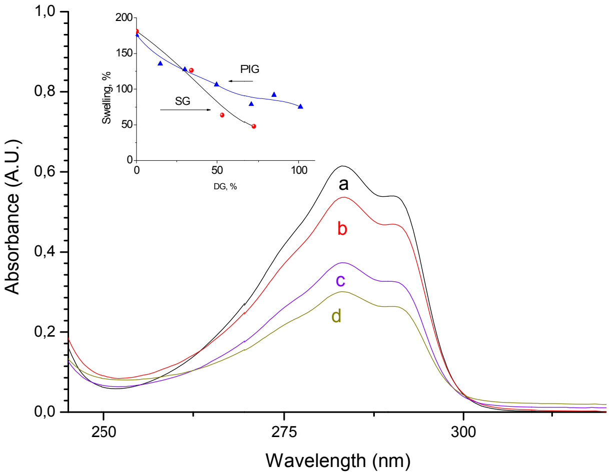

FIG. 15. UV spectra measured in aqueous solution of 2,4–D; a: before, and after adsorption on grafted cellulose using b: PIG, c: SG and d: SG + CD. All DGs were approx. 50% and each sample had approx. the same weight. In approx. the same weight Inset: correlation between swelling in water and DG of pre-irradiated grafted and simultaneously grafted and simultaneously grafted samples.

Experiments for measuring swelling in water were carried out to demonstrate the hydrophilicity of the grafted material. Due to the hydrophobic properties of GMA the swelling in water decreased almost linearly with the DG of the sample. For SG this decrease is significantly larger than for PIG. This is probably because, for the same DG, there is more GMA present on the fibre's surface for SG than for PIG, hindering the fibre's interior for water adsorption. This might be an advantage for filtering purposes, as most contaminants are more hydrophobic. The adsorption properties were tested using UV/VIS spectroscopy and proved the previous supposition. Samples grafted using SG due to their more hydrophobic nature showed better results than the samples grafted using PIG. The functionalization by CD resulted in a further increase in adsorption capacity.

5. CONCLUSIONS

The radiation induced degradation of cotton-cellulose starts at very low doses (5–10 kGy) resulting in a decrease in DP. However, the degradation does not result in a significant change in the mechanical properties.

Optimum conditions for obtaining highest grafting yield with low degradation depend on the monomer structure both for pre-irradiation grafting and for simultaneous grafting.

In the case of pre-irradiation grafting for acrylamide, acrylic acid, and N,N–methylene bis-acrylamide BAAm the highest grafting yield was obtained at: irradiation with 20 kGy absorbed dose, grafting in solution with 2 mol dm^{-3} monomer concentration, at 40°C 60 minutes. For glycidyl methacrylate (GMA) the optimum conditions were: 40 kGy absorbed dose, grafting in solution with 1.5 mol dm^{-3} monomer concentration, at 50°C 60 minutes.

In the case of simultaneous grafting for acrylamide, acrylic acid and BAAm the highest grafting yield was obtained at: irradiation with 20 kGy absorbed dose, monomer solution with 2 mol dm^{-3} concentration, room temperature. For glycidyl methacrylate (GMA) the optimum conditions were: 5 kGy absorbed dose, monomer solution with 0.38 mol dm^{-3} concentration, room temperature.
The swelling in water of cotton-cellulose can be increased by grafting with acrylamide, acrylic acid and N,N'–methylene bis-acrylamide, it can be decreased by grafting with glycidyl methacrylate (GMA). The first three monomers can be applied for adsorption of heavy metal ions. GMA grafted cellulose functionalized with cyclodextrin can be applied for the adsorption of phenol and its derivatives.

The adsorption properties tested using UV/VIS spectroscopy proved to be better for samples grafted with GMA using SG due to their more hydrophobic nature than the samples grafted using PIG. The functionalization by CD resulted in a further increase in adsorption capacity.

Using the mutual grafting method at higher doses the samples were covered by a thick layer while in pre-irradiation method the samples disintegrated. Both phenomena can be called over-grafting. The difference in the appearance of over-grafting between mutual and pre-irradiation grafting is due to the difference in the reaction mechanism. During irradiation radicals are produced not only on the surface of the cellulose but also inside. In the pre-irradiation technique peroxide groups are incorporated both inside and outside. In the heated solution initiation occurs both outside and inside as the monomer could diffuse inside the fibres swollen in aqueous medium. The growing chains inside the fibres cause disintegration. In the case of mutual grafting cellulose radicals initiate the grafting. The grafting starts at surface of the cellulose fibres and the long grafted chains form a dens film on the surface of the fibres forming a barrier layer hindering the diffusion of further monomer molecules inside the fibre.

REFERENCES

[1] JONES, G. K., “Applications of radiation chemistry to understand the fate and transport of emerging pollutants of concern in coastal waters”, PhD dissertation, North Caroline State University, Raleigh, North Carolina (2007).
[2] ZHOU, D., ZHANG, L., ZHOU, J., GUO, S., Cellulose/chitin beads for adsorption of heavy metals in aqueous solution, Water Res. **38** (2004) 2643-2650.
[3] SHIBI, I.G., ANIRUDHAN, T.S., Polymer-grafted banana (Musa paradisiaca) stalk as an adsorbent for the removal of lead (II) and cadmium(II) ions from aqueous solutions: kinetic and equilibrium studies, J. Chem. Technol. Biotechnol. **81** (2006) 433-444.
[4] PETERNELE, W.S., WINKLER-HECHENLEITNER, A.A., GÓMEZ PINEDA, E.A., Adsorption of Cd(II) and Pb(II) onto functionalized formic lignin from sugar cane bagasse, Biores. Technol. **68** (1999) 95-100.

[5] KARNITZ, JR., O., GURGEL, L.V.A., PERIN DE MELO, J.C., BOTARO, V.R., SACRAMENTO MELO, T.M., DE FREITAS GIL, R.P., GIL, L.F., Adsorption of heavy metalion from aqueous single metal solution by chemically modified sugarcane bagasse, Biores. Technol. **98** (2007) 1291-1297.

[6] VAUGHAN, T., SEO, C.W., MARSHALL, W.E., Removal of selected metal ions from aqueous solution using modified corncobs, Bioresour. Technol. **78** (2001) 133-139.

[7] GURGEL, L.V.A., KARNITZ JÚNIOR, O., DE FREITAS GIL, R.P., GIL, L.F., Adsorption of Cu(II), Cd(II) and Pb(II) from aqueous single metal solutions by cellulose and mercerized cellulose chemically modified with succinic anhydride, Bioresour. Technol. **99** (2008) 3077-3083.

[8] ABDEL-AAL, S.E., GAD, Y.H., DESSOUKI, A.M., The use of wood pulp and radiation-modified starch in wastewater treatment, J. Appl. Polym Sci. **99** (2006) 2460-2469.

[9] O'CONNELL, D.W., BIRKINSHAW, C., O'DWYER, T.F., A modified cellulose adsorbent for the removal of nickel (II) from aqueous solutions, J. Chem. Technol. Biotechnol. **81** (2006) 1820-1828.

[10] NAVARRO, R.R., SUMI, K., FUJI, N., MATSUMURA, M., Mercury removal from wastewater using porous cellulose carrier modified with polyethyleneimine, Water Res. **30** (1996) 2488-2494.

[11] KUBOTA, H., SHIGEHISA, Y., Introduction of amidoxime groups into cellulose and its ability to adsorb metal ions, J. Appl. Polym. Sci. **56** (1995) 147-151.

[12] TAMADA, M., SEKO, N., YOSHII, F., Application of radiation-graft material for metal adsorbent and crosslinked natural polymer for healthcare product, Radiat. Phys. Chem. **71** (2004) 223-227.

[13] LIU, S., SUN, G., Radical graft functional modification of cellulose with allyl monomers: Chemistry and structure characterization, Carbohyd. Polym. **71** (2008) 614-625.

[14] MANDAL, P.K., MAJUMDAR, R., MUKHERJEE, K.K., CHAKRABARTI, O., MAITI, H.S., Active cellular perform derived from stems of jute and sticks of cane and their suitability for bulk porous Si/SiC ceramics, J. Porous Mater. **16** (2009) 157-163.

[15] RODRÍGUEZ, A., SERRANO, L., MORAL, A., JIMÉNEZ, L., Pulping of rice straw with high-boiling point organosolvents, Biochem. Eng. J. **42** (2008) 243-247.

[16] KHAN, F., AHMAD, S.R., KRONFLI, E., UV-radiation induced preirradiation grafting of methyl methacrylate onto lignocellulose fiber in an aqueous medium and characterization, J. Appl. Polym. Sci. **91** (2004) 1667-1675.

[17] ORLANDO, U.S., BAES, A.U., NISHIJIMA, W., OKADA, M., Preparation of chelating agents from sugarcane bagasse by microwave radiation as an alternative ecologically benign procedure, Green Chemistry **4** (2002) 555-557.

[18] DUBEY, K.A., PUJARI, P.K., RAMNANI, S.P., KADAM, R.M., SABHARWAL, S., Microstructural studies of electron beam-irradiated cellulose pulp, Radiat. Phys. Chem. **69** (2004) 395-400.

[19] YANG, C., SHEN, Z., YU, G., WANG, J., Effect and aftereffect of gamma radiation pretreatment on enzymatic hydrolysis of wheat straw, Biores. Technol. **99** (2008) 6240-6245.

[20] CHMIELEWSKI, A.G., HAJI-SAEID, M., AHMED, S. Progress in radiation processing of polymers, Nucl. Instr. Meth. Phys. Res. B **236** (2005) 44-54.

[21] ANDREOZZI, L., CASTELVETRO, V., GIARDELLI, G., CORSI, L., FAETTI, M., FATARELLA, E., ZULLI, F., Free radical generation under plasma treatment of cotton fibers and their initiation efficiency in surface-graft polymerization, J. Colloid Interface Sci. **289** (2005) 455-465.

[22] ARTHUR, JR., J.C., Derivatives of cellulose. Reactions induced by high-energy radiation, High Polym. **5** (1971) 937-975.

[23] ARTHUR, JR., J.C., HINOJOSA, Oxidative reactions of cellulose initiated by free radicals, J. Polym. Sci. C **36** (1971) 53-71.

[24] ERSHOV, B.G., The radiation chemistry of cellulose, Russ. Chem. Rev. **53** (1984) 1195-1207.

[25] ERSHOV, B.G., Radiation-chemical transformation of cellulose, Russ. Chem. Rev. **67** (1998) 315-334.

[26] ERSHOV, B.G., ISAKOVA, O.A., Formation and thermal transformations of free radicals in gamma radiolysis of cellulose, Russ. Chem. Bull. **33** (1984) 1171.

[27] KUZINA, S.I., MIKHAILOV, A.I., The oxidation and thermal transformations of macroradicals in gamma irradiated cellulose, Russ. J. Phys. Chem. **80** (2006) 1666-1670.

[28] KOKOT, S., STEWART, S., An exploratory-study of mercerized cotton fabrics by DRIFT spectroscopy and chemometrics, Textil Res. J. **65** (1995) 643-651.

[29] TAKÁCS, E., WOJNÁROVITS, L., FÖLDVÁRY, CS., HARGITTAI, P., BORSA, J., SAJÓ, I., Radiation activation of cotton–cellulose prior to alkali treatment, Res. Chem. Intermed. **27** (2001) 837-845.

[30] TAKÁCS, E., WOJNÁROVITS, L., BORSA, J., PAPP, J., HARGITTAI, P., KORECZ, L.,. Modification of cotton-cellulose by preirradiation grafting, Nucl. Instrum. Meth. Phys. Res. B **236** (2005) 259-265.

[31] CHAUHCAN, G.S., GULEIRA, L.K., SHARMA, R., Synthesis, characterization and metal sorption studies of graft copolymers of cellulose and glycidyl methacrylate and some comonomers, Cellulose **12** (2005) 97-110.

[32] MAO, C., QUI, Y., SANG, H., MEI, H., ZHU, J., SHEN, S., LIN, S., Various approaches to modify biomaterial surfaces for improving hemocompatibility, Adv. Colloid Interface Sci. **110** (2004) 5-17.

[33] PEKEL, N., YOSHII, F., KUME, T., GÜVEN, O., Radiation crosslinking of biodegradable hydroxypropylmethylcellulose, Carbohyd. Polym. **55** (2004) 139.

[34] CHOI, J.I., LEE, H.S., KIM, J.H., LEE, K.W., LEE, J.W., SEO, S.J., KANG, K.W., BYUN, M.W., Controlling the radiation degradation of carboxymethylcellulose solution, Polym. Degrad. Stab. **93** (2008) 310-315.

[35] SHIN, S.J., SUNG, Y.J., Improving enzymatic hydrolysis of industrial hemp (Cannabis sativa L.) by electron beam irradiation, Radiat. Phys. Chem. **77** (2008) 1034-1038.

[36] TAKÁCS, E., MIRZADEH, H., WOJNÁROVITS, L., BORSA, J., MIRZATAHERI, M., BENKE, N., Comparison of simultaneous and pre-irradiation grafting of *N*-vinylpyrrolidone to cotton-cellulose, Nucl. Instrum. Methods Phys. Res. B **265 (**2007) 217-220.

[37] KUMAR, V., BHARDWAY, Y.K., RAWAT, K.P., SABHARWAL, S., Radiation-induced grafting of vinylbenzyltrimethylammonium chloride (VBT) onto cotton fabric and study of its anti-bacterial activities, Radiat. Phys. Chem. **73** (2005) 175.

[38] BENKE, N., TAKÁCS, E., WOJNÁROVITS, L., BORSA, J., Pre-irradiation grafting of cellulose and slightly carboxymethylated cellulose (CMC) fibers, Radiat. Phys. Chem. **76** (2007) 1355-1359.

[39] BHATTACHARYA, A., MISHRA, B.N., Grafting: a versatile method to modify polymers. Techniques, factors and applications, Prog. Polym. Sci. **29** (2004) 767.

[40] SPINKS, J.W.T., WOODS, R.J., An Introduction to Radiation Chemistry, John Wiley and Sons, New York. (1990).

[41] WOODS, R.J., PIKAEV, A.K., Applied Radiation Chemistry: Radiation Processing, John Wiley and Sons, Inc. New York. (1994).

[42] VISMARA, E., MELONEA, L., GASTALDI, G., COSENTINOB, C., TORRI, G., Surface functionalization of cotton cellulose with glycidyl methacrylate and its application for the adsorption of aromatic pollutants from wastewaters, J. Hazard. Mater., **170** (2009) 798–808.

[43] SEKINE, A., SEKO, N., TAMADA, M., SUZUKI, Y., Biodegradable metal adsorbent synthesized by graftpolymerization onto nonwoven cotton fabric, Radiat. Phys. Chem. **79** (2010) 16-21.

[44] WOJNÁROVITS, L., TAKÁCS, E., Irradiation treatment of azo-dye containing wastewater: an overview, Radiat. Phys. Chem. **77** (2008) 225-244.

[45] VONCINA, B., LE MARECHAL, A., Grafting of cotton with beta-cyclodextrin via poly(carboxylic acid), J. App. Polymer Sci. **96** (2005) 1323-1328.

[46] CRINI, G., Kinetic and equilibrium studies on the removal of cationic dyes from aqueous solutions by adsorption onto a cyclodextrin polymer, Dyes and Pigments **77** (2008) 415-426.

[47] ABDEL-HALIM, E.S., FOUDA, M.M.G., HAMDY, I., ABDEL-MOHDY, F.A., EL-SAWY, S.M., Incorporation of chlorohexidin diacetate into cotton fabrics grafted with glycidyl methacrylate and cyclodextrin, Carbohydrate Polymers, **79** (2010) 47-53.

[48] RÁCZ, I., DEÁK, I., BORSA, J., Fibrous carboxymethylcellulose by pad-roll technology, Textil Res. J. **65** (1995) 348-354.

[49] NELSON, M.L., ROUSSELLE, M.A., CANGERNI, S.I., TROUARD, P., The iodine sorption test, factors affecting reproducibility and a semimicro adaptation, Textil Res. J. **40** (1970) 872-880.

[50] TAKÁCS, E., WOJNÁROVITS, L., BORSA, J., FÖLDVÁRY, CS., HARGITTAI, P., ZÖLD, O., Effect of γ-irradiation on cotton-cellulose, Radiat. Phys. Chem. **55** (1999) 663-666.

[51] BADAWY, S.M., DESSOUKI, A.M., NIZAM, EL-DIN, H.M., Direct pyrolysis mass spectrometry of acrylonitrile-cellulose graft copolymer prepared by radiation-induced graft polymerization in presence of styrene as homopolymer suppressor. Radiat. Phys. Chem. **61** (2001) 143–148.

SYNTHESIS OF RADIATION GRAFTED POLYMER MATRICES FOR SEPARATION AND INDUSTRIAL APPLICATIONS

Y.K. BHARDWAJ, K. VIRENDRA, N.K. GOEL, K.S.S. SARMA, S. SABHARWAL

Radiation Technology Development Division
Bhabha Atomic Research Centre
Trombay, MUMBAI-400 085
INDIA

Abstract

Grafting of acrylonitrile onto non-woven porous polypropylene fibre sheet using electron beam was carried out by post-irradiation grafting. Grafting extent of ~125% was achieved. The grafted nitrile groups were amidoximated and studied for uranium uptake from sea water and heavy metal ions (Co^{2+}, Ni^{2+}, Mn^{2+}, and Cd^{2+}) from aqueous solutions. Adsorption and elution of adsorbed ions in suitable eluents was studied. The grafting process was upgraded to pilot scale to obtain 1x1 m^2 sheets. Mutual radiation grafting technique was used for grafting of vinylbenzyltrimethyl ammonium chloride, [2-(methacryloyloxy)ethyl] trimethylammonium chloride and [2-(acryloyloxyethyl)]trimethylammonium chloride onto cotton cellulose substrate. The grafted matrices showed significantly higher water uptake and good water retention properties. The antibacterial efficacy of the grafted products was found to be a function of extent of grafting and the type of bacteria (*Escherichia coli*, *Pseudomonas flourescens*, *Staphylococcus aureus* and *Bacillus cereus*). PVBT-*g*-cotton was studied for its protein adsorption behaviour in continuous column process using Bovine serum albumin (BSA) as a model protein. Mutual radiation grafting technique was used to graft acrylic acid on micrometer thick micro-porous polypropylene membrane. Contact angle measurement studies showed that initial grafting as well as radiation treatment of poly(propylene) in aqueous medium and in presence of Mohr's salt enhances its affinity towards the grafting solution. The enhancement in the polar component of surface energy of treated polypropylene membrane is the primary cause of grafting enhancement. The membranes grafted to an extent of ~20% were found to perform comparably with the battery separator presently being used by battery industry. Acrylic acid was grafted to Teflon scrap by mutual radiation grafting technique. The grafting extent decreased with increasing dose rate and thickness of the substrate. The SEM studies indicate significant difference in bulk and interface due to change in thickness of the Teflon backbone.

1. OBJECTIVE OF THE RESEARCH

The grafted products have potential applications in several industrial applications. The objective of the present investigation was to synthesize radiation grafted products which have immediate or potential applications in industry. The investigation included standardizing various experimental parameters starting from choice of trunk polymer and monomer to be grafted, dose, dose rate, presence of additives and ambient condition etc. to achieve desired grafting extent.

2. INTRODUCTION

Graft polymerization is an easy and efficient technique for modifying base polymers as it results in superposition of properties of backbone and the pendent grafted chains. Grafting can be initiated conventionally using suitable redox system [1] or using radiation [2]. Radiation grafting is an easy and highly efficient procedure for modifying the properties of polymeric substrates of synthetic as well as natural origin [3] and offers some unique advantages over the conventional chemical grafting method [4]. Radiation grafted co-polymers have been investigated for spectrum of applications like metal absorption [5, 6], separation purposes [7, 8], biotechnology [9, 10], electrochemical applications such as electro-dialysis [11], battery separator [12], as solid polymer electrolyte in fuel cells [13, 14] and bio-medical applications [15, 16]. For separation and purification purpose chelating groups like amidoxime [17, 18] have shown to form stable complex with heavy metal ions like uranium, vanadium, cadmium, copper and ion exchange type of matrices have also been tried for the purpose [19, 20].

There are many well-known chemicals, which act as germicides, e.g. halogens, alcohols, peroxygen compounds (H_2O_2, peracetic acid), phenolic compounds, aldehydes and ionic surfactants. Among the various classes of surfactants, particularly the cationic quaternary ammonium compounds are among the most effective germicides. In recent years, trialkyl ammonium chlorides have been reported to possess germicidal effect in dilute aqueous solutions [21]. Thus with a view that radiation grafting of trialkyl ammonium chlorides (Quaternary ammonium salts) like Vinylbenzyltrimethyl ammonium chloride (VBT), [2-(Methacryloyloxy)ethyl]trimethylammonium chloride (MAETC) and [2-(Acryloyloxyethyl)]trimethylammonium chloride (AETC) onto finished cotton cloth may lead to incorporation of anti-bacterial into cotton, grafting of these monomers onto cotton was investigated.

Ion exchange membranes have been investigated for their suitability as battery separator because of their durability, long life, high charge density and appreciable ion exchange capacity at optimum water content which is the most desirable property of the separator membranes [22]. The mutual radiation grafting technique has been used to graft acrylic acid onto micrometer thick polypropylene sheet to get proton exchange membranes (PEM). The grafted membranes were tested under actual battery conditions for their electrical properties.

Polytetrafluoroethylene (PTFE) commercially known as Teflon® is known for its many exceptional properties [23, 24]. However these exceptional properties make its disposal difficult as it does not undergo any degradation under natural conditions. Grafting of acrylic acid onto PTFE scrap was carried out to obtain a matrix which can uptake dyes from industrial effluents and wastewater. This approach would mitigate environmental pollution in two ways by utilizing the PTFE scrap and using the grafted scrap to treat industrial effluents.

3. MATERIALS AND METHODS

3.1. Material

Polymer backbone materials non-woven thermally bonded polypropylene (NWPP) with properties given in Table 1 were obtained from a local supplier, micrometer thick polypropylene (PP) was provided by M/s High Energy Batteries, INDIA was a product of 3M®, USA and used as received. Finished cotton cloth, procured from a local supplier, was washed in ethanol followed by boiling in 1% sodium hydroxide solution for three hours. Treated fabric was then repeatedly washed with distilled water until neutral washings were obtained. The cotton samples thus obtained were dried at 50°C and stored in desiccator for further use. Teflon scrap in ribbon form obtained by machining of Teflon rods was procured from local supplier M/s Max Tools Co. The cleaned PTFE scrap had a bulk density = 2.1 g/cm^3, Melting point = 330°C and surface energy = 22 mJ/m^2.

TABLE 1. DETAILS OF THE NWPP SHEET USED FOR GRAFTING

Property	Value
Weight	525 g/m^2
Thickness	2.7 mm
Breaking strength	90 kgf (for 20 cm × 5 cm strip size)
Busting strength	30-35 kg/cm^2
Operable temperature	90°C
Air permeability	280 (L/dm^2/min)

Commercial grade acrylonitrile (AN) from M/s IPCL India and dimethyl formamide (DMF) from M/s SD Fine chemicals, Mumbai were used. Hydroxylamine hydrochloride, (*ar*-vinylbenzyl)trimethylammonium chloride (VBT), a mixture of 3-vinyl and 4-vinyl isomers, [2-(Methacryloyloxy)ethyl]trimethylammonium chloride (MAETC), Mol wt. = 207.7 in 75% aqueous solution, [2-(acryloyloxy)ethyl]trimethylammonium chloride (AETC), 80 wt.% solution in water from Aldrich were used as received. 2-Hydroxyethyl methacrylate (HEMA), Mol wt. 130.14 from Aldrich chemicals (purity > 97%), was further purified by vacuum distillation at 78°C and 5 mmHg pressure.

Acrylic acid (AA) purity >99% and all other chemicals used were from Aldrich. Himedia (India) nutrient broth (M244S) was used for cultivating bacterial culture and Himedia Plate count Agar (M091) was used for bacterial count experiments. *Escherichia coli* JM109, *Pseudomonas fluorescens* (lab isolate), *Staphylococcus aureus* ATCC 6538P, *Bacillus cereus* MTCC 470 cultures were maintained at 4°C. Before the start of experiment, they were grown on nutrient agar for 2 days at 37°C. The isolates were subcultured twice before inoculation. The long-term storage of cultures was done in 20% glycerol (v/v) at -20°C. All the bacterial counts were done on plate count agar, (Himedia, Mumbai, India) incubated at 37°C for 24 h during the course of this work N_2 and O_2 (purity > 99%) were locally procured. Nanopure water from Millipore was used for all experiments.

3.2. Methods

3.2.1. Irradiation method and sources

Electron beam irradiation of NWPP sheets was carried out using an industrial 2 MeV, 20 kW ILU-6 accelerator (Budker Institute of Nuclear Physics, Russia) under following conditions: energy = 1.8 MeV, current = 10 mA and variable conveyor speed. Grafting was carried out using post irradiation technique i.e. sheets were irradiated prior to immersing them in grafting solution. Gamma chambers having ^{60}Co gamma radiation source GC–5000 and GC–900, supplied by M/s BRIT, India were used for irradiation purpose with suitable lead attenuators to achieve dose rate of 0.5–5 kGy h^{-1}.

3.2.2. Radiation grafting

Post irradiation grafting technique was used to graft AN onto NWPP whereas mutual radiation grafting method was used to graft VBT, MAETC, AETC onto cotton cellulose and to graft AA onto PP and Teflon scrap. For post irradiation grafting the NWPP was irradiated using electron beam and dipped in grafting solution of known composition for desired time. For mutual grafting experiments the backbone polymers were dipped in grafting solution in glass stoppered for at least an hour prior to irradiation in gamma chamber for required doses at desired dose rates. Homo-polymer was extracted from the grafted samples using suitable solvent by Soxhlet extraction for 8 hours. The grafted sample was then dried and grafting yield and grafting efficiency were determined gravimetrically using relations

% Grafting = {(weight after grafting - initial weight)/initial weight} × 100 (1)

% Grafting efficiency = monomer grafted/monomer converted to polymer × 100 (2)

3.2.3. Antibacterial assay

To check whether grafted cotton or radiation polymerized polymers of VBT, MAETC & AETC were bactericidal or bacteriostatic in nature; all four bacterial cultures were inoculated to the level of 10^3 cells/mL in nutrient broth individually. Polymers were added (0.1% w/v) to this and incubated at 37°C for 24 h. Samples were withdrawn at regular intervals and growth was checked by measuring turbidity at 600 nm. The samples were also spread plated to count the colonies after incubation. The minimum bactericidal concentration (MBC) was found out by addition of different concentrations of polymer to 0.1 mol dm^{-3} phosphate buffered saline (PBS) (pH 7.0). The cultures were grown in nutrient broth for 18 h and centrifuged at 6000 rpm for 10 min to harvest the cells. The cells were washed twice with PBS and re-suspended in buffer containing polymers. MBC was defined as the lowest concentration at which complete elimination of cells was achieved at 37°C in 24 h. The antibacterial activity of samples grafted to different extents was assayed by colony count method. Cultures were grown; cells were harvested and suspended in similar way as described above for MBC. Aliquots of samples were withdrawn and spread plated on plate count agar to estimate the initial counts. The grafted sample as well as cotton fabric (control) was then added to this suspension and kept on rotary shaker at 37°C. Cell blank was also included in the experiment. Samples were withdrawn after different intervals of time and spread plated.

3.2.4. U(VI) uptake in amidoximated membrane (AO-membrane)

The uptake studies of U(VI) in AO-membrane from aqueous solutions having pH = 4–8 and seawater were carried out using ^{233}U radiotracer. The amount of ^{233}U spiked in seawater and aqueous samples having different pH was 9.54 μg/mL. This amount of ^{233}U was taken to obtain sufficient α-scintillation counts (≈10 000 cpm (counts per minute)) in 50 μL sample of aqueous feed added to liquid scintillation cocktail. In order to keep the pH of aqueous feed unaltered, the known volume of ^{233}U radiotracer solution was dried under the infrared (IR) lamp, and 100 mg/mL $NaHCO_3$ solution was added to prevent the precipitation of uranium from aqueous feed. The uptake of U(VI) in the membrane sample (2 cm × 1 cm) was monitored by liquid scintillation counting of samples (50–100 μL) of feed solution (15 mL) taken before and after equilibration with the membrane. The uptake of U(VI) in the membrane was obtained from following equation:

$$\% \text{ U(VI) uptake} = \{(C_{before}-C_{after})/C_{before}\} \times 100 \qquad (3)$$

where C_{before} and C_{after} are the α-scintillation counts (cps (counts per second)) of ^{233}U in the samples taken from feed solution before and after equilibrating the AO-membrane sample, respectively.

The equilibration time required for optimum uptake of U(VI) in AO-membrane sample was determined by spiking known radioactivity of ^{233}U in 15 mL seawater, and equilibrating this solution with membrane sample (1 cm × 2 cm) with constant stirring using magnetic stirrer at room temperature. The uptake of ^{233}U in the membrane was monitored by α-scintillation counting of 50 μL samples taken from equilibrating solution at regular time intervals. The U(VI) loading capacity of AO-membrane was measured by drying fixed volume of solution containing known concentration of uranyl nitrate ($^{nat}UO_2(NO_3)_2$) spiked with required radioactivity of ^{233}U, and 15 mL of seawater was added to equilibrate the membrane sample of known weight for 250 min with constant stirring. ^{233}U radiotracer sorbed in the membrane samples was obtained from the difference in total radioactivity of ^{233}U in solution and total radioactivity of ^{233}U in solution left after equilibrating the membrane sample. U(VI) loading capacity of the AO-membrane was calculated from the standard radioactivity comparison method, and knowledge of weight of the membrane sample using following equation:

$$\text{U (VI) uptake capacity (mol/g)} = (A_{mem}/A_{std} \times W_{mem}) \qquad (4)$$

where A_{mem} is the radioactivity (cps) of ^{233}U sorbed in the membrane sample, A_{std} is the radioactivity of ^{233}U (cps) of 1 mol of uranium having same proportion of ^{238}U and ^{233}U as used for loading uranium in the membrane, and W_{mem} is the weight of dry membrane sample.

The value of A_{std} was obtained by taking 100 μL stock solution having known concentration of uranium (^{233}U + ^{238}U) in seawater, and subjecting it to liquid scintillation counting as described above.

3.2.5. Na^+ exchange capacity of AO-membrane

The Na^+ exchange capacity of AO-membrane was measured by equilibrating the membrane sample of known weight with 0.1 mol dm^{-3} NaCl containing known amount of ^{22}Na radioactivity for 3–4 h with constant stirring. ^{22}Na radioactivity in the samples was measured by γ-counting using a well-type NaI(Tl) detector based gamma spectrometer. In order to obtain amount of Na^+ ions sorbed in the membrane, the standard sample was prepared by drying required volume of solution containing known amounts of NaCl, containing same proportion of ^{22}Na radioactivity as that used for equilibrating membrane, on Whatman–41 filter paper having same dimensions as that of membrane samples. The amount of Na^+ ions sorbed in the membrane samples was obtained by measuring γ **activities** of membrane samples and standards under identical sample to detector geometry, and comparing the γ **activity** of the membrane sample with that of standard.

Desorption studies were carried by loading the membrane samples with uranium with known radioactivity of ^{233}U as described above. The release of ^{233}U from the AO–membrane sample in to 15 mL well-stirred solution containing known concentration of desorbing reagents was monitored by taking out 50 µL solution as a function of time, and measuring radioactivity of ^{233}U by liquid scintillation counting. HCl (0.25–1.0 mol dm^{-3}), Na_2CO_3 (0.25–1.0 mol dm^{-3}), and $NaHCO_3$ (1.0 mol dm^{-3}) were used as desorbing reagents.

3.2.6. Metal uptake by grafted matrix

The metal ion concentration in the aqueous solution was estimated on DIONEX–500 ion chromatograph system (DX–500, Dionex) using a column ion pack CS5 containing 2% crosslinked micro porous divinylbenzene-styrene hydrophobic resin core agglomerated with totally permeable latex particles of polyvinylbenzyl quaternary ammonium salts that cause actual anion exchange. Oxalic acid was used as mobile phase and detection was done by absorbance method using (PAR) 4-(2-pyridylazo) resorcinol post column reagent, which has λ_{max} at 520 nm. Sample loop of 25 µL was used.

The equilibrium adsorption study was carried out for metal ions (Co^{2+}, Ni^{2+}, Mn^{2+}, Cd^{2+}) by mixing 0.3 g of AMO-g-PP adsorbent in 25 mL metal ion solution of various known concentrations in 125 mL stoppered conical flasks. The flask containing metal ion solution and adsorbent were placed in motorized thermostatic shaker bath and agitated at 25°C for 5 h until equilibrium was reached. The initial and equilibrium metal ion concentrations of different combinations were measured by ion chromatograph. These data obtained was used to calculate the adsorption capacity of the adsorbent (Q_e) using equation 5.

$$Q_e = (C_0 - C_e)*V/(m \times 1000)\ (mg/g) \tag{5}$$

where C_0 and C_e are the initial and equilibrium liquid phase concentration (mg/L); V is volume of metal ion solution used (mL); m is the mass of adsorbent used (g).

The kinetics of adsorption of AMO-g-PP was carried out under similar conditions for different contact time at 200 ppm ion concentration**.**

3.2.7. Adsorption of Bovine serum albumin (BSA)

All the protein-binding experiments were carried out at 4°C temperature in a cold room, as most of the biological applications are generally carried out at low temperature conditions to avoid the degradation of biomolecules.

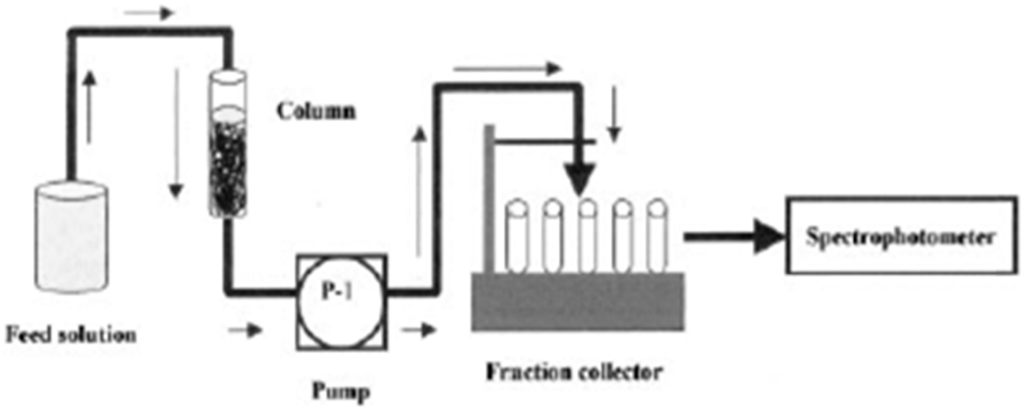

FIG. 1 Schematic representation of experimental setup for protein adsorption data collection in column process.

Schematic representation of experimental setup for protein adsorption data collection in column process is shown in Figure 1. VBT-*g*-cotton cellulose matrix was packed in a glass column (Pharmacia, Sweden) of 50 mm length and 10 mm I.D. The column volume for all the experiments was kept 3.0 mL. The column was equilibrated with buffer solution. The column was attached to a pump (P-1, Pharmacia, Sweden), connected to the fraction collector (Pharmacia, Sweden), wherein effluent passed through the anion exchange PVBT-*g*-Cotton adsorbent was continuously sampled. All experiments were performed at ~0.5 mL/min. flow rate. Protein solution of known concentration was loaded into the column, connected to the buffer solution for washing of unbound protein. After washing, the column was switched to buffer solution containing 1 mol dm^{-3} NaCl solution for elution of bound protein. The concentration of protein in different fractions was estimated by monitoring optical densities of protein solutions at 280 nm referenced with calibration plot using UV−visible spectrophotometer (Chemito UV−Vis 2500, India). Different pH solutions were prepared using buffer solutions namely, pH~4.0 (10 mM acetate buffer), pH~5.6 (10 mM acetate buffer), pH~7.0 (10 mM phosphate buffer), pH~8.6 (10 mM borate buffer).

Binding capacity (BC) and elution percentage (EP) were defined as:

$$\text{BC (mg/g)} = \text{(protein loaded - protein un-adsorbed)/weight of dry adsorbent} \qquad (6)$$

$$\text{EP (\%)} = \text{(amount of protein eluted/ amount of protein adsorbed)} \times 100 \qquad (7)$$

The breakthrough curve was obtained by feeding dilute aqueous solution (0.4 mg/mL) of protein through the column at the flow rate of 0.5 mL/min. The relative concentration of protein in the effluent was plotted against the effluent volume.

The equilibrium binding capacity (EBC) of the anion-exchange grafted matrix was estimated from breakthrough curve using the following relation

$$\text{EBC (mg/g)} = \sum_{i=1}^{s}(C_0 - C_i)V_i/W \qquad (8)$$

where C_0 and C_i are the protein concentration (mg/mL) in the feed and i^th^ fraction of effluent respectively, V_i is the volume (mL) of i^{th} fraction of effluent and W is the weight (g) of the dry anion exchange adsorbent. (i = s when C_i reaches to C_0).

4. RESULTS AND DISCUSSION

4.1. Post-irradiation grafting of AN on NWPP sheet

4.1.1. Parameter standardization for grafting and amidoximation of grafted sheet

After scrutiny of several polymers available in different forms in local market, NWPP was chosen as backbone material because of its ready availability, low cost and higher surface area for grafting of acrylonitrile. The PP backbone was characterized by DSC (endothermic peak at ~165°C corresponding to T_m of PP and by FTIR. Initial experiments indicated post irradiation method using electron beam (EB) to be more suitable for this grafting system. Effect of several experimental variables like dose & dose rate, ambient conditions of irradiation, time of exposure after irradiation, solvent-monomer composition, temperature of grafting, optimum time for grafting and stacking were investigated. Figures 2 and 3 show effect of time spent after irradiation and dose and dose rate on grafting extent. On the basis of this investigation it was found that grafting extent of ~110% could be achieved under following conditions: [25]

- Irradiation for a dose of 200 kGy at the rate of 10 kGy/pass in air;
- Cooling irradiated sheets for 15 minutes in air;
- Grafting solution AN-DMF mixture of composition ratio 70:30 v/v;
- Grafting at a temperature of 60°C.

The cyano group of the grafted NWPP sheet was converted to an amidoxime group by soaking the grafted sheet in 3% hydroxylamine hydrochloride

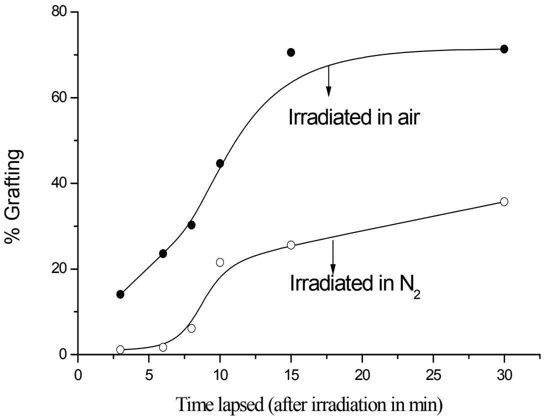

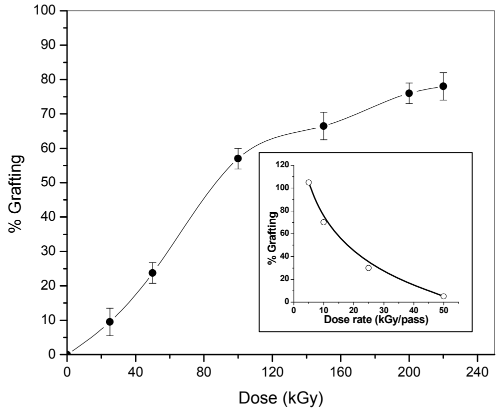

FIG. 2. Effect of retention time of irradiated NWPP on grafting.

FIG. 3. Effect of dose on grafting extent; Dose rate of 10 kGy/pass. Inset: Extent of grafting at different dose rates for total dose of 200 kGy.

The hydroxylamine hydrochloride was neutralized by adding suitable alkaline solution. After the reaction, the sheets were rinsed with water-methanol mixture. ~75–80% of the grafted CN group were amidoximated {-C(NH_2)=NOH} (AO-membrane) within three hours of treatment as estimated by established titration and copper uptake method [26, 27] in accordance with equations below.

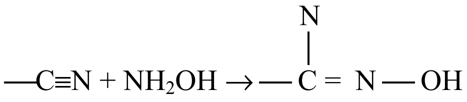

$$—C\equiv N + NH_2OH \rightarrow — \overset{\displaystyle N}{\overset{|}{C}} = N — OH \qquad (9a)$$

$$— NH_2 + HCl \rightarrow NH_3^+Cl^- \qquad (9b)$$

4.1.2. Sorption and desorption of uranium from simulated samples

The alkali treated AO-membrane samples readily sorbed the water, and water uptake capacity of membrane was higher than the weight of dry membrane. The uptake of uranium in the AO-membrane sample from aqueous solutions having pH = 4–8 and seawater was studied by spiking solution with known radioactivity of ^{233}U radiotracer. The uptake of uranium species, existing in these equilibrating solutions, in AO-membrane samples was found to be more than 90%.

The Na^+-exchange capacity of the AO-membrane was found to be $(3.1\pm0.2)\times10^{-4}$ mol/g, which was significantly lower than the calculated functional group density indicating polymer chains bearing amidoxime groups act as weak polyelectrolyte. The saturation uranium uptake in AO-membranes was determined by equilibrating them in solution containing 3–4-fold excess of moles of uranium than the calculated moles of functional groups in the membrane. The profile of sorption rate of uranium in the membrane sample from seawater is shown in Figure 4. Equilibration time was found to be 200 min. The average uranium loading capacity in the AO-membrane was $(1.60\pm0.18)\times10^{-3}$ mole/g [28].

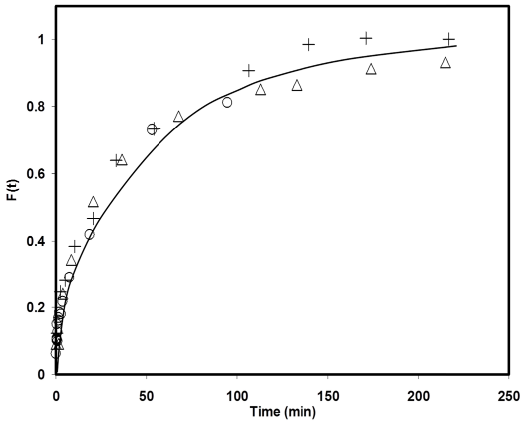

FIG. 4. The fractional attainment of equilibrium uptake of uranium (F(t)) in AO-membrane from seawater spiked with ^{233}U + ^{238}U *as a function of equilibration time.*

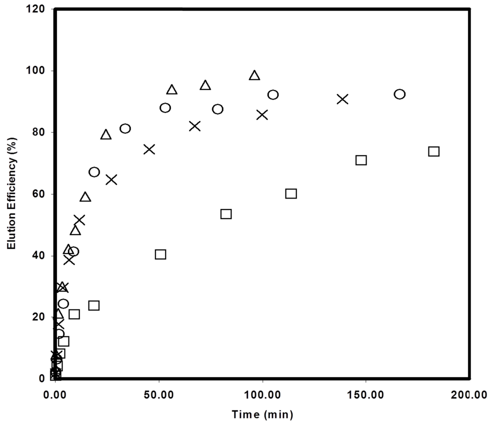

FIG. 5. Desorption of UO_2 *from AO- membrane samples as a function of equilibration time in* Na_2CO_3 *and* $NaHCO_3$*. The symbols* x, Δ, O, *and* □ *represent the* $NaHCO_3$ *(1 M),* Na_2CO_3 *(1 M),* Na_2CO_3 *(0.5 M), and* Na_2CO_3 *(0.25 M).*

The desorption of UO_2^{2+} from membrane was studied by using acids, $NaHCO_3$ and Na_2CO_3. The UO_2^{2+} desorption rate profiles from AO-membrane sample to equilibrating solution containing $NaHCO_3$ or Na_2CO_3 are shown in Figure 5. It can be seen from Fig. 5 that more than 90% of uranium can be desorbed from membrane within 60 min of equilibration time in 0.5 mol dm^{-3} Na_2CO_3 with constant stirring. The desorption of uranium from membrane sample with 1.0 mol dm^{-3} $NaHCO_3$ was found to be 85%, and kinetics of UO_2^{2+} desorption from membrane was slower in $NaHCO_3$ as compared to that in Na_2CO_3. It was observed that UO_2^{2+} loading and subsequent desorption form membrane sample did not require any alkaline treatment or conditioning as the sorption and desorption rate profiles remained same in three cycles.

4.1.3. Metal uptake by amidoximated grafted matrix

Heavy metal ion uptake was monitored by shaking the known weight of grafted matrix with fixed volume of metal ion solution. Figure 6 shows adsorption capacity (Q_e) for metal ions as a function of initial concentration of metal ions (C_i). It can be seen that the adsorption of metal ions follow the order $Cd^{2+} > Co^{2+} > Ni^{2+} > Mn^{2+}$. The adsorption was analyzed using two adsorption models namely, Langmuir [29] and Freundlich isotherms [29]. Different parameters of Langmuir isotherm (Equation 10):

$$C_e/Q_e = 1/K_L + a_L C_e/K_L \qquad (10)$$

where a_L = Langmuir isotherm constant (L/mg)
K_L = Langmuir equilibrium constant (L/g)
C_e = Equilibrium liquid phase ion concentration (mg/L)
Q_e = Equilibrium solid phase ion concentration (mg/g)
K_L/a_L = Maximum adsorption capacity of the adsorbent (mg/g) or theoretical monolayer saturation capacity (q_{max})

and of Freundlich equation obtained are tabulated in Table 2 and Table 3

$$\log Q_e = \log K_f + (1/n) * \log C_e \qquad (11)$$

where K_f= Freundlich constant (L/g) is the relative indicator of adsorption capacity
n = Freundlich exponent is the indication of favourability of adsorption process.

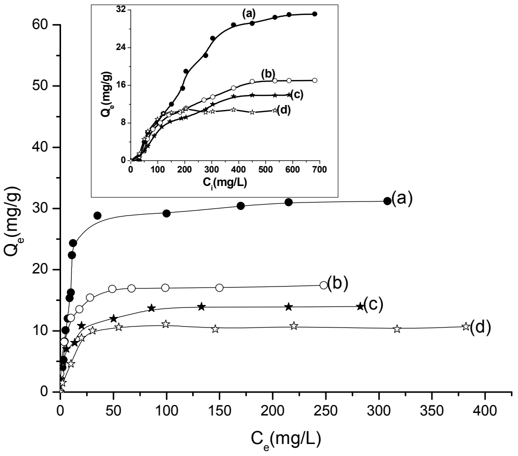

FIG.6. Adsorption isotherm for metal ions (Q_e vs. initial metal ion concentration). (a) Cd^{2+} (b) Co^{2+} (c) Ni^{2+} (d) Mn^{2+}. Inset: Q_e vs. metal ion concentration after adsorption. (a) Cd^{2+} (b) Co^{2+} (c) Ni^{2+} (d) Mn^{2+}.

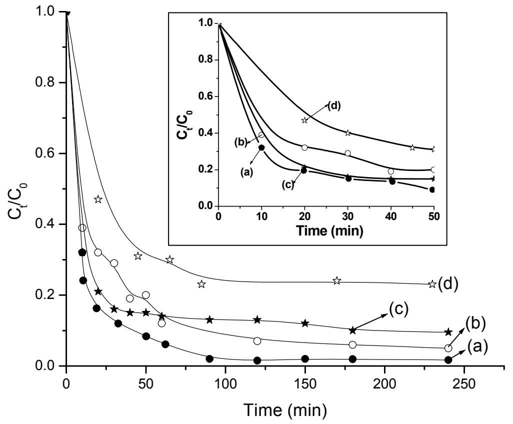

FIG.7. Kinetics of adsorption for metal ions (a) Cd^{2+} (b) Co^{2+} (c) Mn^{2+} (d) Ni^{2+}; initial ion concentration 200 ppm. (Inset: adsorption kinetics at lower time scale (a) Cd^{2+} (b) Co^{2+} (c) Mn^{2+} (d) Ni^{2+}.

Langmuir isotherms were in good agreement with the experimental equilibrium adsorption capacities and also follow the order i.e. $Cd^{2+} > Co^{2+} > Ni^{2+} > Mn^{2+}$. On the other hand Freundlich equation treatment of sorption data for the metal ions showed deviation from linearity and instead showed a two segment relationship.

TABLE 2. LANGMUIR ADSORPTION PARAMETERS OF EB GRAFTED AMO-G-PP ADSORBENT GRAFTING EXTENT ~115% AT 25°C

S. No.	Metal ion	K_L(L/g)	a_L (L/mg)	q_{max} (mg/g)	C.F.*
1.	Cd^{2+}	6.18	0.20	31.58	0.998
2.	Co^{2+}	5.88	0.33	17.57	0.999
3.	Ni^{2+}	2.72	0.19	14.24	0.999
4.	Mn^{2+}	1.91	0.18	10.76	0.998

* *Correlation coefficient.*

TABLE 3. FREUNDLICH ADSORPTION PARAMETERS OF EB GRAFTED AMO-G-PP ADSORBENT GRAFTING EXTENT ~115% AT 25°C

S. No.	Metal ion	K_f (L/g)	n	#C.R. (mg/L)	C.F.*
1.	Cd^{2+}	1.95	1.24	0-300	0.998
2.	Co^{2+}	4.43	2.54	0-215	0.983
3.	Ni^{2+}	4.38	3.93	0-250	0.988
4.	Mn^{2+}	0.79	1.29	0-150	0.989

[#] *Concentration range.*
[*] *Correlation coefficient.*

Adsorption kinetics (Figure 7) shows adsorption rate followed $Cd^{2+} > Mn^{2+} > Co^{2+} > Ni^{2+}$. Among the four ions, Cd^{2+} had the highest adsorption rate; within 1 h more than 90% of the initial 200 ppm Cd^{2+}ions were removed. Meanwhile, Ni^{2+} had the lowest adsorption rate; within 1 h time only up to 70% Ni^{2+} could be removed. It was interesting to see that not only the equilibrium adsorption of the Cd^{2+} ions was highest but also its rate of adsorption was fastest.

Competitive adsorption from aqueous solution containing same concentration (100 ppm) of Cd^{2+}, Co^{2+}, Ni^{2+}, and Mn^{2+} ions was carried out. The equilibrium adsorption from mixed solution followed the pattern $Cd^{2+} > Ni^{2+} > Mn^{2+} > Co^{2+}$ which was different from that obtained in the case of individual ion solution where the order was $Cd^{2+} > Co^{2+} > Ni^{2+} > Mn^{2+}$. These results showed that though uptake of ions like Cd^{2+} were not affected by presence of other metal ions but adsorption of ions like Co^{2+} was affected by presence of other metal ions in the solution [30].

4.1.4. Upgrading of grafting setup for grafting thermally bonded PP sheets

The grafting process developed on laboratory scale was upgraded for grafting sheets of size 1m × 1m. Figure 8 shows the schematic of the grafting setup with all other arrangements for heating, deaeration etc. required for grafting. Figure 9 shows the photograph of the grafting reactor fabricated. The setup is equipped for motorized input of the irradiated sheets to be grafted into the grafting tank for low exposure to monomer fumes during grafting and push fit type of lid for low escape of monomer during grafting. The setup was used for grafting of sheets of desired size and was found to perform satisfactorily.

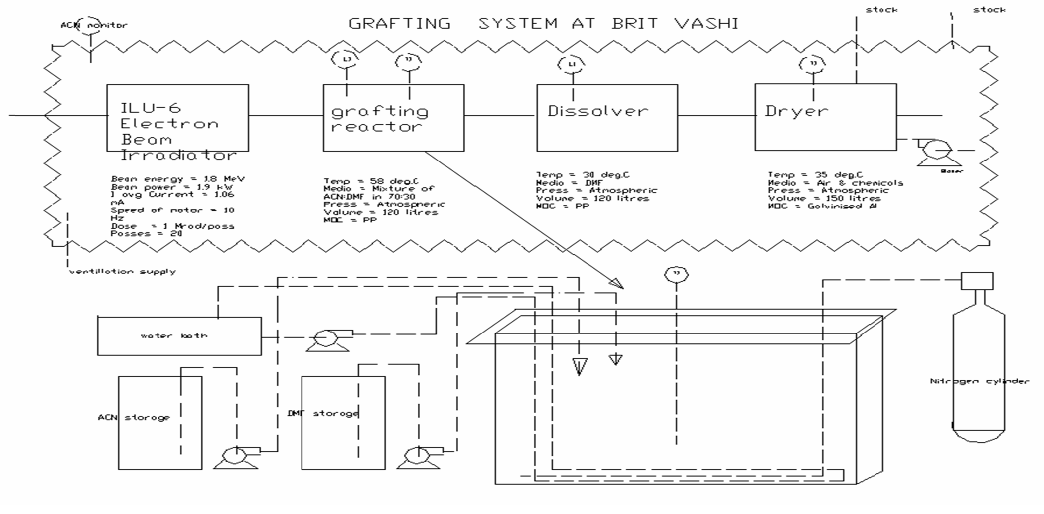

FIG. 8. Schematic diagram of the grafting setup.

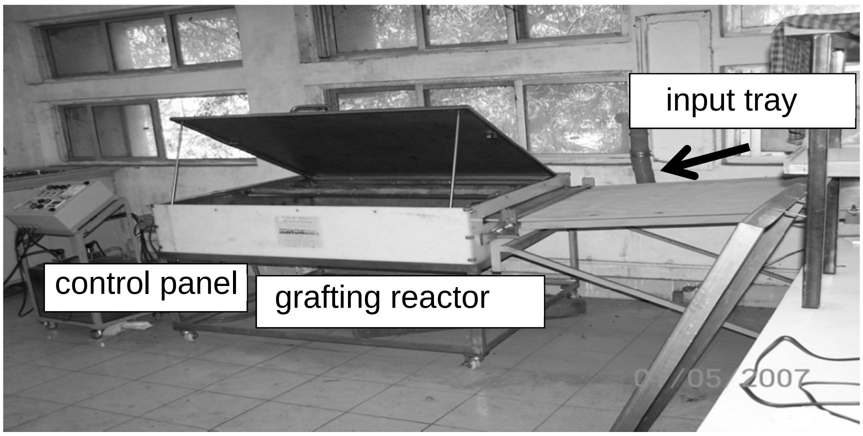

FIG. 9. Grafting setup.

4.2. Mutual radiation grafting of quaternary ammonium salts (QATS) on cotton

4.2.1. Antibacterial properties of quaternary ammonium salts grafted cotton

Grafting of three QATs (structures shown below) onto finished cotton cloth was carried out to introduce antibacterial property.

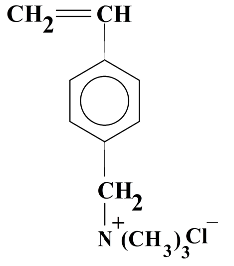

(VBT)

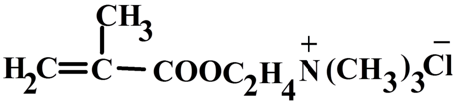

$H_2C{=}\overset{CH_3}{\overset{|}{C}}-COOC_2H_4\overset{+}{N}(CH_3)_3\overset{-}{Cl}$

(MAETC)

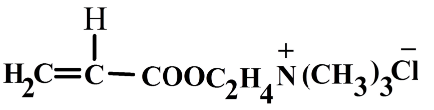

$H_2C{=}\overset{H}{\overset{|}{C}}-COOC_2H_4\overset{+}{N}(CH_3)_3\overset{-}{Cl}$

(AETC)

All three monomers underwent very fast radiation induced polymerization to yield water soluble polymer at appropriate radiation doses. Grafting extent increased with dose and monomer concentration for VBT and MAETC however for AETC increase in grafting extent was observed only in presence of co-monomer HEMA. Inhibitory effect on grafting extent in presence of additives like Mohr's salt, copper salt and inorganic acids was observed. Presence of O_2 hindered the grafting reaction; however de-aeration didn't enhance grafting significantly as shown in Figure 10.

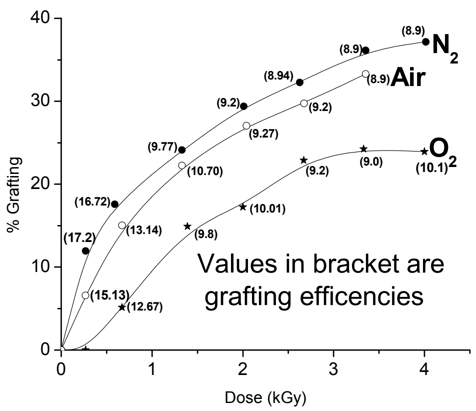

FIG. 10. Effect of ambience on grafting: [VBT] = 20% (w/w) in water, Dose rate: 4.0 kGy h^{-1}.

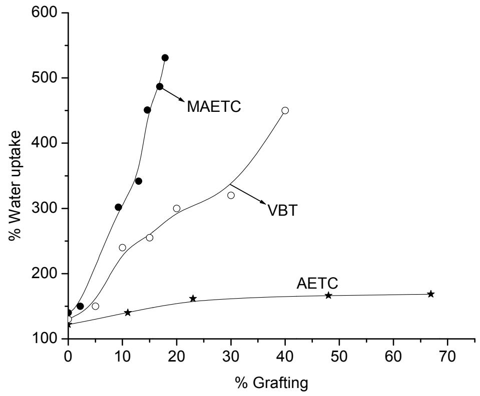

FIG. 11. Water uptake by grafted cotton.

Grafting enhanced the water uptake capacity (Figure 11) and changed the texture of pristine smooth fibre to rough (Figure 12).

Antibacterial activity of the grafted products was studied against gram positive bacteria *Staphylococcus aureus, Bacillus cereus* and gram-negative bacteria like *Escherichia coli*, *Pseudomonas fluorescens*. Antibacterial activity of the grafted cotton was a function of type of monomer grafted [31, 32]. The VBT grafted cotton samples showed excellent anti-bacterial activity against strains *E. coli* and *S. aureus.* Table 4 and Table 5 show time dependent decrease in the counts of *E. coli* and *S. aureus* when VBT-grafted, grafted to different extents were tested for anti-bacterial activity.

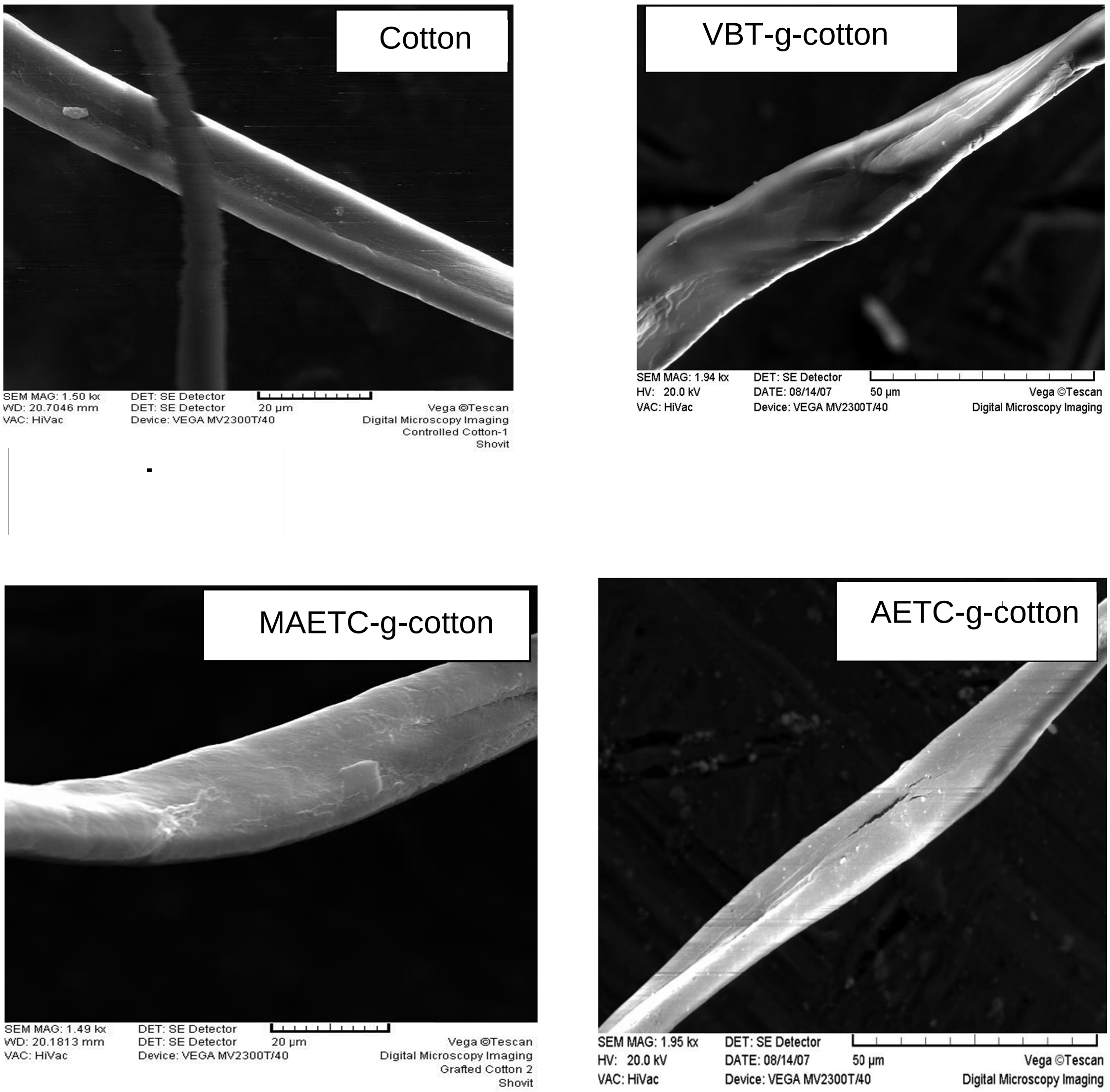

FIG. 12. SEM of pristine and grafted cotton fibrils.

TABLE 4. EFFECT OF GRAFTING EXTENT ON *E. COLI* CELLS

Time of exposure (h)	% Grafting		
	5%	13%	20%
	Counts (CFU/mL)		
0	1.0×10^9	1.1×10^9	1.0×10^9
2	2.8×10^8	4.0×10^4	1.0×10^5
4	2.0×10^8	1.2×10^4	4.0×10^4
6	7.5×10^8		1.0×10^4

TABLE 5. EFFECT OF GRAFTING EXTENT ON S. AUREUS CELLS

Time of exposure (h)	% Grafting		
	5%	13%	20%
	Counts (CFU/mL)		
0	1.0×10^9	1.0×10^9	1.1×10^9
2	1.0×10^9	6.1×10^8	1.0×10^9
4	1.0×10^9	1.8×10^4	1.7×10^4
6	8.0×10^6	3.0×10^4	1.6×10^4

It was observed that grafted samples showed toxicity against both these organisms at grafting levels as low as approximately 5%. The toxicity increased with the grafting extent of 13% and thereafter no significant increase in toxicity was observed. The samples grafted to the extent of ≥13% showed a decrease of about 4–5 log cycles within first two hours for *E. coli* and four hours for *S. aureus.*

The anti-bacterial activity of the grafted cotton samples was retained after several cycles of washing and drying in a commercial detergent powder.

The qualitative test for antibacterial activity of radiation synthesized PMAETC in nutrient broth showed it to be bactericidal as there was no significant increase in turbidity and number of colonies formed on solid media reduced with time. These results indicated the polymer to be bactericidal in nature rather than inhibitory. The MBC of the polymer ranged from 0.025– 0.075% depending on the organism used. The lowest MBC was found to be for *S. aureus*, followed by *E. coli*, *B. cereus* and *P. fluorescens*.

Figure 13(a–d) shows reduction in initial load of *E. coli*, *S. aureus*, *B. cereus* and *P. fluorescens* with time for MAETC grafted samples grafted to different extents. Antibacterial assay showed variations in activity between pure PMAETC and grafted on cotton. The activity of grafted samples was less as compared to pure polymer, which may be due to its bound state on cotton but it was observed that grafted sample showed antibacterial activity against all these organisms at grafting levels as low as 2%. The antibacterial activity increased with extent of grafting up to 19% and thereafter there was no significant increase in activity. Maximum activity was found against *S. aureus,* as there was approximately 5–log cycle kill in 24 h (Figure 13-b). This was expected as PMAETC had lowest MBC against this organism. In case of *B. cereus* (Figure 13-c) and *E. coli* (Figure 13-a), up to 4 log cycle was observed with 19% grafting followed by *P. fluorescens* (Fig 13-d) where only 3 log cycle kill was observed.

The decrease for *E. coli* and *S. aure*us was also monitored with time for sample grafted to an extent of approximately 33%. It was found that reduction in initial count reaches minimum value after 6 hours itself and thereafter no significant decrease in the number of organism is observed. These studies establish that decrease in bacterial count is less than the VBT grafted cotton an reported by us earlier [31] also the decrease is not to that extent as in the earlier case. This indicated that VBT-grafted cotton inhibits the growth of *E. coli* and *S. aureus* more efficiently and effectively in comparison to MAETC grafted cotton.

For AETC-grafted-cotton anti-bacterial activity followed the order: pure polymers>grafted cotton>co-grafted cotton>co-polymer [33]. The lower activity of the grafted matrices may be due to bound state of these polymer/co-polymer chains wherein the flexibility of the grafted chains in restricted which in turn restricts the diffusion of hydrophobic chain into the bacteria once the bacteria held onto by charged interactions [34].

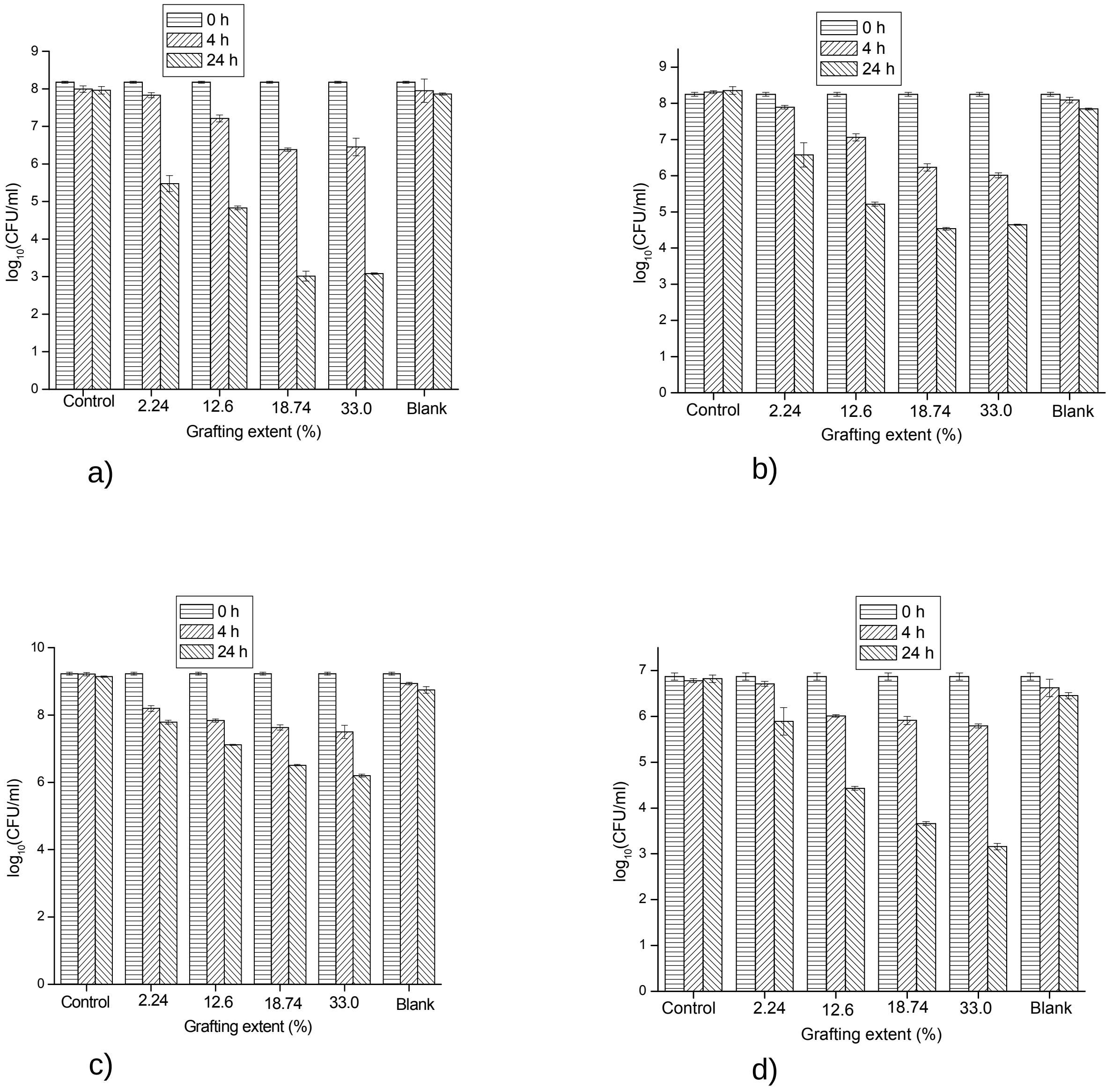

a)
b)
c)
d)

FIG. 13. Anti-bacterial activity of MAETC-g-cotton against (a) E. coli (b) S. aureus (c) B. cereus (d) P. fluorescens.

The AETC-grafted cotton showed antibacterial activity against all these organisms at grafting levels as low as 4.7% and increased with grafting extent. The co-grafted matrices showed noticeable antibacterial activity at much higher grafting extent of ~11% which didn't improve on increase in co-grafting extent. Maximum activity was found against gram positive *S. aureus & B. cereus* and not so significant activity was found against gram negative *E. coli & P. flourescens.* This was on expected lines as poly(AETC) had highest MBC against *E. coli & P. flourescens*. This observation was important in the sense that AETC grafted matrices were effective against gram positive bacteria whereas our earlier studies show that MAETC and VBT [31, 32] were more effective against gram negative organisms which are known to have lipopolysaccharide layer present over their cell walls [35].

4.2.2. Protein binding studies of VBT grafted cotton

PVBT-*g*-cotton, an anion exchange matrix was evaluated for protein adsorption and elution behaviour were investigated in a continuous column process under various experimental conditions, using Bovine serum albumin (BSA) as a model protein. Binding and elution behaviour of the anion exchange matrix was found to depend on different experimental parameters, such as grafting yield, ionic strength, pH of medium and amount of protein loaded. Figure 14 shows binding capacity (BC) of grafted anion-exchange matrix and elution percentage (EP) of the bound protein, as a function of GY. As expected, the protein BC of the adsorbent increased with the increase in GY. Form the elution profile; it was found that up to 10% GY, only about 60% of bound protein could be eluted out. But for adsorbent with GY ≥15%, the EP reached to the saturation value (approximately 95%). In order to estimate the equilibrium binding capacity of 20% GY breakthrough curve were plotted (Figure 15).

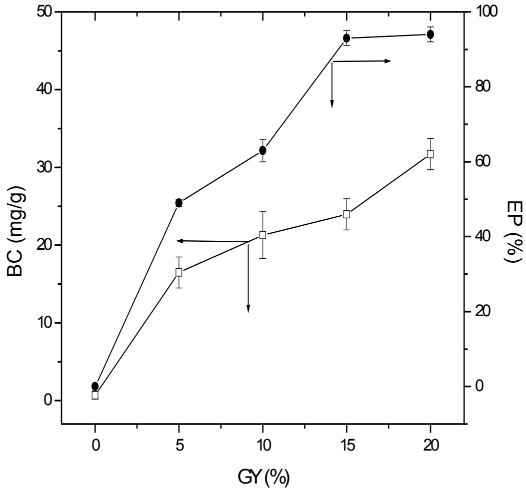

FIG. 14. BC and EP of PVBT-g-cotton cellulose as a function of GY. pH ~7.0 in 10 mM phosphate buffer, protein loaded = 8.9 mg, flow rate = 0.5 mL/min. Data are expressed as mean ± S.D. (n=3).

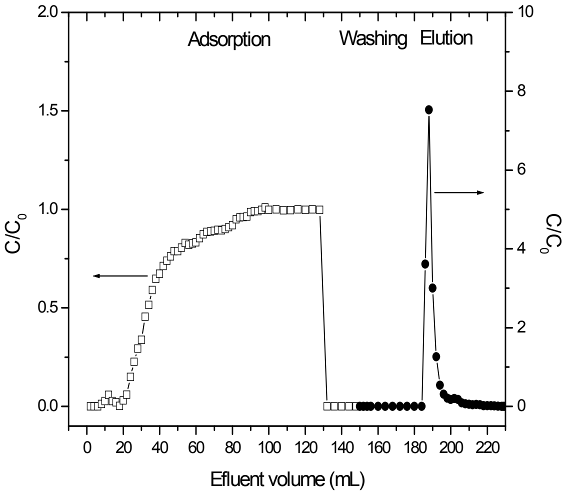

FIG. 15. Breakthrough curve for adsorption of BSA on adsorbent having GY of 20%. BSA concentration in feed solution = 0.4 mg/mL, flow rate = 0.5 mL/min, weight of dry anion exchange matrix=0.2 g.

Data presented in Figure 15 shows that protein content in the unadsorbed fraction increased gradually with the increase in effluent volume, and finally reached to the concentration of feed solution i.e. point of equilibrium at about 100 mL effluent volume. The equilibrated column was then washed and the bound protein was eluted out in 1 mol dm^{-3} NaCl solution. The adsorbed protein could be effectively eluted out in a small volume (~10 mL) of NaCl solution. The equilibrium binding capacity and EP of the PVBT-*g*-cotton cellulose anion exchange adsorbent, estimated from breakthrough curve, was found to be 40.0 mg/g and 94% respectively [36].

4.3. Mutual radiation grafting of AA onto micron thick PP membrane for battery separator applications

For AA-PP grafting system grafting presence of Mohr's salt effectively retarded the polymerization of acrylic acid but did not lead to significant grafting enhancement. Mohr's salt in presence of acids was found to be effective in enhancing the grafting yield. Figure 16 shows effect of combination of salt with acid on grafting extent.

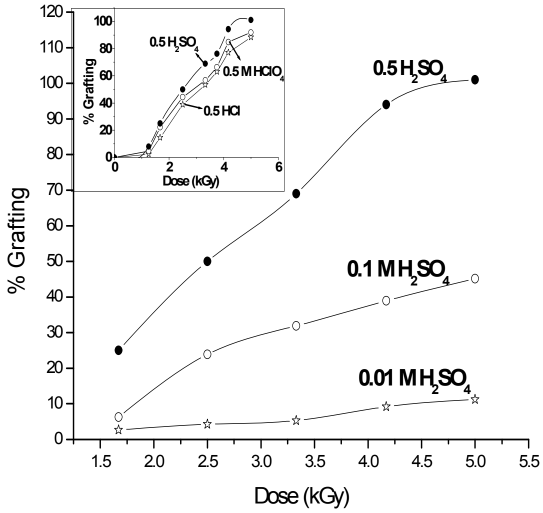

FIG. 16. Effect of H_2SO_4 on grafting in 20% AA + 4% $FeSO_4.(NH_4)_2SO_4$ at a dose rate of 5 kGy h^{-1}.

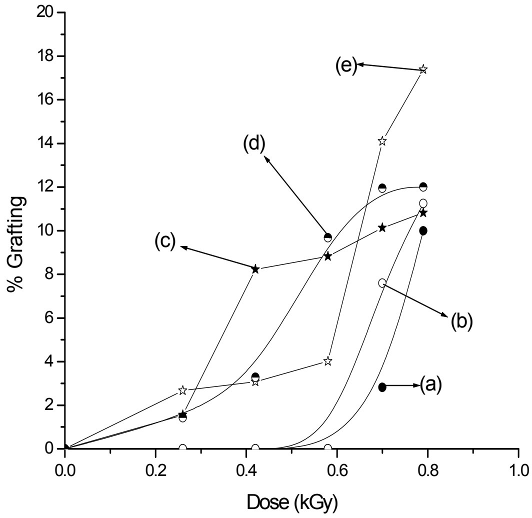

FIG. 17. Grafting of treated (a) untreated (b) Grafted to ~0.99% (c) irradiated in water (d) irradiated in 0.5 mol dm^{-3} H_2SO_4 (e) irradiated in 4% Mohr's salt. Dose rate = 3.2 kGy h^{-1}.

Contact angle measurements of the grafted and radiation treated polypropylene showed that initial grafting as well as radiation treatment of poly(propylene) in aqueous medium and in presence of Mohr's salt enhances its affinity towards the grafting solution (Figure 17). The surface energy measurement using solvents water and diiodomethane with Owens-Wendt method [37] indicated enhancement in the polar component of surface energy of treated polypropylene membrane is the primary cause of surface energy increase.

The developed grafted AA grafted PP sheet was tested for its performance under actual battery conditions vis-à-vis the battery separator membrane presently used by Indian battery industry. For testing the grafted samples, the samples grafted to different extent were put in one Ni/2Cd electrode cells and soaked with KOH electrolyte. All the cells were subject to C/5 charging and 1C rate discharging. Those samples, which enabled the cells to pass 60 minutes of discharging, were considered to be working satisfactorily. Samples grafted to different extents were tested. Figures 18 and 19 show the results of some of the samples. It was seen that samples grafted to extent of 10% did not give satisfactory results. The samples grafted to extent >20% only gave satisfactory results. The sample grafted to an extent of 21% was also used for a full cell consisting of 17 Ni and 16 Cd electrodes. The performance was at par with the cell assembled using battery separator presently used by the industry. The actual testing results indicated that grafting not only converts the hydrophobic PP into battery active hydrophilic state but also helps to retain the hydrophilic state over longer storage period, which is a necessity for Ni-Cd batteries [38].

4.4 Teflon scrap based cation exchanger by radiation grafting

High-energy gamma radiation from ^{60}Co-gamma radiation source has been used to covalently link acrylic acid to Teflon by mutual radiation grafting technique.

The grafting extent decreased with increasing dose rate and increased with monomer concentration and optimum concentration of Mohr's salt and sulphuric acid. As shown in Figure 20 the extent and depth of grafting was strong function of the backbone thickness.

The crystallinity of the PTFE increased on irradiation (Figure 21). As during grafting the bulk of the backbone could further crystallize and hinder immediate grafting reaction.

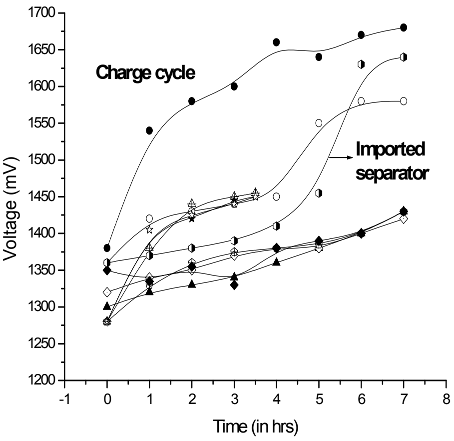

FIG. 18. Profiles for charge cycles.

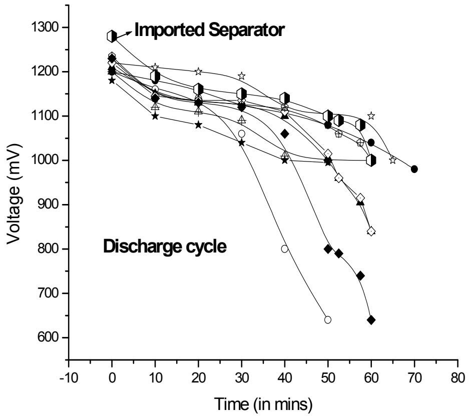

FIG. 19. Profiles for discharge cycles.

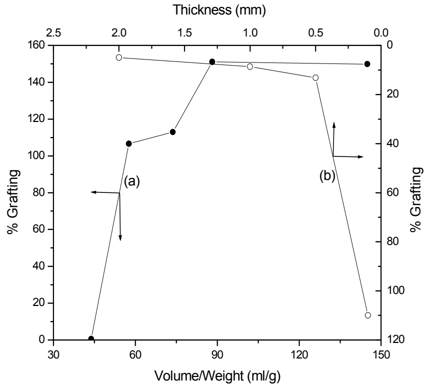

FIG. 20. Grafting in 20% AA solution containing 4% Mohr's salt, 0.5 mol dm^{-3} H_2SO_4; Dose rate 3 kGyhr^{-1}; dose 15 kGy (a) PTFE thickness = 0.1 mm & varying volume/initial weight (b) volume/initial weight ~73.5 and varying thickness.

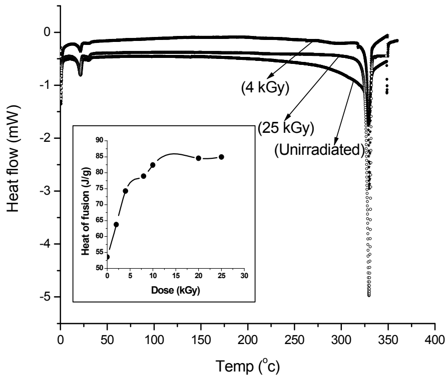

Figure 21. DSC thermograms (thickness = 0.5 mm) irradiated at dose rate of 3 kGy/h.
Inset: heat of fusion.

AFM image studies and kurtosis of the AFM images (Figure 22) clearly showed that radiation grafting does not uniformly take place over whole surface. The surface in fact showed more uniformity (less spread) only on higher grafting as reported earlier [39]. Dynamic contact angle measurement studies of the grafted and radiation treated Teflon® showed that initial grafting as well as radiation treatment of Teflon® enhances its hydrophilicity as shown in Figure 23. In order to quantify the change in hydrophobic character of PTFE on treatment and grafting surface energy of the samples was estimated by dynamic contact angle analysis [37]. Table 6 shows results of these studies. It is clear from the values in Table 6 that irradiation of PTFE in water does not affect the surface energy significantly but presence of Mohr's salt and acid during irradiation does enhance the surface energy when irradiated to higher doses. Probably the increase in surface energy (polar component) in presence of Mohr's salt and acid is among the reasons which contribute to affinity enhancement of the PTFE for grafting solution which results in higher extent of grafting.

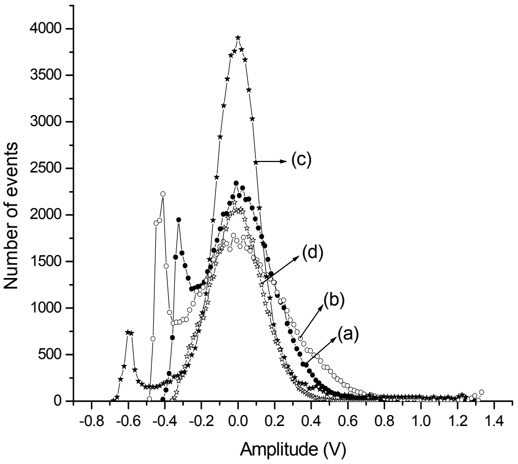

FIG. 22. Surface kurtosis studies of the AFM images (a) Un-irradiated thickness 0.5 mm (b) Grafted 5.59%, 0.5 mm, 2.8kGy (c) Grafted 17.75%, 0.5 mm, 5.6 kGy (d) PTFE irradiated in solution 0.5 mm, 20 kGy.

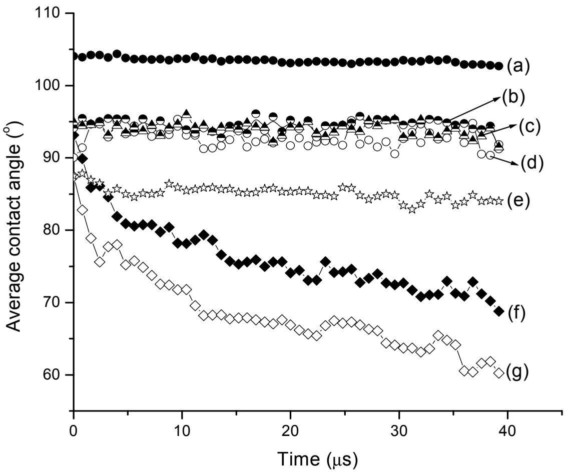

FIG. 23. Change in contact angle with time against water (a) PTFE (b) PTFE irradiated in water ~24 kGy (c) PTFE irradiated in solution 4% $FeSO_4(NH_4)_2SO_4.6H_2O$ *+ 0.5 mol* dm^{-3} H_2SO_4 *24 kGy (d) PTFE grafted ~1.87% (e) PTFE grafted ~8.51% (f) PTFE grafted ~13.57% (g) PTFE grafted ~21.43%.*

TABLE 6. SURFACE ENERGY OF SAMPLES

Sample	Surface energy (mJ/m^2)		
	Total Energy	Polar component	Dispersive component
Ungrafted Teflon	22.5	1.2	21.3
Teflon grafted 1.89%	24.9	1.3	23.6
Teflon grafted 3.48%	28.4	2.7	25.6
Teflon grafted 8.51%	29.1	4.3	24.8
Teflon grafted 13.57%	32.9	6.9	23.6
Teflon grafted 21.43%	41.3	14.6	26.7
Teflon irradiated in aqueous solution containing 4% Mohr's salt + 0.5 mol dm^{-3} H_2SO_4 (Dose = 4 kGy)	25.4	1.8	23.6
Teflon irradiated in aqueous solution containing 4% Mohr's salt + 0.5 mol dm^{-3} H_2SO_4 (Dose = 18 kGy)	30.5	8.7	21.8
Teflon irradiated in water (4 kGy)	22.8	2.5	20.3
Teflon irradiated in water (18 kGy)	23.1	2.8	20.4

5. CONCLUSIONS

Post irradiation and mutual radiation grafting technique, both can be used for grafting of desired monomers on commercially available polymer backbones to get products which have applications in separation, health-care and waste water treatment industry. High energy radiation sources electron beam or gamma radiation both can be utilized for irradiation purpose depending on the backbone polymer. In general for all grafting systems the grafting extent is a function of dose, dose rate, homo-polymerization inhibitor, additives like acid and ambiance of grafting. As grafting leads to co-grafted product having properties of both the parent precursors, by judicious choice of pre-cursors and experimental conditions a polymer like cotton prone to bacterial and fungal attack can be made antibacterial which will retain all properties of cotton and also highly hydrophobic PTFE can be converted to a hydrophilic polymer.

ACKNOWLEDGEMENTS

Authors acknowledge the partial financial support from International Atomic Energy Agency under the CRP Project Research Contract Number 14643/RO and sincerely thank Mr K. P. Rawat & Ms M. S. Rao for carrying out anti-bacterial tests Dr Ajay Singh and Mr C. Tinaharan for SEM and Mr S. P. Shejwal for the technical help provided during the work.

REFERENCES

[1] FANTA, G.F., Block and Graft Copolymerization, Vol I. Ceresa, R.J. (Ed.), Wiley London (1973).

[2] CHAPIRO, A., ”Preparation of graft copolymers with the aid of ionizing radiation”. In Radiation chemistry of polymeric systems. John Wiley & Sons, New York, (1962).

[3] STANETT, V., Radiation grafting state of the art, Radiat. Phys. Chem. **35** (1990) 82-87.

[4] GARNETT, J.L., Grafting, Radiat. Phys. Chem. **14** (1979) 79-99.

[5] SAHINER, A., PEKEL, N., GUVEN, O., Radiation synthesis, characterization and amidoximation of N-vinyl-2-pyrrolidone/acrylonitrile interpenetrating polymer networks, React. Funct. Polym. **39** (1999) 139-146.

[6] ZHAO, D., SENGUPTA, A.K., STEWART, L., Selective removal of Cr(VI) oxyanion with a new anion exchanger, Ind. Eng. Chem. Res. **37** (1998) 4383.

[7] KATAKAI, A., SUGO, T., MAKUUCHI, K., Water selective separation of ethanol-water mixture through acrylic acid grafted membrane prepared by radiation grafting, Nippon Kagaku Kaishi **1** (1994) 68-73.

[8] ROPER, D. K., LIGHTFOOT, E. N., Separation of biomolecules using adsorptive membranes, J. Chromatogr A. **702** (1995) 3-26.

[9] KIM, M., KOJIMA, J., SAITO, K., FURUSAKI, S., SUGO, T., Reduction of non-selective adsorption of proteins by hydrophilization of microfiltration membranes by radiation induced grafting, Biotechnol. Prog. **10** (1994) 114-120.

[10] INTERNATIONAL ATOMIC ENERGY AGENCY, Radiation Technology for Immobilization of Bioactive Materials, IAEA-TECDOC-486, IAEA, Vienna (1988) 35-61.

[11] KOSTOV, G.K., TURMANOVA, S.C., ATANASSOV, A.N., Properties of cation-exchange membranes prepared by radiation grafting of acrylic acid onto tetrafluoroethylene-ethylene copolymers, Electron. Electr. Eng. Res. Stud. Electron Mater. Ser. **1** (1995) 676-679.

[12] CHAKRAVORTY, B., MUKHERJEE, R.N., BASU, S., Synthesis of ion-exchange membranes by radiation grafting, J. Membr. Sci. **41** (1989) 155-161.

[13] MASSON, J.P., MOLINA, R., ROTH, E., GAUSSENS, G., LEMAIRE, F., Obtention and evaluation of polyethylene-based solid polymer electrolyte membranes for hydrogen production, Adv. Hydrog. Ener. **2** (1981) 99-105.

[14] KABANOV, V. YA., Preparation of polymer membranes for fuel cells by radiation graft polymerization, High Energ. Chem. **38** (2004) 57-65.

[15] DONG, L.C., HOFFMAN, A.S., A new method for immobilization of biomolecules using preirradiation grafting at low temperature, Radiat. Phys. Chem. **28** (1986) 177-182.

[16] CARENZA, M., Recent achievements in the use of radiation polymerization and grafting for biomedical applications, Radiat. Phys. Chem. **39** (1992) 485-493.

[17] SAITO, K., HORI, T., FURUSAKI, S., SUGO, T., OKAMOTO, J. Porous amidoxime group containing membrane for the recovery of uranium from sea water, Ind. Eng. Chem. Res. **26** (1987) 1977-1983.

[18] SUGO, T., Selective collection of rare elements dissolved in trace amounts in the sea by using polymer adsorbent, Nippon Kaisui Gakkai-Shi. **51** (1997) 20-29.

[19] TAHER, N.H., DESSOUKI, A. M., KHALIL, F.H., Radiation grafting of acrylic acid onto polypropylene films, Radiat. Phys. Chem. **36** (1990) 785-790.

[20] HEGAZY, E.S., ABD EL-REHIM H., KHALIFA, N., ATWA, S., SHAWKY, H., Anionic/cationic membranes obtained by radiation grafting method for use in waste water treatment, Polym. Int. **43** (1997) 321-333.

[21] SENUMA, M., IWAKURA, M., EBIHARA, S., SHIMURAB, Y., KERIYAMA, K. Antibacterial activity of copolymers of trialkyl(4-vinylbenzyl)ammonium chlorides with acrylonitrile, Angew. Makromol. Chem. **204** (1993) 119-124.

[22] GUPTA, B., ANJUM, N., JAIN, R., REVAGADE, N., SINGH, H., Development of membranes by radiation induced graft polymerization of monomer onto poltethylene, J. Macromol. Sci. Part-C, Polym. Rev. **C44** (2004) 275-309.

[23] BRADY, JR. R.F., Fluoropolymers, Chem. Br. **26** (1990) 427-430.

[24] PLUNKETT, R.J., ”The history of polytetrafluoroethylene: discovery and development”, in High Performance Polymers: Their Origin and Development. Seymour, R. B., Kirshenbaum, G. S. (Eds.), Elsevier, New York, (1986) pp 267.

[25] BHARDWAJ, Y.K., VIRENDRA KUMAR, SARMA, K.S.S., KHADER, S.A., SABHARWAL, S., “Development of electron beam grafted co-polymer membranes for recovery of uranium from seawater: Process parameter standardization” BARC technical report No. BARC/2006/E/004 (2006)

[26] CHOI, S., NHO, Y.C., Adsorption of UO_2^+ by polyethylene adsorbent with amidoxime, carboxyl and amidoxime/carboxyl groups, Radiat. Phys. Chem. **57 (**2000) 187-193.

[27] OKAMOTO, J., SUGO, T., KAKATAI, A., OMICHI, H., Amidoxime-group-containg adsorbents for metal ions synthesized by radiation-induced grafting, J. Appl. Polym. Sci. **30** (1985) 2967-2973.

[28] DAS, S., PANDEY, A.K., ATHWALE, A., VIRENDRA KUMAR, BHARDWAJ, Y. K., SABHARWAL, S. MANCHANDA, V. K., Chemical aspects of uranium recovery from sea water by amidoximated electron-beam-grafted polypropylene membranes, Desalination **232** (2008) 243-253.

[29] RUTHVEN, D. M., Principles of Adsorption and Adsorption Process, Wiley, New York, (1984).

[30] VIRENDRA K., BHARDWAJ, Y.K., TIRUMALESH, K., DUBEY, K.A., CHAUDHARI, C.V., BISWAL, J., SABHARWAL, S., Electron beam grafted polymer adsorbent for removal of heavy metal ion from aqueous solution, Sep. Sci & Technol. **41** (2006) 3123-3140.

[31] VIRENDRA K., BHARDWAJ, Y.K., RAWAT, K.P., SABHARWAL, S., Radiation induced grafting of vinylbenzyltrimethylammmonium chloride (VBT) onto cotton fabric and study of its anti-bacterial activities, Radiat. Phys. Chem. **73** (2005) 175-182.

[32] GOEL, N. K., RAO, M. S., VIRENDRA K., BHARDWAJ, Y. K., CHAUDHARI, C. V., DUBEY, K. A., SABHARWAL, S. Synthesis of antibacterial cotton fabric by radiation induced grafting of [2-(Methacryloyloxy)ethyl] trimethylammonium chloride (MAETC) onto cotton, Radiat. Phys. Chem. **78** (2009) 399-406.

[33] GOEL, N.K., RAO, M.S., VIRENDRA K., BHARDWAJ, Y.K., SABHARWAL, S., Synthesis of antibacterial cotton fabric by radiation induced co-grafting of [2-(Acryloyloxyethyl)]trimethylammonium chloride and 2-hydroxyethyl methacrylate onto cotton fibrils, React. Functl. Polym. submitted.

[34] SUVET, G., DUPOND, S., KAZMIERSKI, K., CHOJNOWSKI, J., Biocidal polymers active by contact. V. Synthesis of polysiloxanes with biocidal activity, J. Appl. Polym. Sci. **75** (2000) 1005-1012.

[35] BOZJA, J., SHERRILL, J., MICHIELSEN, S., STOJILJKOVIC, I., Porphyrin bases light activated antimicrobial materials, J. Polym. Sci. Part A-Polym. Chem. 41, (2003) 2297-2303.

[36] VIRENDRA K., BHARDWAJ, Y. K., JAMDAR, S. N., GOEL, N. K., SABHARWAL, S., Preparation of anion exchange adsorbent by radiation induced grafting of vinylbenzyltrimethylammonium chloride onto cotton cellulose and its application for protein adsorption, J. Appl. Polym. Sci. **102** (2006) 5512-5521.

[37] THOMAS S.P., THOMAS S., ABRAHAM, R., BANDYOPADGYAY S., Polystyrene/calcium phosphate nanocomposites: Contact angle studies based on water and methylene iodide, Express Polym. Lett. **2** 7 (2008) 528–538.

[38] GOEL, N.K., BHARDWAJ, Y.K., MANOHARAN, R., VIRENDRA K., SABHARWAL, S., Physicochemical and electrochemical properties of radiation grafted micro-porous polypropylene membranes, Express Polym. Lett. **3** 5 (2009) 267–278.

[39] CHAUDHARI, C.V., PAUL, J., PANICKER, L., DUBEY, K.A., KUMAR, V., GOEL, N.K., BHARDWAJ, Y.K., SABHARWAL, S., Teflon scrap based cation exchanger by radiation graftin: Process parameter standardization and characterization, Environ. Prog. Sustain. Ener. (In print) doi: 10.1002/ep.10533.

DEVELOPMENT OF HIGHLY EFFICIENT GRAFTING TECHNIQUE AND SYNTHESIS OF NATURAL POLYMER-BASED GRAFT ADSORBENT

Y. UEKI, N. SEKO, M. TAMADA

Japan Atomic Energy Agency,
Quantum Beam Science Directorate,
Takasaki,
JAPAN

Abstract

In the framework of the CRP, Japan has focused on the development of fibrous adsorbents for removal of toxic metal ions and recovery of significant metal ions from industrial wastewater and streaming water. Graft polymerization was carried out by using gamma irradiation facility and electron beam accelerator. Emulsion grafting is a novel topic for synthesis of metal ion adsorbents which are prepared from fibrous trunk polymers such as polyethylene fibre and biodegradable nonwoven fabrics. The emulsion grafting, where monomer micelles are dispersed in water in the presence of surfactant, is a highly efficient and economic grafting technique as compared to general organic solvent system. The resultant cotton-based adsorbent has high adsorption efficiency and high adsorption capacity for Hg, besides, it is biodegradable. Polylactic acid can also be used as a trunk material for the grafting.

1. OBJECTIVE OF THE RESEARCH

Fibrous metal adsorbents have been developed by radiation induced grafting. The grafted adsorbents can selectively and swiftly adsorb toxic metal ions. However, these adsorbents have some drawbacks such as high production cost and high environmental burden. For practical use, these drawbacks must be reduced.

The objective was focused on the development of fibrous metal adsorbent by highly efficient and economic grafting technique. Furthermore, from the view point of the reduction of environmental burden, natural polymer was used as the trunk material for the grafting.

2. INTRODUCTION

Japan Atomic Energy Agency (JAEA) has 11 sites of research institutes. Takasaki site, JAEA carries out application R&D of radiation processing using of facilities such as gamma source, electron beam accelerator, and ion accelerators. Two divisions, environment and industrial materials research division and radiation-applied biology division, of quantum beam science directorate are located in Takasaki site. Environmental polymer group in environment and industrial materials research division applied to this CRP in the research subject of ‘Development of fibrous adsorbents for toxic metal ions in streaming water’. Environmental polymer group has studied radiation processing of polymer to apply the resulting materials to the fields of environmental preservation and the resources conservation.

Fibrous adsorbents for toxic ions were synthesized by graft polymerization and they were adapted to the purification of contaminated streaming water. The adsorbent can be applied to the remove significant metals as well as toxic ions from the water. The purification of streaming water is important for the environment.

In the case of recovery of significant metal ions, no slag was produced in the collection process since the adsorbent collected the metal directly from the water. The adsorbent can be used repeatedly after the adsorbed metal was eluted. By using fibrous graft adsorbents, it was successfully achieved the recovery of U from seawater [1, 3] the recovery of Sc from hot spring water [4, 5] and removal of Cd from scallop processing [2, 6], respectively. Currently, this research focuses on two subjects: these are development of low-cost production method and reduction of environmental burdens.

It was developed a new highly efficient and economic grafting technique and synthesized natural polymer-based graft adsorbent to reduce environmental burden.

3. GRATING FOR METAL ION ADSORBENT

Generally, the trunk polymers in various shapes, such as fabric, film, hollow fibre, particle, and fibre are available. Especially, nonwoven fabric enables the swift adsorption and easy handling because of its large surface area and its unique shape. In the present work nonwoven fabric is mainly used as a trunk polymer and pre-irradiation grafting is adopted to synthesize a metal adsorbent. First, the trunk polymer was placed into polyethylene bag and the air was replaced with nitrogen gas. Then, this trunk polymer was irradiated with electron beam. The irradiated polymer was reacted with the monomer to initiate graft chains onto trunk polymer. These graft chains have strong affinity for metal ions.

Figure 1 shows comparison of the granular resin and our fibrous graft adsorbent shape. The granular resin is close-packed in the column and its porosity is very low, limiting the flow rate. Therefore, resin can limit only under the low flow rate condition. On the other hand, the fibrous graft adsorbent has high porosity and large surface. The porosity of our nonwoven fabric is over 70%.

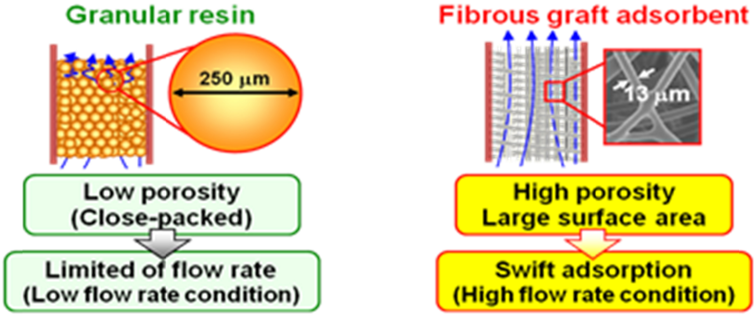

FIG. 1. Comparison of the granular resin and fibrous graft adsorbent shape.

4. CURRENT DEVELOPMENT

4.1. Emulsion grafting

Radiation-induced graft polymerization is favourable and simple technique; allowing the introduction of various functional groups onto various shaped polymers. The fibrous graft adsorbents, which are synthesized by grafting onto fibrous trunk polymers, are attracting a lot of attention as sophisticated metal adsorbents because they can rapidly remove and effectively recover metal ions from water resources. However, these fibrous graft adsorbents can hardly be commercialized due to their high production cost. For practical applications of fibrous graft adsorbent, its production cost should be reduced. The production cost consists of 50% labour cost, 40% irradiation cost and 10% material and reagent costs. Although the reduction of labour cost is not easily achievable, the other two costs, such as irradiation cost and material and reagent costs, can be reduced. By reducing the dose necessary for grafting the production cost will decrease. To achieve the development of low-cost production method, it’s desirable to find out a new better grafting method, such as emulsion grafting.

Therefore, it was investigated whether or not the emulsion grafting could be adapted into the low-cost production method of the fibrous graft adsorbent. Water has an essential and important role in the emulsion grafting. Therefore, the effect of water on the graft polymerization was investigated.

In this experiment, polyethylene (PE) fibre and glycidyl methacrylate (GMA) were used as trunk polymer and monomer, respectively. The Degree of grafting (Dg) was defined by the following equation:

$$\mathrm{Dg}\ [\%] = (W_1 - W_0)/W_0 \times 100 \qquad (1)$$

where W_0 and W_1 are the dry weights of the polyethylene fibre before and after grafting, respectively.

Figure 2 shows typical tendency of grafting, the graft polymerization was carried out at 200 kGy and 40°C. By using water, the grafting reaction occurred considerably faster than in organic solvent system such as dimethyl sulfoxide (DMSO), and Dg in water became 7-folds higher than that in DMSO. After grafting for 5 h Dg reached 92% and 13% in water and in DMSO, respectively, indicating that water was better solvent for graft polymerization than DMSO. However, this Dg is not enough for making a metal adsorbent, and the Dg of over 150% was needed as a precursor of a metal adsorbent. Monomer concentration was increased in order to get higher Dg. Below 2% GMA, the monomer solution is homogeneous. However, above 2% GMA phase separation occurred. A surfactant such as sodium n-dodecylsulfate (SDS) was added into the phase-separating monomer solution [7]. After adding surfactant, the monomer layer disappeared and the monomer solution colour became milky white indicating formation of emulsion. The monomer is localized in the micelles and these micelles are dispersed uniformly into the water. Figure 3 shows the comparison of Dg of each condition. The Dg of emulsion grafting with 2% GMA and 5% GMA became 1.5- and 2-times higher than that in pure water. Based on these results, it was found that the emulsion grafting was a highly efficient and economic grafting technique compared to the general organic solvent system.

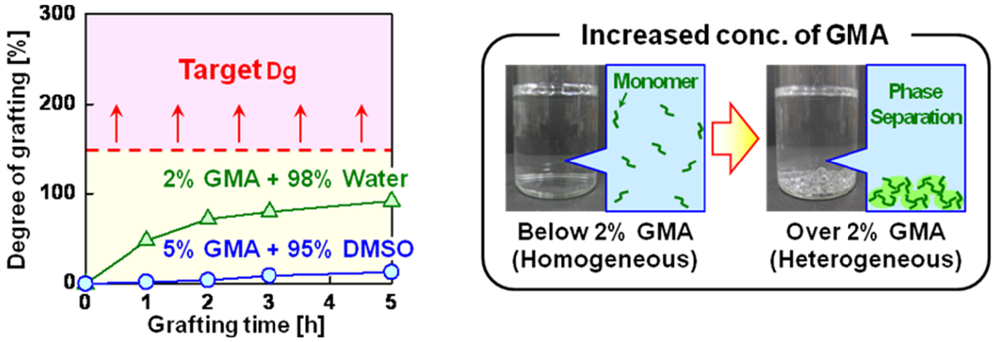

FIG. 2. Effect of water on graft polymerization.

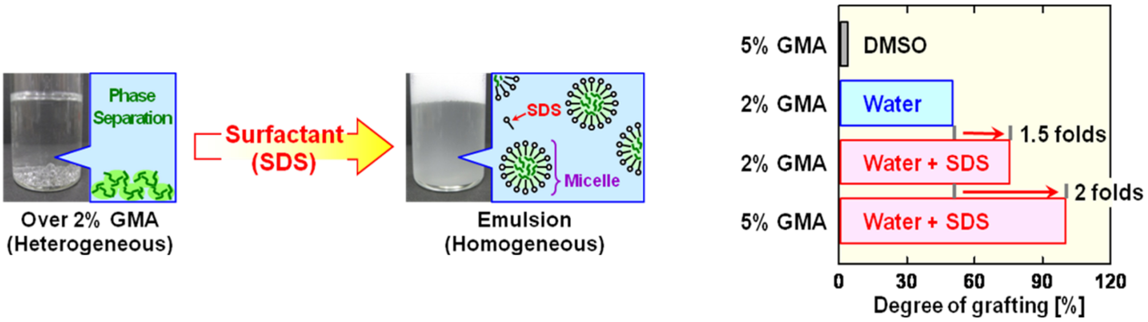

FIG. 3. Effect of emulsion grafting on Dg.

An interesting phenomenon was observed: Dg was improved by increasing the surfactant concentration with constant monomer concentration, such as 2% GMA. It was supposed that, in emulsion grafting, grafting rate was affected by the micelle diameter. Therefore, the relationship between micelle size and Dg was investigated. In this experiment, micelle diameter was measured by the dynamic light scattering (DLS) method. In DLS method, the laser beam hit the micelles in monomer solution, after that specific scattering lights corresponding to the micelle diameter were produced. By measuring these specific scattering lights, micelle diameter and distribution were estimated. Figure 4 shows the relationship between micelle diameter and Dg. In this case, GMA concentration was 5%, and the graft polymerization was carried out at 100 kGy, 40°C, and 3 h. The micelle diameter of GMA emulsion decreased with the decrease of SDS concentration. The micelle diameter of GMA emulsion were about 0.42, 0.85, 1.25, and 1.84 µm for the SDS concentration of 4%, 8%, 12%, and 16%, respectively. The Dg of smaller micelle was higher than that of larger micelle, and the Dg after grafting for 3 h reached 120, 75, 40, and 18% at the SDS concentration of 4%, 8%, 12%, and 16%, respectively. These results indicated that emulsion grafting with smaller micelle was more efficient.

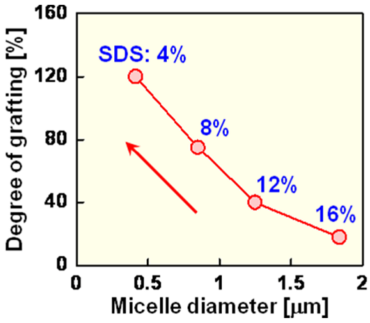

FIG. 4. Effect of SDS concentration on micelle diameter and Dg.

Reaction mechanism for emulsion grafting was suggested. In aqueous system the monomers are dispersed uniformly into the water, and therefore, monomers can react with trunk polymer slowly. On the other hand, in emulsion the monomers are localized and concentrated in the micelle. In the case of the emulsion polymerization 2 types of reaction mechanisms are considered; type 1 is 'leaked monomers from micelle attaches on trunk surface', and type 2 is 'localized and concentrated monomer in micelle attaches directly on trunk surface'. If type 1 is correct, the grafting in emulsion will be less efficient than in aqueous system. On the contrary, in the case of the type 2, the local monomer concentration is very high. Therefore, the grafting reaction proceeds efficiently and continuously, as a result, grafting efficiency is dramatically improved.

The contact area of micelle is also an important factor for the grafting efficiency. The relationship between SDS concentration, surface area of micelle covering PE fibre, and Dg was investigated and these results were shown in Figure 5. GMA concentration was 5%, and the emulsion grafting was carried out at 100 kGy, 40°C, and 3 h.

Surface area of micelle was estimated by the following equation:

$$\text{Surface area of micelle covering PE fiber [cm}^2\text{]} = \frac{\text{Amount of attached monomer on PE fiber [mg/g]}}{\text{Micelle diameter [µm]}} \tag{2}$$

As shown in Figure 5, the micelle surface area which could contact the PE fibre surface decreases with increasing SDS concentration, due to the steric hindrance between larger micelles. On the other hand, smaller micelles could cover a lager surface area of PE fibre enhancing the grafting efficiency. Based on these results, it was found that Dg was improved by the emulsion grafting with smaller micelle.

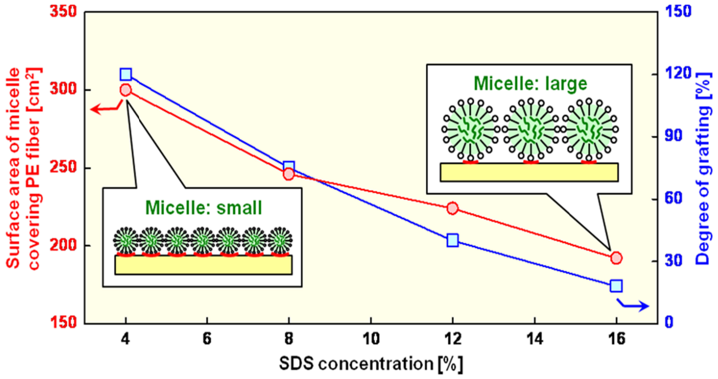

FIG. 5. Effect of SDS concentration on surface area of micelle covering PE fiber and Dg.

For further improvement of Dg, it was aimed to decrease the micelle diameter by using several types of surfactant. The smallest micelle was prepared by Tween 20 (polyoxyethylene (20) sorbitan monolaurate) which is one of the nonionic surfactant, and the micelle diameter of GMA emulsion, which consisted of 5% GMA, 0.5% Tween 20 and 94.5% water, was 0.08 µm [8]. The resulting GMA emulsion was in a milky state and the milky state was stable for 48 h without phase separation and disruption of micelles. This micelle stability was enough for graft polymerization since the grafting time generally needs several hours. Figure 6 shows the results obtained in Tween 20 emulsion, SDS emulsion and in organic solvent. The GMA concentration was 5%, and the graft polymerization was carried out at 40°C. In the presence of Tween 20 Dg was dramatically improved, and even at 10 kGy dose, the Dg reached 100% within only 1 h. Based on above result, it was found that emulsion grafting had some advantages. These advantages were the reduction of absorbed dose from 200 kGy to 30 kGy, consequently, the required grafting time could be reduced from 24 h to 2 h and the reduction of reagent and waste by substituting organic solvent with water. These advantages lead to the reduction of the production cost. By this technology a new graft adsorbent for ultra-pure water production in the field of semiconductor manufacturing was developed, and this new graft adsorbent was commercialized since September 2010 [9].

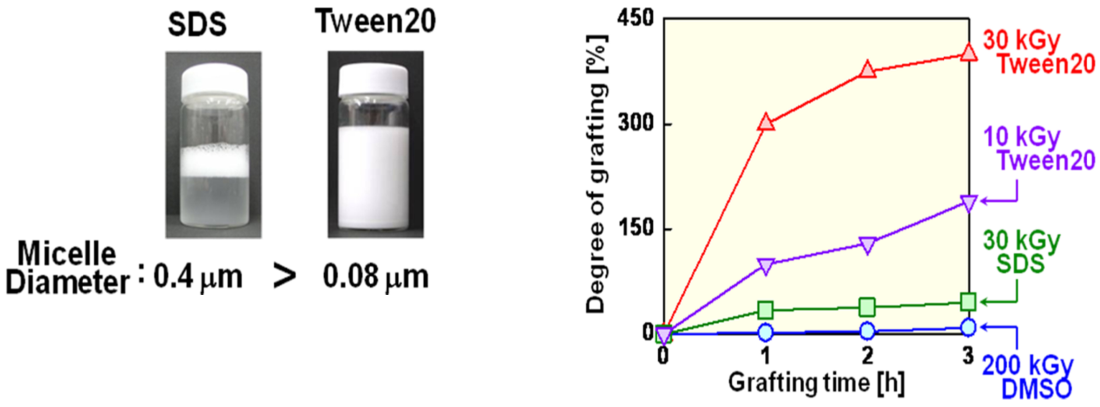

FIG. 6. Improvement of degree of grafting by smaller micelle.

4.2. Cotton-based graft adsorbent

Natural polymers, such as cellulose are difficult to use as a trunk material for grafting, because cellulose is radiation degradable. Emulsion grafting developed by our group was highly efficient grafting technique, and therefore the required dose of the emulsion grafting was lower compared to general organic solvent system. As a result, the emulsion grafting has high potential for natural polymer to use as a trunk material for grafting. A fibrous adsorbent for Hg ions was synthesized by radiation-induced emulsion graft polymerization of glycidyl methacrylate (GMA) onto a nonwoven cotton fabric (NWCF) and subsequent chemical modification with ethylenediamine (EDA) [10]. The emulsion was composed of 2% of GMA, 0.05% Tween 20 and 97.95% water, and the graft polymerization was carried out at 40°C for 1 h. Figure 7 shows the relationship between Dg and the tensile strength at breaking point of un-grafted NWCF for pre-irradiation doses up to 50 kGy. The value of Dg monotonously increased with increasing doses and reached 280% at 50 kGy. During high-energy irradiation radicals are created on the trunk polymer and these radicals initiate the grafting reaction, but, simultaneously, induce degradation of the trunk polymer, as well. The tensile strength of NWCF decreased with increasing dose, becoming half of its initial value at 50 kGy due to the degradation. To minimize the effects of radiation damage on the mechanical strength of NWCF, 10 kGy pre-irradiation dose was used. Figure 8 shows the effect of amination time on the EDA group density for the GMA-grafted NWCF having Dg of 120%. The EDA group density levelled off after 1 h amination time. The EDA density after amination for 1 h reached 3.5 mmol-EDA/g-adsorbent and the conversion ratio of epoxy group in adsorbent was 97%, this EDA density was equivalent to the granular commercial resin.

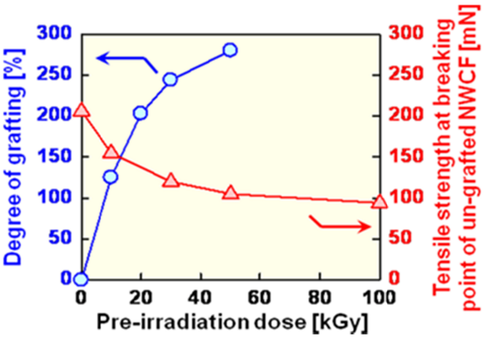

FIG. 7. Effect of pre-irradiation dose on Dg and and tensile strength at breaking point.

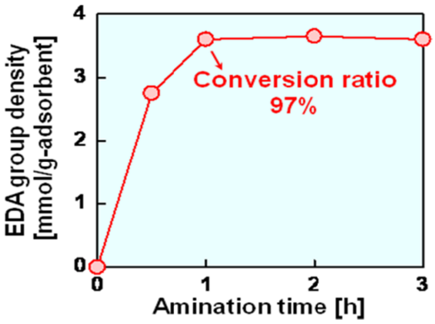

Fig. 8. Effect of amination time on EDA group density in adsorbent.

To evaluate the absorption performance the cotton-based graft adsorbent of 2.7 mmol-EDA/g-adsorbent was soaked in 50 mL of Hg solution having a concentration of 100 ppb at pH 3. As shown in Figure 9, the adsorption rate of the cotton-based graft adsorbent was higher than that of the granular commercial resin. About 80% of Hg was adsorbed on the cotton-based graft adsorbent within only 5 min in Hg solution and, after 60 minutes the cotton-based graft adsorbent collected 98% of Hg ions. To investigate the effect of pH on Hg adsorption, the cotton-based graft adsorbent was also tested for 2 h in 50 mL of Hg solution of 100 ppb in the pH range from 1 to 9. Figure 10 shows the effect of pH on the distribution coefficient for Hg adsorption with cotton-based graft adsorbent. Distribution coefficient was defined by the following equation:

$$\text{Distribution coefficient [-]} = \frac{\text{Hg weight in adsorbent [g]}}{\text{Micelle diameter [}\mu\text{m]}} \qquad (3)$$

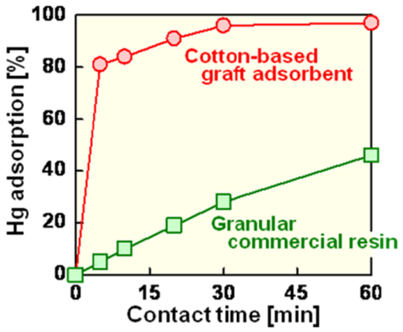

FIG. 9. Batch evaluation of Hg adsorption with cotton-based graft adsorbent.

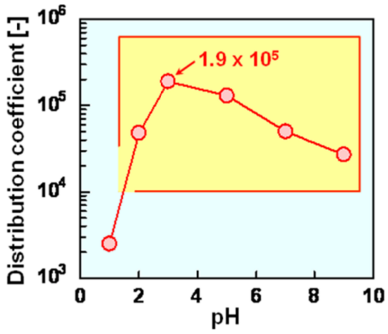

FIG. 10. Effect of pH on distribution coefficient for Hg adsorption.

The highest distribution coefficient, 1.9 × 10^5, was obtained at pH 3. It was found that the cotton-based graft adsorbent had high affinity for Hg ions in the pH range from 2–9. Additionally, adsorbed Hg on the cotton-based graft adsorbent could be eluted by hydrochloric acid. After the elution of Hg ions, the cotton-based graft adsorbent could be used repeatedly without any significant loss of its adsorption performance. Based on the above results, it was found that the cotton-based graft adsorbent could be used for the removal of Hg ions from wastewater at the pH range from 2–9.

The biodegradability of the NWCF and cotton-based graft adsorbent was evaluated with a microbial oxidative degradation analyzer (MODA) assembled by following the ISO14855 protocol. Figure 11 shows the biodegradability of NWCF and the cotton-based graft adsorbent. The NWCF was decomposed by microorganisms, and about 60% of the carbon contained in the NWCF was converted to CO_2 after 120 days. Almost of all degradation occurred within 60 days. In this experiment, the maximum degradation rate was 60%, because 40% of CO_2 was consumed as energy of microorganism. On the other hand, the degradation of cotton-based graft adsorbent proceeded in two steps. Firstly, the cotton part of cotton-based graft adsorbent had decomposed within 30 days, and subsequently the degradation of GMA-graft chain occurred after 60 days. Consequently, the degradation percentage of cotton-based graft adsorbent reached 60% at 120 days. These results indicate that the cotton-based graft adsorbent synthesized by using biodegradable NWCF can be degraded by microorganism in compost and it can lead to the reduction of environmental burden.

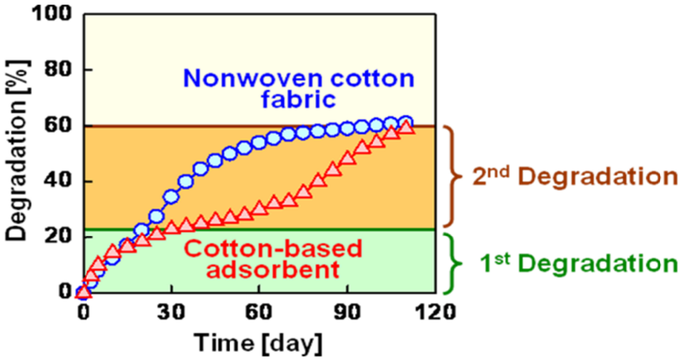

FIG.11. Microbial degradation of cotton-based graft adsorbent and NWCF.

4.3. Polylactic acid-based graft adsorbent

Polylactic acid (PLA) one of biodegradable polymers, is particularly attractive as a sustainable alternative to petrochemical derived products as it is manufactured from the fermentation of agricultural by-products such as corn starch, maize, wheat, etc. However, PLA has poor chemical resistance to alkalis, although its radiation resistance is better as compared to cotton. The PLA was hydrolyzed easily and readily by basic compounds and, consequently, its mechanical strength decreased. In order to synthesize PLA-based graft adsorbent with adequate metal adsorption capacity and sufficient mechanical strength, the controls of both grafting and PLA hydrolysis are necessary. PLA-based graft adsorbent was synthesized by radiation-induced emulsion graft polymerization of glycidyl methacrylate (GMA) [11] or chloromethylstyrene (CMS) [12] onto a nonwoven PLA fabric and subsequent chemical modification with iminodiacetic acid disodium (IDA-Na). GMA emulsion was composed of 2% GMA, 0.05% Tween 20 and 97.95% water and the CMS emulsion was composed of 3% GMA, 0.3% Tween 20 and 96.7% water, respectively. Graft polymerization was carried out at 40°C for 4 h. As shown in Figure 12 at 100 kGy, Dg of GMA reached 120%, and Dg of CMS reached 80%. At 100 kGy the tensile strength was maintained at 70% of original value, and this value was enough for using as a metal adsorbent. Based on above results, to combine the adequate Dg and sufficient mechanical strength, the optimal pre-irradiation dose of PLA was determined to be 100 kGy.

GMA-grafted PLA fabric of 200% Dg was utilized as metal adsorbent. When, the modification of GMA-grafted PLA treated with IDA-Na, PLA hydrolysis reaction also occurred simultaneously, as well as modification of GMA-graft chain. Therefore, in the modification, control of PLA hydrolysis was very important. Figure 13 shows the results of modification of GMA-grafted PLA with IDA-Na in various types of modification medium to control PLA hydrolysis [11]. The IDA group density in graft adsorbent increased with the increase of the methanol (MeOH) concentration. However, the IDA group density which was actually available was limited to below 0.6 mmol-IDA/g-adsorbent, because, over this value, the mechanical strength of PLA-based graft adsorbent became lower and the damaged adsorbent was difficult to handle as a metal adsorbent. To minimize the effects of hydrolysis damage, the optimal IDA group density of PLA-based graft adsorbent was determined to be 0.6 mmol/g adsorbent.

With 0.6 mmol-IDA/g adsorbent the selectivity of the PLA-based graft adsorbent for various metal ions was evaluated by batch adsorption tests. The order of metal ion selectivity of the fibrous metal adsorbent was $Cu^{2+} > Pb^{2+} > Ni^{2+} > Zn^{2+} > Cd^{2+} > Co^{2+} > Ca^{2+} > Mg^{2+}$, and these equilibrium adsorption capacities were 0.49, 0.42, 0.42, 0.32, 0.28, 0.24, 0.21 and 0.11 mmol/g-adsorbent, respectively. Although this selectivity was in the same order of that of the commercial granular resin with IDA group (DIAION CR11), its adsorption capacities for heavy metal ions were within the range from 30–80% of those of the DIAION CR11. This difference of the adsorption capacities was caused by the lower conversion rate, below 25%, of the GMA-grafted chains in order to maintain the sufficient mechanical strength of the fabrics

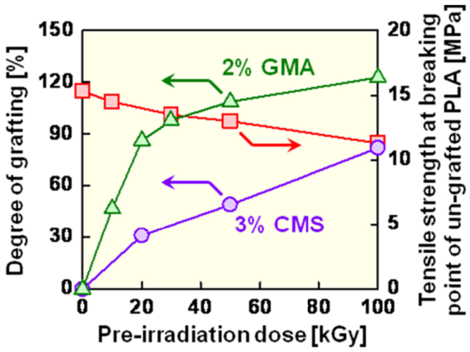

FIG. 12. Effect of pre-irradiation dose on Dg of GMA, Dg of CMS and tensile strength at breaking point.

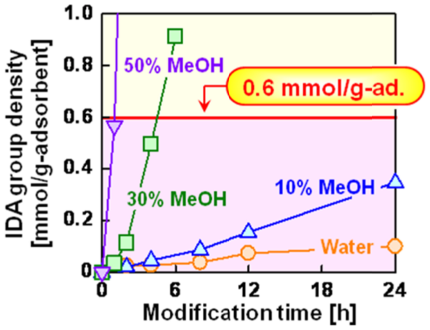

FIG. 13. Effect of MeOH concentration on IDA groups density.

5. INDUSTRIAL APPLICATION

5.1. Preliminary test of graft adsorbent for applying purification system of circulating cooling water

Due to the increasing demand for air conditioning, the purification of circulating water for cooling system in buildings is important issue from the view point of economy and environmental preservation. Generally, the circulating water flows in the pipes and circulates, and is used for a long term continuously. In the long time usage, many type of sludge such as ferric oxides, silica, and calcium-compounds deposit in the pipes (Figure 14). These solids cause corrosion and decrease in the electric power efficiency. A current purification method is treatment with chemicals. These chemicals cause environmental pollution.

Unused pipes   Long-usage pipe

FIG. 14. The deposit of pipe-inside of circulating water.

5.1.1. Batch adsorption test

The effect of circulating time on Fe(III) removal was studied. A rinsed FPA one disk was filled into an adsorption column, and an aqueous 1 mg/L and 5 mg/L Fe(III) solution was passed through into the column. Figure 15 shows the relationship between the circulation time of operations and Fe(III) concentration. After passed through of these solutions, 1 mg/L of Fe(III) could be reduced to 0.1 mg/L only 2 time operations, and in the case of 5 mg/L of Fe(III) solution, the Fe(III) concentration was able to be remove to 0.1 mg/L of the regulatory limit by doing 7 time operations. In the second stage of bench scale of 300 L, this pilot system was evaluated by using underground water. Table 1 summarized the initial and final Fe(III) concentration of the water in the circulation adsorption experiment for 2 times of one week operation. Both tests indicated that the FPA adsorbent could be removed until regularity limit during only one week operation.

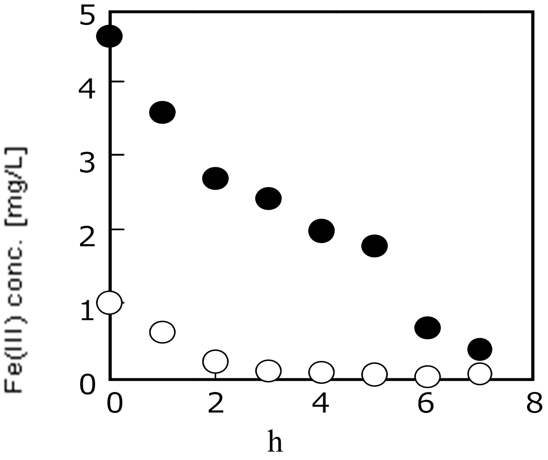

FIG.15. Adsorption ability of FPA adsorbent with the circulating of Fe(III) solution thrown times (●):5mg/L/pH 3.8, (○):1mg/L/pH 4.3.

TABLE 1. THE CHANGES OF Fe(III) CONCENTRATION IN THE BENCH SCALE TEST

	Initial Fe(III) (ppm)	Final Fe(III) (ppm)
Test 1	6.6	0.02
Test 2	8.3	0.14

5.1.2. *Pilot scale adsorption test*

In the pilot scale experiment 90 tons of water was circulated. One operating period was 7 days, and the circulating water was running through the adsorbent stacks continuously meanwhile. Figure 16 shows the tendency of Fe(III) removal vs. contact days. Since the amount of ferric was large though the concentration was low, the ratio of Fe removal was almost changeless in the first week. From the second week, however, Fe(III) concentration decreased rapidly, and removed from 0.3 mg/L to 0.1 mg/L in 8 weeks. At each operation (one week), to elute the adsorbed Fe(III) the adsorbent stacks were dipped into a 5% HCl solution. The adsorbed Fe(III) could be eluted by HCl completely, and there were used 5 times in this preliminary test.

In the preliminary experiment of pilot scale, Fe(III) in the 90 ton circulating water could be reduced from 0.3 to 0.1 mg/L during only 2 months operating of this system. This implied that graft adsorbent was promising material for adapting environmental purification.

The adsorbents can be used to treat water in case of emergency for the removal of metal e.g. copper. It can be provisionally calculated that about 17 000 people can use it for one month as urgent daily life water for the disaster in the storage water of 1 000 m3.

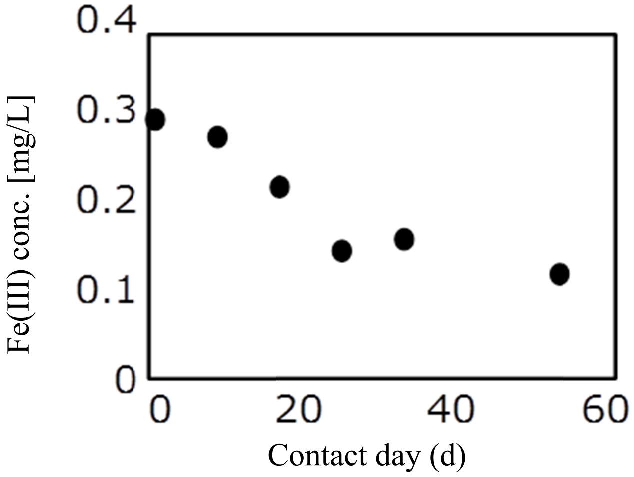

FIG. 16. Adsorption performance of Fe(III) removal in the pilot scale experiment.

6. CONCLUSIONS

Economic cost of a fibrous graft adsorbent could be achieved by using emulsion grafting technique uniformly dispersing monomer micelles in water with a surfactant. The emulsion grafting was highly efficient and economic grafting technique compared to general organic solvent system. It was found that smaller micelles could improve grafting yield, because they could contact a larger surface area of trunk polymer. The micelle diameter of emulsion was controlled by ratio of monomer to surfactant concentration. The smallest micelle of 0.08 μm was obtained in emulsion with composition of 5% GMA, 0.5% Tween 20 and 94.5% water. In this emulsion 100% Dg onto PE fibre was reached in one hour, with a pre-irradiation dose of 10 kGy and reaction temperature of 40°C. The emulsion grafting has inherently the following advantages: (1) required absorbed dose could be reduced to 1/5 (2) required reaction time is reduced to 1/3 (3) amount of organic wastewater could be reduced to 1/20. By using this emulsion system, the fibrous graft adsorbent for ultra-pure water production was commercialized. For reduction of environmental burden, natural polymer-based metal adsorbents were synthesized by emulsion grafting onto the nonwoven cotton fabric and used to effectively adsorb Hg ion. This adsorbent was degraded by microorganism in compost during 120 days. PLA-based metal adsorbent was also synthesized and used as metal adsorbent with ion selectivity of $Cu^{2+} > Pb^{2+} > Ni^{2+} > Zn^{2+} > Cd^{2+} > Co^{2+} > Ca^{2+} > Mg^{2+}$.

REFERENCES

[1] TAMADA, M., SEKO, N., UEKI, Y., “Development of Fibrous Adsorbents for Toxic Metal Ions in Streaming Water”, Report of the 1st RCM on “Development of Novel Adsorbents and Membranes by Radiation-induced Grafting for Environmental and Industrial Applications”, IAEA (2008) 93–99.

[2] SEKO, N., UEKI, Y., TAMADA, M., “Development of Fibrous Adsorbents by Toxic Metal Ions in Streaming Water”, Report of the 2nd RCM on “Development of Novel Adsorbents and Membranes by Radiation-induced Grafting for Selective Separation Purposes”, IAEA (2009) 145–152.

[3] TAMADA, M., “Current status of technology for collection of uranium from seawater”, International Seminar on Nuclear War and Planetary Emergencies - 42nd Session, Erice, (2009) 243–252.

Contact day [d]

[4] SEKO, N., HOSHINA, H., KASAI, N., UEKI, Y., TAMADA, M., KIRYU, T., TANAKA, K., TAKAHASHI, M., Novel recovery system of scandium from hot spring water by fibrous graft adsorbent, J. Ion Exch. **21** (2010) 117–122.

[5] BASUKI, F., SEKO, N., TAMADA, M., Recovery of scandium by phosphoric chelating adsorbent by directly synthesized radiation graft polymerization, J. Ion Exch. **21** (2010) 127–130.

[6] NAKAI, H., SEKO, N., TAMADA, M., TEMMA, T., OGUMA, M., Study of system to utilize the waste of scallop processing, J. Ion Exch. **15** (2004) 10–15.

[7] SEKO, N., NINH, N.T.Y., TAMADA, M., Emulsion grafting of glycidyl methacrylate onto polyethylene fiber, Radiat. Phys. Chem. **79** (2010) 22–26.

[8] SEKO, N., BANG, L.T., TAMADA, M., Syntheses of amine-type adsorbents with emulsion graft polymerization of glycidyl methacrylate, Nucl. Instr. Meth. B **265** (2007) 146–149.

[9] TAKEDA, T., TAMADA, M., SEKO, N., UEKI, Y., Ion exchange fabric synthesized by graft polymerization and its application to ultra-pure water production, Radiat. Phys. Chem. **79** (2010) 223–226.

[10] SEKINE, A., SEKO, N., TAMADA, M., SUZUKI, Y., Biodegradable metal adsorbent synthesized by graft polymerization onto nonwoven cotton fabric, Radiat. Phys. Chem. **79** (2010) 16–21.

[11] UEKI, Y., SEKO, N., HOSHINA, H., TAMADA, M., Preparation of polylactic acid nonwoven fabric-based metal adsorbent by radiation-induced graft polymerization, J. Ion Exch. **18** (2007) 214–219.

[12] NAYANAJITH, L.D.C., UEKI, Y., SEKO, N., HOSHINA, H., TAMADA, M., Aminated adsorbent synthesized by radiation-induced graft polymerization of 4-chloromethylstyrene onto nonwoven polylactic acid fabric and its adsorption capacity for metal ions, J. Ion Exch. **21** (2010) 123–126.

[13] SEKO, N., YOSHII, A., SHIOZAWA, T., TSUNODA, Y., OTANI, H., INOUE, A., HOSHINA, H., UEKI, Y., TAMADA, M., Development of purification system for circulative cooling water by radiation graft, EcoDesign, **39** (2009) 1191-1194.

RADIOLYTICAL PREPARATION OF A POLY(VINYLBENZYL SULFONIC ACID)-GRAFTED FEP MEMBRANE AND CHARACTERIZATION AS POLYMER ELECTROLYTES FOR DIRECT METHANOL FUEL CELLS

Y-C. NHO, J. SHIN, J-Y. SOHN, G. FEI

Radiation Research Division for Industry & Environment,
Korea Atomic Energy Research Institute,
1266 Sinjeong-dong, Jeongeup-si, Jeollabuk-do 580-185,
REPUBLIC OF KOREA

Abstract

In this study, a novel polymer electrolyte membrane, poly(vinylbenzyl sulfonic acid)-grafted poly(tetrafluoroethylene-co-hexafluoropropylene) (FEP-g-PVBSA), has been successfully prepared by simultaneous irradiation grafting of vinylbenzyl chloride(VBC) monomer onto a FEP film and taking subsequent chemical modification steps to modify the benzyl chloride moiety to the benzyl sulfonic acid moiety. The chemical reactions for the sulfonation were carried out via the formation of thiouronium salt with thiourea, base-catalyzed hydrolysis for the formation of thiol, and oxidation with hydrogen peroxide. Each chemical conversion process was confirmed by FTIR, elemental analysis, and SEM-EDX. A chemical stability study performed with Fenton's reagent (3% H_2O_2 solution containing 4 ppm of Fe^{2+}) at 70°C revealed that FEP-g-PVBSA has a higher chemical stability than the poly(styrene sulfonic acid)-grafted membranes (FEP-g-PSSA). An EDX analysis was also used to observe the cross-sectional distribution behaviors of the hydrophilic sulfonic acid groups and hydrophobic fluorine groups. The characteristics of an ion-exchange capacity (IEC), water and methanol uptake, methanol permeability, and proton conductivity as a function of the degree of grafting were also studied. The IECs and water uptakes of membranes with different degrees of grafting (36–102%) were measured to be in the range of 0.8–1.62 meq/g, and 10–30%, respectively. When the degree of grafting reached 60% the proton conductivity was higher than that of a Nafion® 212 membrane (6.1E-02 S/cm). The methanol permeability and uptake of the FEP-g-PVBSA membrane was significantly lower than that of the Nafion® 212 membrane, and even the degree of grafting reached 102%.

1. OBJECTIVE OF THE RESEARCH

This study aims to develop fuel cell membranes with higer chemical stability against the radical attack by introducing poly(vinylbenzyl sulfonic acid)-graft polymer chains onto a fluoropolymer film using a radiaton grafting method. The sulfonic acid group of the membranes was designed to be indirectly connected to the benzene ring of the graft chain with a methylene spacer group, and this structural change of the substituent was expected to change the benzyl radical stability of the graft chain.

2. INTRODUCTION

Among the many global efforts to solve serious energy and environmental problems concerning the consumption of fossil fuels and pollutant emissions, fuel cells have been considered as a very attractive alternative for fossil fuel based power generation systems ranging from stationary power generation to automotive transportation. Nafion® membrane is a polymer electrolyte that has typically been used in the fuel cells since it shows good chemical and mechanical properties as well as high proton conductivity. However, the disadvantages of the Nafion® membranes such as high production cost and high methanol cross-over in direct methanol fuel cell (DMFC) have limited their practical applications [1] and thus have led many researchers to develop promising alternative membranes that can overcome the problems associated with the Nafion® membranes.

By utilizing a radiation grafting process [2], poly(styrene sulfonic acid) chains could be easily grafted onto various fluorinated polymer films with strong chemical, mechanical and thermal properties, and the grafted membranes have been studied as a fuel cell polymer electrolyte [2–6]. According to these studies, the membranes showed promising electrochemical performances but the lower chemical stability of the membranes resulting from the graft chain scission was also observed [1, 2, 7, 8]. This graft chain scission is known to occur at the benzyl position of the graft chain, by radicals produced in the fuel cell environment. In order to overcome the chemical stability problem of the membranes, two strategies have been extensively studied. The first is to utilize the more stable substituted monomers such as α,α,β-trifluorostyrene (TFS) and α-methylstyrene (AMS), [2, 7] which cannot generate a labile benzylic hydrogen atom after graft polymerization. However, these monomers are usually expensive and/or show slow kinetics. The second is to add crosslinkers such as divinylbenzene (DVB), bis(vinyl phenyl)ethane (VBPE) and triallylcyanurate (TAC) during the radiation grafting process to produce a cross-linked network that can improve the chemical and mechanical properties [2, 5, 7, 9]. The crosslinking strategy is relatively simple; however, it only retards the degradation rate without changing the inherent reactivity of the benzyl position against the radical attack.

It has been reported that benzyl radical stability could largely be influenced by various substituents on the benzene ring [10–13]. Both electron donating and electron withdrawing substituents have been reported to stabilize the benzyl radical in these studies. This result implies that the sulfonic acid substituent on the benzene ring of the graft chain could enhance the benzyl radical stability, and this can facilitate the formation of radicals on the graft chain that cause the graft chain scission.

In this study, a novel polymer electrolyte membrane with a methylene sulfonic acid substituent on the benzene ring of the graft chain has been prepared. The sulfonic acid group of the membrane was designed to be indirectly connected to the benzene ring of the graft chain with a methylene spacer group, and this structural change of the substituent was expected to change the benzyl radical stability of the graft chain. In order to obtain the desired membrane, a FEP-g-PBVC film prepared by a simultaneous irradiation grafting of vinylbenzyl chloride (VBC) [14] was utilized as a starting material. The benzyl chloride moiety of the graft chain was then converted to the benzyl sulfonic acid moiety. FEP-g-PVBC films prepared by a pre-irradiation grafting of VBC have been applied to prepare anion exchange membranes by amination [15–20] and a cation exchange membrane by phosphonation [21]. However, no sulfonation of the membrane has been attempted as far as it's expected.

This paper describes the preparation method of the desired FEP-g-PVBSA membrane and the relative chemical stability of the membrane against radicals. The physio-chemical properties, including IEC value, water and methanol uptake, methanol permeability, and proton conductivity of the FEP-g-PVBSA membranes with various DOGs, were also evaluated for direct methanol fuel cell application.

3. SIMULTANEOUS RADIATION GRAFTING OF VINYLBENZYL CHLORIDE (VBC) ONTO POLY(TETRAFLUOROETHYLENE-CO-HEXAFLUOROPROPYLENE) (FEP) FILMS

3.1. Materials and methods

3.1.1. Materials

The poly(tetrafluoroethylene-co-hexafluoropropylene) (FEP) films with 25, 50, and 100 μm thickness (UNIVERSAL Co. Ltd., Japan) were used as the base films. All reagents including the VBC monomer (a mixture of m- and p-isomers, 96% purity, Acros Organics) and thiourea (99%, extra pure, Acros Organics) were used as received from the commercial suppliers.

3.1.2. ^{1}H NMR study for the radiolytic polymerization of VBC in $CDCl_3$

NMR spectroscopy (JEOL, 500 MHz for ^{1}H NMR) was used to monitor the radiolytic polymerization of VBC in $CDCl_3$. VBC and $CDCl_3$ were mixed in small vials prior to a nitrogen purging. The mixtures (VBC: $CDCl_3$, 10:0, 5:5, volume ratio) were exposed to γ ray irradiation for 20 h at does rates of 2 and 4 kGy/h. Small portions of the irradiated samples were diluted with $CDCl_3$ for the ^{1}H NMR analysis. When pure VBC (10:0) was exposed to irradiation, it became very rigid so it could not be dissolved in $CDCl_3$.

3.1.3. Simultaneous radiation grafting of VBC onto FEP films

Generally, a FEP film (25 μm thickness) cut into 2 cm × 3 cm, was immersed in a vial containing a VBC monomer and $CHCl_3$ with a 1:1 volume ratio. A series of mixture samples containing a FEP film, VBC, and $CHCl_3$ was purged with nitrogen gas for 10 min to remove the oxygen, and then subjected to a γ ray irradiation up to a total dose of 40 kGy at dose rates of 1, 2, and 4 kGy/h for the grafting of VBC onto the FEP films. The PVBC grafted FEP films were washed with DCM three times to remove the unbound homopolymers and the excess VBC monomer. After drying the films in a vacuum oven at 60°C overnight, the degrees of grafting (DOG) of the grafted films were calculated as shown below. (W_o: original sample weight, W_g: grafted sample weight).

$$\text{DOG } (\%) = [(W_g - W_o)/W_o] \times 100 \quad (1)$$

3.1.4. Characterization of the PVBC grafted FEP films

IR spectra of the PVBC grafted FEP films were obtained by using the FTIR spectrometer Tensor-37 (Brucker, Germany) at ambient conditions in the transmittance mode. The spectra were measured in a wave number range of 400–4000 cm^{-1}. The thermal property of the PVBC grafted FEP films was investigated by a thermogravimetric analysis (TGA). The samples were heated from 40 to 650°C at a rate of 10°C min^{-1} under a dry nitrogen atmosphere.

SEM EDX (SIRION, FEI Company) measurement was conducted to investigate the distribution of the PVBC grafting polymer on the cross-section of the FEP-g-PVBC films. The grafted films were broken in liquid nitrogen and placed between two silicon wafers. These samples were coated with platinum and subjected for a SEM EDX analysis. The SEM EDX operating conditions were set as follows: accelerating voltage with 20 kV, spot size of 4 and a working distance of 5~10 mm for obtaining CPS: 1500. In the EDX mode, the relative content of the chlorine atom over the cross-section of the FEP-g-PVBC films presented in a diagram.

3.2. Result and discussion

3.2.1. ^{1}H NMR study of the polymerization of VBC in $CDCl_3$

Mixtures of VBC monomer and $CDCl_3$ (1:1 volume ratio) were exposed to γ ray up to 80 kGy at a dose rate of 4 kGy/h. Small amounts of the irradiated samples were diluted with $CDCl_3$ prior to the 1H NMR analysis. The ^{1}H NMR spectra of the pure VBC and the irradiated VBC samples are illustrated in Figure 1. The multiplets at 7.25–7.44 ppm correspond to four aromatic hydrogen of VBC and the three peaks at 5.28, 5.76, and 6.70 ppm correspond to three hydrogen at the C=C double bond of VBC, respectively. A sharp singlet observed at 4.59 ppm can be assigned to the methylene peak of the chloromethyl group of VBC. As shown in Figure 1 (B) and (C), new broad peaks resulting from the polymerization of VBC appeared at around 1.4, 1.7, 4.4, 6.5 and 7.0 ppm and theses intensities of the peaks increased as the radiation dose increased. These spectra show that the peaks from the aromatic hydrogen of VBC were slightly shifted to 6.5 and 7.0 ppm, whereas the peaks from the hydrogen at the C=C double bond of VBC were significantly shifted to a downfield region (1.4 and 1.7 ppm) due to a change of the C=C double bond to a single bond. These spectra also show that the methylene peak resulting from the chloromethyl moiety of VBC was shifted from 4.59 ppm to 4.4 ppm with a line broadening response. By comparing the integral values of the peaks arising from VBC and PVBC, it can be concluded that the chloromethyl moiety of VBC is fairly stable at the given irradiation conditions (up to 80 kGy) and therefore could be applied for a simultaneous radiation grafting onto a polymer film.

The usage of a suitable solvent for a simultaneous irradiation grafting polymerization could not only improve the grafting efficiency but also minimize the homopolymerization [22, 23]. This can be attributed to the facts that the diffusion of the monomer onto the grafting sites is largely determined by the swellability of the polymer in a solvent. The reactivity and lifetime of the radicals generated during an irradiation are also affected by the solvent [24].

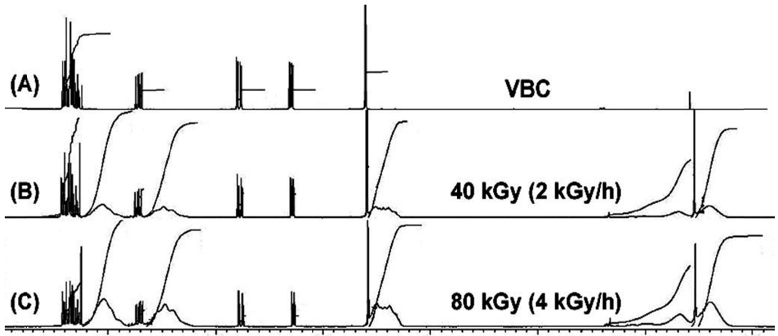

FIG. 1. The ^1H NMR spectra of pure VBC (A) and the irradiated VBC samples (50% VBC in $CDCl_3$) at doses of 40 kGy (B) and 80 kGy (C), respectively.

Several solvents including halogenated, aromatic, and aliphatic hydrocarbon solvents were tested to find a suitable solvent for the grafting of VBC onto a FEP film. A piece of FEP film was immersed in a mixtures containing VBC and a solvent at a ratio of 1:1 (v/v), and then irradiated at doses of 20 and 40 kGy with a dose rate of 2 kGy/h. The degree of grafting (DOG) of the samples irradiated in various solvents are calculated and shown in Figure 2. Among the used solvents, hexane, methanol, and isopropanol are excluded from this figure since too much insoluble VBC homopolymer was formed in these solvents. The homopolymer formation increases the viscosity of the grafting solutions and reduces the monomer diffusion onto a polymer film [25]. As shown in Figure 2, higher grafting efficiencies were observed from the halogenated solvents (excep CCl_4). For the VBC grafting onto FEP, chloroform was found to be a better solvent than dichloromethane which has normally been used as a solvent for a simultaneous irradiation grafting of polystyrene (PS) onto a polymer film [22]. Although a moderate grafting efficiency was observed from toluene, the film grafted in toluene was found to be brittle. Based on this study, chloroform was selected as the solvent for simultaneous grafting of VBC onto a FEP film.

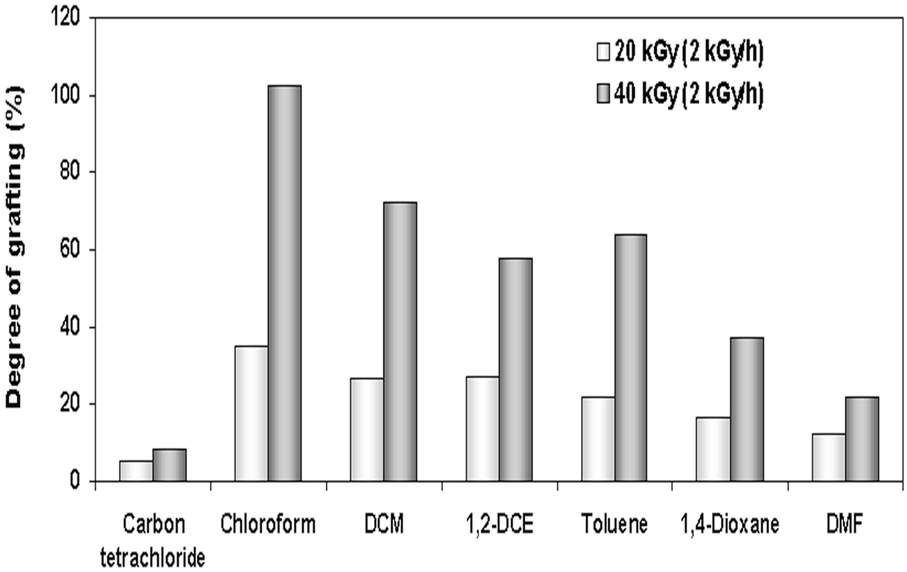

FIG. 2. The degree of grafting of the PVBC-grafted FEP films prepared in various solvents; carbon tetrachloride, chloroform, DCM (dichloromethane), 1,2-DCE (1,2-dichloroethane), toluene, 1,4-dioxane, DMF (N,N-dimethylformamide). Each sample containing a FEP film and a VBC/solvent (1:1 v/v) mixture was irradiated at doses of 20 and 40 kGy with a dose rate of 2 kGy/h.

3.2.2. Simultaneous grafting of VBC onto FEP films

Figure 3 (A) shows the variation of the degree of grafting with the absorbed dose at various VBC concentrations (30, 40 and 50% v/v in $CHCl_3$) during a simultaneous irradiation grafting of VBC onto a FEP film. The VBC grafting solutions containing FEP film were irradiated at doses of 10, 20, 30 and 40 kGy with a dose rate of 2 kGy/h. As shown in the figure, the degree of grafting increases as the radiation dose and VBC concentration increase. This behavior can be explained easily by considering the increase in the radical yield with the dose and the enhancement in the accessibility of VBC monomers near graft sites, which subsequently lead to an increase of the graft yields. To investigate the effects of the dose rate on a simultaneous irradiation grafting of VBC, samples containing a FEP film and a mixture of VBC and $CHCl_3$ (50:50 volume ratio) were irradiated at dose rates of 1, 2 and 4 kGy/h. As shown in Figure 3 (B), the degree of grafting decreases with an increasing dose rate when the same irradiation dose is employed since a prolonged irradiation time at a low dose rate can provide a sufficient time for a survival of the radicals and a polymer chain growth. The PVBC-grafted FEP films prepared at the conditions shown in Figure 3 are flexible and have a good shape while the grafted films prepared in a high VBC concentration solution (70%) at a dose rate of 4 kGy/h are somewhat brittle. At high VBC concentration conditions, a significant formation of homopolymer, resulting in a lower grafting efficiency was also observed. Therefore, these grafting studies, presented in Figure 3 and discussed here, suggest that 40~50% of VBC in chloroform (v/v) at dose rates of 1~2 kGy/h seem to be suitable conditions for the grafting of VBC onto a FEP film.

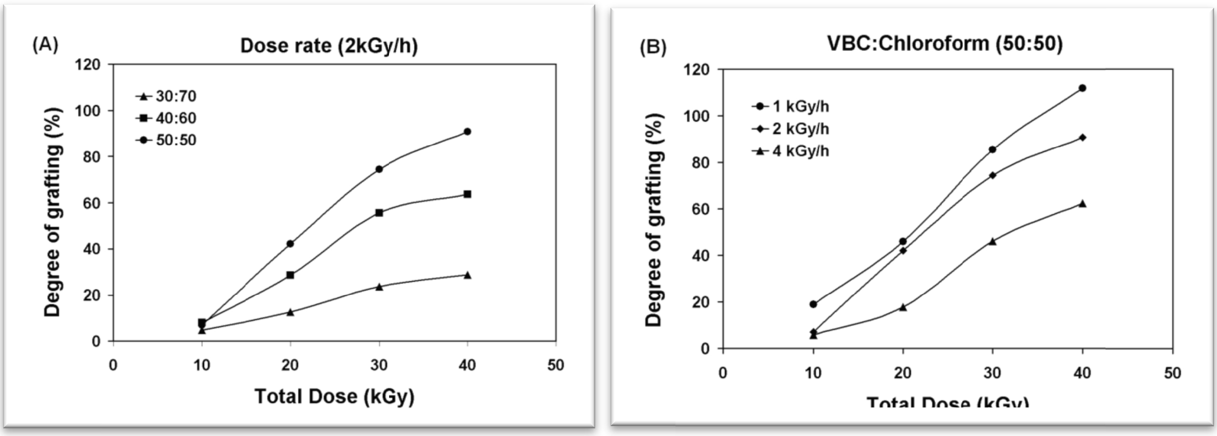

FIG. 3. (A) The degree of grafting vs. dose at different VBC concentrations (2 kGy/h dose rate). (B) The degree of grafting vs. dose at different dose rates (VBC:chloroform 50:50 (v/v)).

Figure 4 shows the effects of the monomer concentration in two different halogenated solvents (dichloromethane and chloroform) on the degree of grafting of VBC on the FEP films. As shown in the figure, DOG increased with increasing VBC monomer concentration up to 60% in dichloromethane and up to 50% in chloroform because of the increased monomer accessibility at the grafting sites. However, the DOG decreased above these concentrations, which was similar to the results that were observed when styrene was used as a grafting monomer during the radiation grafting procedure in previous literature [5, 6, 23, 26]. The homopolymer formation at higher VBC concentrations caused an increase in the viscosity of the grafting solution, which limited the diffusion of the VBC monomer into the polymer matrix [6, 23, 27, 28]. Different grafting behaviors were observed for the two halogenated solvents because of the different radical chain-transfer constants of dichloromethane (0.15) [23, 24] and chloroform (0.5) [29]. A previous report showed that a solvent with a low chain-transfer constant could slow down the chain growth and chain-termination processes, which could eventually increase the DOG [30–32]. From Figure 4, chloroform was a suitable solvent at a VBC concentration of 50% or lower, whereas dichloromethane was a good solvent at a VBC concentration of 60%. In this study, chloroform and a VBC concentration of 50% were chosen as the solvent and the VBC concentration, respectively, for the following experiments.

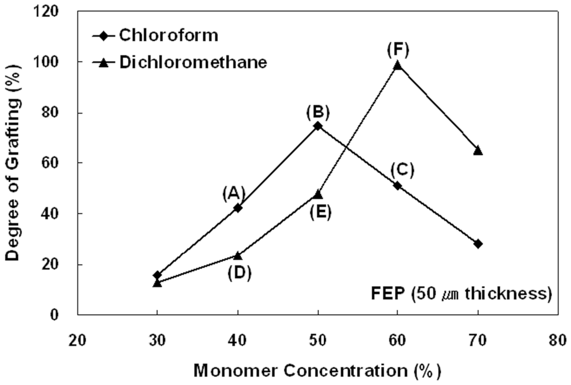

FIG. 4. The degrees of grafting of the VBC on the FEP films that were irradiated at various VBC concentrations in dichloromethane and chloroform solvents at a total dose of 40 kGy and a dose rate of 2 kGy/h.

Figure 5 shows the change in the DOG of the grafted films (25, 50, 100 µm) with respect to the doses. The grafting processes were conducted at a VBC concentration of 50% in the chloroform solution, and the doses ranged from 10 to 80 kGy at a dose rate of 2 kGy/h. As shown in Figure 5, the DOG increased as the dose increased, and the thinner films exhibited higher DOG values at the same dose.

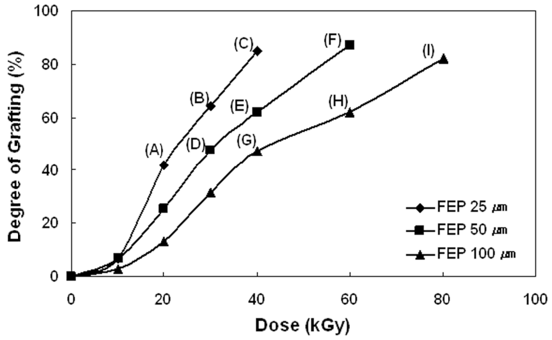

FIG. 5. The degrees of grafting of the VBC monomer onto the FEP films with thicknesses of 25, 50, and 100 µm. These samples were irradiated in a VBC/chloroform (50/50, v/v) solution at a dose rate of 2 kGy/h.

3.2.3. Characterization of the PVBC grafted FEP films

The FTIR-ATR spectrum (Figure 6) of the original FEP film showed strong bands at 1150–1250 cm^{-1} and a sharp band at around 980 cm^{-1} arising from the -C-F stretching vibration of the FEP polymer [24]. The spectrum of the FEP-g-PVBC film showed all the signals assignable to the FEP base film and the new absorption bands arising from the grafted PVBC components, indicating a successful grafting of VBC onto a FEP film [17, 19]. The aromatic absorption bands of the grafted PVBC appeared at 3050 cm^{-1} (=C-H stretching vibration) and at 1450–1600 cm^{-1} (C=C stretching vibrations), respectively. The aliphatic absorption bands were observed at 2800–2900 cm^{-1} (-C-H stretching vibration) and a characteristic band of the chloromethyl group (-C-Cl stretching vibration) of the grafted PVBC was also observed at 820 cm^{-1} [19].

Figure 7 shows the TGA thermograms of the ungrafted FEP film and the grafted (FEP-g-PVBC) films. The grafted FEP-g-PVBC films were found to undergo a two step degradation at 360 and 490°C, whereas the ungrafted FEP film exhibited a one-step degradation where it maintains a temperature up to 490°C. These results indicate that the incorporation of PVBC grafts in the FEP matrix does not bring about any changes to the inherent decomposition of the FEP backbone and the mass loss of the PVBC decreases with the extent of the radiation grafting of the PVBC [1, 33].

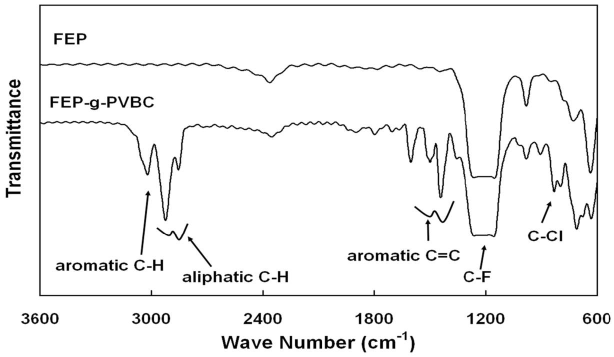

FIG. 6. The FTIR-ATR spectra of the original FEP film and the FEP-g-PVBC film.

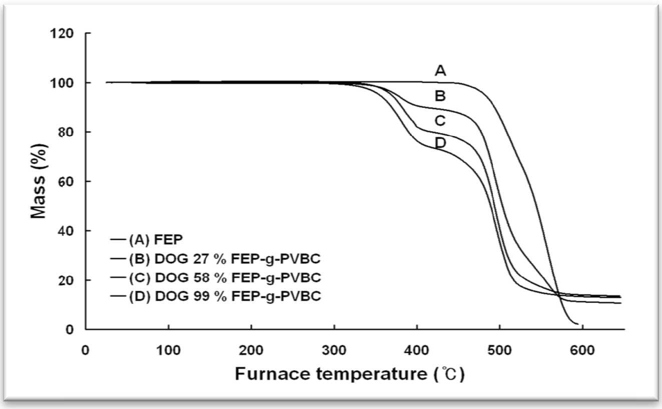

FIG. 7. TGA thermograms of the PVBC grafted FEP films with different degrees of grafting: FEP-g-PVBC with (A) ungrafted FEP, (B) 27% DOG, (C) 58% DOG, and (D) 99% DOG.

3.2.4. A Study on the cross-sectional distribution of poly(vinylbenzyl chloride)-grafted polymer onto a FEP film

To observe the distribution profile of the PVBC grafts over the cross-section of a FEP film, the SEM EDX technique was utilized in this study. EDX result in Figure 8 shows three major peaks: carbon, fluorine and chlorine atoms. Among those atoms, the chlorine atom was chosen for the distribution study of the PVBC grafts since it only exists in the PVBC grafts. This means that the distribution profile of the chlorine atoms corresponds to that of the PVBC grafts. The SEM EDX data shows that chlorine atoms are uniformly distributed over the cross-section of a grafted FEP film with a 64 % DOG, indicating that the VBC monomer was evenly grafted from the surface to the inner of a FEP film by a simultaneous radiation method.

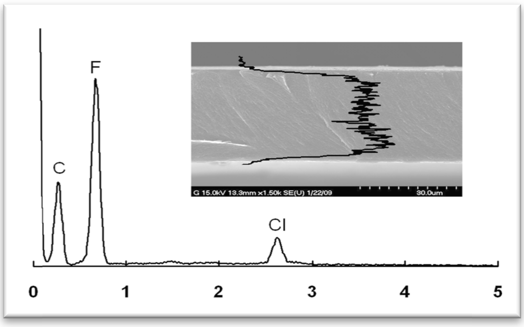

FIG. 8. Cross-sectional SEM micrograph image of the grafted FEP film (64% DOG) with the chlorine distribution profile and the EDX spectrum of the grafted FEP film.

3.3. Conclusions

It was demonstrated that a simultaneous irradiation method could be applied for the grafting of VBC onto FEP films without a noticeable degradation of the chloromethyl group. It is also concluded that chloroform is a more effective solvent than the other solvents including dichloromethane during a radiation grafting of VBC onto a FEP film. Studies showed that the degree of grafting of the FEP-g-PVBC increased with an increasing irradiation dose and the monomer concentration increased. The optimum radiation grafting conditions were also determined to be in the ranges of 1~2 kGy/h for the dose rate and 40~50% (v/v) for the VBC concentration in chloroform. Several instruments such as FTIR, TGA and SEM EDX were utilized to characterize the prepared FEP-g-PVBC films and the results support a successful grafting of VBC onto a FEP film via a simultaneous irradiation method.

4. PREPARATION AND CHARACTERIZATION OF A POLY(VINYLBENZYL SULFONIC ACID)-GRAFTED FEP MEMBRANE AS POLYMER ELECTROLYTES FOR DIRECT METHANOL FUEL CELLS

4.1. Materials and methods

4.1.1. Materials

VBC (a mixture of m- and p-isomers, 96% purity) and thiourea (99% purity) were purchased from Acros Organics and used as received. Other chemicals (sodium sulfite, sodium bisulfite, and sodium hydroxide) and solvents used are of reagent or higher grade, and used without further purification. A FEP film of 25 μm thickness was supplied by the Universal Company (Japan).

4.1.2. Preparation of poly(vinylbenzyl sulfonic acid)-grafted FEP membrane (FEP-g-PVBSA)

PVBC-grafted FEP film (FEP-g-PVBC) was prepared by simultaneous radiation grafting of PVBC onto FEP films as described in previous-section. In brief, a FEP film (4 cm × 30 cm) with 25 μm thickness was washed with acetone and dried prior to immersing it in a VBC/chloroform (40/60 volume ratio) mixture. The mixture containing the FEP film was purged with nitrogen for 10 mins and then irradiated by γ–ray from ^{60}Co source at a dose of 40 and 50 kGy with a dose rate of 2 kGy/h at room temperature. The irradiated film was washed with dichloromethane several times and dried in a vacuum oven for 12 h at 60°C to give the grafted film. DOG values of the prepared films were 64% (at 40 kGy) and 73% (at 50 kGy). Anal. Calcd. (%) for the film of 64% DOG: C, 42.3; H, 2.3. Found (%): C, 42.9; H, 3.37.

4.1.3. Preparation of poly(vinylbenzyl thiouronium salt)-grafted FEP film (FEP-g-PVBTS)

The prepared FEP-g-PVBC film (3 cm × 4 cm) was immersed in 0.13 M thiourea ethanol solution. The mixture was reacted at 40°C for 6 h to convert the chloride of the film to the thiouronium salt. The prepared film was several times washed with ethanol and dried at 60°C in a vacuum oven. Anal. calcd (%): C, 35.2; H, 2.2; N, 4.8; S, 5.5. Found (%): C, 37.1; H, 3.6; N, 5.7; S, 6.6.

4.1.4. Preparation of poly(vinylbenzyl thiol)-grafted FEP film (FEP-g-PVBSH)

The prepared FEP-g-PVBTS film was immersed in a 0.25 M sodium hydroxide aqueous solution at room temperature for 8 h. The film was washed three times with dilute hydrochloric acid and with distilled water until the pH of the washing solution was neutral. The washed films were dried at 60°C in a vacuum oven. Anal. calcd (%): C, 42.7; H, 2.6; S, 8.3. Found (%): C, 40.9; H, 2.8; S, 7.0.

4.1.5. Preparation of Poly(vinylbenzyl sulfonic acid)-grafted FEP membrane (FEP-g-PVBSA)

The prepared FEP-g-PVBTS film was added in a mixture of 30% hydrogen peroxide and acetic acid solution (40/60 volume ratio). The mixture was then reacted at room temperature for 12 h. The prepared membrane was washed several times with distilled water and then dried at 60°C in a vacuum oven. Anal. calcd (%): C, 36.0; H, 1.9; O, 9.4; S, 6.3. Found (%): C, 36.0; H, 3.0; O, 30.7; S, 5.2.

4.1.6. Instrumental analysis

Infrared (IR) spectra of the prepared membrane and intermediates were obtained by using a FTIR spectrometer Tensor-37 (Brucker, Germany) at ambient conditions in the transmittance mode. SEM EDX (7200-H, HORIBA Company) measurements were conducted to investigate the relative distribution patterns of the graft polymers on the cross-section of the prepared films. The prepared films were broken in liquid nitrogen and then coated with platinum for SEM EDX analysis. The SEM EDX operating conditions were set as follows: accelerating voltage with 15 kV and working distance 12 mm for getting CPS: 2200. Elemental analysis (Vario-EL Elemental Analyzer, Germany) measurements were conducted to determine C, N, S, H and O contents of the samples. 2 mg of each sample was subjected to the high temperature combustion mode (1150°C) for the complete combustion of the sample.

4.1.7. Ion exchange capacity (IEC) and degree of sulfonation (DOS)

Ion exchange capacity (IEC) of the prepared membranes was determined by acid-base titration. The membrane samples in acid form were immersed into a 3 mol dm^{-3} NaCl solution overnight at room temperature. The protons (H^+) released in the solution were titrated with standardized 0.1 mol dm-3 NaOH solution by using an automatic titrator (DL22, Mettler Toledo Company). The IEC value was calculated as below,

$$IEC_{exp} = [0.1 \times V_{NaOH}]/W_{dry} \qquad (2)$$

where, V_{NaOH} is the volume of 0.1 mol dm^{-3} NaOH aqueous solution consumed for the volumetric titration, and W_{dry} is the dry weight of the membrane. The degree of sulfonation (DOS) was defined as follows,

$$DOS (\%) = (IEC_{exp}/IEC_{theor}) \times 100 \qquad (3)$$

where, the IEC_{theor} is the theoretical ion exchange capacity calculated from the degree of grafting (DOG) and can be expressed by the following formula,

$$IEC_{theor} = 1000 \times DOG/(100M_{VBC} + DOG \times M_{PVBSA}) \qquad (4)$$

where, M_{VBC} is the molar weight of VBC monomer, and M_{PVBSA} is the molar weight of sulfonated VBC monomer.

4.1.8. Chemical stability

The chemical stability of the prepared FEP-g-PVBSA membrane was assessed by measuring the weight change of the swollen membrane in an aqueous H_2O_2/Fe^{2+} solution [7, 8, 34]. In this study, a membrane with a size of 2 cm × 3 cm was first soaked in distilled water at 70°C until a maximum swelling was achieved (original wet weight). The swollen membrane was then transferred to an aqueous 3% H_2O_2 solution containing 4 ppm Fe^{2+} (Fenton's reagent), and the solution was shaken in water bath at 70°C. The weight change of the swollen membrane was intermittently measured every 20~30 minutes after wiping off solvent from the surface.

4.1.9. Water and methanol uptake

Water uptake and methanol uptake of the prepared FEP-g-PVBSA membranes were measured by immersing the membranes in distilled water and 10 M methanol solution for 24 h at room temperature, respectively. Before measuring the weight of the swollen membranes, the adhering water (or methanol) was wiped off from the membrane surface. The water uptake (WU) and methanol uptake (MU) can be calculated as below,

$$\text{WU (or MU) (\%)} = [(W_w - W_d)/W_d] \times 100 \qquad (5)$$

where, W_w and W_d were the weights of wet and dried membranes, respectively.

4.1.10. Methanol permeability

The methanol permeability of prepared membrane was measured at room temperature by using a membrane-separated diffusion cell method. The prepared membrane was placed between a distilled water chamber (120 mL) and a 10 mol dm-3 methanol solution chamber (120 mL). The amount of methanol passed though the membrane to the distilled water side was measured by a gas chromatography (Shimadtzu, GC-14B, Tokyo, Japan). The methanol concentration in the water chamber as a function of time was given by,

$$g = \frac{C_B}{(t - t_0)} \qquad (6)$$

where, g was the slope, C_B was the methanol concentrations in distilled water chamber (%), t and t_0 were the experimental time (s) and the start of experimental time (s), respectively.
The methanol permeability (P, cm^2/s) was calculated as bellow,

$$P = \frac{g V_B L}{C_A A} \qquad (7)$$

where, V_B, L, A, and C_A were the volume of water chamber (cm^3), the thickness of the membrane (cm), the size of aperture (cm^2), the methanol concentrations in 10 mol dm-3 methanol solution chamber (%), respectively.

4.1.11. Proton conductivity

The proton conductivity of the prepared FEP-g-PVBSA membranes was measured by using an AC impedance analyzer. (SI 1260, Solatron Company) The impedance measurements were carried out in the frequency region from 0.01–100 kHz. The membranes were hydrated in distilled water at room temperature for 24 h prior to the measurement. The proton conductivity (σ, S/cm) was calculated as below,

$$\sigma = L/(AR) \qquad (8)$$

where, L is the distance between the two probes (cm), A was the cross-sectional area of the membrane (cm^2), and R was the electrical resistance (Ω).

4.2. Results and discussion

4.2.1. Preparation of FEP-g-PVBSA membrane

For the conversion of the benzyl chloride moiety of the PVBC-grafted FEP film to the benzyl sulfonic acid moiety, several synthetic routes have been employed in this study. Firstly, direct sulfonation [35,36] with a sulfite ion to replace the chloride has been attempted under several reaction conditions, but no noticeable reaction progress was observed according to IR spectra of the samples. The failure of the reaction was a result of the sulfite ions with low permeability and low reactivity in the perfluoropolymer-based polymer matrix. Therefore, the reaction with the sulfite ion was indirectly attempted after the conversion of the benzyl chloride moiety of the film to dimethylanilinium salt by the reaction with *N*,*N*-dimethylaniline [37], but no reaction with the sulfite ion also occurred under several reaction conditions. The reaction progress and the formation of dimethylanilinium salt in the grafted film were assessed by FTIR and TGA data (data not shown). Due to the failure of the attempted reactions of the sulfite ion with leaving groups of the grafted film, a synthetic pathway utilizing the oxidation of thiol was applied to prepare the desired membrane.

Figure 9 shows a reaction scheme for the preparation of the FEP-g-PVBSA membrane starting from the FEP-g-PVBC film. The poly(vinylbenzyl chloride)-grafted FEP film was prepared by immersing a FEP film in a vinylbenzyl chloride/chloroform (40/60 volume ratio) mixture and then irradiating by γ–ray from ^{60}Co source at a dose of 40 kGy with a dose rate of 2 kGy/h at room temperature using a simultaneous irradiation grafting method [14]. Similar membranes could also be prepared by using a pre-irradiation method [15, 17, 18].

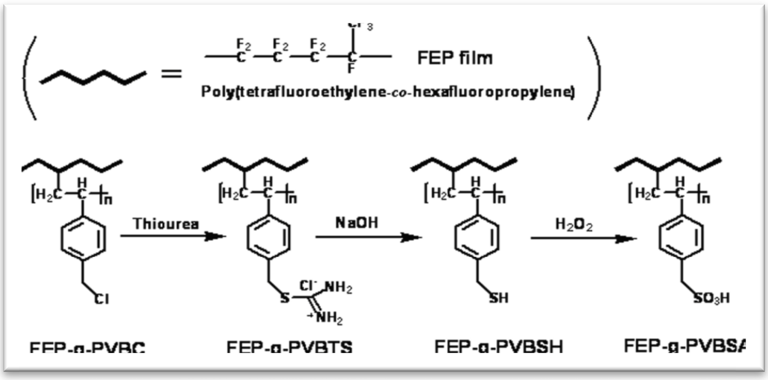

FIG. 9. Chemical reaction scheme for the FEP-g-PVBSA membrane.

Thiourea, a good organic nucleophile was applied to convert the benzyl chloride moiety of FEP-g-PVBC film to the benzyl thiol moiety [37–39]. In this reaction, a FEP-g-PVBC film with a degree of grafting of 64% was reacted with thiourea in an ethanol solution to give the desired FEP-g-PVBTS film. The reaction progress was monitored by IR spectroscopy (Figure 10A and 10B). The spectrum of FEP-g-PVBC shows absorption bands resulting from FEP base film (strong bands around 1150–1250 cm^{-1} for CF$_2$ stretching, and a sharp band at around 980 cm^{-1} arising from the C-F stretching vibration of the CF$_3$ group) and grafted PVBC (2800–3100 cm^{-1} for C–H stretching and 820 cm^{-1} for C-Cl stretching) [14]. After completion of the reaction, new absorption bands resulting from the formation of thiouronium salt (1641 cm^{-1} for C=N stretching [38] and a very broad band around 3200 cm^{-1} for N–H stretching and O–H stretching from water present as an impurity) appeared while a characteristic C–Cl band of FEP-g-PVBC disappeared, as shown in Figure 10B. The prepared FEP-g-PVBTS film was then subjected to hydrolysis by immersing it in an aqueous solution of sodium hydroxide at room temperature. The successful conversion to the FEP-g-PVBSH film was proved by IR spectral data as shown in Figure 10C. In this spectrum, the characteristic absorption bands of thiouronium salt completely disappeared, and a very similar spectral pattern to that of FEP-g-PVBC (Figure 10A) except an absorption band at 2590 cm^{-1} (S–H stretching vibration) was observed. For the final step, hydrogen peroxide was used to oxidize the thiol moiety of the grafted film to give a desired sulfonated membrane [37, 39–41]. In this reaction, the FEP-g-PVBSH film was treated with a mixture of 30% hydrogen peroxide and acetic acid solution at room temperature, and the reaction progress was monitored by IR spectroscopy and by measuring the IEC of the film (Figure 3). In the IR spectrum of the final membrane (Figure 10D), the strong absorption bands resulting from the formation of the sulfonic acid moiety (1045 cm^{-1} for O=S=O stretching and a broad absorption band at 3100–3700 cm^{-1} for O-H stretching from sulfonic acid and remaining water in the membranes) were observed.

The ion exchange capacity (IEC), which provides an indication of the content of acid groups in the membrane, was utilized to investigate the effect of oxidation time, and the result is shown in

Figure 11. The theoretical IEC of the FEP-g-PVBSA membrane having degree of grafting 73% is found to be 2.44 meq/g. The experimental IEC value continuously increased with the reaction time up to 1.6 meq/g for 12 h with 66% DOS, and then slowly decreased. The decrease of the IEC value after 12 h is considered due to the possible decomposition of the grafted polymer under the oxidative reaction conditions.

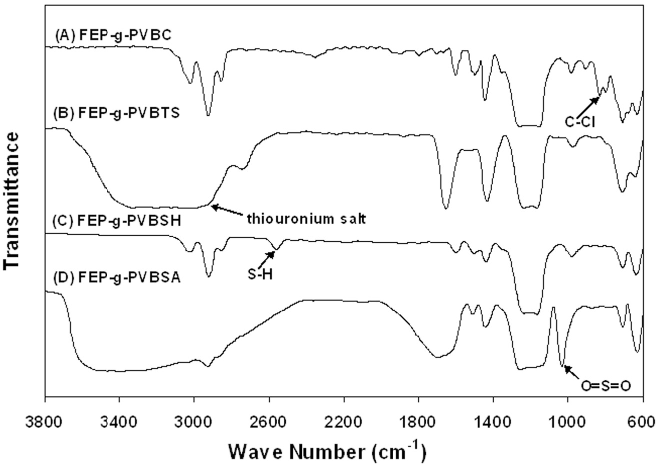

FIG. 10. FTIR spectra of (A) FEP-g-PVBC, (B) FEP-g-PVBTS, (C) FEP-g-PVBSH, and (D) FEP-g-PVBSA.

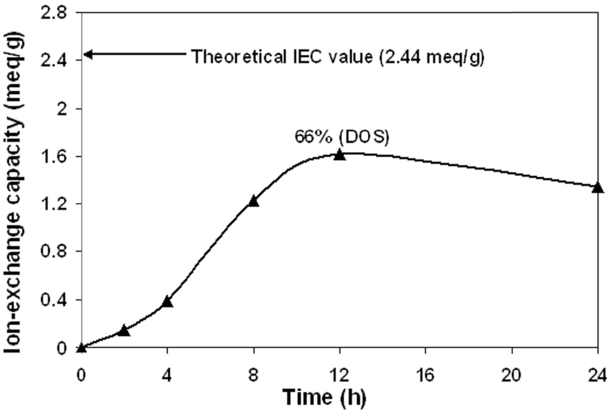

FIG. 11. Monitoring of oxidation process performed in hydrogen peroxide/water/acetic acid (12/28/60) at room temperature.

The conversion progress and success of each reaction step starting from a FEP-g-PVBC to a FEP-g-PVBSA membrane were also confirmed by the elemental analysis study of the samples using an EDX instrument (Figure 12). The EDX data obtained from the cross-sectional surface of the prepared films show several peaks corresponding to carbon, fluorine, chlorine, sulfur, and oxygen atoms. After formation of the thiouronium salt in the grafted film, a peak of sulfur atom with a relatively high atomic number appeared on the spectrum while a peak of nitrogen atom with a low atomic number was not detected due to the low intensity of the atom in this EDX mode. A peak for chlorine atom present as a counter anion in the spectrum 12B completely disappeared in the spectrum 12C indicating successful conversion of a FEP-g-PVBTS to a FEP-g-PVBSH film. After treatment of the FEP-g-PVBTS film with hydrogen peroxide, a peak for an oxygen atom appeared in the spectrum 12D indicating successful oxidation of the thiol moiety in the grafted film to the sulfonic acid moiety.

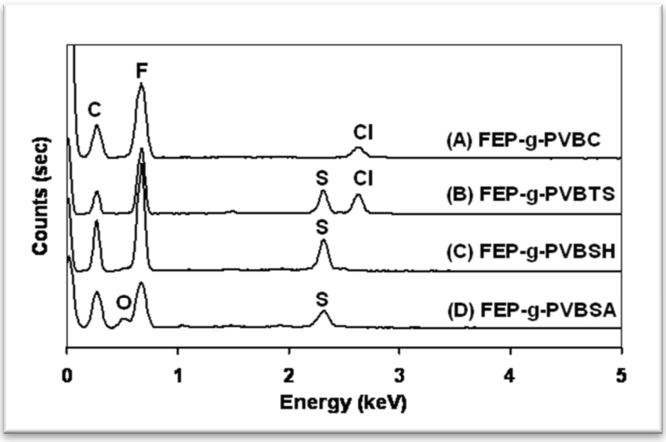

FIG. 12. EDX spectra of (A) FEP-g-PVBC, (B) FEP-g-PVBTS, (C) FEP-g-PVBSH, and (D) FEP-g-PVBSA.

Currently, the SEM-EDX instrument with fast scanning and multiple-sample loading ability has widely been applied to investigate the element distribution of films and monitor the conversion progress [22, 42]. Figure 13 shows the element distribution profiles of the characteristic atoms over the cross-section of the grafted FEP samples (64% DOG), observed by SEM-EDX. As shown in the chlorine atom distribution profile of the FEP-g-PVBC film (Figure 13A), the grafted film with a relatively even grafting profile over the cross-section was employed to prepare the desired FEP-g-PVBSA membrane in this study [14]. The nearly identical distribution profiles of the chlorine and sulfur atoms observed in Figure 13B indicate an effective conversion to the desired FEP-g-PVBTS through the inner portion of the film. Furthermore, the reduction of the chlorine atom to a low level (possibly noise level) observed in Figure 13C also indicates that the thiouronium chloride salt in the grafted film was effectively converted to the desired FEP-g-PVBSH through the inner portion of the film. The intensity of the distribution profile of oxygen atom in Figure 13D is somewhat lower compared to other heavier atoms such as chlorine and sulfur due to its lower sensitivity in the standard EDX detector, but the oxygen profile still supports the successful formation of the sulfonic acid moiety in the grafted film.

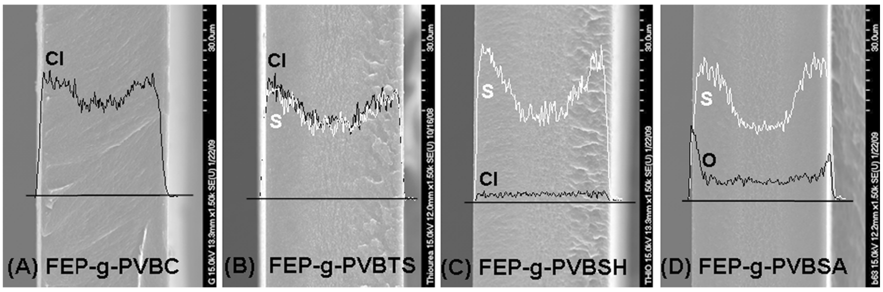

FIG 13. Cross-sectional SEM micrographs and characteristic element distribution profiles of (A) FEP-g-PVBC, (B) FEP-g-PVBTS, (C) FEP-g-PVBSH, and (D) FEP-g-PVBSA.

Elemental analysis was also conducted by a combustion method to determine the element (C, N, S, H, and O) contents of each prepared film. The experimental results were in good agreement with the theoretical results, except that the oxygen content of the FEP-g-PVBSA membrane was higher than the theoretical value. This difference can be attributed to the water molecules associated with sulfonic acid groups in the membrane.

4.2.2. Chemical stability of FEP-g-PVBSA membrane

In general, the chemical stability of poly(styrene sulfonic acid)-grafted fluoropolymer membranes is lower than that of Nafion® membranes against peroxy radical attack during the fuel cell operation, and this low stability of the membranes has hampered their use as fuel cell membranes even though they have showed promising performances [1, 7, 8, 34]. The lower chemical stability of the poly(styrene sulfonic acid)-grafted fluoropolymer membranes is due to the labile benzyl position of the graft chain that causes the graft chain scission [1, 2, 7, 8]. An approach to improve the chemical stability of the radiolytically prepared membranes is to utilize the substituted styrene as a grafting monomer, thus enhancing the chemical stability of the membrane prepared with the substituted styrene [7]. The sulfonic acid moieties in the prepared FEP-g-PVBSA membrane were not directly connected to the benzene rings of the graft chains, and this structural change could also change the chemical stability of the membrane by changing the radical stability of the benzyl position of the graft chain.

To evaluate the relative chemical stability of the prepared membranes, a FEP-g-PVBSA membrane (A: DOG 73%, IEC 1.23 meq/g) and two FEP-g-PSSA membranes (B: DOG 24%, IEC 1.4 meq/g, C: DOG 79%, IEC 2.4 meq/g) were subjected for a simple chemical stability test utilizing Fenton's reagent containing 3% H_2O_2 and 4 ppm of Fe^{2+}. The results are shown in Figure 14. In this experiment, three samples were soaked in distilled water at 70°C until they reached the maximum swelling, and then they were transferred to Fenton's reagent pre-equilibrated at 70°C. The decrease of the wet-weight of the membranes observed in Figure 14 can be attributed to both the cleavage of the hydrophilic graft-chain and the resulting water loss from the swollen membrane.

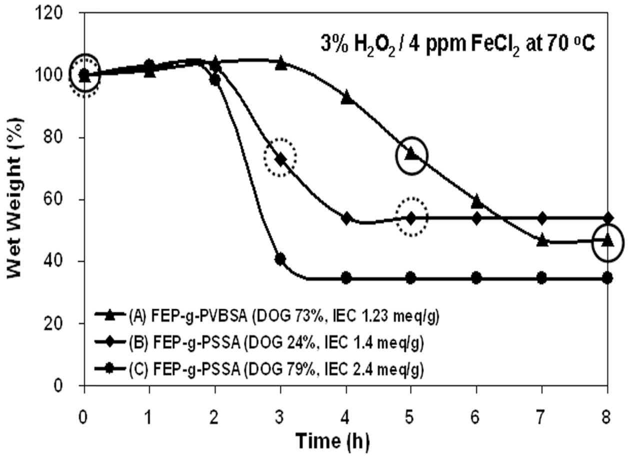

FIG.14. The chemical stability test of the prepared (A) FEP-g-PVBSA (DOG 73%, IEC 1.23meq/g), (B) FEP-g-PSSA (DOG 24%, IEC 1.4 meq/g), and (C) FEP-g-PSSA (DOG 79%, IEC 2.4 meq/g) membranes in 3% H_2O_2 *solution containing 4 ppm* Fe^{2+} *at 70 °C.*

The FEP-g-PVBSA membrane 14A (DOG 73%, IEC 1.23 meq/g) shows higher chemical stability than FEP-g-PSSA membranes 14B and 14C, as shown in Figure 14. The wet–weight of the FEP-g-PVBSA membrane 14A began to decrease from 3 h and remained constant after 7 h, while those of two FEP-g-PSSA membranes 14B and 14C began to decrease at 2 h and remained constant within 4 h. The faster wet-weight loss was observed from the membrane with a higher DOG value (Figure 14C) and this can be attributed to the higher uptake of Fenton's reagent that causes the chain scission. Both the beginning time of the wet-weight loss and the decrease rate show that the prepared FEP-g-PVBSA membrane has higher chemical stability than the FEP-g-PSSA membrane.

The degradation processes of the FEP-g-PSSA and FEP-g-PVBSA membranes were also monitored by IR spectroscopy (Figure 15A and 15B). During the wet–weight loss periods (3 h for 15A and 5 h for 15B, respectively), the decreased IR band intensities of each graft chain were observed. No significant IR bands of each graft chain were observed after the end of the wet–weight loss time (5 h for 15A and 8 h for 15B, respectively) while IR bands corresponding to the CF_2 groups of the FEP film still exist. This observation indicates that the wet-weight loss is due to the loss of the sulfonated graft chain in the presence of the Fenton's reagent and, furthermore, supports that the chemical stability of the FEP-g-PVBSA membrane is better than those of the FEP-g-PSSA membranes.

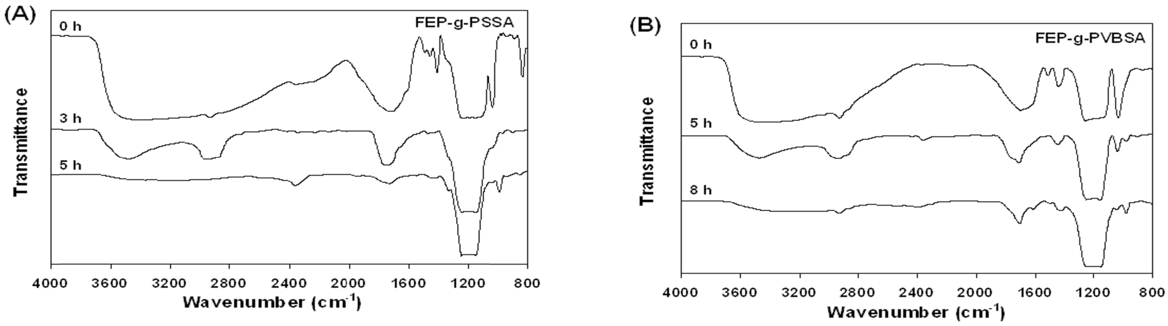

FIG. 15. FTIR spectra of (A) the FEP-g-PSSA membranes: (DOG 24%, IEC 1.4 meq/g) soaked in Fenton's reagent for 3 and 5 h, and (B) the FEP-g-PVBSA membranes (DOG 73%, IEC 1.23 meq/g) soaked in Fenton's reagent for 5 and 8 h.

4.2.3. Characterization of FEP-g-PVBSA membranes as polymer electrolytes for direct methanol fuel cells

To investigate the physio-chemical properties of the prepared membranes as polymer electrolytes for direct methanol fuel cell, three membranes with various the degree of grafting were prepared as shown in Table 1 and applied for the characterization study.

TABLE 1. PREPARATION OF MEMBRANES

	Nafion®212	DOG 36	DOG 61	DOG 102
Dose (kGy)		30	60	60
VBC concentration (vol.%)		40	40	50
Dry thickness (μm)	50	35	38	44
Wet thickness (μm)	64	38	40	50

To observe the cross-sectional distribution behaviors of the graft polymer in the prepared membranes with various the degrees of grafting, the relative intensities of the sulfur and fluorine atoms across the cross-section were investigated by using an EDX instrument (Figure 16). The cross-sectional distribution profile of the membrane, with 36% DOG, exhibited higher sulfur atom distribution near the surface region and relatively higher fluorine atom distribution near the middle of the membrane. It was well known that the irradiation grafting process starts at the surface of the base film and progresses to the diffusion of the monomer through the grafted layers into the inside of the film. At a low degree of grafting (36%), the PVBC grafts were mainly located near the surface of the film, and this could exert high local resistance and obstruct proton transfer near the middle of the film. Whereas, as the DOG increased, the distribution profiles of sulfur and fluorine atoms became flatter (from 36% to 102% DOG) indicating that the grafts are evenly distributed across the membrane.

The IEC value was a very important factor determining fuel cell membrane properties since it provided an indication of the content of sulfonic acid groups in the membrane, which was closely related to proton conductivity. Figure 17 shows the IEC values of the FEP-g-PVBSA membranes as a function of the degree of grafting. As the degree of grafting increased, the IEC values increased. This tendency can be attributed to the increased number of sulfonic acid groups incorporated in the FEP-g-PVBSA membranes with the increase in the degree of grafting. In comparison with the theoretical IEC values, the experimental IEC values were measured to be about 60% of the theoretical IEC values. As shown in Figure 17, the FEP-g-PVBSA membrane, with 36% DOG, exhibited a slightly lower IEC value (0.8 meq/g) than the Nafion® 212 membrane (0.9 meq/g). Considering the uneven distribution of the membrane with the low DOG shown in Figure 16, the membranes with higher DOG values were considered to be suitable for fuel cell application.

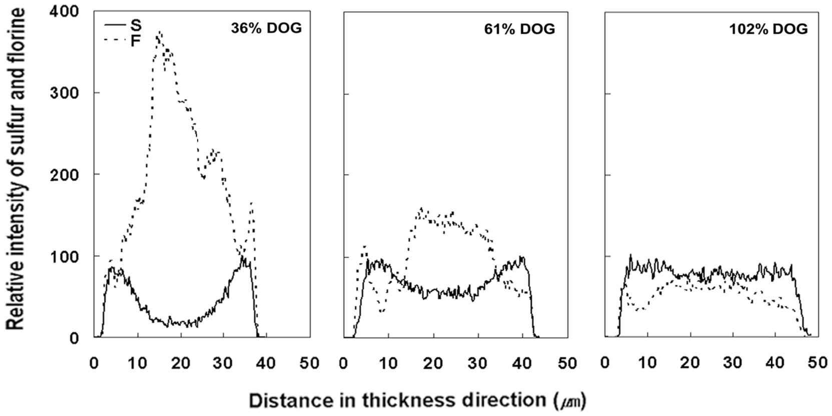

FIG. 16. Comparison of sulfur and fluorine distributions of FEP-g-PVBSA membranes.

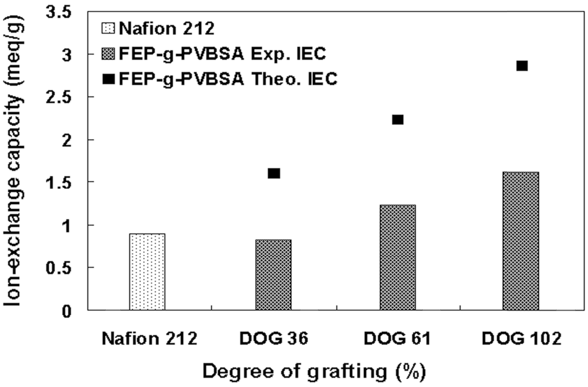

FIG. 17. The ion-exchange capacities of the prepared FEP-g-PVBSA membranes as a function of the degree of grafting. The theoretical IEC value curve and Nafion 212 are also plotted.

The water uptake of the fuel cell membrane was also an important factor because high water uptake could lead to problems concerning dimensional stability and mechanical properties. Figure 18 shows the water uptakes of the prepared membranes as a function of degree of grafting. The water uptake also increased with increasing the degree of grafting that is the membranes became more hydrophilic by the incorporation of more sulfonic acid groups on the membranes. In this study, the water uptake of the membranes increased from 10–30% as the degree of grafting increased from 36–102%. The water uptake of the Nafion® 212 membrane was measured to be 17% under the same experimental conditions.

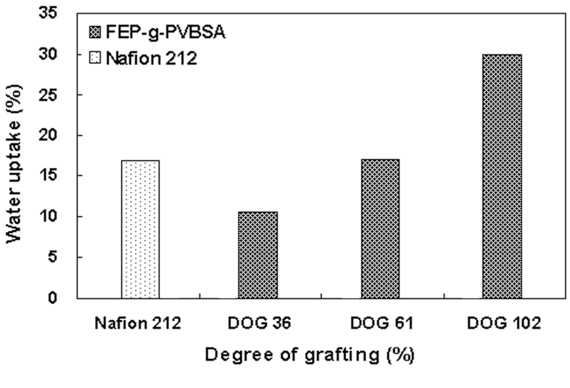

FIG. 18. The water uptakes of the prepared FEP-g-PVBSA membranes as a function of the degree of grafting at room temperature.

Figure 19 shows the proton conductivity of the membranes as a function of DOG. The proton conductivity of the membranes was measured in their water-saturated state at room temperature. The results show that the proton conductivities increased with the increasing DOG due to the increase of the proton exchangeable sulfonic acid groups in the membranes. Similar results were also observed from the water uptake experiments, as shown in Figure 18. Compared with the Nafion® 212 membrane (6.1E-02 S/cm), the prepared membrane showed higher proton conductivity when the degree of grafting reached 60%.

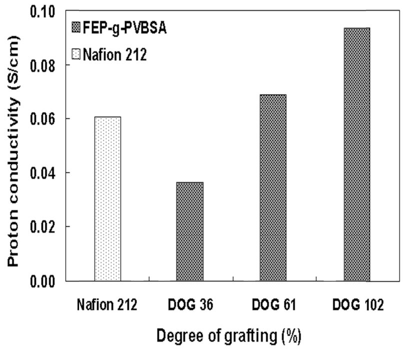

FIG. 19. The proton conductivities of the prepared FEP-g-PVBSA membranes as a function of the degree of grafting at room temperature.

Methanol used as a fuel for DMFC can also permeate through the hydrophilic regions of the polymer electrolyte membrane, and this methanol crossover phenomenon was known to decrease the cell performance via fuel consumption and the catalyst poisoning process. Since higher methanol feed concentration can provide a higher overall cell voltage and power density, it was also necessary to develop the membranes with lower methanol crossover so that they could be used at a higher methanol concentration. In particular, the Nafion® membrane known to have high methanol crossover was considered to be inappropriate for a DMFC application. Figure 20(A) shows the methanol permeability of the membranes as a function of the degree of grafting. Even though these methanol-related properties increased with the increasing of the degree of grafting, the prepared membranes still showed considerably lower methanol permeability than that of Nafion 212 at the given range of the degree of grafting (up to 102%). This lower methanol permeability was considered due to the inherent properties of the membranes grafted with a hydrocarbon based polymer, PVBSA that had a lower affinity with methanol, compared to Nafion® composed of fully fluorocarbon based chain. The methanol uptakes of the prepared membranes were presented in Figure 20(B) and the results were well in conformity with the methanol permeability results shown in Figure 20(A).

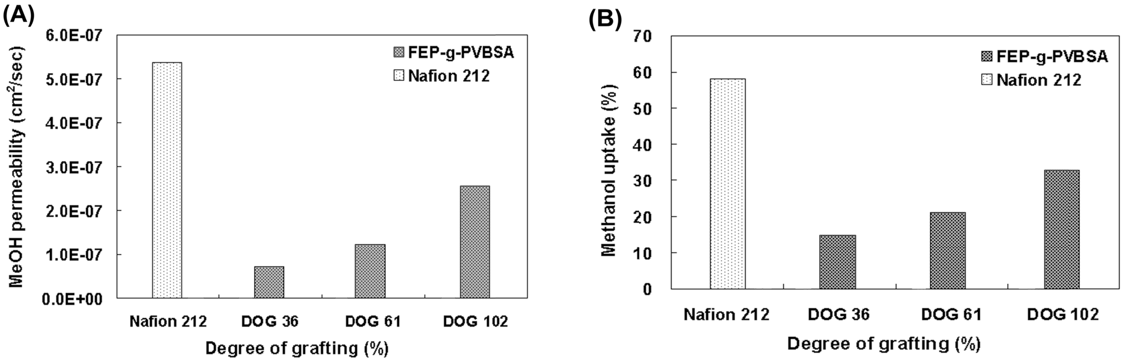

FIG.20. The methanol permeability (A) and methanol uptake (B) of the prepared FEP-g-PVBSA membranes as a function of the degree of grafting at room temperature.

4.3. Conclusions

A novel FEP-g-PVBSA polymer membrane with improved chemical stability was successfully prepared by the chemical modification of the radion grafted FEP-g-PVBC film. The reactions for the introduction of the sulfonic acid moiety to the graft chain were carried out via the formation of thiouronium salt with thiourea, base-catalyzed hydrolysis for the formation of thiol, and oxidation with hydrogen peroxide. FTIR, elemental analysis, and SEM-EDX results indicated that each chemical conversion step was processed. The chemical stability test performed with Fenton's reagent indicated that the FEP-g-PVBSA membrane had better chemical stability compared to the FEP-g-PSSA membranes. The characteristic studies of the membranes for DMFC application including IEC, water and methanol uptake, methanol permeability, and proton conductivity indicated that the FEP-g-PVBSA membrane could be utilized as a polymer electrolyte membrane for DMFC application.

ACKNOWLEDGEMENT

This work was supported by Nuclear R & D Program through the Korea Science and Engineering Foundation funded by the Ministry of Education, Science, and Technology, Korea.

REFERENCES

[1] NASEF, M.M., SAIDI, H., NOR, H.M., FOO, O.M., Cation exchange membranes by radiation-induced graft copolymerization of styrene onto PFA copolymer films. II. Characterization of sulfonated graft copolymer membranes, J. Appl. Polym. Sci. **76** (2000) 1-11.

[2] GUBLER, L., GÜRSEL, S.A., SCHERER, G.G., Radiation grafted membranes for polymer electrolyte fuel cells, Fuel Cells **5** (2005) 317-335.

[3] LI, J., SATO, K., ICHIDURI, S., ASANO, S., IKEDA, S., IIDA, M., OSHIMA, A., TABATA, Y., WASHIO, M., Pre-irradiation induced grafting of styrene into crosslinked and non-crosslinked polytetrafluoroethylene films for polymer electrolyte fuel cell applications. I: Influence of styrene grafting conditions, Eur. Polym. J. **40** (2004) 775-783.

[4] SHERAZI, T.A., AHMAD, S., KASHMIRI, M.A., GUIVER, M.D., Radiation-induced grafting of styrene onto ultra-high molecular weight polyethylene powder and subsequent film fabrication for application as polymer electrolyte membranes: I. Influence of grafting conditions, J. Membr. Sci. **325** (2008) 964-972.

[5] NASEF, M.M., Gamma radiation-induced graft copolymerization of styrene onto poly(ethylene terephthalate) films, J. Appl. Polym. Sci. **77** (2000) 1003-1012.

[6] NASEF, M.M., SAIDI, H., NOR, H.M., Proton exchange membranes prepared by simultaneous radiation grafting of styrene onto poly(tetrafluoroethylene-co-hexafluoropropylene) films. I. Effect of grafting conditions, J. Appl. Polym. Sci. **76** (2000) 220-227.

[7] CHEN, J., ASANO, M., YAMAKI, T., YOSHIDA, M., Preparation and characterization of chemically stable polymer electrolyte membranes by radiation-induced graft copolymerization of four monomers into ETFE films, J. Membr. Sci. **269** (2006) 194-204.

[8] FU, R.Q., WOO, J.J., SEO, S.J., LEE, J.S., MOON, S.H., Sulfonated polystyrene/polyvinyl chloride composite membranes for PEMFC applications, J. Membr. Sci. **309** (2008) 156-164.

[9] NASEF, M.M., SAIDI, H., Preparation of crosslinked cation exchange membranes by radiation grafting of styrene/divinylbenzene mixtures onto PFA films, J. Membr. Sci. **216** (2003) 27-38.

[10] DUST, J.M., ARNOLD, D.R., Substituent effects on benzyl radical ESR hyperfine coupling constants. The σα·scale based upon spin delocalization, J. Am. Chem. Soc. **105** (1983) 1221-1227.

[11] LIU, L., CHENG, Y.H., FU, Y., CHEN, R., GUO, Q.X., The nonpolar resonance effects and the non-hammett behaviors, J. Chem. Inform. Computer Sci. **42** (2002) 1164-1170.

[12] PRATT, D.A., WRIGHT, J.S., INGOLD, K.U., Theoretical study of carbon-halogen bond dissociation enthalpies of substituted benzyl halides. How important are polar effects, J. Am. Chem. Soc. **121** (1999) 4877-4882.

[13] SINGH, N.K., POPELIER, P.L.A., O'MALLEY, P.J., Substituent effects on the stability of para substituted benzyl radicals, Chem. Phy. Lett. **426** (2006) 219-221.

[14] SHIN, J., GENG, F., KANG, S.A., KO, B.S., KANG, P.H., NHO, Y.C,. Simultaneous radiation grafting of vinylbenzyl chloride onto poly(tetrafluoroethylene-co-hexafluoropropylene) films, J. Appl. Polym. Sci. **113** (2009) 2858-2862.

[15] DANKS, T.N., SLADE, R.C.T., VARCOE, J.R., Alkaline anion-exchange radiation-grafted membranes for possible electrochemical application in fuel cells, J. Mater. Chem. **13** (2003) 712-721.

[16] ALEXANDRATOS, S.D., ZHU, X., Amination of poly(vinylbenzyl chloride) with N,N-dimethylformamide, Macromol. **36** (2003) 3436-3439.

[17] DANKS, T.N., SLADE, R.C.T., VARCOE, J.R., Comparison of PVDF- and FEP-based radiation-grafted alkaline anion-exchange membranes for use in low temperature portable DMFCs, J. Mater. Chem. **12** (2002) 3371-3373.

[18] HERMAN, H., SLADE, R.C.T., VARCOE, J.R., The radiation-grafting of vinylbenzyl chloride onto poly(hexafluoropropylene-co-tetrafluoroethylene) films with subsequent conversion to alkaline anion-exchange membranes: Optimisation of the experimental conditions and characterization, J. Membr. Sci. **218** (2003) 147-163.

[19] CHOI, Y.J., KANG, M.S., CHO, J., MOON, S.H., Preparation and characterization of LDPE/polyvinylbenzyl trimethyl ammonium salts anion-exchange membrane, J. Membr. Sci. **221** (2003) 219-231.

[20] SLADE, R.C.T., VARCOE, J.R., Investigations of conductivity in FEP-based radiation-grafted alkaline anion-exchange membranes, Solid State Ionics **176** (2005) 585-597.

[21] SCHMIDT-NAAKE, G., BÖHME, M., CABRERA, A., Synthesis of proton exchange membranes with pendent phosphonic acid groups by irradiation grafting of VBC, Chem. Eng. Tech. **28** (2005) 720-724.

[22] DARGAVILLE, T.R., GEORGE, G.A., HILL, D.J.T., WHITTAKER, A.K., High energy radiation grafting of fluoropolymers, Prog. Polym. Sci. **28** (2003), 1355.

[23] CARDONA, F., GEORGE, G.A., HILL, D.J.T., RASOUL, F., MAEJI, Copolymers obtained by the radiation-induced grafting of styrene onto poly(tetrafluoroethylene-co-perfluoropropylvinyl ether) substrates. 1. Preparation and structural investigation, Macromolecules **35** (2002) 355-364.

[24] NASEF, M.M., Effect of solvents on radiation-induced grafting of styrene onto fluorinated polymer films, Polym. Int. **50** (2001) 338-346.

[25] CARDONA, F., GEORGE, G.A., HILL, D.J.T., PERERA, S.J., Spectroscopic study of the penetration depth of grafted polystyrene onto poly(tetrafluoroethylene-co-perfluoropropylvinylether) substrates. 1. Effect of grafting conditions, Polym. Sci. **40** (2002) 3191-3199.

[26] LI, Y., DESIMONE, J.M., POON, C.D., SAMULSKI, E.T., Photoinduced graft polymerization of styrene onto polypropylene substrates, J. Appl. Polym. Sci. **64** (1997) 883-889.

[27] NASEF, M.M., SAIDI, H., NOR, H.M., DAHLAN, K.Z.M., HASHIM, K., Cation exchange membranes by radiation-induced graft copolymerization of styrene onto pfa copolymer films. i. preparation and characterization of the graft copolymer, J. Appl. Polym. Sci. **73** (1999) 2095-2101.

[28] BRACK, H.-P., BÜHRER, H.G., BONORAND, L., SCHERER, G.G., Grafting of pre-irradiated poly(ethylene-alt-tetrafluoroethylene) films with styrene: Influence of base polymer film properties and processing parameters, J. Mater. Chem. **10** (2000) 1795-1803.

[29] WALLING, C., Free Radical in Solution, 1st ed. Wiley, California, (1957) 152.

[30] CAMBRON, R.T., HARRIS, J.M., Time-resolved photothermal grating calorimetry for investigating kinetics of free-radical chain reactions, Anal. Chem. **67** (1995) 365-373.

[31] MIYASAKA, H., KHAN, S.R., ITAYA, A., Solvent effect of the hole migration along a poly(N-vinylcarbazole) chain as revealed by picosecond transient absorption and dichroism measurements, J. Phys. Chem. A. **106** (2002) 2192-2199.

[32] SAYED, W.M., Preparation of modified polystyrene with maleic anhydride in the presence of different solvents, J. Appl. Polym. Sci. **109** (2008) 4099-4104.

[33] BÜCHI, F.N., GUPTA, B., HAAS, O., SCHERER, G.G., Study of radiation-grafted FEP-G-polystyrene membranes as polymer electrolytes in fuel cells, Electrochim. Acta. **40** (1995), 345-353.

[34] BELECKI, K., BERLINER, M., BIBART, R.T., MELTZ, C., NG, K., PHILLIPS, J., RIPIN, D.H.B., VETELINO, M., Route development and bulk synthesis of CP-865,569, Org. Proc. Res. Develop. **11** (2007) 754-761.

[35] CHEN, Y.T., XIE, J., SETO, C.T., Peptidic α-ketocarboxylic acids and sulfonamides as inhibitors of protein tyrosine phosphatases, J. Org. Chem. **68** (2003) 4123-4125.

[36] CLEMENS, D.H., LANGE, R.J., Method of preparing resins containing sulfonic acid functionality involving oxidation of thiouronium salts with hydrogen peroxide, U.S. Patent 3944507 (1976).

[37] HUBER, W., BUBENDORF, A., GRIEDER, A., OBRECHT, D., Monitoring solid phase synthesis by infrared spectroscopic techniques, Anal. Chim. Acta **393** (1999) 213.

[38] MCALLISTER, L.A., BRAND, S., GENTILE, R.D., PROCTER, D.J., The first Pummerer cyclisations on solid phase. Convenient construction of oxindoles enabled by a sulfur-link to resin, Chem. Comm. **18** (2003) 2380-2381.

[39] LLAUGER, L., HE, H., CHIOSIS, G., Synthesis of 8-arylsulfoxyl/sulfonyl adenines, Tetra. Lett. **45** (2004) 9549-9552.

[40] SHYLESH, S., SHARMA, S., MIRAJKAR, S.P., SINGH, A.P., Silica functionalised sulphonic acid groups: Synthesis, characterization and catalytic activity in acetalization and acetylation reactions, J. Mol. Cat. A: Chem. **212** (2004) 219-228.

[41] GUPTA, B., BÜCHI, F.N., SCHERER, G.G., CHAPIR, A., Crosslinked ion exchange membranes by radiation grafting of styrene/divinylbenzene into FEP films, J. Membr. Sci. **118** (1996) 231-238.

[42] KIMURA, Y., ASANO, M., CHEN, J., MAEKAWA, Y., KATAKAI, R., YOSHIDA, M., Influence of grafting solvents on the properties of polymer electrolyte membranes prepared by γ-ray preirradiation method, Rad. Phys. Chem. **77** (2008) 864-870.

[43] GUO, Q., PINTAURO, P.N., TANG, H. S., O'CONNOR, Sulfonated and crosslinked polyphosphazene-based proton-exchange membranes, J. Membr. Sci. **154** (1999) 175-181.

DEVELOPMENT OF LESS WATER-DEPENDENT RADIATION GRAFTED PROTON EXCHANGE MEMBRANES FOR FUEL CELLS

M.M. NASEF, A. AHMAD, H. SAIDI, K.Z.M. DAHLAN

Institute of Hydrogen Economy
Energy Research Alliance (ERA)
International Campus
Univeristi Teknologi Malaysia
Jalan Semarak, Kuala Lumpur

Radiation Processing Division
Malaysian Nuclear Agency
Bangi, Kajang
MALAYSIA

Abstract

The aim of these studies was the development of proton exchange membranes for polymer electrolyte membrane (PEM) fuel cell operated above 100°C, in order to obtain less water dependent, high quality and cheap electrolyte membrane. Sulfonic acid membranes were prepared by radiation induced grafting (RIG) of sodium styrene sulfonate (SSS) onto electron beam (EB) irradiated poly(vinylidene fluoride) (PVDF) films in a single step reaction for the first time using synergetic effect of acid addition to grafting mixture under various grafting conditions. The fuel cell related properties of the membranes were evaluated and the in situ performance was tested in a single H_2/O_2 fuel cell under dynamic conditions and compared with a similar sulfonated polystyrene PVDF membrane obtained by two-step conventional RIG method i.e. grafting of styrene and subsequent sulfonation. The newly obtained membrane (degree of grafting, G% = 53) showed an improved performance and higher stability together with a cost reduction mainly as a result of elimination of sulfonation reaction. Acid-base composite membranes were also studied. EB pre-irradiated poly(ethylene-*co*-tetrafluoroethylene) (ETFE) films were grafted with N-vinyl pyridine (NVP). The effects of monomer concentration, dose, reaction time, film thickness, temperature and film storage time on G% were investigated. The membranes were subsequently doped with phosphoric acid under controlled condition. The proton conductivity of these membranes was investigated under low water conditions in correlation with the variation in G% and temperature (30–130°C). The performance of 34 and 49% grafted and doped membranes was tested in a single fuel cell at 130°C under dynamic conditions with 146 and 127 mW/cm^2 power densities. The polarization, power density characteristics and the initial stability of the membrane showed a promising electrolyte candidate for fuel cell operation above 100°C.

1. OBJECTIVE OF THE RESEARCH

The main objective of this research is to develop highly conductive, stable and less water-dependent radiation grafted membranes PEM for fuel cells operation above 100°C. The scope of the work also involves development of sulfonic acid membranes for low temperature fuel cell operation using shorter radiation induced grafting route to improve the properties of the membranes and reduce their cost of preparation.

2. INTRODUCTION

The search for new alternative cost effective electrolyte membranes for polymer electrolyte membrane (PEM) fuel cell continues to attract an increasing worldwide attention in the field of advanced materials and electrochemical systems. Various approaches have been explored by many research groups to obtain highly conductive, stable and cost effective materials. This includes formation of Nafion® composites or modification of Nafion® membranes by surface coatings. Direct sulfonation of non-fluorinated polymer backbones such as polystyrene, polyphosphazene, polyphenylene oxide, polysulfone, polyether sulfone, polyether ether ketone, polybenzimidazole and polyimides was also adopted. The challenge in this approach is to achieve sufficient sulfonation for high proton conductivity in the membranes without the polymer becoming soluble. Another approach involves sulfonation of pendent aromatic rings attached to a variety of copolymer (grafted) films obtained by chemical plasma, thermal or radiochemical graft copolymerization of styrene monomer was pursued. The various approaches for membrane preparation were recently reviewed [2]. Radiation-induced graft copolymerization has been found to be an effective method for preparation of alternative cost effective PEM for fuel cells [3, 4]. The membranes obtained by this method have the advantages of ease of preparation, compositional controllability and absence of shaping problem.

Radiation grafted fuel cell membranes are commonly prepared by grafting of styrene onto fluorinated polymer films followed by sulfonation reaction. However, the obtained membranes have been found to lack chemical and mechanical stabilities as indicated by short life time in fuel cell [5]. To enhance the stability of the polystyrene sulfonic acid membranes and to meet the durability demands in fuel cell, research workers used various strategies including crosslinking with agents such as divinylbenzene (DVB) [6–10], grafting of substituted styrene monomers such as α-methylstyrene [11, 12] and α,β,β-trifluorostyrene [13], grafting of a comonomer with styrene or substituted styrene [14–16]. However, proton transport in sulfonic acid bearing membranes such as Nafion and their analogous commercial or developmental counterparts takes place in the aqueous phase of these membranes and therefore it is necessary to have an adequate membrane humidification during fuel cell operation. Both excess and less water in the membranes hinder the performance of fuel cell. This also limits the usage of these membranes to application having fuel cell operating below 100°C (60–80°C) [17, 18]. At temperatures above 100°C Nafion loses water and conductivity leading to a sharp drop in the PEM fuel cell performance [19]. This trend together with the high cost has motivated the search for new membranes for higher temperature operation. Technically, operating fuel cell at temperature above 100°C makes water management easier because water molecules exist in a gaseous state. Furthermore, the high temperature operation enhances the catalytic activity at the electrodes and reduces the poisoning by CO [20].

Various approaches have used to develop alternative membranes for high temperature fuel cell operation: 1) modification of Nafion® membranes with inorganic conductors/fillers such as zirconium phosphate, zirconium oxide or silica to enhance water retention within the membrane [19, 21], 2) loading of Nafion® with less water dependent proton conductor such as phosphoric acid [22], *N*-heterocycles [23] or ionic liquids [24] and 3) formation of acid-base composites of basic polymers, like poly(ethylene oxide) [26] and poly(4-vinylimidazole) [27], doped with various organic and inorganic acids (mostly phosphoric acid) [28, 29]. Most of these membranes acquire sufficient proton conductivities whereas their mechanical stabilities are deemed to be low particularly at higher acid doping levels.

Applying radiation induced grafting method to prepare fuel cell membranes for higher temperature operation has been very scarce. Grafting monomers such as N-vinylpyridine (NVP) onto radiation resistant fluorinated polymer such as ETFE films followed by doping with phosphoric acid provide acid-base composite membranes that can reduce the reliance of the ionic conductivity on the water absorbance.

3. MATERIALS AND METHODS

3.1. Materials

ETFE films with various thicknesses (50–120 μm) were obtained from Nowofol GmbH (Germany) and used as polymer substrates for preparation of the membranes in this study. Pieces of ETFE film of surface area of 10 cm × 10 cm were used as standard samples. NVP of purity more than 95% (Aldrich) was used immediately after purification by vacuum distillation under reduced pressure (6.7 mbar, 54°C). Other solvents such as acetone, isopropanol, tetrahydrofuran, methanol and toluene were research grade and used as received.

3.2. Preparation of the membranes

3.2.1. Irradiation of polymer films

ETFE or PVDF films were washed with acetone or ethanol and dried in a vacuum oven at 70°C for 1 hour. The initial weights of the film samples were recorded. The films were irradiated by electron beam (EB) accelerator (NHV-Nissin high voltage, EPS 3000, Cockroft Walton type, Japan) with doses ranging from 20–100 kGy at 10 kGy per pass under N_2 atmosphere. Details of parameters of EB accelerator and irradiation conditions are given in Table 1. After irradiation, the irradiated films were quickly sealed in evacuated thin polyethylene bag and kept in a low temperature freezer at - 60°C.

TABLE 1. PARAMETERS OF EB ACCELERATOR AND IRRADIATION CONDITIONS OF ETFE FILMS

EB acceleration parameters:	
Accelerating voltage	200 keV (PVDF) 500 keV (ETFE)
Beam current	2.0 mA
Dose per pass	10 kGy
Irradiation conditions:	
Dose range	20–100 kGy
Atmosphere	N_2
Temperature	ambient

3.2.2. Grafting of N–vinylpyridine

Graft copolymerization of NVP onto ETFE films was carried out using the grafting system shown in Fig. 1. The irradiated ETFE film was placed in a glass reactor, which was tightly sealed then evacuated to remove air using a vacuum pump (10 mbar). In the meantime, a bubbler containing a solution of the monomer/solvent (with a specified composition) was bubbled with purified N_2 gas for 10 minutes to remove air. The deaerated grafting solution was then transferred to the evacuated glass reactor containing ETFE film through a tri-way stopcock and the reactor side inlet was carefully sealed under N_2 atmosphere and eventually detached from the rest of the system. To allow the graft copolymerization reaction to be initiated, the glass reactor was placed in a thermostatic bath at specified temperature for a desired period of time. After completion of the grafting reaction, the grafted films were removed and extracted with methanol and tetrahydrofuran under ultrasonication for one day to remove the excess monomer and the homopolymer occluded in the surfaces of the films. The grafted films were dried under vacuum (10 mbar) at 70°C until a constant weight was obtained. The grafted films were then weighed and the degree of grafting (G%) was calculated by considering the percent of weight increase in the grafted film using Eq. (1).

$$G\% = \frac{W_g - W_o}{W_o} \times 100 \qquad (1)$$

where W_o and W_g are the weights of original and grafted PVDF films, respectively.

3.2.3. Phosphoric acid doping grafted ETFE films

The grafted films were doped with phosphoric acid using procedure reported in Ref. 19. The grafted films were immersed in 85% and 70% aqueous phosphoric acid for various periods of time at room temperature. The weight gain due to both water and phosphoric acid was obtained by comparing the weight change before and after doping. The doped polymer membranes were dried at 110°C under vacuum until no weight change was reached to separate the doping acid and water uptake. The acid doping was estimated using eq. (2).

$$\text{Acid doping } \left(mol\frac{of H_3PO_4}{PNVP}\right) = \frac{\text{Weight increase}}{\text{Initial weight of grafted film}} \, x \, \frac{105\ (MW\ of\ PNVP)}{98\ (MW\ of\ H_3PO_4)} \quad (2)$$

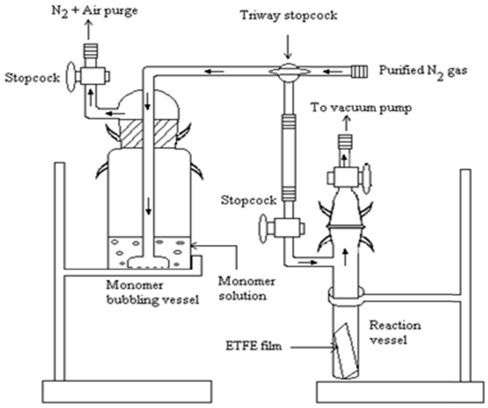

FIG. 1. Schematic diagram of the grafting system.

3.2.4. Grafting of sodium styrene sulfonate

Grafting of SSS (Aldrich) started by placing EB (Curetron, EBC-200-AA2, Nisshin High Voltage Kabushiki Kaisha, Japan) irradiated PVDF film (Goodfellow) in a glass ampoule tightly sealed and evacuated to remove air. A nitrogen-bubbled monomer solutions composes of SSS/DMF/H_2SO_4 (aqueous) with prescribed concentrations and volumes were introduced to the film-containing ampoule through a special connection and the reaction was allowed for 24 h at a temperature of 60°C. More details on the effect of grafting parameters on the degree of grafting was detailed in an earlier report [31].The grafted film was removed and extracted in a hot water-containing vessel placed in an ultrasonic machine for several hours to remove the un-reacted monomer. The obtained membrane having sulfonic acid moiety was dried under vacuum and the degree of grafting (G%) was calculated. The membranes were subsequently treated with 1 mol dm^{-3} HCl for 16 h then wash acid free with deionized water several times. Similar membrane obtained by conventional two-step radiation grafting of styrene and subsequent sulfonation under controlled conditions was used as a reference.

3.3. Characterization of the membranes

3.3.1. FTIR analysis

Fourier transform infrared (FTIR) spectra of the membranes were recorded on a Digilab-FTS7000 spectrophotometer in a transmittance mode over a range of 4 000–500 cm^{-1} with a resolution of 4 cm^{-1}. The spectra were detected and analyzed using WIN-IR Pro^{TM} (DIGILAB$^{®}$) commercial software.

3.3.2. Ion exchange capacity

Ion exchange capacity (IEC) was measured on membrane samples converted to H^+-form by treating with 1M HCl solution. The membranes were removed and washed acid free with deionized water several times. The samples were subsequently immersed in a 0.1 N NaCl aqueous solution at room temperature for 16 h under continuous stirring conditions. The H^+ released in the solution was titrated against a standardized 0.5 NaOH solution using an automatic titrator (Metrohom, Switzerland) until pH 7 was reached. IEC per unit mass of the dry membrane (mmol g^{-1}) was calculated by taking the concentration and the volume of NaOH solution consumed in titration into account.

3.3.3. Water uptake

The water uptake of the membranes was determined by soaking the membrane samples in deionized water until a swelling equilibrium was achieved. Samples were removed and the excess water adhered to their surfaces was quickly blotted by tissue papers and then weighed. The water uptake was determined as the weight gain of the membrane in the wet state compared to the dry one. The hydration number or the number of sorbed water molecules per sulfonic acid group was calculated using taking water uptake, water molecular weight and IEC into consideration.

3.3.4. Thermal gravimetric analysis (TGA)

TGA analysis of the membranes was performed using Perkin-Elmer TGA-7. All the heating runs were made in a temperature range of 50–650°C at a constant heating rate of 20°C/min and under N_2 atmosphere.

3.3.5. Differential scanning calorimetry (DSC)

DSC measurements were recorded on a Perkin Elmer Pyris-1 calorimeter under N_2 atmosphere. The degree of crystallinity of the membranes was calculated by correcting their recorded ΔH_m by dividing over the weight fraction of PVDF in the investigated grafted films and sulfonated membranes.

3.3.6. X ray diffraction analysis (XRD)

XRD measurements were performed using a Philips, PW 1840, X ray diffractometer. The diffractograms were collected at ambient temperature in scanning range of 2θ 5–50° by means Cu-Kα radiation (λ = 1.54nm) and monochromated by means of Nickel filter.

3.3.7. STEM analysis

Scanning transmission electron microscope (STEM) measurements were conducted using SEI Quanta 400 microanalyzer. The samples were mounted on a sample holder by double sided tape and gold sputtered after being sliced with a microtome.

3.3.8. Ionic conductivity (IC)

IC of both polymer electrolyte membranes was measured at room temperature by complex AC impedance spectroscopy. Measurements were carried using frequency response analyser (Autolab PGSTAT 30) at frequency range of 0.01–100 kHz. Analysis was conducted on membrane samples dried at 110°C for 8 h. Circular samples were sandwiched between two stainless steel electrodes having round-end discs (20 mm diameter) hosted into self-made Teflon® cell. The two halves of the cell were clamped in a way that prevents the samples from being squeezed between the two discs of the electrodes when the cell is assembled. Freshly polished electrodes were always used to ensure exclude microscopic corrosion. The IC of the polymer electrolyte membranes was calculated by taking the resistance obtained from the intercept on the real axis at the high frequency end of the Nyquist plot of complex impedance into consideration. Measurements of IC of PVDF-g-PSSA membrane were conducted under fully hydrated conditions where those of phosphoric acid dopes ETFE-g-PNVP membranes were conducted under dry conditions. The conductivity measurements were repeated at various temperatures by placing the conductivity cell in a modified oven in a temperature range of 30–130°C.

3.4. Fuel cell testing

3.4.1. Single fuel cell test for PVDF-g-PSSA membranes

The performance of the membranes was tested in a single fuel cell of 5 cm^2 (Globe Tech., Inc., USA). The cell was operated under: humidifier temperature: T_{H2}/T_{O2} = 75/65°C; cell temperature: 60 ± 2°C;

gas pressure: $PH2/P_{O2}$ = 0.20/0.20MPa; gas purity: 99.96% for H_2 and 99.90% for O_2. Commercial gas diffusion electrodes (Pt/C, 0.4 g/cm^2 Pt loading, E-Tek, USA) coated with a Nafion solution (0.5–0.8 mg/cm^2) were sandwiched with the fully hydrated membrane and hot-pressed at 110°C and 15 kg cm^2 for 1–2 min to form membrane/electrode assembly (MEA). The life test was performed at 150 mA/cm^2 with a cell voltage of recorded as a function of time.

3.4.2. Single fuel cell test for phosphoric acid doped ETFE-g-PNVP membranes

A preliminary fuel cell test was conducted in a single fuel cell of 5 cm^2 under dry gases conditions with a pressure of 3 bars. The electrodes having high platinum loading (Pt/C, Pt loading 1.5 g/cm^2, E-Tek, USA) were hot pressed onto both sides of the membrane at 130°C and 15 kg cm^2 for several minutes. A phosphoric acid electrolyte diluted solution was used to coat both the membrane and the electrodes.

4. RESULTS AND DISCUSSION

4.1. Grafting of SSS onto PVDF films and sulfonate membrane preparation

The grafting of SSS onto PVDF was found to be remarkably enhanced by the addition of acid. The synergetic role of addition of various acids with different concentrations and volumes to grafting mixtures, in boosting grafting level to high values suitable for fuel cell application was further investigated [32]. The addition of acid was found to be essential for the grafting to embark from negligible levels to values suitable for fuel cell application. The grafting reaction was found to proceed by front mechanism [33]. The role of acid in boosting the degree of grafting followed the sequence: H_2SO_4>HCl>CH_3COOH>HNO_3. The acid concentration and volume were found to heavily affect G%. The highest G (65%) was achieved with an aqueous solution of sulphuric acid having concentration of 0.2 mol dm^{-3} at 10 vol% of the total volume of SSS diluted with DMF. The synergetic acid effect was attributed to increase in monomer supply to graft growing chains under the influence of portioning effect, the inhibition of termination by recombination in the graft propagating chains and suppression of homopolymer by Na-salt formed in the grafting solution. G% was also found to be function of monomer concentration and irradiation dose under constant values of acid concentration and volume. G% was found to increase as SSS concentration increased from 0.6 to 1.0 mol dm^{-3}. G% was also found to increase with the increase in monomer concentration as indicated from Fig. 2.

G% was found to increase with the increase in the dose in the range of 20–100 kGy (as indicated from Fig. 3) and this mostly caused by increase in the amount of radical generated in the films. The reaction kinetic dependence on the dose was found to be with an order of 1.2 which is higher than theoretical value of free radical polymerization (0.5). Such high dependency on the dose reflects a high possibility of decay or mutual recombination of some of the trapped radicals caused by reduction in polymer chain mobility under the influence of partial crosslinking mostly took place upon irradiation of PVDF. In the first 24 h, the degree of grafting is not only a function of monomer diffusion but also the amount of radiation formed in the polymer films.

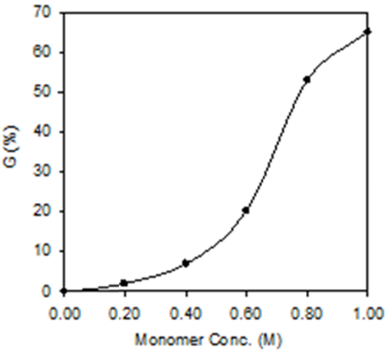

FIG. 2. Variation of degree of grafting with monomer concentration: dose 100 kGy, volume of acid solution (0.2 mol dm^{-3}) 1:10 v/v of total solution, temperature, 60^{o}C, reaction time, 24 h.

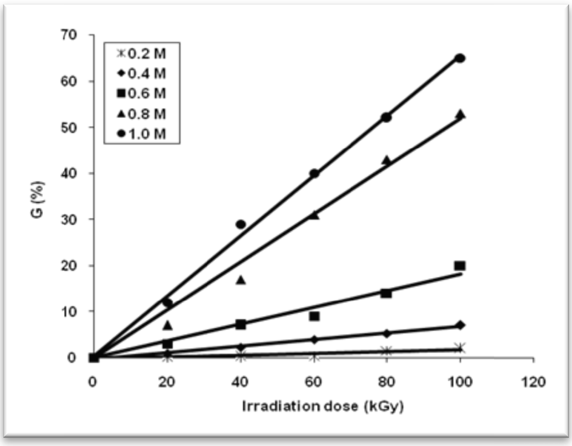

FIG. 3. Variation of degree of grafting with monomer concentration different doses: volume of acid solution (0.2 mol dm-3) 1:10 v/v of total solution, temperature, 60 °C reaction time, 24 h.

G% was found to increase with temperature increase from 30–60 °C as shown in Fig. 4 and this due to the increase in the reactivity of the thermally decomposed trapped radicals coupled with an enhancement in the monomer diffusion. Activation energy of 11.36 kJ/mol was obtained for grafting reaction and this is caused by synergetic effect of acid addition that led to rapid monomer diffusion which outweighs the rapid radicals decay and the increase in the chain mobility.

The variation of the thickness of PVDF film from 50–125 μm was accompanied by a decrease in G% as deduced from Fig. 5. The grafting front is suggested to meet faster in thinner films than thicker ones. The radicals formed in the film were found to survive for more than 180 days as indicated by the negligible variation G% obtained from grafting reaction. More details on the effect grafting parameters on the degree of grafting and the SSS kinetic behaviour during grafting can be found elsewhere [33].

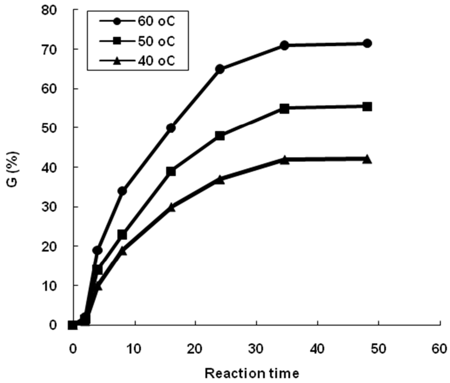

FIG. 4. Kinetics of grafting at different temperature: reaction parameters are as in Fig. 2.

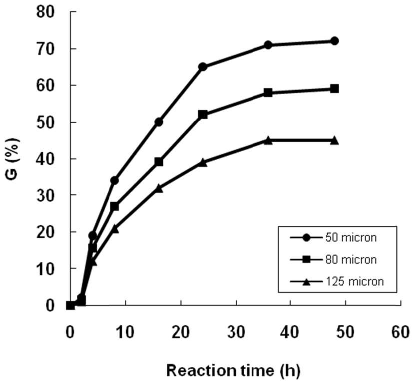

FIG. 5. Kinetics of grafting at different film thicknesses: reaction parameters are as in Fig. 2.

FTIR spectra of the membrane shown in Fig. 6 provides a strong evidence of grafting of SSS as indicated by presence of the bands at 2930 and 2850 cm^{-1} which are due to the asymmetric and symmetric stretching vibrations of CH_2 of PVDF matrix. The incorporation of sulfonated aromatic ring was confirmed by the presence of the features established by skeletal C=C in plate-stretching vibrations in the range of at 1493 and 1602 cm^{-1} together with C-H aromatic stretching vibrations at 3100 and 3026 cm^{-1}. The band at 1040 cm^{-1} is due to the in-plane C-H bending vibration of the di-substituted benzene ring, and the 1007 and 1126 cm^{-1} bands are due to the symmetric S-O stretching vibration of the $–SO_3^-$ group. The band at 3550 cm^{-1} is due to –OH group of the water associated with $–SO_3^-$ group by hydrogen bonding. Accordingly a schematic representation for preparation of PVDF-g-PSSA membrane is presented in Fig. 7.

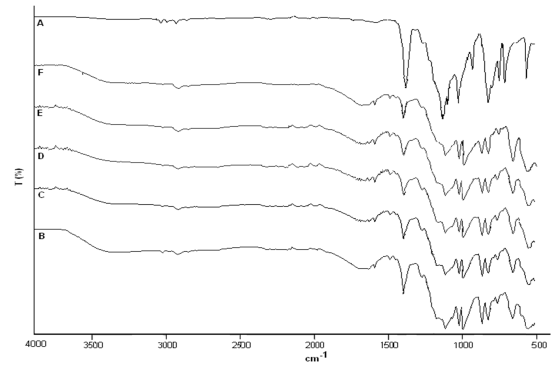

FIG. 6. FTIR spectra of: A) original PVDF film and sulfonic acid polystyrene grafted PVDF membranes with various degrees of grafting, B) 12%; C) 29%; D) 44%; E) 53%.

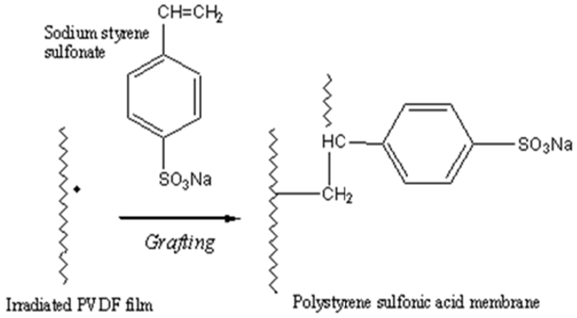

FIG.7. Schematic representation of preparation of sulfonic acid membrane by a single-step radiation induced grafting.

DSC data presented in Table 2 which depicts variation of T_m and degree of crystallinity revealed that SSS grafting takes place in the amorphous region of the PVDF film without causing partial disruptions in inherent crystallinity as indicated by the absence shifts in the melting endothermic peaks of membranes and the calculated degree of crystallinity at various G%. This observation was confirmed by XRD results. Thus, grafting of polystyrene of the amorphous nature has a dilution effect on the crystalline structure of obtained membranes and such effect is a function of G%. Interestingly, the reduction in the crystallinity of similar membranes obtained by conventional two-step radiation grafting was found to be higher suggesting the presence of partial distortion which was avoided in the new membranes by elimination of sulfonation reaction. As a result better thermal and mechanical properties were achieved in the new membranes.

TABLE 2. DSC DATA FOR VARIATION OF THE MELTING TEMPERATURE (T_M) AND DEGREE OF CRYSTALLINITY WITH THE DEGREE OF GRAFTING FOR MEMBRANES PREPARED BY TWO DIFFERENT METHODS

Single step grafting method			Conventional, two step grafting method		
IEC (mmol g^{-1})	Crystallinity (%)	T_m (C°)	IEC (mmol g^{-1})	Crystallinity (%)	T_m (C°)
0.00	38	167.9*	0.00	37.2	167.9*

**Refers to the main melting peak.*

TGA results suggest the membranes have multi-step degradation pattern due to dehydration of water, desulfonation, depolymerisation and decomposition of PVDF backbone. The membranes are thermally stable up to ~200°C which is most suitable for PEM fuel cell operation. However, the membrane obtained by the new method showed higher stability than counterpart obtained by conventional method.

The properties such as ion exchange capacity, water uptake, hydration number, ionic conductivity of the obtained membranes were found to be functions of the content of the grafted ionic moiety [31]. The membranes were found to attain very good combination of physico-chemical properties suitable for fuel cell application as shown in Table 3. The membranes were also found to have superior properties compared to those obtained by conventional two-step grafting method as far as fuel cell requirements are concerned [34]. A summary of the membranes obtained by single step grafted method is shown in Table 4.

TABLE 3. SUMMARY OF THE PHYSICO-CHEMICAL PROPERTIES OF THE MEMBRANES OBTAINED BY SINGLE-STEP GRAFTING METHOD

Degree of grafting (%)	Thickness (µm)	WU (g/g)	IEC (mmol/g)	Proton conductivity (mScm^{-1})
44	56	57	2.30	63
53	58	71	2.63	87
65	61	92	2.90	114

TABLE 4. SUMMARY OF THE PHYSICO-CHEMICAL PROPERTIES OF A MEMBRANE OBTAINED BY SINGLE-STEP GRAFTING AND COUNTERPART OBTAINED BY CONVENTIONAL GRAFTING METHOD

Method/DG (%)	Thickness (µm)	WU (g/g)	IEC (mmol/g)	Proton conductivity (mS cm^{-1})	Permeability (Barrer)	
					P_{H2}	P_{O2}
New method (53%)	58	0.63	2.63	87	24.2	11.9
Conventional (53%)	63	0.92	2.90	114	26.5	13.4

Figures 8 and 9 show current-voltage characteristics of MEAs with PVDF-*g*-PSSA membranes. The current−voltage characteristics of the three MEAs have a similar trend with a maximum power density of 67−78 mW/cm^2 can be observed with the variation of *G* in the range of 44–65%. This indicates that increasing G% improves the polarization characteristics of the membrane. Such behaviour may be attributed to the higher proton conductivity and water uptake at high G% values, both of which reduce the membrane resistance to proton transfer. The high open circuit values in all membranes (982 ± 3 mV) indicate that the tested PVDF-*g*-PSSA membranes are gas tight and H_2 or O_2 permeation is independent of the thickness. The membrane obtained by new method (G = 53%) showed also better performance than the counterpart (G = 53%) obtained by conventional method despite the slightly higher conductivity in the latter as shown in Fig. 10. Furthermore, the membrane obtained by new method (G = 53%) showed better durability than the counterpart (G = 53%) obtained by conventional method with ~30% increase in lifetime.

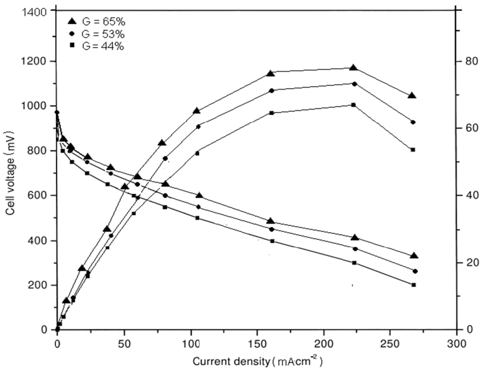

FIG. 8. Current-voltage and power density characteristics of PEM fuel cell with PVDF-g-PSSA with various G%.

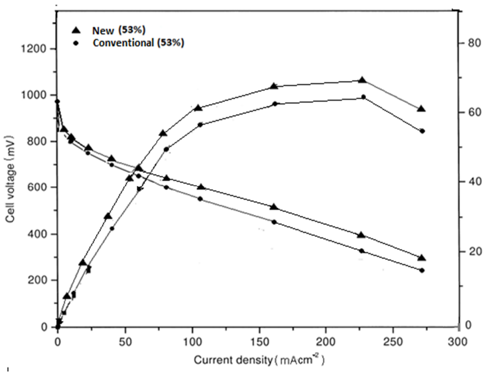

FIG. 9. Current-voltage and power density characteristics of PEM fuel cell with PVDF-g-PSSA membranes obtained by new grafting method and counterparts prepared by conventional grafting.

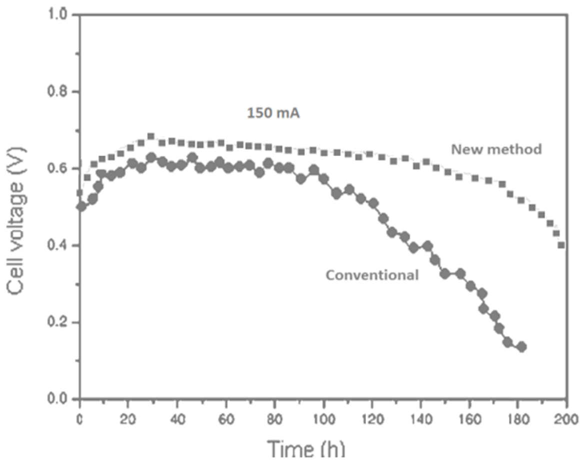

FIG. 10. Lifetime of PVDF-g-PSSA membrane obtained by new grafting method vs. counterpart obtained by conventional method.

4.2. Grafting of N-vinyl pyridine onto ETFE films

4.2.1. Effect of monomer concentration

Figure 11 shows the relationship between the monomer concentration and the degree of grafting for grafting of NVP onto ETFE films. As can be seen, G% increases gradually with the increase in the monomer concentration. The grafting kinetics at different monomer concentrations show a quazi-plateau after 6 h as depicted in Fig. 12. This behaviour can be attributed to the enhancement of the diffusion of NVP monomer to the grafting sites which leads to availability of more NVP molecules involved in the grafting reaction. As reaction time increased more than 4 h, the viscosity of the grafting zone increases and G% slows down.

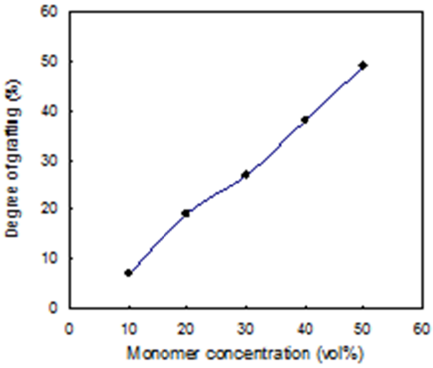

FIG. 11/ Degree of grafting vs. monomer concentration for grafting of NVP onto ETFE films. Dose 100 Gy; reaction time 6 h, temperature 60^{o}C.

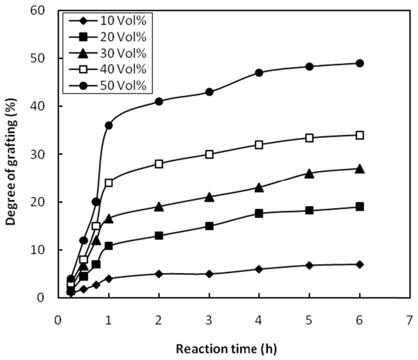

FIG. 12. Degree of grafting vs. Reaction time for grafting of NVP onto ETFE films. Dose 100 kGy; reaction time 6 h, temperature 60 °C.

4.2.2. Effect of dose

Figure 13 shows the effect of the irradiation dose on the degree of grafting of NVP onto ETFE films. G% was found to increase steeply with the increase in the irradiation dose. The grafting kinetics (Fig. 14) shows an increase in the reaction rate all doses. This behaviour can be attributed to the increase in the amount of radicals formed in the film which is most likely accompanied by a predominant propagation. These results suggest that the degree of grafting in the present system is a function of amount of radicals formed in the polymer films and the concentration of the monomer in the grafting sites.

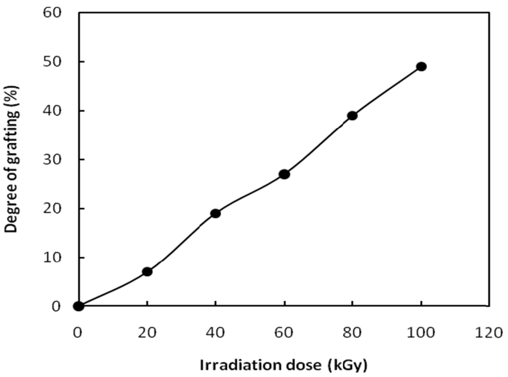

FIG. 13. *Degree of grafting vs. dose for grafting of NVP onto ETFE films. NVP concentration 50vol%; reaction time 6 h, temperature 60 °C.*

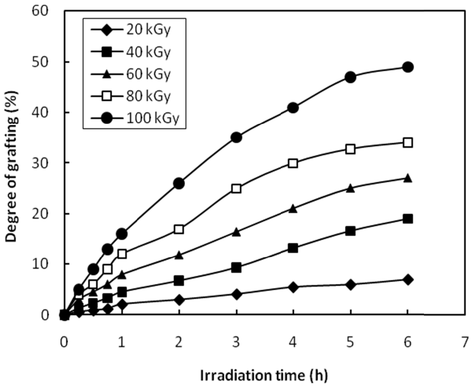

FIG. 14. *Degree of grafting vs. time at various doses for grafting of NVP onto ETFE films. NVP concentration 50vol%; reaction time 6 h, temperature 60 °C.*

4.2.3. Effect of temperature

Figure 15 shows the variation of the degree of grafting with temperature of the grafting of NVP onto ETFE film. G% was found to increase with the increase in the temperature and achieved a maximum at 60°C beyond which is dropped. The grafting kinetics at different temperatures concentrations show a quazi- plateau after 4 h as depicted in Fig. 16. The drastic increase in G% up to 60°C can be attributed to the increase in the reactivity of the thermally decomposed trapped radicals with the rise in temperature.

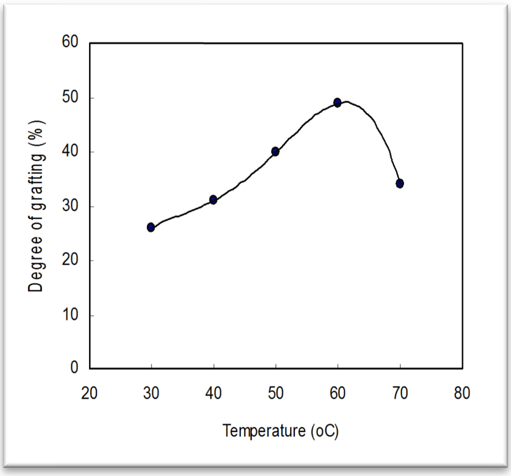

FIG. 15. Variation of the degree of grafting with temperature for grafting of NVP onto ETFE films. Dose 100 kGy, the rest of reaction conditions are as in Fig. 13.

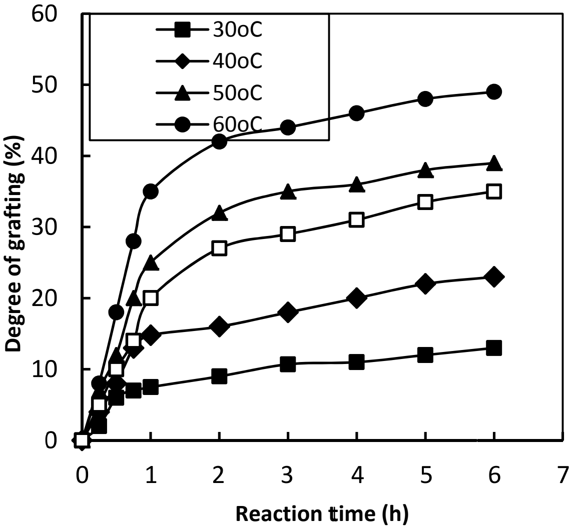

FIG. 16. Variation of the degree of grafting with reaction timeat various temperatures for grafting of NVP onto ETFE films. Dose 100 kGy, the rest of reaction conditions are as in Fig. 13.

This is mostly accompanied by an enhancement in the monomer diffusion in the base polymer. Consequently, the initiation and propagation rates are enhanced. The decrease G% at 70°C is not only caused by mutual recombination of trapped radicals taking place before reacting with the diffused monomer molecules but also by bimolecular termination of the graft growing chains enhanced at higher temperatures.

4.2.4. Effect of solvent type

The effect of the solvent in correlation with the degree of grafting was investigated and the data obtained was plotted in Fig. 17. Tetrahydrofuran (THF) was found to give the highest G% compared to method and isopropanol. Therefore, THF was used as a diluting agent in all experiments.

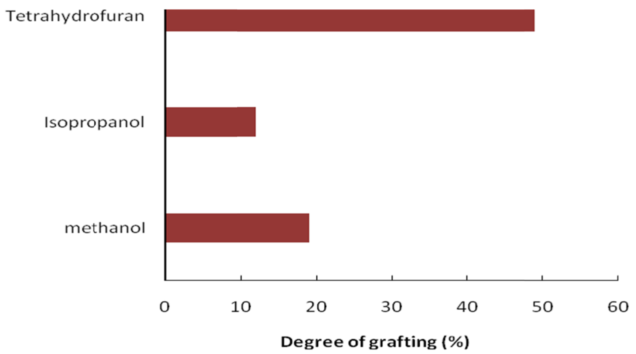

FIG. 17. Variation of the degree of grafting with solvent type. Dose 100 kGy, reaction conditions are as in Fig. 13.

4.2.5. Effect of film thickness

The variation of the degree of grafting with the film thickness is shown Fig. 18. G% was found to the increase with the increase in film thickness and this is due to availability of polymer volume for more propagation of graft growing chains in thicker film unlike thinner films where the growing chains meets faster across the thickness of the film.

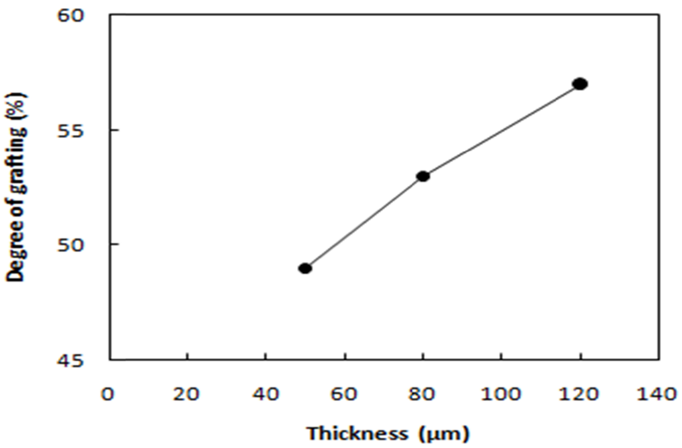

FIG. 18. Varation of the degree of grafting with film thickness. Dose 100 kGy, reaction conditions as in Fig. 13.

4.2.6. Effect of storage time

Figure 19 shows the variation of the degree of grafting with storage time up to 180 days. No significant changes in G% could be observed suggesting that no serious loss in radicals reactivity i.e. radicals survive for more than 6 month under -60°C giving ETFE film an advantages for preirradiation method.

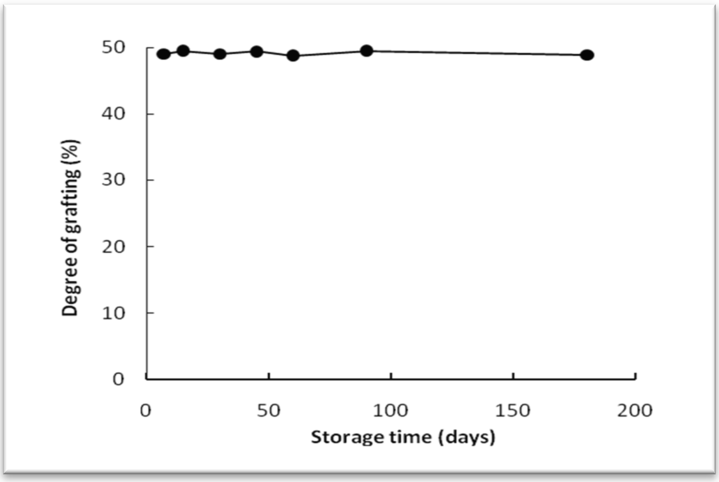

FIG. 19. Varation of the degree of grafting with storage time. Dose 100 kGy, reaction conditions as in Fig. 13.

4.3. Phosphoric acid doping of grafted PNVP films

The acid doping increases sharply with the increase in the reaction time and tend to level off and achieve a plateau after 42 h giving acid dope of 10 and 12 H_3PO_4 mol/unit of PNVP for 34 and 49 % grafted membranes, respectively (Fig.20).

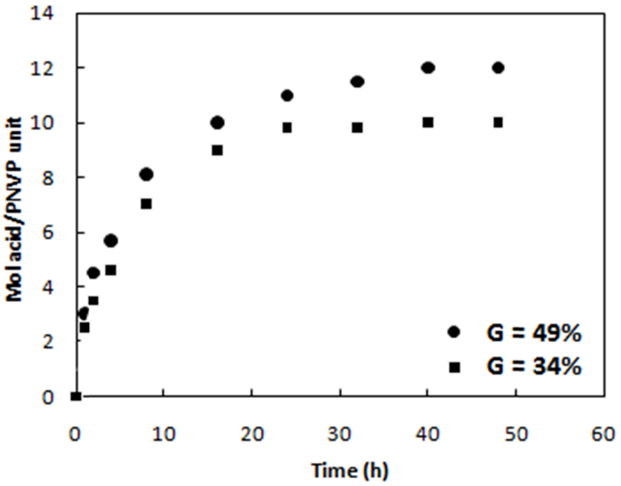

FIG. 20. Variation of phosphoric acid (85 wt%) doping with time.

4.4. Characterization of ETFE-g-PNVP membranes

4.4.1. Evidence of NVP grafting and subsequent acid doping

The FTIR spectra of NVP grafted ETFE film compared to the respective original ETFE film and PVP film are shown in Figs 21 and 22. Compared to the spectrum of the original ETFE and pure PNVP films, the spectrum of NVP grafted film contains a characteristic absorption band at 1602 cm^{-1} which is associated with the pyridine ring stretching modes of the grafted NVP polymer. This confirms grafting of NVP onto ETFE films. The loading of phosphoric acid leads to obvious changes in range of 2000–3500 cm^{-1}. The broad at 2000–2400 cm^{-1} can be attributed to the phosphoric acid that takes place on the nitrogen group of the ring of PNVP that causes stretching vibration of NH^+. The small band at about 2500 to 3000 cm-1 should be related to the protonation of the nitrogen of the –N- by transferring one proton from H_3PO_4 to –N- groups of PNVP as in the plausible mechanism shown in Fig. 23.

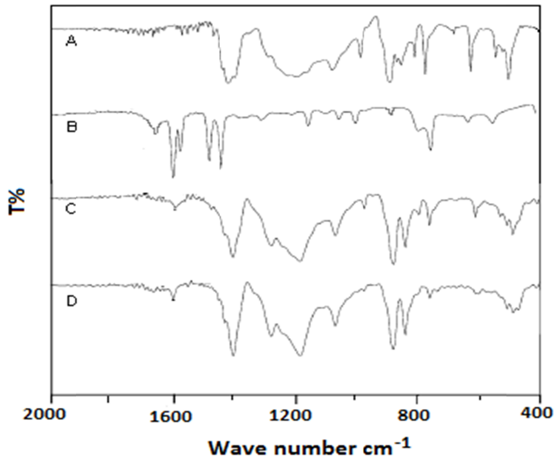

FIG. 21. Typical FTIR spectra of: A) original ETFE film, B) PNVP film, C) 28% and D) 49% ETFE-g-PNVP films.

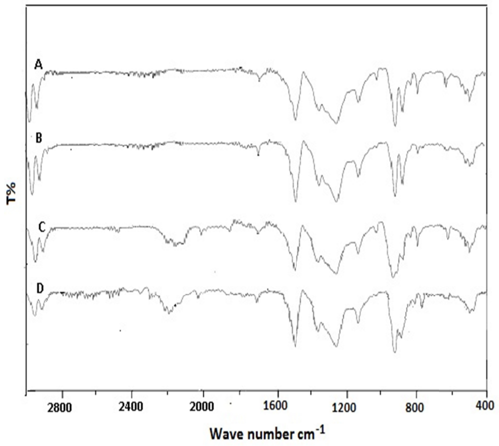

FIG. 22. Typical FTIR spectra of: A)& B) 28% and 49% ETFE-g- PNVP films, C) & D) phosphoric acid doped 28% and 49% PNVP-g-ETFE films.

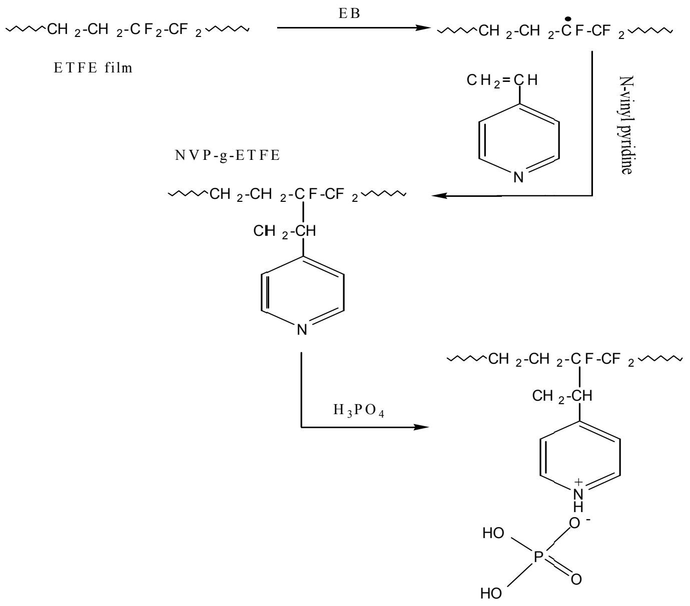

FIG. 23. Plausible mechanism of preparation of phosphoric ad doped PNVP-g-ETFE membrane by radiation induced grafting.

4.4.2. Thermal stability

Figure 24 shows thermograms of original, NVP grafted ETFE films having various degrees of grafting. All the degradation temperatures were measured onset. The original ETFE film was found to have a single-step degradation pattern at 380°C corresponding to the thermal degradation of ETFE main chains. The PNVP grafted ETFE films (B-D) showed a two-step degradation pattern primary due to the weight loss started at 340°C and caused by PNVP degradation followed by the decomposition of the ETFE matrix at 400°C. It can be seen that the presence of PVP grafts in the grafted film increased the inherent decomposition temperature of the ETFE matrix. The PNVP grafts are incompatible with ETFE matrix due the difference in nature between PNVP grafts and ETFE matrix. As a result phase-separated microdomains are formed in the grafted film. Doping the grafted films with phosphoric acid leads to a multi-step degradation pattern including removal of acid, decomposition of PNVP and ETFE matrix in the membranes as shown in Fig. 25. Membrane stability up to 250°C can be suggested. A complex of C, N and P prevented the membranes from complete degradation at the end of heating run.

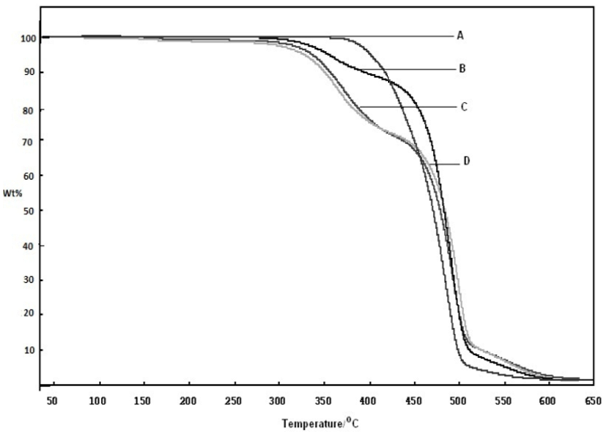

FIG. 24. TGA thermograms of: A) original ETFE film and PNVP-g-ETFE films having various degrees of grafting: B) 19%, C) 36% and D) 49%.

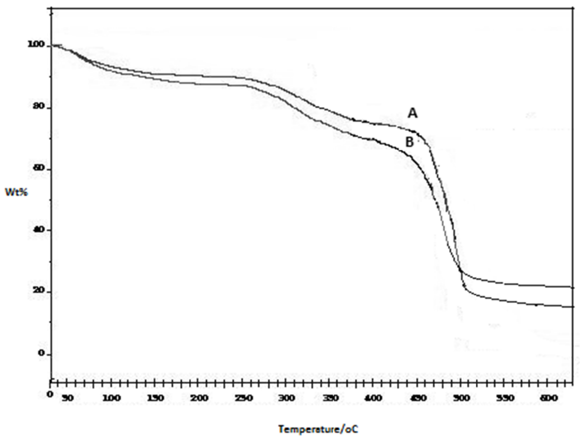

FIG. 25. TGA thermograms of phosphoric acid doped PNVP-g-ETFE films having various degrees of grafting: A) 36% and B) 49%.

4.4.3. Structural changes

Diffractograms of the original and grafted ETFE films are shown in Fig. 26. It can be obviously seen that a remarkable decrease in the degree of crystallinity takes place as a result of NVP grafting and the amount of such decrease depends mainly on *G%*.

Higher G% leads to lower degrees of crytallinity and vice versa as illustrated form the inverse proportional relationship between the peak intensity and G%. The effect of grafting on the crystallinity for all grafted films shows no shift in the angle (2θ) compared to the original film which reflects no change in the crystal size. These results suggest that the reduction in the crystallinity of PNVP grafted films is due to the dilution of ETFE structure with the amorphous PNVP grafts. Similar decreasing trend in the crystallinity could be observed when membranes were doped with phosphoric acid and such decrease is also a function of G% as shown in Fig. 27. No shift in the peak position suggesting that acid doping further exerted dilution in the crystalline structure with crystal disruption.

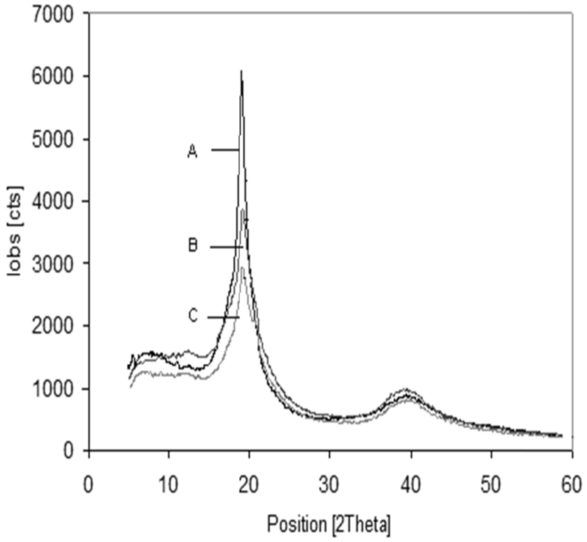

FIG. 26. XRD diffractograms of: A) original ETFE film and PNVP grafted ETFE films having various degrees of grafting: B) 19% and C) 49%.

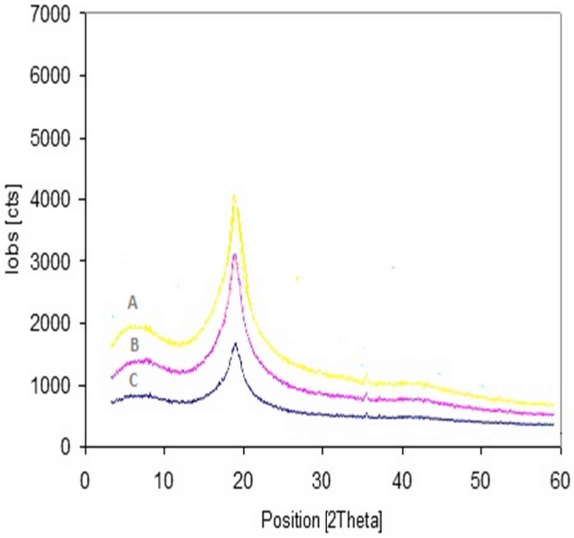

FIG. 27. XRD diffractograms of acid doped PNVP-g-ETFE membranes having various degrees of grafting: A) 19% B) 34% and C) 49%.

4.4.4. Mechanical properties

The changes in tensile strength and elongation% at break for the ETFE-*g*-PNVP films before and after doping with phosphoric acid were studied as a function of degree of grafting as shown in Figs 28 and 29. It can be noticed that the tensile strength and the elongation percent decreased with the increase in the degree of grafting in un-doped films and acid doped membrane and with the latter attaining higher reduction in both mechanical properties. Such results were expected from the structural changes in the ETFE film upon the introduction of the amorphous PNVP grafts leading to the reduction in the crystallinity content in the grafted film with the increase in the degree of grafting. Doping with phosphoric acid further increased the reduction in the crystallinity and mechanical properties in turn. However, the membranes show reasonable mechanical properties at G% up to 49%, suitable for fuel cell application.

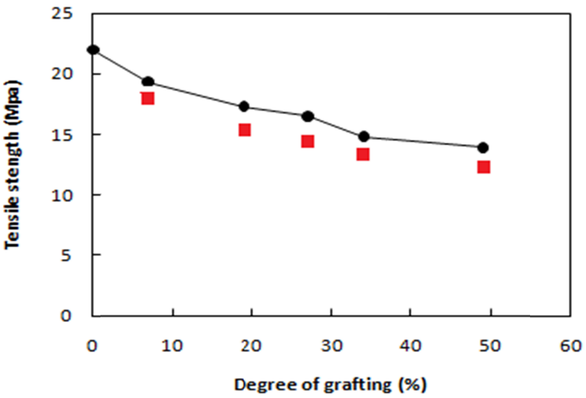

FIG. 28 Variation of tensile strength with degree of grafting before (●) and (■) after phosphoric acid doping.

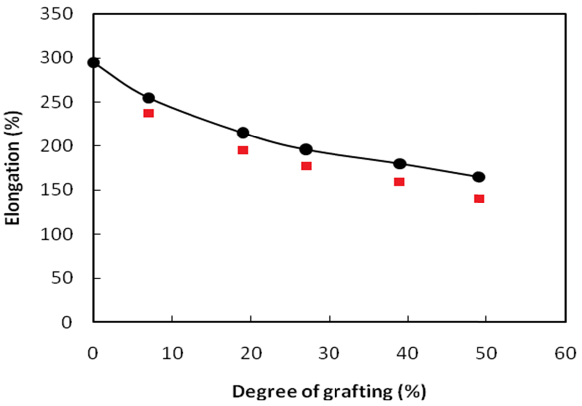

FIG. 29 Variation of elongation with degree of grafting before (●) and (■) after phosphoric acid doping.

4.4.5. Morphological changes

The micrograph of the original ETFE film, 34% grafted PVP and corresponding phosphoric acid doped membrane of the same degree of grafting is shown in Fig. 30. As can be seen the original ETFE film has very smooth surface showing faint lining developed during the processing of the polymer films. Grafting of PVP has introduced some changes to the grafted samples in a form of straps of bright colour with equal distribution across the sample. Doping the grafted sample with phosphoric acid has brought further changes in the sample represented by network of straps with obvious swelling in the whole samples as indicated by the bright spots. The uniform appearance of the membranes is a possible sign for the formation of a homogenous structure. STEM results further confirm the grafting of PNVP onto ETFE films and their subsequent phosphoric acid doping.

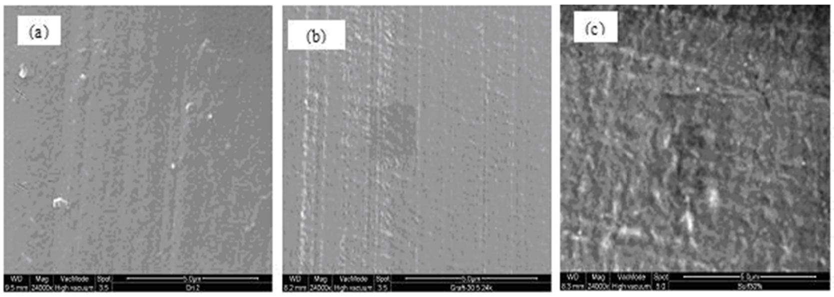

FIG. 30. STEM micrograph of (a) ETFE Original, b) grafted PNVP grafted ETFE (c) phosphoric acid doped membrane.

4.4.6. Proton conductivity

Figure 31 shows an increase of proton conductivity with the increase in the degree of grafting in the membranes at room temperature. This trend could be understood based on the fact that the increase in G% provides more –N- for more phosphoric acid loading in the membrane. Figure 32 shows the Arrhenius plot for proton conductivity of phosphoric acid doped membranes of G% of 34 and 49% doped with 85 wt% acid concentration. As can be seen, proton conductivity increases with the increase in the temperature with the conductivity values of 49% grafted membrane higher than corresponding one with G of 34% at all temperatures. The conductivity rising trend is most likely due to the enhancement in the chain mobility, the dissociation of phosphoric acid groups and the ionic mobility across the membrane. The observed linear dependence of proton conductivity of the membrane on the temperature follows Arrhenius law. The membrane of G equals 49% was found to have stable ionic conductivity for than 100 h at a temperature of 130°C as shown in Fig. 33 and this is a good indication for suitability of fuel cell operation above 100°C.

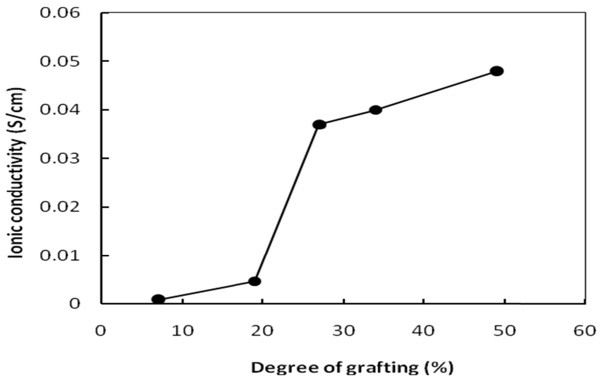

FIG. 31. Variation of ionic conductyivity of phosphoric acid doped membrane with degree of grafting.

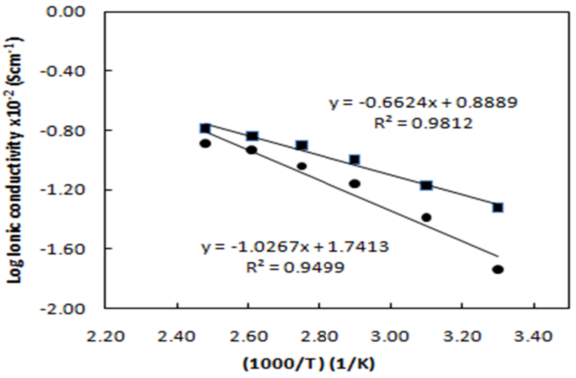

FIG. 32. Arrhenius plot for proton conductivity of phosphoric acid doped membrane at: 34% (■) and 49% (●) degree of grafting.

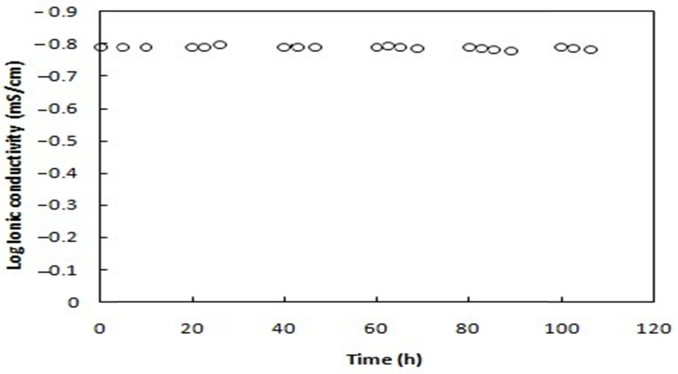

FIG. 33. The ionic conductivity versus time for phosphoric acid doped membrane (G = 49%) with 85% acid concentration. Sample was kept at 130°C.

4.5. Fuel cell testing above 100°C

4.5.1. Performance of single fuel cell

The preliminary performance of single fuel cell showed a typical polarization characteristic with power densities of 146 mW/cm² for membrane having G of 49% and 127 mW/cm² for the membrane with G of 34% as prevailed from Figs 34 and 35. These results are considered reasonable for such membranes in the early stage. Long term stability test is undergoing to further optimize the performance and determine the life time of the membranes.

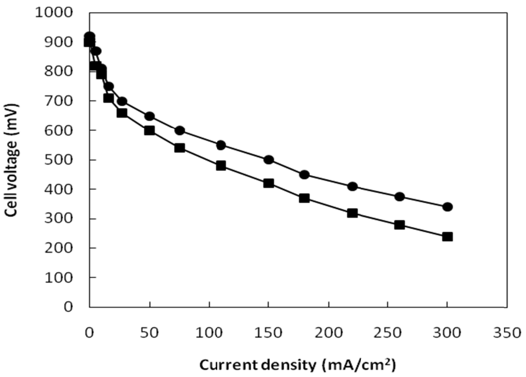

FIG. 34.Current-voltage characteristics of PEM fuel cell with phosphoric acid doped membranes at: 34% (●) and 49% (■) degree of grafting.

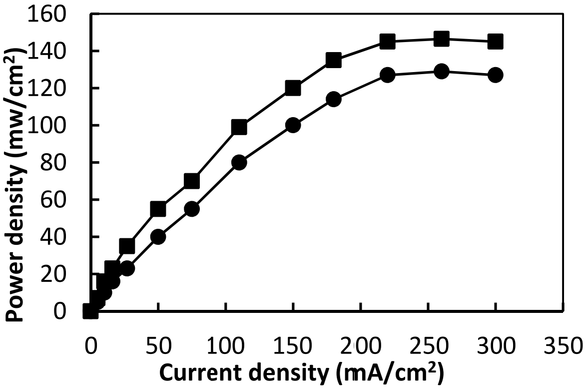

FIG. 35.Current-power density characteristics of PEM fuel cell with phosphoric acid doped membranes at: 34% (●) and 49% (■) degree of grafting.

5. CONCLUSIONS

Two types of proton exchange membranes for fuel cell application for operation below and above 100°C were prepared, characterized and tested. In the first part of the work, a new method was successfully used to prepare PVDF-*g*-PSSA membranes by radiation induced grafting of SSS onto PVDF films. This method provides a shorter route to prepare sulfonic acid membranes with improved properties together with cost and time reduction through eliminating the hazardous sulfonation reaction. The degree of grafting was synergized by the addition of acid and depended on the reaction parameters upon acid addition and this provides means to control the level of grafted moiety and the properties of membranes. The PVDF-*g*-PSSA membranes possess reasonable water uptake, high ion exchange capacity, high proton conductivity, excellent thermal stability, and low H_2 and O_2 permeabilities rendering them suitable for PEM fuel cell. The membranes obtained by a single-step grafting method were found to have better properties compared to those prepared by conventional grafting method and this was marked by a higher durability of 30% in fuel cell at 60°C under dynamic conditions. The performance of these membranes can be further improved toward high temperature operation by impregnation of inorganic filler such as zirconium phosphate or zirconium oxide. Also, crosslinking during grafting reaction would help to improve stability. This could result in low cost membranes suitable for use in low temperature fuel cells.

In the second part of the project, preparation of phosphoric acid doped composite membranes by radiation induced grafting of NVP onto ETFE films was successfully carried out under controlled conditions. The degree of grafting in the obtained membranes was found to be a function of grafting parameters and the optimum membrane structure was found to rely on the availability of the right combination of irradiation and grafting parameters. The phosphoric acid doping was found to depend on time. The obtained phosphoric acid doped composite membranes showed high proton conductivity suitable for fuel cell (level of 10^{-2} S/cm). The conductivity is also a function of G% and follows Arrhenius law when tested at temperatures in the range of 30–130°C. The preliminary performance of two phosphoric acid doped membranes having G% of 34 and 49 under dry conditions showed a power density of 146 and 127 mW/cm², respectively. The performance of these membranes needs to be further investigated under various conditions including concentration of doping acid and temperature of doping followed by stability test. Finally, it can be suggested that grafting of NVP onto fluorinated polymer films followed by phosphoric acid doping is a promising alternative route to prepare less water dependent acid/base phosphoric acid membranes which have strong potential for operating PEM fuel cell above 100°C.

ACKNOWLEDGEMENT

The authors wish to thank Malaysian Ministry of Science, Technology and Innovation (MOSTI) for funding the major part of this project. Thanks are also due International Atomic Energy Agency (IAEA) for partial financial support under CRP mechanism. Amgad Ali, Inderiani and Nor Hafizan are thanked for conducting some of the experiments.

REFFERENCES

[1] SMITHA, B., SRIDHAR, S., KHAN, A.A., Solid polymer electrolyte membranes for fuel cell applications – a review, J. Membr. Sci. **259** (2005) 10-26.

[2] KARIDURAGANAVAR, M.Y., NAGARALE, R.K., KITTUR, A.A., KULKARNI S.S., Ion-exchange membranes preparative methods for electrodialysis and fuel cell applications, Desalination **197** (2006) 225-246.

[3] NASEF, M.M., HEGAZY, E.A., Preparation and applications of ion exchange membranes by radiation-induced graft copolymerization of polar monomers onto non-polar films, Prog. Polym. Sci. **29** (2004) 499-561.

[4] GUBLER, L., GÜRSEL, S.A., SCHERER, G.G., Radiation grafted membranes for polymer electrolyte fuel cells, Fuel Cells **5** (2005) 317-335.

[5] BÜCHI, F.N., GUPTA, B., HAAS, O., SCHERER, G.G., Study of radiation-grafting FEP-g-polystyrene membrane as polymer electrolyte in fuel cells, Electrochem. Acta **40** (1995) 345-353.

[6] GUPTA, B., BÜCHI, F., SCHERER, G.G., CHAPIRO, A., Crosslinked ion exchange membranes by radiation grafting of styrene/divinylbenzene into FEP films, J. Membr. Sci. **118** (1996) 231-238.

[7] GUBLER, L., KUHN, H., SCHMIDT, T.J., SCHERER, G.G., BRACK, H-P., SIMBECK, K., Performance and durability of membrane electrode assemblies based on radiation-grafted FEP-g-polystyrene membranes, Fuel Cells **4** (2004) 196-205.

[8] NASEF, M.M., SAIDI H., Preparation of crosslinked cation exchange membranes by radiation grafting of styrene/divinylbenzene mixtures onto PFA films, J. Membr. Sci. **216** (2003) 27-38.

[9] ARICÓ, A.S., BAGLIO, V., CRETI, P., DI BLASI, A., ANTONUCCI, V., BRUNEA, J., CHAPOTOT, A., BOZZI, A., SCHOEMANS, J., Investigation of grafted ETFE-based polymer membranes as alternative electrolyte for direct methanol fuel cells, J. Power Sour. **123** (2003) 107-115.

[10] GUBLER L., PROST, N., GÜRSEL, S.A., SCHERER, G.G., Proton exchange membranes prepared by radiation grafting of styrene/divinylbenzene onto poly(ethylene-alt-tetrafluoroethylene) for low temperature fuel cells, Solid State Ionics **176** (2005) 2849- 2860.

[11] CHEN J., ASANO, M., YAMAKI, T., YOSHIDA, M., Preparation and characterization of chemically stable polymer electrolyte membranes by radiation-induced graft copolymerization of four monomers into ETFE films, J. Membr. Sci. **269** (2006) 194-204.

[12] LI, J., MUTO, F., MIURA, T., OSHIMA, A., WASHIO, M., IKEDA, S., IIDA, M., KATSUMURA, Y., Improving the properties of the proton exchange membranes by introducing α-methylstyrene in the pre-irradiation induced graft polymerization, Euro. Polym. J. **42** (2006) 1222-1228.

[13] GÜRSEL, S.A., YANG, Z., CHOUDHURY, B., ROELOFS, M.G., SCHERER, G.G., Radiation-grafted membranes using a trifluorostyrene derivative, J Electrochem. Soc. **153** (2006) A1964-A1970.

[14] BECKER, W., SCHMIDT-NAAKE, G., Properties of polymer exchange membranes from irradiation introduced graft polymerization, Chem. Eng. Technol. **24** (2001) 1128-1132.

[15] GUBLER, L, SLASKI, M, WOKAUN, A, SCHERER, G.G., Advanced monomer combinations for radiation grafted fuel cell membranes, Electrochem. Commun. **8** (2006) 1215–1219.

[16] ROHANI, R., NASEF, M.M., SAIDI, H., DAHLAN, K.Z.M., Effect of reaction conditions on electrons induced graft copolymerization of styrene onto poly(ethylene-*co*-tetrafluoroethylene) films: kinetics study, Chem. Eng. J. **132** (2007) 27-35.

[17] HAMROCK, J., YANDRASITS, M.A., Proton exchange membranes for fuel cell applications, J. Macromol. Sci. Part C: Polym. Rev. **46** (2006) 219–244.

[18] STAITI, P., MINUTOLI, M., HOCEVAR, S., Membranes based on phosphotungstic acid and polybenzimidazole for fuel cell application, J. Power Sour. **90** (2000) 231–235.

[19] LI, Q., HE, R., JENSEN, J.O., BJERRUM, N.J., Approaches and recent development of polymer electrolyte membranes for fuel cells operating above
100 °C, Chem. Mater. **15** (2003) 4896–4915.

[20] ZHANG, J., ZHONG, X., TANG, Y., SONG, C., High temperature PEM fuel cells, J. Power Sources **160** (2006) 872-891.

[21] HOGARTH, W.H.J., DINIZ DA COSTA, J.C., LU, G.Q., Solid acid membranes for high temperature (>140 °C) proton exchange membrane fuel cells, J. Power Sources **142** (2005) 223–237.

[22] SAVINELL, R., YEAGER, E., TRYK, D., LANDAU, U., WAINRIGHT, J., WENG, D., LUX, K., LITT, M., ROGERS, C., A polymer electrolyte for operation at a temperature up to 200 °C, J. Electrochem. Soc. **141** (1994) L46-L48.

[23] SUN, J.*,* JORDAN, L.R.*,* MACFARLANE, D.R., Acid–Organic base swollen polymer membranes, Electrochim. Acta **46** (2001) 1703-1708.

[24] CHO, E.K., PARK, J-S., SEKHON, S.S., PARK, G-G., YANG, T-H., LEE, W-Y. KIM, C-S, PARK, S-B., A study on proton conductivity of composite membranes with various ionic liquids for high-temperature anhydrous fuel cells, J. Electrochem. Soc. **156** (2009) B197-B202.

[25] SCHUSTER*,* M.F.H.*;* MEYER*,* W.H., Anhydrous proton-conducting polymers. Annu*.* Rev*.* Mater*.* Res*.* **33** (2003) 233-261.

[26] TANAKA, R., YAMAMOTO, H., SHONO, A., KUBO, K., SAKURAI, M., Electrochim. Acta **45** (2000) 1385-1392.

[27] BOZKURT, A., MEYER, W.H., GUTMANN, J., WEGNER, G., Proton conducting copolymers on the basis of vinylphosphonic acid and 4-vinylimidazole, Solid State Ionics **164** (2003) 169-176.

[28] MA, Y., WAINRIGHT, J., LITT, M., SAVINELL, R., Conductivity of PBI membranes for high-temperature polymer electrolyte fuel cells, J. Electrochem. Soc. **151** (2004) A8-A16.

[29] XIAO, L., ZHANG, H., SCANLON, E., RAMANATHAN, L., CHOE, E., ROGERS, D., High temperature polybenzimidazole fuel cell membranes via a sol-gel process, Chem. Mater. **17** (2005) 5328-33.

[30] LI, M., SHAO, Z., SCOTT, K., A high conductivity Cs2.5H0.5PMo12O40/ polybenzimidazole (PBI)/H_3PO_4 composite membrane for proton-exchange membrane fuel cells operating at high temperature, J. Power Sources **183** (2008) 69-75.

[31] NASEF, M.M., SAIDI, H., DAHLAN, K.Z.M., Single-step radiation induced grafting for preparation of proton exchange membranes for fuel cell, J. Membr. Sci., **339** (2009) 115-119.

[32] NASEF, M.M., SAIDI, H., DAHLAN, K.Z.M., Acid synergized grafting of sodium styrene sulfonate onto electron beam irradiated poly(vinylidene fluoride) films for preparation of fuel cell membrane, J. Appl. Polym. Sci., **118** (2010) 2801–2809.

[33] NASEF, M.M., SAIDI, H., DAHLAN, K.Z.M., Kinetic investigation of graft copolymerization of sodium styrene sulfonate onto poly(vinylidene fluoride) films, Radiation Physics and Chemistry*,* **80** (2011) 66-75.

[34] NASEF, M.M., SAIDI, H., DAHLAN, K.Z.M. Comparative investigations on radiation grafted proton exchange membranes prepared by single-step and conventional two-steps radiation induced grafting methods, Polym. Int. (2010) published online: 21 Sep. 2010.

FUNCTIONALIZATION OF POLYMER SURFACES BY RADIATION-INDUCED GRAFTING FOR SEPARATION OF HEAVY METAL IONS

G. PRZYBYTNIAK, E.M. KORNACKA, L. FUKS, M. WALO, K. ŁYCZKO, K. MIRKOWSKI

Institute of Nuclear Chemistry and Technology,
Dorodna 16, 03-195 Warsaw,
POLAND

Abstract

The reported investigations were focused on the elucidation of the most important factors influencing radiation-induced grafting; particularly (1) the effect of radical population generated in polymeric matrix on degree of grafting, (2) parameters determined grafting and its procedure, (3) correlation between layer structure formed via copolymerization and content of monomers in the initial solution. Sorption capacity of the adsorbants was evaluated using $^{152}Eu^{3+}$ as a marker monitoring depletion of the radioisotope from the initial solution by gamma radiometer. Electron spin resonance spectroscopy (EPR) and gas chromatography (GC) studies confirmed that yield of radiation-induced radicals increases in the following order polystyrene (PS) < polypropylene (PP) < polyethylene (PE). The same relationship was found for efficiency of radiation grafting. It was concluded that under comparable conditions the content of radicals in polymeric matrices determines grafting degree. It was found that application of the simultaneous method of grafting introduces to the grafted layers crosslinking or/and branching as well as degradation of functional groups. All these phenomena reduce access of Eu^{3+} to the studied sorbent therefore sorption capacity of the polyamide functionalized via pre-irradiation (indirect) method is higher than that determined for the sorbent prepared by simultaneous method of grafting. When two monomers, acrylic acid (AAc) and acrylamide (AAm) , contributed in the formation of grafted layer, their input into copolymerization was not proportional to the concentrations in the feed solution. It was confirmed that grafting of the monomers shows synergetic effect as the yield of copolymerization exceeds degree of grafting achieved for individual components

1. OBJECTIVE OF THE RESEARCH

Radiation induced grafting offers many advantages that might be commercialized: simplicity in controlling parameters of processing, uniform grafting of monomers or other low molecular weight moieties at ambient temperature, flexibility and good reproducibility of treatment. The adsorbent fabricated in this way can be applied to concentrate radioactive isotopes that possess chemical affinity to ligands present in grafted layers. Therefore, selection of suitable radiation grafted groups complexing with chosen metal ions seems to be promising way for working out novel separation technique. The results might contribute in the development of radiation technologies for the production of adsorbents of trivalent ions demonstrating similar chemical properties, e.g. Lanthanides.

2. INTRODUCTION

Several methods have been developed for the metal ions separation or their recovery from dilute solutions such as industrial fluids and wastewater [1–3]. Among them is sorption of metal ions on the polymers containing nitrogen, oxygen or sulphur donor atoms, i.e. groups that usually demonstrate coordination ability. Radiation induced graft polymerization is one of the most promising methods for obtaining materials having desired properties. Introducing different functional groups bonded covalently with polymeric matrix, the chemically active layers are formed that might be used as sorbents of heavy and/or radioactive metal ions. High concentrations of ligands localized in the layers and their ability to coordinate metal ions by several functional groups, similarly to the multidentate complexing agents, are the most important requirements for such type of sorbents. Great variety of monomers may be used to produce reactive macromolecules containing appropriate ligands, e.g. amino, carboxylic, hydroxyl, and amidoxime groups. It was chosen vinyl monomers comprising in the structure oxygen and/or nitrogen atoms, namely N-vinylpyrrolidon, (NVP), acrylamide (AAm) and acrylic acid (AAc) that are classified as ligands able to form mono- or polydentate polymer-metal complexes. However, as was confirmed by Kaliyappan and Kannan [4], due to steric obstruction, chance for binding metal ion by the second ligand positioned at the same chain seems to be limited. Utility of the grafted layers and their potential application depend not only on the introduced monomer but also on the method of grafting [5] which to some extend determines the structure of grafted layers and their final features. The following aspects of radiation-induced grafting are reported:

a) The influence of radicals generated in polymeric matrix and in monomer solutions on radiation yield of grafting. The simultaneous radiation grafting of acrylic acid (AAc) onto polyethylene (PE), polypropylene (PP) and polystyrene (PS) films was investigated. The contribution of processes initiated by active sites situated in the matrices was determined and analyzed.
b) The influence of grafting method using simultaneous and pre-irradiation procedures on ability to sorption of europium-152 on the surface modified with two vinyl monomers – NVP and AAm.
c) Graft copolymerization of two monomers, AAc and AAm, in order to improve sorption capacity of radioactive isotopes. Studies of simultaneous grafting of two components were performed to find if the introduction of carboxyl groups increasing hydrophilic properties of the polymeric matrix (polypropylene) enhances affinity towards cation attraction, and subsequently production of complex/chelate compounds.

Characterization of the sorbents at each step of their production was carried out using gravimetric method, EPR spectroscopy, ATR-FTIR, thermal and contact angle measurements. Sorption properties of the prepared materials were determined using LG-1 gamma radiometer, constructed at the Institute of Nuclear Chemistry and Technology, by the measurements of solutions radioactivity before and after sorption. The sorption capacity indirectly reveals construction of the grafted layers as well as their usefulness for coordination of the selected metal ions. It is known that the coordination chemistry of trivalent lanthanides does not differ neither along the series nor from the actinide series [6] thus obtained data can be extrapolated for both groups of elements.

3. MATERIALS AND METHODS

3.1. Materials and their irradiation

Following materials used in this work were commercially available LDPE - Malen FGNX 23D-022, PP - Malen P J601 and PS - GPPS - Owispol 525 0001TH supplied from PKN Orlen S.A. PA 6,10 polyamide and PP filter of microporous structure (20 µm) were studied as matrices. Acrylic acid (AAc), N-vinyl-pyrrolidone (NVP) and acrylamide (AAm), ferric chloride and Mohr's salt were purchased from Aldrich Chemical Company Inc. and used without any purification. Methanol was delivered from Chempur Co. The polymers in form of tape or PP filter were washed with water in ultrasonic bath and dried at 60°C under vacuum. Before irradiation the materials were kept 24 h in solvents.

The samples were irradiated with a 10 MeV electron beam generated by an Elektronika accelerator in air atmosphere at room temperature. The total doses were obtained by multipass exposure (ca. 25 kGy per one pass). For some samples ^{60}Co source Issledovatiel (dose rate 1.14–0.97 kGy/h) was applied for simultaneous grafting.

3.2. EPR spectroscopy

The radicals produced in the polymeric matrices were monitored and identified by electron paramagnetic resonance (EPR) spectroscopy using X-band ESP 300 Bruker spectrometer equipped with the Apollo software.

3.3. Gas chromatography

The radiation yields of hydrogen in the gas phase evolved from irradiated polymers were determined with a gas chromatograph Shimadzu – 14B. 1 m long column was packed with molecular sieves of 5 Å; the thermoconductivity method was used for detection. The carrier gas was argon; calibration was performed with hydrogen of purity 99.99%.

3.4. Thermal analysis

Thermal properties were investigated using DSC technique. Phase transitions were determined by a TA Instruments apparatus with nitrogen flow and heating rate of 10°C/min. The crystallization and melting behaviour of the samples were studied during first heating/cooling cycle or after erasing of the thermal and mechanical history of samples in the second run. Measurements were performed in the temperature range from 25–200°C. About 5 mg of the sample inserted in the pan was heated, then kept for 5 min at 200°C and gradually cooled. Afterwards, the second run was performed applying the same conditions as for the first cycle. Thermal decomposition of the polymers was performed on a TA Instruments TGA Q500 apparatus. Analyses were conducted over the temperature range from 30°C to 600°C with a programmed temperature increment of 10°C/min under nitrogen atmosphere.

3.5. Swelling measurements

Swelling of the polymeric material was examined by immersing *ca.* 0.025 g samples in distillated water or in the aqueous solutions of monomers at 40°C for 18 h, when saturation was reached. Subsequently, the samples were dried carefully with the filter paper and immediately weighed. Swelling was calculated by the following equation:

$$\text{Swelling (\%)} = [(w_s - w_o)/w_o] \times 100\% \qquad (1)$$

were w_s and w_o represent the weights of swelled and initial (dry) samples, respectively.

3.6. Radiation-induced grafting

Simultaneous grafting was performed using aqueous solutions of NVP and AAm at concentrations indicated in Figures 8 and 9. Tapes of PA immersed in the solutions containing an inhibitor of homopolymerization (20 mmol dm^{-3} $CuCl_2$) and monomers were irradiated either in gamma source at ambient temperature or in accelerator Elektronika. For pre-irradiation grafting, polyamide was exposed to electron beam in an accelerator Elektronika under air atmosphere and subsequently contacted with aqueous solutions of monomer at 40°C.

Upon grafting, the samples made from PA covered with the layers of polymerized NVP or AAm were washed for 0.5 h in ultrasonic water bath and dried under vacuum at 80°C until a constant weight was reached. The degree of grafting was determined gravimetrically and expressed as follows:

$$\text{Degree of grafting (\%)} = [(w_g - w_o)/w_o] \text{ x } 100\% \qquad (2)$$

where w_g and w_o represent the weights of grafted and initial samples, respectively.

For PP filter, grafting was performed from methanol solution of AAc and AAm. The procedure applied after grafting was analogous to that one described above.

3.7. Dynamic contact angle measurements

The surface of the grafted polyamide was characterized by dynamic contact angle measurements carried out by means of Wilhelmy method using Krűss Tensjometer K100. The presented data were calculated on a basis of eight independent assays.

3.8. ATR-FTIR spectroscopy

ATR-IR spectra were recorded with a Bruker Equinox 55 FT-IR spectrometer. The spectra were collected in the range of 4000–650 cm^{-1} at a resolution of 4 cm^{-1} by means of an accessory designed for single reflection ATR technique equipped with ZnSe crystal.

3.9. Sorption

The grafted polymeric samples, before using as a sorbent, were activated by 0.5 h treatment with 1.0 mol dm^{-3} HCl, 1.0 mol dm^{-3} NaCl and water. Europium radioisotope ^{152}Eu^{3+} (10^{-7} mol dm^{-3} in 1 mol dm^{-3} NaCl solution) was used as a marker monitoring sorption capacity. pH values of the initial solutions were adjusted by adding 0.05 mol dm^{-3} NaOH or HCl and were controlled using a combined glass electrode connected to a pH meter (of the HI-221 type, Hanna Instruments Co.). It was found that batch sorption equilibrium was reached after 2 h shaking using programmable roto–shaker MultiBio RS-24 (Biosan, Latvia). Home-made gamma radiometer LG-1 was used to determine the initial and equilibrium radioactivity of the solutions.

4. RESULTS AND DISCUSSION

4.1. Influence of radicals generated in polymeric matrix and in monomer solutions on radiation yield of grafting

Generally, grafting yield is determined predominantly by the level of radicals initiated both in polymeric matrix and in solvent. The analysis of paramagnetic species performed by EPR spectroscopy enables to estimate contribution of particular polymers to radiation induced formation of radicals what indirectly reveals their ability to construct covalent bonds with monomers.

PS is considered as the most radiation resistant polymer since efficient conversion of absorbed radiation energy into the heat by aromatic rings. Thus, radiation processes are very limited and radiation yield of the radicals in PS is much lower than that found in other polymers. According to Clough et al. [6] three radicals can be identified – two of them are formed upon abstraction of hydrogen and one is created *via* addition of hydrogen to aromatic ring. The EPR spectrum measured upon irradiation with a dose of 25 kGy (Fig. 1) is uncharacteristic and of low intensity what reveals low efficiency of the radical processes influencing yield of radiation-induced grafting.

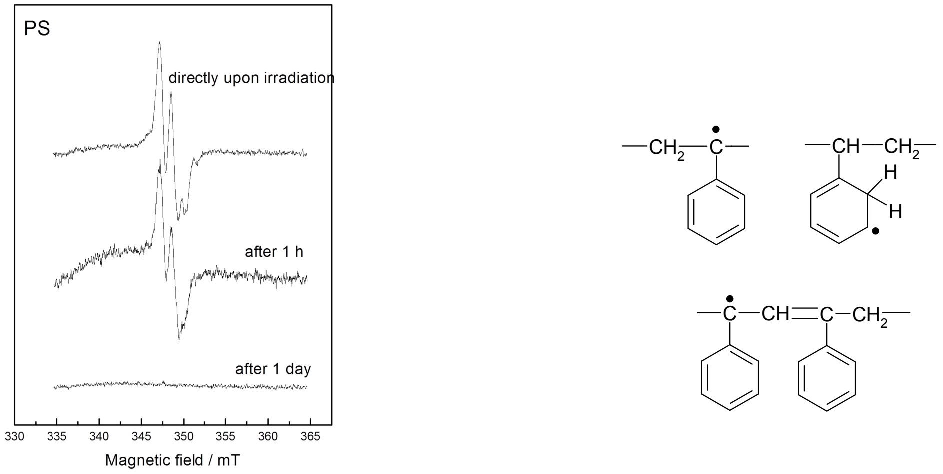

FIG. 1. EPR spectra of radicals formed in PS by ionizing radiation with a dose of 25 kGy (electron beam, air atmosphere) and expected radical structures [7].

Figure 2 shows the spectra of the radicals formed in PP upon exposure to an electron beam. A dominant product is third ordered alkyl radical that fast undergoes oxidation. Formed peroxyl radical is very stable and can be detected even many months upon irradiation thus PP seems to be a proper substrate for applying pre-oxidation method of grafting. However such a procedure requires exposure of the polymer to much higher doses than in simultaneous method, thus the risk of polymer degradation increases. The level of radicals, as was roughly determined by double integration of obtained EPR signal is more than 4 times higher in PP than in PS.

PE is also considered as a radiation resistant polymer but the background of the phenomenon is different than in the case of PS. A dominant factor determining final effect of irradiation is formation of bonds between main chains that occurs in amorphous phase. Except effective cross-linking, ionizing radiation induces residual radicals in crystalline phase. The experimental spectrum of PE is a composite signal arising from various contributions of several radical individuals, Fig. 3. Deconvolution of the experimental spectra leads to the conclusion that eventually alkyl, allyl and polyenyl radicals are produced under vacuum (in Fig. 3 dotted lines present spectra reconstructed on a basis of the signals of individual species).

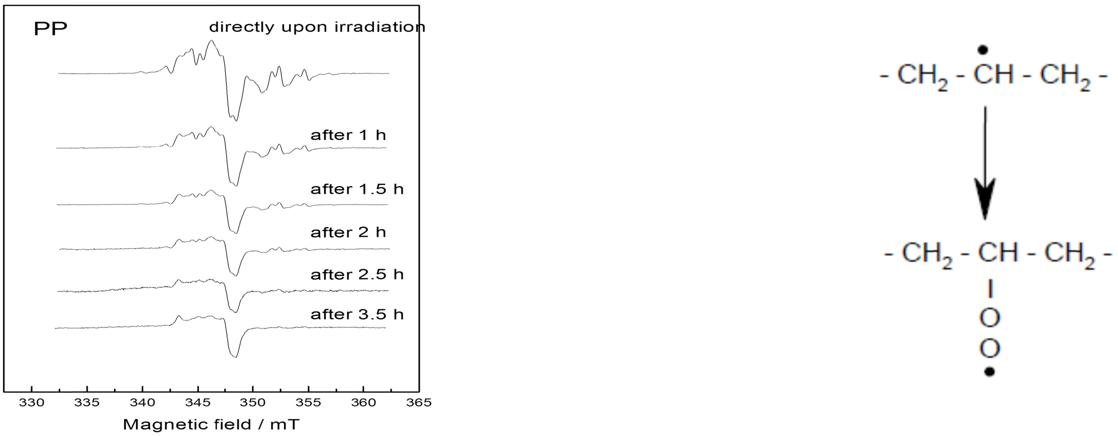

FIG. 2. EPR spectra of radicals formed in PP by ionizing radiation with a dose of 25 kGy (electron beam, air atmosphere) and expected radical structures [7].

The dominant intermediate is a second ordered alkyl radical; less populated are allyl type radicals and polyenyl radicals that might be selected upon partial decay of the main product. Significant level of paramagnetic species should facilitate formation of covalent bonds during grafting. The concentration of radicals in PE estimated directly upon irradiation overcome that found in PP. It must be emphasized that used polymers are commercial products thus observed variations among population of radicals concern these particular materials.

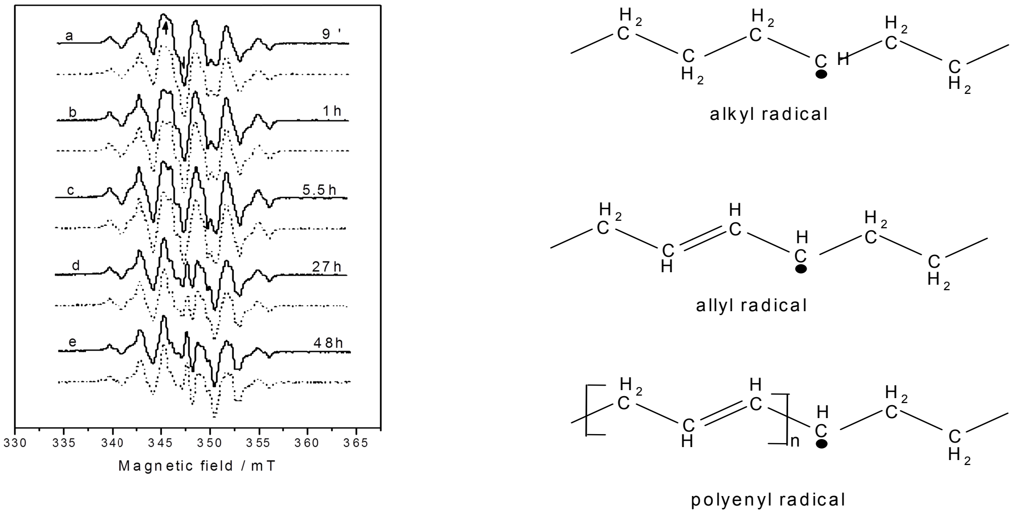

FIG. 3. EPR spectra of radicals formed in PE by ionizing radiation with a dose of 25 kGy (electron beam, vacuum) and expected radical structures [7].

The radicals formed in the studied polymers, PS, PP and PE, are predominantly generated upon abstraction of hydrogen. Consequently, radiation yield of hydrogen reflects indirectly level of formed paramagnetic species. Values of radiation yield of hydrogen, G(H_2), in Table 1 reveal great discrepancies among particular polymers. The most intensive is emission of hydrogen from PE (0.46 µmol/J), smaller from PP (0.27 µmol/J) and the smallest from PS (0.036 µmol/J). Dehydrogenation results in the production of alkyl radicals as well as cross-linking, and the last process is the most significant in PE.

TABLE 1. RADIATION YIELD OF HYDROGEN G (H_2)

Polymer	Radiation yield of hydrogen µmol/J
PP	0.27
PS	0.036
PE	0.46

Then, an influence of the radical population on efficiency of simultaneous grafting was investigated. Figures 4 A, B and C illustrate relationships between grafting degree and concentration of the agent inhibiting homopolymerization observed for PS, PP and PE matrices, respectively. For PS, even upon a relatively high dose, 25 kGy, yield of the process is insignificant at concentration of 50% of AAc and negligible at 25%. EPR and GC results indicate that the level of radicals in PS is very low. Therefore, lack of noticeable changes reveals that the radicals occurred in the matrix have dominant influence on the initiation of grafting. Additionally, life-time of intermediates in PS is shorter than in irradiated PE and PP thus conversion to diamagnetic product competes with grafting processes.

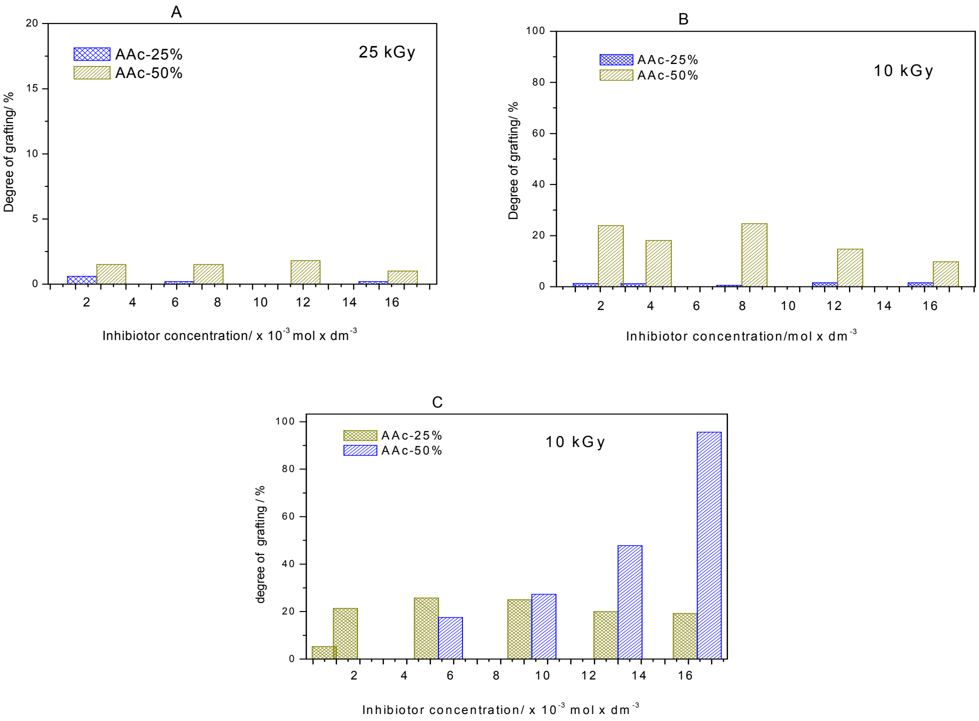

FIG. 4. Effects of concentration of homopolymerization inhibitor ($Fe(SO_4).(NH_4)_2(SO_4)$) on the degree of grafting of AAc onto PS (A), PP (B) and PE (C) [7].

The grafting degree on PP as a function of Mohr's salt concentration is shown in Fig. 4B. If concentration of the inhibitor exceeds 2 μmol/dm^3 degree of grafting was found to be independent on amount of the additive till 8 μmol/dm^3 and subsequently diminishes. Probably the following fraction of Fe^{2+} contributes in termination of the grafting processes: $-CH_2\ CH^{\bullet}COOH + Fe^{2+} + H^+ \rightarrow -CH_2\ CH_2COOH + Fe^{3+}$. Under experimental conditions the yield of AAc grafting on PP does not exceed 30% in presence of 50% AAc.

For PE the increase in inhibitor concentration results in increase in grafting degree. Two different tendencies support the process: high level of AAc monomers that avoid homopolymerization due to raising contents of ferrous ions and large population of radical centres situated in the matrix since concentration and stability of radicals generated in PE backbone is higher than in irradiated PS and PP.

The degree of radiation-induced grafting of AAc is the highest for PE matrix, lower for PP and negligible for PS, under comparable conditions. Radiation processes in the solutions are independent on the character of immersed polymeric samples. Thus, the radicals generated in the matrices have to be responsible for differences in the degree of grafted monomer. Analyzing population of unpaired spins by double integration of EPR spectra it was found that concentration of the radicals is consistent with increasing efficiency of grafting. The changes in radiation yield of hydrogen emitted from PS, PP and PE also confirmed such a tendency.

4.2. Functionalization of polyamide surface by radiation-induced grafting of N-vinyl pyrrolidone and acrylamide

As it was earlier confirmed, the content of radicals generated by ionizing radiation in polymeric matrices has significant influence on grafting degree [7]. Therefore, in the second stage of the reported investigations, stability and decay of paramagnetic active centres as well as their relative concentrations were determined. The EPR spectra detected upon irradiation with a dose of 28 kGy are presented in Fig. 5. For PA the radicals stable at room temperature show a quartet of hyperfine splitting (hfs) about 2.3 mT and a singlet in the centerfield revealed one day after irradiation. Storage of the sample results in decrease in the signal intensity and in insignificant changes in proportion among peaks.

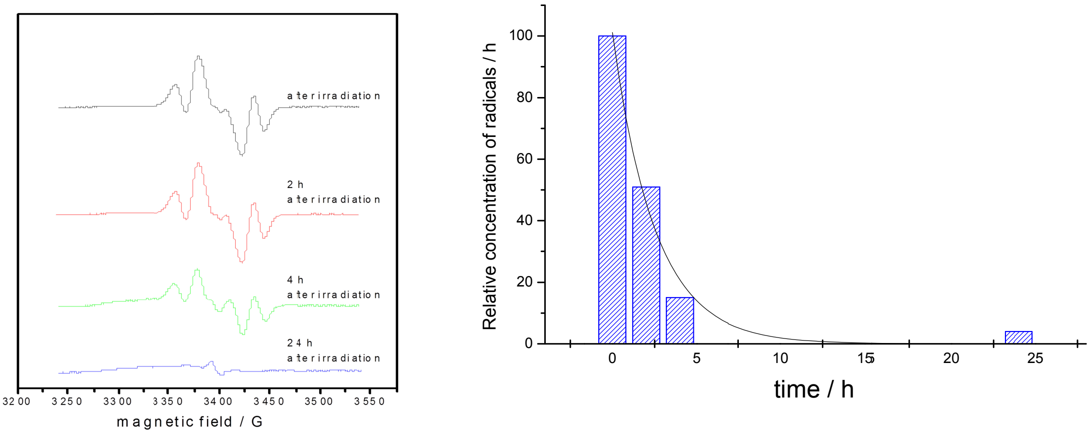

FIG. 5. Left side: EPR spectra of PA detected at room temperature. Right side: kinetics of radical decay in PA [8].

Interpretation of the EPR results was performed on a basis of literature data [9, 10] as well as on analysis of the obtained signals. The character of the recorded spectra suggests interaction between unpaired electron and hydrogen atoms, due to characteristic hfs values, typical for alkyl radicals. Nevertheless, the radical shown below and similar ones (radical centre localized at carbon atom other than C_α) ought to demonstrate a sextet originated from the interaction of unpaired spin with five nearly equivalent protons, similarly to other hydrocarbon macromolecules, e.g. polyethylene. Such a pattern is not observed in any of the recorded spectrum. Additionally, the range of EPR spectrum is much lower than 10,0 mT thus a number of hydrogen atoms affecting radical centre must be less than 5.

$$—CO—NH—CH_2—\dot{C}H—CH_2—$$

As was suggested earlier by Takigami et al. [10], the PA spectrum corresponds probably to the radical which centre is localized at α position towards amide group (see below). In such a case EPR spectrum reveals interaction of unpaired electron and protons at α and β carbon atoms.

$$—CO—NH—\dot{C}H—$$

During the last stage of radical processes disproportionation might lead to the production of unsaturated bonds and eventually to the conjugated double bond systems that are able to stabilize unpaired spin efficiently. Such a product reveals EPR spectrum in form of singlet, analogously to irradiated polyethylene. The last observed in PA spectrum might be assigned to that type of intermediate. The kinetics of radical decay shown in Fig. 4 reveals that paramagnetic species are stable in PA matrix only for 24 h. The EPR data demonstrate that (i) the radical centred at α position towards amide group is a precursor of vinyl monomer grafting and (ii) in pre-irradiation grafting the matrix has to be contacted with monomers during first few hours after irradiation. Two different monomers containing nitrogen and oxygen donor atoms that form complexes of high stability with many metal ions were used for radiation induced grafting. These were namely N-vinyl pyrrolidone (NVP) and acrylamide (AAm) dissolved in double distilled water.

Swelling of PA matrix was determined using aqueous solutions containing monomers at various concentrations. The process might facilitate penetration of monomer molecules into the external layer of matrix. For 40% solutions swelling reaches 10% and 12% for NVP and AAm, respectively, Fig. 6.

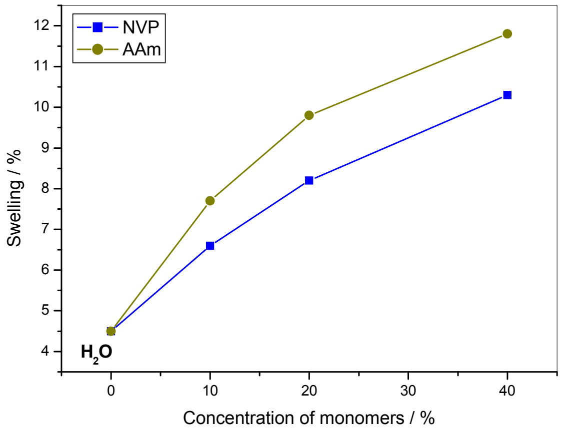

FIG. 6. Swelling of PA in aqueous solution of NVP and AAm [8].

In order to carry out grafting by means of simultaneous method, the dose was split and delivered in portions of 25 kGy. Figure 7A shows a relationship between absorbed dose and grafting degree of NVP in presence of air. The function is linear and depends considerably on the monomer concentration. If the concentration is doubled, then also the grafting process is almost twice more efficient. In order to detect exothermic effect of the growing NVP chain, a rise in temperature was measured after each pass under electron beam (Fig. 7B). The increase in temperature results not only from the simple conversion of radiation energy into the heat but also from exothermic radical polymerization since the observed effect depends on the monomer concentration and consequently degree of grafting.

The AAm monomer was grafted using simultaneous and indirect procedures (Fig. 8). As was expected, efficiency of AAm grafting per 1 kGy of absorbed energy was much higher when simultaneous method of grafting was applied. In such a procedure just for doses in the range of 2–5 kGy the degree of grafting reaches 20% and 80% at concentrations of 10% and 40% AAm, respectively, whereas for pre-irradiation method the yield of grafting is much lower, as seen in Fig. 8B and 8C. The kinetics of AAm pre-irradiation grafting shows that at 40°C the maximal effect is reached just after 1 h. The final result is strongly influenced by absorbed dose. For pre-irradiation method the grafting yield is growing with the monomer concentration only till 30% and for higher content of AAm changes are insignificant.

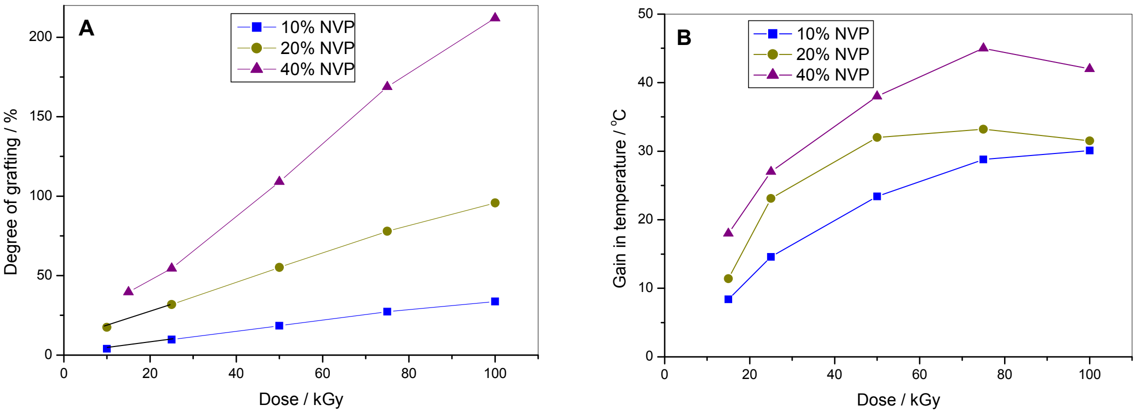

FIG. 7. A - Relationship between absorbed dose and degree of grafting for PA/NVP system (simultaneous grafting, EB). B – Increase in temperature after each pass under electron beam for NVP grafting on PA [8].

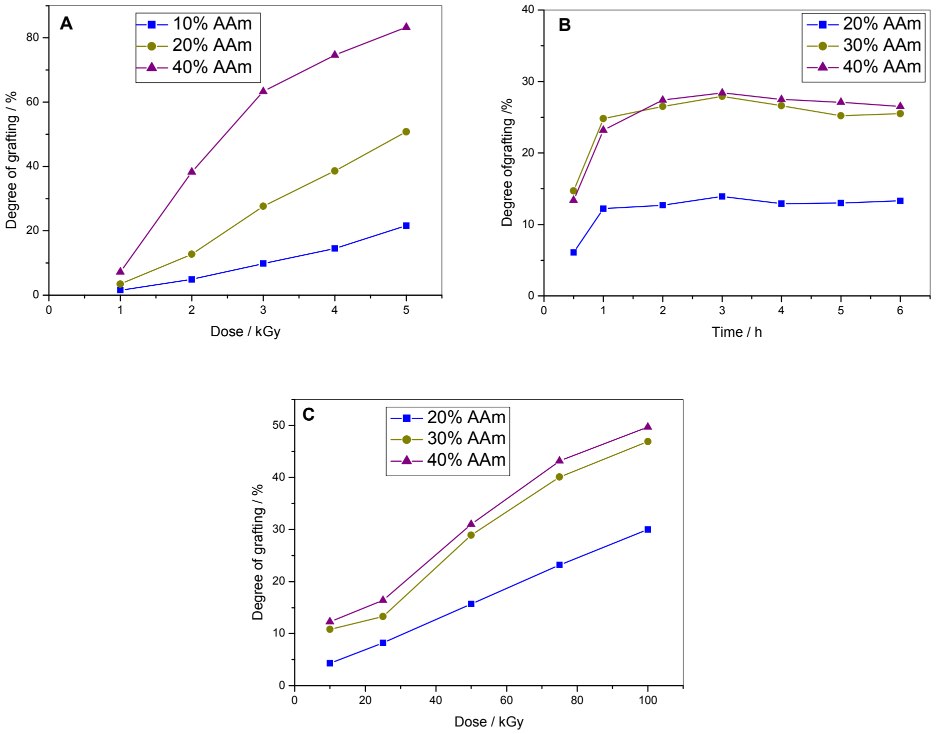

FIG. 8. A - Relationship between absorbed dose and degree of grafting for PA/AAm system (simultaneous grafting, gamma source). B - Optimization of the reaction time for pre-irradiation grafting of AAm on PA for a dose of 25 kGy; C - Function of grafting degree versus absorption dose at various concentrations of AAm [8].

An increase in hydrophilic properties of the PA surface covered with grafted AAm and NVP macromolecules was monitored by the dynamic contact angle measurements. The data obtained for advanced angle do not reflect wettability correctly since the system was far from reaching equilibrium with water. Thus, only recede angle clearly confirms considerable raise of hydrophilicity (Table 2). Low values of contact angle are attributed to the surfaces of enhanced ability towards attraction of polar moieties what can support metal ion sorption.

Sorption properties of the grafted polymeric materials have been determined using radioactive isotope ^{152}Eu. Initial pH of 10^{-7} M Eu^{3+} aqueous solution in NaCl was 4.55. Solution acidity, upon contacting with the grafted samples, remarkable decreases (equilibrium pH for the studied samples is shown in Table 3).

TABLE 2. EXAMPLES OF RECEDE CONTACT ANGLE OF PA BEFORE AND AFTER GRAFTING, 25°C

PA	$CA_{Rec.}$ (deg)
0 kGy	32
20 kGy	40
Pre-irradiation grafting 20% NVP	23
Pre-irradiation grafting 30% AAm	15

TABLE 3. UPTAKE OF EUROPIUM IONS BY GRAFTED LAYERS OF NVP AND AAM ON PA MATRIX. AVERAGE RADIOACTIVITY WAS CALCULATED ON A BASIS OF THREE INDEPENDENT MEASUREMENTS

Sorbent	Grafted layer/mass of PA (mmol/g)	pH after grafting	Radioactivity kBq/g (grafted layer)
NVP Simultaneous grafting	15.2	5.27	310
AAm Simultaneous grafting	6.0	4.90	586
AAm Pre-irradiation grafting	4.2	5.05	1283

It is known that up to about pH = 6.0 europium exists predominantly in form of trivalent ion, however for more basic solutions, the trivalent cation undergoes hydrolysis forming $Eu(OH)^{2+}$ and $Eu(OH)_2^+$ structures [11, 12]. On the other hand, sorption from the acidic solutions is limited due to competition between the excess of H^+ ions and cationic species. The process was confirmed by Sharma and Tomar [13] who investigated influence of pH on sorption of some lanthanides onto the analogue of mesolite. According to the results, below pH = 5.5 the removal of U(IV), Th(IV) and Eu(III) decreased considerably, reaching at pH = 1 level more than three times lower than at pH = 5. Since the trivalent europium ion sorption significantly depends on pH, increasing basicity during sorption (Table 2) is supposed to enhance the efficiency of metal ion binding. Therefore, the resulting pH seems to improve conditions for sorption of the studied cation.

In model studies europium ion is frequently used as an analogue to trivalent actinides and applied as a tracer of radionuclide migration in the geosphere. In these investigations various minerals were applied as potential complexing agents, e.g. hydrous silica [14], Gorleben sand and humic substances [15] and analogue of mesolite [13]. Two types of Eu^{3+} bonding to mineral surfaces have been distinguished: (i) electrostatic interaction with negatively charged surface sites and (ii) formation of surface complexes with oxygen containing polar groups. The second mechanism was also confirmed in some other organic europium complexes – in conjugated Eu^{3+} complexes involving carbonyl and pyridine groups [16] as well as in complexes with pyridyl oxadiazole derivative and dibenzoylmethane [17]. These organic compounds served as ligands delivering oxygen and nitrogen atoms bonded with the central ion. Complexes of Eu^{3+} with grafted layers of AAm and NVP probably also are formed with contribution of the heteroatom. Bidentate ligands based on oxygen and nitrogen atoms present in each monomer are responsible for the capacity of europium ion sorption. The neighbouring mers provide subsequent pairs of functional groups that might contribute in Eu^{3+} complexation. Such a system characterizes a considerable hydrophilization of the surface and efficient sorption of selected metal ions.

4.3. Copolymerization of AAm and AAc on PP filters

In order to intensify sorption capacity, PP filter of extended boundary surface facilitating penetration of low molecular species was applied as a matrix. Polyacrylamide which, as was found in the previous studies, efficiently forms complexes with europium ion, was enriched with AAc mers that additionally increased hydrophilic properties of the product and enhanced affinity towards cations due to introduction of carboxyl groups.

Grafting yield measurements: The PP-g-AAc-AAm sorbent was prepared via simultaneous grafting applying methanol solvents of monomers in various concentrations with AAc:AAm ratio was as follows: 0:100, 20:80, 40:60, 60:40, 80:20, 100:0, (Fig. 9). The obtained data indicated that grafting of acrylamide is more efficient than acrylic acid, and the highest yield was achieved when the mixture of both components was in the proportion of AAc/AAm = 40:60.

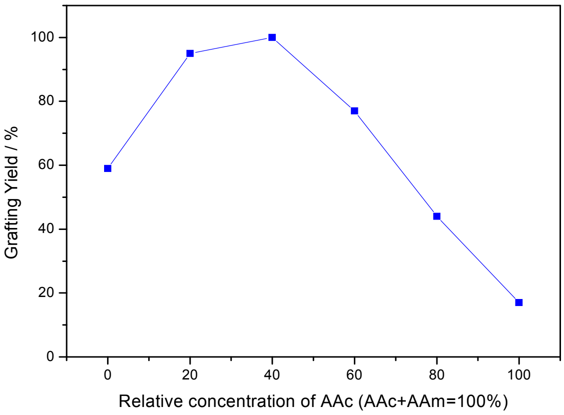

FIG. 9. Effect of monomer concentration on the grafting yield for the system PP-g-AAc-AAm. Grafting conditions were as follows: total concentration of monomers in methanol: 30%, inhibitor concentration ($CuCl_2$):$5x10^{-4}$ mol dm^{-3}, dose: 10 kGy, temperature: 50°C.

The profile of grafting yield unambiguously reveals that radiation induced processes in the system comprising two monomers, namely AAc and AAm, demonstrates synergetic effect as under such conditions the efficiency of the reaction exceeds yields achieved for the individual components.

Thermogravimetric analysis in ambient gas (nitrogen): Thermal stability of grafted PP depends on the nature of mers. The initial weight loss was due to the presence of small amount of moisture in the samples, Fig. 10. The thermographs of PP-g-AAc and PP-g-AAm show one distinct zone of thermal degradation of maximal decay rate (T_{m3}) at about 460°C. For PP-g-AAc the small peak below 400°C is due to the decarboxylation combined with the emission of carbon dioxide.

Contrary to this findings, the PP-g-AAc-AAm system is more thermally sensitive as the first step of decay starting at low temperatures achieves maximal decay rate just at T_{m1} = 217°C, and second one at T_{m2} = 390°C, Fig. 10. In both stages the thermal decomposition deepens with increasing concentration of AAm and reaches maximum for AAc: AAm=20:80 (Fig. 9, right side). Position of the signals is in correlation with T_{m3} which increases insignificantly when thermal decay at T_{m1} and T_{m2} becomes more intensive. The first stage decomposition at around T_{m1} was due to dehydration as well as loss of ammonia by AAc-AAm copolymer followed by the formation of imide group via cyclisation. The second stage at T_{m2} might correspond to degradation of the network structures or main chain scissions.

Considerable decompositions at T_{m1} and T_{m2} do not develop in mono-monomer grafting system thus it seems that they might be attributed to the chains constructed from two types of mers that form defined structure of features determined by the ratio between used components.

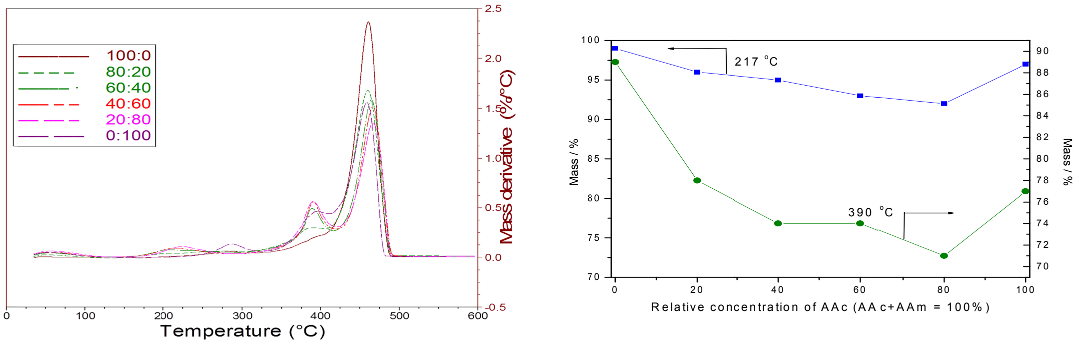

FIG.10. Left side: DTGA thermographs of PP-g-AAc-AAm. Right side: thermally induced mass loss at 217 °C and 390 °C for PP-g-AAc-AAm in nitrogen atmosphere.

The results confirm that during grafting the uniform layer of copolymer is produced which shows specific, well defined parameters.

Differential scanning calorimetry: During the first run of heating melting point of PP before and after grafting is situated at the same position, i.e. at around 160°C and the peak is getting smaller when the material is grafted (Fig. 11). Moreover, very broad exothermic transition related to the presence of moisture emerge in the region below 100°C. Intensity of all peaks corresponding to melt and crystallization transitions are the highest for PP-g-AAc, then diminishes with increasing AAm concentration till ratio AAc:AAm = 40:60 and subsequently the peaks are partly restored. Additionally, with increasing AAm concentration, monomodal exothermic crystallization transition is converted into bimodal one.

During the second cycle of DSC measurements positions of melting points as well as areas under the peaks corresponding to the melting transition were determined (Fig. 12). It was confirmed, in accordance with previous studies, that enthalpy of fusion ΔH reflecting degree of PP crystallinity decreases after AAc and AAm grafting. The loss of rigid phase caused by AAc mer is the lowest and grows when graft copolymerization is performed. Thus, as in previous studies, the modification of matrix is the highest when co-mer layers are formed.

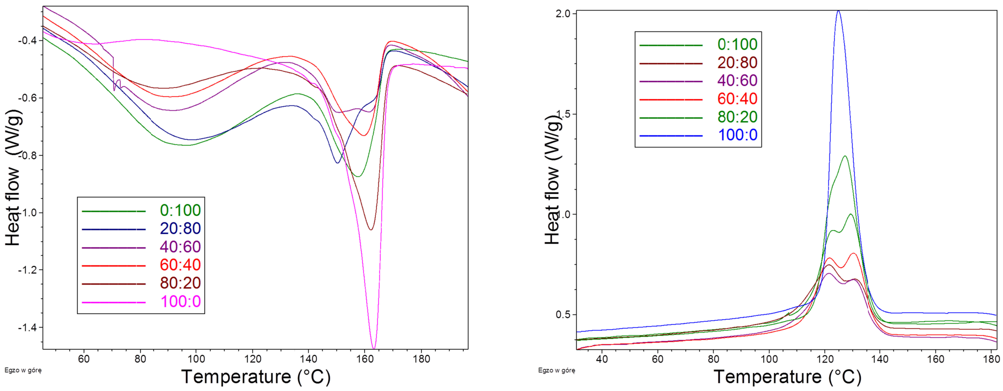

FIG. 11. Thermographs presenting phase transitions of PP-g-AAc-AAm detected during the first heating/cooling cycle. Left side: heating, right side: cooling.

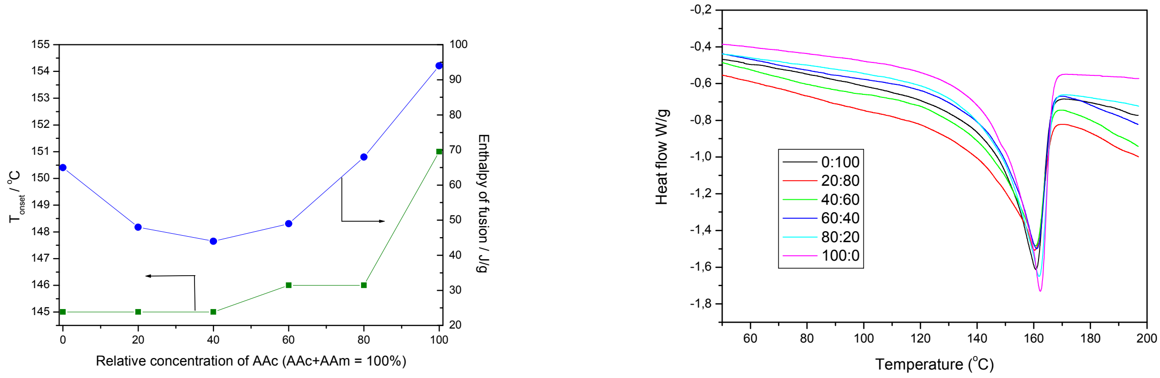

FIG. 12. Left side: thermographs presenting phase transitions of PP-g-AAc-AAm detected during the second heating. Right side: changes of melting point and enthalpy of fusion determined on a basis of the graphs shown nearby.

EPR spectroscopy gives insight into radical processes initiated during exposition to ionizing radiation. As in solutions the generated intermediates are unstable at room temperature, the following systems were frozen in liquid nitrogen: AAc/methanol, AAm/methanol, AAc/AAm/methanol, AAc/AAm/methanol/PP. Then, upon irradiation, the EPR spectra were recorded using Bruker EPR spectrometer. As expected, the character of all spectra is comparable (Fig. 13). It seems that the radical showed below is generated in the main chains of growing macromolecules:

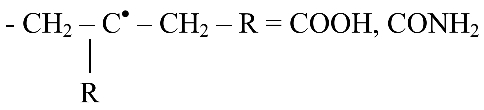

$$-\,CH_2 - \underset{\textstyle R}{\underset{|}{C^\bullet}} - CH_2 - \quad R = COOH,\ CONH_2$$

The unpaired spin interacts with four almost equivalent protons at β position revealing hyperfine splitting (hfs) near 2.4 mT. Before annealing poorly resolved lines attributed to γ-hydrogen atoms appear in all recorded spectra as well as triplet corresponding to methanol radical. However, after heating to -113°C, only distinct quintet is observed (Fig. 13 (b)) that at elevated temperatures, e.g. at -53°C, is converted to the spectrum comprising anisotropic signal of oxidative degradation products (Fig. 13 (c)).

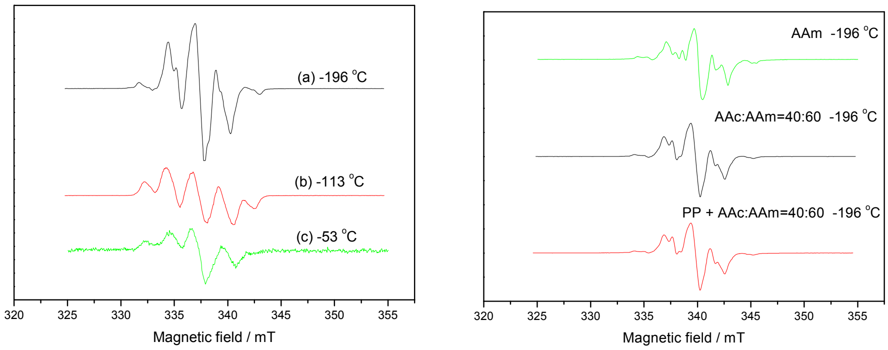

FIG. 13. Left side: EPR spectra of AAc. Right side: EPR spectra of AAm, AAc + AAm and PP + AAc + AAm.

The following terminal radical responsible for graft polymerization was not found in the analyzing EPR spectra:

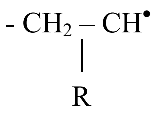

$$-\,CH_2 - \underset{\textstyle R}{\underset{|}{CH^\bullet}}$$

This radical is supposed to demonstrate quartet of hfs typical for alkyl radicals that was not identified in the detected spectra. Such a product due to high reactivity is efficiently consumed during the chains grow. Thus, initiated by ionizing radiation primary species were not detected even under cryogenic conditions and radicals formed in the grafted products provide evidence that polymerization proceeds very efficiently.

ATR-FTIR spectroscopy: the ratio between AAc and AAm monomers in the solution needs not reflect the contribution of AAc and AAm mers in the grafted layer. In order to estimate the correlation between participation of the particular components in growing chains of copolymers and their concentration in the initial methanol solution, IR spectra were recorded using ATR-FTIR spectroscopy. Many various bands were detected revealing complexity of the system. Two of them were selected in order to monitor the contribution of amide group in the studied system.

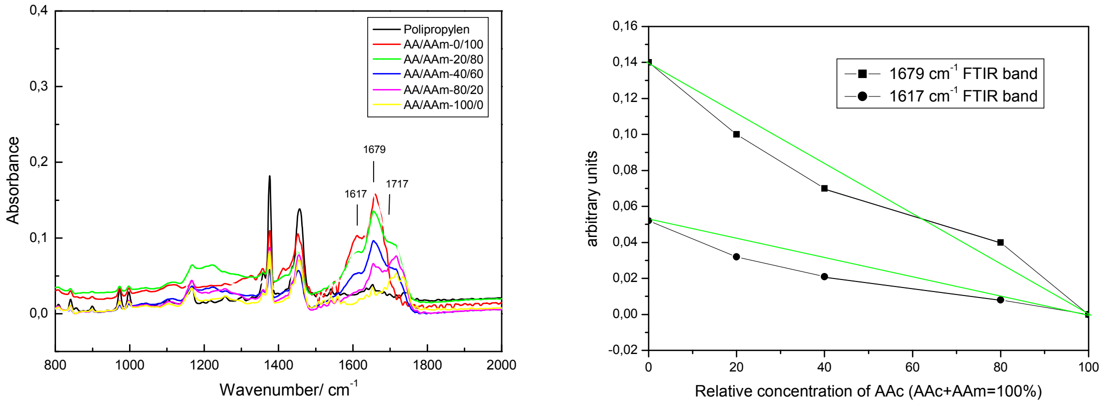

FIG. 14. Left side: ATR-FTIR spectra of PP-g-AAc-AAm. Right side: decrease in intensity of N-H bending vibration – II amide band (1617 nm) and interference of C=O stretching vibrations – I amide band (1679).

If the contribution between mers in grafted copolymer is additive, the relationship between AAc concentration and diminishing intensity of 1679 and 1617 cm^{1-} bands would demonstrate a green line (Fig. 14, right diagram). However, for the solutions containing 20 and 40% of AAm, the contribution of acrylamide component in the grafted layer is not directly proportional to the concentration in the solutions and the results are ca. 20 and 30 % smaller, respectively.

Adsorption of europium ion: The sorption capacity of produced sorbents is changing significantly depending on the ratio between components. It was found that the highest radioactivity per gram of grafted layer was determined for grafted polyacrylic acid homopolymer (Fig. 15). About 40% lower values were achieved for polyacrylamide only and for copolymer comprising mers in the proportion of AAm:AAc = 20:80. However, depletion of europium ions by grinded grafted filters from the aqueous solutions was substantial for all prepared sorbents and reaches above 93%. As seen in Fig. 9 degree of grafting for AAc was the lowest thus sorption calculated per gram of layer is the highest. It seems that the internal fractions of the grafted layers do not contribute in the sorption and predominantly the external functional groups are engaged in bounding of europium ions. Thus, the yield of sorption for all studied homo- and co-polymers is comparable (Table 4).

TABLE 4. DEPLETION OF THE $^{152}EU^{3+}$ RADIONUCLIDE FROM 10^{-7} mol dm^{-3} AQUEOUS SOLUTION

Relative concentration of AAc (%)	0	20	40	60	80	100
Decrement of radioactivity in $^{152}Eu^{3+}$ solution (%)	95	98	99	98	99	99

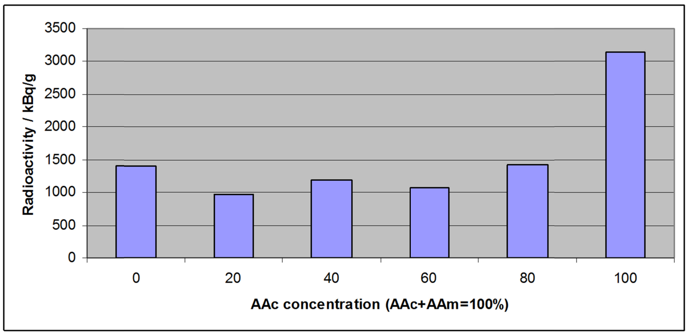

FIG. 15. Radioactivity per gram of grafted layers resulting from sorption of europium radioisotope $^{152}Eu^{3+}$.

5. CONCLUSIONS

Analyzing population of unpaired spins by double integration of EPR spectra it was found that concentration of the radicals is consistent with increasing efficiency of grafting. The changes in radiation yield of hydrogen emitted from PS, PP and PE also confirmed such a tendency. Under comparable conditions the degree of radiation-induced grafting of AAc is the highest for PE matrix, lower for PP and insignificant for PS. Radiation processes in the solutions are independent on the character of polymeric samples. Thus, the radicals generated in the matrices have to be responsible for the differences in the degree of grafting.

It has been confirmed that sorption efficiency is determined by the grafting method. For PA/AAm system the uptake of trivalent europium ions for the sorbents prepared by indirect grafting method is twice higher than for the sorbents produced according to simultaneous procedure. The effect can be explained in terms of two factors: (i) steric effect, which is determined by the conformation and density of the grafted chain, and (ii) special environment constituted by polymer ligand domains. Features and sorption capacity of the grafted layers depend, except many other factors and parameters, on grafting method. Simultaneous grafting is the simplest radiation technique for the preparation of grafted polymers. However, the process has some limitations arising from the high level of homopolymer formation. Additionally, crosslinking and branching of the growing chains as well as degradation of the functional groups might occur. These consequences hinder diffusion processes and ability to metal-ion sorption, diminishing expected effect. To some extend these phenomena are possible also when pre-irradiation process is applied. However, at elevated temperature the growth of grafted macromolecules develops relatively fast and side-effects seem to be limited. There are not reactions induced by indirect effect of ionizing radiation when intermediates generated in solvent (water) and solute (monomer) contribute in the undesired destruction of grafted functional groups or interrupt radical polymerization. Pre-irradiation grafting seems to be more appropriate for the preparation of efficient sorbents of the heavy/radioactive metal ions.

The grafted AAm layer reveals higher affinity towards sorption of trivalent europium ions than grafted NVP macromolecules. The following factors contribute in the observed effects: (i) the position of nitrogen atom in AAm molecule is more accessible, (ii) AAm is more hydrophilic than NVP thus stronger attracts polar species, and (iii) swelling of PA matrix by AAm solution is more efficient than by NVP solution, consequently penetration of ions in the former system is facilitated. Surface charge of the metal binding sites can be modified by changing the pH of the solution. The parameter influences also chemical form of solutes. Nevertheless, the fluctuations of pH in the narrow range of 4.9–5.3 are not supposed to influence the chemical form of europium ions as, according to the literature data reported by Sharma and Tomar [13], for pH between 4.5–5.5 the highest sorption capacity is expected.

It seems that the fraction of AAm in grafted layers is lower than that expected on a basis of AAc:AAm ratio in solution (ATR-FTIR measurements). On the other hand, addition of acrylamide intensifies significantly grafting efficiency of AAc (synergetic effect) and influences thermal characteristic of the grafted matrix measured by means of TGA and DSC methods. Graft copolymerization affects matrix crystallinity, particularly when AAm is used. This can be explained by effective chain transfer reactions during polymerization of AAm. The following factors determine sorption capacity: availability of heteroatoms contributed in the formation of complexes, hydrophilic properties of introduced functional groups and pH of feed solution. Only external layers of the grafted homopolymers (PAAc and PAAm) and copolymers (P(AAc + AAm)) contribute in sorption of radioactive europium ions. Depletion of the radionuclide from 10^{-7} mol dm^{-3} aqueous solution is above 93% for all prepared adsorbents. The final product can be exploited for the preconcentration and removal of cations including lanthanide from very dilute solutions as well as for the decontamination and treatment of radioactive waste water.

REFERENCES

[1] HEGAZY, E.A., ABD EL-REHIM, H.A., ALI, A.M.I, NOWIER, H.G., ALY, H.F., Characterization and application of radiation grafted membranes in treatment of intermediate active waste, Nucl. Instr. Meth. Phys. Res. B **15** (1999) 393-398.

[2] HEGAZY, E.A., KAMAL, H., MAZIAD, N., DESSOUKI, A.M., Membranes prepared by radiation grafting of binary monomers for adsorption of heavy metals from industrial wastes, Nucl. Instr. Meth. Phys. Res. B **151** (1999) 386-392.

[3] HEGAZY, E.A., ABDEL REHIM, A.H., KAMAL, H., KANDEEL, K.A., Advances in radiation grafting, Nucl. Instr. Meth. Phys. Res. B **185** (2001) 235-240.

[4] KALIYAPPAN, T., KANNAN, P., Co-ordination polymers, Prog. Polym. Sci. **25** (2000) 343-370.

[5] NASEFA, M.M., HEGAZY, E.A., Preparation and applications of ion exchange membranes by radiation-induced graft copolymerization of polar monomers onto non-polar films, Prog. Polym. Sci. **29** (2004) 499–561.

[6] CLOUGH, R.L., MALONE, G.M., GILLEN, T.K., WALLACE, J.S., SINCLAIR, M.B., Discoloration and subsequent recovery of optical polymers exposed to ionizing radiation, Polym. Degrad. Stabil. **49** (1995) 305-313.

[7] PRZYBYTNIAK, G., KORNACKA, E.M., MIRKOWSKI, K., WALO, M., ZIMEK, Z., Functionalization of polymer surfaces by radiation-induced grafting, Nukleonika **53** (2008) 89-95.

[8] PRZYBYTNIAK, G., KORNACKA, E., FUKS. L., Functionalization of polyamide surface by radiation-induced grafting of N-vinyl pyrrolidone and acrylamide, J. Polym. Res. (in press).

[9] SIMON, P., ROCKE, A., MAUER, AZORI, M., ESR study of irradiated nylon 6; conformational isomerism of free radicals, Eur. Polym. J. **13** (1997) 189-192.

[10] TAKIGAMI, S., MATSUMOTO, I., NAKAMURA, Y., Electron spin resonance study of γ-irradiated nylon 6, J. Appl. Polym. Sci. **26** (1981) 4317-4330.

[11] BAES JR, C.F., MESMER, R.E., The Hydrolysis of Cations, Wiley, New York (1976).

[12] RAMÍREZ-GARCÍA, J.J., SOLACHE-RÍOS, M., JIMÉNEZ-REYES, M., ROJAS-HERNÁNDEZ, A., Solubility and hydrolysis of La, Pr, Eu, Er, and Lu in 1 M NaCl ionic strength at 303 K, J. Solution Chem. **32** (2003) 879-895.

[13] SHARMA, P., TOMAR, R., Synthesis and application of an analogue of mesolite for the removal of uranium(VI), thorium(IV), and europium(III) from aqueous waste, Micropor. Mesopor. Mat. **116** (2008) 641–652.

[14] PATHAK, P.N., CHOPPIN, G.R., Sorption studies of europium(III) on hydrous silica, J.Radioanaly. Nucl. Chem. **270** 2 (2006) 277–283.

[15] BENEŠ, P., ŠTAMBERG, K., ŠIROKÝ, L., MIZERA, J., Radiotracer study of sorption of europium on Gorleben sand from aqueous solutions containing humic substances, J. Radioanal. Nucl. Chem. **254** 2 (2002) 231–239.

[16] AN, B-L., GONG, M-L., LI, M-X., ZHANG, J-M., CHENG, Z-X., Synthesis and luminescence of a novel conjugated europium complex with 6-aniline carbonyl 2-pyridine carboxylic acid, J. Fluoresc. **15** (2005) 613-617.

[17] LIU, Y., LIANG, B., XIAO, D., ZHUA, M., ZHUA, W., Synthesis and characteristics of a europium complex using pyridyl oxadiazole derivative as a secondary ligand, J. Alloy Compd. **469** (2009) 370–373.

RADIATION GRAFTED POLYMER MEMBRANES FOR FUEL CELL APPLICATIONS

G.G. SCHERER, F. WALLASCH, H. BEN YOUCEF, L. GUBLER

Electrochemistry Laboratory
Paul Scherrer Institut
CH-5232 Villigen
SWITZERLAND

Abstract

Partially fluorinated proton exchange membranes prepared via radiation induced graft copolymerization (‘radiation grafting’) offer the prospect of cost-effective and tailor made membrane electrolytes for the polymer electrolyte fuel cell (PEFC). The composition and structure of radiation grafted membranes can be adjusted in a broad range to balance the different requirements of proton transport and mechanical robustness. Based on the earlier work on Styrene grafting, the novel monomer combination α-methyl-styrene/methacrylonitrile (AMS/MAN) is introduced for improved stability in the prevailing fuel cell environment. Successful fuel cell experiments proved the concept.

1. OBJECTIVE OF THE RESEARCH

Fuel cells play an important role in the future energy conversion technology. For mobile applications polymer electrolyte fuel cells (PEFCs) are considered to be applied. PEFCs utilize a proton-conducting polymer membrane as solid electrolyte. The objective of the present work was to prepare partially fluorinated proton exchange membranes via radiation induced graft copolymerization in order to obtain cost-effective and tailor made membrane electrolytes for polymer electrolyte fuel cells (PEFC). A further objective was to achieve improved stability in the prevailing fuel cell environment by introducing novel monomer combination of α-methyl-styrene-methacrylonitrile (AMS/MAN).

2. INTRODUCTION

Fuel cells are efficient electrochemical energy converters and considered to play an important role as a future energy conversion technology. Among the various types of fuel cells, polymer electrolyte fuel cells (PEFCs) are considered to be applied for mobile applications. PEFCs utilize a proton-conducting polymer membrane as solid electrolyte. The polymer membrane has to fulfil three functions:

- Electrolyte, bulk and surface ionic/protonic conduction;
- Separator for the reactant gases H_2 and O_2;
- Part of the gasket design.

A scheme of a PEFC is displayed in Fig. 1.

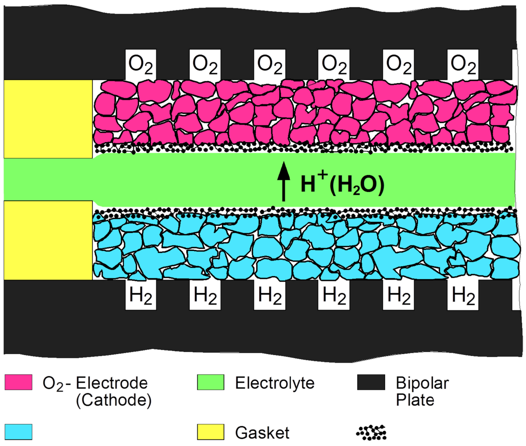

FIG. 1. Scheme of a polymer electrolyte fuel cell.

As a consequence, a multiple optimization of the membrane towards their necessary properties is required, as indicated in Fig. 2.

In addition to the optimization of the physico-chemical properties of the membrane, the cost issue is of paramount importance. Currently used membranes (Nafion® type) are by a factor of 100 and more away from the cost target set by the US DOE for fuel cell membranes for transportation applications (Fig. 3)

Radiation grafting and subsequent sulfonation offers the possibility to convert a base polymer film into a proton conducting membrane at potentially low cost [1, 2, 3, 4].

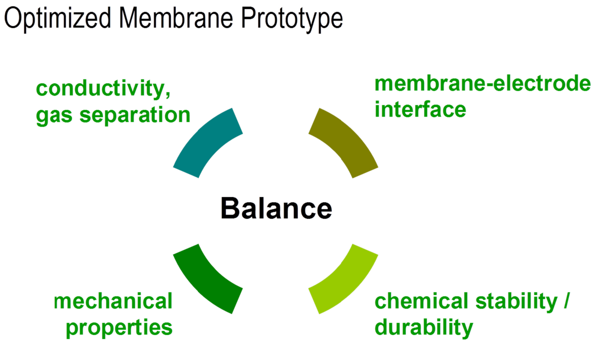

FIG. 2. Important membrane properties and their interaction for fuel cell application.

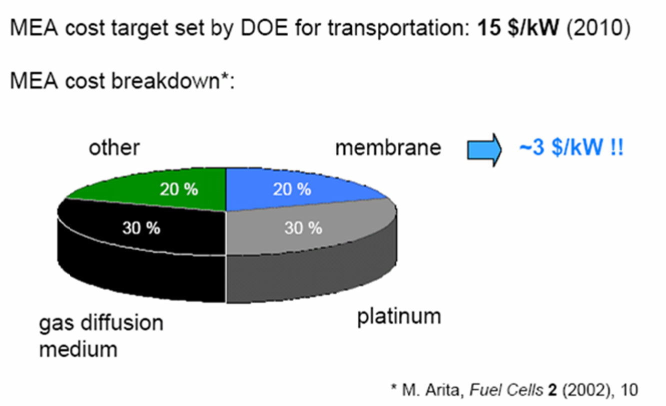

FIG 3. DOE cost target for the fuel cell membrane electrode assembly (MEA) for the year 2010.

3. PREPARATION OF RADIATION GRAFTED AND SULFONATED POLYMER MEMBRANES

3.1. Base polymer films

Base polymers utilized for the preparation of proton-conducting membranes are *commercial* films available in different thicknesses, e.g. 25 µm thick films of FEP or ETFE (supplier: DuPont, Nowofol, others). More recently, emphasis has been placed on ETFE as base material, due to its advantageous mechanical properties. Before irradiation and grafting, these films undergo a quality control process: control of thickness, crystallinity (DSC), etc. If necessary, all parameters have to be checked with reference to machining and transverse orientation and also to thickness.

Films are electron irradiated (1 MeV) in air prior to the grafting process and immediately stored at -80°C until their use as base polymer. It's important to point out that these films are commodities and their properties may change over time, due to undisclosed changes of the specifications by the supplier.

3.2. Monomers

Due to the importance of the cost issue, as indicated above, in the past styrene as the main graft component and divinyl benzene (DVB) as crosslinker have been employed in technical grade. In this contribution, the emphasis is placed on the monomer combination α-methyl-styrene/methacrylonitrile (AMS/MAN). In AMS, the α–hydrogen atom in styrene is substituted by a methyl group, hence avoiding the formation of resonance stabilized phenyl rings and thus decreasing chain scission of the polystyrene graft component. Further on, the grafting solution may contain non solvents, like water/alcohol mixtures. Grafting kinetics is investigated with respect to various grafting parameters like temperature, concentrations, time, etc. As a first indicator, the degree of grafting is used for further optimization.

3.3. Sulfonation

Sulfonation is carried out utilizing chlorosulfonic acid out to introduce proton conductivity. A defined protocol is applied afterwards to swell membranes in water to the required water content.

4. EX SITU CHARACTERIZATION

4.1. Pristine and grafted films and membranes

4.1.1. Mechanical properties

Mechanical properties in machining directions of pristine FEP- and ETFE films, 25 µm each, were characterized by stress-strain measurements under defined conditions in a climate chamber at a temperature of 25°C and a relative humidity at 35%. Young's modulus, tensile strength, and elongation at break are plotted in Fig. 4 for different irradiation doses for these two base polymers. As a result, it can clearly be seen that ETFE has favourable properties with respect to the requirements of the application. However, in view of the application as solid electrolyte particular attention has to be paid to minimize the necessary dose for grafting and, as a consequence, minimize degradation of mechanical properties [5, 6].

The mechanical properties in transverse direction display similar behaviour; however the absolute values are different.

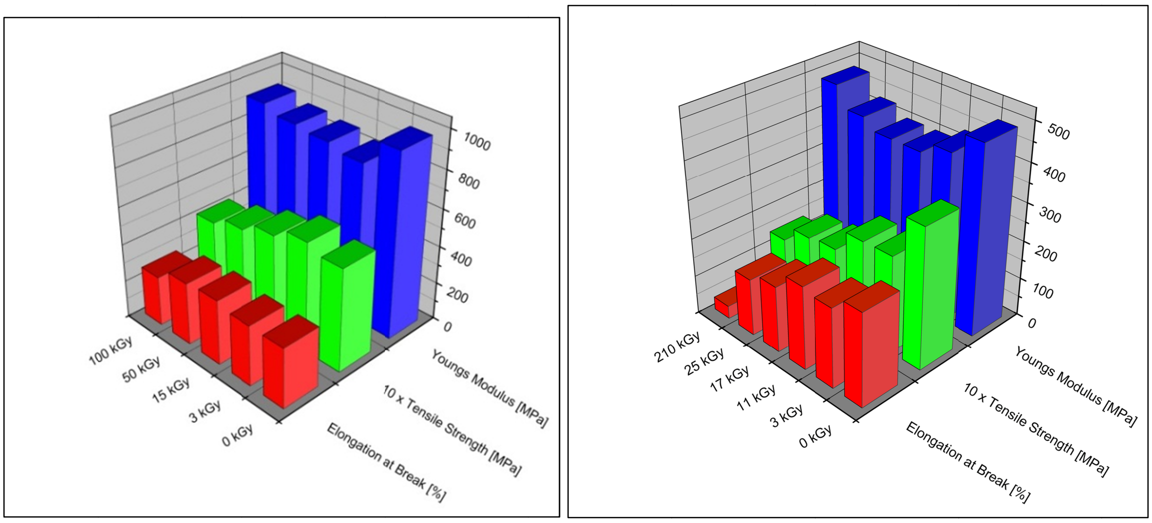

FIG. 4. Young's modulus, tensile strengths, and elongation at break measured for 25 µm thick FEP- (left) and ETFE films (right). Temperature 25 °C, relative humidity 35%.

4.1.2. Morphology

Comprehensive characterization of pristine, grafted films and membranes (stress strain, DSC, TGA, FTIR, FTIR ATR, SANS, others) is carried out to learn about mechanical, thermal, morphological, and other important properties and their changes due to the grafting process.

To substantiate the influence of the grafting and sulfonation process on the morphology of the semi-crystalline base polymer (FEP, ETFE), further characterization by SANS, DSC, etc. has been carried out recently [7, 8, 9, 10]. Essentially, these recent results give proof of the pictorial description, as displayed in Fig. 5. Grafting essentially takes place in the amorphous regions of the semi-crystalline polymer, while the crystalline phase remains more or less unaltered after grafting.

Small angle X Ray scattering (SAXS) was carried out on DIPB-crosslinked membranes (0–20% DIPB in grafting solution). The scattering patterns of dry and fully (100°C) hydrated membranes are displayed in Fig. 6 (left side).These patterns are anisotropic, due to scattering differences in machining (MD) and transverse (TD) direction. Differences also occur for dry and hydrated membranes. In combination with integral (volume) data of water uptake and specific conductivity, the morphology was reconstructed as a function of water content (right side).

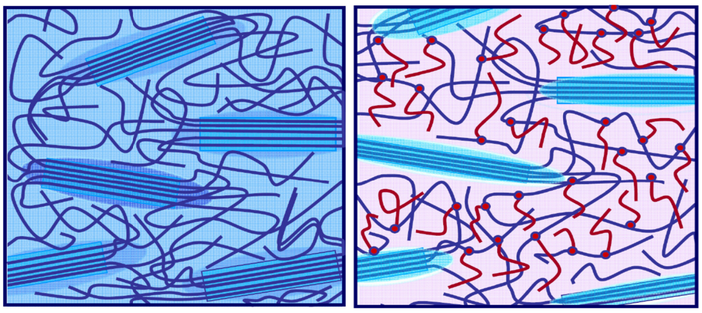

a) FEP b) FEP-*g*-PS

FIG. 5. Scheme of morphology (crystallinity vs. amorphous phase) for pristine FEP and FEP grafted polystyrene films as deduced from DSC and SANS measurements.

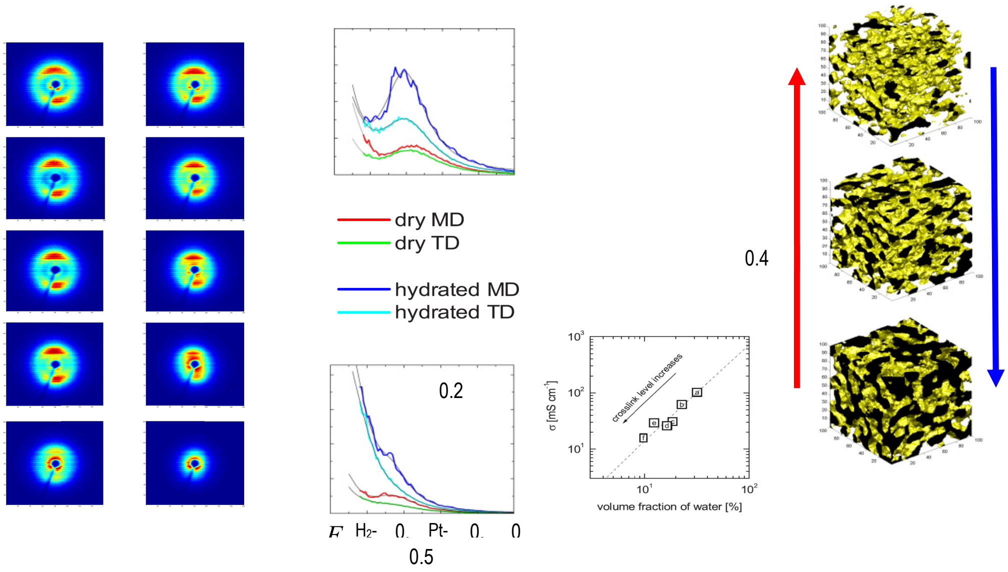

FIG. 6. Small angle X ray scattering of DIPB crosslinked (0–20%) dry and water-swollen membranes. Reconstruction of morphology.

4.1.2. Grafting kinetics

The kinetics of the grafting process has been followed by confocal Raman microscopy. For MAN grafting only, a clear front mechanism has been observed (Fig. 7, left). [11, 12]. Based on these experimental results, a model can be developed, which allows describing the grafting kinetics [13].

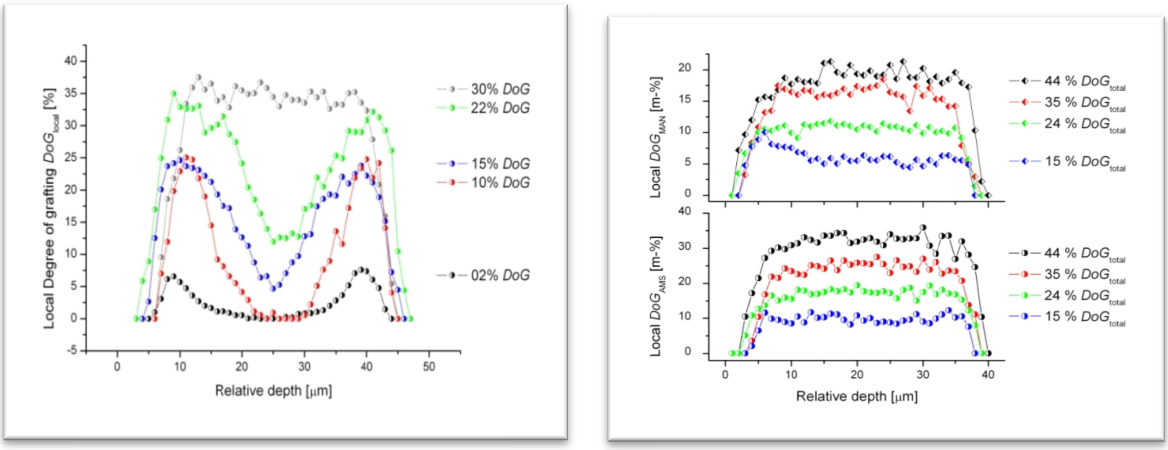

FIG. 7. Local degree of grafting of p-MAN over film thickness for different degrees of grafting (left) and grafting of p-co-AMS-MAN (right), as characterized by locally resolved Raman microscopy.

Co–grafting of MAN and AMS renders drastically the graft component distribution over the film thickness. Due to the slow grafting kinetics of AMS, the grafting front mechanism no longer prevails and a homogeneous distribution of both components is detected by confocal Raman spectroscopy in the investigated range of degree of grafting (Fig. 7, left).

From these measurements, the molar fraction of AMS in the grafted films was determined as a function of the molar fraction in the grafting solution (Fig. 8). The respective grafting conditions were: temperature 50°C, monomer concentration 30 v %, solvent isopropanol/water.

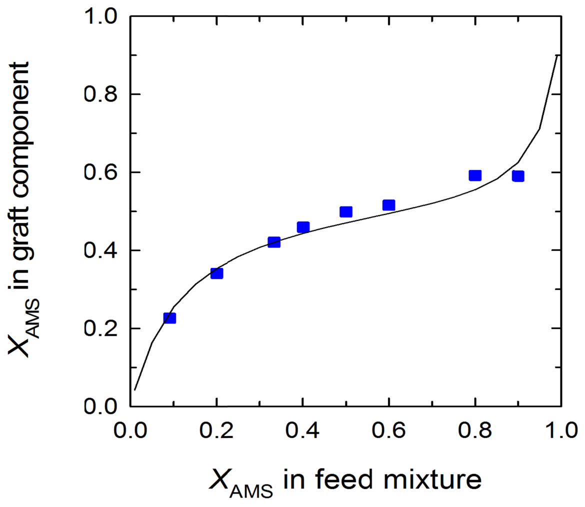

FIG. 8. Molar fraction of AMS in graft component as a function of molar fraction in feed mixture (graft solution). (Preparation conditions see text.)

Reaction rates for the copolymerization of AMS and MAN were evaluated from this data. The values determined are $r_{\mathrm{AMS}} = 0.08 \pm 0.02$ and $r_{\mathrm{MAN}} = 0.22 \pm 0.03$, which compare favourably with values from solution polymerization, $r_{\mathrm{AMS}} = 0.06$ and $r_{\mathrm{MAN}} = 0.28$. Hence, the probability of an alternating AMS–MAN chain is concluded.

5. IN SITU CHARACTERIZATION

5.1. Performance and longevity

Membranes are characterized in fuel cells under defined standard conditions for their performance (power output) and longevity [14, 15, 16, 17, 18]. Results of the fuel cell performance of uncrosslinked AMS/MAN grafted membranes with different $R_{m,sol}$ (ratio of AMS versus MAN in the grafting solution) are depicted in Fig. 9. It can be concluded from these results that membranes with high R_m yield the best performance, due to their higher conductivity, respectively higher p-AMS content.

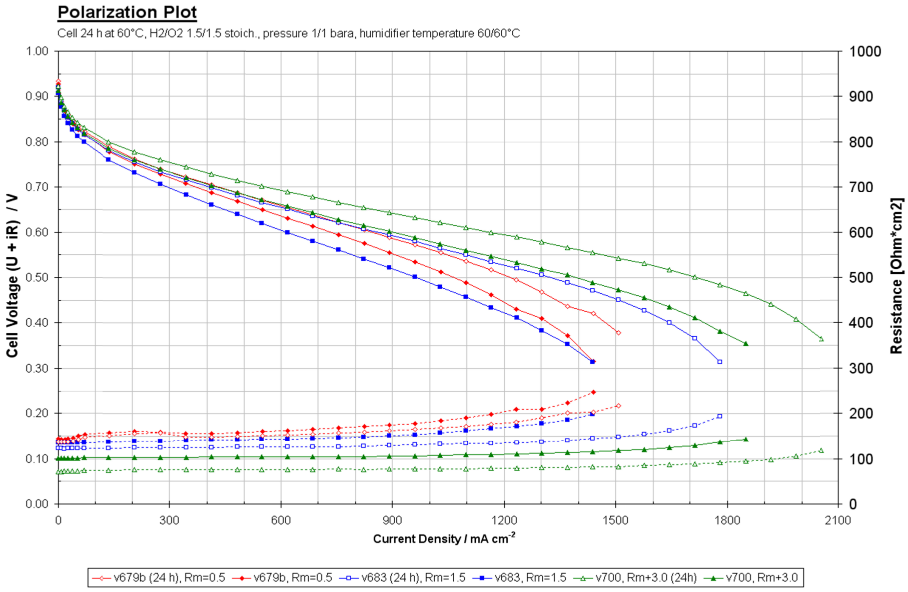

FIG. 9. Comparison of fuel cell current-voltage curves for AMS/MAN grafted membranes as solid electrolyte. Fuel cells were operated in H_2/O_2 and H_2/Air mode at 60°C.

Under a steady state protocol (constant current density of 500 mA/cm^2) lifetimes in the order of at least 1000 h could be demonstrated in laboratory size fuel cells (30 cm^2) for these *uncrosslinked* membrane materials [10]. These first successful fuel cell experiments give proof of the concept to substitute styrene as a monomer, prone to α–H abstraction, by the low cost monomer α–methylstyrene as species to be sulfonated.

As a next step, x-linking was introduced into AMS/MAN grafted films and membranes and their *ex situ* and *in situ* properties were optimized with respect to fuel cell performance.

In Figure 10 more recent fuel cell testing results are displayed for three membranes: The commercial standard membrane Nafion® 212, a styrene:DVB grafted membrane (DoG ~25%) (Generation 1), and an AMS:MAN:DVB grafted membrane (DoG ~40%) (Generation 2), both grafted onto a 25 µm thick ETFE film. The Gen 1 membrane displayed an ion exchange capacity of 1.7 meq/g and a specific conductivity of 62 mS/cm (RT). The respective values for the Gen 2 membrane were 1.7 meq/g and 64 mS/cm, respectively. The fuel cell test conditions were as follows: H_2/O_2 fully humidified, stoichiometries 2/2, ambient pressure, 80°C. The differences in voltage values at constant current densities are mainly due to the differences *in situ* Ohmic resistance, as indicated by the overlap for the iR-corrected current density-voltage curves for all three tested membranes.

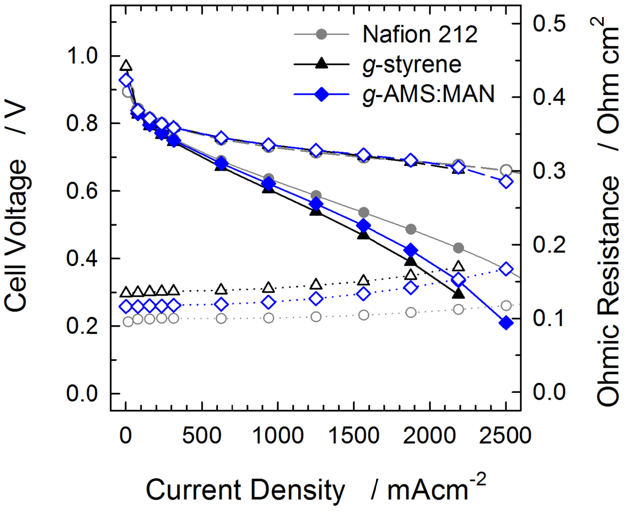

FIG. 10. Current density–voltage and current density–Ohmic resistance curves for cells with three different membranes. Test conditions: 80°C, H_2/O_2 fully humidified, stoichiometry 2/2, ambient pressure.

In situ degradation studies of Gen 1 and Gen 2 membranes, un-crosslinked and crosslinked show distinct differences in IEC-loss after defined testing times (please observe logarithmic scale of IEC-Loss). DVB-crosslinking of Gen 1 membranes improves dramatically stability under fuel cell conditions (see conditions mentioned in Fig. 10), typically by more than a factor of 100 compared to un-crosslinked ones.

The concept to substitute the α–hydrogen atom in polystyrene could be proven to be very effective by decreasing IEC-loss by a factor of approximately 30. A further decrease can be observed for crosslinking these Gen 2 membranes, which are currently not fully optimized. Hence, a further improvement can be expected, even under non-steady state testing conditions, resembling closer the duty cycle of automotive application.

Fuel cell testing under OCV-hold conditions at higher pressure is one of the most severe conditions for the membrane. Membrane stability was detected by following the membrane resistance over time. Again, the higher stability of the Gen 2 membrane is displayed. The increase in Ohmic resistance indicates loss of the grafted component, including the ion-containing group responsible for proton-conduction.

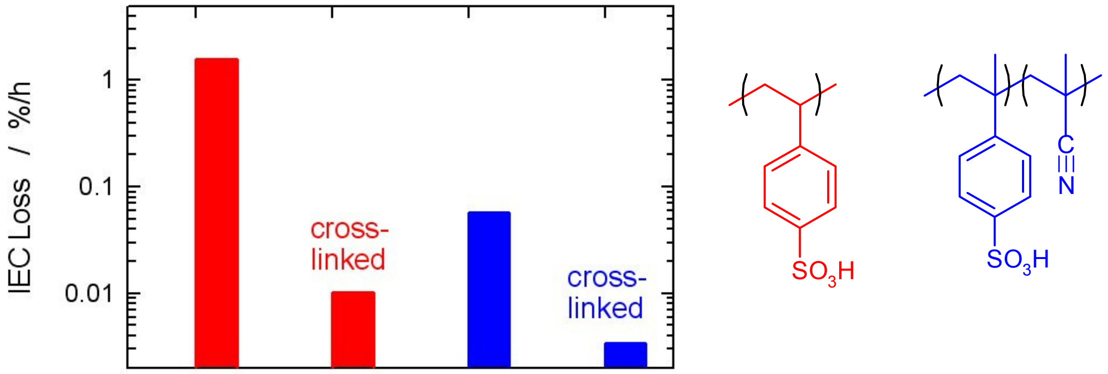

FIG. 11. Ion Exchange capacity (IEC) loss in %/h for Gen 1 (styrene and styrene/DVB) and Gen 2 (AMS/MAN and AMS/MAN/DVB) membranes under typical fuel cell conditions: 80 °C, H_2/O_2, OCV, 100% r.h., 3bar$_a$

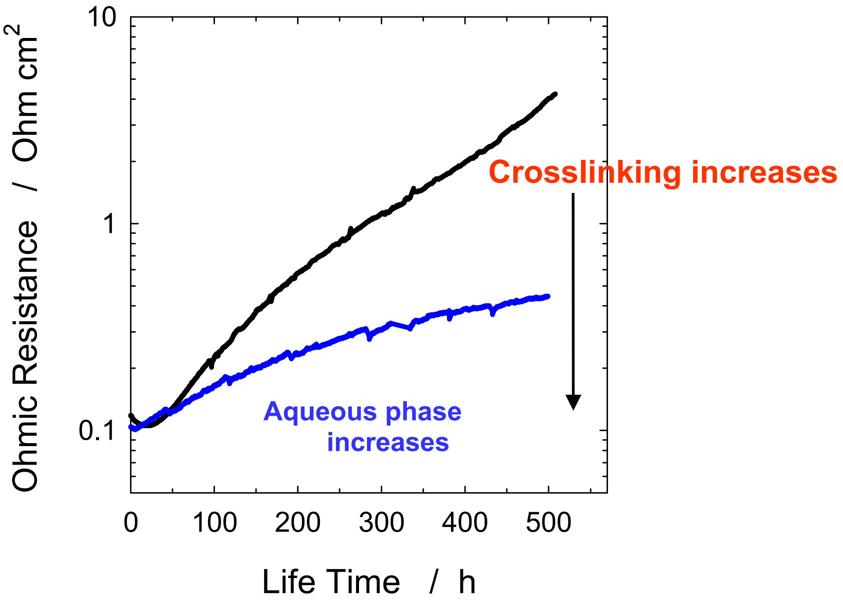

FIG. 12. Ohmic resistance development over life time for OCV hold test of Gen 1 and Gen 2 membranes, based on 25 μm thick ETFE-films.

6. CONCLUSIONS

Several fundamental aspects of synthesis, characterization, and fuel cell testing of radiation grafted membranes have been addressed. Progress in terms of stability under fuel cell operating conditions has been achieved in moving from Gen 1 to Gen 2 membranes. Crosslinking is important for both generations of membranes, indicating the importance of water uptake respectively gas cross-over for the longevity of membrane properties under in situ conditions.

REFERENCES

[1] GUBLER, L., SCHERER, G.G., “Radiation-grafted proton conducting membranes” in Handbook of Fuel Cells: Advances in Electrocatalysis, Materials, Diagnostics and Durability, Volumes 5&6, W. Vielstich, H.A. Gasteiger, H. Yokokawa (Editors), John Wiley & Sons Ltd, Chichester, United Kingdom, 313–321 (2009).

[2] ALKAN-GÜRSEL, S., GUBLER, L., GUPTA, B., SCHERER, G.G., Radiation grafted membranes, Adv. Polym. Sci. **215** (2008) 157–217.

[3] GUBLER, L., SCHERER, G.G., “Durability of radiation-grafted fuel cell membranes” in: F.N. Büchi, M. Inaba, T.S. Schmidt (eds.), Polymer Electrolyte Fuel Cell Durability, , Springer Science + Business Media, LLC, 133–155 (2009).

[4] GUBLER, L., SCHERER, G.G., Trends for fuel cell membrane development, Desalination **250** (2010) 1034–1037.

[5] BEN YOUCEF, H., ALKAN GÜRSEL, S., WOKAUN, A., SCHERER G.G., The influence of crosslinker on the properties of radiation-grafted films and membranes based on ETFE, J. Membr. Sci. **311** (2008) 208–215.

[6] BEN YOUCEF, H., ALKAN GÜRSEL, S., BUISSON, A., GUBLER, L., WOKAUN, A., SCHERER G.G., Influence of radiation-induced grafting process on mechanical properties of ETFE-based membranes for fuel cells, Fuel Cells **10** (2010) 401–410.

[7] ALKAN GÜRSEL, S., SCHNEIDER, J., BEN YOUCEF, H., WOKAUN, A., SCHERER, G.G., Thermal properties of proton-conducting radiation grafted membranes, J. Appl. Polym. Sci. **108** (2008) 3577–3585.

[8] MORTENSEN, K., GASSER, U., ALKAN GÜRSEL, S., SCHERER, G.G., Structural characterization of radiation-grafted block copolymer films using SANS technique, J. Polym.

Sci.: Part B: Polym. Phys. **46** (2008) 1660–1668.

[9] BALOG, S., GASSER, U., MORTENSEN, K., GUBLER, L., BEN YOUCEF, H., SCHERER, G.G., Correlation between morphology, water uptake, and proton conductivity in radiation-grafted proton-exchange membranes, Macromol. Chem. Phys. **211** (2010) 635–643.

[10] BALOG, S., GASSER, U., MORTENSEN, K., BEN YOUCEF, H., GUBLER, L., SCHERER, G.G., Nano-scale morphology in graft copolymer ion-exchange membranes cross-linked with DIPB, J. Membr. Sci. (submitted).

[11] WALLASCH, F., ABELE, M., GUBLER, L., WOKAUN, A., MÜLLER, K., SCHERER, G.G., Characterization of radiation grafted polymer films using CP/MAS NMR spectroscopy and confocal Raman microscopy, PCP, (submitted).

[12] WALLASCH, F., Dissertation ETH Zürich (2010).

[13] GUBLER, L., WALLASCH, F., WOKAUN, A., SCHERER, G.G., “An enhanced radiation grafting model comprising monomer transport”, (PSI Electrochemistry Laboratory - Annual Report 2008) ISSN **6** (2008) 1661–5379.

[14] GUBLER, L., BEN YOUCEF, H., ALKAN GÜRSEL, S., WOKAUN, A., SCHERER, G.G., Cross-linker effect in ETFE-based radiation-grafted proton-conducting membranes. I. Properties and fuel cell performance characteristics, J. Electrochem. Soc. **155** (2008) 9 B921–B928.

[15] BEN YOUCEF, H., GUBLER, L., YAMAKI, T., SAWADA, S.-I., ALKAN GÜRSEL, S., WOKAUN, A., SCHERER, G.G., Cross-linker effect in ETFE-based radiation-grafted proton-conducting membranes. II. Extended fuel cell operation and degradation analysis, Electrochem. Soc. **156** (2009) 4 B532–B539.

[16] BEN YOUCEF, H., ALKAN GÜRSEL, S., WOKAUN, A., SCHERER, G.G., The influence of crosslinker on the properties of radiation-grafted films and membranes based on ETFE, J. Membr. Sci. **311** (2008) 208–215.

[17] BEN YOUCEF, H., GUBLER, L., ALKAN GÜRSEL, S., HENKENSMEIER, D., WOKAUN, A., SCHERER, G.G., Novel ETFE based radiation grafted poly(styrene sulfonic acid-co methacrylonitrile) proton conducting membranes with increased stability, Electrochem. Commun. **11** (2009) 941–944.

RADIATION INDUCED PREPARATION OF POLYMER MEMBRANES GRAFTED WITH BASIC AND ACIDIC MONOMERS FOR APPLICATION IN WASTEWATER TREATMENT

Z. AJJI

Polymer Technology Division, Radiation Technology Department,
Atomic Energy Commission of Syria (AECS)
17th Nissan Street, Kafar Sousah, Damascus
SYRIAN ARAB REPUBLIC

Abstract

Polymer membranes (PP and PE) had been grafted with basic and acidic functional groups using gamma radiation. Two binary mixtures had been used for the grafting reactions: acrylic acid/N-vinyl pyrrolidone, and acrylic acid/N-vinyl imidazole. The influence of different reaction parameters on the grafting yield had been investigated as: type of solvent and solvent composition, comonomer concentration and composition, addition of inhibitors, and dose. Water uptake with respect to the grafting yield had also been evaluated. The ability of PP films, grafted with acrylic acid/ vinyl pyrrolidone, to uptake heavy metal ions such as Hg^{2+}, Pb^{2+}, Cd^{2+}, Co^{2+}, Ni^{2+} and Cu^{2+} was elaborated. The uptake of the metal ions increases with increasing the grafting yield. Furthermore, the Pb^{+2} uptake was much higher than the uptake of the Hg^{2+} and Cd^{2+} ions. The membranes may be considered for the separation of Pb^{2+} ions from Hg^{2+} or Cd^{2+} ions. Also the ability of PE films, grafted with acrylic acid/ N-vinyl imidazole to uptake heavy metal ions such as Pb^{2+}, Cd^{2+}, Co^{2+} and Ni^{2+} was elaborated. An increase in the uptake of the metal ions was observed as the grafting yield increased.

1. OBJECTIVE OF THE RESEARCH

The Syrian contribution in the CRP project is a part of national project concerning the preparation of polymeric membranes for different applications, which are grafted with basic and acidic functional groups using gamma radiation. The present project was intended to prepare polyethylene and polypropylene membranes grafted with two binary mixtures of acrycilic acid/N-vinyl pyrrolidone, and acrylic acid/N-vinyl imidazole using gamma radiation. The factors affecting the grafting process and the possible use of the modified membranes in the field of ion adsorption have been investigated.

2. INTRODUCTION

The effective treatment of heavy metals in the environment has become one the major issues of public interest due to their toxicity. The treatment of aqueous waste, including soluble heavy metals, needs concentration of the metallic solution into small volume, followed by recovery or secure disposal. The modification of hydrophilic polymer membranes to an adsorbent has been reported to be useful for collecting target ions and molecules [1].

Gamma radiation induced graft copolymerization of vinyl monomers onto different substrates has attracted the interest of many researchers since different types of polymer chains containing various functional groups can be introduced in the structure of trunk polymers used. The conditions of grafting reactions can be manipulated and graft copolymer with desired properties may be obtained; extensive work has already been performed on methods for optimization of the reaction yield [2–3]. The use of a mixture of monomers may also influence the extent of grafting of the individual monomer onto the substrate polymers, especially when of synergism occurs during such reaction [4]. Such grafting reactions can also give more economical grafts under the most favourable reaction conditions [5].

The goal of the present project was the preparation of polymeric membranes grafted with basic and acidic functional groups using gamma radiation. The factors affecting the grafting process and the possible use of the modified membranes in the field of ion adsorption.

3. MATERIALS AND METHODS

3.1. Materials

Polypropylene (PP) films (thickness: 20 μm) were supplied by the company ERGIS S.A., Poland. Polyethylene films (thickness 100 μm) were obtained from the company PKN Orlen S. A., Poland. Various chemicals were supplied by Merck, Germany as: N-vinyl pyrrolidone (purity > 99%), methanol (purity > 99.8), acetone (purity > 99.8). N-vinyl imidazole (purity > 99%) and acrylic acid (purity > 99%), were purchased from Fluka, Germany. Ethanol was obtained from Riedel de Haën, Germany (purity 99.8%).

3.2. Graft copolymerization

The direct radiation-induced grafting of acrylic acid and N-vinyl pyrrolidone or acrylic acid/ N-vinyl imidazole monomers onto PP and PE films was used as a preparation technique in an air atmosphere. PP or PE strips were washed with acetone, dried at 50°C, weighed and then immersed in the monomer or binary monomer solution in glass ampoules. The glass ampoules containing all the reactants and polymer substrates were subjected to ^{60}Co gamma rays in N_2 gas atmosphere. The grafted films were removed and washed thoroughly with suitable solvent to extract the residual monomer or homopolymer may be accumulated in the grafted films. The films were then dried in an oven at 50°C. The degree of grafting was determined by the percent increase in weight as follow:

$$\text{Degree of Grafting}\,\% = \frac{W_g - W_o}{W_o} \times 100$$

where W_o and W_g are the weights of initial and grafted films, respectively.

3.3. Maximum swelling

The clean dried grafted films of known weight (after the washing procedure mentioned above) were immersed in distilled water until a constant weight was reached (equilibrium swelling); the films were then removed, blotted quickly with absorbent paper and weighed. The maximum swelling (S_{max}%) was then calculated by the following equation:

$$S_{\max}\,\% = \frac{W_S - W_o}{W_o} \times 100$$

where W_S is the weight of membrane at equilibrium, and W_o is the weight of dried membrane.

3.4. Ion uptake

The dry membranes were immersed in the metal feed solution of concentration 2000 ppm. An atomic absorption instrument (Avanta; GBC scientific equipment) was utilized to determine the remaining metal salt in their feed solutions using lamps for Pb, Cd, and Hg. The ion uptake was calculated according to the following equation:

$$\text{Metal ion uptake} = \frac{\text{uptaken metal ions (mg)}}{\text{weight of the dry gel (g)}}$$

3.5. Mechanical measurements

The tensile strength was determined using an Instron instrument Model 1011; for each point, the average of five specimens was calculated.

4. RESULTS AND DISCUSSION

4. 1. Grafting of polypropylene and polyethylene with N-vinyl pyrrolidone and acrylic acid

4.1.1. Effect of inhibitor concentration

Addition of inhibitors to grafting solutions is an essential step towards overcoming the problem of homopolymerization, which affects the grafting reactions and the degree of grafting in membranes. The suppression of homopolymer formation is of utmost importance when reactive monomers such as acrylic acid and methacrylic acid are grafted [6–9].

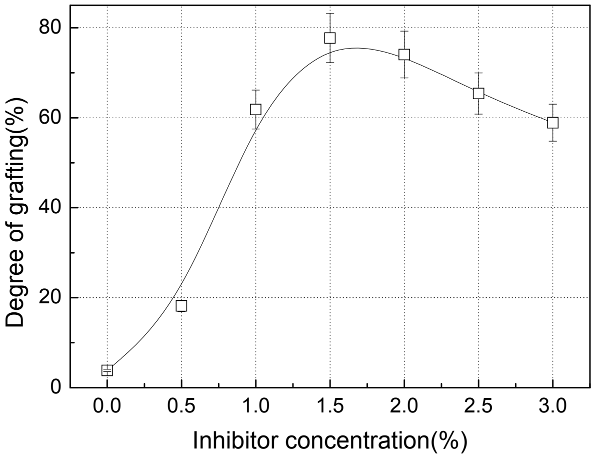

FIG. 1. Grafting yield on PP with respect to the inhibitor concentration in aqueous solution; dose = 25 kGy; monomer concentration = 20%; comonomer composition (AAc:VP = 3:1).

The influence of inhibitor concentration on the grafting yield of AAc/VP onto PP and PE was investigated, and the results are represented in Figs 1 and 2 (dose = 25 kGy; AAc:VP = 3:1; monomer concentration = 20%). The data show that the grafting yield increases in presence of the inhibitor ($FeCl_3$) achieving the highest value at an inhibitor concentration of 1.5%. Thereafter, the grafting yield decreases with increasing the concentration of the inhibitor.

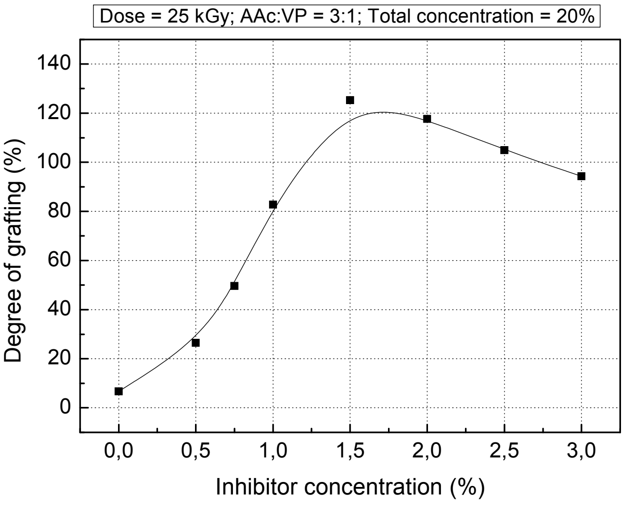

FIG. 2. Effect of inhibitor concentration ($FeCl_3$) on the grafting yield of AAc/VP onto PE, comonomer composition: 3/1: AAc/VP; dose = 25 kGy; comonomer concentration = 20wt%.

4.1.2. Effect of comonomer composition

The synergistic effect of two monomers may lead to more efficient grafting processes [4]. Therefore, the influence of the comonomer composition on the grafting process has been studied. The grafting yield of AAc/VP binary monomer systems of various relative compositions was determined with respect to the comonomer composition (inhibitor = 1.5%; dose = 25 kGy; comonomer concentration = 20wt% in water), and the obtained data are represented in Fig. 3 and 4. It is obvious that the grafting yield increases with increasing the content of AAc in comonomer solution to reach a maximum grafting yield at an AAc/VP composition of 75/25 mol/mol in the presence of both monomers in the feed solution. The grafting of pure AAc onto PP was higher than that of the comonomer.

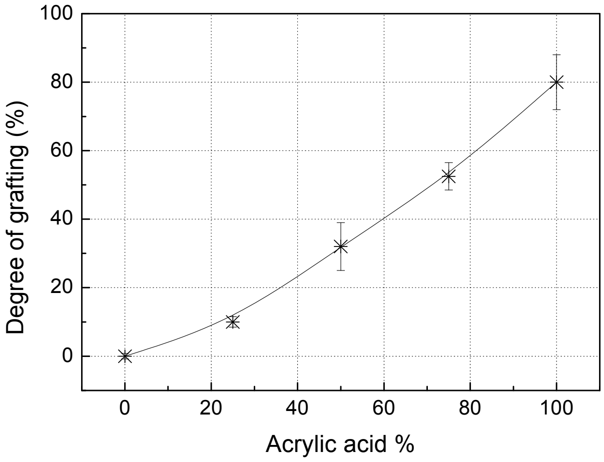

FIG. 3. Grafting yield with respect to the comonomer composition (VP:AAc); dose = 25 kGy; monomer concentration = 20%; inhibitor concentration $FeCl_3$ = 1.5% ; solvent is water.

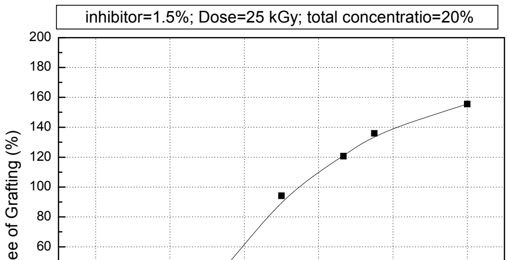

FIG. 4. Degree of grafting onto PE films vs. AAc/VP comonomer composition; comonomer concentration = 20%; inhibitor concentration ($FeCl_3$) = 1.5%; dose = 25 kGy.

4.1.3. Effect of comonomer concentration

The concentration of the monomer to be grafted has a significant role to play during membrane preparation by radiation-induced graft copolymerization method. The content of the monomer in the bulk solution strongly affects its diffusivity to the grafting zone and consequently the rate as well as the final degree of grafting varies [10]. The comonomer concentration during radiation grafting may affect the kinetic parameters of this process. Therefore, the suitable comonomer concentration differs from system to another, depending on the diluent used, type of polymer support materials, comonomer composition, irradiation dose and dose rate etc. The effect of dilution of AAc/VP binary monomers mixture at a comonomer composition (3/1, mol/mol) on the graft copolymerization onto PP and PE is investigated and the results are represented in Figs 5 and 6. It can be seen that the degree of grafting increases with increasing the comonomer concentration in the reaction medium. The high concentration of free radicals at grafting sites favours propagation of growing chains and consequently, the grafting yield increases [5].

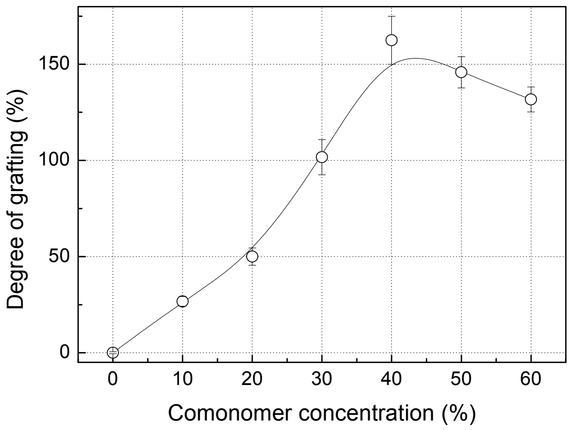

FIG. 5. Grafting yield on PP vs. comonomer concentration (VP: AAc); dose = 25 kGy; inhibitor $FeCl_3$ = 1.5%; comonomer composition (VP: AAc =1:3); solvent is water.

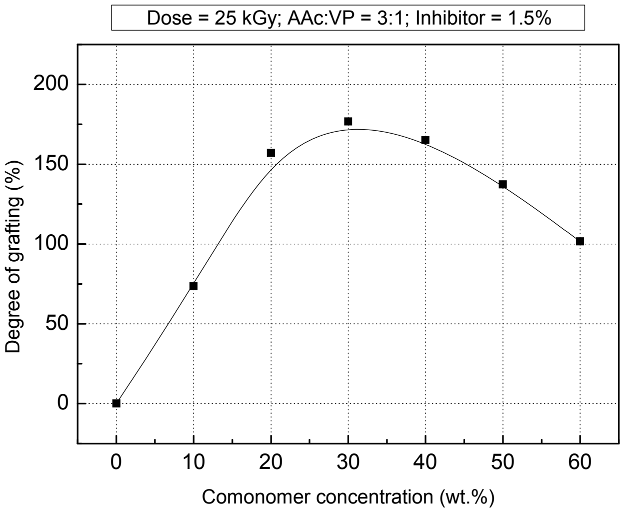

FIG. 6. Grafting yield of AAc/VP on PE films vs. comonomer concentration on; comonomer composition of 3/1: AAc/VP; dose = 25 kGy; inhibitor concentration = 1.5%.

4.1.4. Effect of absorbed dose

The influence of absorbed dose, on the grafting yield of AAc/VP binary monomers onto PP and PE films is investigated, and the results are illustrated in Figs 7 and 8. It can be seen that the grafting yield becomes higher as the absorbed dose increases. From results, it can be assumed that the increase in exposure dose resulted in increasing the concentration of free radicals formed in the polymer substrate as well as in the AAc/VP comonomer.

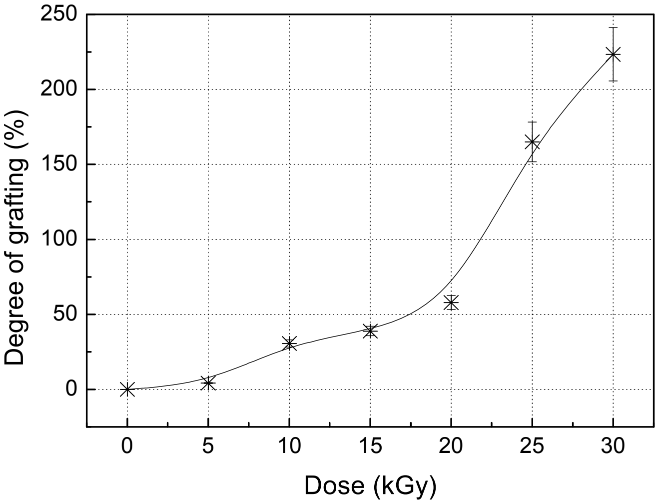

FIG. 7. Grafting yield on PP with respect to dose; $FeCl_3$ = 1.5%; comonomer composition (VP: AAc =1:3); monomer concentration (VP: AAc) = 40%; solvent is water.

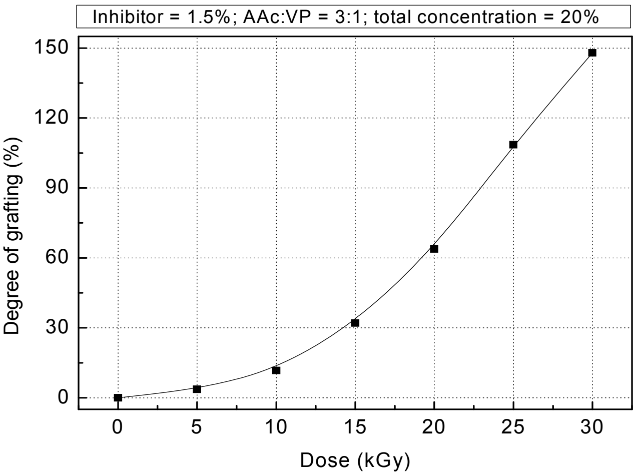

FIG. 8. Effect of absorbed dose on the degree of grafting of AAc/VP onto PE films; comonomer composition of 3/1: AAc/VP; $FeCl_3$ = 1.5%; comonomer conc. = 30wt%.

4.1.5. Swelling behaviour

Figures 9 and 10 show the water uptake percent for the untreated PP-g-AAc/VP and PE-g-AAc/VP grafted membranes, and also for membranes treated with NaOH. It can be seen that the water uptake increases with increased grafting yield, which could be explained with higher content of hydrophilic groups in the graft copolymer. It can also be seen that the chemically treated grafted copolymers possessed higher water uptake compared with untreated membranes. This behaviour could be due to the formation of easily ionizable carboxylate groups, which have good hydrophilic properties. Such hydrophilic grafted material may be of interest for the use as biomaterial.

4.1.6. FTIR spectroscopy

Figures 11 and 12 show FTIR spectra of the PP, PP-g-AAc/VP, PE, PE-g-AAc/VP films. It can be seen according to the presence of the carbonyl bands that both monomers are grafted onto the polymer substrates. The carbonyl bands centred at around 1720 cm^{-1} can be assigned to the carboxylic acid. The bands centred around 1549 cm^{-1} can be assigned to vinyl pyrrolidone.

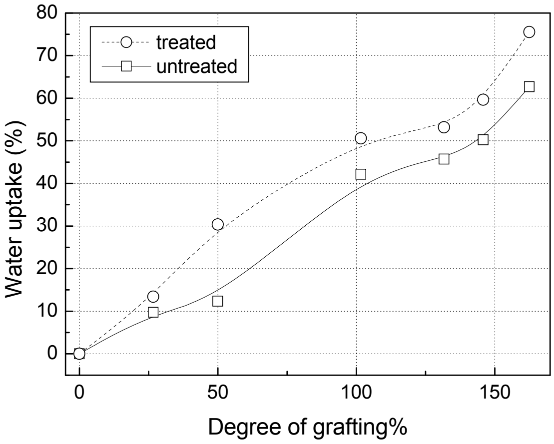

FIG. 9. Water uptake versus grafting yield of AAc/VP onto PP films; comonomer composition of 3/1: AAc/VP; inhibitor concentration = 1.5%; comonomer concentration = 40 wt%.

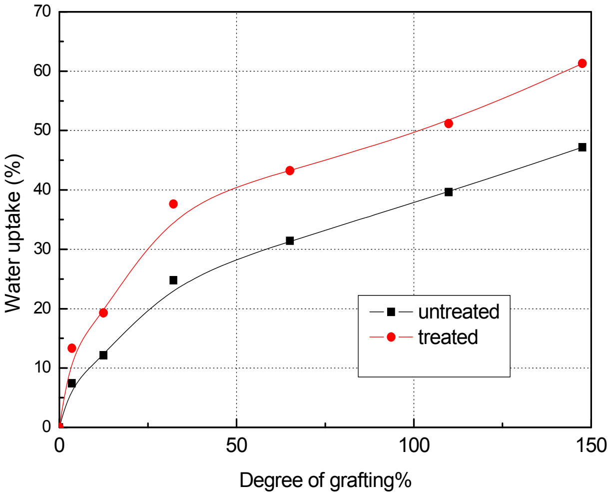

FIG. 10. Water uptake vs. grafting yield of AAc/VP onto PE films; comonomer composition of 3/1: (AAc/VP); inhibitor concentration = 1.5 %; comonomer concentration = 30 wt%.

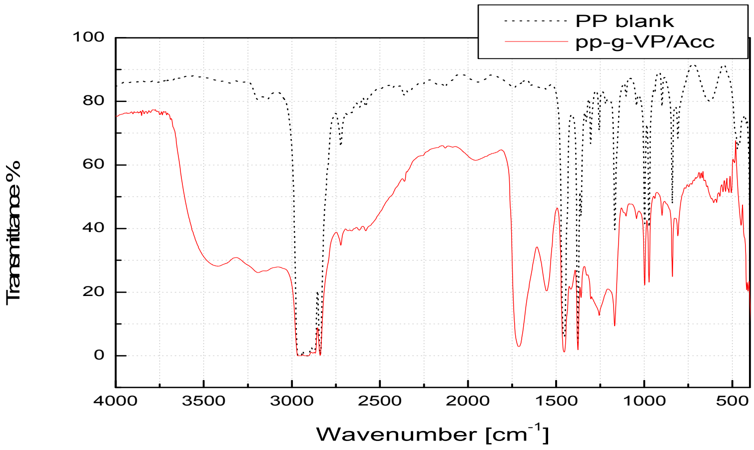

FIG. 11. Spectra of the original PP and PP-g-AAc/VP films.

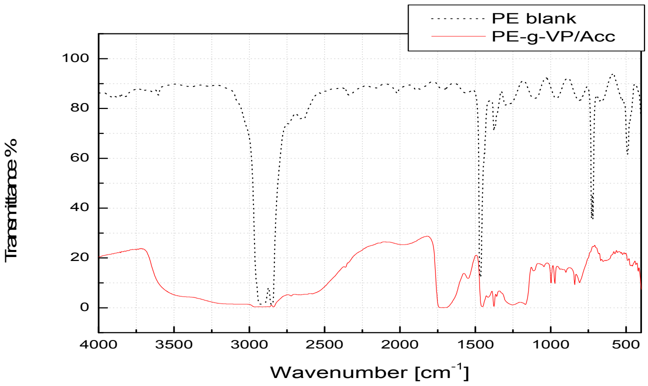

FIG. 12. FTIR spectra of PE and PE-g-AAc/VP films.

4.1.7. Mechanical properties

Figure 13 represents the stresses at break of the PE-g-AAc/VP films versus the grafting yield; the preparation conditions were as follows: inhibitor concentration ($FeCl_3$) = 1.5%; comonomer composition of 3/1: (AAc/VP); dose = 25 kGy; comonomer conc. = 30 wt%. The stress at break rises with increasing grafting yield due to the increase of the crosslink density.

The strain % is illustrated in Fig. 14 with respect to degree of grafting %. It can be seen that the strain % decreases significantly as the grafting yield increases, which can be explained with an increase of the cross-link density due to irradiation as mentioned above.

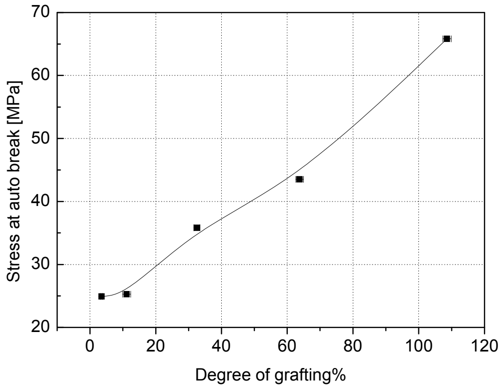

FIG. 13. Stress at auto break with respect to degree of grafting; $FeCl_3$ = 1.5%; comonomer composition 3/1: (AAc/VP); 25 kGy; comonomer concentration = 30 wt%.

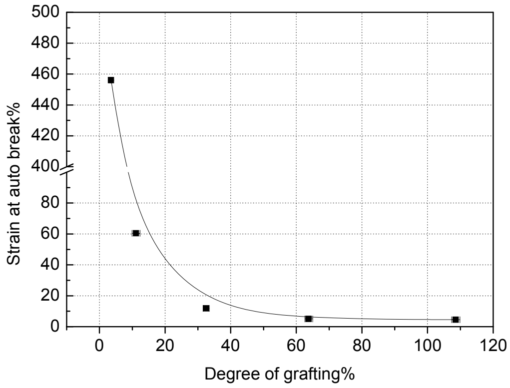

FIG. 14. Strain at auto break with respect to degree of grafting; $FeCl_3$ = 1.5%; comonomer composition 3/1: AAc/VP; dose = 25 kGy; concentration wt% = 30%.

4.1.8. Ion uptake

The ion uptake of PP-g-VP/AAc membranes versus the degree of grafting is represented in Fig. 15 and 16. As the degree of grafting increases, the ion uptake of the membrane increases. This behaviour can be reasonably attributed to the increase in the number of functional groups (carboxylic and amide groups) grafted onto the polymer backbone in the membrane with the increase in the degree of grafting. It is also observed that the efficiency of PP-g-VP/AAc membrane having degree of grafting 166.7% is very high, and the amount of recovered Pb^{2+} ions attained is about 749.5 mg/g. This result can be explained with the availability of different functional groups, which can interact with lead ions in various ways forming ionic bonds (carboxyl group) or/ and complex bonds (hydroxyl or N-amide group).

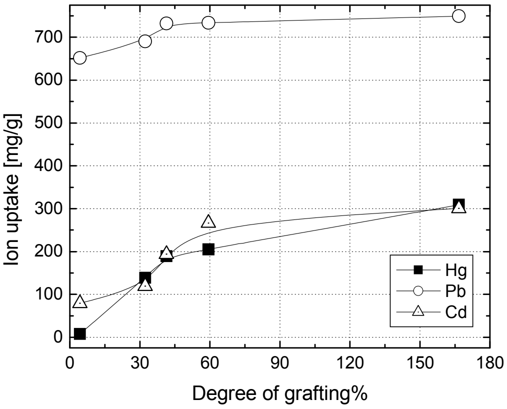

FIG. 15. Uptake of Hg^{2+}, Pb^{2+} and Cd^{2+} ions versus grafting yield of PP-g-AAc/VP; initial feed concentration = 2000 ppm; time = several days; temperature = 22℃.

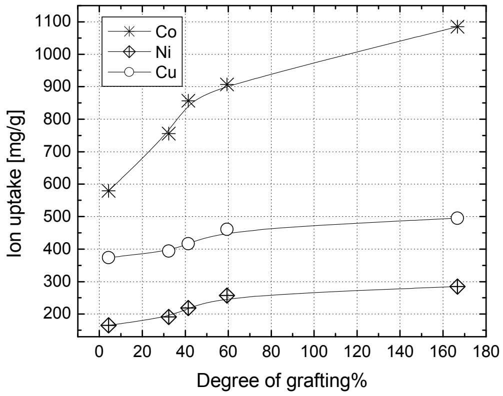

FIG. 16. Uptake of Co^{2+}, Ni^{2+} and Cu^{2+} ions versus the grafting yield of PP-g-AAc/VP; initial feed concentration = 2000 ppm; time = several days; temperature = 22℃.

4.2. Grafting of polypropylene and polyethylene with N-vinyl imidazole and acrylic acid

4.2.1. Effect of solvent Type

Solvents play an important role in enhancing the grafting process of a monomer onto a trunk polymer. The solvent may influence the grafting process by diluting the monomer, thus reducing the rate of propagation and kinetic chain length. The solvent may also swell the polymer substrate to facilitate accessibility and diffusion of the monomer to the active sites and/or may modify the thermodynamic equilibrium of the copolymer in the particular monomer solvent mixture.

The grafting yield of vinyl imidazole (Azole) and acrylic acid (AAc) onto polypropylene and polyethylene are shown in Fig. 17 and 18 with respect to solvent type and its mixture with water. It can be seen that acetone as solvent leads to the highest grafting yield onto polypropylene and polyethylene.

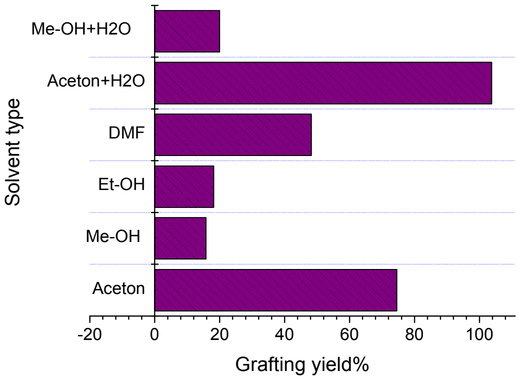

FIG. 17. Grafting yield in different solvents; dose = 30 kGy; monomer concentration = 20%; $FeCl_3$ = 1%; comonomer composition Azole/AAc=1:3.

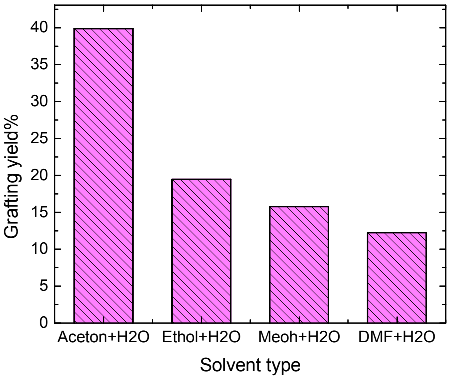

FIG. 18. Grafting yield in different solvents; dose = 30 kGy; monomer concentration = 20%; $FeCl_3$ = 1%; comonomer composition Azole/AAc=1:3.

4.2.2. Effect of inhibitor concentration

The influence of inhibitor concentration on the grafting yield of AAc/Azole onto PP and PE was investigated, and the results are presented in Figs 19 and 20. The data show that the grafting yield increases in the presence of the inhibitor with a maximum at 0.5% inhibitor concentration for PP. For PE the grafting yield increased up to 4% of inhibitor, and did not show a maximum. The maximum value seems to lay at higher values.

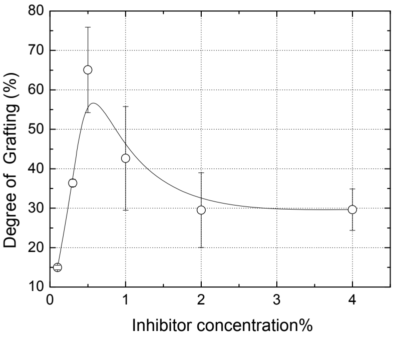

FIG. 19. Grafting yield onto PP with respect to the inhibitor concentration; dose = 30 kGy; monomer conc. = 20%; Azole:AAc = 3:1; acetone/water composition = 40:60(%).

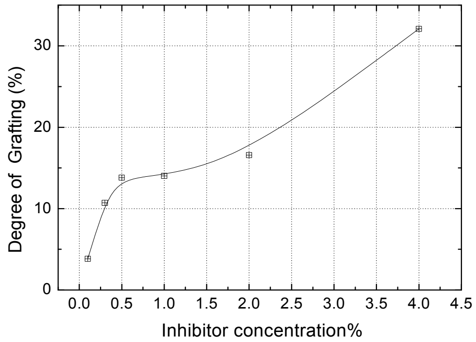

FIG. 20. Grafting yield onto polyethylene with respect to the inhibitor concentration; at 30 kGy; monomer conc. = 20%; Azole:AAc=3:1; acetone/water composition = 30:70(%).

4.2.3. Effect of solvent composition

The influence of the solvent composition on the grafting process has been investigated for all three polymer substrates. Figures 21 and 22 present the grafting yield with respect to the water/ solvent content in the solution; other reaction parameters are constant. A water content of 60–80% is necessary to achieve the highest grafting yield. The presence of water has an enhancing effect on the grafting process. This behaviour can be explained by the fact that the reactive intermediates formed in water radiolysis (hydrogen atom and hydroxyl radical) attack the polymer chain and activate the polymer substrate by H atom abstraction:

$$H_2O \xrightarrow{\hspace{2cm}} R^{\bullet}\ (H^{\bullet} + OH^{\bullet})$$
$$R^{\bullet} + \text{Polymer} \xrightarrow{\hspace{2cm}} RH + \text{Polymer}^{\bullet}$$

However, at higher water content beyond optimum, radiolysis of water produces a radical species, which annihilate the growing grafted chains leading to decrease in percent grafting.

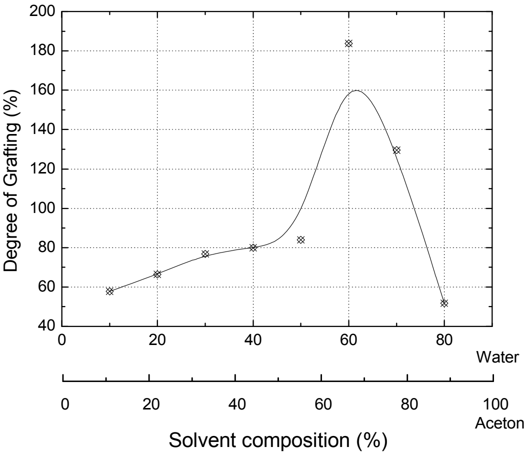

FIG. 21. Grafting yield onto polypropylene vs. solvent composition; dose = 30 kGy; monomer concentration = 20%; FeCl$_3$ = 1%; Azole/AAc = 1:3.

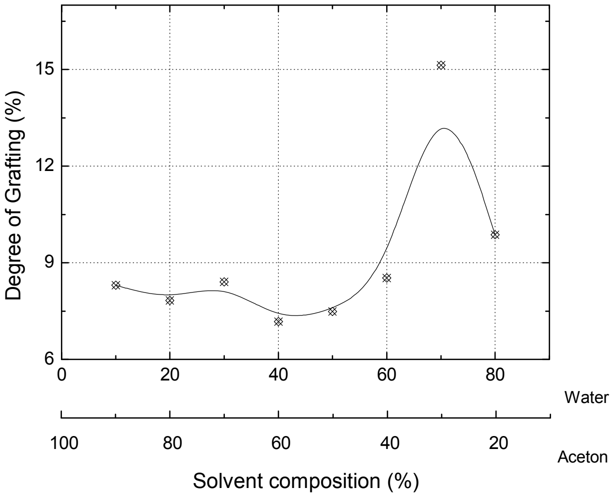

FIG. 22. Grafting yield onto PP with respect to solvent composition; dose = 30 kGy; monomer concentration = 20%; $FeCl_3$ = 1%; comonomer composition Azole/AAc=1:3.

4.2.4. Effect of comonomer composition

The influence of the comonomer composition on the grafting process has been studied because of the synergistic effect of two monomers, which may lead to more efficient grafting processes. The grafting yield of AAc/Azole binary monomer systems of various relative compositions was determined with respect to the comonomer composition; the other reaction parameters were held constant as optimized in previous experiments (inhibitor concentration, irradiation dose, total comonomer concentration), and the obtained data are represented in Fig. 23 and 24. It is obvious that the grafting yield increases with increasing the content of AAc in comonomer solution.

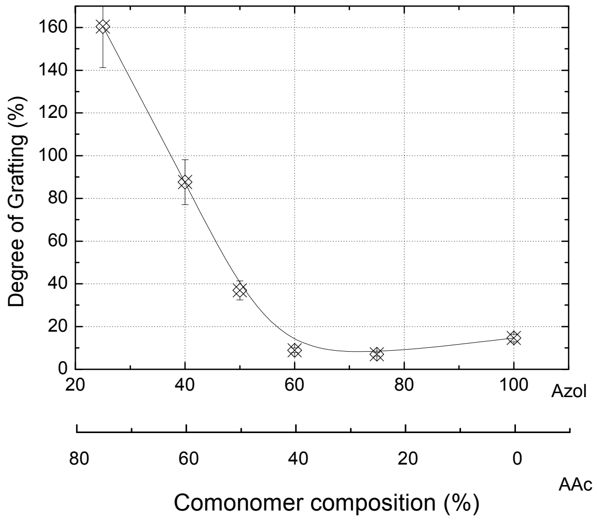

FIG. 23. Grafting yield onto polypropylene with respect to the comonomer composition (Azole/AAc); dose = 30 kGy; monomer concentration = 20%; $FeCl_3$ = 0.5%; solvent composition (acetone/water) = 40:60(%).

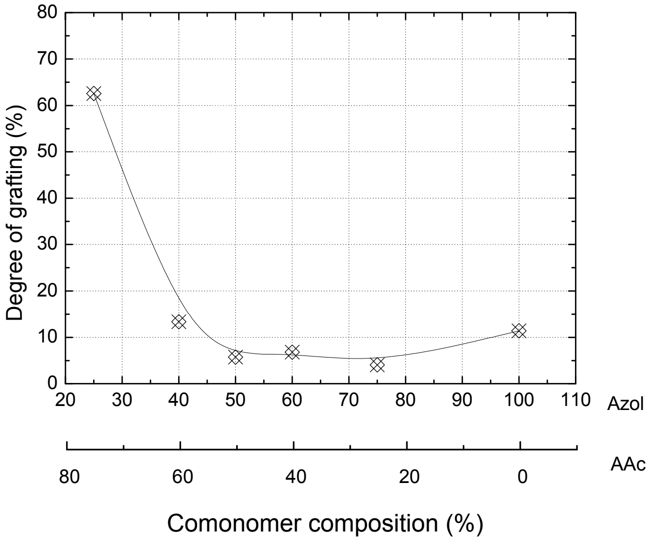

FIG. 24. Grafting yield onto polyethylene vs. comonomer composition (Azole/AAc); dose = 30 kGy; monomer concentration = 20%; $FeCl_3$ = 4%; acetone/water = 30:70(%).

4.2.5. Effect of comonomer concentration

The influence of comonomer concentration during radiation grafting may affect the kinetic parameters of this process. Therefore, the suitable comonomer concentration differs from one system to another, depending on the diluent used, type of polymer support materials, comonomer composition, irradiation dose and dose rate etc.

The effect of dilution of AAc/Azole monomers mixture on the graft copolymerization onto PP and PE has been investigated and the results are presented in Fig. 25 and 26. It can be seen that the degree of grafting increases with increasing the comonomer concentration. The increase in the grafting yield with comonomer concentration may be due to the increase in diffused monomer into the bulk polymer. The high concentration of free radicals at grafting sites favours propagation of growing chains and consequently the grafting yield increases.

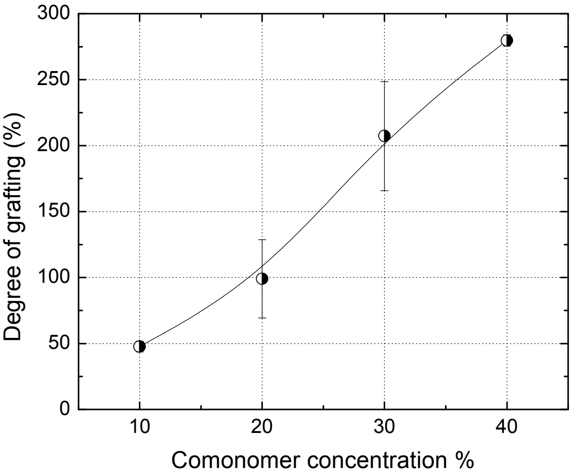

FIG. 25. Grafting yield onto PP with respect to comonomer concentration; dose = 30 kGy; $FeCl_3$ = 0.5%; comonomer composition (Azole/AAc=1:3); acetone: water = 40:60(%).

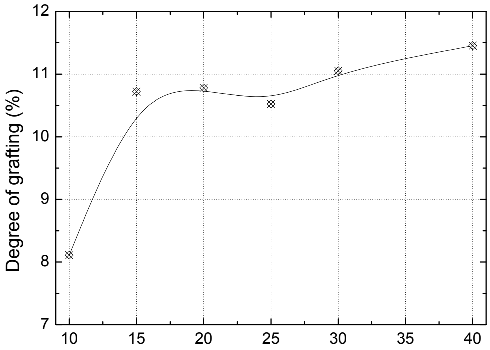

FIG. 26. Grafting yield onto PE with respect to comonomer concentration; dose = 30 kGy; $FeCl_3$ = 1%; comonomer composition (Azole/AAc=1:3); acetone: water = 70:30(%).

4.2.6. Effect of absorbed dose

The increase in the irradiation dose results in increase in the concentration of free radicals formed in the polymer substrate as well as in the monomer itself. The influence of dose on the grafting yield of AAc/Azole binary monomers onto PP and PE films was investigated. The results are illustrated in Fig. 27 and 28. The grafting yield generally increases with increasing dose till a maximum, and then tends to level off or to decrease due to degradation.

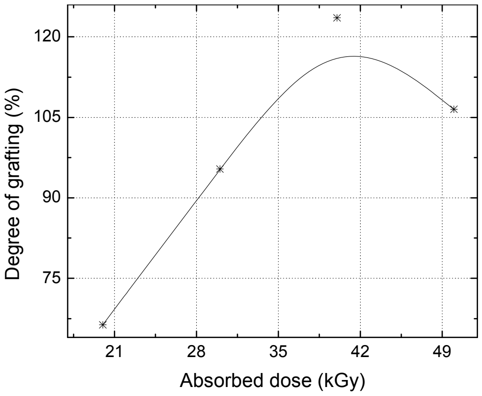

FIG. 27. Grafting yield onto PP with respect to the dose; comonomer concentration = 40%; $FeCl_3$ = 0.5%; comonomer composition (Azole/AAc=1:3); acetone:water = 40:60 (%).

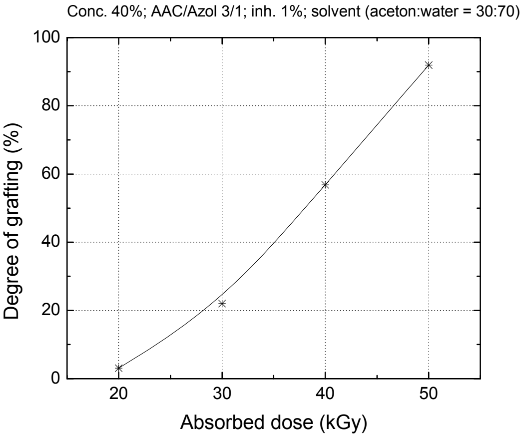

FIG. 28. Grafting yield onto PE with respect to the dose; comonomer concentration = 40%; $FeCl_3$ = 1%; Azole/AAc=1:3; acetone: water = 30:70 (%).

4.2.7. FTIR spectroscopy

Figures 29 and 30 show FTIR spectra of the original PE, PP-g-AAc/Azole, original PE, PE-g-AAc/Azole films. The carbonyl bands centred at around 1720 cm^{-1} can be assigned to the carboxylic acid. The band appearing at 3160 cm^{-1} can be assigned to the C–H (ring) stretching mode for poly(vinyl imidazole).

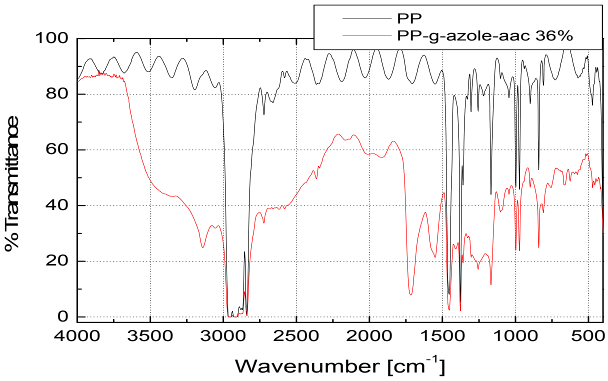

FIG. 29. FRIR spectra of PP and PP-g-AAc/Azole films.

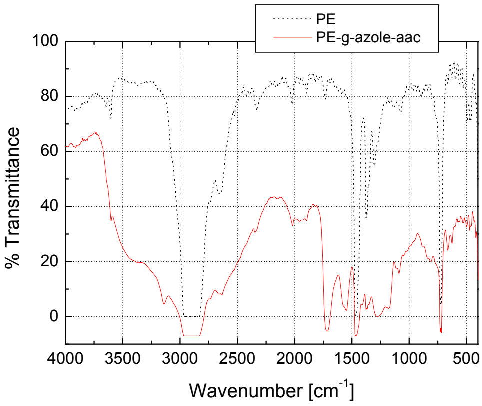

FIG. 30. FTIR spectra of PE and PE-g-AAc/Azole films.

4.2.8. Ion Uptake

The ion uptake of PE-g-Azole/AAc membranes versus the degree of grafting is represented in Fig. 31. As the degree of grafting increases, the ion uptake of the membrane increases. This behaviour can be reasonably attributed to the increase in the number of functional groups grafted onto the polymer backbone.

5. CONCLUSION

Polypropylene and polyethylene films were grafted with acrylic acid/N-vinyl imidazole or acrylic acid/N-vinyl pyrrolidone binary mixtures using gamma radiation. The grafting conditions were determined regarding their influence on the grafting yield as: type of solvent and solvent composition, comonomer concentration and composition, addition of inhibitor, and absorbed dose. The ability of the grafted films to adsorb heavy metal ions was evaluated with respect to the grafting yields. It increases with increasing the grafting yield. Because of their basic/acidic character the prepared membranes may be considered for removal of the studied ions from wastewater. Further work is in progress to elaborate the use of the prepared membranes in separation processes.

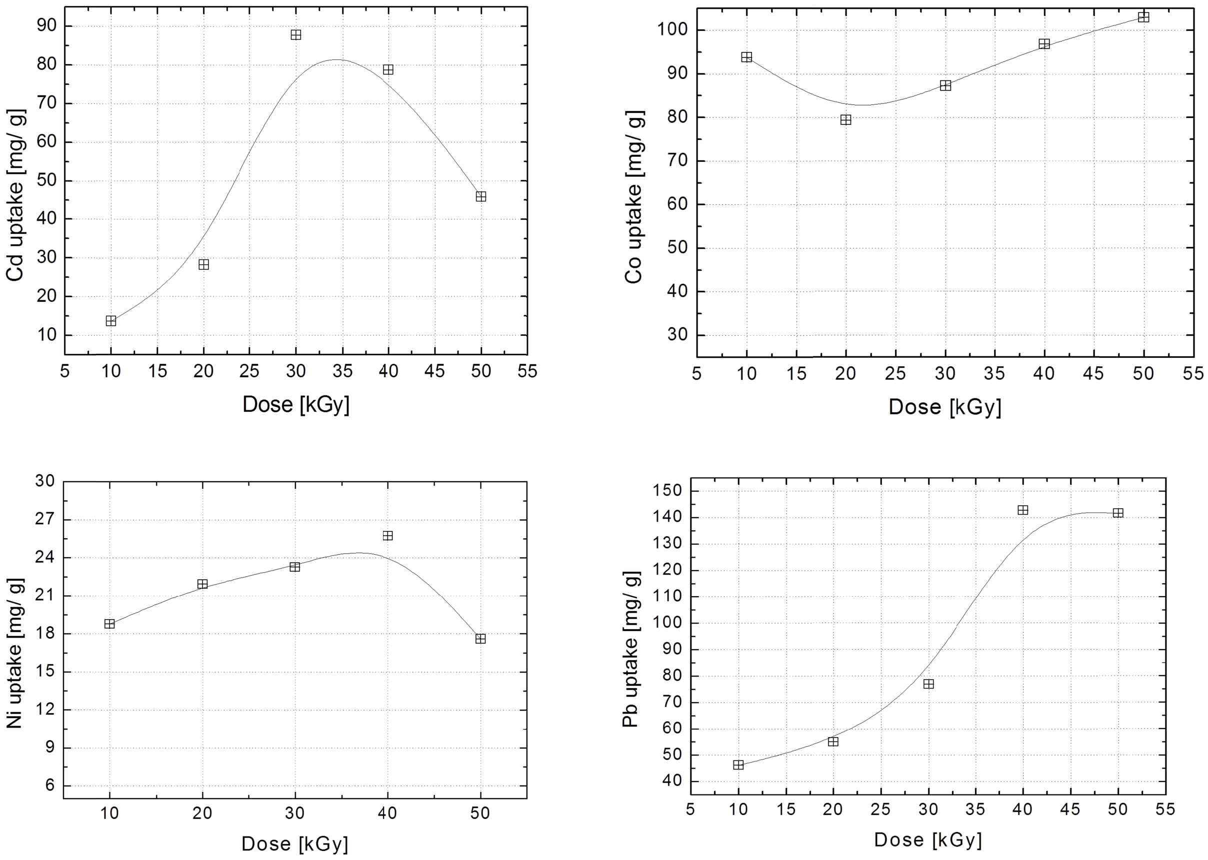

FIG. 31. Uptake of Co^{2+}, Pb^{2+},Ni^{2+} and Cd^{2+} ions vs. grafting yield of PE-g-AAc/Azole; initial feed concentration = 2000 ppm; time = several days; temperature = 22°C.

REFERENCES

[1] KIM, M., SAITO, K., Radiation-induced graft polymerization and sulfonation of glycidyl methacrylate on to porous hollow-fiber membranes with different pore sizes, Radiat. Phys. Chem., **57** (2) (2000) 167-172.

[2] CHAPIRO, A., Radiation Chemistry of Polymeric Systems. Interscience, New York (1962).

[3] GARNETT, J.L., Grafting, Radiat. Phys.Chem. **14** (1979) 79-99.

[4] HEBEISH, A., SHALABY, S., BAYAZEID, A., H_2O_2-induced graft polymerization of acrylic acid/styrene mixtures on poly(ethylene terephthalate) fibers, J. Appl. Polym. Sci. **27** (1982) 197.

[5] LOKHANDE, H.T., TELI, M.D., Grafting onto polyester fibers: IV. Synergism during graft copolymerization of binary mixture of vinyl monomers onto polyester fibers, J. Appl. Polym. Sci. **29** (1984) 1843.

[6] AOUADJ, S., CHAPIRO, A., Preparation of hydrophilic membranes by grafting acrylic acid onto pre-irradiated Teflon-FEP films, Angew. Makromol. Chem. **235** (1996) 73–80.

[7] TAHER, N., DESSOUKI, A., KHALIL, F., EL-ARNAOUTY, M., Preparation and properties of cationic membranes obtained by radiation grafting of vinyl monomers onto poly(tetrafluoroethyleneperfluoropropylvinyl ether) (PFA) films, Polym. Int. **41** (1996) 383–389.

[8] ISHIGAKI, I., SUGO, T., TAKAYAMA, T., OKADA, T., OKAMOTO, J., MACHI, S., Graft polymerization of acrylic acid onto polyethylene film by preirradiation method. II. Effects of oxygen at irradiation, storage time after irradiation, Mohr's salt, and ethylene dichloride, J. Appl. Polym. Sci. **27** (1982) 1043–1051.

[9] MISRA, B., KUMAR, D., KAUR, I., Preparation and characterization of Teflon-FEP films grafted with acrylic acid by radiochemical method, J. Appl. Polym. Sci. **56** (1995) 1133–1139.

[10] NASEF A.M.M., HEGAZY, E.A., Preparation and applications of ion exchange membranes by radiation-induced graft copolymerization of polar monomers onto non-polar films, Prog. Polym. Sci., **29** (2004) 499-561.

[11] LUO, C.S., HUANG, S., Adsorption of copper ion with metal hydroxide from ammonia solution, Separation Science Technology **28** 6 (1993) 1253.

METAL ADSORBENT PREPARED FROM POLY(METHYL ACRYLATE)-GRAFTED CASSAVA STARCH VIA GAMMA IRRADIATION

P. SUWANMALA, K. HEMVICHIAN, W. SRINUTTRAKUL

Nuclear Research and Development Group
Thailand Institute of Nuclear Technology
Bangkok,
THAILAND

Abstract

Metal adsorbent containing hydroxamic acid groups was successfully synthesized by radiation-induced graft copolymerization of methyl acrylate (MA) onto cassava starch. The optimum conditions for grafting were studied in terms of % degree of grafting (Dg). Conversion of the ester groups present in poly(methyl acrylate)-grafted-cassava starch copolymer into hydroxamic acid was carried out by treatment with hydroxylamine (HA) in the presence of alkaline solution. The maximum percentage conversion of the ester groups of the grafted copolymer, %Dg = 191 (7.63 mmol/g of MA), into the hydroxamic groups was 70% (5.35 mmol/g of MA) at the optimum conditions: in a mixture solution of 20% HA (w/v) and methanol solution (methanol:H_2O = 5:1) 300 mL, pH 13, reaction time 2 h, and 20 g of grafted copolymer. The adsorbent was characterized by FTIR, TGA, and DSC. The presence of electron donating groups in adsorbent containing hydroxamic acid groups gives the ability to form polycomplexes with metal ions. The ability of the adsorbent to adsorb various metals was investigated in order to evaluate the possibility of its use in metal adsorption. The adsorbent exhibited a remarkable % adsorption for Cd^{2+}, Al^{3+}, $UO_2{}^{2+}$, V^{5+} and Pb^{2+} at pH 3, 4, 5, 4, and 3, respectively. The adsorbent of 191%Dg had total adsorption capacities of 2.6, 1.46, 1.36, 1.15, and 1.6 mmol/g adsorbent for Cd^{2+}, Al^{3+}, $UO_2{}^{2+}$, V^{5+} and Pb^{2+}, respectively, in the batch mode adsorption.

1. OBJECTIVE OF THE RESEARCH

This research project aimed to apply radiation processing to synthesize metal adsorbents with specific affinity to particular metal ions. Native natural polymers, cassava starch, was be used as starting materials. The monomers with desired functional groups were grafted onto the backbone of natural polymers via radiation-induced graft polymerization. Various factors were investigated in order to determine the optimum conditions for the graft copolymerization. Chemical modification was employed to improve the efficiency of the copolymers so that they have specific affinities towards particular metal ions. The optimum conditions for the chemical modifications were verified. Subsequently, the properties and efficiency of the obtained adsorbents were examined in order to evaluate the possibility of their used for environmental applications.

2. INTRODUCTION

In recent years, there has been considerable interest in the design, synthesis, and application of polymers having functional group that can form coordinate bonds with heavy metals [1–3]. Polymeric chelating resin containing the hydroxamic acid group has been found to be an effective chelating ligand with a wide range of metals [3]. Polymeric chelating resins bearing hydroxamic acid group have been used for extraction and separation of metal ions due to the hydroxamic acid groups can form complexes with various metal ions [3,4,5,6,7] such as Cd^{2+}, V^{5+}, Fe^{2+}, Fe^{3+}, Zn^{2+}, Pb^{2+}, Ni^{2+}, Hg^{2+}, Au^{3+}, Ag^{+}, Cu^{2+}, Co^{2+}, Cr^{3+}, and $UO_2{}^{+2}$. Starch is a renewable natural polymer that can be modified by chemical reaction to give novel properties for different purposes [3, 7, 8]. A number of studies have investigated the graft copolymerization of vinyl monomers on starch [2, 3, 9] and concluded that this chemical modification can expand the range of its utilization.

Radiation–induced graft polymerization (RIGP) is a powerful method for preparation of polymeric materials with new properties for practicable applications. The advantages of this method include: (1) it can give uniform and rapid creation of active radical sites allowing a high degree of penetration of graft chains to the polymer matrix, (2) it can be effectively and conveniently carried out at room temperature, (3) polymer chains containing functional groups can be added without significant changes in the properties of the trunk polymers, (4) various side reactions are minimal, (5) a wide range of shapes and qualities of polymers can be selected as a trunk polymer according to mechanical, thermal, and chemical stability required by the practicable applications, (6) the distribution of the introduced functional groups is easily achieved by controlling the irradiation energy. RIGP has been used for preparation of metal adsorbents [9–16].

The main objective of this research is to convert cassava starch into useful products for environmental applications. In the present work, an adsorbent containing hydroxamic acid groups was synthesized by radiation-induced graft copolymerization of methyl acrylate (MA) onto cassava starch (Fig. 1). Graft polymerizations were studied with regard to various parameters of importance: dose, the amount of MA, and the amount of cassava starch. Conversion of the ester groups of the grafted copolymer into the hydroxamic groups was performed by treatment with an alkaline solution of hydroxylamine (HA). The experimental parameters such as concentration of HA, reaction time, reaction medium methanol-water ratio, pH, and the amount of grafted copolymer were investigated. In addition, the adsorption behaviour of chelating resin toward metal ions was investigated.

a.) Poly(methyl acrylate)-grafted-cassava starch via gamma irradiation.

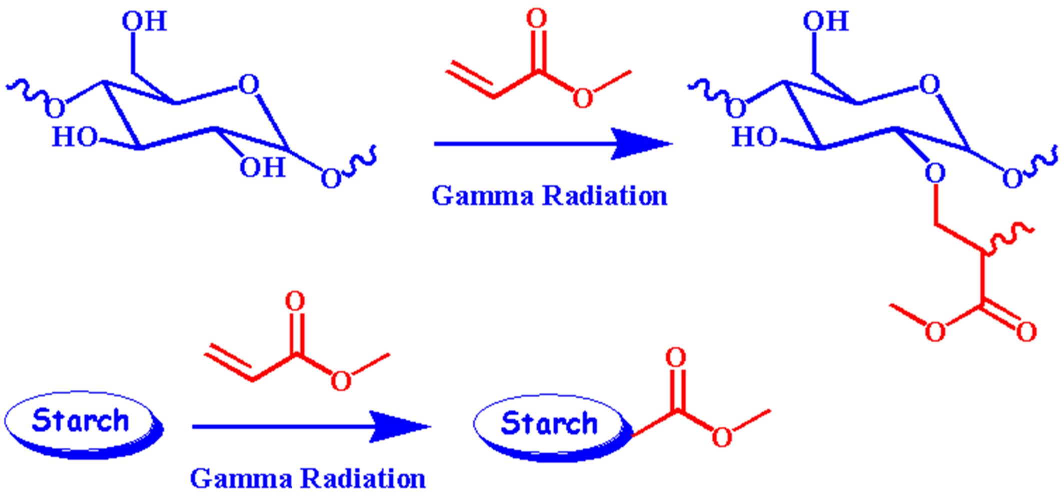

b.) Modification of poly(methyl methyl acrylate)-grafted-cassava starch.

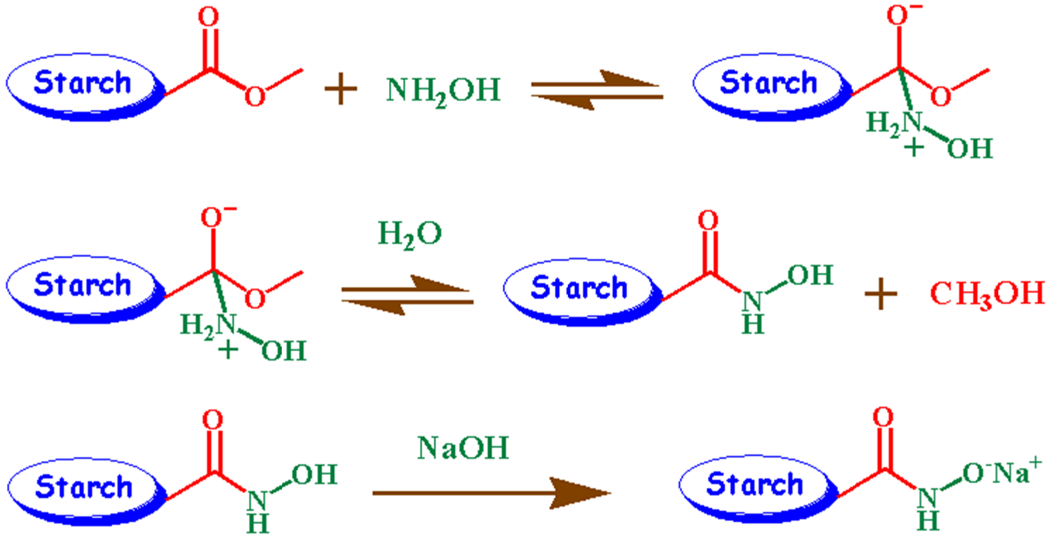

FIG. 1. Preparation of adsorbent containing hydroxamic acid by radiation-induced grafting.

3. MATERIALS AND METHODS

3.1. Materials

Commercial cassava starch was obtained from Siam Ouality Starch Co., Ltd. Methyl acrylate was purchased from Aldrich and was used as received. Hydroxylamine hydrochloride was obtained from Fluka. All other chemicals and solvents were also used without further purification.

3.2. Adsorbent preparation

3.2.1. Radiation-induced graft polymerization

In a gelatinization reactor, 20 g of cassava starch was mixed with 190 mL of distilled water. The mixture was continuously stirred using a mechanical stirrer under nitrogen atmosphere. The mixture was gradually heated from ambient temperature to 80°C and held at this temperature for one hour. The mixture was left to cool down to room temperature to yield the gelatinized starch. The obtained gelatinized cassava starch was mixed with 45 mL of methyl acrylate. The mixture was stirred under nitrogen atmosphere at room temperature for one hour to form a homogeneous mixture. The gelatinized starch–methyl acrylate mixture was transferred into the glass bottle and purged with nitrogen gas for 5 minutes. The bottle was tightly closed with cap, and then irradiated under gamma radiation in Gammacell 220 Excel (^{60}Co source) at a dose rate of 0.14 kGy/min and a dose of 7.5 kGy. After irradiation, the crude product was precipitated in methanol, filtered, and then dried at 50°C in vacuum oven. PMA homopolymer formed during the graft copolymerization was separated from the grafted copolymer by washing several times with methanol: water (4:1). Then, the product was dried in vacuum oven at 50°C. The degree of grafting was determined by the following equation:

$$Dg\ (\%) = 100\ [(W_2 - W_1)/W_1]$$

where W_1 and W_2 are the weights of cassava starch and graft copolymer, respectively.

3.2.2. Preparation of hydroxylamine (NH_2OH) solution

Hydroxylamine hydrochloride ($NH_2OH.HCl$) 20% (w/v) was dissolved in a 300 mL methanol solution ($MeOH:H_2O$ = 5:1) The HCl was neutralized by the NaOH pellets. The precipitated NaCl was separated by filtration. The pH of the reagent was adjusted to pH 13 by addition of the NaOH pellets.

3.2.3. Modification of graft copolymer

The graft copolymer (20 g) was placed in the reactor which was equipped with a mechanical stirrer and condenser and the hydroxylamine solution was added. The reaction was carried at 75°C for 2 hours. After completion of the reaction, the modified graft copolymer was washed several times with a methanol solution (methanol:water = 4:1) then, it was dried in vacuum oven at 50°C overnight.

Finally, the modified graft copolymer was treated with 100 mL of methanol HCl solution (0.2 M) for 10 minutes, washed several times with the methanol solution (methanol:water = 4:1) and then dried in vacuum oven at 50°C.

3.3. Fourier transform infrared spectroscopy

Fourier transform infrared (FTIR) spectra were recorded by FTIR spectrometer (Tensor 27, BRUKER) using the KBr disc technique at a resolution of 4 cm^{-1} and 16 co-added scans. The spectral scan range was 4000–500 cm^{-1}.

3.4. Thermogravimetric analysis

Thermogravimetric analysis (TGA) experiments were performed using a TGA/SDTA851^e from Mettler Toledo. The analyses were carried out in nitrogen atmosphere in the temperature range from 25–800°C at a heating rate of 10°C/min with a N_2 flow rate of 90 mL/min.

3.5. Differential scanning calorimeter

Differential scanning calorimetric (DSC) experiments were performed with a DSC822^e/700 from Mettler Toledo with the N_2 flow rate set at 50 mL/min and a heating rate of 10°C/min.

3.6. Elemental analysis

Elemental analysis provides accurate information of the conversion of poly(methylacrylate ester) into poly(hydroxamic acid) via treatment with hydroxylamine in an alkaline medium. It can be used to determine the conversion of poly(methylacrylate ester) into poly(hydroxamic acid) because the modified graft copolymer has nitrogen atoms in its molecular structure, but unmodified graft copolymer does not. Elemental analysis of the modified copolymer was carried out with a CHNS/O 2400 Series II element analyzer (Perkin Elmer). The percent conversion of poly(methylacrylate ester) into poly(hydroxamic acid) was calculated as follows:

Amount of hydroxamic acid groups (X):

$$\mathrm{X} = \left(\frac{W_s.N}{100}\right)/14x10^3$$

where W_s denotes the weight of sample, and N denotes the percentage of nitrogen.

Density of hydroxamic acid group (Y):

$$\mathrm{Y} = \frac{X}{W_s}$$

Conversion(%):

$$\%\ \mathrm{Conversion} = \frac{Y}{Z}x100$$

$$\mathrm{Z} = \left(\frac{W_1 - W_0}{86.09}\right)/W_1$$

where W_0 and W_1 are the weights of cassava starch, and PMA-grafted copolymer. The factor 86.09 corresponds to the molecular weight of MA.

3.7. Metal absorption

The adsorbent (0.5 g) was soaked into metal solution and shaken using a rotary shaker at room temperature. After equilibration was completed, a 5 mL supernatant was collected for metal ion determination.

3.8. Inductively coupled plasma mass spectroscopy

The initial and final metal concentrations were determined by an inductively coupled plasma mass spectroscopy (ICP-MS, 4500 Series, Hewlett Packard).

4. RESULTS AND DISCUSSION

4.1. Radiation-induced graft polymerization

4.1.1. Effect of dose on degree of grafting

As shown in Fig. 2 the degree of grafting increased with increasing dose up to 7.5 kGy and then decreased with increasing dose. The increase in the dose enhances the formation of radicals, resulting in high degree of grafting. The degree of grafting reached about 135% at the absorbed dose of 7.5 kGy. At the absorbed doses higher than 7.5 kGy, the degree of grafting decreased, which may be due to the degradation of cassava starch.

4.1.2. Effect of the concentration of methyl acrylate on degree of grafting

The effect of methyl acrylate on the grafting of methyl acrylate on cassava starch is presented in Fig. 3. As the monomer concentration increased, the degree of grafting increased as well. At higher monomer concentration, radical generated on the trunk polymer are able to interact with more monomer molecules.

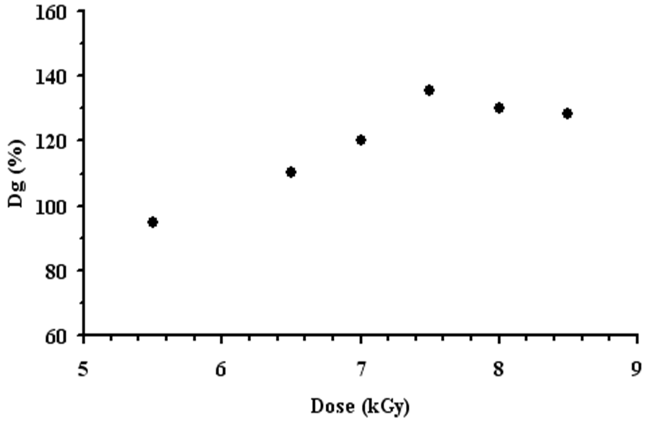

FIG. 2. Effect of absorbed dose on degree of grafting.

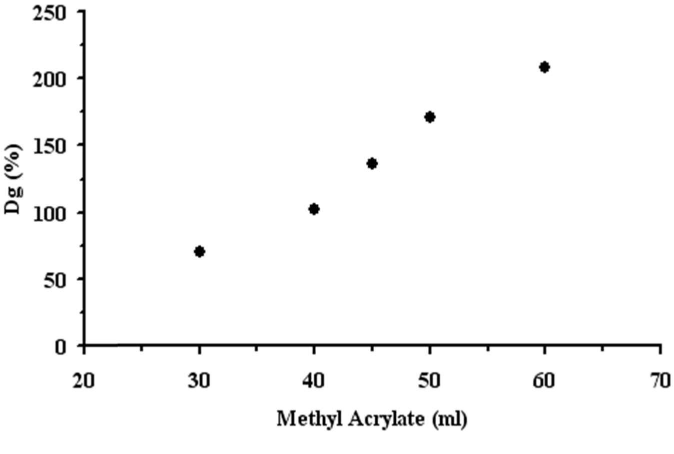

FIG. 3. Effect of methyl acrylate on degree of grafting.

4.1.3. Effect of the amount of cassava starch on degree of grafting

Figure 4 represents the effect of the amount of cassava starch on degree of grafting. The degree of grafting decreased with increasing the amount of cassava starch.

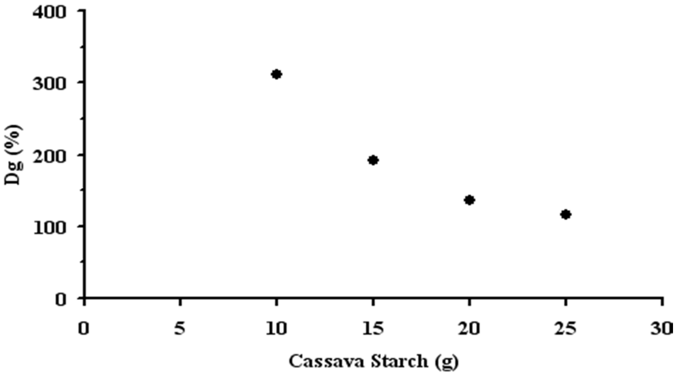

FIG. 4. Effect of the amount of cassava starch on degree of grafting.

4.2. Modification of grafted copolymer

The ester group of the PMA-grafted copolymer was converted into the hydroxamic acid group by treatment of an ester with hydroxylamine in an alkaline solution. Modification parameters were determined in relation to % nitrogen.

4.2.1. Effect of HA concentration on % conversion

The effect of concentration of HA on % conversion of poly(methylacrylate ester) into poly(hydroxamic acid) is presented in Fig. 5. The maximum percentage of conversion 70% (5.35 mmol/g of hydroxamic acid groups) was observed at 20% (w/v MeOH:H_2O = 5:), and thereafter gradually decreased until it levelled off.

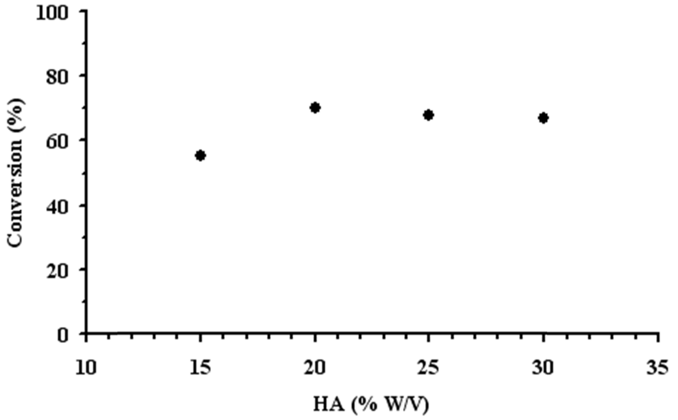

FIG. 5. Effect of HA concentration on conversion of poly(methylacrylate ester) into poly(hydroxamic acid); 20 g of grafted copolymer (Dg = 191%, 7.63 mmol/g of MA group), methanol:H_2O = 5:1, reaction time 2 h, pH 13.

4.2.2. Effect of reaction time on the conversion

Figure 6 shows the effect of reaction time on % conversion of poly(methylacrylate ester) into poly(hydroxamic acid). The percentage conversion increased with an increasing reaction time up to 2 h. This reaction time gave the maximum degree of grafting of 70%.

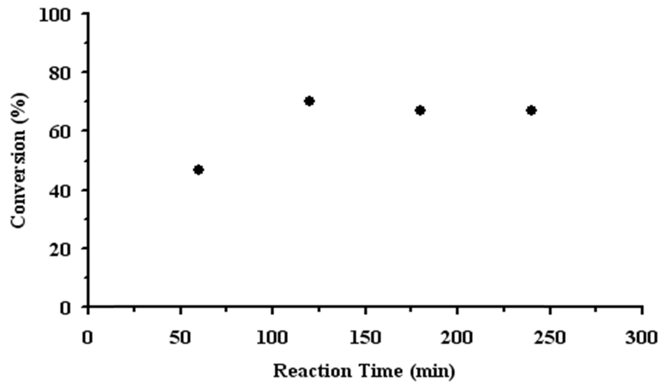

FIG. 6. Effect of reaction time on conversion of poly(methylacrylate ester) into poly(hydroxamic acid); 20 g of grafted copolymer, 20% w/v HA, methanol: H_2O = 5:1, pH 13.

4.2.3. Effect of reaction medium methanol-water ratio on the conversion

It can be observed from Fig. 7 that conversion increases with increasing methanol-water ratio up to MeOH:H_2O ratio of 5:1. The maximum percentage of conversion was obtained in the presence of MeOH:H_2O ratio of 5:1.

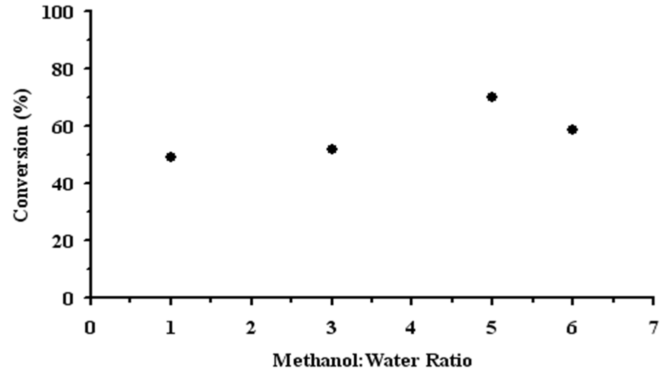

FIG. 7. Effect of reaction medium methanol-water ratio on the conversion of poly(methylacrylate ester) into poly(hydroxamic acid); 20 g of grafted copolymer, 20% w/v HA, reaction time 2 h, and pH 13.

4.2.4. Effect of pH on % conversion

The effect of pH on conversion of poly(methylacrylate ester) into poly(hydroxamic acid) shown in Figure 8 indicates that conversion increases with increasing pH up to pH 13. This pH gave the maximum conversion of 70%.

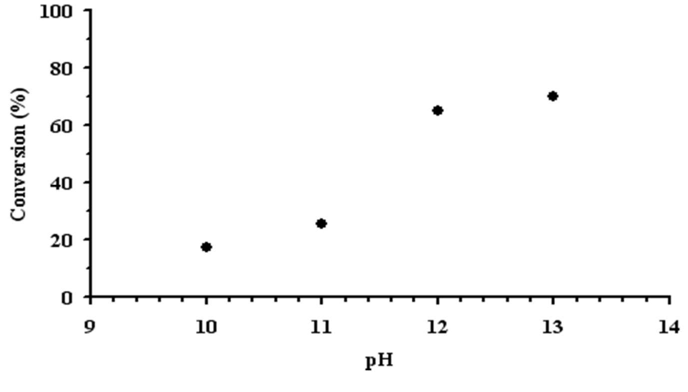

FIG. 8. Effect of pH on conversion of poly(methylacrylate ester) into poly(hydroxamic acid): 20 g of grafted copolymer, 20% w/v HA, reaction time 2 h, methanol:H_2O ratio = 5:1.

4.2.5. Effect of the amount of graft copolymer on conversion

The effect of the amount of grafted copolymer on conversion is shown in Fig. 8. The percentage conversion of poly(methylacrylate ester) into poly(hydroxamic acid) increased with increasing the amount of grafted copolymer up to 20 g of grafted copolymer, and then levelled off. Maximum conversion was obtained at 20 g of grafted copolymer.

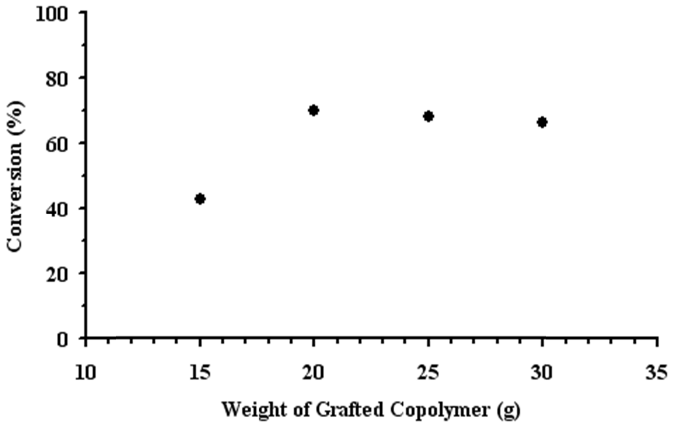

FIG. 9. Effect of the amount of grafted copolymer on conversion of poly(methylacrylate ester) into poly(hydroxamic acid); 20% w/v HA, reaction time 2 h, methanol:H_2O ratio 5:1, pH 13.

4.3. Fourier transformed infrared spectroscopy

FTIR spectra of cassava starch, PMA-g-starch, and adsorbent containing hydroxamic acid groups are shown in Fig. 10. The FTIR spectrum of cassava starch shows the following characteristic absorption bands: 3200–3600 cm^{-1} (H-bonded OH), 2932 cm^{-1} (C-H stretch), 1155 cm^{-1} (tertiary C-OH), 1078 cm^{-1} (C-O stretch), 1016 cm^{-1} (asymmetric C-O-C) and 927 cm^{-1} (cyclic C-O-C), while that of PMA-g-starch shows similar pattern with an extra band at 1740 cm^{-1} due to C=O stretching vibration. In the FTIR spectrum of the adsorbent the strong band at 1740 cm^{-1} disappears, whereas two new bands associated with hydroxamic acid (amide C=O stretching at 1638 cm^{-1} and amide N-H bending at 1560 cm^{-1}) become visible. These provide strong evidence for the presence of hydroxamic acid groups in the grafted copolymer.

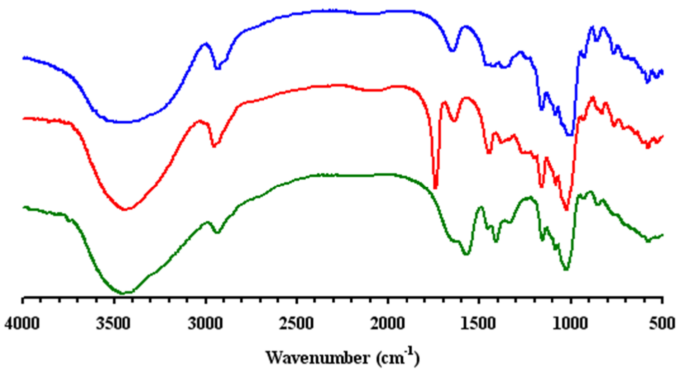

FIG. 10. FTIR spectra of cassava starch (top), PMA-grafted-starch (middle) and adsorbent (bottom).

4.4. Differential scanning calorimeter (DSC)

The DSC curves of the starch, PMA-grafted-starch, and adsorbent are presented in Fig. 11. The melting peak of cassava starch is centred at approximately 85°C, while those of PMA-g-starch and chelating resin shifts to higher temperature at around 155 and 163°C, respectively.

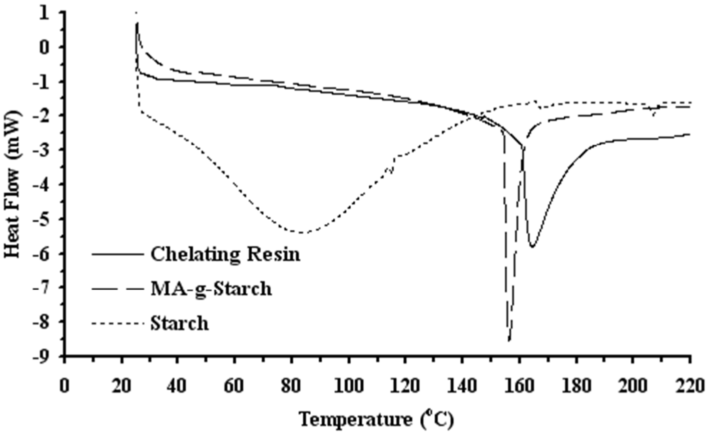

FIG. 11. DSC thermo grams of cassava starch, PMA-grafted-starch and adsorbent.

4.5. Thermogravimetric analysis (TGA)

Figure 12 shows that on the TGA thermo gram of cassava starch a major one-stage weight loss process appears, with the highest rate of weight loss at approximately 334°C. Unlike cassava starch, PMA-g-starch displays a well-separated two-stage weight loss process. The first process coincides with the thermogram of cassava starch, confirming the presence of cassava starch in the copolymer. The second process represents the thermal degradation of PMA grafted onto the backbone of cassava starch, resulting in a 6% final char yield at 800°C. TGA thermogram of the adsorbent also shows a two-stage weight loss process. However, it is obvious that, at 800°C the char yield of adsorbent (28%) is significantly higher than that of PMA-g-starch. This indicates that adsorbent is thermally more stable than PMA-g-starch, probably due to the enhanced interaction between the carbonyl groups of hydroxamic acid and the hydroxyl groups in the cassava starch. It also confirms that the copolymer and the chelating resin are different, both chemically and structurally.

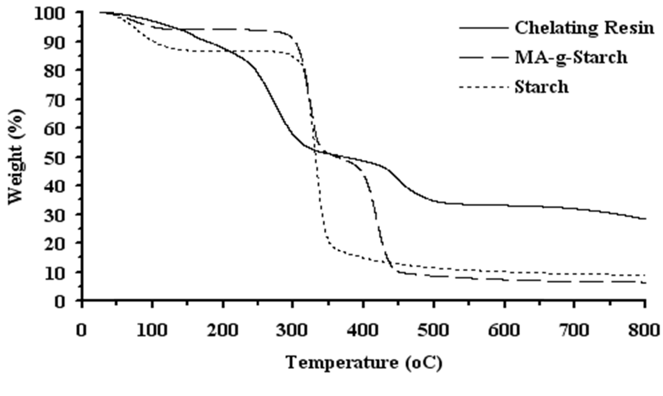

FIG. 12. TGA thermograms of cassava starch, PMA-grafted-starch and adsorbent.

4.6. Metal adsorption

The presence of electron donating groups in adsorbent containing hydroxamic acid groups gives the ability to form polycomplexes with metal ions. The ability of the adsorbent to adsorb various metals was carried out in order to evaluate the possibility of their uses in metal adsorption. 0.5 g of adsorbent was soaked into 100 mL of 100 ppb metal solution and stirred at room temperature for 24 hours. A diagram showing the percentage adsorption of adsorbents for various metals is shown in Fig. 13. It was found that adsorbent containing hydroxamic acid groups can adsorb various metal ions. Each metal ion has its own optimum pH at which it shows maximum percentage adsorption. The adsorbent exhibited a remarkable adsorption for Cd^{2+} and Pb^{2+} at pH 3, as shown in Fig. 14 and 15.

In order to investigate the adsorption properties of the synthesized adsorbent, the set of batch experiments towards Al(III), V(V), Pb(II), Cd(II) and U(VI) ions in aqueous solution (pH 3) was performed. 0.5 g of adsorbent was treated with 100 ppb metal ion solutions. The adsorption test results for five metal ions are shown in Fig. 16. High adsorption rates are observed within 30 min with 63, 51, 71, 75, 60% uptake for Al(III), V(V), Pb(II), Cd(II) and U(VI) ions, respectively. The adsorbent showed a good affinity towards chelating with five metals. Equilibrium adsorption values of 93, 98, 99, 99.5 and 75% were reached for Al(III), V(V), Pb(II), Cd(II) and U(VI) ions after 24 h.

The values of the adsorption capacity of the synthesized adsorbent towards Cd^{2+}, Al^{3+}, UO_2^{2+}, V^{5+} and Pb^{2+} ions have been evaluated. The adsorbent exhibited a remarkable adsorption for Cd^{2+}, Al^{3+}, UO_2^{2+}, V^{5+} and Pb^{2+} at pH 3, 4, 5, 4, and 3, respectively (Fig. 17). The adsorbent of 191% Dg had total adsorption capacities of 2.6, 1.46, 1.36, 1.15, and 1.6 mmol/g adsorbent for Cd^{2+}, Al^{3+}, UO_2^{2+}, V^{5+} and Pb^{2+}, respectively, in the batch mode adsorption.

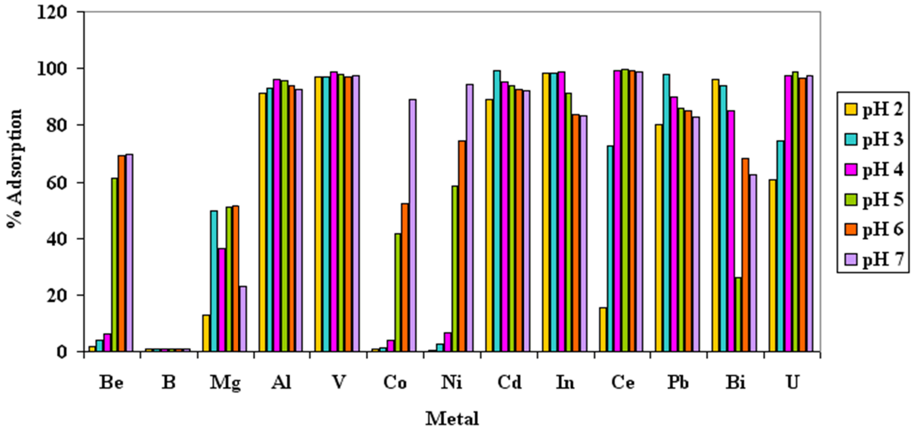

FIG. 13. Adsorption of different metals by the adsorbent containing hydroxamic acid groups.

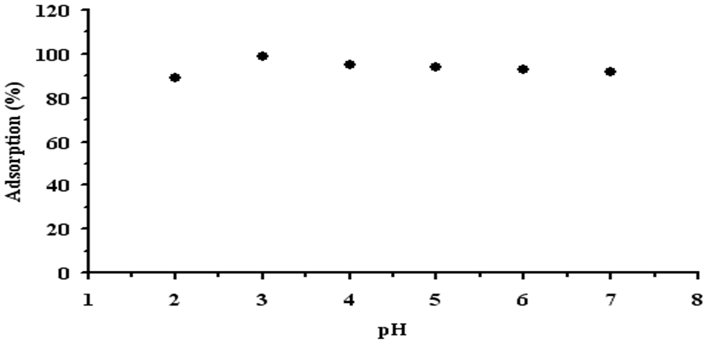

FIG. 14. Effect of pH on Cd^{2+} adsorption.

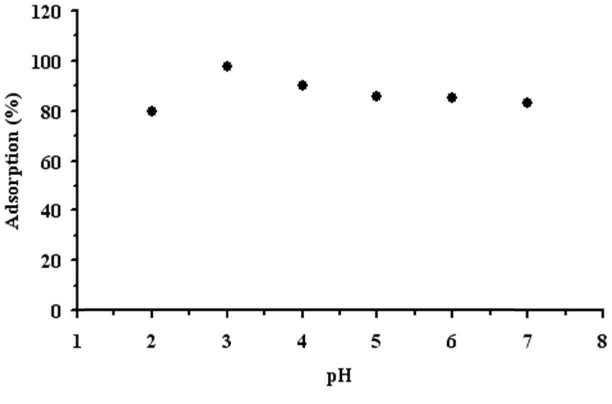

FIG. 15. Effect of pH on Pb^{2+} adsorption.

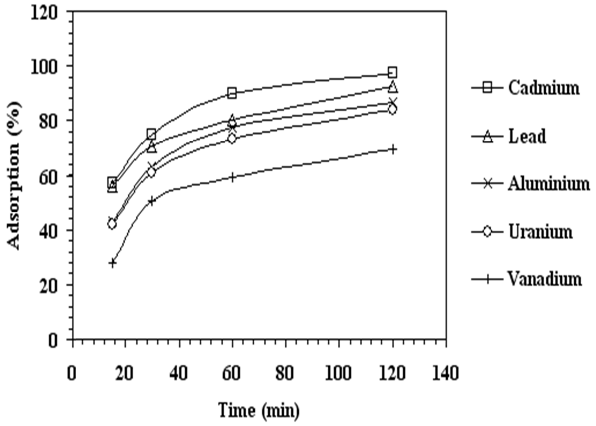

FIG. 16. Adsorption kinetics of Al(III), V(V), Pb(II), Cd(II) and U(VI) ions from 100 ppb initial concentrations.

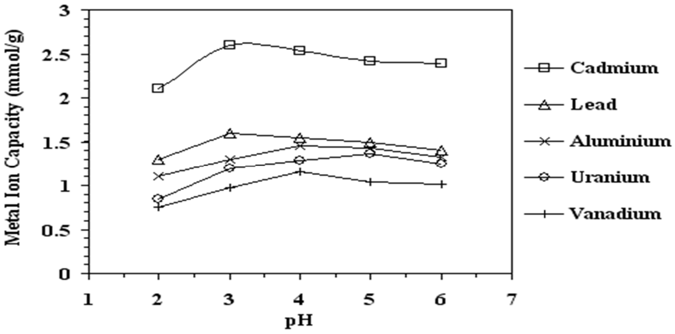

FIG. 17. Metal ion capacities of adsorbents containing hydroxamic acid as a function of pH.

Cellulose adsorbent containing hydroxamic acid groups was successfully prepared by graft copolymerization of methyl acrylate (MA) onto cotton fabric by simultaneous gamma irradiation. Conversion of the ester groups present in poly(methyl acrylate) (PMA) grafted cellulose fibre copolymer into hydroxamic acid was performed by treatment with hydroxylamine (HA) in the presence of alkaline solution. Major parameters for graft copolymerization including dose, and monomer concentration were investigated. Cotton fabric with weight to surface ratio of 150 g/cm^3 was used as a trunk polymer. The optimum condition for grafting methyl acrylate onto cotton fabric was found at the following condition: 45% MA (v/v) in solvent mixture containing ethanol:H_2O = 1:1 dose of 50 kGy. The degree of grafting at this condition was 133 (6.63 mmol/g of MA group). The maximum percentage conversion of the ester groups of the grafted copolymer, %Dg = 133 into the hydroxamic groups was 55% (3.67 mmol/g of hydroxamic acid) at the optimum condition: in a mixture solution of 25% HA (w/v) in solution methanol:H_2O = 5:1, 300 mL, pH 13, reaction time 2 h, and reaction temperature 75°C. The adsorbent was characterized by FTIR, TGA, and DSC. The adsorbent exhibited a remarkable adsorption for Cd^{2+}, Al^{3+}, UO_2^{2+}, V^{5+} and Pb^{2+} at pH 3, 4, 5, 4 and 3, respectively. The adsorbent of 133% Dg had total adsorption capacities of 2.1, 1.04, 1.01, 0.7 and 1.36 mmol/g adsorbent for Cd^{2+}, Al^{3+}, UO_2^{2+}, V^{5+} and Pb^{2+}, respectively, in the batch mode adsorption. Its selectivity toward the metal ions used is in the following order: $Cd^{2+} > Pb^{2+} > Al^{3+} > UO_2^{2+} > V^{5+}$.

5. CONCLUSIONS

Adsorbent containing hydroxamic acid groups was successfully prepared by radiation grafting of methyl acrylate onto two natural polymers cassava starch, and cotton fabric, followed by treatment with hydroxylamine. The characterizations of adsorbent were performed by FTIR, DSC, and TGA. The presence of hydroxamic acid groups was confirmed by the formation of dark purple colour when the adsorbent was mixed with vanadium ions. The selectivity of adsorbent towards the metal ions is in the following order: $Cd^{2+} > Pb^{2+} > Al^{3+} > UO_2^{2+} > V^{5+}$.

REFERENCES

[1] HEGAZY, E.A., ABD EL-REHIM, H.A., SHAWKY, H.A., Investigation and characterization of radiation grafted copolymers for possible practical use in waste water treatment, Radiat. Phys. Chem. **57**(1) (2000) 85-95.

[2] LUTFOR, M.R., SILONG, S., ZIN, W.M., AB RAHMAN M.Z.A., AHMAD, M., HARON, J., Preparation and characterization of poly(amidoxime) chelating resin from polyacrylonitrile grafted sago starch, Eur. Polym. J. **36** (2000) 2105-2113.

[3] LUTOR, M.R., SIDIK, W.M., WAN YUNUS, W.M.Z., RAHMAN, M.Z.A., MANSOR, A. HARON, M.J., Synthesis and characterization of poly(hydroxamic acid) chelating resin from poly(methyl acrylate)-grafted sago starch, J. Appl. Polym. Sci. **79** (2001) 1256-1264.

[4] YALE, H.L., The hydroxamic acids, Chem. Rev. **33** (1943) 209-256.

[5] MENDEZ, R.M., PILLAI, V.N.S., Synthesis, characterization and analytical application of a hydroxamic acid resin, Talanta **37** (1990) 591-594.

[6] AGRAWAL, Y.K., KAUR, H., MENON, S.K., Poly(styrene-p-hydroxamic acids): synthesis, and ion exchange separation of rare earths, React. Funct. Polym. **39** (1999) 155-164.

[7] PHILIPS, R.J., FRITZ, J.S., Synthesis and analytical properties of an n-phenyl-hydroxamic acid resin, Anal. Chim. Acta. **121** (1980) 225-232.

[8] VERNON, F., DHAD, T., The extraction of uranium from seawater by poly(amidoxime)/poly(hydroxamic acid) resins and fibre, Reac. Polym. **1** (1983) 301-308.

[9] ATHAWALE, V.D., LELE, V., Graft copolymerization onto starch. II. Grafting of acrylic acid and preparation of its hydrogels, Carbohyd. Polym. **35** (1998) 21-27.

[10] SHIRAISHI, T., TAMADA, M., SAITO, K., SUGO, T., Recovery of cadmium from waste of scallop processing with amidoxime adsorbent synthesized by graft-polymerization, Radiat. Phys. Chem. **66** (2003) 43-47.

[11] BASAKI, F., SEKO, N., TAMADA, M., SUGO, T., KUME, T., Direct synthesis of adsorbent having phosphoric acid with radiation induced graft polymerization, J. Ion Exchange **14** (Supplement) (2003) 209-212.

[12] CHOI, S., NHO, Y. Adsorption of UO_2^{+2} by polyethylene adsorbents with amidoxime, carboxyl, and amideoxime/carboxyl group, Radiat. Phys. Chem. **57** (2000) 187-193.

[13] CHOI, S., LEE, K., LEE, J., NHO, Y., Graft copolymer-metal complexes obtained by radiation grafting on polyethylene film, J. Appl. Polym. Sci. **77** (2000) 500-508.

[14] ZHU, X., JYO, A., Column-mode phosphate removal by a novel highly selective adsorbent, Water Research **39** (2005) 2301-2308.

[15] KUGARA, J., TROBRADOVIC, H., JYO, A., SUGO, T., TAMADA, M., KATAKAI, A., Behavior of iminodiacetate fiber in column-mode adsorption of lead (III), J. Ion Exchange **14** (Supplement) (2003) 77-80.

[16] BONDAR, Y., KIM, H.J., YOON, S.H., LIM, Y.J., Synthesis of cation-exchange adsorbent for anchoring metal ions by modification of poly(glycidyl methacrylate) chains grafted onto polypropylene fabric, React. Funct. Polym. **58** (2004) 43-51.

RADIATION-INDUCED GRAFTING FOR THE SYNTHESIS OF ADSORBENTS FOR PHOSPHATE AND CHROMATE REMOVAL FROM AQUEOUS SYSTEMS

P.A. KAVAKLI, C. KAVAKLI, O. GÜVEN

Department of Chemistry
Hacettepe University
Beytepe, 06800, Ankara
TURKEY

Abstract

Nonwoven fabrics made of PE coated PP fibres were irradiated by accelerated electrons in inert atmospheres for grafting of two different monomers, glycidyl methacrylate and dimethylaminoethyl methacrylate. Grafting conditions were optimized by a systematic investigation of the effects of absorbed dose, monomer concentration, grafting reaction temperature and duration. 150% grafted copolymers were later modified by protonation and quaternization of poly(dimethylaminoethyl methacrylate) chains and by Cu(II) loading of dipyridyl amine modified poly(glycidyl methacrylate) graft chains. The PE/PP based adsorbents thus prepared were used for their suitability of removing phosphate and chromate ions from aqueous systems. Adsorption/removal studies were carried out in both batch and continuous flow type systems. The selectivity of adsorption of phosphate ions in the presence of other competing anions were also checked showing the enhanced selectivity for phosphate ions.

1. OBJECTIVE OF THE RESEARCH

To develop nonwoven fabric based adsorbents by radiation-induced grafting of some selected monomers for further functionalization toward efficient removal of anions and in particular phosphate and chromate ions from aqueous systems.

2. INTRODUCTION

Water resources have been and continue to be contaminated with biologically and environmentally resistant pollutants from industrial, municipal and agricultural discharges. Pollution coming from these resources includes untreated sewage, chemical discharges, petroleum leaks and spills and agricultural chemicals that are washed off from farm fields.

The short and long term consequences of these polluted waters causing a serious threat to mankind have led the scientists and technologists to look for developing new technologies for treatment of wastewaters. A variety of methods based on biological, chemical, photochemical and electrochemical processes are being explored for treating the chemical and biological contaminants present in wastewaters. The number and kind of chemical and biological species causing pollution in especially drinking water sources are enormous mainly consisting of ionic and molecular products. Among the ionic pollutants phosphorus containing anionic species requires special attention.

Phosphates are not toxic to people or animals unless they are present in very high levels. Digestive problems could occur from extremely high levels of phosphate. Phosphorus can provide an additional nutrient for growth of photosynthetic macro- and microorganisms in aquatic bodies, but also leading to the eutrophication problem especially in enclosed water bodies. The removal of phosphate from waters can be an effective method for the control of eutrophication in natural waters. Phosphorus concentrations in excess of 0.03–0.05 mg/L have been associated with algae blooms, which lead to the eutrophication of lakes and rivers [1–3]. In order to decrease eutrophication in lakes and other water sources, concentration of phosphorus must be limited to 0.01 mg/L or less [4]. Extensive studies on the effective treatment of phosphates in water systems have been previously conducted [5–8]. The major methods for the removal of phosphate include precipitation and coagulation, as well as adsorption or ion exchange process. The precipitation and coagulation processes with iron (III) [9], aluminium [10], calcium [11], and lanthanum salts [12], which convert anions into insoluble form, have been widely used. Although the precipitation and coagulation method is simple and economical, this process will result in a wet bulky sludge disposal problem and requires final filtration for secondary treatment.

Moreover, the ion–exchange process using ion exchangers has also been identified as a treatment method for phosphate removal [8]. The process development for the removal and recovery of phosphorus from wastewater using enhanced activated alumina has been published in a series by Urano and Tachikawa [13]. They reported that the enhanced activated alumina can adsorb various inorganic phosphorus species in a pH range of 4–7. Recently, a new class ion-exchange sorbent after treatment of commercial DOW 3N polymer with copper solution which is designated as DOW 3N-Cu or PLE (polymeric ligand exchanger) used for the selective removal of phosphates from contaminated water [7]. A PLE consists of a polymer with chelating functional groups that can bind tightly to a transition metal, which can remove anions from water by complex formation. PLE used in the above mentioned work is basically a copper-loaded chelating ion exchanger with styrene-divinylbenzene polymer matrix designed to effectively remove divalent phosphate ion (HPO_4^{2-}) at above neutral pH. The results appeared technically feasible. However, in actual municipal and industrial wastewater, where the pH widely varies, the existence of other forms of phosphate ions such $H_2PO_4^-$, HPO_4^{2-} and PO_4^{3-} or other species is inevitable due to nature of phosphate originating from a polyprotic acid. In such a case, PLE sorbent becomes technically ineffective unless those phosphate species are first converted into divalent form and then the pH of the solution is adjusted to above the neutral range for adsorption. Therefore, it is very important to use an adsorbent that can adsorb various species of phosphates and that can work effectively in a wide range of pH.

Chromium compounds are extensively used in electroplating, anodizing operations in the surface finishing industry, corrosion control, oxidation, leather industry and various other industrial applications. The effluents from these industries contain Cr(III) and Cr(VI) with the latter being the most toxic form. The discharge of Cr(VI) into surface water is regulated to be below 0.05 mg/L while total Cr (including Cr(III), Cr(VI) and other forms) is regulated to be below 2 mg/L. Cr(III) is not a significant groundwater contaminant whereas Cr(VI) is approximately 100 times more toxic than Cr(III).

Graft polymerization on polymeric matrixes followed by functionalization is widely used for the surface modification of adsorbent materials. The polymeric adsorbents prepared in different forms (hollow fibre, nonwoven fabric, film) with varied concentration of ion-exchange groups enhance adsorption efficiency of the adsorbents [14–17]. Graft polymerization can be initiated by using γ rays, electron beams, ultraviolet, plasma treatment, and chemical initiators. Among these methods, ionizing radiation is one of the most promising methods, because of ease of creation of active sites for initiating grafting through the polymeric substrate and moderate reaction conditions. Radiation–induced grafting being a clean technique [18] is a convenient method for the modification of physical and chemical properties of polymeric materials [19–21]. Radiation grafted adsorbents have been used usually for separation and wastewater treatment processes [22–26]. Several types of ion exchange matrices have been prepared by grafting monomers like acrylic acid, methacrylic acids, acrylonitrile on trunk materials like polyethylene and polypropylene [27–29].

3. MATERIALS AND METHODS

3.1. Radiation–induced grafting of functional monomers onto PE/PP non-woven fabric

3.1.1. Grafting of glycidyl methacrylate (GMA)

The preparation of nonwoven fabric adsorbents based on GMA grafting and further functionalization requires two steps: (1) grafting of an epoxide group containing monomer, glycidyl methacrylate (GMA) by preirradiation grafting technique and (2) modification of epoxy group with a proper ligand.

First GMA was grafted onto PE coated PP nonwoven fibres by preirradiation technique as described above. The concentration of GMA solution was set at 10% (w/w) in methanol as the solvent. The degree of grafting was calculated as described above. GMA grafted fabrics with 150% graft ratio was used for the further characterizations and modifications as this graft ratio was found to be the optimum in one of our previous publications [30].

Functionalization of GMA grafted fabrics

Following the grafting of GMA, epoxide groups in grafted nonwoven fabric were reacted with different chemicals such as triazol, dipicolylamine, dipyridylamine (DPA). In this second step, effect of solvent, ligand concentration and the reaction time were investigated to achieve an optimized reaction condition. Modifications were performed in four solvents; methanol, ethanol, dimethylsulfoxide (DMSO) and dioxane. In a typical modification reaction, approximately 0.5 g of GMA grafted nonwoven fabric was immersed in 25 mL of DPA containing solutions. Three different DPA concentrations were examined: 5%, 10% and 15%, w/v. The reaction was performed at 80°C for different time periods to construct the conversion curve. After binding of DPA onto the epoxide group of GMA grafted polymer, the remaining unreacted epoxy groups were hydrolyzed with acid solution for 2 h at 80°C. Subsequently nonwoven fabric was washed with methanol and then was dried at room temperature and in a vacuum oven at 40°C. The percent replacement of the epoxide groups with DPA was calculated as follows:

$$\text{Conversion (\%)} = \text{mmol DPA} / \text{mmol GMA} \qquad (1)$$

Preparation of Cu-loaded polymeric ligand exchangers

Preparation of polymeric ligand exchanger (PLE) was conducted by loading Cu(II) onto DPA modified PP/PE fabric. For this purpose approximately 0.5 g of DPA immobilized fabric was placed into 200 mL of 1500 ppm Cu(II) ion solution at pH~4 in a bottle stirred magnetically at moderate rpm for a given time period. The time needed was predetermined in a separate adsorption kinetics study. In order to determine the amount of Cu(II) ions loaded onto the fabric, Cu(II) ion concentration remaining in the solutions was determined by using an UV-Vis spectroscopic technique [31]. The amount of Cu(II) ion adsorbed per unit mass of PP/PE fabric was evaluated using the following expression,

$$q_e = \frac{(C_e - C_0) \times V}{W} \qquad (2)$$

where, q_e is the amount of Cu(II) ions adsorbed onto unit dry mass of PP/PE fabric (mg/g); C_0 and C_e are the concentrations of Cu(II) ion solutions (mg/L) prior and after the treatment for a certain period of time, respectively; V is the volume of aqueous phase (L) and W is the amount of dry fabric used (g).

3.1.2. Grafting of dimethylaminoethylmethacrylate (DMAEMA)

A new adsorbent was prepared by radiation-induced graft polymerization of DMAEMA onto polyethylene/polypropylene (PE/PP) nonwoven fabric. The PE/PP nonwoven fabrics cut into pieces of 10 cm by 5 cm were sealed in polyethylene bags purged with nitrogen gas. The trunk polymer was irradiated by an electron beam (2 MeV, 3 mA) at dry-ice temperature to different doses. The irradiated fabrics were immersed in different concentrations of DMAEMA solutions ranging from 5% (w/w) to 20% in water at different temperatures. After a pre-determined period, the DMAEMA grafted nonwoven fabrics were removed from the grafting solution, washed several times with distilled water and methanol to remove the homopolymer and residual monomer and dried under reduced pressure. The degree of grafting was determined gravimetrically as a function of dose, monomer concentration, temperature, and reaction time.

The degree of DMAEMA grafting (Dg) was determined by using the following expression:

$$\text{Dg (\%)} = [(W_1 - W_0)/W_0] \times 100 \qquad (3)$$

where W_0 and W_1 are the weights of the trunk and DMAEMA grafted nonwoven fabrics in dry state.

3.1.2.1. Protonation of the DMAEMA grafted fabrics

Grafting conditions were optimized, and DMAEMA grafted polymer was later protonated by using acid solution to prepare an adsorbent for the removal of anions. DMAEMA grafted nonwoven fabric was placed into 1 M HCl solution for 24 h at room temperature. The protonated DMAEMA grafted nonwoven fabric was removed from the solution and washed with distilled water to remove unreacted acid and kept in wet form for the adsorption tests.

3.1.2.2. Quaternization of the DMAEMA grafted fabrics

Particular amount of DMAEMA grafted fabric was immersed in DMF solution of dimethyl sulphate. The grafted fabrics placed in this solution were heated in thermostated oil bath at 65°C under nitrogen atmosphere for 24 h with stirring. The fabric was removed from reaction medium and then washed with DMF, water and methanol several times and dried under vacuum at room temperature, according to literature [32]. After quaternization, the sulphate form of fabric adsorbent was converted to chloride form by using HCl.

3.2. Continuous flow adsorption tests

By dissolving analytical grade sodium dihydrogen phosphate (NaH_2PO_4) in water 100 ppb phosphate (as P) solution was prepared. The solution was passed through protonated DMAEMA grafted nonwoven fabric adsorbent-packed in 7 mm inner diameter column. The phosphate solution was fed into fabric adsorbent-packed column at two flow rates (space velocities, SV) 250 h^{-1} and 1000 h^{-1}. Column effluents were collected by a fraction collector (Advantec SF2100). The concentration in each fraction was measured by an inductively coupled plasma-optical emission spectrometer (ICP-OES, Perkin Elmer, Optima 5200).

3.3. Batch adsorption experiments

Batch adsorption experiments with quaternized DMAEMA grafted fabrics for phosphate and chromate removal were conducted by using both low (0.5–25 ppm) and high ion concentrations (50 – 1000 ppm). The effect of pH on phosphate and chromate adsorption was studied at different pH values with the same initial phosphate and chromate concentration (100 mg anion/L). Competitive adsorption experiments were also carried out with two concentration levels (low concentration: 1 ppm phosphate, 1 ppm bromide, 1 ppm nitrite, 10 ppm sulphate and 10 ppm nitrate mixture and high concentration: 50 ppm phosphate, 50 ppm bromide, 50 ppm nitrite, 500 ppm sulphate and 500 ppm nitrate mixture). The pH of the solution was adjusted by either HCl or NaOH solution. The phosphate and chromate ion concentrations in the equilibrated solutions were measured with the UV-Visible Spectrophotometer (Carry 100, Varian) by using ammonium molybdate method and diphenylcarbazide method, respectively [33–34]. Phosphate, bromide, nitrite, sulphate and nitrate analyses were carried out by using a Dionex Ion Chromatograph (DIONEX ICS 3000, USA).

4. RESULTS AND DISCUSSION

4.1. Grafting of glycidyl methacrylate (GMA) and functionalization of GMA grafted fabrics

DPA was immobilized onto GMA grafted nonwoven fabric with 150% graft ratio by a reaction between the epoxy rings of GMA grafts and the amine group of DPA (the details of the preparation of GMA grafted fabric can be found in our previous publication) [16]. The percent replacement of the epoxide groups by DPA was calculated by eq. (1) and the modifications were tested in four different solvents; methanol, ethanol, dioxane and DMSO. Modifications in methanol and ethanol resulted in similar DPA replacement ratios which were lower than those obtained in other two solvents. The conversion (i.e. replacement) ratio obtained in DMSO was slightly lower than that observed in dioxane (both were around 70% at 80 h). As the boiling point of dioxane is lower than DMSO, we preferred this solvent as it offers an easier removal after the modification. The effect of DPA concentration on the conversions was also investigated in three solvents having different amounts of DPA (i.e., 5%, 10% and 15% DPA (w/v)) in dioxane (Figure 1). Figure 1 shows that the conversion of epoxides has not been fully completed (most probably due to inactivation of some epoxy rings during the grafting process and difficulty in access to sterically hindered ones) and a maximum of ~70% conversion has been achieved for all concentrations examined at the end of 80 h reaction time. Figure 1 indicates that the effect of DPA amount is more distinct at lower reaction times, e.g. the conversion is around 8%, 44% and 49% for the solutions having 5%, 10% and 15% DPA, respectively at 40 h. This shows that the replacement of epoxy groups by DPA is quicker at high concentrations. However, the difference becomes indistinct in longer time, and the maximum conversion reaches to ~70% at 80 h for all the concentrations studied. Functionalization of GMA grafted nonwoven fabrics was therefore achieved in 5% DPA (w/v) containing solutions for monomer saving and these adsorbents (the exact conversion value is 76%) were used in all experimental characterizations and further metal ion uptake studies. The detail preparation condition and results were given in our previous paper [35].

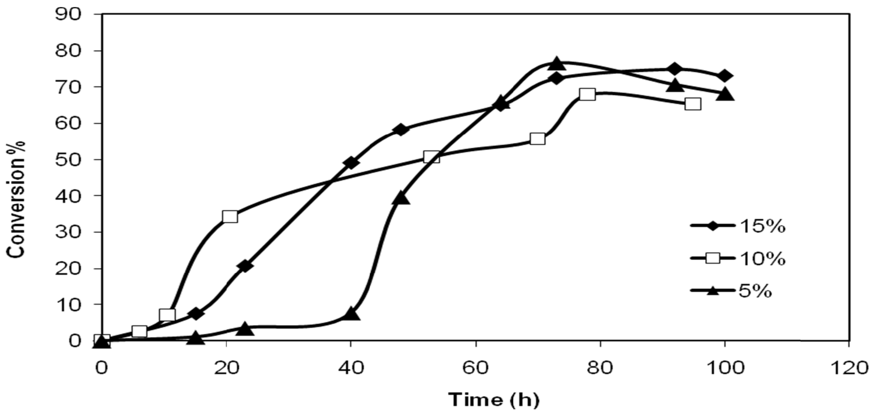

FIG. 1. Effect of DPA concentration (w/v) on the conversion of epoxide groups of GMA; GMA grafted nonwoven fabric with 150% grafting, in dioxane as, at 80°C.

4.2. Preparation of the protonated and quaternized DMAEMA grafted nonwoven fabric

The preparation of DMAEMA grafted nonwoven fabric requires two steps as shown in Fig. 2. (1) Grafting of DMAEMA monomer by pre-irradiation grafting technique and (2) Protonation of amine groups by using acid solution.

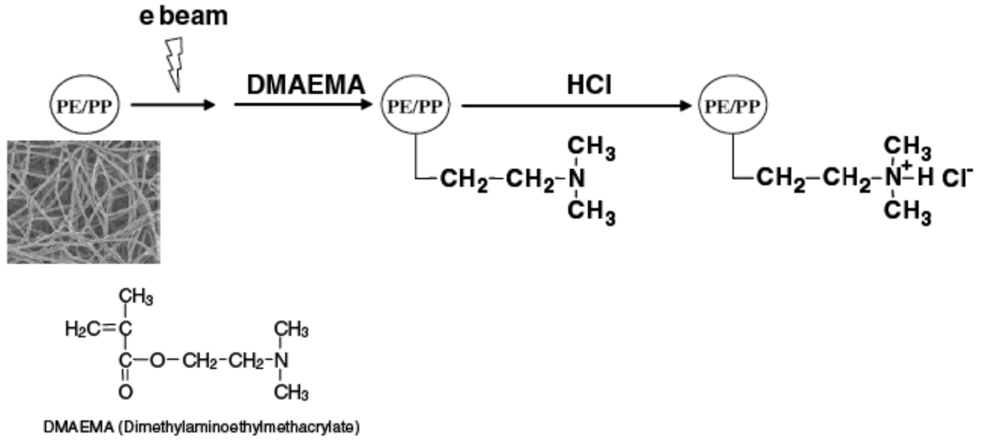

FIG. 2. Schematic preparation of DMAEMA grafted nonwoven fabric adsorbent.

The effect of dose and initial monomer concentration on degree of grafting (Dg) of DMAEMA were investigated. For this purpose, PE/PP nonwoven fabric was irradiated at four different doses (30, 50, 100 and 200 kGy) by an electron accelerator in nitrogen atmosphere at dry ice temperature (-20ºC). Irradiated nonwoven fabrics were then reacted with three different monomer concentrations (5%, 10% and 15%). The results shown in Fig. 3 indicate that the maximum grafting was achieved at 200 kGy dose and 15% monomer concentration at 4 hours reaction time. The grafting yield of DMAEMA increases with the increasing dose due to the formation of more free radicals at higher doses. But this reaction medium was not chosen as the optimum grafting condition due to reduced flexibility of the nonwoven fabric at this dose. It was also observed that at higher degrees of grafting (>200%), the cloth became even brittle. Considering these unwanted properties, 50 kGy dose, 15% monomer concentration and 4 h reaction time were selected as optimum conditions for the preparation of DMAEMA grafted nonwoven fabrics. The detailed preparation conditions of DMAEMA grafted fibres were given in our previous paper [30]. Recently, DMAEMA grafting onto polypropylene films by using radiation induced graft polymerization has been reported by Chen et al. [17]. 170% degree of grafting for DMAEMA was obtained at 200 kGy dose, 20% DMAEMA concentration and 4 h reaction times in EtOH/H_2O.

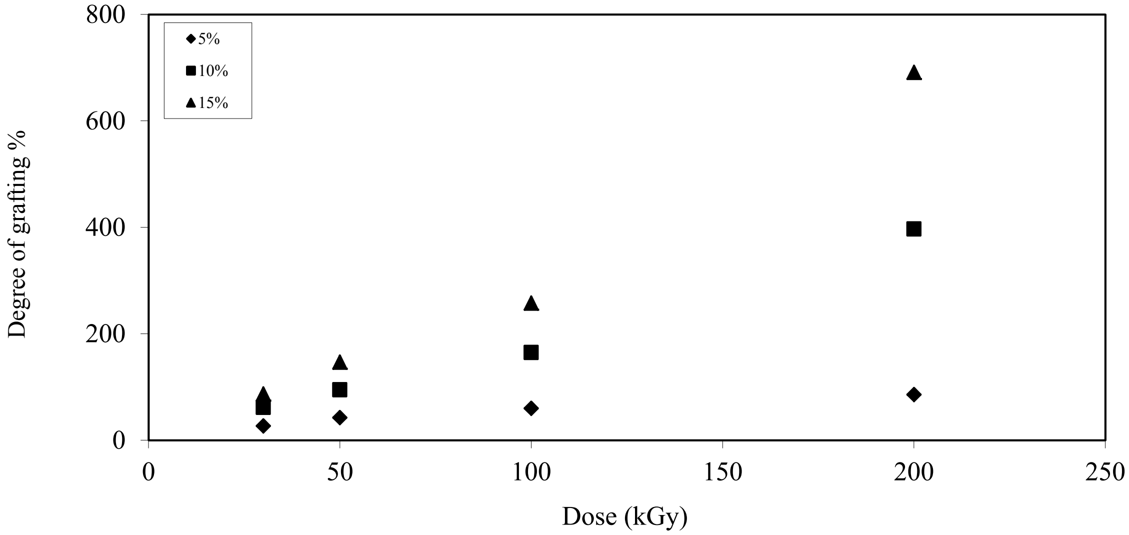

FIG. 3. Change in degree of grafting with dose for fabrics at indicated DMAEMA concentrations.

After grafting of DMAEA, the tertiary amine group of DMAEMA graft chain was then protonated by using acid solution and chemically treated with dimethyl sulphate to obtain quaternized DMAEMA grafted nonwoven fibre having ion exchange properties. Approximately 90% quaternization was obtained in 24 hours.

4.3. Adsorption of phosphate

4.3.1. Adsorption of phosphate by using DPA modified GMA grafted nonwoven fabric

The performance of polymeric ligand exchanger (PLE) was investigated with respect to adsorption kinetics, adsorption and desorption behaviour and pH effects toward the target phosphate anion. The pH of the aqueous solution is an important variable influencing the adsorption process especially in ion exchangers. Phosphate species present in water include H_3PO_4, $H_2PO_4^-$, HPO_4^{2-} and PO_4^{3-}, and their relative amounts depend on the pH of the medium. Experiment was performed for five different pH values ranging from 5 to 9 and it was observed that phosphate adsorption did not change virtually within the studied pH range. This shows that adsorbent material can effectively remove different forms of phosphate ions, namely H_3PO_4, $H_2PO_4^-$, HPO_4^{2-} and PO_4^{3-} from aqueous solution at each pH value where these species exist.

The effect of initial concentration of phosphate on the adsorption behaviour of PLE was determined in 8 h contact time for five solutions (50 mL) with different phosphate concentrations (10, 50, 100, 250, and 500 ppm) at pH 7 and the adsorption amounts were given in Figure 4. Figure 4 shows that, the new PLE exhibited a very high affinity for phosphate at low concentration levels reaching a value of 16 mg of phosphate/g dry PLE from 10 ppm phosphate solution. It was found that adsorption of phosphate by Cu-loaded fabrics increased with increasing phosphate concentration and 101 mg/g dry PLE phosphate adsorption was obtained from 500 ppm phosphate solution.

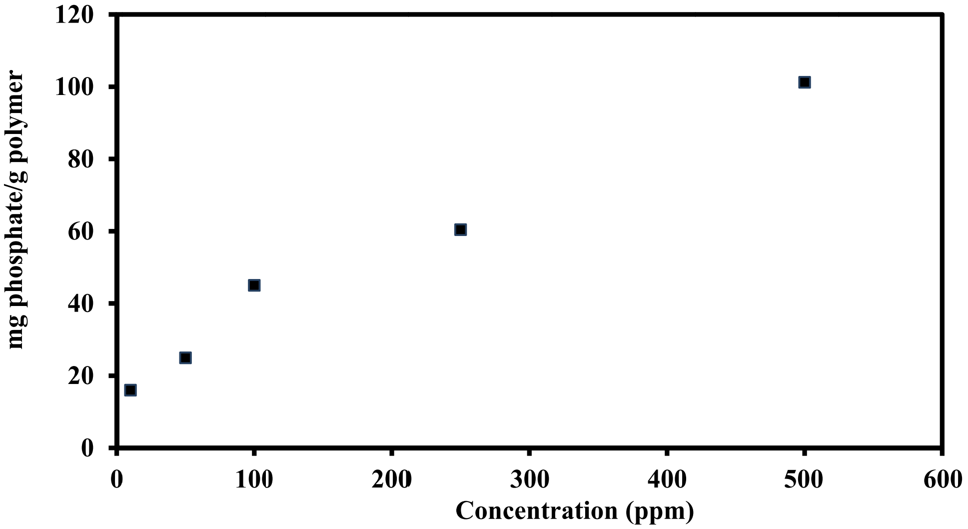

FIG. 4. Effect of initial concentration of phosphate on the adsorption behaviour of the PLE.

Anion selectivity studies were also achieved using ion chromatography and the quantitative determination of anions was presented in Figure 5. For the solution with low concentrations, phosphate adsorption is the significantly highest one among the others with a removal of around 82%. The adsorption order is phosphate >> nitrate ≈ bromide > nitrite ≈ sulphate. However for the solution with high concentration the selectivity among the anions disappears; all the anions present a removal ratio ranging between 38% and 26%. This shows that although the adsorbent is selective to phosphate at lower concentrations, it also adsorb competing ions among them phosphate ion at high concentrations. Therefore can be concluded that the prepared PLE is suitable for the specific removal of trace amounts of phosphate from aqueous solution.

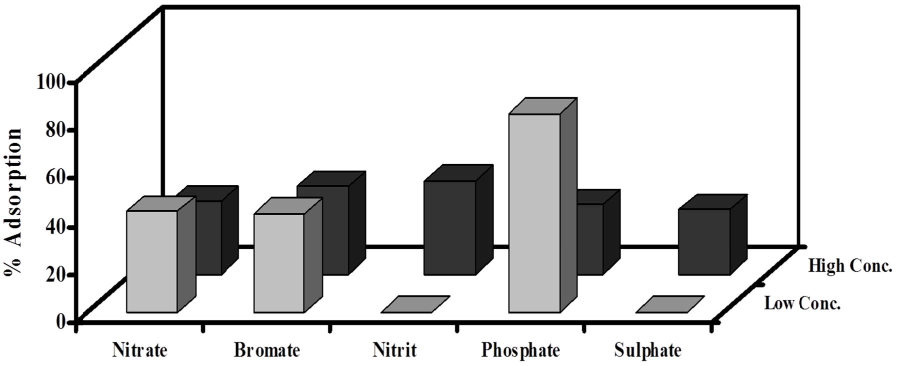

FIG. 5. Adsorption selectivity of PLE. Low concentration: 1 ppm phosphate, 1 ppm bromide, 1 ppm nitrite, 10 ppm sulphate and 10 ppm nitrate. High concentration: 50 ppm phosphate, 50 ppm bromide, 50 ppm nitrite, 500 ppm sulphate and 500 ppm nitrate.

The PLEs should be suitable for efficient regeneration so that they can be used for multiple cycles of operations. Sodium chloride is an ideal regenerator as it is easily available, inexpensive and nontoxic. Therefore, 6% of NaCl solution was used for regeneration of phosphate adsorbed by the PLEs. Ion chromatography was used for the determination of regeneration amount. PLEs easily desorbed the loaded phosphate under given conditions and were reusable. High regeneration efficiencies were achieved with a phosphate recovery of nearly 100%.

4.3.2. Adsorption of phosphate by using protonated DMAEMA grafted nonwoven fabric

Adsorption experiments were performed in column mode for removal of phosphate ions by using protonated DMAEMA grafted nonwoven fabric. Figure 6 shows the adsorption characteristics of phosphate ions on protonated DMAEMA grafted nonwoven fabric by plotting C/C_0 vs. bed volumes. Here C and C_0 are effluent and feed solution concentrations of anion and bed volume is defined as the ratio of feed solution volume to the fixed polymer bed volume (mL feed solution/mL polymer). Flow rate is calculated as the bed volumes of feed solution hourly provided (h^{-1} in space velocity) [36]. Approximately 2000 bed volumes (BV) of phosphate-free water can be produced from 10 ppb phosphate solution at low (250 SV) and high (1000 SV) space velocities. After 2000 BV, phosphate adsorption showed breakthrough gradually.

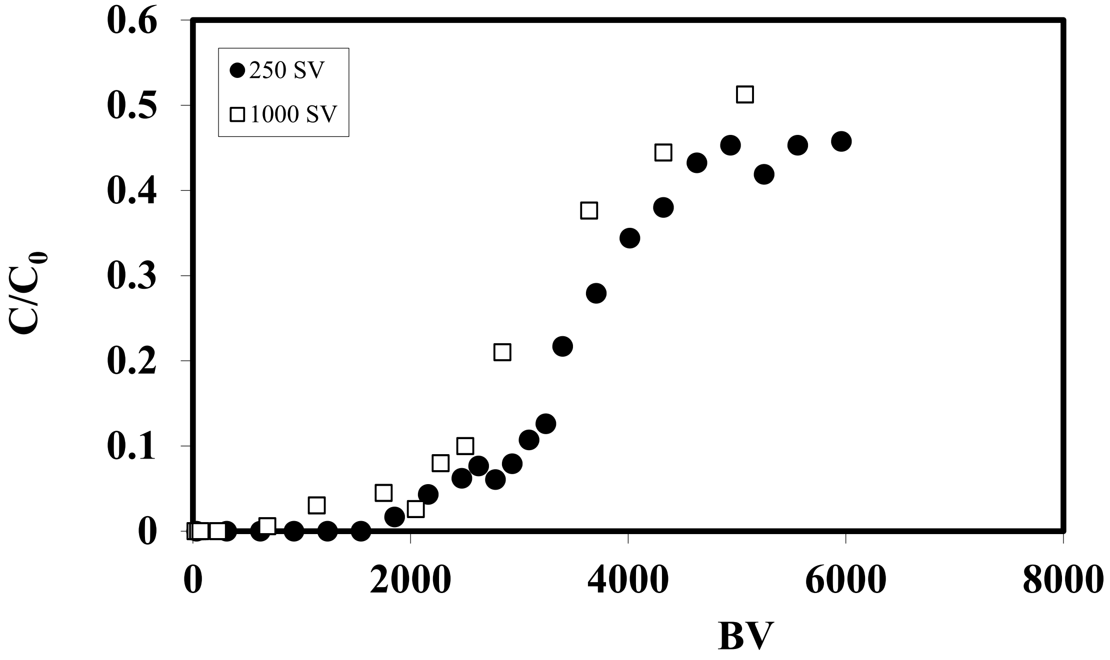

FIG 6. Breakthrough curves for phosphate removal at indicated space velocities (SV).

4.3.3. Adsorption of phosphate by using quaternized DMAEMA grafted nonwoven fabric

Figure 7 and 8 show adsorption of phosphate ions at low phosphate concentrations (0.5–25 ppm) and high phosphate concentrations (50–1000 ppm) at pH 7.00 on quaternized DMAEMA grafted fabrics, respectively. Both results showed that the adsorption of phosphate ions increases linearly with increasing the initial feed concentration both at low and high phosphate concentrations due to density of ion exchange sites on the adsorbent. Adsorbed phosphate amounts were found to be 63 mg phosphate/g polymer and 512 mg phosphate/g polymer for low phosphate concentration (25 ppm) and high phosphate concentration (1000 ppm), respectively. This result shows that the adsorbent material quite effective in removing phosphate in wide concentration range. Detailed adsorption results were given in our previous paper [37].

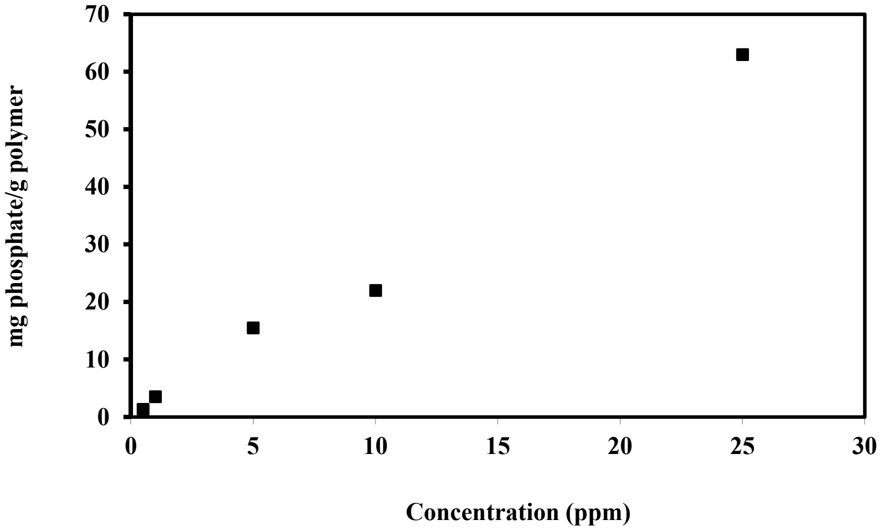

FIG. 7. Phosphate uptake onto quaternized DMAEMA grafted nonwoven fabric at low phosphate concentrations at pH 7.

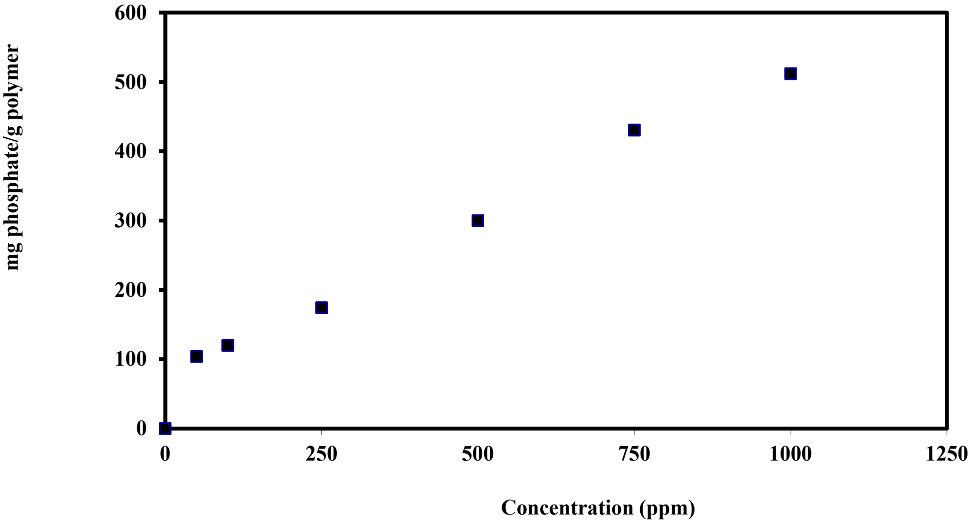

FIG. 8. Phosphate uptake onto quaternized DMAEMA grafted nonwoven fabric at high phosphate concentrations at pH 7.

4.4. Effect of competing anions on phosphate adsorption

Figure 9 shows the effect of competing ions at two concentration levels at pH 7. Phosphate adsorption on quaternized DMAEMA grafted nonwoven fabric was higher than the other competing ions at two concentration levels. At high concentration level, the adsorption order was phosphate > nitrite > bromide > sulphate > nitrate and at low concentration level, the adsorption order was phosphate ≅ sulphate > bromide > nitrite > nitrate, respectively. These results indicate that adsorbent can also adsorb competing ions beside phosphate ion which is a normal (expected result) effect due to relative affinities of anions toward adsorbent. 6% of NaCl solution was used for regeneration of phosphate adsorbed quaternized DMAEMA grafted nonwoven fabric. High regeneration efficiencies were achieved with a phosphate recovery of nearly 100%.

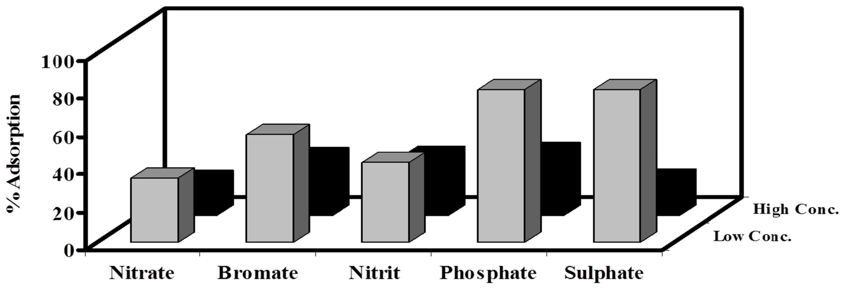

FIG. 9. Adsorption selectivity of quaternized DMAEMA grafted nonwoven fabrics for indicated anions: 50 ppm and 1 ppm of phosphate, bromide, nitrite and 500 ppm and 10 ppm of sulphate and nitrate, respectively.

It was concluded that the protonated and quaternized DMAEMA grafted nonwoven fabric have higher adsorption capacity for phosphate ions than the DPA modified GMA grafted nonwoven fabric. The explanation can be given as follows; DMAEMA grafted nonwoven fabric was obtained as a homopolymer directly from dimethylaminoethylmethacrylate monomer but the DPA modified GMA grafted nonwoven fabric was firstly grafted with GMA (glycidyl methacrylate) and then modified with 2,2'- dipyridylamine (DPA) with a maximum of ~70% conversion.

4.5. Adsorption of chromate by using quaternized DMAEMA grafted nonwoven fabric

In order to investigate the adsorption kinetics of chromate ion onto quaternized DMAEMA grafted nonwoven fabric, approximately 0.015 g of adsorbent was treated with 100 ppm chromate solution at pH 6. Figure 10 shows the adsorption kinetic of chromate ion onto quaternized DMAEMA grafted PE/PP nonwoven fabric. The adsorbed amounts are given as the percentage of metal ions initially present. High adsorption rate is observed for chromate ion and the plateau values (i.e., adsorption equilibrium) were reached approximately at 100% removal of chromate within 10 min.

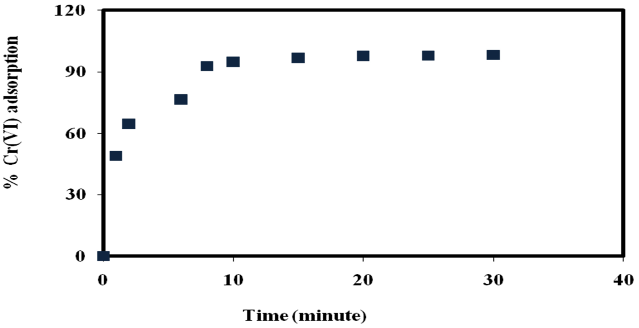

FIG. 10. Adsorption kinetics of chromate ion from 100 ppm chromate solution.

Figure 11 shows the relationships between chromate adsorption and solution pH. The quaternized DMAEMA grafted fabric adsorbs chromate over a wide pH range (4–8). This trend shows that quaternized DMAEMA grafted nonwoven fabric can be effectively used for removing chromate from water at about pH 7.

Figures 12 and 13 show adsorption of chromate ions at 0.5–5 ppm and at 50–1000 ppm concentrations (pH 6) on quaternized DMAEMA grafted fabrics, respectively. Both results showed that the adsorption of chromate ions increases with increasing initial feed concentration both at low and high chromate concentrations due to density of ion exchange sites on the adsorbent. Adsorbed amounts were 1.3 mg chromate/g polymer and 125 mg chromate/g polymer for 5 ppm and 1000 ppm chromate concentration, respectively. Table 1. shows that quaternized DMAEMA grafted PE/PP nonwoven fabric is quite effective in removing chromate as compared with similar adsorption studies in literature.

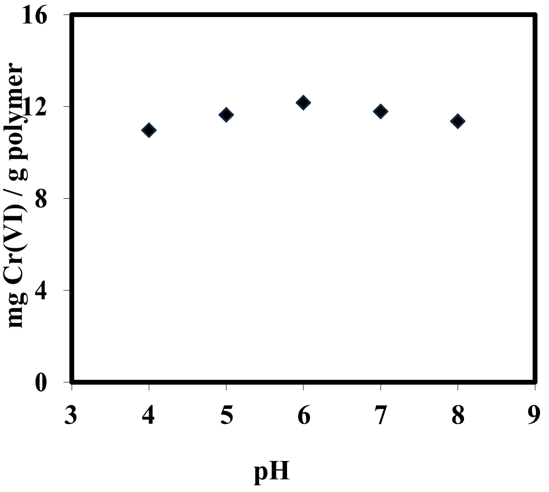

FIG.11. pH effect on chromate uptake onto quaternized DMAEMA grafted nonwoven fabric from 100 ppm chromate solution.

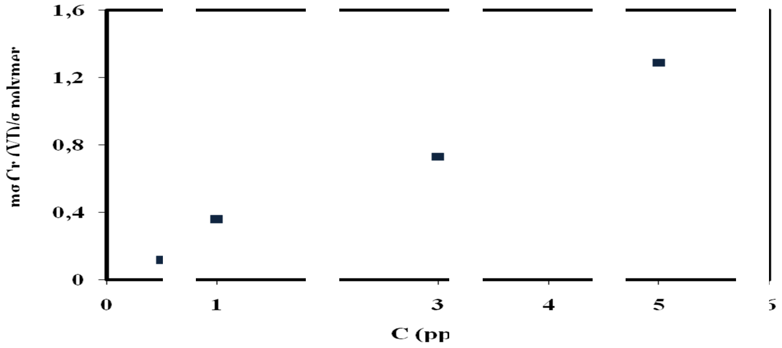

FIG. 12. Chromate uptake onto quaternized DMAEMA grafted nonwoven fabric at low concentration levels at pH 6.

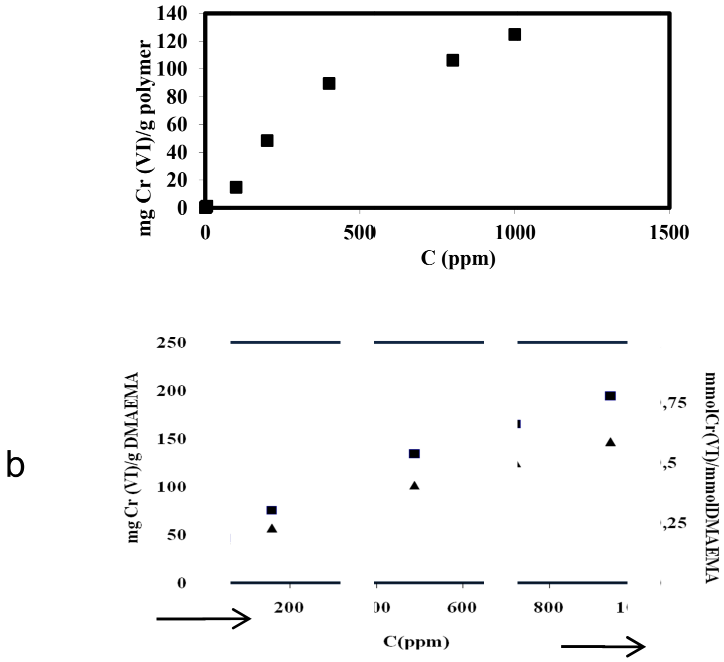

FIG. 13. Dependence of Cr(VI) uptake on the initial concentrations of Cr(VI) ion a) as milligram of adsorbed Cr(VI) per gram polymer b) as milligram of adsorbed Cr(VI) per gram DMAEMA unit and mill molar of adsorbed Cr(VI) per gram DMAEMA unit at high concentration levels at pH 6.

TABLE 1. A COMPARISON OF Cr(VI) ADSORPTION USING VARIOUS POLYMERIC ADSORBENTS

Polymeric Adsorbent	mg Cr(VI)/g polymer
Solvent impregnated resins containing Aliquat 336 [38]	48
Quaternary ammonium moieties immobilized on glycidylmethacrylate/N,N-methylene bis-acrylamide resin. [39]	50
This work	125

5. CONCLUSIONS

Radiation-induced graft polymerization is an easy and highly efficient surface modification procedure for functionalization of polymeric materials. Environmentally stable PE/PP nonwoven fibres were used as base material for the synthesis of a new adsorbent for anions. To introduce specific functional groups to the trunk polymer, GMA and DMAEMA were grafted onto preirradiated fabrics. Following the grafting of GMA and DMAEMA, epoxide groups in GMA grafted nonwoven fabric were reacted with DPA and the tertiary amine group of DMAEMA graft chains were protonated by using acid solution and quaternized by using dimethyl sulphate for removal of phosphate ions in aqueous solutions. The protonated and quaternized DMAEMA grafted nonwoven fabrics were found to have higher adsorption capacity for phosphate ions than the DPA modified GMA grafted nonwoven fabric. The quaternized DMAEMA grafted nonwoven fabric have also high adsorption capacity for chromate ions from aqueous media containing different concentrations in wide pH range.

REFERENCES

[1] BHARGAWA, D.S., SHELDARKAR, S.B., Use of TNSAC in phosphate adsorption studies and relationships – literature, experimental methodology, justification and effects of process variables, Water Res. **27** (1993) 303-312.

[2] CHEUNG, K.C., VENKITACHALAM, T.H., Improving phosphate removal of sand infiltration system using alkaline fly ash, Chemosphere **41** (2000) 243-249.

[3] UĞURLU, A., SALMAN, B., Phosphorus removal by fly ash, Environ. Int. **24** (1998) 911-918.

[4] KNEY, A. D., ZHAO, D., A pilot study on phosphate and nitrate removal from secondary wastewater effluent using a selective ion exchange process, Environ. Technol. **25** (2004) 533-542.

[5] ZHAO, D., SENGUPTA, A.K., Selective removal and recovery of phosphate in a novel fixed-bed process, Water Sci. Technol. **33** (1996) 139-147.

[6] ZHAO, D., SENGUPTA, A.K., Ultimate removal of phosphate from wastewater using a new class of polymeric ion exchangers, Water Res. **32** (1998) 1613-1625.

[7] ZHAO, D., SENGUPTA, A.K., Ligand separation with a copper(II)-loaded polymeric ligand exchange, Ind. Eng. Chem. Res. **39** (2000) 455-462.

[8] BOKI, K., TANADA, S., Phosphate removal by adsorption to activated carbon, Jpn. J. Hygiene, **42** (1987) 710.

[9] CHEN, S.L., DZENG, S.R., YANG, M.H., CHIU, K.H., SHIEH, G.M., WAI, C.M., As species in groundwaters of the black-foot disease area, Taiwan, Environ. Sci. Technol. **28** (1994) 877-881.

[10] McNEILL, L.S., EDWARDS, M.J., Predicting arsenic removal during metal hydroxide, J. Environ. Eng. **123** (1997) 453-460.

[11] SORG, T.J., in Proc. Water Qual. Technol. Conf. (1993).

[12] TOKUNAGA, S., YOKOYAMA, S., WASAY, S.A., Removal of arsenic(III) and arsenic(V) ions from aqueous solutions with lanthanum(III) salt and comparison with aluminium(III), calcium(II), and iron(III) salts, Water Environ. Res. **71** (1999) 299-306.

[13] URANO, K., TACHİKAWA, H., Process development for removal and recovery of phosphorus from wastewater by a new adsorbent. 1. Preparation method and sorption capacity of a new adsorbent, Ind. Eng. Chem. Res. **30** (1991) 1893-1896.

[14] SAITO, K., ITO, M., YAMAGISHI, H., FURUSAKI, S., SUGO, T., OKAMOTO, J., Novel hollow fiber membrane for the removal of metal ion during permeation: preparation by radiation-induced cografting of a crosslinking agent with reactive monomer, Ind. Eng. Chem. Res. **28** (1989) 1808-1812.

[15] KAWAKITA, H., UEZU, K., TSUNEDA, S., SAITO, K., TAMADA, M., SUGO, T., Recovery of Sb(V) using a functional-ligand-containing porous hollow-fiber membrane prepared by radiation-induced graft polymerization, Hydrometallurgy **81** (2006) 190-196.

[16] AKKAŞ KAVAKLI, P., SEKO, N., TAMADA, M., GÜVEN, O., Radiation-induced graft polymerization of glycidyl methacrylate onto PE/PP nonwoven fabric and its modification toward enhanced amidoximation, J. Appl. Polym. Sci. **105** (2007) 1551-1558.

[17] CHEN, J., WU, Z., YANG, L., ZHANG, Q., SUN, J., SHI, Y., XIA, L, KAETSU, I., Grafting copolymerization of N,N-dimethyacrylaminoethylmethacrylate (DMAEMA) onto preirradiated polypropylene films, Radiat. Phys. Chem. **76** (2007) 1367-1370.

[18] SEKO, N., TAMADA, M., YOSHII, F., Current status of adsorbent for metal ions with radiation grafting and crosslinking technique, Nucl. Instrum. Meth. Phys. Res. B **236** (2005) 21-29.

[19] SATOSHI, T.S., SAITO, K., MITSUHARA, H., SUGO, T., Novel ion exchange membranes for electrodialysis is prepared by radiation induced graft polymerization, J. Electrochem. Soc. **142** (1995) 3659-3663.

[20] NASEF, M.M., SAIDI, H., Structure of polyethylene-graft-polystyrene sulfonic acid membranes prepared by radiation-induced grafting, Int. J. Polym. Mater. **53** (2004) 1027-1043.

[21] KUMAR, V., BHARDWAJ, Y.K., DUBEY, K.A., CHAUDHARI, C.V., GOEL, N.K., BISWAL, J., SABHARWAL, S., TIRUMALESH, K., Electron beam grafted polymer adsorbent for removal of heavy metal ion from aqueous solution, Sep. Sci. Technol. **41** (2006) 3123-3139.

[22] AKKAŞ KAVAKLI, P., SEKO, N., TAMADA, M., GÜVEN, O., Adsorption efficiency of a new adsorbent towards uranium and vanadium ions at low concentrations, Sep. Sci. Technol. **39** (2004) 1631-1643.

[23] AKKAŞ KAVAKLI, P., SEKO, N., TAMADA, M., GÜVEN, O., A highly efficient chelating polymer for the adsorption of uranyl and vanadyl ions at low concentrations, Adsorption **10** (2004) 309-315.

[24] SHIRAISHI, T., TAMADA, M., SAITO, K., SUGO, T., Recovery of cadmium from waste of scallop processing with amidoxime adsorbent synthesized by graft-polymerization, Radiat. Phys. Chem. **66** (2003) 43-47.

[25] SEKO, N., BASUKI, F., TAMADA, M., YOSHII, F., Rapid removal of arsenic(V) by zirconium(IV) loaded phosphoric chelate adsorbent synthesized by radiation induced graft polymerization, React. Funct. Polym. **59** (2004) 235-241.

[26] HEGAZY, E.A., KAMAL, H., MAZIAD, N., DESSOUKI, A., Membranes prepared by radiation grafting of binary monomers for adsorption of heavy metals from industrial wastes, Nucl. Instrum. Meth. Phys. Res. B **151** (1999) 386-392.

[27] MUKHERJEE, A.K., GUPTA, B.D., Radiation-induced graft copolymerization of methacrylic acid onto polypropylene fibers. II. Effect of solvents, J. Appl. Polym. Sci. **30** (1985) 2643-2661.

[28] GUPTA, B., CHAPIRO, A., Preparation of ion-exchange membranes by grafting acrylic acid into pre-irradiated polymer films-1. grafting into polyethylene, Eur. Polym. J. **25** (1989) 1137-1143.

[29] KAWAI, T., SAITO, K., SUGITA, K., KAWAKAMI, T., KANNO, J., KATAKAI, A., SEKO, N., SUGO, T., Preparation of hydrophilic amidoxime fibers by cografting acrylonitrile and methacrylic acid from an optimized monomer composition, Radiat. Phys. Chem. **59** (2000) 405-411.

[30] AKKAŞ KAVAKLI, P., KAVAKLI, C., SEKO, N., TAMADA, M., GÜVEN, O., Radiation-induced grafting of dimethylaminoethylmethacrylate onto PE/PP nonwoven fabric, Nucl. Instrum. Meth. Phys. Res. B **265** (2007) 204-207.

[31] ÖZMEN, F., AKKAŞ KAVAKLI, P., GÜVEN, O., Removal of phosphate by using copper-loaded poly(N-vinylimidazole) hydrogels as polymeric ligand exchanger, J. Appl. Polym. Sci. **119** (2011) 613-619.

[32] BÖHMER, M.R., WILLIAM H.A. HEESTERBEEK, W.H.A., DERATANI, A., RENARD, E., Adsorption of partially quarternised poly(vinyl imidazoles) onto SiO_2 and Y_20_3, Coll. Surf. A: Physicochem. Eng. Aspects **99** (1995) 53-64.

[33] INTERNATIONAL ORGANIZATION FOR STANDARDIZATION, Water quality – Spectrometric determination of phosphorus using ammonium molybdate, ISO 6878:1998, ISO, Geneva (1998).

[34] UNITED STATES ENVIRONMENTAL PROTECTION AGENCY, Chromium hexavalent (colorimetric), EPA METHOD 7196A, USA, (1992).

[35] BARSBAY, M., AKKAŞ KAVAKLI, P., GÜVEN, O., Removal of phosphate using copper-loaded polymeric ligand exchanger prepared by radiation grafting of polypropylene/polyethylene (PP/PE) nonwoven fabric, Radiat. Phys. Chem. **79** (2009) 227-232.

[36] HELFFERICH, F., Ion Exchange McGraw – Hill, New York, NY, (1962).

[37] AKKAŞ KAVAKLI, P., KAVAKLI, C., GÜVEN, O., Preparation of quaternized dimethylaminoethylmethacrylate grafted nonwoven fabric for the removal of phosphate, Radiat. Phys. Chem. **79** (2009) 233-237.

[38] KABAY, N., ARDA, M., SAHA, B., STREAT, M., Removal of Cr(VI) by solvent impregnated resins (SIR) containing Aliquat 336, React. Funct. Polym. **54** (2003) 103–115.

[39] ATIA, A.A., Synthesis of a quaternary amine anion exchange resin and study its adsorption behaviour for chromate oxyanions, J. Haz. Mater. B **137** (2006) 1049.

ELECTRON-BEAM INDUCED GRAFTING OF ISOPROPYLACRYLAMIDE TO A POLY(ETHYLENE-TEREPHTHALATE) MEMBRANE FOR CELL SHEET DETACHMENT AND FUEL CELL MEMBRANE

L. SHAHAMAT, M. AL-SHEIKHLY

Department of Materials Science and Engineering,
College Park, Maryland,
UNITED STATES OF AMERICA

Abstract

Using high-energy irradiation initiation, isopropylacrylamide (IPAA) was grafted to a porous membrane dish composed of poly(ethylene terephthalate) (PET). IPPA demonstrates a transition from a hydrophobic to a hydrophilic structure with a simple change in temperature. The dishes were used for cell grow. Cells generally grow in an environment set at 37°C, at which the IPAA polymer exhibits its hydrophobic structure. IPAA was attached uniformly to a cell culture surface, and cells were able to grow on top of the IPAA while it was in its hydrophobic state. Cells were easily removed from the surface of the dishes after changing the temperature below the LCST of IPAA. By changing the temperature polymer altered its structure to a hydrophilic state and no longer provided a suitable surface for the cells to adhere to. This caused the cells to lift off the culture surface without the use of a destructive enzyme such as trypsin or dispase. These cell sheets are useful to cell sheet engineering because the cells will retain both their extracellular matrix (ECM) and cell-to-cell junctions, which are normally lost in the harvest of cells. Poly(tetrafluoroethylene-co-hexefluoropropylene) (FEP) is a material under investigation as a polymer electrolyte membrane for fuel cells. In order to make it ionically conductive, styrene was grafted to it and then subsequently sulfonated. Grafting of styrene to FEP was performed by simultaneous irradiation of the monomer and substrate to initiate the reaction, followed by a heat treatment to allow the reaction to undergo propagation. The effects of dose rate and heat treatment time on the weight percent yield of grafting and uniformity as a function of depth in the substrate was investigated. A 38.5 wt% graft was obtained after a 50 kGy dose of electron irradiation at a dose rate of 2,8 Gy/pulse and post-irradiation heat treatment of 60°C for three hours. FTIR analysis of 10 µm sections of material grafted under these conditions indicated that styrene had been grafted through the entire depth of the 125 µm FEP substrate, as could be seen by the presence of bands at 2910, 2940, 1597, 1490 and 1444 cm^{-1} which correspond to styrene. Additional characterization of the morphology and chemical composition of the material (on the surface and cross-section) was performed by atomic force microscopy (AFM), scanning electron microscopy (SEM), energy dispersive X ray spectroscopy (EDS), and X ray photoelectron spectroscopy (XPS).

1. OBJECTIVE OF THE RESEARCH

The objective of the research was to prepare membrane dishes with smart surface for cell sheet grows. Using porous membrane dishes composed of poly(ethylene terephthalate) (PET) as trunk material and grafting a temperature sensitive monomer, isopropylacrylamide (IPAA) to its surface the hydrophilic-hydrophobic properties of the surface can be changed by simply changing the temperature allowing the easy removal of the cell sheets. The other objective of the work was the preparation of a polymer electrolyte membrane for fuel cells. It is necessary to make poly(tetrafluoroethylene-co-hexafluoropropylene) (FEP) ionically conductive, therefore styrene was grafted to it and then subsenquently sulfonated.

2. INTRODUCTION

2.1. Cell sheets

Polymers sensitive to a particular stimulus, often called ‘smart’ polymers, have been increasingly employed in biomedical and medicinal applications. The temperature sensitive polymer isopropylacrylamide (IPAA) has been a very useful polymer in the research being conducted in tissue engineering. IPAA demonstrates a transition from a hydrophobic to a hydrophilic structure with a simple change in temperature. The lower critical solution temperature (LCST) of IPAA is around 32°C. Above this temperature, IPAA behaves like a hydrophobic polymer while below this temperature, it behave like a hydrophilic polymer. Since this temperature lies near a physiologically favourable temperature, it is understandable why IPAA has been used for so many biological applications.

Cells generally grow in an environment set at 37°C, at which the IPAA polymer exhibits its hydrophobic structure. If the IPAA is attached uniformly to a cell culture surface, cells are able to grow on top of the IPAA while it is in its hydrophobic state. Once the temperature is dropped below the LCST of IPAA, the polymer alters its structure to a hydrophilic state and no longer provides a suitable surface for the cells to adhere to. This causes the cells to lift off the culture surface without the use of a destructive enzyme such as trypsin or dispase.

By avoiding the use of a destructive enzyme, cells can be harvested in sheets as opposed to single cells. These cell sheets are useful to cell sheet engineering because the cells will retain both their extracellular matrix (ECM) and cell-to-cell junctions, which are normally lost in the harvest of cells. The ECM is vital to the adherence, growth, and differentiation of cells, making its preservation quite significant to tissue engineering [1–6]. Either single or multiple layer cell sheets hold the potential to be transplanted into a host system without the use of additional materials, such as a polymer scaffold [7–10]. Foreign materials implanted in a host can often cause negative effects in the organism, so eliminating them from the process would solve some of the problems afflicting tissue engineering.

Several methods can be used to attach, or graft, IPAA to the culture surface. This experiment explored the use of radiation, in the form of high energy electrons, to initiate the formation of free radicals, both on the culture surface and on the IPAA monomers themselves. The culture surface in this experiment was a porous membrane dish composed of poly(ethylene terephthalate) (PET). The free radicals created in both materials can react with one another to stabilize by forming covalent bonds. The covalent connection of the PET polymers with IPAA is known as a graft co-polymer. The radiation also could cause the IPAA monomers to react with one another. This could either produce polymer chains grafted to the surface of the PET or simply homopolymers. Homopolymers are the result of IPAA covalently bonding to itself instead of to the PET surface.

The chemical structures of the IPAA and PET are shown in Figure 1. The carbon-carbon double bond in the IPAA is the bond that breaks when IPAA is grafted to PET or forms a homopolymer with itself. The aromatic ring in PET makes it relatively radiation resistant, but since the membrane dish is small and frail, the amount of radiation it can tolerate is less than usual. Due to the radiation resistance of PET, this experiment utilizes the method of pre-irradiation in an attempt to activate the PET surface before the IPAA solution is deposited.

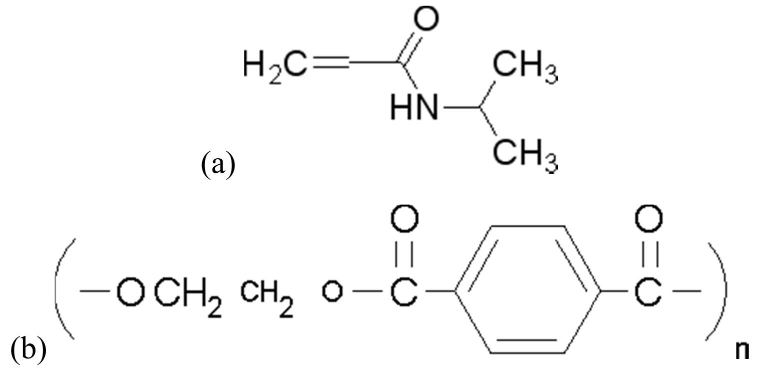

FIG. 1. Chemical structures of (a) isopropylacrylamide and (b) poly(ethylene terephthalate).

Oxygen is a known inhibitor of polymerization when radiation is used as the initiator of free radicals. If a large enough dose of radiation is applied to the solution, the oxygen will eventually be consumed and free radicals will be able to form on the PET membrane and on the IPAA. This phenomenon is called the inhibition period. Bubbling the solution with argon is a technique used to lower the concentration of oxygen in the solution. Since argon is much heavier than oxygen, it would displace the oxygen from the solution. Blowing argon on the surface of the membrane during irradiation is another technique. This process would create an inert atmosphere with less oxygen near the surface of the membrane. Oxygen would thus have been prevented from reintroducing itself back into the solution when the solution was deposited on the surface. Since it was desirable to use a lower dose on the PET membranes in this experiment, it was useful to eliminate the inhibition period as much as possible. The main objectives of this experiment were (1) to graft IPAA polymers uniformly to the surface of the PET membrane using a low dose of radiation and (2) to use a change in temperature to cause the spontaneous detachment of a cell sheet cultured on the surface of the grafted membrane.

2.2. Fuel cell membranes

Poly(tetrafluoroethylene-co-hexafluoropropylene) (FEP) is a material under investigation as a polymer electrolyte membrane for fuel cells. In order to make it ionically conductive, styrene is grafted to it and then subsequently sulfonated. Grafting of styrene to FEP was performed by simultaneous irradiation of the monomer and substrate to initiate the reaction, followed by a heat treatment to allow the reaction to undergo propagation. The effects of dose rate and heat treatment time on the weight percent yield of grafting and uniformity as a function of depth in the substrate was investigated. A 38.5 wt% graft was obtained after a 50 kGy dose of electron irradiation at a dose rate of 2.8 Gy/pulse and post-irradiation heat treatment of 60°C for three hours. FTIR analysis of 10 μm sections of material grafted under these conditions indicated that styrene had been grafted through the entire depth of the 125 μm FEP substrate, as could be seen by the presence of bands at 2910, 2840, 1597, 1490, and 1444 cm^{-1} which correspond to styrene. Additional characterization of the morphology and chemical composition of the material (on the surface and cross-section) was performed by atomic force microscopy (AFM), scanning electron microscopy (SEM), energy dispersive X ray spectroscopy (EDS), and X ray photoelectron spectroscopy (XPS).

3. CELL SHEETS PROJECT

3.1. Materials and methods

3.1.1. Materials

The *N*-isopropylacrylamide (IPAA) monomer and the poly(ethylene glycol)-methacrylate (PEG-methacrylate) polymer (MW 526) used in this experiment were purchased from Sigma-Aldrich. Isopropanol was the chosen solvent for dissolving these two materials. The Cell Culture Inserts^{TM}, or porous membrane dishes, with a pore size of 0.45 μm, a pore density of $1.6 \times 10^6/cm^2$, and a surface area of 4.2 cm^2 were obtained from VWR. The cell line, phosphate-buffered saline (PBS), trypsin-0.53 mM EDTA solution, and Fetal Bovine Serum (FBS) were purchased from ATCC. The cell line used consisted of human prostate epithelium cells (HPECs). The medium used to nourish the cells was prepared using a kit purchased from Invitrogen. This kit contained Keratinocyte Serum Free Media (K-SFM), bovine pituitary extract (BPE), and human recombinant epidermal growth factor (EGF).

3.1.2. Solution preparation

The solution containing the temperature sensitive monomer was the first item to be prepared. A basic stock solution with a 60 wt% IPAA and 40 wt% isopropanol composition was created. The IPAA was in the form of a powder, and it was added to the isopropanol solvent, which was mixed with a magnetic stirrer until it was completely dissolved. During the dissolving process, the flask containing the solution was covered with aluminium foil to limit the UV exposure of the solution. Once dissolved, the solution was bubbled with argon gas for about 30 minutes to minimize the concentration of oxygen in the solution. After the bubbling was completed, the flask was sealed and covered with aluminium foil. This stock solution was stored in the refrigerator for later use.

A portion of the stock solution was set aside for further preparation. The final solution had a composition consisting of a 99.5 wt% of the stock solution and a 0.5 wt% of poly(ethylene glycol) methacrylate (PEG-methacrylate). In order to determine the necessary proportions needed of these materials, the density of the stock solution was calculated. By determining the weight and volume of a small sample of the stock solution, the density was calculated and determined to be approximately 0.9645 g cm^{-3}. Once this density was determined, the proper amount of PEG-methacrylate was added to create the complete IPAA solution.

3.1.3. Irradiation

The membrane dishes needed to be placed in an inert environment prior to their pre-irradiation. This was done by packing each individual membrane dish to be irradiated in its own foil pouch composed of an aluminium and polyester material (MIL-B-131H, Bell Fibre Products Corp., Columbus, GA). Each pouch was purged with argon gas for 15 minutes and subsequently sealed to create the inert environment desired.

The prepared IPAA solution was bubbled gently for about 5 minutes with argon gas prior to irradiation. It was also necessary to bubble the solution with argon for about 2 minutes in between each individual irradiation process for half of the samples to make sure the concentration of oxygen in the solution remained as low as possible.

A 9 MeV electron beam accelerator was the apparatus used in this experiment to produce the desired radiation. After dosimetry was conducted, the membrane dishes were pre-irradiated in their inert, argon environment. Pre-irradiation doses used were 1 kGy and 2 kGy. The dose rate for the experiment conducted was approximately 21 Gy/pulse. Following the pre-irradiation, the membrane dish was removed from its inert environment while argon was blown on the surface. The membrane was attached to clamp stand set-up shown in Figure 2. The clamp suspended the membrane dish in the air, so it would not be in contact with another surface during irradiation. The location that the membrane dish was placed with respect to the electron beam was determined using the inverse square law equation along with the values obtained from the dosimetry.

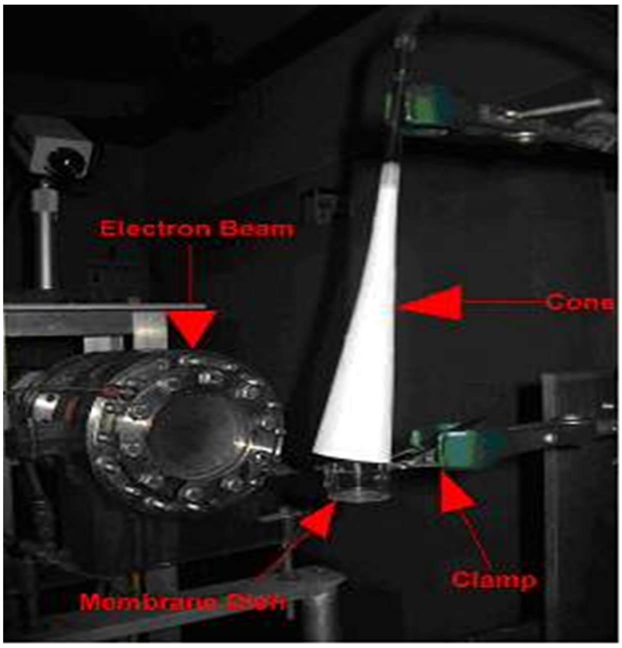

FIG. 2. Clamp stand set-up for irradiation of membrane dish samples.

Once the membrane was in its proper position, 30 µL of the prepared solution was deposited on the surface of the membrane dish using a micro-pipette. During the irradiation, argon was blown on the surface of the membrane for most of the samples using a cone with an opening similar to the size of the membrane dish attached to the tubing delivering the argon. A dose of 25 kGy was applied to each individual membrane dish with a dose rate of about 21 Gy/pulse. It was necessary to conduct all of the above mentioned steps following the pre-irradiation as quickly as possible in order to preserve the free-radicals that had been produced. Certain samples with a 1 kGy pre-irradiation dose were also subjected to irradiation without their argon blowing on them, without their solution being bubbled beforehand, or without both their argon blowing on them and their solution being bubbled beforehand. A slightly lower dose of 20 kGy was also used for these varied samples instead of a dose of 25 kGy.

A membrane dish with 30 μL of the prepared solution was also subjected to a very high dose of 200 kGy at 25 Gy/pulse. Its solution was not bubbled prior to irradiation, the sample was not pre-irradiated, and argon was not blown on the surface of the membrane in this part of the experiment. This sample was done to make a comparison of the effects of a high dose on the PET membrane dish with the effects of a lower dose. A table containing the details about all the samples irradiated is shown in Table 1.

TABLE 1. SUMMARY OF ALL THE COMBINATIONS USED WHEN MEMBRANES WERE IRRADIATED

Irradiation summary			
Pre-irradiation dose (kGy)	Dose (kGy)	Solution bubbled	Argon blowing
1	20	no	no
1	20	no	yes
1	25	yes	no
1	25	yes	yes
2	25	yes	no
2	25	yes	yes
0	200	no	no

3.1.4. Washing procedure

Once the irradiation was complete, the membrane dish was washed vigorously with distilled water to remove any unreacted monomer or unattached homopolymer. After this preliminary washing, FTIR measurements were taken of the membrane dish surface. Once these measurements were completed, the membrane was washed in an ultrasonic cleaner for 60 minutes. The temperature in the ultrasonic cleaner was monitored and not allowed to rise above 30°C. More FTIR measurements were taken after the ultrasonic cleaning to determine if this more thorough cleansing removed the polymer present on the surface of the membrane dish.

3.1.5. Membrane surface analyses

The main method employed to characterize the surface of the membrane dish before and after irradiation was Fourier transform infrared (FTIR) spectroscopy. A Nicolet Magna 550 IR Spectrometer was used to conduct FTIR spectrometry on all the samples. The results of FTIR spectroscopy allowed for the functional groups present on the surface of the membrane to be ascertained. FTIR measurements were taken before and after all stages of washing.

3.1.6. Cell culture

The HPECs were growth and subcultured based on the instructions given in the Product Information Sheet for ATCC® CRL-11609™. The medium was prepared using the base medium of K-SFM plus 0.05 mg/mL BFE and 5 ng/mL EGF. The medium was incubated at 37°C before it was used in the culture in order to raise its pH to an acceptable level. The cells were thawed in a 37°C water bath and centrifuged at 125 × g for 6 minutes. The supernatant was disposed of and the cell pellet suspended in fresh growth medium. The resuspended cells were transferred to a polystyrene cell culture flask and supplied with a suitable amount of growth medium. This flask was placed in an incubator set at 37°C, and the HPECs were allowed to grow for several days before they were subcultured.

In order to subculture the cells, the growth medium was removed using a vacuum pump. The cells attached to the flask were rinsed with PBS. Then a 1:1 solution of Trypsin-EDTA and PBS was added to the flask and placed in an incubator set at 37°C for 6 minutes in order to dissociate the cells from the surface. A solution containing 2% FBS in PBS was added to the flask to inhibit the trypsin, and the contents of the flask were gently pipetted. The flask contents were centrifuged at 125 × g for 6 minutes. The supernatant was disposed of and the cell pellet was suspended into three new culture flasks with fresh growth medium. These flasks were placed in an incubator set at 37°C, and the HPECs were allowed to grow for several days before they were subcultured in the membrane dishes.

When the HPECs were subcultured in the membrane dishes, the membranes were held in a six-well plate because of their pores. The same subculturing steps mentioned above were used. Only the steps following the suspension of the centrifuged cell pellet in fresh growth medium were altered. First, the concentration of the cell suspended solution was ascertained using a haemocytometer, which was found to be approximately 2×10^6 cells/mL. Each membrane was then situated in its own well in the six-well plate along with 5 mL of growth medium and 0.5 mL (1×10^6 cells) of the cell suspended solution. Membrane dishes with both 1 kGy and 2 kGy pre-irradiation doses were used. Unirradiated membrane dishes were used as a control group. Table 2 shows the pre-irradiation dose, dose, and amount of solution added to the membranes that were selected to culture the cells.

TABLE 2. SELECTION OF MEMBRANE DISHES USED FOR CELL CULTURE

Membranes dishes for cell culture		
Pre-irradiation dose (kGy)	Dose (kGy)	Solution deposited (µL)
0	0	0
1	20	30
1	25	30
2	25	30

3.1.7. Cell sheet release

The HPECs were cultured in the membrane dishes for 4.5 days. The cells were removed from the incubator set at 37°C and placed at room temperature (approximately 24°C), which was below the LCST of IPAA. The cells were observed and photographed after the cells had been placed at room temperature. The time which was required for detachment of the cell sheets to be achieved was also recorded.

4. RESULTS

4.1. Presence of IPAA solution

The membrane dishes illustrated visible changes following their irradiation with the prepared IPAA solution. When removed from their sterile casing, each membrane dish consisted of a smooth, transparent membrane and housing composed of PET. The monomer solution was transparent as well, but it had a light yellow colour. When the solution was deposited on the membrane, it seemed to distribute itself across the entire membrane surface. The layer of solution was respectively very thin given that only 30 µL was deposited. Since the membrane used was porous, the solution was able to diffuse through the pores during the irradiation procedure. Due to this diffusion, the membrane was suspended in the air during the experiment to prevent it from sticking to the surface it was irradiated on.

Some areas on the membrane where the polymer had seemingly attached itself during the irradiation process were visible to the naked eye. However, these areas were not uniformly distributed over the surface of the membrane. These polymer regions on the membrane looked uneven and translucent, not smooth and transparent like the remainder of the membrane. The portions of the membrane that did not have polymer on them looked similar to an unirradiated membrane surface. FTIR measurements were taken of the unirradiated membranes as well as the polymer and non-polymer regions of the irradiated membranes. A comparison of these three different spectrums for one sample is shown in Figure 3. These FTIR measurements showed the presence of additional functional groups on the irradiated membranes in Figures 3b and 3c that were not present on the unirradiated membrane in Figure 3a. The peak near the 1750 wavelength was highly characteristic of PET, which is the polymer the membrane was composed of. All three spectra in Figure 3 displayed this peak, meaning the PET was distinguished in all the samples. This peak was attributable to the ester carbonyl functional group found in PET which is not present in IPAA, as can be seen in their structures shown in Figures 1a and 1b [12]. The peaks on the spectra around the 1650 and 3300 wavelengths were indicative of the presence of IPAA because they were visible on the spectra of the irradiated membranes but not the unirradiated membrane. The 1650 wavelength fell in the range for the FTIR absorption frequency of the amide carbonyl functional group, while the 3300 wavelength fell in the range of the amine functional group [12]. Both of these functional groups were present in the IPAA structure but not the PET structure, which can again be compared in Figures 1a and 1b. Whenever FTIR measurements were taken and the peaks at the 1650 and 3300 wavelengths were not detected, it was assumed that there was no IPAA present on the membrane [12]. Also, due to the very small concentration of PEG-methacrylate in the solution, no identifying peaks were able to be detected for this portion of the solution.

4.2. Anaerobic condition

The purpose of using argon to bubble the solution and blow the surface during irradiation was to lessen the concentration of oxygen. The polymeric regions on the membrane after irradiation varied in appearance based on whether or not the solution was bubbled directly before being deposited on the membrane. When bubbled directly before irradiation, the polymeric region looked smoother and more uniform. If the solution was not bubbled directly before irradiation, the polymeric region appeared uneven and not uniformly distributed. There were some discrepancies with the solution bubbled directly before the irradiation of the membranes irradiated with a 2 kGy pre-dose and a 25 kGy dose. The solution had started to become thicker and was not as aqueous as it had been for the other samples. This caused the polymeric region formed on these membranes to be more uneven than the samples whose bubbled solution was smoother.

The blowing of argon on the surface of the solution had several different effects on the outcome of the polymer formed on the irradiated membrane. If the argon was blowing in a stream that was too concentrated and powerful, the solution on the surface of the membrane was disturbed and splashed around. This resulted in a non-uniform coating of the polymer regions on the membrane. The blowing also seemed to produce bubbles in the polymeric regions of the irradiated membranes. A cone with an opening similar to the size of the membrane dish was therefore attached to the end of the piping that delivered the argon gas. This successfully reduced the strength of the stream of argon gas and distributed it more uniformly across the surface of the membrane.

Membranes that did not have argon gas blowing on them did not have a uniform polymeric covering like the samples that did have argon blown on them. The FTIR measurements of the membranes with argon blowing showed a higher absorbance for the presence of IPAA than the membranes without argon blowing, as shown in Figure 4.

The higher absorbance shown in Figure 4b may have been a result of the polymer regions on the membranes blown with argon being thicker than the polymer regions of the membranes without argon blown. This meant that after irradiation, more polymer was present on the membrane surfaces that had argon blowing on them than the surfaces without it.

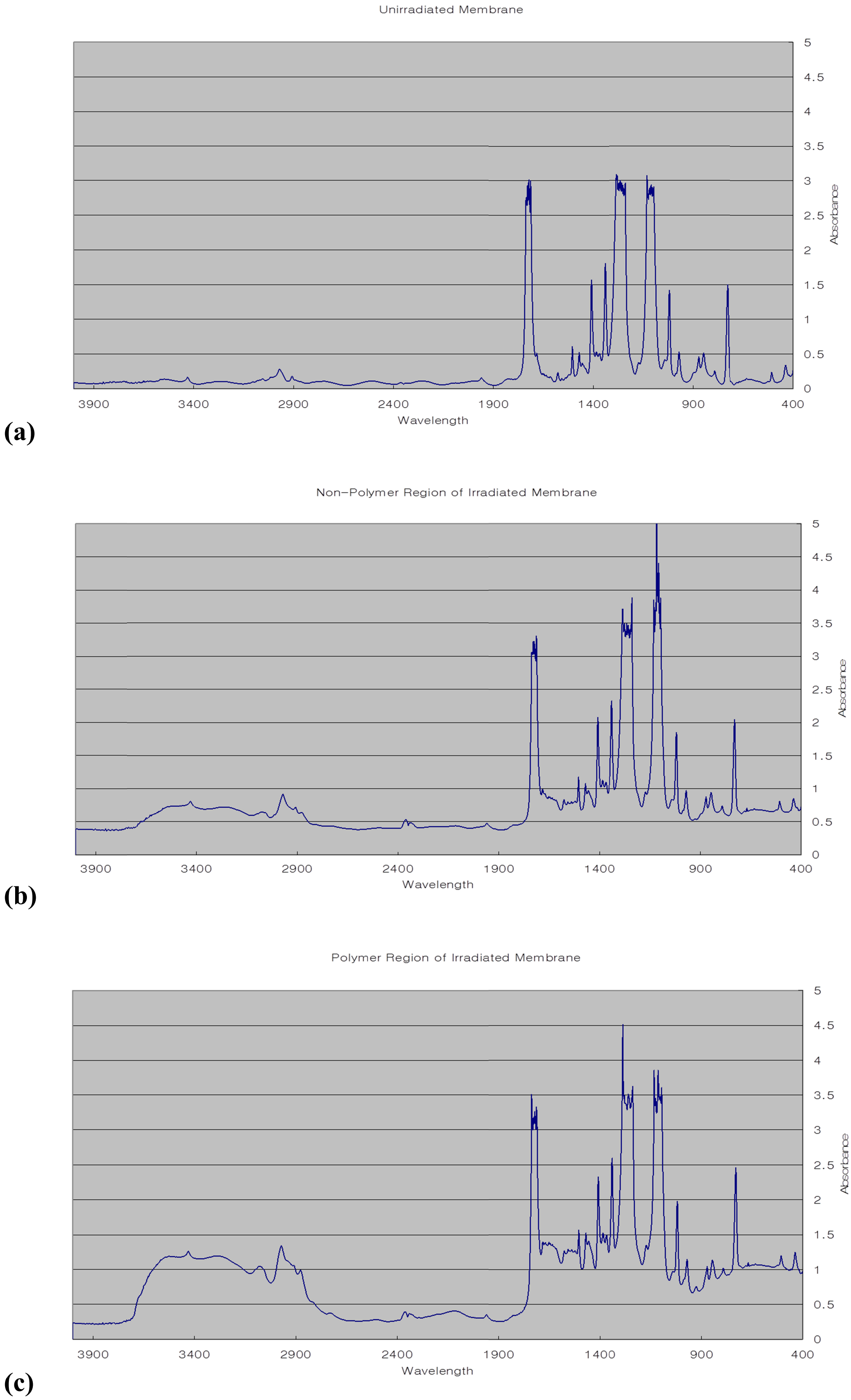
Unirradiated Membrane

Non-Polymer Region of Irradiated Membrane

Polymer Region of Irradiated Membrane

FIG. 3. FTIR spectrum of (a) an unirradiated membrane and a (b) non-polymeric and (c) polymeric region of an irradiated membrane (2 kGy pre-dose, 25 kGy dose, vigorously washed).

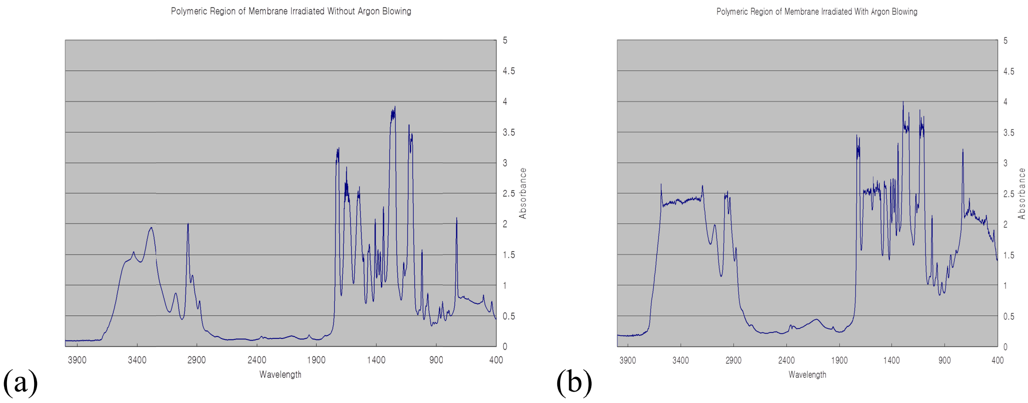

FIG. 4. FTIR spectrum of an irradiated membrane (1 kGy pre-dose, 25 kGy dose, vigorously washed) (a) without and (b) with argon blown during irradiation.

4.3. Effect of washing technique

The washing technique used significantly affected the presence of IPAA on the surface of an irradiated membrane. Originally, the membranes were only washed vigorously with distilled water, but this caused the membrane to exhibit a sticky quality believed to be excess polymer not grafted to the surface.

The process of using an ultrasonic cleaner in addition to the vigorous washing was developed in order to wash the membranes more thoroughly. The ultrasonic cleaner was very effective at removing the IPAA polymer from the surface of the membrane. After the membranes were sonicated, the majority of the visible polymer regions were removed. FTIR measurements were taken on the membranes before and after sonication, further revealing the effectiveness of the cleaner at removing the ungrafted IPAA polymer. The spectra for two samples after being vigorously washed and then after being ultrasonically washed are shown in Figure 5.

It was hard to predict whether the ultrasonic washing would reveal results like those in Figures 5a and 5b or whether the results would be like the ones in Figures 5c and 5d. Although the pre-irradiation and irradiation doses were different for these two samples, these differences did not seem to affect the outcome of the ultrasonic washing. The main difference in the irradiation procedure for which a trend could be established between these washing results was the sample in Figure 5a and 5b had its solution bubbled immediately before irradiation while the sample in Figure 5c and 5d did not. Bubbling the solution before irradiating seemed to cause the ultrasonic washing to remove more of the polymer regions from the membranes than it did for membranes whose solution had not been bubbled.

The vigorously washed membrane often caused problems with the FTIR measurements by over-saturating the absorbance measured for certain wavelengths. If this happened, the spectra obtained for the vigorously washed sample had no discernable peaks, making it difficult to quantify. Saturated spectra were discarded, and more measurements were taken of different areas on the membrane until enough useful data was obtained. This inconsistency truly showed that the polymer regions on the irradiated membrane were not distributed uniformly over the surface of the membrane, since some areas were able to saturate the absorbance of the spectra while others could not.

The ultrasonic cleaning caused a problem as well. It seemed that 1 hour of sonicating could be detrimental to the membrane. Not all of the membranes demonstrated this problem, but after being washed in the ultrasonic cleaner for this amount of time, some of the membranes appeared to deteriorate slightly. Small dots formed on the surface that looked like the membrane was being damaged by the sonication. Although the general condition of the membrane seemed to be unaffected by these dots, they were not considered beneficial and should be avoided.

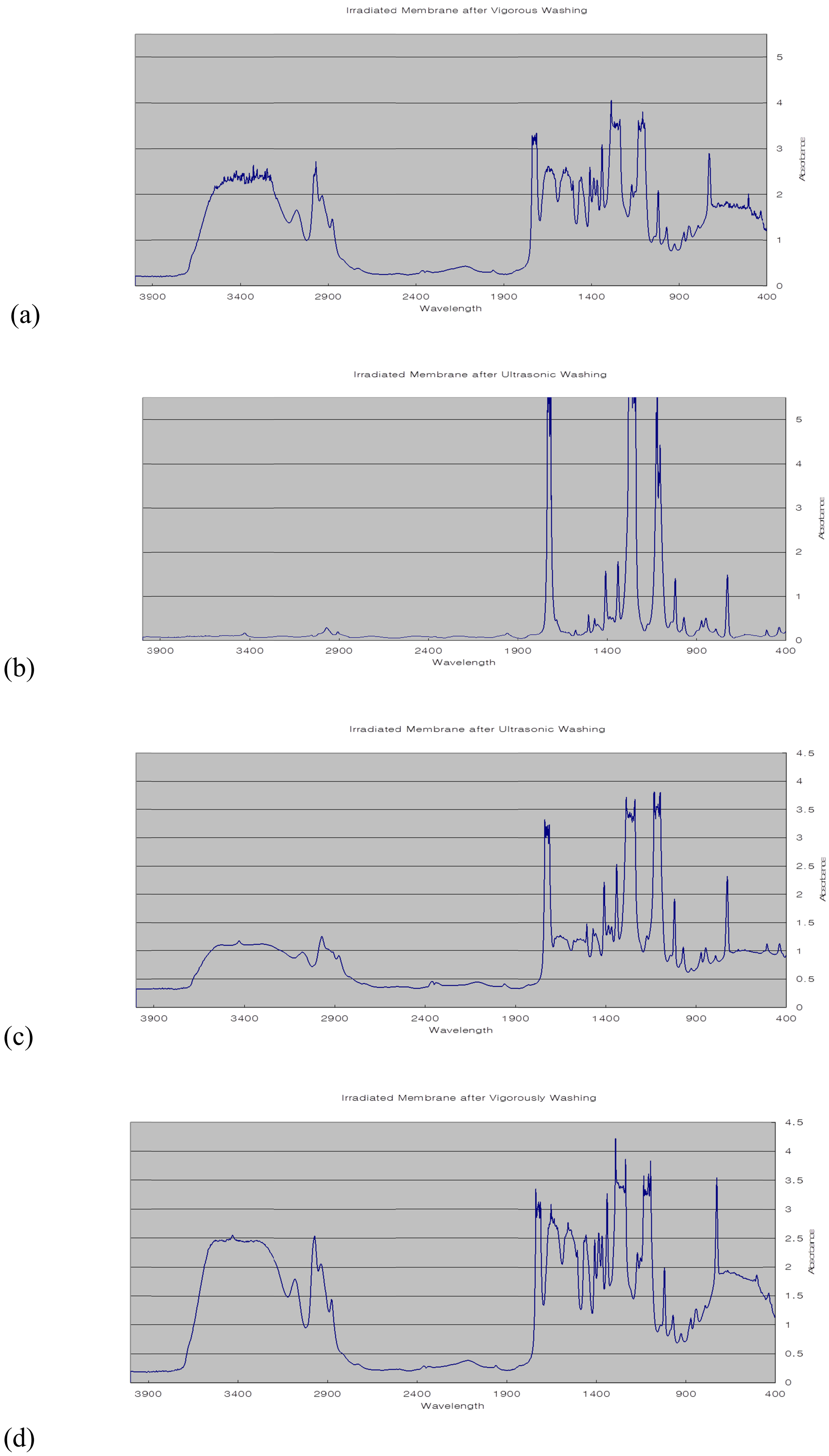

FIG. 5. FTIR spectra of (a) vigorously washed and (b) ultrasonically washed membrane (2 kGy pre-dose, 25 kGy dose). FTIR spectra of (c) vigorously washed and (d) ultrasonically washed membrane (1 kGy pre-dose, 20 kGy).

4.4. Effect of high dose

The majority of the membrane dishes were irradiated with a dose of less than 30 kGy. One sample was irradiated with a high dose of 200 kGy to see its effect on the membrane. It was very easy to see that the membrane dish was damaged by the high dose. The PET housing was discoloured and warped, and the PET membrane itself had become brittle. When a lower dose of radiation was used, the membrane dish did not appear to be physically damaged.

A picture of the membrane dish before and after irradiation with a 200 kGy dose is shown in Figure 6. The white spot on the irradiated membrane in Figure 6b was the location where the electron beam had hit the sample during irradiation. This white spot did not appear on any of the samples with lower doses. Also, the polymer regions formed on the surface of the membrane were not improved by the higher dose.

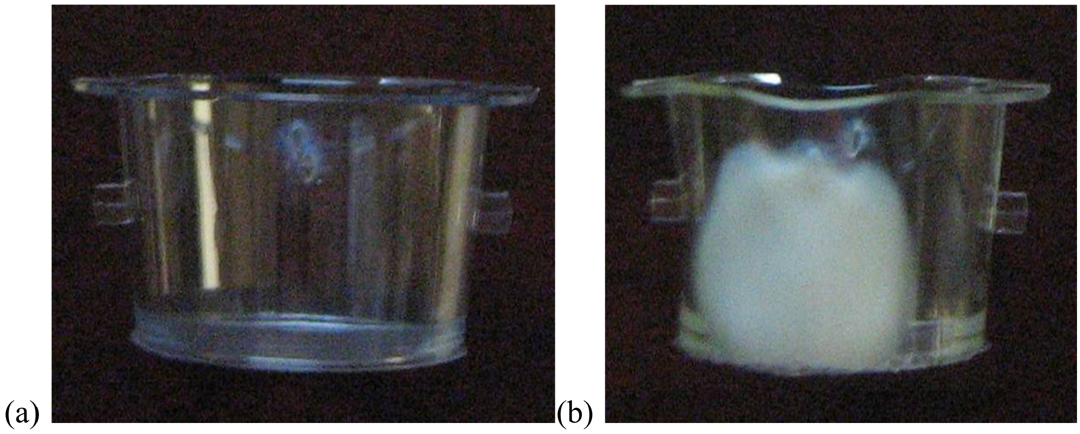
(a) (b)

FIG. 6. Photograph of the membrane dish (a) before and (b) after irradiated with 200 kGy.

5. FUEL CELL MEMBRANE

5.1. Materials

Poly(tetrafluoroethylene-co-hexafluoropropylene) (FEP) sheets of 25 μm and 125 μm thickness were cut into strips of desired size, approximately 5 cm by 5 cm. Styrene was used as received. A solution of 0.2 M chlorosulfonic acid in dichloromethane was prepared.

5.2. Ionizing radiation techniques

Two types of ionizing radiation were used in this work: (i) electron radiation from a pulsed electron linear accelerator (Varian Model 5V-7715, 7 MeV energy, 3 μs pulse length, 60 Hz pulse frequency, 2–4 Gy dose per pulse), and (ii) gamma radiation from a ^{60}Co source (Neutron Products Model 200364, 1.7×10^{13} Bq activity, 0.17 Gy/s dose rate in water). The absorbed dose was calibrated using nine Far West film dosimeters placed in an array which covered the area of the FEP film.

5.3. Grafting

The electron beam grafting procedure involved immersion of the film in pure styrene monomer which was heat-sealed inside an aluminized polyethylene bag. The sample was then irradiated with the electron beam to the desired absorbed dose. Immediately after irradiation, the sealed specimen was placed in an oven at a temperature of either 45°C or 60°C for a varying period of time. After this post-irradiation heat treatment, the film was removed from the aluminized polyethylene pouch, sonicated in a xylene bath to remove residual styrene monomer and homopolymer, and dried in air.

The ^{60}Co gamma irradiation procedure involved the immersion of the FEP film in pure styrene inside an aluminium container, shown in Figure 7. The FEP substrate was held in place by clamping it at either end with aluminium clamps which were screwed together. The system was bubbled with argon gas during the irradiation. After the irradiation, samples were removed from the aluminium container, washed in xylene and dried in air.

(a)

(b)

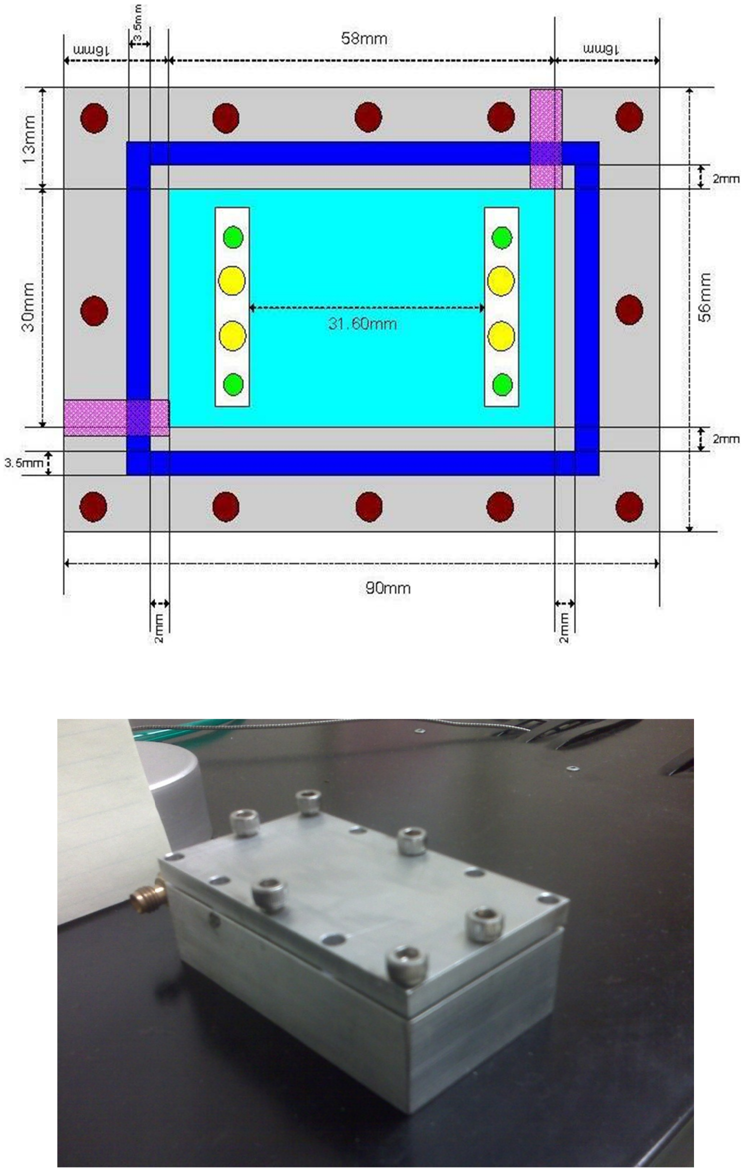

FIG. 7. (a) Schematic and (b) photograph of the aluminium container used to simultaneously graft styrene monomer to FEP by ^{60}Co gamma irradiation.

5.4. Sulfonation

The styrene-grafted FEP films were sulfonated by immersing them in a boiling 0.2 M chlorosulfonic acid/dichloromethane solution at 60°C for eight hours. After washing with water, the sulfonated films were hydrated in water at 80°C for twelve hours. These samples were stored in deionized water at room temperature.

5.5. Characterization

The extent of grafting was determined through measurement of the change in weight before (W_o) and after (W_g) grafting in equation 1:

$$Degree\,of\;grafting\,(wt\%) = \frac{W_g - W_o}{W_o} \times 100 \qquad (1)$$

Fourier transform infrared (FTIR) analysis was performed using a Nicolet Magna 550 spectrometer to verify successful formation of the grafted material. Each spectrum was determined from 32 scans measured with a resolution of 4 cm^{-1}. Two different types of FTIR analysis were performed. One technique involved the measurement of the transmittance spectrum of the entire 125 μm film. The other technique involved microtoming the grafted 125 μm film into cross-sections of 10 μm thickness, followed by measurement of the transmittance spectrum of each section corresponding to successive thicknesses.

5.6. Morphology

Analysis of changes in the morphology of the surface and cross-section of the grafted films as a function of various synthesis conditions was performed by atomic force microscopy (AFM) and scanning electron microscopy (SEM). Samples were embedded in epoxy and sputtered with gold prior to SEM analysis. Energy dispersive X ray spectroscopy (EDS) was employed to measure the chemical composition of the material along its cross-section, thereby confirming the graft uniformity as a function of depth.

X ray photoelectron spectroscopy (XPS) was performed on a Kratos Axis 165 X ray photoelectron spectrometer operating in hybrid mode using monochromated Al Kα X radiation (1486.6 eV) at 300 W. Charge neutralization was used to minimize sample charging and the pressure of the system was maintained at 1×10^{-8} Torr or lower throughout the experiment.

Survey spectra and high resolution spectra were collected at pass energies of 160 eV and 20 eV, respectively. Some sample degradation was noted during XPS data collection evidenced by a gradual decrease in the C/F ratio, corresponding to changes in C 1s peak shape and yellowing of sample with increased analysis time [11]. XPS data presented here were collected from samples exposed to X rays for a maximum of 20 minutes.

5.7. Ion conductivity

Proton conductivity was measured at 80°C and a fixed humidity using an AC impendence method at 3M Company. The humidity was started at 70% RH and measurements were collected at successive 10 RH percentage point reductions. Additionally, measurements were taken as the humidity was increased from 20% RH by units of 10 percentage points up to 90% RH. A standard PFSA membrane with an equivalent weight of 825 g/mol was used to compare proton conductivity to the styrene-grafted films.

6. RESULTS

6.1. Radiation-induced grafting of styrene to FEP

Figure 8 shows the degree of grafting as a function of post-irradiation heat treatment time for FEP/styrene grafted simultaneously with electron beam irradiation. At each heat treatment time employed, the degree of grafting was observed to increase with temperature. This is due to the enhancement of the diffusivity of the styrene monomer through the FEP film as temperature increases, which causes the rate of initiation and propagation of the grafting copolymerization reaction to increase. At each of the temperatures employed, the rate of grafting was observed initially to increase rapidly with heat treatment time, then to increase more slowly at longer heat treatment times. A similar pattern of change in the rate of grafting was reported by Gupta [12], in which the initial rapid increase in grafting was attributed to the predominance of the initiation and propagation steps of the reaction, while the slower changes in rate of grafting at longer times were due to the increased significance of the termination reaction.

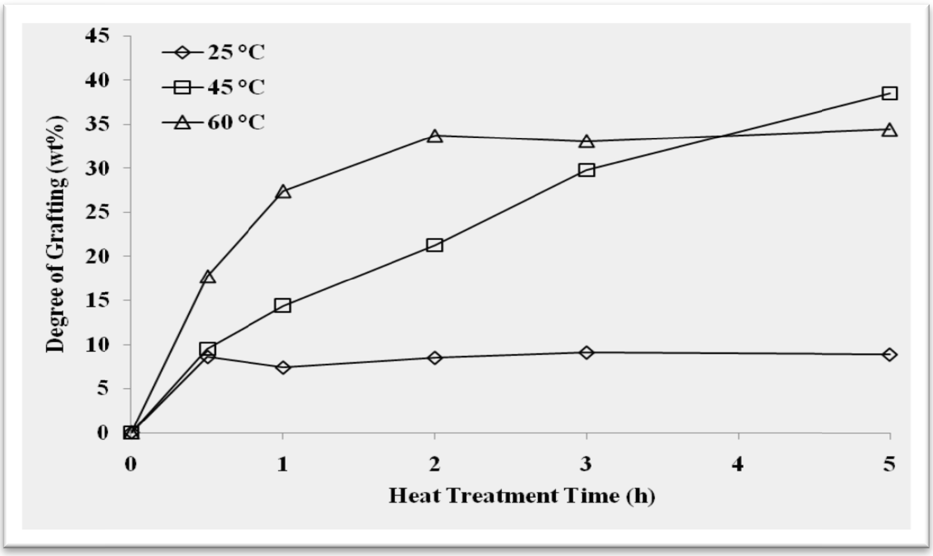

FIG. 8. Degree of grafting (wt%) as a function of heat treatment time (h) at 25 (◊), 45 (□), and 60 (Δ) ℃. FEP film (125 μm) and styrene monomer were simultaneously irradiated with pulsed electron beam to a dose of 50 kGy at 2.8 Gy/pulse.

Figure 9 shows SEM cross-section micrographs of FEP before and after electron beam grafting of styrene. Substrate and monomer were simultaneously irradiated to 50 kGy dose, and then subjected to heat treatment at 60°C for up to 5 h. The uniformity of the morphology of the cross-section increases with heat treatment time. During the first hour of heat treatment (see figures 9(b) and 9(c)), the cross-section of the film is divided into three distinct regions. The outer regions of the film are grafted with styrene, while the central region contains ungrafted FEP substrate material. After two hours of heat treatment (see figures 9(d) and 9(e)), the grafted regions meet each other at the centre of the film, and the morphology of the cross-section becomes homogeneous. These images show that styrene grafting is initiated at the surfaces of the FEP film, and then proceed towards the centre of the film to produce a graft which extends through the entire depth of the film.

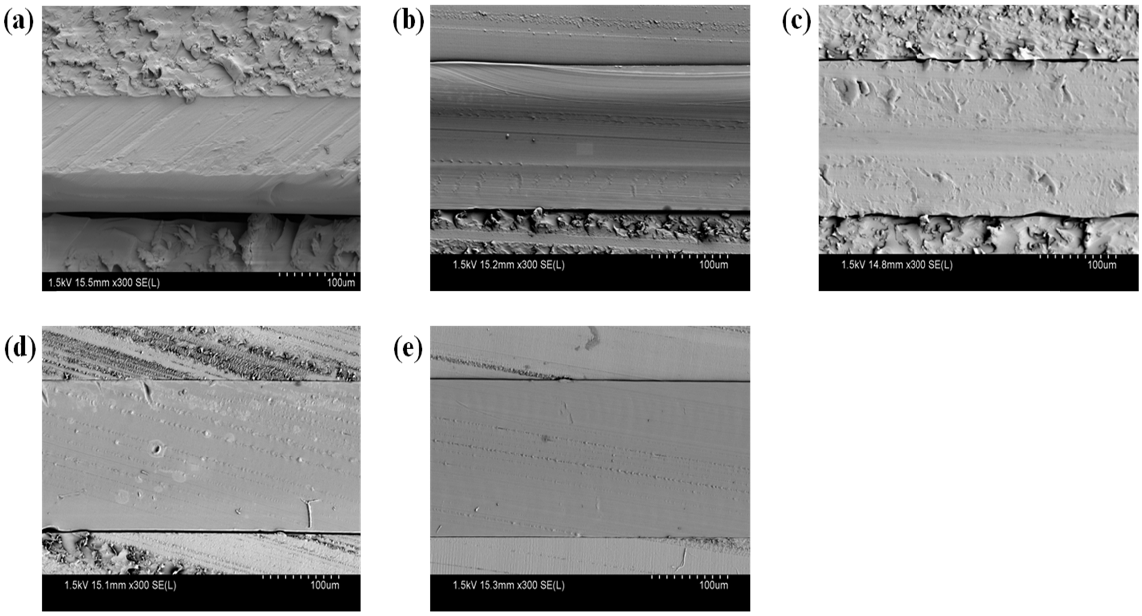

FIG. 9. SEM cross-section micrographs of (a) unirradiated FEP (125 μm), and electron beam irradiated FEP/styrene (50 kGy, 2.8 Gy/pulse) with post-irradiation heat treatment at 60℃ for (b) 0.5 h, (c) 1 h, (d) 2 h, and (e) 5 h.

Although the initiation and propagation steps of the reaction predominate during the early stages of the grafting process, while the termination step predominates at later times in the grafting process for all temperatures investigated, the rates of each of these steps in the reaction are enhanced at higher temperatures. This can clearly be seen by comparison of the rate of grafting at 45 and 60°C. When a heat treatment temperature of 60°C is employed, the termination of primary radicals after five hours of heat treatment becomes so enhanced that the rate of grafting is reduced to below the rate at which grafting would occur if a heat treatment temperature of 4°C were used.

Figure 10 shows the EDS line scans of FEP after electron beam grafting with styrene at various heat treatment times. This analysis serves as an additional way to observe the uniformity of the depth of the graft by monitoring the elemental composition along a cross-section of the material. The ungrafted FEP substrate contains a higher concentration of fluorine than carbon through the entire depth of the material. All of the data shown in figure 4 are from samples which have been irradiated with a 50 kGy dose of radiation and stored in an oven at 60°C for varying lengths of time. The sample treated for 30 minutes exhibits a concentration of carbon exceeding that of fluorine from either edge until 50 µm into the film.

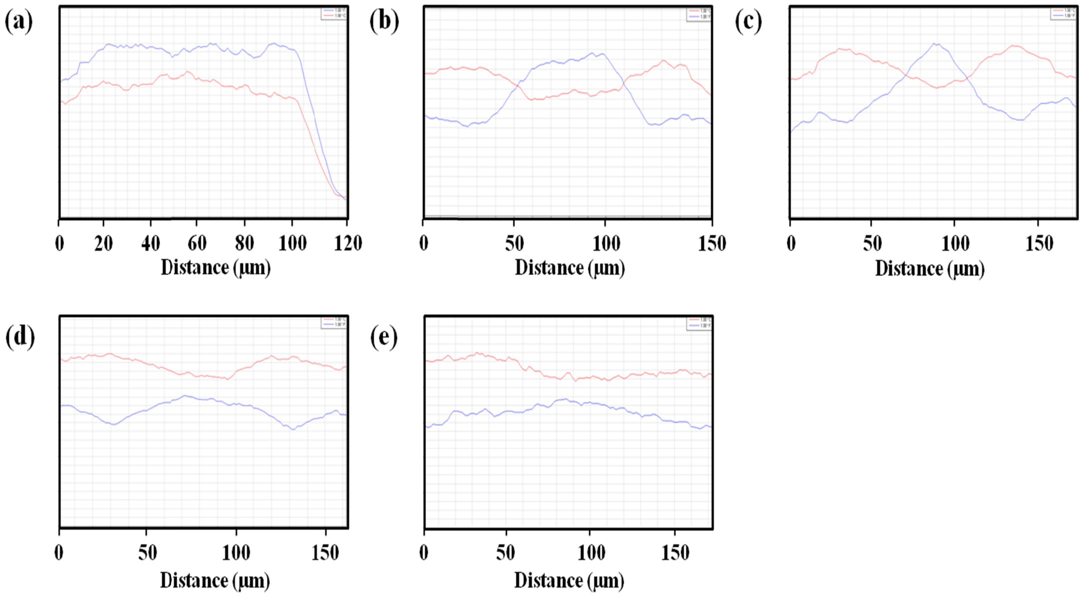

FIG. 10. EDS line scans of fluorine (blue) and carbon (red) across the cross-sections of (a) unirradiated FEP (125 µm), and electron beam irradiated FEP/styrene (50 kGy, 2.8 Gy/pulse) with post-irradiation heat treatment at 60 ℃ for (b) 0.5 h, (c) 1 h, (d) 2 h, and (e) 5 h.

These regions of higher carbon content are regions which are grafted with styrene. The depth of these grafted regions increases until after a 2 hour heat treatment, where carbon concentration exceeds that of fluorine for the entire depth of the film. The increasing heat treatment times show the increase in graft uniformity, which is observed by the formation of a more even profile for both carbon and fluorine with greater heat treatment time. This also corresponds to an increasing grafting percentage up to 2 hours of heat treatment, as shown in Figure 8.

Figure 11 shows the SEM image and EDS line scans a 125 µm FEP film which has been grafted with styrene by electron beam radiation followed by a heat treatment for three hours at 45°C. The cross-section appears to contain three distinct regions, and the atomic composition of each of these regions is analyzed by EDS. In the central region of the film, which is approximately 70 µm in thickness, fluorine is the predominant element. The outer regions of the film located on either side of this central region, which is approximately 50 µm in thickness, both contain carbon as the predominant element. This indicates that under the grafting conditions employed to synthesize this material, the styrene grafting front has penetrated to a depth of 50 µm on either side of the FEP film.

The SEM and EDS measurements shown in Figure 11 of partially grafted FEP indicate that the copolymerization of styrene with FEP proceeds through what is known as a „grafting front mechanism” [13]. During the initial stages of the reaction, styrene grafts to the surface of the FEP film. This outer layer of grafted material swells in the styrene monomer within which it is immersed. The monomer then is able to diffuse through this swollen grafted region and continue the grafting reaction at greater depths within the FEP film. Eventually, the grafted regions which formed on either surface of the FEP film encounter each other near the centre of the film. A homogeneous graft distribution across FEP is necessary for its proper functioning as a fuel cell membrane, because it requires hydrophilic paths along which protons can be transported from the anode to the cathode.

Figure 12 shows the FTIR spectra of a 125 µm FEP film before and after grafting styrene with electron beam radiation and post-irradiation heat treatment of three hours at 60°C. The grafted film was sliced into 10 µm-sections, and the transmittance spectrum of each slice was measured. The absorptions near 1265–1110 cm^{-1} and 975 cm^{-1} correspond to the CF$_2$ and CF$_3$ stretching vibrations of the FEP substrate [14]. New bands arise in the spectrum, which are attributed to styrene, and are present in the spectrum of every slice analyzed, which verifies that grafting had taken place through the entire depth of the FEP film. The bands near 3200–3000 cm^{-1} are associated with the stretching vibration of aromatic =CH groups of the grafted styrene. The bands at 2910 and 2840 cm^{-1} are the asymmetric and symmetric stretching vibrations of CH$_2$. The bands at 1597 and 1490 cm^{-1} are the stretching vibrations of C=C.

The band at 1444 cm^{-1} is associated with CH$_2$ bending. FTIR analysis of each of these slices of the grafted film offer clear evidence of the production of a homogeneous styrene graft within FEP. Although the measurement of the transmittance spectrum of the entire film would indicate that styrene grafting had occurred, by examination of individual slices we can see to what depth within the base polymer the styrene has grafted.

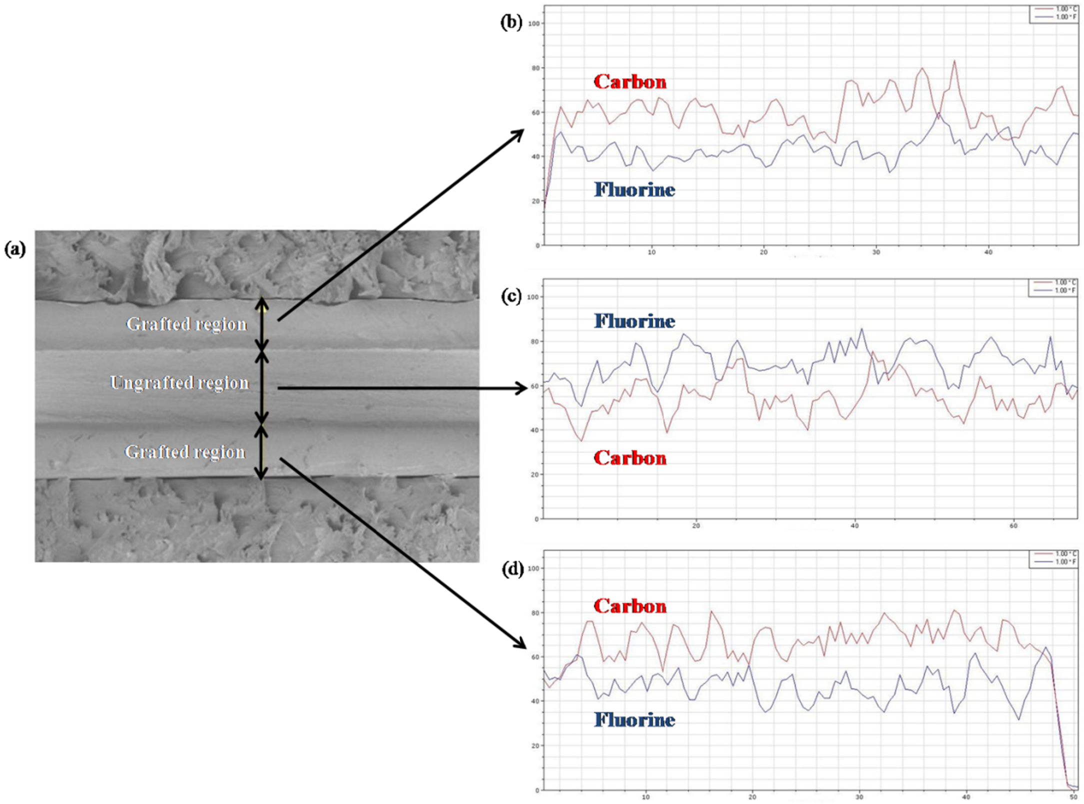

FIG. 11. SEM cross-section image (a) and EDS line scans of styrene-grafted (b, d), and ungrafted (c) regions of FEP film (125 µm). Grafting was performed through simultaneous irradiation of FEP and styrene with electron beam (50 kGy, 2.8 Gy/pulse), followed by heat treatment at 45 ℃ for 3 h. Degree of grafting: 24.3 wt%.

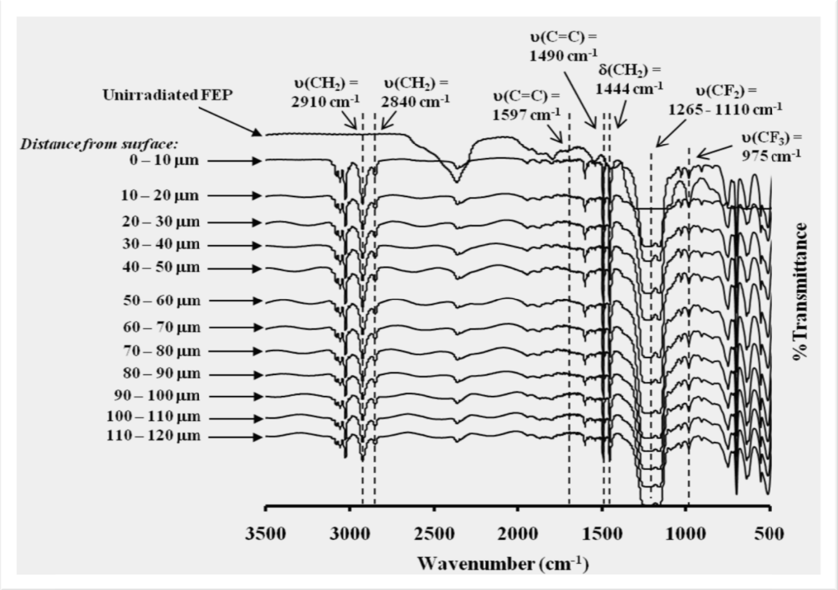

FIG. 12. FTIR spectra of unirradiated FEP film (125µm) and FEP/styrene grafted film sliced into 10 µm sections parallel to film thickness. Grafting was performed through simultaneous irradiation of FEP and styrene with electron beam (50 kGy, 2.8 Gy/pulse), followed by heat treatment at 60ºC for 3 h. Degree of grafting: 38.5 wt%.

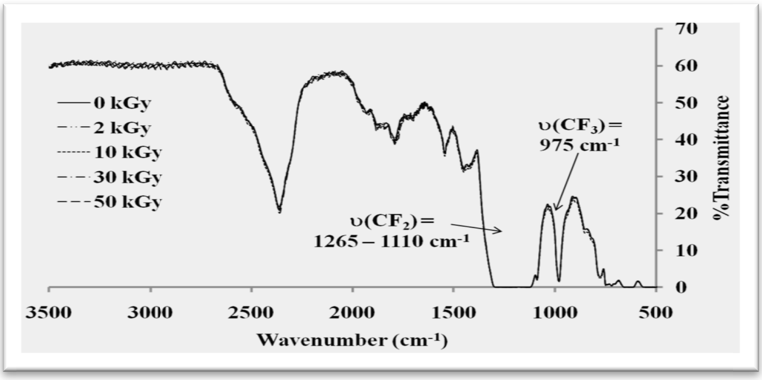

FIG. 13. FTIR spectra of FEP film (125 µm) before and after ^{60}Co γ irradiation in air at a dose rate of 0.17 Gy/s to doses of 2, 10, 30, and 50 kGy.

Figure 13 shows an overlay of the FTIR spectra of FEP (125 µm) before and after ^{60}Co γ irradiation in air to doses of 2–50 kGy. No significant changes in the spectra of FEP were observed after irradiation, which indicated that this material is relatively stable when irradiated to doses up to 50 kGy. Therefore the use of ionizing radiation to graft styrene will not negatively affect the integrity of the FEP film.

The degree of grafting as a function of dose and FTIR spectra for FEP/styrene grafted simultaneously with ^{60}Co γ irradiation under argon-saturated conditions (no post-irradiation heat treatment was used) are shown in Figure 14 and 15, respectively. The spectra indicate the formation of a styrene graft, as could be observed by the appearance of styrene bands. Gravimetric measurements indicate that not only does the degree of grafting increase with dose, but also that γ radiation generates grafting yields comparable to those obtained using electron radiation under similar conditions. For example, a 50 kGy dose of electron irradiation gave an 8.9 wt% graft at five hours after the irradiation at room temperature, while the same dose of γ radiation gave an 8.4 wt% degree of grafting. The ability to obtain similar degrees of grafting despite the large difference in dose rate and atmospheric conditions indicate the significance of the post-irradiation heat treatment as a means of enhancing the grafting yield.

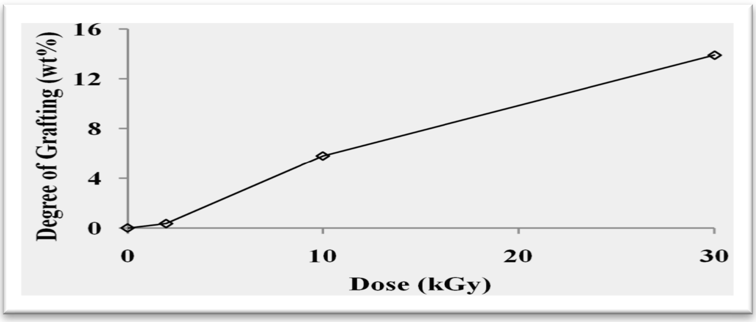

FIG. 14. Degree of grafting (wt%) as a function of gamma irradiation dose. FEP film (125 µm) and styrene monomer were simultaneously irradiated with ^{60}*Co* γ *radiation at 0.17 Gy/s.*

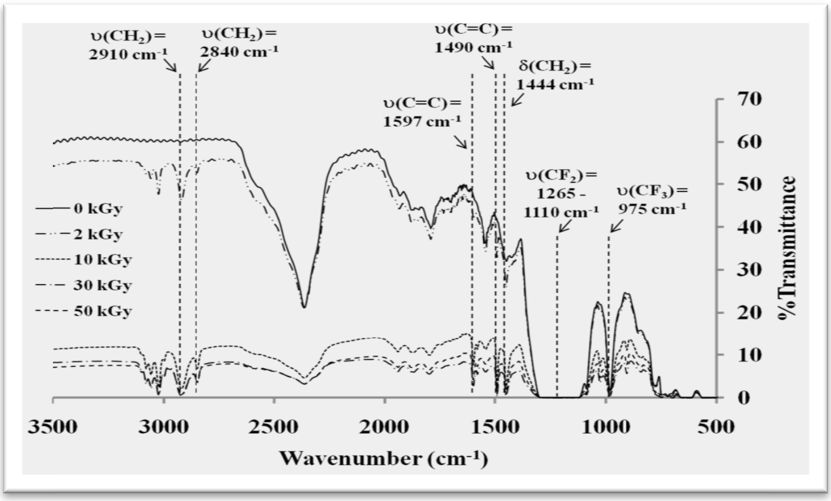

FIG. 15. FTIR spectra of FEP film (125 µm) before and after styrene grafting by simultaneous ^{60}*Co* γ *irradiation in argon at a dose rate of 0.17 Gy/s to doses of 2, 10, 30, and 50 kGy.*

Figure 16 shows the SEM image and EDS analysis of the cross-section of styrene-grafted FEP which was produced by simultaneous gamma irradiation to a dose of 50 kGy. According to the composition profile shown in figure 16(c), carbon is the predominant element in the outer 10 µm of the film, while fluorine predominates within the innermost regions of the film. This indicates that a uniformly grafted material was not generated under these synthesis conditions.

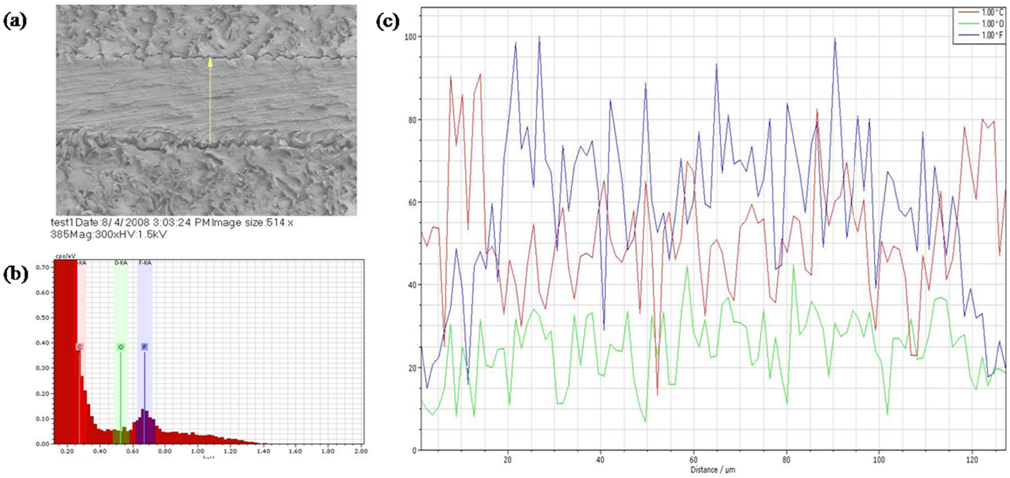

FIG. 16. (a) SEM image and (b, c) EDS analysis of the cross-section of FEP (125 µm) grafted with styrene by ^{60}*Co* γ *irradiation to a dose of 50 kGy at 0.17 Gy/s under argon-saturated conditions. Degree of grafting: 8.4 wt%.*

6.2.Surface composition and morphology of FEP-g-Sty

Figure 17 shows surface and cross-sectional SEM images of FEP before and after electron beam grafting of styrene with a dose of 50 kGy and post-irradiation heat treatment at 60°C for 3h. According to EDS measurements, the grafting conditions employed to produce these materials generated a uniform styrene content through the entire thickness of the FEP substrate. Although these grafting conditions caused the material to swell to a thickness of approximately 160 μm, no major irregularities in the morphology of the surface could be observed.

XPS spectra were analyzed using CASA XPS software, quantification was based on relative sensitivity factors obtained from the Kratos Vision library, 1.000 for fluorine and 0.278 for carbon. The C 1s spectra were fit with peaks of equal full-width at half maximum, with a 50% Gaussian/50% Lorentzian product function peak shape after removal of a Shirley background. Data were collected for three samples, an unirradiated FEP substrate (Figure 18(a)), an electron-beam styrene-grafted FEP (Figure 18(b)) and a ^{60}Co γ-grafted FEP (Figure 20).

Figure 18(a) shows the C1s and F 1s regions for the unirradiated FEP substrate for which the calculated F/C ratio is 2.2. The C 1s can be fit to 5 peaks and assuming minimal sample degradation, this is consistent with the structure expected. Peaks 1 and 2 probably occur due to sample degradation and a small amount of oxidized hydrocarbon contamination, which can be expected on the surface of all samples exposed to atmosphere, to some extent [15]. Figure 18(b) shows the C 1s and F 1s spectra after electron beam grafting of styrene. The calculated F/C ratio was 0.69; this marked decrease in fluorine concentration would be expected with increased carbon due to significant styrene incorporation in the film. The C 1s spectrum shows an almost complete disappearance of the peak due to CF_2 at ~290.0 eV, while there is still a significant peak due to CF_3 at ~292.2 eV. This indicates that the styrene bonds preferentially at the CF_2 group. Additionally styrene incorporation is evidenced by the large increase in C-C and C-H bonds. Angle resolved spectra (not shown here) demonstrated that the grafting of the styrene was homogeneous up to the depth at which XPS is sensitive, ~10 nm.

(a) **Unirradiated FEP**

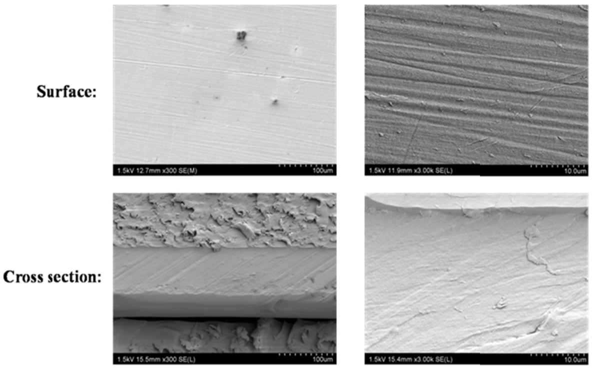

(b) **Electron-irradiated FEP/Styrene**

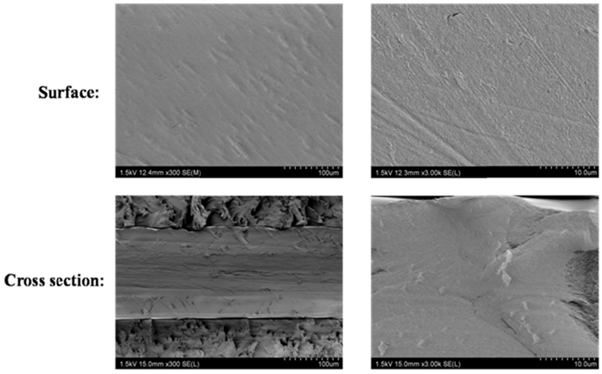

FIG. 17. SEM micrographs of the surface and cross-sections of (a) unirradiated FEP (125 μm) film and (b) electron beam irradiated to a dose of 50 kGy with 2.8 Gy/pulse and heat treatment for 3 hours at 60ºC.

(a) Unirradiated FEP

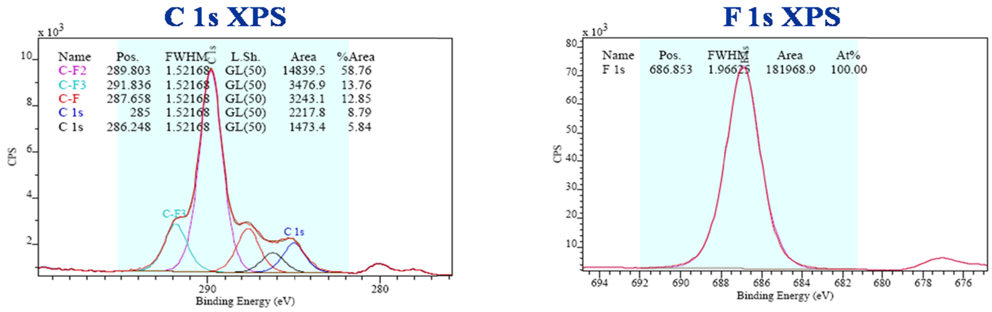

(b) Electron-irradiated FEP/Styrene

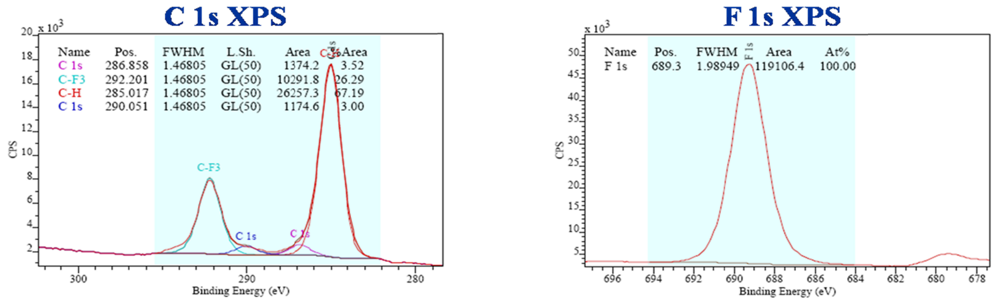

FIG. 18. C 1s and F 1s XPS of (a) unirradiated FEP (125 µm) and (b) FEP/styrene grafted by simultaneous electron beam irradiation to a dose of 50 kGy at 2.8 Gy/pulse, followed by heat treatment at 60℃ for 3 h. Degree of grafting: 38.5 wt%.

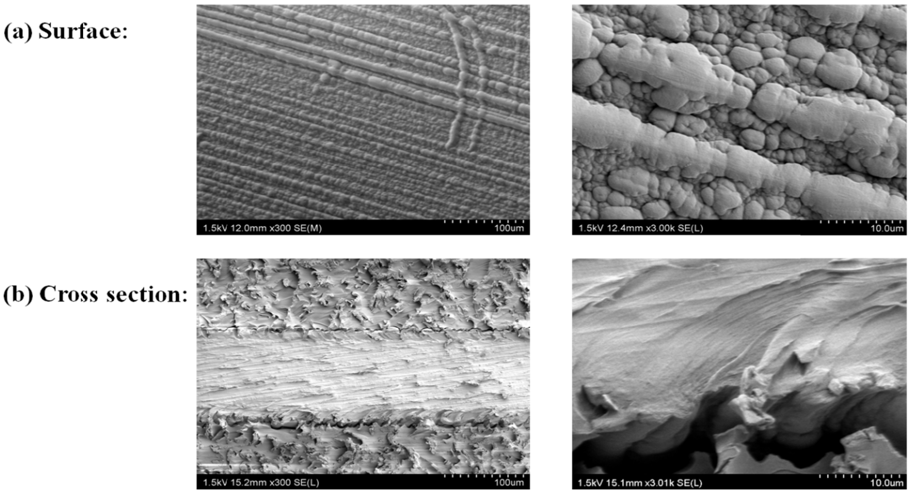

FIG. 19. SEM micrographs of the surface and cross-sections of FEP (125 µm) simultaneously ^{60}Co γ-irradiated in argon with styrene monomer to a dose of 50 kGy at 0.17 Gy/s. Degree of grafting: 8.4 wt%.

The SEM micrographs FEP films after styrene grafting with γ irradiation to a dose of 50 kGy are shown in Figure 19. The striated distributions of material on the surface of the grafted films are more pronounced after γ irradiation than after electron beam irradiation. An increase in surface roughness has also been reported by Machi et al., [16], in which a bubble morphology formed on polyethylene after radiation grafting with styrene. These bubbles were demonstrated to contain collections of styrene homopolymer which swell in benzene solvent. The slower rate of grafting which takes place during gamma irradiation may explain the inhomogeneities which were observed in FEP-g-Sty. Under the lower dose rate conditions provided by gamma radiation, the rate of the grafting reaction may slow down so much that it becomes comparable to the rate of the styrene homopolymerization reaction. Styrene homopolymer formation may therefore become much more significant, thereby placing mechanical stresses on the FEP substrate that enhance the surface roughness.

Figure 20 shows the C 1s and F 1s spectrum for ^{60}Co γ-grafted FEP, the C 1s spectrum is characteristic of pure styrene with a peak due to C-C/C-H at 285 eV and a $\pi \rightarrow \pi^*$ shake-up satellite peak at ~ 292.0 eV. The ratio of F/C of the γ-grafted film is very low: 0.006. The XPS technique will only generate atomic bonding information from the top surface, to a maximum depth of 10 nm, and since the results show almost no fluorine and only C-C bonding, it is likely only styrene is present on the top surface. Due to the low dose rate of γ radiation, instead of a rapid production of free radicals on both styrene monomer and FEP, it is possible that polystyrene polymerization occurs. Thus the top surface would have a layer of polystyrene or styrene monomer.

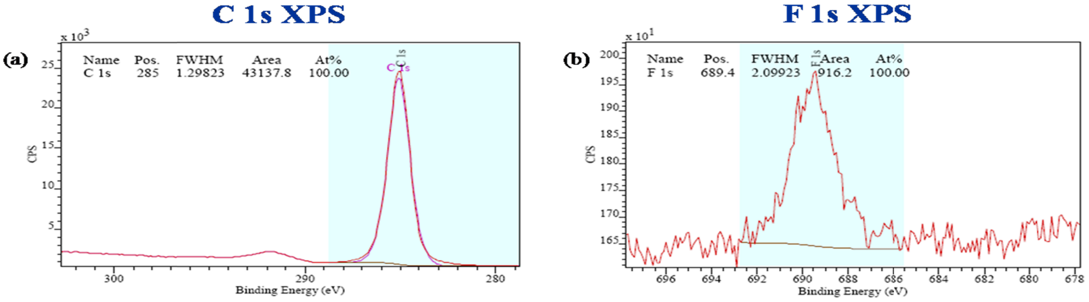

FIG. 20. C 1s and F 1s XPS of FEP film (125 μm) grafted with styrene by ^{60}Co γ irradiation to 50 kGy at 0.17 Gy/s in argon. Degree of grafting is 8.4 wt%.

Figure 21 shows AFM measurements of the surface morphology of the FEP/styrene grafted material produced by ^{60}Co γ irradiation and electron beam irradiation. γ-Irradiation was observed to produce broader irregularities on the surface of the FEP film than electron beam irradiation. For example, the larger features in the gamma-irradiated sample shown in figure 21(a) are on the order of 10 μm in width, whereas those in the electron-irradiated sample shown in figure 21(b) are approximately 2–3 μm in width. The height of the irregular features produced by gamma irradiation is also greater than that produce by electron beam irradiation. A typical peak-to-valley distance in height produced by gamma irradiation is on the order of 500 nm, whereas that produced by electron irradiation is on the order of 30 nm.

(a) ^{60}Co γ-irradiated FEP/Styrene

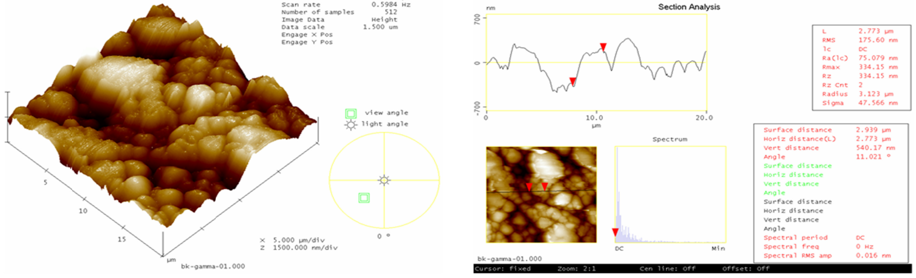

Digital Instruments NanoScope
Scan size 20.00 μm
Scan rate 0.5984 Hz
Number of samples 512
Image Data Height
Data scale 1.500 um
Engage X Pos
Engage Y Pos

X 5.000 μm/div
Z 1500.000 nm/div

L 2.773 μm
RMS 175.60 nm
lc DC
Ra(lc) 75.079 nm
Rmax 334.15 nm
Rz 334.15 nm
Rz Cnt 2
Radius 3.123 μm
Sigma 47.566 nm

Surface distance 2.939 μm
Horiz distance(L) 2.773 μm
Vert distance 540.17 nm
Angle 11.021 °
Surface distance
Horiz distance
Vert distance
Angle
Surface distance
Horiz distance
Vert distance
Angle
Spectral period DC
Spectral freq 0 Hz
Spectral RMS amp 0.016 nm

(b) Electron-irradiated FEP/Styrene

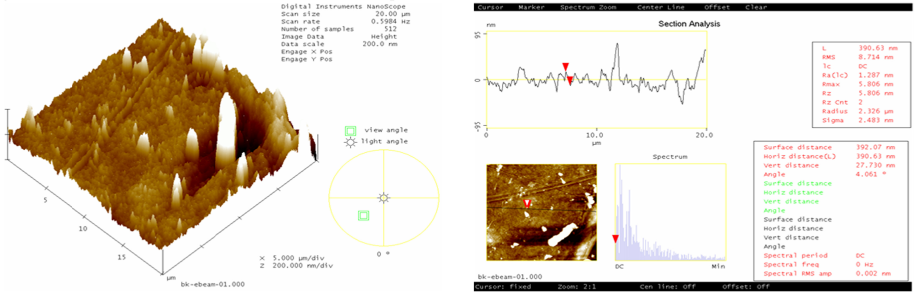

Digital Instruments NanoScope
Scan size 20.00 μm
Scan rate 0.5984 Hz
Number of samples 512
Image Data Height
Data scale 200.0 nm
Engage X Pos
Engage Y Pos

X 5.000 μm/div
Z 200.000 nm/div

L 390.63 nm
RMS 8.714 nm
lc DC
Ra(lc) 1.287 nm
Rmax 5.806 nm
Rz 5.806 nm
Rz Cnt 2
Radius 2.326 μm
Sigma 2.483 nm

Surface distance 392.07 nm
Horiz distance(L) 390.63 nm
Vert distance 27.730 nm
Angle 4.061 °
Surface distance
Horiz distance
Vert distance
Angle
Surface distance
Horiz distance
Vert distance
Angle
Spectral period DC
Spectral freq 0 Hz
Spectral RMS amp 0.002 nm

FIG. 21. AFM analysis of FEP (125 μm) grafted with styrene by (a) ^{60}Co γ irradiation to a dose of 50 kGy at 0.17 Gy/s in argon (degree of grafting is 8.4 wt%), and (b) electron beam irradiation to a dose of 50 kGy at 2.8 Gy/pulse in air followed by heat treatment at 60 ℃ for 3 h. Degree of grafting: 38.5 wt%.

6.3. Ion conductivity of FEP-g-SSA membrane

The proton conductivity measurements acquired with an AC impedance value are presented in Figure 21. The 25 μm FEP styrene-grafted films yielding the closest proton conductivity to the standard had weight grafting percentages of 21.8% and 24% with medium absorbed grafting dose (62 kGy and 81 kGy, respectively) yet used very different 60ºC heat treatment times (2 hours and 24 hours, respectively). Yet on the contrary, a FEP specimen with 23 % grafting using a 86 kGy absorbed dose and 5 hour 60ºC heat treatment yielded much lower conductivity. Additionally, a second sample using 63 kGy and 2 hour heat treatment times yielded very low conductivity as compared to the specimen yielding conductivity close to the standard. This discrepancy between specimens having similar gravimetric grafting rates can be postulated to depend on the uniformity of the graft.

One specimen in which the FEP film was pre-irradiated and to which styrene was then immediately added, yielded only a 1.8% of grafting and exhibited low proton conductivity. This may indicate that the simultaneous grafting method is much more efficient in yielding high grafting percentages (Table 3)

TABLE 3. FEP FILMS FOR PROTON CONDUCTIVITY WITH ELECTRON BEAM IRRADIATION DOSE, HEAT TREATMENT TIME AND RESULTING % STYRENE GRAFTING IN ORDER OF DECREASING CONDUCTIVITY

Absorbed Dose (kGy)	H.T. Time (h)	H.T. Temp (°C)	Irrad. Method	Grafting (%)
81.2	24	60	Simultaneous	24.1
62	2	60	Simultaneous	21.8
86.2	5	60	Simultaneous	22.8
23.5	5	60	Pre-irradiated	1.8
25.1	25	60	Simultaneous	8.9
63	2	60	Simultaneous	20.6

7. DISCUSSION

The most effective technique of styrene grafting to FEP investigated in this work involved the simultaneous electron beam irradiation followed by post-irradiation heat treatment. This approach produced a styrene graft through the entire thickness of the FEP film, with a degree of grafting of over 30 wt% and a smooth surface morphology. The uniformity of grafting as a function of depth in the FEP substrate was observed by EDS to be highly dependent on the length of time that the irradiated samples were exposed to heat treatment. The data presented through FTIR, SEM micrographs, and EDS line scans indicate that after a 50 kGy dose of electron irradiation and two hours of 60°C heat treatment, a uniform graft forms within the FEP film. Shorter heat treatment times produce ’grafting fronts’ which indicate that the styrene has only diffused partially through the film

During the simultaneous irradiation of styrene and FEP, both species are expected to form carbon-centred free radicals. The high electronegativity of fluorine causes the C-F bonds in FEP to be sensitive to radiation-induced scission, and would be expected to generate radicals much more rapidly and with higher yields than would be produced from the styrene monomer. The radicals on the styrene and FEP combine with each other to form a covalent bond, or graft.

Grafting performed using ^{60}Co γ radiation generated yields which were comparable to those produce with the same dose of electron beam radiation without post-irradiation heat treatment. This result illustrates the importance of exposing the irradiated FEP/styrene to elevated temperatures in order to achieve uniformly grafted materials. It is proposed that under low dose rate and room temperature conditions after irradiation, the styrene will graft to the surface and outer regions of the FEP film, then homopolymerize to form long polystyrene chains that extend out from and/or lay on the surface of the substrate. The high concentrations of C-C and C=C bonds observed in the XPS spectra of the grafted material indicates that there is a relatively high concentration of styrene and/or polystyrene near the surface of the film. Styrene appears to graft only near the surface of each side of the FEP film under low dose rate and room temperature conditions, rather than penetrating through the film.

Additionally, SEM micrographs and AFM images point to the uneven morphology of the γ-grafted surface. These striations may be associated with the polystyrene agglomerations caused by homopolymerization. The use of ^{60}Co γ irradiation to graft styrene monomer to FEP without post-irradiation heat treatment causes agglomeration on the surface of the film instead of diffusion into the thickness of the film for grafting.

The proton conductivity measurements showed mixed results. There was no clear pattern in achieving higher proton conductivity between dose or heat treatment time. Some of the specimens used in proton conductivity measurements exhibited behaviour close to the control at the high RH and were somewhat lower at the lower RH. This behaviour is typical for hydrocarbon based membranes. Generally, a medium absorbed dose (60–80 kGy) yielded the highest proton conductivity. Doses below 40 kGy yielded low grafting percentages and conductivity measurements. Additionally, doses above 80 kGy reduced the conductivity slightly, possibly due to FEP film degradation. Beyond two hours, heat treatment time did not have a significant effect on conductivity as grafting reaches a plateau. For specimens yielding generally low conductivity, the apparent increase in conductivity at lower RH is noise in the measurement rather than a true effect. Overall, these samples show 100–1000 times lower conductivity than the other samples and are near the detection limit.

Generally, the use of a hydrocarbon based fuel cell membrane is likely to yield these types of proton conductivity results. While the 125 μm films allow us to probe the morphology and mechanisms of grafting, this study is limited by the use of two FEP film thicknesses. Characterization with 25 μm thin films would produce a stronger correlation between absorbed dose, dose rate and heat treatment time. Also, the higher doses used with conductivity samples was not probed for degradation. While it was achieved a very uniform graft even through a thickness of 125 μm, and presumably with the 25 μm film, the styrene graft must be made shorter. As was shown with the γ-irradiated specimens, a low dose rate will produce a long styrene chain off the surface. The use of an even higher dose rate than achieved with the pulsed electron beam will likely yield more favourable proton conductivities even closer to the standard sample.

8. CONCLUSIONS

Simultaneous electron beam irradiation of FEP and styrene followed by post-irradiation heat treatment has been demonstrated to be a successful technique of production of a polymer electrolyte membrane for substrate thicknesses of 25–125 μm. A uniform styrene graft as a function of depth within the FEP substrate was observed when the system was irradiated with a dose of 50 kGy of electron irradiation and held at either 45°C for three hours or 60°C for two hours after irradiation. Although lower levels of grafting were achieved using gamma irradiation, this method was unable to produce uniformly grafted materials. The graft uniformity therefore appears to be highly dependent on the radiation dose rate, whereas the degree of grafting depends heavily on the heat treatment conditions. The simultaneous grafting method followed by heat treatment reported in this work can be used to successfully produce polymer electrolyte membranes with significant levels of proton conductivity.

REFERENCES

[1] GUBLER, L., SCHERER, G.G., A proton-conducting polymer membrane as solid electrolyte – function and required properties, Adv. in Polymer Sci. **215** (2008) 1.

[2] GÜRSEL, S.A., GUBLER, L., GUPTA, B., SCHERER, G.G., Radiation grafted membranes, Advances in Polymer Science **215** (2008) 157 – 217.

[3] COSTAMAGNA, P., SRINIVASAN, S., Quantum jumps in the PEMFC science and technology from the 1960s to the year 2000 Part I. Fundamental scientific aspects, Journal of Power Sources **102** (2001) 242 – 252.

[4] ACRES, G.J.K., Recent advances in fuel cell technology and its applications, Journal of Power Sources **100** (2001) 60 – 66.

[5] STANIS, R.J., YAKLIN, M.A., CORNELIUS, C.J., TAKATERA, T., UMEMOTO, A., AMBROSINI, A., FUJIMOTO, C.H., Evaluation of hydrogen and methanol fuel cell performance of sulfonated Diels Alder poly(phenylene) membranes, Journal of Power Sources **195** (2010) 104 – 110.

[6] KIM, B.N., LEE, D.H., HAN, D.H., Characteristics of fuel cell membranes prepared by EB radiation grafting onto FEP with styrene derivatives, styrene and 2-methylstyrene, Journal of the Electrochemical Society **155** (2008) B680 – B685.

[7] KIM, B.K., LEE, D.H., LEE, S.W., HAN, D.H., Improvement of polymer electrolyte membrane by radiation-induced grafting of styrene onto FEP Film with subsequent sulfonation, Korean Journal of Chemical Engineering **25** (2008) 1212 – 1220.

[8] GUBLER, L., SCHERER, G.G., A proton-conducting polymer membrane as solid electrolyte – function and required properties, Advances in Polymer Science **215** (2008) 1 – 14.

[9] GUBLER, L. GURSEL, S.A., SCHERER, G.G., Radiation grafted membranes for polymer electrolyte fuel cells, Fuel Cells **5** (2005) 317 – 335.

[10] KIM, B.N., LEE, D.H., LEE, S.W., HAN, D.H., Improvement of polymer electrolyte membrane by radiation-induced grafting of styrene onto FEP film with subsequent sulfonation, Korean Journal of Chemical Engineering **25** (2008) 1212 – 1220.

[11] FERRARIA, A.M., LOPES, D.A., SILVA, J.D. BOTELHO DO REGO, A.M., Polymer **44** (2003) 7241 – 7249.

[12] GUPTA, B., BÜCHI, F.N., SCHERER, G.G., Cation exchange membranes by pre-irradiation grafting of styrene into FEP films. I. Influence of synthesis conditions, Journal of Polymer Science Part A **32** (1994) 1931 – 1938.

[13] CHAPIRO, A., Radiation induced grafting, Radiat. Phys. Chem. **9** (1977) 55 – 67.

[14] LI, J., SATO, K., ISHIZURI, S., ASANO, S., IKEDA, S., IIDA, M., OSHIMA, A., TABATA, Y., WASHIO, M., Pre-irradiation induced grafting of styrene into crosslinked and non-crosslinked polytetrafluoroethylene films for polymer electrolyte fuel cell applications. II: characterization of the styrene grafted films, European Polymer Journal **41** (2005) 547 – 555.

[15] BRIGGS, D., SEAH, M.P., Eds. Practical Surface Analysis, Volume 1: Auger and X-Ray Photoelectron Spectroscopy. 2nd ed. John Wiley & Sons. (1994).

[16] MACHI, S., SILVERMAN, J., Bubble formation in radiation-induced grafting of styrene to polyethylene, Journal of Polymer Science, Part A-1 Polymer Chemistry **7** (1969) 2737 – 2740.

PUBLICATIONS RESULTING FROM THE COORDINATED RESEARCH PROJECT

1. ARGENTINA

MAZZEI, R., BERMÚDEZ, G.G., FERNÁNDEZ, A., TORRES, A., BETZ, N., TADEY, D., Grafting of PNIPAAm on PVDF submicroscopic tracks induced by the active sites remainders of the etching process, Nuclear Instruments and Methods in Physics Research B **266** (2008) 937–943.

MAZZEI, R., FERNÁNDEZ, A., BERMÚDEZ, G.G., TORRES, A., GUTIERREZ, M.C., MAGNI, M., CELMA, G., TADEY, D., Grafting of acrylic acid on etched latent tracks induced by swift heavy ions on polypropylene films, Nuclear Instruments and Methods in Physics Research B **266** (2008) 937–943.

MAZZEI, R., BERMÚDEZ, G.G, ARBEITMAN, C.R., DEL GROSSO, CHAPPA, M.F., New membranes obtained by grafted implanted PVDF foils, (in preparation).

MAZZEI, R., CAMPOROTONDI, D., LOMBARDO, J., TADEY, D., BERMÚDEZ, G.G., Immobilization of biological substances in membranes obtained grafting PVDF implanted with Ar^+ ions, (in preparation).

2. BRAZIL

MOURA, E., SOMESARI, E., SILVEIRA, C., PAES, H. A., SOUZA, C.A., FERNES, W., MANZOLI, J.E., GERALDO, A.B.C., Influence of physical parameters on polymer mutual grafting by electron beam irradiation, Radiation Physics and Chemistry, **80** (2011) 175–181.

MANZOLI, J.E., ARAÚJO, F.D.C., PANZARINI, L.C.G.A., DUARTE, C., SOMESARI, E., SILVEIRA, C., PAES, H.A., Phthalate Migration Study from PVC Grafted by Gamma Radiation, Arab Journal of Nuclear Science and Applications **42** (2009) 433–439.

PANZARINI, L.C.G.A., MANZOLI, J.E., ARAÚJO, F.D.C., MARTINELLO, V.C., SOMESARI, E., SILVEIRA, C., PAES, H.A., MOURA, E.S., Dose rate effect on grafting by gamma radiation of DMAEMA onto flexible PVC, Arab Journal of Nuclear Science and Applications **42** (2009) 425–431.

AUGUSTO, C.G., MOURA, E., SOMESSARI, E.S.R., SILVEIRA, C.G., PAES, H. A., SOUZA, C.A., FERNES,W., MANZOLI, J.E., GERALDO, A.B.C., "Chemical functionalization of styrene grafted polymers", Paper presented at 9th Meeting of the Ionizing Radiation and Polymer Symposium, Maryland, USA, October 25 to 29 2010.

MANZOLI, J.E., MOURA, E., SOMESSARI, E.S.R., SILVEIRA, C.G., PAES, H.A., SOUZA, C.A., FERNES, W., GERALDO, A.B.C., "Radiation induced peroxidation on polypropylene", Paper presented at 9th Meeting of the Ionizing Radiation and Polymer Symposium, Maryland, USA, October 25 to 29 2010.

MOURA, E., CARDOZO, P., SOMESARI, E., SILVEIRA, C., PAES, H. A., SOUZA, C.A., FERNES, W., MANZOLI, J.E., GERALDO, A.B.C., "Perfluorinated polymer grafting: influence of pre-irradiation conditions", Paper presented at International Nuclear Atlantic Conference, Rio de Janeiro, Brazil, September 27 to October 6 2009.

MOURA, E., SOMESARI, E., SILVEIRA, C., SOUZA, C.A., FERNES, W., MANZOLI, J. E., GERALDO, A.B.C., "Physical parameters influence at polymer mutual grafting by electron beam irradiation", Paper presented at 11th Pacific Polymer Conference, Cairns, Australia, December 6–10 2009.

CARDOZO, P., MANZOLI, J.E., GERALDO, A.B.C., SOMESARI, E., SILVEIRA, C., PAES, H.A., FERNES, W., SOUZA, C.A., “Vacuum chamber with heating up to 300°C dispositive: application on grafting process by electron beam irradiation”, Paper presented at 11th Pacific Polymer Conference, Cairns, Australia, December 6–10 2009.

MANZOLI, J.E., MAZZEI, R., GERALDO, A.B.C., MOURA, E., BERMÚDEZ, G.G., DEL GROSSO, M.F., CHAPPA, V.C., ARBEITMAN, C., “Cationic membranes produced by swift heavy ions to be applied in PEM fuel cells”, Paper presented at 8th Meeting of the Ionizing Radiation and Polymer Symposium, Angra dos Reis, Brazil, October 12 to 17 2008.

MANZOLI, J.E., ARAÚJO, F.D.C., PANZARINI, L.C.G.A., DUARTE, C., SOMESARI, E., SILVEIRA, C., PAES, H.A., “Phthalate migration study from PVC grafted by gamma radiation”, Paper presented at 9th Radiation Physics and Protection Conference, Cairo, Egypt, November 15 to 19 2008.

PANZARINI, L.C.G.A., MANZOLI, J.E., ARAÚJO, F.D.C., MARTINELLO, V.C., SOMESARI, E., SILVEIRA, C., PAES, H.A., MOURA, E.S., “Dose rate effect on grafting by gamma radiation of DMAEMA onto flexible PVC”, Paper presented at 9th Radiation Physics and Protection Conference, Cairo, Egypt, November 15 to 19 2008.

3. EGYPT

KAMAL, H., HEGAZY, E.A., SOLIMAN, E.A., ABD ELMAKSOD, A., SAYED A., Radiation and physicochemical properties of ion exchange membranes by simultaneous radiation grafting of styrene-Methacrylic acid comonomers onto LDPE film, Journal of Radiation Research and Applid Science, (submitted).

EL-SAWY, N.M., HEGAZY, E.A., EL-HAG ALI, A., ABDEL MOTLAB, M.S., AWADALLAH-F., A., Physicochemical study of radiation-grafted LDPE copolymer and its use in metal ions adsorption, Nuclear Instruments and Methods in Physics Research Section B: Beam Interactions with Materials and Atoms **264** (2007) 227–234.

KAMAL, H., ABD EL-REHIM, H.A., HEGAZY, E.A., Radiation syntheses of molecularly imprinted grafted polymer for metal ion selective separation, Nuclear Instruments and Methods in Physics Research Section B: Beam Interactions with Materials and Atoms, (submitted).

EL-HAG ALI, A., KAMAL H., ABD EL-REHIM DALIA H.A., HEGAZY, E.A., Selective separation of metal ions by poly (vinyl alcohol), 2- grafted acrylamido-2-methyl propane sulfonic acid and acrylic acid or acrylamide ter-polymers prepared by ionizing radiation, Separation and Purification Technology, (submitted).

4. FRANCE

WADE, T., CLOCHARD, M-C., Nano-valve device comprising nanoporous membrane, Demande de brevet européen n°09 305 252.0 du 20 mars 2009.

WADE, T., CLOCHARD, M-C., Method and device using nanoporous membranes for detecting and quantifying heavy metal ions in a fluid, European patent June 2008 EP08305237. Extension PCT/EP2009/056967.

BESSBOUSSE, H., NADHAKUMAR, I., DECKER, M., BARSBAY, M., CLOCHARD, M-C., WADE, T.L., Analytical Chemistry, (submitted).

5. HUNGARY

TAKÁCS, E., WOJNÁROVITS, L., BORSA, J., HARGITTAI, P., RÁCZ, I., ”Modification of the water adsorbance of cellulose by radiation induced grafting”, Paper presented at 8th International Conference on Ionizing Radiation and Polymers, Angra dos Reis, Brazil, October 11−17, 2008.

TAKÁCS, E., WOJNÁROVITS, L., BORSA, J., RÁCZ, I., Hydrophilic/hydrophobic character of grafted cellulose, Radiat. Phys. Chem. **79** (2010) 467–470.

WOJNÁROVITS, L., FÖLDVÁRY, CS., TAKÁCS, E., Radiation-induced grafting of cellulose for adsorption of hazardous water pollutants. A review, Radiat. Phys. Chem. **79** (2010) 848−862.

TAKÁCS, E., DESMET, G., WOJNÁROVITS, L., BORSA, J., ”Functionalization of cotton-cellulose by radiation induced grafting and cyclodextrin immobilization”, Invited lecture presented at 9th International Conference on Ionizing Radiation and Polymers, College Park, USA, October 25−29 2010.

TAKÁCS, E., DESMET, G., WOJNÁROVITS, L., BORSA, J., Functionalization of cotton-cellulose via high-energy irradiation initiated grafting of glycidyl methacrylate and cyclodextrin immobilization, Radiat. Phys. Chem. (accepted).

6. INDIA

GOEL, N.K., RAO, M.S., VIRENDRA, K., BHARDWAJ, Y.K., CHAUDHARI, C.V., DUBEY, K.A., SABHARWAL, S., Synthesis of antibacterial cotton fabric by radiation induced grafting of [2-(Methacryloyloxy)ethyl] trimethylammonium chloride (MAETC) onto cotton, Radiat. Phys. Chem. **78** (2009) 399–406.

DAS, S., PANDEY, A.K., ATHWALE, A., VIRENDRA KUMAR, BHARDWAJ, Y.K., SABHARWAL, S. MANCHANDA, V. K., Chemical aspects of uranium recovery from sea water by amidoximated electron-beam-grafted polypropylene membranes, Desalination **232** (2008) 243−253.

GOEL, N.K., BHARDWAJ, Y.K., MANOHARAN, R., VIRENDRA, K., DUBEY, K.A., CHAUDHARI, C. V., SABHARWAL, S., Physicochemical and electrochemical properties of radiation grafted micro-porous polypropylene membranes, eXpress Polym. Lett. **3(5)** (2009) 268−278.

CHAUDHARI, C. V., PAUL, J., PANICKER, L., DUBEY, K.A., KUMAR, V., GOEL, N.K., BHARDWAJ, Y.K., SABHARWAL, S., Teflon scrap based cation exchanger by radiation grafting: Process parameter standardization and characterization, Environ. Prog. & Sustain. Ener. (In print) doi: 10.1002/ep.10533.

GOEL, N.K., RAO, M.S., VIRENDRA, K., BHARDWAJ, Y.K., DUBEY, K.A., CHAUDHARI, C. V., SABHARWAL, S., Synthesis of antibacterial cotton fabric by radiation induced co-grafting of [2-(acryloyloxyethyl)] trimethylammonium chloride and 2-hydroxyethyl methacrylate onto cotton fibrils, Radiat. Phys. Chem. **80** (2011) 1233−1241.

7. JAPAN

SEKO, N., NINH, N.T.Y., TAMADA, M., Emulsion grafting of glycidyl methacrylate onto polyethylene fiber, Radiat. Phys. Chem. **79** (2010) 22−26.

SEKO, N., HOSHINA, H., KASAI, N., UEKI, Y., TAMADA, M., KIRYU,T.,TANAKA, K., TAKAHASHI, M., Novel recovery system of scandium from hot spring water by fibrous graft adsorbent, J. Ion Exchange **21** (2010) 117−122.

NAYANAJITH, L.D.C., UEKI, Y., SEKO, N., HOSHINA, H., TAMADA, M., Aminated adsorbent synthesized by radiation-induced graft polymerization of 4-chloromethylstyrene onto nonwoven polylactic acid fabric and its adsorption capacity for metal ions, J. Ion Exchange **21** (2010) 123−126.

HOSHINA, H., SEKO, N., UEKI, Y., IYATOMI, Y., TAMADA, M., Evaluation of graft adsorbent with N-methyl-D-glucamine for boron removal from groundwater, J. Ion Exchange **21** (2010) 153−156.

SEKINE, A., SEKO, N., TAMADA, M., SUZUKI, *Y.,* Biodegradable metal adsorbent synthesized by graft polymerization onto nonwoven cotton fabric, Radiat. Phys. Chem. **79**, (2010) 16–21.

BASUKI, F., SEKO, N., TAMADA, M., Recovery of scandium by phosphoric chelating adsorbent by directly synthesized radiation graft polymerization, J. Ion Exchange **21** (2010) 127−130.

PHIRIYATORN, S., HOSHINA, H., SEKO, TAMADA, M., Adsorption of metals by adsorbent containing hydroxamic acid groups synthesized by radiation induced graft polymerization, J. Ion Exchange **21** (2010) 157−160.

TAKEDA, T., TAMADA, M., SEKO, N., UEKI, Y., Ion exchange fabric synthesized by graft polymerization and its application to ultra-pure water production, Radiat. Phys. Chem. **79** (2010) 223–226.

IYATOMI, Y., HOSHINA, H., SEKO, N., SHIMADA, A., OGATA, N., SUGIHARA, K., KASAI, N., UEKI, Y., TAMADA, M., Investigation to increase the efficiency of fluorine and boron removal from groundwater using radiation-induced graft polymerization adsorbent, Trans. Atom. Energy Soc. Jpn. **9**(3) (2010) 330–338.

SEKO, N., YOSHII, A., SHIOZAWA, T., TSUNODA, Y., OTANI, H., INOUE, A., HOSHINA, H., UEKI, Y., TAMADA, M., Development of purification system for circulative cooling water by radiation graft adsorbent, EcoDesign **39** (2009) 1191−1194.

HOSHINA, H., PHIRIYATORN, S., SEKO, N., TAMADA, M., New adsorbent containing hydroxamic acid groups synthesized by radiation induced graft polymerization, EcoDesign **39** (2009) 1195−1198.

SEKO, N., YOSHII, A., TSUNODA, Y., Development of metal adsorbent for water treatment, Radiation & Industries (Japan), **123** (2009) 15−18.

SEKO, N., Development of novel adsorbents for rare metals form hot spring water, J. Soc. Automotive Engineer. (Japan) **63**, (2009) 102−105.

SEKO, N., Current status of metal adsorbent for recover from seawater and the prospect of coexistence with fishing industry, Bull. Soc. Sea Water Sci., (Japan), **63** (2009) 221–225.

TAMADA, M., Fibrous metal ion adsorbent synthesized by radiation processing, Polymers (Japan) **58** (2009) 397–400.

TAMADA, M., ”Current status of technology for collection of uranium from seawater”, Paper presented at International Seminar on Nuclear War and Planetary Emergencies - 42nd Session, 243−252 (2009)

UEKI, Y., SEKO, N., HOSHINA, H., TAMADA, M., Preparation of metal adsorbent with sulfo groups by radiation-induced grafting of ethyl p-styrenesulfonate, JAEA-Review 2008-055, **39** (2008)

HOSHINA, H., SEKO, N., N. KASAI, N., UEKI, Y., IYATOMI, Y., N. OGATA, N., TAMADA, M., Preliminary evaluation of fibrous boron adsorbent with groundwater, JAEA-Review 2008–055, **40** (2008)

8. MALAYSIA

NASEF, M.M., SAIDI, H., DAHLAN, K.Z.M., Single-step radiation induced grafting for preparation of proton exchange membranes for fuel cell, J. Membr. Sci. **339** (2009) 115–119.

NASEF, M.M., SAIDI, H., DAHLAN, K.Z.M., Acid synergized grafting of sodium styrene sulfonate onto electron beam irradiated poly(vinylidene fluoride) films for preparation of fuel cell membrane, J. Appl. Polym. Sci. **118** (2010) 2801–2809.

NASEF, M.M., SAIDI, H., DAHLAN, K.Z.M., Radiation grafted poly(vinylidene fluoride)-graft-polystyrene sulfonic acid membranes for fuel cells: Structure-property relationships, Chinese J. Polym. Sci. **28** (2010) 761–770.

NASEF, M.M., SAIDI, H., DAHLAN, K.Z.M., Comparative investigations on radiation grafted proton exchange membranes prepared by single-step and conventional two-steps radiation induced grafting methods, Polym. Int. **60** (2011) 186-193.

NASEF, M.M., SAIDI, H., DAHLAN, K.Z.M., Kinetic investigation of Graft copolymerization of sodium styrene sulfonate onto poly(vinylidene fluoride) films, Radiation Physics and Chemistry **80** (2011) 66–75.

NASEF, M.M., Radiation grafted membranes for fuel cells: current trends and future directions, Chem. Rev. accepted.

NASEF, M.M., SAIDI, H., DAHLAN, K.Z.M., ”Sulfonic acid membranes by a new radiation induced grafting method”, Paper presented at the 8th International Symposium on Ionizing Radiation and Polymers (IRAP 2008), Angra dos Reis, Rio de Janeiro, Brazil, 12–17 November 2008.

NASEF, M.M., SAIDI, H., DAHLAN, K.Z.M., ”Radiation induced grafting of styrene onto partially fluorinated films for preparation of proton exchange membranes: The role of liquid additives”, Paper presented at The 7th International Conference on Membrane Science and Technology, MST2009, Kuala Lumpur, Malaysia,12–15 May 2009.

NASEF, M.M., SAIDI, H., DAHLAN, K.Z.M., ”Radiation induced grafting of styrene onto partially fluorinated films for preparation of proton exchange membranes: The role of liquid additives”, Paper presented at The 7th International Conference on Membrane Science and Technology, MST2009, Kuala Lumpur, Malaysia,12–15 May 2009.

NASEF, M.M., ”Development of polymer electrolyte membranes by electron beam irradiation”, Invited paper presented at International Conference on Electron Beam Irradiation – an Eco-friendly Technology for Processing of Food and Industrial Products, New Delhi, India, July 30–31 2009.

NASEF, M.M., ”Polymer electrolyte membranes for fuel cells by radiation induced grafting with electron beam irradiation: state-of-the-art”, Invited lecture presented at The second International conference on radiation sciences and its applications (ICRSA 2010), Marsa Alam, Egypt. 28/3/2010–1/4/2010.

NASEF, M.M., ”Is single-step radiation grafting method better than its counterpart conventional two-step method in preparation of proton exchange membranes for fuel cell?” Paper presented at the 8th International Conference on Membrane Science and Technology, Institute Teknologi Bandung (ITB) Bandung, Indonesia, 30th Nov – 1st Dec 2010.

NASEF, M.M., ”Fuel cell membranes by radiation-induced graft copolymerization: current status, challenges, and future directions”, in ZAIDI, S.M.J. and MATSUURA, T., (eds.) Polymer Membranes for Fuel Cells, Springer Science, New York, (2008) pp. 87–114.

9. POLAND

PRZYBYTNIAK, G., KORNACKA, E.M., MIRKOWSKI, K., WALO, M., ZIMEK, Z., Functionalization of polymer surfaces by radiation-induced grafting, Nukleonika **53** (3) (2008) 89–95.

PRZYBYTNIAK, G., KORNACKA, E., FUKS, L., Functionalization of polyamide surface by radiation-induced grafting of N-vinylpyrrolidone and acrylamide, J. Polym. Res. on line.

KORNACKA, E., PRZYBYTNIAK, G., MIRKOWSKI, K., ”Radiation-induced grafting monomers onto Polyamide 6,10,” Paper presented at the 26th Miller Conference on Radiation Chemistry, Keszthely, Hungary, 28.08–02.09.2009.

WALO, M., PRZYBYTNIAK, G., KAVAKLI, P.A., BARSBAY, M., GÜVEN, O., ”Radiation-induced graft modification of polyurethanes based on isophorone diisocyanate for biomedical applications”, Paper presented at the 9th Meeting of the Ionizing Radiation and Polymers Symposium (IRaP2010), College Park, Maryland, USA, 25.10–29.10.2010.

WALO, M., PRZYBYTNIAK, G, KAVAKLI, P.A., BARSBAY, M., GÜVEN, O., Radiation-induced graft modification of polyurethanes based on isophorone diisocyanate for biomedical applications, To be submitted to *Radiat. Phys. Chem.*

PRZYBYTNIAK, G., KORNACKA, E. FUKS, L., MIRKOWSKI, K., ŁYCZKO, K., Radiation-induced co-grafting of acrylamide and acrylic acid of polypropypene filter, To be submitted.

10. REPUBLIC OF KOREA

GENG, F., SHIN, J., KANG, S.A., KO, B.S., KANG, P.H., LEE, Y.S., NHO, Y.C., Preparation and Characterization of a Poly(vinylbenzyl sulfonic acid)-grafted FEP membrane, J. Polym Sci. Part A: Polym. Chem. **48** (2010) 563–569

GENG, F., KANG, S.A., SHIN, J., KO, B.S., NHO, Y.C., Influence of the radiation grafting conditions on the cross-sectional distribution of poly(vinylbenzyl chloride) grafted polymer onto poly(tetrafluoroethylene-co-hexafluoropropylene) films, J. Appl. Polym. Sci. **117** (2010) 2380–2385.

GWON, S.J., CHOI, J.H., SOHN, J.Y., IHM, Y.E., NHO, Y.C., Preparation of a new micro-porous poly(methyl mehtacrylate)-grafted polyethylene separator for high performance Li secondary battery, Nucl. Instr. Methods Phys. Res. Sect. B **267** (2009) 3309–3313.

LEE, J.Y., LEE, Y.M., BHATTACHARYA, B., NHO, Y.C., PARK, J.K., Separator grafted with siloxane by electron beam irradiation for lithium secondary batteries, Electrochim. Acta **54** (2009) 4312-4315.

LEE, J.Y., BHATTACHARYA, B., NHO, Y.C., PARK, J.K., New separator prepared by electron beam irradiation for high voltage lithium secondary batteries, Nucl. Instr. Methods Phys. Res. Sect. B **267** (2009) 2390–-2394.

SHIN, J., KO, B.S., KANG, S.A., GENG, F., NHO, Y.C., KANG, P.H., A Study on the distribution of polystyrene sulfonic acid grafts over the cross-section of a PFA film, Nucl. Instr. Methods Phys. Res. Sect. B **267** (2009) 791–794.

GWON, S.J., CHOI, J.H., SOHN, J.Y., LIM, Y.M., NHO, Y.C., Battery performance of PMMA-grafted PE-separators prepared by pre-irradiation grafting techinique, J. Ind. Eng. Chem. **15** (2009) 748–751.

KANG, S.A., SHIN, J., GENG, F., KO, B.S., KIM, C.Y., KANG, P.H., NHO, Y.C., Preparation of crosslinked polystyrene grafted PFA films by a simultaneous irradiation method, J. Ind. Eng. Chem. **15** (2009) 748–751.

GWON, S.J., CHOI, J.H., SOHN, J.Y., Y IHM, O.E., NHO, Y.C., Radiation grafting of methyl methacrylate onto polyethylene separators for lithium secondary batteries, Nucl. Instr. Methods Phys. Res. Sect. B **266** (2008) 3387–3391.

CHOI, J.H., GWON, S.J., SOHN, J.Y., JUNG, C.H., IHM, Y.E., LIM, Y.M., NHO, Y.C., Preparation of polystrylene-grafted poly(vinylidene fluoride)membranes for lithium secondary batteries, J. Ind. Eng. Chem. **14** (2008) 116–119.

KANG, S.A., SHIN, J., GENG, F., KO, B.S., KIM, C.Y., NHO, Y.C., Radiolytic preparation of poly(styrene sulfonic acid)-grafted poly(tetrafluoroethylene-co-perfluorovinylether) membranes with highly cross-linked networks, Nucl. Instr. Methods Phys. Res. Sect. B **268** (2010) 3458–3463.

SOHN, J.Y., LIM, J.S., GWON, S.J., CHOI, J.H., SHIN, J., IHM, Y.E., NHO, Y.C., Preparation and characterization of a PVDF-HFP/PEGDMA-coated PE separator for lithium-ion polymer battery by electron beam irradiation, Radiat. Phys. Chem. **78** (2009) 505–508.

11. SWITZERLAND

BEN YOUCEF, H., ALKAN GÜRSEL, S., WOKAUN, A., SCHERER, G.,G.The influence of crosslinker on the properties of radiation-grafted films and membranes based on ETFE, J. Membr. Sci. **311** (2008) 208–215.

GUBLER, L., BEN YOUCEF, H., ALKAN GÜRSEL, S., WOKAUN, A., SCHERER, G.G. Cross-linker effect in ETFE-based radiation-grafted proton-conducting membranes. I. Properties and fuel cell performance characteristics, J. Electrochem. Soc. **155** (9) (2008) B921–B928.

BEN YOUCEF, H., GUBLER, L., YAMAKI, T., SAWADA, S.-I., ALKAN GÜRSEL, S., WOKAUN, A., SCHERER, G.G. Cross-linker effect in ETFE-based radiation-grafted proton-conducting membranes. II. Extended fuel cell operation and degradation analysis, J. Electrochem. Soc. **156** (4) (2009) B532–B539.

BEN YOUCEF, H., GUBLER, L., ALKAN GÜRSEL, S., HENKENSMEIER, D., WOKAUN, A., SCHERER, G.G. Novel ETFE based radiation grafted poly(styrene sulfonic acid-co methacrylonitrile) proton conducting membranes with increased stability, Electrochem. Commun. **11** (2009) 941–944.

GUBLER, L., SLASKI, M., WALLASCH, F., WOKAUN, A., SCHERER, G.G. Radiation grafted fuel cell membranes based on co-grafting of alpha-methylstyrene and methacrylonitrile into a fluoropolymer base film, J. Membr. Sci. **339** (2009) 68–77.

BALOG, S., GASSER, U., MORTENSEN, K., GUBLER, L., SCHERER, G.,G. BEN YOUCEF, H. Correlation between morphology, water uptake, and proton conductivity in radiation-grafted proton-exchange membranes, Macromol. Chem. Phys. **211** (2010) 635–643.

BEN YOUCEF, H., ALKAN GÜRSEL, S., BUISSON, A., GUBLER, L., WOKAUN, A., SCHERER, G.G. Influence of radiation-induced grafting process on mechanical properties of ETFE-based membranes for fuel cells, Fuel Cells **10** (2010) 401–410.

GUBLER, L., SCHERER, G.G. Trends for fuel cell membrane development, Desalination **250** (2010) 1034–1037.

WALLASCH, F., ABELE, M., GUBLER, L., WOKAUN, A., MÜLLER, K., SCHERER, G.G. Characterization of radiation grafted polymer films using CP/MAS NMR spectroscopy and confocal Raman microscopy, Phys. Chem. Phys. (submitted).

BALOG, S., GASSER, U., MORTENSEN, K., BEN YOUCEF, H., GUBLER, L., SCHERER, G.G. Nano-scale morphology in graft copolymer ion-exchange membranes cross-linked with DIPB, J. Membr. Sci. (submitted).

12. THAILAND

SUWANMALA, P., HEMVICHAIN, K., SRINUTTRAKUL, W., Cadmium adsorbent prepared from poly(methyl acrylate) grafted cassava starch via gamma irradiation, Thai Journal of Physics, In press.

HEMVICHIAN, K., SUWANMALA, P., PIBANWONG, W., SIRI-UPATHUM, C., preparation of hydroxamic acid-containing cellulose adsorbent by radiation-induced grafting, Thai Journal of Physics, In press.

13. TURKEY

BARSBAY, M., AKKAŞ KAVAKLI, P., GÜVEN, O. Removal of phosphate using copper-loaded polymeric ligand exchanger prepared by radiation grafting of PP/PE nonwoven fabric, Rad. Phys. Chem. **79** (2010) 227.

AKKAŞ KAVAKLI, P., KAVAKLI, C., GÜVEN, O. Preparation of quaternized dimethylaminoethylmethacrylate grafted fabric for removal of phosphate, Radiat. Phys. Chem. **79** (2010) 233.

14. UNITED STATES OF AMERICA

CHUMAKOV, M.K., LAYLA SHAHAMAT’ ALIA WEAVER, LEBLANC, J., MAHNAZ CHAYCHIAN, SILVERMAN, J., RICHTER, K.B., WEISS, D., AL-SHEIKHLY, M., Electron-beam induced grafting of n-isopropylacrylamide to a poly(ethylene-terephthalate) membrane for rapid cell sheet detachment, Radiat. Phys. Chem. **80** (2011) 182–189.

ABBREVIATIONS

β–PVDF	β–poly(vinylidene fluoride)
AAc	acrylic acid
AAm	acrylamide
AAs	atomic absorption instruments
AETC	[2-(Acryloyloxyethyl)] trimethylammonium chloride
AFM	atomic force microscopy
AMPS	2-acrylamido-2-methyl propane sulfonic acid
AMS	α-methyl-styrene
ASV	anodic stripping voltammetry
Azole	imidazole
BAAm	N,N–methylene bis-acrylamide
CD	β–cyclodextrin
CSLM	confocal scanning laser microscopy
DEHP	di-2-ethyl hexyl phthalate
Dg, DG, DOG, DoG	Degree of grafting
DMAEMA	dimethyl aminoethyl methacrylate
DOS	degree of sulfonation
DP	degree of polymerization
DSC	differential scanning calorimetry
DVB	divinyl benzene
EDS	energy dispersive x ray spectroscopy
FEP	poly(tetrafluoroethylene-co-hexafluoropropylene
FESEM	field-emission scanning electron microscopy:
FME	functionalized membrane electrodes
FTIR	Fourier transform infrared spectroscopy
GMA	graft glycidyl methacrylate
HA	hydroxylamine
HEMA	2–hydroxyethyl methacrylate
HPA	2–hydroxypropyl acrylate
ICP-MS	inductively coupled plasma-mass spectrometer
ICP-OES	inductively coupled plasma-optical emission spectrometer
IEC	Ion exchange capacity
MAAc	methacrylic acid
MAETC	[2-(Methacryloyloxy) ethyl]trimethylammonium chloride
MAN	methacrylonitrile
MIPS	molecular imprinted polymers
NIPAAm	N-isopropylacrylamide
NMR	nuclear magnetic resonance
NVP	N-vinylpyrrolidone
PE	polyethylene
PEFCs	polymer electrolyte fuel cells
PET	poly(ethylene terephthalate)
PIG	pre-irradiation grafting
PLA	polylactic acid
PLE	polymeric ligand exchanger
PP	polypropylene
PTFE	polytetrafluoroethylene, Teflon
PVA	poly(vinyl alcohol)
PVC	poly(vinyl chloride)
PVDF	poly(vinylidene fluoride)
RIGP	Radiation–induced graft polymerization
SEM	scanning electron microscopy
SG	simultaneous irradiation grafting

Sty	styrene
TEM	transmission electron microscopy
TGA	thermogravimetric analysis
VBC	vinylbenzyl chloride
VBT	vinylbenzyltrimethyl ammonium chloride
XPS	x ray photoelectron spectroscopy

LIST OF PARTICIPANTS

Ajji,Z.	Atomic Energy Commission of Syria (AECS) 17th Nissan Street, Kafar Sousah, P.O. Box: 6091 Damascus, Syrian Arab Republic Tel.: +963-11-611-19 26/7, 213 25 80 atomic@aec.org.sy, Zajji64@gmail.com, zajji@gmx.net
Al-Sheikhly, M.	University of Maryland Dept. of Materials & Nuclear Eng. College Park MD 20742-2115, United States of America Tel.: +301-405-5214 mohamad@umd.edu
Bhardwaj, Y.K.	Bhabha Atomic Research Centre RTDD, HIRUP Building Trombay - MUMBAI-400085, India Tel.: +91-022-25590178 ykbhard@barc.gov.in
Clochard, M.-C.	CEA – LSI, Ecole Polytechnique 91128 – Palaiseau, France Tel.: +33 (0) 1 69 33 45 26 marie claude.clochard@polytechnique.edu
Gueven, O.	Department of Chemistry Hacettepe University 06532 Ankara, Turkey Tel.: + 90 – 312 – 297-7977 guven@hacettepe.edu.tr
Hegazy, E.-S. A.	National Center for Radiation Research & Technology 3 Ahmed El-Zomor, P.O. Box 29, Madinat Nasr, Cairo Egypt Tel.: + 202-2876031 hegazy_ea@hotmail.com
Manzoli, J. E.	Instituto de Pesquisas Energeticas e Nucleares (IPEN) Comissao Nacional de Energia Nuclear (CNEN) Av. Prof.Lineu Prestes, 2242 - Cidade Universitaria 05508-000 Sao Paulo, Brazil Tel.: +55-11-31339865 jmanzoli@ipen.br
Mazzei, R.	Comisión Nacional de Energía Atómica (CNEA) Avda del Libertador 8250 C 1429BNP Buenos Aires, Argentina Tel.: +54-11-6779-8571 mazzei@cae.cnea.gov.ar
Nasef, M. M. E.-S	Faculty of Chemical & Natural Resources Engineering Universiti Teknologi Malaysia 81310 Utm Skudai, Joho, Malaysia Tel.: +607-5535561 mahmoudeithar@fkkksa.utm.my

Nho, Y.-C.	Korea Atomic Energy Research Institute (KAERI) 1266 Sinjeong, Jeongup Jeonbuk-Do, 580-185 Republic of Korea Tel.: +82-63-570-3060 ycnho@kaeri.re.kr
Przybytniak, G.	Institute of Nuclear Chemistry and Technology (INCT) Dorodna Str. 16, 03-195 Warsaw, Poland Tel.: + 48-22-504-13 84, + 48 22 504-10-94 przybyt@ichtj.waw.pl
Scherer, G. G.	Paul Scherrer Institut CH-5232 Villigen, Switzerland Tel.: +41-563-102-362 guenther.scherer@psi.ch.
Suwanmala, P.	Ministry of Science and Technology (MOST) Thailand Institute of Nuclear Technology (TINT) 16 Vibhavadi Rangsit Road, Chatuchak, Bangkok 10900 Thailand Tel.: +66- 257-95230, Ext. 2323 phiriyatorn@hotmail.com
Takács, E.	Institute of Isotopes Hungarian Academy of Sciences Konkoly Thege ut 29-33 H-1121 Budapest, Hungary Tel: + 36-1-392-2612 takacs@iki.kfki.hu
Ueki, Y.	Japan Atomic Energy Agency (JAEA) 1233 Watanuki Takasaki, 370-1292, Takasaki, Japan Tel.: +81-27-346-9394 ueki.yuji@jaea.go.jp

Research Coordination Meetings
Vienna, Austria: 19–23 November 2007
Aargau, Switzerland: 15–19 June 2009
Budapest, Hungary: 6–10 December 2010

No. 22

IAEA
International Atomic Energy Agency

Where to order IAEA publications

In the following countries IAEA publications may be purchased from the sources listed below, or from major local booksellers. Payment may be made in local currency or with UNESCO coupons.

AUSTRALIA
DA Information Services, 648 Whitehorse Road, MITCHAM 3132
Telephone: +61 3 9210 7777 • Fax: +61 3 9210 7788
Email: service@dadirect.com.au • Web site: http://www.dadirect.com.au

BELGIUM
Jean de Lannoy, avenue du Roi 202, B-1190 Brussels
Telephone: +32 2 538 43 08 • Fax: +32 2 538 08 41
Email: jean.de.lannoy@infoboard.be • Web site: http://www.jean-de-lannoy.be

CANADA
Bernan Associates, 4501 Forbes Blvd, Suite 200, Lanham, MD 20706-4346, USA
Telephone: 1-800-865-3457 • Fax: 1-800-865-3450
Email: customercare@bernan.com • Web site: http://www.bernan.com

Renouf Publishing Company Ltd., 1-5369 Canotek Rd., Ottawa, Ontario, K1J 9J3
Telephone: +613 745 2665 • Fax: +613 745 7660
Email: order.dept@renoufbooks.com • Web site: http://www.renoufbooks.com

CHINA
IAEA Publications in Chinese: China Nuclear Energy Industry Corporation, Translation Section, P.O. Box 2103, Beijing

CZECH REPUBLIC
Suweco CZ, S.R.O., Klecakova 347, 180 21 Praha 9
Telephone: +420 26603 5364 • Fax: +420 28482 1646
Email: nakup@suweco.cz • Web site: http://www.suweco.cz

FINLAND
Akateeminen Kirjakauppa, PO BOX 128 (Keskuskatu 1), FIN-00101 Helsinki
Telephone: +358 9 121 41 • Fax: +358 9 121 4450
Email: akatilaus@akateeminen.com • Web site: http://www.akateeminen.com

FRANCE
Form-Edit, 5, rue Janssen, P.O. Box 25, F-75921 Paris Cedex 19
Telephone: +33 1 42 01 49 49 • Fax: +33 1 42 01 90 90
Email: formedit@formedit.fr • Web site: http://www. formedit.fr

Lavoisier SAS, 145 rue de Provigny, 94236 Cachan Cedex
Telephone: + 33 1 47 40 67 02 • Fax +33 1 47 40 67 02
Email: romuald.verrier@lavoisier.fr • Web site: http://www.lavoisier.fr

GERMANY
UNO-Verlag, Vertriebs- und Verlags GmbH, Am Hofgarten 10, D-53113 Bonn
Telephone: + 49 228 94 90 20 • Fax: +49 228 94 90 20 or +49 228 94 90 222
Email: bestellung@uno-verlag.de • Web site: http://www.uno-verlag.de

HUNGARY
Librotrade Ltd., Book Import, P.O. Box 126, H-1656 Budapest
Telephone: +36 1 257 7777 • Fax: +36 1 257 7472 • Email: books@librotrade.hu

INDIA
Allied Publishers Group, 1st Floor, Dubash House, 15, J. N. Heredia Marg, Ballard Estate, Mumbai 400 001,
Telephone: +91 22 22617926/27 • Fax: +91 22 22617928
Email: alliedpl@vsnl.com • Web site: http://www.alliedpublishers.com

Bookwell, 2/72, Nirankari Colony, Delhi 110009
Telephone: +91 11 23268786, +91 11 23257264 • Fax: +91 11 23281315
Email: bookwell@vsnl.net

ITALY
Libreria Scientifica Dott. Lucio di Biasio “AEIOU”, Via Coronelli 6, I-20146 Milan
Telephone: +39 02 48 95 45 52 or 48 95 45 62 • Fax: +39 02 48 95 45 48
Email: info@libreriaaeiou.eu • Website: www.libreriaaeiou.eu

JAPAN
Maruzen Company, Ltd., 13-6 Nihonbashi, 3 chome, Chuo-ku, Tokyo 103-0027
Telephone: +81 3 3275 8582 • Fax: +81 3 3275 9072
Email: journal@maruzen.co.jp • Web site: http://www.maruzen.co.jp

REPUBLIC OF KOREA
KINS Inc., Information Business Dept. Samho Bldg. 2nd Floor, 275-1 Yang Jae-dong SeoCho-G, Seoul 137-130
Telephone: +02 589 1740 • Fax: +02 589 1746 • Web site: http://www.kins.re.kr

NETHERLANDS
De Lindeboom Internationale Publicaties B.V., M.A. de Ruyterstraat 20A, NL-7482 BZ Haaksbergen
Telephone: +31 (0) 53 5740004 • Fax: +31 (0) 53 5729296
Email: books@delindeboom.com • Web site: http://www.delindeboom.com

Martinus Nijhoff International, Koraalrood 50, P.O. Box 1853, 2700 CZ Zoetermeer
Telephone: +31 793 684 400 • Fax: +31 793 615 698
Email: info@nijhoff.nl • Web site: http://www.nijhoff.nl

Swets and Zeitlinger b.v., P.O. Box 830, 2160 SZ Lisse
Telephone: +31 252 435 111 • Fax: +31 252 415 888
Email: infoho@swets.nl • Web site: http://www.swets.nl

NEW ZEALAND
DA Information Services, 648 Whitehorse Road, MITCHAM 3132, Australia
Telephone: +61 3 9210 7777 • Fax: +61 3 9210 7788
Email: service@dadirect.com.au • Web site: http://www.dadirect.com.au

SLOVENIA
Cankarjeva Zalozba d.d., Kopitarjeva 2, SI-1512 Ljubljana
Telephone: +386 1 432 31 44 • Fax: +386 1 230 14 35
Email: import.books@cankarjeva-z.si • Web site: http://www.cankarjeva-z.si/uvoz

SPAIN
Díaz de Santos, S.A., c/ Juan Bravo, 3A, E-28006 Madrid
Telephone: +34 91 781 94 80 • Fax: +34 91 575 55 63
Email: compras@diazdesantos.es, carmela@diazdesantos.es, barcelona@diazdesantos.es, julio@diazdesantos.es
Web site: http://www.diazdesantos.es

UNITED KINGDOM
The Stationery Office Ltd, International Sales Agency, PO Box 29, Norwich, NR3 1 GN
Telephone (orders): +44 870 600 5552 • (enquiries): +44 207 873 8372 • Fax: +44 207 873 8203
Email (orders): book.orders@tso.co.uk • (enquiries): book.enquiries@tso.co.uk • Web site: http://www.tso.co.uk

On-line orders
DELTA Int. Book Wholesalers Ltd., 39 Alexandra Road, Addlestone, Surrey, KT15 2PQ
Email: info@profbooks.com • Web site: http://www.profbooks.com

Books on the Environment
Earthprint Ltd., P.O. Box 119, Stevenage SG1 4TP
Telephone: +44 1438748111 • Fax: +44 1438748844
Email: orders@earthprint.com • Web site: http://www.earthprint.com

UNITED NATIONS
Dept. I004, Room DC2-0853, First Avenue at 46th Street, New York, N.Y. 10017, USA
(UN) Telephone: +800 253-9646 or +212 963-8302 • Fax: +212 963-3489
Email: publications@un.org • Web site: http://www.un.org

UNITED STATES OF AMERICA
Bernan Associates, 4501 Forbes Blvd., Suite 200, Lanham, MD 20706-4346
Telephone: 1-800-865-3457 • Fax: 1-800-865-3450
Email: customercare@bernan.com · Web site: http://www.bernan.com

Renouf Publishing Company Ltd., 812 Proctor Ave., Ogdensburg, NY, 13669
Telephone: +888 551 7470 (toll-free) • Fax: +888 568 8546 (toll-free)
Email: order.dept@renoufbooks.com • Web site: http://www.renoufbooks.com

Orders and requests for information may also be addressed directly to:

Marketing and Sales Unit, International Atomic Energy Agency
Vienna International Centre, PO Box 100, 1400 Vienna, Austria
Telephone: +43 1 2600 22529 (or 22530) • Fax: +43 1 2600 29302
Email: sales.publications@iaea.org • Web site: http://www.iaea.org/books

12-44681

This publication summarizes the results of a coordinated research project on the Development of Novel Adsorbents and Membranes by Radiation-induced Grafting for Selective Separation Purposes. Radiation-induced grafting is a technique that uses readily available, low cost synthetic and natural polymers to prepare novel materials for use where the requirements for bulk properties and surface properties cannot be readily met using a single polymeric material. The objective of the coordinated research project was to use gamma rays, electron beams and swift heavy ions to graft various monomers onto natural and synthetic polymers for the development of novel adsorbents and membranes for environmental and industrial applications. The publication provides a summary of the project results and includes reports by the participants.

INTERNATIONAL ATOMIC ENERGY AGENCY
VIENNA
ISBN 978–92–0–134010–8
ISSN 2225–8833